

Copyright is owned by the Author of the thesis. Permission is given for a copy to be downloaded by an individual for the purpose of research and private study only. The thesis may not be reproduced elsewhere without the permission of the Author.

# Characterisation and Numerical Simulation of the Lower Manawatu Catchment Hydrogeological System

A thesis presented in partial fulfilment of the  
requirements for the degree of

Doctor of Philosophy

in

Earth Sciences

at Massey University, Manawatu, New Zealand



**MASSEY UNIVERSITY**

Hisham Ibrahim Sabri Zarour

2018

Characterisation and numerical simulation of the Lower Manawatu Catchment hydrogeological system. A thesis presented in partial fulfilment of the requirements for the degree of Doctor of Philosophy in Earth Sciences at Massey University, Manawatu, New Zealand

Copyright © 2018 Hisham Zarour

Supervisor:

Dr Alan Palmer, School of Agriculture and Environment, Massey University.

Co-Supervisor:

Dr John Begg, GNS Science.

Doctoral Oral Exam Convenor:

Professor Huia Jahnke, School of Maori Knowledge, Massey University

Internal Examiner:

Associate Professor David Horne, School of Agriculture and Environment,  
Massey University

New Zealand Examiner:

Dr Clint Rissmann, Adjunct Senior Fellow, Waterways Centre, University of  
Canterbury/Lincoln University

Overseas Examiner:

Professor John Tellam, University of Birmingham, United Kingdom

**Entia non sunt multiplicanda praeter necessitatem**

Occam's razor – the principle of parsimony

To my mother Samia

In memory of my father Ibrahim

With love and eternal appreciation.

## Abstract

The Lower Manawatu Catchment (LMC) hydrogeological system presents an example of extensive stratified heterogeneous aquifers. A conceptual model was developed for the system through systematic characterisation of its geology, soil, climate, hydrology, hydrogeology and hydrochemistry. Numerical groundwater flow modelling provided an effective integrated framework for the analysis. The developed knowledge and models are useful for the identification and comparison of land and water resources management options in the catchment.

The research involved the development of a soil moisture balance modelling code to evaluate recharge. Stratigraphical modelling has been possible through incorporating imaginary lithological well logs and stratigraphical cross-sections in data-sparse areas. Geological material heterogeneity was represented in the groundwater flow model through hybridising zonal and pilot point calibration techniques. The developed soil moisture, geology and heterogeneity modelling techniques have universal applications.

The study indicates that the LMC hydrogeological system is more suitably represented as a continuous groundwater flow system rather than a sequence of discrete aquifers and aquitards. Average groundwater recharge is estimated at about 25% of average rainfall. Average baseflow is estimated at about 10% of the average runoff, the equivalent to more than half the estimated average recharge.

The LMC groundwater resource is mainly tapped at shallow depths, the locus where most of the interaction with surface water occurs. Catchment-scale steady-state numerical groundwater flow modelling suggests that in average groundwater abstraction may have been depleting overall surface water flow by about 5%.

Groundwater levels in the LMC were found to be generally stable, implying sustainable resource development. Rising groundwater levels noted in the eastern and southern outskirts of Palmerston North may be related to prolonged practice of

irrigation. No evidence of land use impacts on groundwater quality was found in the catchment. Nitrate concentrations are believed to have been kept at acceptable levels in groundwater due to denitrification stimulated by extensive organic content in some geological units.

This thesis represents a one stop shop for information on groundwater in the LMC. The knowledge and tools developed through this research have immediate use in the LMC and elsewhere, and they provide solid basis for further work.

## Acknowledgements

This thesis would not have been completed without the relentless support of my supervisor, Dr Alan Palmer. I am greatly indebted to him and grateful for his guidance. I am also thankful to Dr John Begg of GNS Science for co-supervising my research and for his invaluable insights and reviews. Alan's and John's encouragement meant a lot to me and I cannot thank them enough.

Gratitude is due to Dr Jon Roygard for encouraging me to start this journey and providing essential resources at the initial stages of the research. I also thank Clare Houlbrooke for introducing me to the Manawatu geology and hydrogeology.

This research would have been greatly lacking without the virtual climate data provided by Dr Andrew Tait of NIWA. Other important data have been provided by good colleagues in Horizons Regional Council. I particularly acknowledge help from Maree Patterson, Abby Matthews, Stacey Binsted, Stephen Collins, Sean Hodges, Ron Estall, Brent Watson, Raelene Mercer and Jeff Watson.

Peter Hurn collected most of the groundwater level data used in this thesis. I acknowledge his dedication and punctuality in gathering that information. Acknowledgements are similarly due to the drillers in the region who have been unremittingly collecting and reporting lithological information from the wells they drilled, particularly Lyle Sharratt of Wanganui Well Drillers Ltd, Neil Richardson of Richardson Drilling Co, Richard Webb of Richard Webb Limited, and Philip Webb of Nevill Webb & Son Ltd. That data have been critical to the research.

The support of my wife Amal, our daughters Karma and Dalia and sons Ibrahim and Mohamed has been inestimable, and I would like to thank them wholeheartedly for that.

I dedicate this thesis to Professor Zekai Şen of Istanbul Medipol University and Professor John Lloyd of the University of Birmingham for whom I owe my passion for hydrogeology.

# Contents

<b>Abstract</b>	<b><i>i</i></b>
<b>Acknowledgements</b>	<b><i>i</i></b>
<b>List of Figures</b>	<b><i>ix</i></b>
<b>List of Tables</b>	<b><i>xv</i></b>
<b>Chapter 1 Introduction</b>	<b>1</b>
1.1 Background	1
1.2 Research objectives	2
1.3 Hypothesis and challenges	3
1.4 Methods and material	5
1.5 The study area	8
1.6 Previous work	10
1.6.1 Hydrogeology	10
1.6.2 Hydrochemistry	13
1.7 Thesis organisation	22
<b>Chapter 2 Groundwater modelling methodology</b>	<b>23</b>
2.1 Introduction	23
2.1.1 Fitness for purpose	23
2.1.2 Understanding through modelling	24
2.1.3 Limitations and challenges	24
2.2 Flow in porous media	25
2.2.1 Darcy's law	26
2.2.2 Reynolds number	27
2.3 Groundwater flow governing equations	28
2.3.1 Laplace equation	29
2.3.2 Unconfined aquifers	30
2.4 Analytical solutions	30
2.5 Numerical solutions	32

---

2.5.1	Finite difference methods	33
2.5.2	Finite element methods	36
<b>2.6</b>	<b>Modelling method and code selection</b>	<b>37</b>
2.6.1	Code verification	39
2.6.2	Water budget calculations	39
2.6.3	Proven track record	40
2.6.4	Availability and capabilities of GUIs	41
<b>2.7</b>	<b>Modelling software package selection</b>	<b>42</b>
<b>2.8</b>	<b>Modelling approach</b>	<b>44</b>
<b>2.9</b>	<b>Calibration</b>	<b>47</b>
2.9.1	Targets	48
2.9.2	Calibration goodness circumstantial and statistical assessment	49
<b>Chapter 3</b>	<b><i>Geology and soil</i></b>	<b>51</b>
<b>3.1</b>	<b>Introduction</b>	<b>51</b>
<b>3.2</b>	<b>Geological and conceptual uncertainty</b>	<b>51</b>
<b>3.3</b>	<b>Data sources</b>	<b>52</b>
3.3.1	Ground elevation data	52
3.3.2	Geological maps	53
3.3.3	Horizons Regional Council groundwater database	55
3.3.4	Soil data	60
<b>3.4</b>	<b>Regional geological setting</b>	<b>60</b>
<b>3.5</b>	<b>Structure</b>	<b>65</b>
3.5.1	Subduction interface	67
3.5.2	Faults and Folds	67
	Wellington Fault	69
	Ruahine Fault	69
	Northern Ohariu Fault	69
	Pohangina structure/Pohangina Anticline	69
	Mt Stewart-Halcombe fault/Anticline	70
	Feilding fault/Feilding Anticline	70
<b>3.6</b>	<b>Physiographical setting</b>	<b>70</b>
<b>3.7</b>	<b>Landforms</b>	<b>73</b>

---

<b>3.8</b>	<b>Landform classification</b>	<b>74</b>
	Slope	74
	Local relief	75
	Tableland setting	77
	Profile	77
<b>3.9</b>	<b>Landform types</b>	<b>81</b>
3.9.1	Mountains and steep land	81
3.9.2	Strongly dissected terrace remnants and moderate hills	82
3.9.3	Dissected terraces	85
3.9.4	Weakly dissected terraces	85
3.9.5	Flat plains	86
<b>3.10</b>	<b>Stratigraphy</b>	<b>87</b>
3.10.1	Greywacke basement rocks	90
3.10.2	Plio-Pleistocene marine rocks	91
3.10.3	Middle-Late Quaternary strata (Hawera Series)	93
3.10.4	Holocene alluvium and dune sands	96
<b>3.11</b>	<b>Interplay between alluvial deposition and sea level change</b>	<b>97</b>
<b>3.12</b>	<b>Geological history</b>	<b>99</b>
<b>3.13</b>	<b>Soil</b>	<b>103</b>
<b>Chapter 4</b>	<b><i>Climate, soil moisture and groundwater recharge</i></b>	<b>112</b>
<b>4.1</b>	<b>Introduction</b>	<b>112</b>
<b>4.2</b>	<b>Pathway of precipitation water</b>	<b>112</b>
<b>4.3</b>	<b>Soil moisture</b>	<b>114</b>
4.3.1	Conditions and definitions	114
4.3.2	Influence over evapotranspiration	115
4.3.3	Influence over surface water runoff	117
4.3.4	Influence over groundwater recharge	118
4.3.5	Modelling	118
<b>4.4</b>	<b>Potential and actual evapotranspiration</b>	<b>118</b>
<b>4.5</b>	<b>Climatic data availability</b>	<b>120</b>
4.5.1	Monitoring network	120
4.5.2	Virtual climate stations	122

---

<b>4.6</b>	<b>LMC climate</b>	<b>123</b>
4.6.1	General setting	123
4.6.2	Precipitation	124
4.6.3	Evapotranspiration	131
4.6.4	Hydrological year	134
<b>4.7</b>	<b>LMC soil moisture balance modelling</b>	<b>136</b>
4.7.1	Set up	136
4.7.2	Results	141
4.7.3	Limitations	146
4.7.4	Verification	147
<b>Chapter 5</b>	<b>Hydrology</b>	<b>149</b>
<b>5.1</b>	<b>Introduction</b>	<b>149</b>
<b>5.2</b>	<b>Springs, seeps, lakes and wetlands</b>	<b>149</b>
<b>5.3</b>	<b>Rivers and streams</b>	<b>153</b>
<b>5.4</b>	<b>Surface water monitoring and surveys</b>	<b>153</b>
<b>5.5</b>	<b>Units and conventions</b>	<b>155</b>
<b>5.6</b>	<b>Hydrological statistics</b>	<b>157</b>
<b>5.7</b>	<b>General flow statistics</b>	<b>157</b>
5.7.1	Mean flow	157
5.7.2	Median flow	158
<b>5.8</b>	<b>Flow variability</b>	<b>158</b>
5.8.1	Yearly variability	158
5.8.2	Seasonal variability	159
5.8.3	Flow distribution	160
<b>5.9</b>	<b>Flow extremes</b>	<b>160</b>
5.9.1	Mean annual flood	160
5.9.2	Mean annual low flow	162
<b>5.10</b>	<b>Surface water-groundwater interaction</b>	<b>162</b>
<b>5.11</b>	<b>Surface water abstraction</b>	<b>164</b>
<b>5.12</b>	<b>Catchment water budget</b>	<b>164</b>
<b>Chapter 6</b>	<b>Hydrogeology</b>	<b>166</b>

---

<b>6.1</b>	<b>Introduction</b>	<b>166</b>
<b>6.2</b>	<b>Hydrogeological classification of geological material</b>	<b>166</b>
<b>6.3</b>	<b>Hydrolithostratigraphical setting</b>	<b>167</b>
6.3.1	Greywacke basement rocks	167
6.3.2	Plio-Pleistocene marine rocks	168
6.3.3	Middle-Late Pleistocene strata	168
6.3.4	Holocene alluvium and sands	169
<b>6.4</b>	<b>Aquifer properties</b>	<b>170</b>
6.4.1	Grain-size distribution analysis	170
6.4.2	Pumping tests	173
<b>6.5</b>	<b>Groundwater piezometry</b>	<b>175</b>
6.5.1	Groundwater level variability in time	176
6.5.2	Groundwater level change with depth	179
6.5.3	Piezometry and groundwater flow	179
<b>Chapter 7</b>	<b>Hydrochemistry</b>	<b>185</b>
<b>7.1</b>	<b>Introduction</b>	<b>185</b>
<b>7.2</b>	<b>Processes controlling groundwater quality</b>	<b>185</b>
<b>7.3</b>	<b>Material and methods</b>	<b>189</b>
<b>7.4</b>	<b>Data availability</b>	<b>191</b>
<b>7.5</b>	<b>Data reliability</b>	<b>193</b>
7.5.1	Quality control (QC)	194
7.5.2	Quality assurance (QA)	195
<b>7.6</b>	<b>Groundwater quality temporal variability</b>	<b>198</b>
<b>7.7</b>	<b>Representative samples</b>	<b>204</b>
<b>7.8</b>	<b>Hydrogeochemical facies (multi-ion ratios and water types)</b>	<b>205</b>
<b>7.9</b>	<b>Alkalinity and hardness</b>	<b>216</b>
<b>7.10</b>	<b>Redox conditions and nitrate concentrations</b>	<b>219</b>
<b>7.11</b>	<b>Groundwater quality variability with depth</b>	<b>226</b>
<b>7.12</b>	<b>Groundwater suitability for various uses</b>	<b>233</b>

---

<b>7.13</b>	<b>Summary</b>	<b>235</b>
<b>Chapter 8</b>	<b><i>LMC groundwater flow model</i></b>	<b>237</b>
<b>8.1</b>	<b>Introduction</b>	<b>237</b>
<b>8.2</b>	<b>Objectives and strategy</b>	<b>237</b>
<b>8.3</b>	<b>Hydrolithostratigraphical framework</b>	<b>238</b>
8.3.1	Data sources, limitations and uncertainty	238
8.3.2	Stratigraphical modelling methodology	244
8.3.3	LMC stratigraphical model	250
<b>8.4</b>	<b>LMC conceptual hydrogeological model</b>	<b>254</b>
8.4.1	Assumptions	254
8.4.2	Uncertainty and limitations	256
<b>8.5</b>	<b>Groundwater numerical model implementation</b>	<b>257</b>
8.5.1	Temporal discretisation	257
8.5.2	Spatial discretisation	258
8.5.3	Model code and software	261
<b>8.6</b>	<b>Boundary conditions</b>	<b>262</b>
8.6.1	The coastline	263
8.6.2	Water divides and basement rocks	264
8.6.3	The water table	264
8.6.4	Surface water features	265
<b>8.7</b>	<b>Groundwater abstraction</b>	<b>266</b>
8.7.1	Well depths and screen lengths	266
8.7.2	Pumping rates	269
<b>8.8</b>	<b>Model parametrisation</b>	<b>269</b>
<b>8.9</b>	<b>Initial conditions</b>	<b>270</b>
<b>8.10</b>	<b>Set up and calibration</b>	<b>270</b>
8.10.1	Initial parametrisation and manual calibration	272
8.10.2	Homogeneous layers calibration and parameter sensitivity	276
8.10.3	Heterogeneous layers calibration and parameter sensitivity	280
<b>8.11</b>	<b>Usability and confidence level</b>	<b>285</b>
<b>8.12</b>	<b>Uncertainty and limitations</b>	<b>287</b>

---

8.13	Key findings	289
<b>Chapter 9</b>	<b>Conclusion and recommendations</b>	<b>294</b>
9.1	Introduction	294
9.2	The modelling process and techniques	294
9.3	Main results	297
9.4	Further work	298
	<b>References</b>	<b>305</b>
<b>Appendix A</b>	<b>Rainfall maps</b>	<b>323</b>
<b>Appendix B</b>	<b>Surface water hydrographs</b>	<b>328</b>
<b>Appendix C</b>	<b>Groundwater level data and hydrographs</b>	<b>336</b>
<b>Appendix D</b>	<b>Groundwater quality data</b>	<b>381</b>
<b>Appendix E</b>	<b>LMC groundwater model data and figures</b>	<b>424</b>

## List of Figures

<i>Figure 1-1. Groundwater modelling process (after Barnett et al., 2012).</i> .....	6
<i>Figure 1-2. Location map showing position, extent and main features in the study area.</i> .....	9
<i>Figure 1-3. Piper trilinear diagram for groundwater samples collected from the Oroua Downs area around 1977 (after Mark-Brown, 1978).</i> .....	15
<i>Figure 2-1. Schematic represent of Darcy’s experimental apparatus illustrating the terms in Darcy’s Law (after Younger, 2007).</i> .....	26
<i>Figure 2-2. Schematic illustration of mass balance for a representative fixed control volume element (RFCVE).</i> .....	28
<i>Figure 2-3. Graphical illustration of approximation used to linearise Eq. 2-21.</i> .....	34
<i>Figure 2-4. Finite-difference (FD) grid and notation (after Anderson et al., 2015).</i> .....	36
<i>Figure 2-5. Two-dimensional (2D) horizontal finite-element mesh with triangular elements and notation (after Anderson et al., 2015).</i> .....	37
<i>Figure 2-6. Flow chart illustrating the typical sequence of steps involved in groundwater modelling (after Younger, 2007).</i> .....	46
<i>Figure 2-7. Model calibration target.</i> .....	49
<i>Figure 3-1. Physiographical map sourced from digital elevation model data.</i> .....	54
<i>Figure 3-2. Geological map based on digital QMAP data (Heron, 2014).</i> .....	58
<i>Figure 3-3. New Zealand and international geological timescales (Extracted from GNS Science, 2015).</i> ..	59
<i>Figure 3-4. Tectonic setting of New Zealand.</i> .....	61
<i>Figure 3-5. Schematic of plate interface beneath southern North Island viewed from Cook Strait (modified after Little, 2013).</i> .....	62
<i>Figure 3-6. Three-dimensional impression of the southern North Island showing effect of tectonic setting on structural geological setting.</i> .....	63
<i>Figure 3-7. Sketch section between Tangimoana and the Ruahine Ranges showing the relationship between structure and relief (after Heerdegen &amp; Shepherd, 1992).</i> .....	64
<i>Figure 3-8. Structural geological map for LMC and surrounds based on digital QMAP data (Heron, 2014).</i> .....	66
<i>Figure 3-9. Interpreted seismic line from Melhuish et al. (1996) across the Mt Stewart-Halcombe Anticline and associated faults indicating the style of deformation that might be expected near at least some of the other faults and folds in the LMC area.</i> .....	68
<i>Figure 3-10. Cross-sectional profile through the lower part of the interfluvies-river valleys area in the LMC.</i> .....	72

Figure 3-11. Slope rise, local relief, upland/lowland setting and profile calculations in 900 m radial moving window calculated from 15x15 m digital elevation model to enable landform classification using a modification of the Hammond (1954 & 1964) approach to suit local conditions and study objectives. .	76
Figure 3-12. Hammond (1954 & 1964) landform classification method criteria.....	78
Figure 3-13. Landform classes calculated using the Hammond (1954 & 1964) method with modifications to suit local conditions.....	79
Figure 3-14. Landform types in the LMC. ....	80
Figure 3-15. Surface drainage density in the LMC.....	84
Figure 3-16. Simplified geological map for the LMC.....	89
Figure 3-17. Schematic drawing illustrating the formation of terraces in the LMC (adapted after Fair, 1968). ....	94
Figure 3-18. Method to calculate incision /uplift rates in deformed, terraced areas.....	100
Figure 3-19. Schematic cross-section showing the relation between the Plio- Pleistocene sequence and basement rocks in the Wanganui Basin (after Lee et al., 2011).....	102
Figure 3-20. Soil classification orders in the LMC drawn using Fundamental Soil Layers (FSLs) digital data by Landcare Research (Hewitt, 2010).....	106
Figure 3-21. Soil classification groups in the LMC drawn using Fundamental Soil Layers (FSLs) digital data by Landcare Research (Hewitt, 2010).....	107
Figure 4-1. Schematic diagram showing the apportionment of precipitation and/or irrigation water reaching the ground surface. ....	113
Figure 4-2. Possible soil moisture conditions, corresponding plant and hydrological conditions. ....	114
Figure 4-3. Schematic diagram showing relationship between soil texture, field capacity (FC), permanent wilting point (PWP) and total available water (TAW) (after McLaren & Cameron, 1996). ....	116
Figure 4-4. Water stress coefficient (Ks) under various soil moisture conditions (after Allen et al., 1998). ....	116
Figure 4-5. Climatic and virtual climatic stations in and near the LMC. ....	121
Figure 4-6. Virtual climate stations (VCS), Thiessen polygons for climatic parameter calculations and mean annual rainfall isohyetal map for the period 1971-2000 (based on digital map by Tait & Sturman, 2008). ....	126
Figure 4-7. Mean annual rainfall calculated from VCS data for the period 1985 – 2015.....	127
Figure 4-8. Monthly rainfall at Palmerston North for the period 1985-2015. ....	129
Figure 4-9. Yearly rainfall at Palmerston North.....	130
Figure 4-10. Monthly rain cumulative deviation from mean (CDFM) at Palmerston North for the period 1985-2015. ....	131
Figure 4-11. Mean annual potential evapotranspiration calculated from VCS data for the period 1985 – 2015. ....	133

Figure 4-12. Mean rainfall ( $P$ ) compared to calculated maximum, mean and minimum monthly potential evapotranspiration ( $ET_p$ ) at Palmerston North Aws station (data sourced from Chappell, 2015). .....	134
Figure 4-13. Mean annual difference between rainfall and potential evapotranspiration calculated from VCS data for the period 1985–2015. ....	135
Figure 4-14. Screenshot of the user interface for the LMC SMB model. ....	137
Figure 4-15. Ministry for the Environment 2012 land use map. ....	139
Figure 4-16. Long-term mean annual actual to potential evapotranspiration ratio. ....	143
Figure 4-17. Long-term mean annual surface runoff depth. ....	144
Figure 4-18. Long-term mean annual groundwater recharge depth. ....	145
Figure 5-1. Possible relationships between groundwater, wetlands and lakes (after Winter et al., 1998). .....	150
Figure 5-2. Possible relationships between groundwater, rivers and streams (after Winter et al., 1998). .....	151
Figure 5-3. Method for determining stream-groundwater relationship using groundwater level contour maps (after Winter et al., 1998). ....	151
Figure 5-4. Lake distribution in relation to landforms and geological structure. ....	152
Figure 5-5. Environmental river classification (REC), river catchments and surface water data availability in the LMC. ....	154
Figure 5-6. Flow variability percentiles for selected surface waterways (data from Henderson & Diettrich, 2007). ....	159
Figure 5-7. Flow duration curve (FDC) for the Manawatu River at three locations in the LMC showing percentage of time flows are equalled or exceeded (data from Henderson & Diettrich, 2007). ....	161
Figure 5-8. Conceptual presentation of main rivers and streams and their mean annual flows. ....	163
Figure 6-1. Effect of terraces on groundwater flow (after Winter et al., 1998). ....	169
Figure 6-2. Constant rate pumping test time-drawdown semi-log plot for Well 336093 (40 m deep) in Aokautere, east of Palmerston North. The S-shaped time-drawdown curve is typical of unconfined aquifer with delayed yield (figure sourced from Schumacher, 1999). ....	175
Figure 6-3. Comparison of hydraulic conductivity values obtained from pumping tests in the LMC to literature values (figure sourced from Schumacher, 1999). Screen length is used in the calculations as a proxy to aquifer thickness. ....	176
Figure 6-4. Example of groundwater level hydrograph plots presented in Appendix C. ....	177
Figure 6-5. Groundwater level trends in the LMC. ....	178
Figure 6-6. Hydrogeological fence diagram (after Schumacher, 1999). ....	180
Figure 6-7. Relation between screen depth and head as observed in the Whakarongo multi-level piezometer setup (after Zarour, 2008). ....	180
Figure 6-8. Piezometric map for the LMC drawn using long-term average groundwater level and surface water stage monitoring data. ....	182

---

Figure 6-9. Schematic diagram for a topographically controlled groundwater system and flow times (after Buchanan & Buddemeier, 2005).....	183
Figure 6-10. Schematic diagram showing multi-scale flow system (after Winter et al., 1998).....	184
Figure 7-1. Location map showing groundwater quality sampling sites and depths in the LMC until the end of 2007. ....	192
Figure 7-2. Depth range of sampled wells in the LMC. ....	193
Figure 7-3. Map showing location and depth of wells with complete, acceptable groundwater quality samples in the LMC until the end of 2007. ....	197
Figure 7-4. Depth range of wells with acceptable samples in the LMC. ....	198
Figure 7-5. Frequency plot of CAB values for samples from LMC until the end of 2007.....	198
Figure 7-6. Location map showing wells with long-term groundwater quality record until the end of 2007 in the LMC. ....	200
Figure 7-7. Groundwater chemistry hydrograph for Well 316037. Representative sample date (28/05/2002) indicated by red arrow. ....	201
Figure 7-8. Groundwater chemistry hydrograph for Well 336113. Representative sample date (4/03/1998) indicated by red arrow. ....	201
Figure 7-9. Groundwater chemistry hydrograph for Well 336114. Representative sample date (30/10/1996) indicated by red arrow. ....	202
Figure 7-10. Groundwater chemistry hydrograph for Well 337005. Representative sample date (29/09/1995) indicated by red arrow. ....	202
Figure 7-11. Groundwater chemistry hydrograph for Well 352271. Representative sample date (10/09/1987) indicated by red arrow. ....	203
Figure 7-12. Groundwater chemistry hydrograph for Well 353015. Representative sample date (2/10/1995) indicated by red arrow. ....	203
Figure 7-13. Groundwater chemistry hydrograph for Well 354011. Representative sample date (18/12/1995) indicated by red arrow. ....	204
Figure 7-14. Procedure to plot samples on the Expanded Durov Diagram (adapted after Younger, 2007). ....	207
Figure 7-15. Interpolation of the Expanded Durov Diagram (Modified after Younger, 2007). Field numbers can be used to typify the water and labelled arrows indicate evaluation processes for samples on the same flow path (A: ion exchange, B: dissolution and/or mixing, C: reverse ion exchange). ....	208
Figure 7-16. Expanded Durov plot of samples from the LMC (continued overleaf).....	209
Figure 7-17. Groundwater quality types in the LMC.....	212
Figure 7-18. $\text{HCO}_3^-$ : $\text{Na} +$ relationship for LMC groundwater. ....	215
Figure 7-19. pH values for representative groundwater samples in LMC.....	217
Figure 7-20. Relationship between calculated $\text{pCO}_2$ and measured $\text{CO}_2$ values in LMC groundwaters. ....	218

---

Figure 7-21. Redox groundwater types in the LMC. ....	221
Figure 7-22. Location map showing detections of peat/organic matter reported in drillers' well logs. .	222
Figure 7-23. Redox ladder: electron acceptors and donors. ....	223
Figure 7-24. Nitrate concentration in mg/L NO <sub>3</sub> – in the LMC. ....	225
Figure 7-25. Plot of calculated total dissolved solids (TDS) against well nominal depth.....	227
Figure 7-26. Plot of calculated total dissolved solids (TDS) against elevation of well nominal bottom. .	227
Figure 7-27. Location map showing well clusters used to investigate groundwater quality-depth relationship. ....	228
Figure 7-28. Change in hydrogeochemical parameters with depth in selected areas across the LMC (continued overleaf). ....	229
Figure 7-29. Wilcox plot for representative groundwater samples from the LMC. ....	235
Figure 8-1. Location map showing wells with drillers' description in the LMC, real and imaginary wells and cross-sections used in the construction of the stratigraphical model presented in Section 8.3.3. ....	240
Figure 8-2: Flow chart illustrating attempted and abandoned stratigraphical model construction methodology. ....	247
Figure 8-3. Stratigraphical cross-sections extrapolated between imaginary wells to help with 3D stratigraphical modelling. ....	248
Figure 8-4. Perceived possible extent of stratigraphical units.....	251
Figure 8-5. Block diagram presenting the stratigraphical framework in the LMC. ....	252
Figure 8-6. Fence diagram presenting the stratigraphical framework in the LMC.....	253
Figure 8-7. Approaches for superimposing stratigraphical models on finite difference grid (after Aquaveo, 2017). ....	260
Figure 8-8. Idealised sketch of the relationship between fresh groundwater and seawater in an unconfined coastal aquifer (after Todd and Mays, 2005). ....	264
Figure 8-9. Surface water features and monitoring data incorporated in the LMC groundwater flow model. ....	267
Figure 8-10. Average groundwater abstraction rates included in the groundwater flow model. ....	268
Figure 8-11. Model calculated head distribution (in masl) for the topmost layer from manual calibration. ....	274
Figure 8-12. Scatter plot of measured heads against manually calibrated model calculated heads using initial estimates of hydraulic conductivity values presented in Table 8-3 and river/stream bed conductance values presented in Figure 8-9. ....	275
Figure 8-13. Cross-section through row 41 in the homogeneous stratigraphical strata model showing the overlay of geology on the groundwater flow model finite difference grid, flow velocity vectors (black arrows) and the water table (Blue line).....	278
Figure 8-14. Sensitivity evaluation of hydraulic conductivity (top) and bed conductance (bottom) values obtained from automated parameter estimation assuming homogeneity of geological strata. ....	280

---

<i>Figure 8-15. Error bars at observation points showing the degree of fitness between calculated and observed heads from automated parameter estimation assuming heterogeneity of hydrolithostratigraphical units within the LMC model area. ....</i>	<i>282</i>
<i>Figure 8-16. Sensitivity evaluation of hydraulic conductivity (top) and bed conductance (bottom) values obtained from automated parameter estimation assuming heterogeneity of geological strata. ....</i>	<i>285</i>
<i>Figure 8-17. Flow velocity vectors showing groundwater flowing mainly towards rivers in Layer 1 of the LMC model. ....</i>	<i>291</i>
<i>Figure 8-18. Cross-section through the Square at the centre of Palmerston North, showing vertical groundwater flow components. ....</i>	<i>292</i>
<i>Figure 9-1. Groundwater level hydrographs for Well 336651. ....</i>	<i>366</i>

## List of Tables

<i>Table 2-1. GMS supported MODFLOW packages (modules).</i>	44
<i>Table 3-1. Geological units and map codes.</i>	56
<i>Table 3-2. Land slope classes (adapted after Dikau et al., 1991).</i>	75
<i>Table 3-3. Land relief classes (adapted after Dikau et al., 1991).</i>	75
<i>Table 3-4. Upland/lowland classification (adapted after Dikau et al., 1991).</i>	77
<i>Table 3-5. Land profile classes (adapted after Dikau et al., 1991).</i>	78
<i>Table 3-6. Soil Orders and Groups in the LMC.</i>	108
<i>Table 3-7. Quaternary terraces ages, names and loess cover in the LMC (after Begg et al., 2005).</i>	111
<i>Table 3-8. General order of magnitude for saturated hydraulic conductivity for soil horizons in loessial soils (after Poulsen, 2013).</i>	111
<i>Table 4-1. Palmerston North climatic stations.</i>	120
<i>Table 4-2. Reported daily rainfall for stations Palmerston North Aws (old) and Palmerston North Ews (new) during their co-operating period.</i>	122
<i>Table 4-3. Long-term mean climatic parameter values for Palmerston North (mainly compiled from Chappell, 2015).</i>	125
<i>Table 4-4. Annual mean rain rates and volumes over the LMC area for the periods 1985-2015 calculated from VCS data.</i>	128
<i>Table 4-5. Mean and median rain rates and volumes over the LMC area for the periods 1971-2000 and 1978-2007 (estimated from digital maps by Tait &amp; Sturman, 2008).</i>	128
<i>Table 4-6. Typical soil water characteristics for various USDA-STC classes (after Allen et al., 1998), correlated to LMC soils based on NZ FSL.</i>	138
<i>Table 4-7. SMB model calculated mean annual rain, potential evapotranspiration, irrigation, actual evapotranspiration, surface runoff and groundwater recharge over the periods 1985-2015.</i>	142
<i>Table 4-8. Ratios between SMB model calculated mean annual hydrological parameters over the periods 1985-2015.</i>	142
<i>Table 4-9. Overall LMC SMB model results for the periods 1985-2015 assuming only dry land farming conditions.</i>	142
<i>Table 5-1. Continuous river level and flow monitoring sites operated by Horizons and basic flow statistics.</i>	156
<i>Table 5-2. Consented surface water takes active during the period 2010-2015.</i>	164
<i>Table 5-3. LMC water balance parameters.</i>	165
<i>Table 6-1. Typical Hydraulic conductivity values for selected rocks and sediments (compiled from Bear, 1972; Heath, 1983; Younger, 2007).</i>	167

<i>Table 6-2. Hydraulic conductivity calculations based on grain-size distribution data reported in Cooper (1999).</i> .....	172
<i>Table 7-1. Status of available groundwater quality records in and within 2 km of the Lower Manawatu Catchment until the end of 2007.</i> .....	196
<i>Table 7-2. Status of available groundwater quality records in and within 2 km of the Lower Manawatu Catchment until the end of 2007.</i> .....	199
<i>Table 7-3. Classification of LMC representative samples using the Expanded Durov Diagram hydrogeochemical facies typifying.</i> .....	213
<i>Table 7-4. important water quality guideline values in the DWSNZ and ANZECC 2000 (after Daughney et al., 2009)</i> .....	234
<i>Table 8-1. Commonly used drillers' descriptions of rock and soil units in well logs and their most likely lithological interpretation (adapted after Schumacher, 1999).</i> .....	242
<i>Table 8-2. Upper Wanganui Series and Haweran Series stratigraphical units (adapted after Begg et al., 2005).</i> .....	243
<i>Table 8-3. LMC stratigraphical model units.</i> .....	245
<i>Table 8-4. Groundwater boundary conditions (Barnett et al., 2012; Franke et al., 1987).</i> .....	262
<i>Table 8-5. Surface water calibration targets'</i> .....	271
<i>Table 8-6. Manually calibrated model main results and basic calibration metrics.</i> .....	276
<i>Table 8-7. Automated estimates of hydraulic conductivity and riverbed conductance assuming homogeneity in geological strata.</i> .....	279
<i>Table 8-8. Main results and basic calibration metrics for the automated parameter estimation model assuming hydraulic conductivity homogeneity in each hydrolithostratigraphical unit.</i> .....	279
<i>Table 8-9. Hydraulic conductivity ranges estimated for hydrolithostratigraphical units in the LMC using zoned pilot point calibration.</i> .....	283
<i>Table 8-10. Main results and basic calibration metrics for the automated parameter estimation model assuming hydraulic conductivity heterogeneity in hydrolithostratigraphical material.</i> .....	283
<i>Table 8-11. Heterogeneous hydrolithostratigraphical units model calculations of overall average effects of groundwater abstraction on main river flows and other elements of the water budget.</i> .....	293

# Chapter 1 Introduction

## 1.1 Background

One of our most valuable resources is the water in the ground beneath our feet (McCarron & Zarour, 2005). Toebes (1972) estimated that 80%, or  $1.7 \times 10^{12} \text{ m}^3$ , of New Zealand's fresh water lies under the ground. Stewart and Bidwell (2008) contemplate that in 2007 groundwater accounted on the national-scale for nearly 10% of the water used by industry, 25% of the water used for domestic supply, and 80% of the water used by agriculture. Groundwater springs and baseflow are also important in sustaining flows in rivers, maintain wetland ecosystems and support many subterranean life forms, particularly during dry periods. Nevertheless, groundwater is often the least-understood component of the hydrological cycle and is commonly undervalued (White & Rosen, 2001). In part, this may be due to its nature as a dynamic, invisible resource that makes it difficult to conceptualise. Another possible reason could be that historically surface water was easier to exploit in New Zealand, so there has been limited interest in gathering hydrogeological data and undertaking groundwater studies.

With increasing demand and environmental restrictions on surface water, groundwater is becoming the preferred and perhaps even the only available water supply option in some areas in New Zealand (Zarour, 2008). Groundwater is also becoming more valued by the community due to the increased awareness of its interconnectedness with surface water and that quantity and quality of surface water and groundwater are inseparable.

In the Manawatu-Wanganui region, within which the Lower Manawatu Catchment (LMC) is located, groundwater provides more than 40% of the overall consumptive water demand (Horizons, 2007). Licenced groundwater abstraction in the region has nearly doubled over the period 1997–2007 (Zarour, 2008). In the LMC groundwater is used for human and animal drinking purposes, irrigation, some

industries and supports wetlands and other surface water forms. Zarour (2008) estimated that  $53 \times 10^6 \text{ m}^3$  of groundwater were extracted for various purposes from c. 5,400 wells through the LMC in the hydrological year 2007/2008.

Despite its obvious importance to the environment, the community and the economy, groundwater in the LMC remains poorly understood and largely an underrated resource. The hydrogeology of parts of the LMC had been studied but many areas have never been investigated and the catchment's groundwater system has not been considered holistically. Moreover, previous studies commonly derived conflicting conclusions regarding the extent, nature and dynamics of the hydrogeological system and there has been a lack of suitable methods to satisfactorily represent the area's hydrolithostratigraphy and realistically simulate its complex hydrogeology. A sound and comprehensive understanding of the resource is fundamental to managing it beneficially and sustainably and new techniques are needed to enable sound hydrogeological analysis of the stratified heterogeneous aquifer system in the LMC.

## 1.2 Research objectives

This thesis is principally aimed at establishing a robust understanding of the groundwater system in the LMC through systematic conceptualisation and numerical modelling. Achieving this objective required the development of a new geological modelling technique that employs imaginary wells and cross-sections and a new aquifer parametrisation procedure that amalgamates zonal and pilot point model calibration methods to appropriately represent geological stratification and hydraulic heterogeneity in the studied aquifer system. The conceptual model presented provides a realistic framework for effective environmental planning and decision-making and the developed numerical models can be used as tools for assessing the feasibility of various environmental management options. The developed new geological and hydrogeological modelling approaches can be utilised in geological and hydrogeological work globally.

### 1.3 Hypothesis and challenges

Most previous investigators were inclined to define the LMC groundwater system as a sequence of alternating glacial-time, gravel dominated alluvial aquifers and interglacial-time, sand dominated marine aquitards and aquicludes, in which upward hydraulic gradients can occur only due to aquifer confinement by aquitard or aquiclude strata. This research hypothesises and proves that the LMC hydrogeological system is more appropriately conceptualised and modelled as an integral groundwater flow system that comprises a sequence of glacial and interglacial times sediments that are hydraulically continued throughout the entire three-dimensional (3D) extent of the hydrogeological system, which is hydraulically connected to surface water in the catchment. Within this conceptual framework, downward hydraulic gradients characterise recharge area settings and upward hydraulic gradients depict discharge area settings (Freeze & Cherry, 1979; Tóth, 2009).

Legitimate models simplify reality without forgoing important components or traits of the simulated systems. They must be based on correct and sufficient data, realistic assumptions and implement sound and defensible methods. The conceptualisation of the LMC groundwater flow system presented in this thesis is based on interdisciplinary synthesis of various types of data including information and knowledge on soil, geology, climate, hydrology, hydrogeology, hydrochemistry and land use. Numerical modelling in this study is intended to provide an ultimate integrated framework for hydrogeological analysis.

From the onset of the research, it was clear that the modelling of the LMC groundwater system would be a challenging undertaking due to data limitations and the lack of readily usable methods for realistic simulation of the system. Special analyses had to be undertaken to generate some necessary datasets and new techniques had to be developed to be able to realistically model the LMC stratified, heterogeneous aquifer system. Modelling the LMC groundwater system involved the following challenges and workarounds:

1. Poor definition of recharge areas, mechanisms and rates:

Geology, geomorphology, soil, land use, land cover, climate and surface water data have been analysed to define recharge areas and a soil moisture balance (SMB) model was developed based on the United Nations Food and Agriculture (FAO) Penman–Monteith equation (Allen *et al.*, 1998). It was necessary to correlate soil types from the New Zealand Fundamental Soil Layer (FSL) (Hewitt, 2010) to the United States Department of Agriculture (USDA) Soil Texture Classification (STC) soil types to enable this analysis.

The developed SMB model can be easily accustomed to other locations in New Zealand and internationally, providing a simple useful tool to assess groundwater recharge, crop water demand and surface runoff. It could be further enhanced to calculate contaminant loads (e.g. nutrients) resulting from various historical and planned land use scenarios.

2. Ambiguity of lithological well–log data (drillers’ descriptions of drilling cuttings):

An approach had to be devised to transform drillers’ lithological descriptions of borehole drilling cuttings into lithostratigraphical units usable in 3D geological modelling. This approach is particularly relevant to young (Pliocene to Present) glacio–eustasy sequences. It can be used in similar geological settings in New Zealand and other countries to help with general geological research and natural resources investigations.

3. Inadequate spatial coverage of lithological well–log data:

A new geological modelling methodology had to be developed using imaginary wells and cross–sections to compensate for the unrepresentativeness of certain areas and depths in the available lithological well logs dataset. The developed method assimilates conventional manual geological cross–section drawing practices with modern, computerised geostatistics–based geological modelling techniques. It has global

applications and can facilitate the construction of geological models for various purposes. There is potential to integrate more data types into the process, including surface and subsurface geophysical data, structural geology measurements and remote sensing.

#### 4. Aquifer stratification and heterogeneity:

Existing aquifer parametrisation techniques can be used to simulate stratified heterogeneous aquifers like the LMC sequence. However, the resultant simulations would not be realistic as they either assume homogeneity within individual model layers or unrealistically oversimplify the lithology of the modelled aquifer by discarding geological contacts and assuming uninterrupted heterogeneity throughout the entire modelled hydrolithostratigraphical sequence. A new method had been developed by coupling zonal and pilot point calibration techniques to simulate hydraulic properties heterogeneity in hydrolithostratigraphical units. The new technique to represent aquifer stratification and heterogeneity has global applications and a great potential to assist in making groundwater models more realistic. It could be beneficial to the modellers as well as to the users of the models, including resource managers and regulators.

### 1.4 Methods and material

The theme of this research is the use of numerical modelling as an integrated framework for developing a defensible understanding of the groundwater system. The research follows a systematic model development process that progresses through a series of interdependent stages with frequent feedback loops to earlier stages as recommended in the Australian groundwater modelling guidelines (Barnett *et al.*, 2012) (Figure 1–1). The model development process is described in detail in Chapter 8.

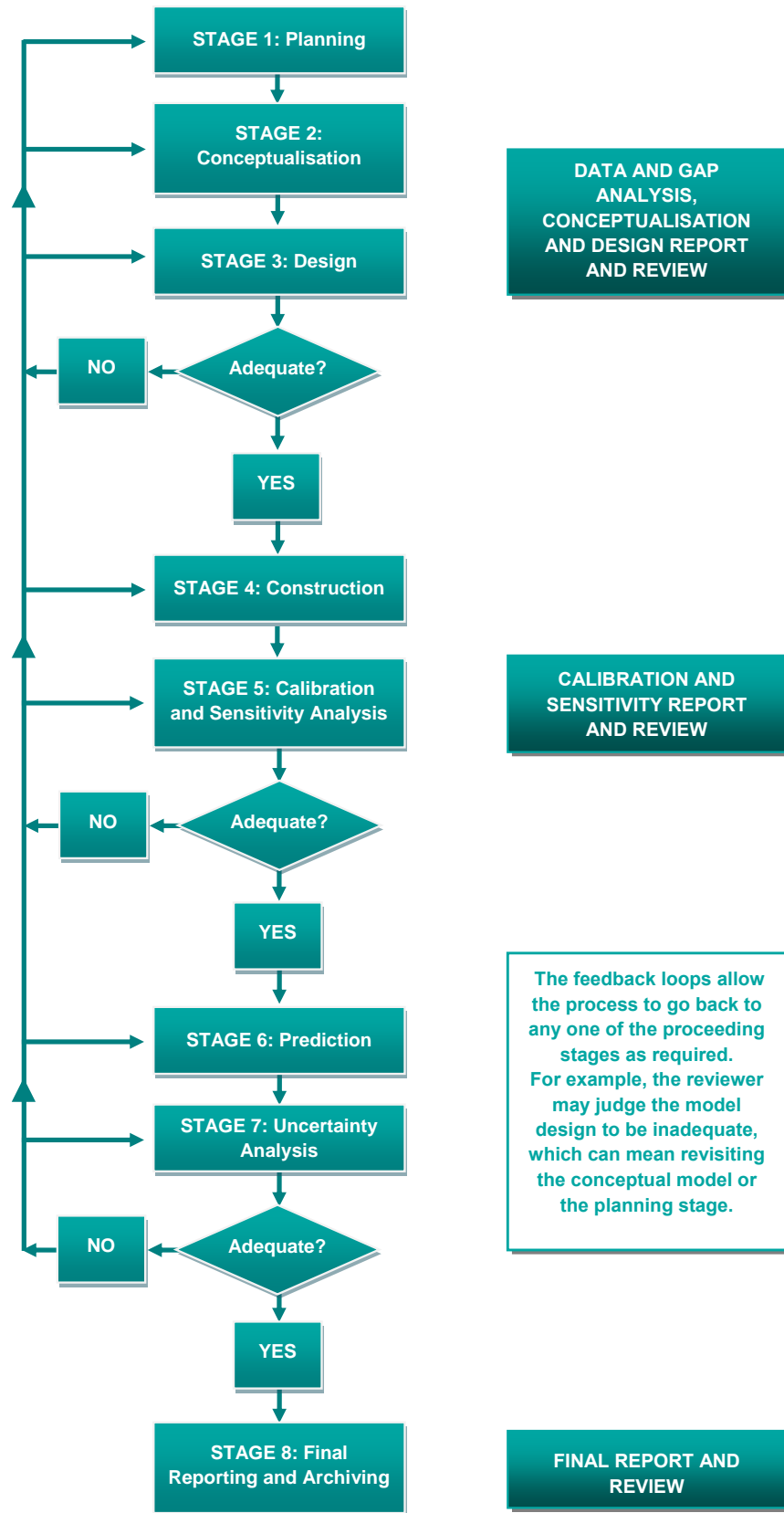


Figure 1-1. Groundwater modelling process (after Barnett *et al.*, 2012).

Numerical groundwater modelling requires vast amounts of data of various types, including information on physiography, soils, geology, climate, hydrology, hydrogeology, hydrochemistry, groundwater abstraction, land cover and use. Often, it is argued that there are not enough data for modelling, but the qualifier ‘enough’ is subjective. All models are based on available data and knowledge of the modelled system at the time of model development. During their development and use, models can help identify knowledge gaps and guide the collection of further data. Subsequently, models can be improved by incorporating the new acquired data and knowledge. Therefore, groundwater modelling may appear to be a never-ending undertaking. To be practical, however, groundwater modelling starts by identifying the research objective/s and ends by reporting on the process and results.

A good volume of data needed to understand and model the LMC groundwater system has been found to be available. Most of the data used in this research had been obtained from Horizons Regional Council (Horizons)<sup>1</sup>, which holds data on wells, drillers’ lithology description, groundwater level and quality. Hydrological data are also mainly sourced from Horizons. Geological information was sourced from GNS Science and published work. Climate data were obtained from the National Institute of Water and Atmospheric Research (NIWA) and from their publicly accessible web pages. Data availability and use in this research are described in more detail in relevant chapters.

Limited fieldwork, mainly reconnaissance visits, has been undertaken for this research. The investigation is focused on amalgamating available data to generate new knowledge rather than the generation of new raw data. It identifies data gaps and priorities that need to be addressed by relevant institutions and proposing new methods and techniques to facilitate the development of more realistic geological and hydrogeological models.

---

<sup>1</sup> Horizons Regional Council (Horizons™) is the trading name of the Manawatu–Wanganui Regional Council, the organisation responsible for managing the natural resources of the Manawatu–Wanganui region, within which the study area is located.

## 1.5 The study area

The greater Manawatu River catchment straddles the eastern and western flanks of the Ruahine and Tararua axial ranges in the southern North Island of New Zealand. The Manawatu River is antecedent to the Kaikoura Orogeny that formed the ranges and continues to drain water from the Upper Manawatu Catchment (UMC) to the east into the LMC to the west through the Manawatu Gorge. The river ultimately drains into the Tasman Sea. The North Island central ranges effectively separate the groundwater systems in the eastern and western parts of the Manawatu Catchment, albeit allowing surface water flow from the upper catchment to the lower catchment through the Manawatu Gorge. Hence, the LMC can be considered as a separate hydrogeological system from the UMC.

The LMC is part of the Wanganui basin, which is traversed by a series of northeast–southwest trending folds that subdivide it into similarly oriented catchments, including the LMC. The study area is conveniently defined as the Lower Manawatu surface water catchment (Figure 1–2). It includes about 2,678 km<sup>2</sup> of land area. Based on evidence presented in the following chapters, the surface water catchment and the groundwater catchment are considered coincidental. Notwithstanding, parts of the surface water catchment area have little or no groundwater potential due to the very low permeability of underlying rocks. Consequently, the area of the groundwater resource is smaller than that of the catchment area.

The LMC is drained by the Manawatu River and its tributaries the Oroua River and the Pohangina River. The area can be subdivided into four zones, namely: (1) the Pohangina Valley, (2) the Lower Manawatu Valley (LMV), (3) the Oroua Valley, and (4) the Manawatu Plains. The lower sections of the valleys and the Manawatu Plains form an area with an extensive groundwater resource potential.

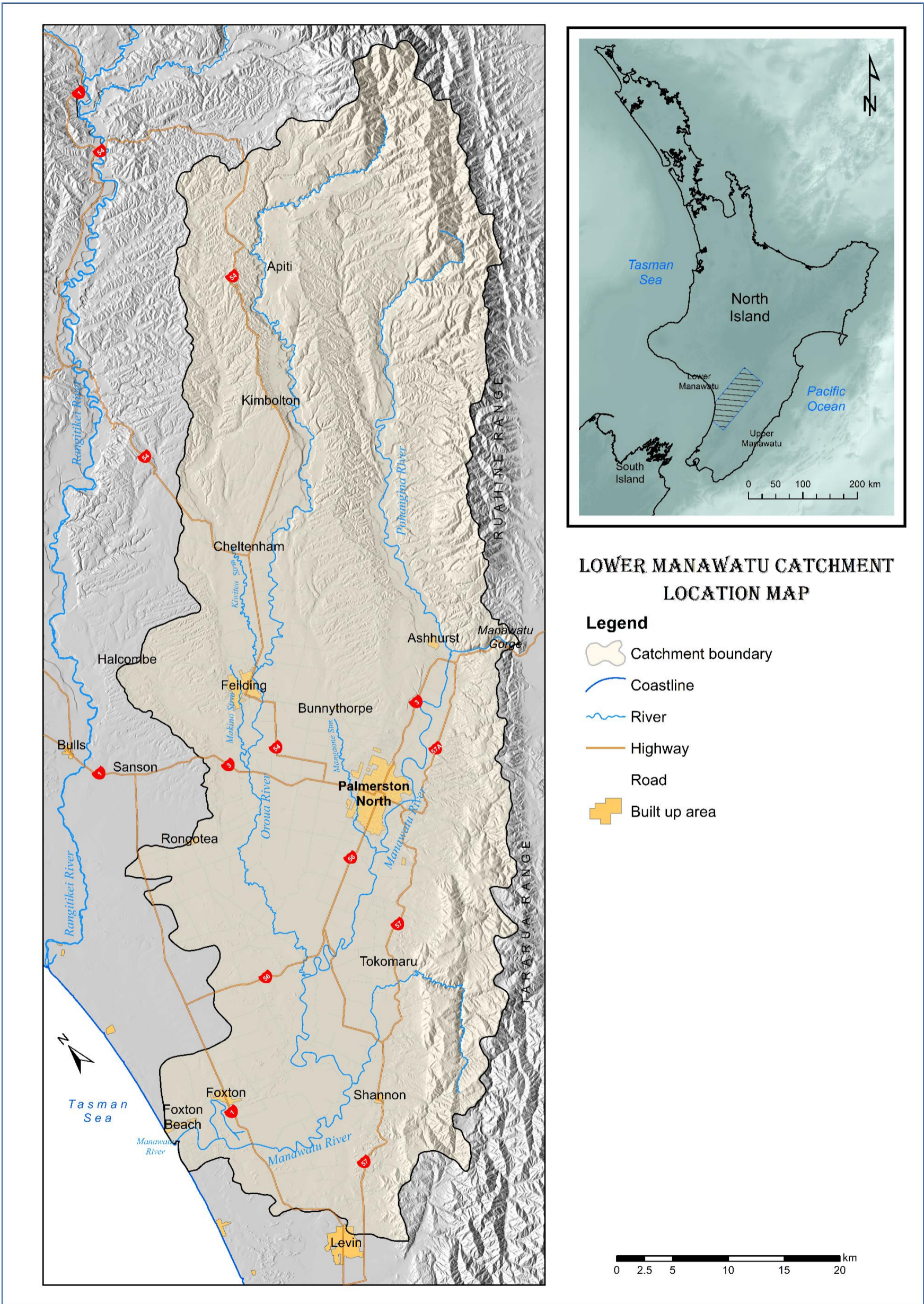


Figure 1-2. Location map showing position, extent and main features in the study area.

The Wanganui Basin contains one of the most complete late Neogene marine stratigraphical records in the world (Carter & Naish, 1998b). The basin depocentre lies c. 20 km to the south of Wanganui and the maximum sedimentary fill thickness is about 4,000 m (Anderton, 1981). In the LMC, the sedimentary sequence maximum thickness is over 1,100 m (Melhuish *et al.*, 1996). However, water wells are normally less than 100 m deep with only few wells exceeding the 200 m depth mark and very few wells in the 300–350 m depth range (Zarour, 2008). Available records provide that the median and average depths of water wells in the LMC are 30 m and 48.75 m, respectively. Accordingly, it has been hypothesised that there is no real hydrogeological interest below 350 m from the ground level. The zone of interest encompasses the entire sedimentary sequence and excludes basement rock, covering c. 2,150 km<sup>2</sup> of the LMC area. On these bases, the bottoms of the geological and hydrogeological models have been set at the contact between the Late Tertiary–Quaternary sedimentary sequence and the unconformably underlying greywacke basement rock, or 350 m below the ground surface, whichever is shallower.

The horizontal–scale and resolution of the investigation and models are constrained by the scale of the used geological maps (1:250,000) and the groundwater flow model grid spacing (500x500). The vertical resolution of the study is controlled by the model layer thickness (50 m). Hence the information presented in this thesis is usable for large– or catchment– scale purposes and should not be used in site–specific and small–scale interpretations. The study uses and produces average and representative values and the flow models are steady–state, so they cannot be directly used in transient analyses and interpretations. Notwithstanding, subsequent site–specific and transient analyses and models can be effectively based on the findings of this study and the models presented in it.

## 1.6 Previous work

### 1.6.1 Hydrogeology

Zarour (2008) summarised earlier groundwater investigations related to the LMC. Not much work has been done since then. Review of previous work reveals

reasonably good understanding of the area's geology. However, this cannot be said about its hydrogeology. So far, the well-developed geological knowledge has not been effectively incorporated in a defensible and agreed conceptual hydrogeological model for the LMC.

Parts of the LMC groundwater resource have been studied but, until now, there has not been a complete study of the resource over the whole catchment. The first known groundwater investigation in the study area is attributed to Marchbanks (1898). He looked at the artesian<sup>2</sup> wells at Longburn, conceptualising them as part of a groundwater flow system that extends up catchment to reach Ashhurst.

Most previous investigators explicitly or implicitly recognised that cyclic lithology related to global glacio-eustasy characterises the geological system in the LMC. As a result, many advocated subdivision of the hydrogeological system in the area into a series of distinct aquifers and aquitards, inaccurately associating groundwater only with cold/glacial times gravel deposits and designating all warm/interglacial periods medium- to fine-grained sediments (mainly sand) as non-water bearing aquitard material (e.g. Martley, 2001). Sand is the dominant lithology beneath the Manawatu Plains. Sand is permeable and generally makes good aquifers (e.g. Fetter, 2013; Freeze & Cherry, 1979; Todd & Mays, 2005). In addition, many investigators confused lithostratigraphical units with hydrolithostratigraphical units (e.g. McCarron & Zarour, 2005) and some misconstrued legitimate, arbitrary mathematical modelling layers as being genuine hydrostratigraphical units (e.g. Gyopari, 2005).

There have been few proposals to subdivide the LMC hydrogeological system into discrete aquifer units based on arbitrary boundaries like depth ranges (e.g. Lieffering, 1990). Such proposals are not useful. Catuneanu (2006) contends that '*the concept of sequence* [such as a hydrogeological system of aquifers and aquitards] *is as good, or acceptable, as the boundaries that define it.*' He further argues that: '*as a matter of principle, it is useless to formalise a unit* [such as an

---

<sup>2</sup> Old workers tended to describe tube wells as artesian wells.

aquifer] *when the definition of its boundaries is left to the discretion of the individual practitioner.*'

In the Wanganui Basin, structural geology knowledge was mostly not incorporated in delineating the areal extent of groundwater systems (Schumacher, 1999). The interplay of tectonic uplift and glacio–eustatic sea level created terraced valleys in the Wanganui Basin and contributed to its geomorphological development (Fair, 1968). The bearing of tectonism coupled with glacio–eustacism on the area's hydrogeology has been considered by Begg *et al.* (2005) who noted that local–scale deformation has controlled and restricted fluvial erosion, sediment transport and deposition in the area for the last 400 ka<sup>3</sup>. Most of the area's groundwater resource relates to this period – the Haweran Series.

In addition to misunderstanding the real influence of the geology on the area's hydrogeology, many of the previous conceptual models include basic hydrogeological oversight. For instance, Ongley (1945) regarded clay as potential aquifer material because of its high porosity, but he implied that its groundwater yield potential may be restricted because of its low permeability. In doing that, he considered that groundwater resource potential is principally controlled by total porosity rather than permeability, effective porosity and hydraulic conditions.

Upward hydraulic gradient in places in the LMC also proved to be particularly challenging for many previous investigators. Subdividing the system into discrete aquifers and claiming they occur under confined conditions offered a convenient explanation for the artesian conditions noticed in areas in the LMC (e.g. Bekesi, 1991). Such conceptual models failed to appreciate that, by definition, groundwater head increases with depth in discharge zones (e.g. Freeze & Cherry, 1979). They assumed that confining layers provide the only possible explanation for increasing groundwater head with depth. Zarour (2008) noted that evidence from a multi–level piezometer in the LMV suggests a proportional linear relationship between well depth and groundwater head, an indication of hydraulic continuity

---

<sup>3</sup> ka: thousand years.

rather than abrupt change. The conceptual models of stacked distinct aquifers in the area have not been able to explain the recharge mechanism for the confined aquifers.

The remarkable disagreement amongst the conceptual hydrogeological models presented by various researchers for the LMC represents a serious challenge to environmental authorities and the resource users. Miscorrelation of the geology and hydrogeological of the LMC groundwater system has been costly to the community. For example, many dry wells have been drilled in unsuitable places, including the 181 m deep well drilled by the Kiwitea Rural Water Supply Scheme in 2009. Additionally, many wells across the LMC had to be backfilled to a shallower depth because deeper strata proved unproductive. Flawed hydrogeological conceptualisation may have also contributed to unreliable environmental planning and resource management decisions.

### 1.6.2 Hydrochemistry

Few investigators studied the groundwater quality in the LMC but none of them focused only on the catchment or covered its entire area. There is still scope and need for specialised and thorough hydrogeochemical investigation of groundwater in the LMC to strengthen the hydrogeological knowledge of the resource.

Marchbanks (1898) considered groundwater quality in his assessment of water wells at Longburn, on the southwestern outskirts of Palmerston North. He reported that at the time the area's groundwater was good, soft, and suitable for use in locomotive boilers. He noted that the water was *'clear, colourless and feebly alkaline water, containing 12.22 gr.<sup>4</sup> of fixed salts per gallon. These salts are principally sodic chloride and carbonate and calcic chloride. The proportion of lime in the water is 4.28 gr., and of silica 3.01 gr., per gallon. Only traces of sulphates and magnesia are present. As lime, magnesia, and silica are not present in this water in proportions greater than are here stated, ...'*

---

<sup>4</sup> gr.: grain.

Petricevich (1970) believed that the existence of fresh groundwater in the immediate vicinity of wells in the Palmerston North area and surrounds reflects local recharge. He believed that low chloride ( $Cl^-$ ) content groundwater flowing from the Tararua Range (direct rainfall recharge) mixes with high  $Cl^-$  groundwater near Bunnythorpe to the north of Palmerston North.

Mark-Brown (1978) studied the water quality in Oroua Downs, a coastal area located just to the north of the Manawatu coastal plains. He used the Piper trilinear diagram (Figure 1-3) to classify groundwater quality samples from what he conceptualised as a three-aquifer groundwater system. Figure 1-3 shows that all the samples can be generally typified as calcium-bicarbonate ( $Ca^{2+} - HCO_3^-$ ) water. However, it seems that samples from the shallow wells have higher relative concentrations of  $Cl^-$ , which he believed to be related to contamination of shallow groundwater by sea spray. Mark-Brown (1978) noted that groundwater in all the three aquifers that he defined is dominated by alkaline earths as samples plotted in the carbonate hardness area in the Piper diagram. He noted that he did not detect an obvious seasonal pattern in the groundwater quality.

Russell (1989) noticed that groundwater salinity,  $Cl^-$  and sodium ( $Na^+$ ) content increase in the horizontal direction of flow, and that iron ( $Fe$ ) and fluoride ( $F^-$ ) concentrations increase with upward flow, resulting in lowered water quality in local and regional discharge areas. He highlighted that ion ratios in groundwater and in the Manawatu River water are similar, but ion concentrations are much higher in the former due to less dilution and longer residence time of water in the aquifers. Russell (1989) hypothesised that the increased salinity noticed in the Manawatu River at low flows is due to the dominance of base flow at such times. He believed that  $Na^+ - Cl^-$  water type surficial recharge mixes with upward leaking  $Ca^{2+} - HCO_3^-$  water type in the Lower Manawatu Valley area. Russell (1989) found no hydrochemical evidence of separate and distinctive aquifer units in the Manawatu plains and no indications of seawater intrusion in the coastal area.

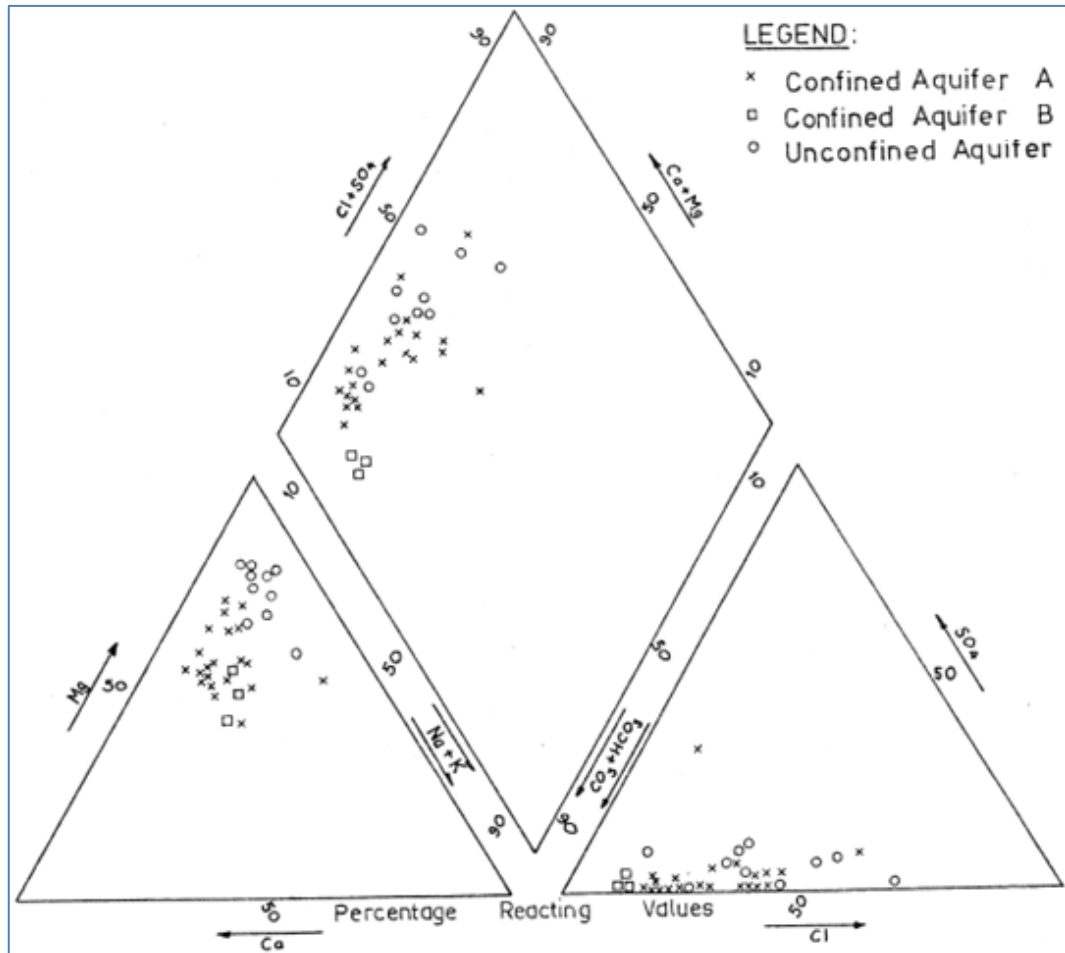


Figure 1–3. Piper trilinear diagram for groundwater samples collected from the Oroua Downs area around 1977 (after Mark–Brown, 1978).

Lieffering (1990) divided the ‘Palmerston North region’ into five hydrochemical districts but did not provide justification for that. He constructed isoconcentration maps for major constituents and few other parameters. Noticeably, many of his isoconcentration maps show zero concentration isolines, which is unrealistic. Lieffering (1990) found that the groundwater in the Palmerston North area is overall fresh, with total dissolved solids (*TDS*) generally less than 400 parts per million (ppm). However, higher salinity values reaching around 700 ppm occur to the north of the Oroua River. Lieffering (1990) suggested that the freshest groundwater occurs in the area adjacent to the Manawatu River. He noted that nitrate ( $NO_3$ ) concentrations in the area are generally very low (<0.2 ppm) but he did not clarify whether that is a measure of nitrate ion ( $NO_3^-$ ) or nitrate–nitrogen ( $NO_3^- - N$ )<sup>5</sup>. He

<sup>5</sup> 1 mg/L  $NO_3^- - N \approx 4.43$  mg/L  $NO_3^-$ .

also noted that *Fe* concentrations in the area are low (<6 ppm) and manganese (*Mn*) concentrations are very low (<0.1 ppm). He concluded that in the Palmerston North region groundwater salinity and the concentrations of all parameters except sulphate ( $SO_4^{2-}$ ) increase from east to west, increase in the direction of flow in the Manawatu River (northeast–southwest), and decrease with depth. He supposed that  $SO_4^{2-}$  concentration increases from west to east. Lieffering (1990) tried to relate groundwater quality to the three aquifers that he arbitrarily defined at three depth ranges (<60 mbgl<sup>6</sup>, 60–120 mbgl, and >120 mbgl). He suggested that higher salinity in the shallow groundwater might be due to increased dissolution of minerals by water flowing upwards from deeper levels. In addition, he suggested that pollution from agricultural land use and sea spray carried inland by westerly winds may be a reason for higher salinity in shallow groundwater in the Palmerston North area.

Bekesi (1991) believed that in the Lower Manawatu Valley, *TDS* in groundwater increase along the north–northwest flow path. He hypothesised that  $Na^+ - HCO_3^-$  water type derived from gravels overlying greywacke basement evolves into  $Ca^{2+} - HCO_3^-$  water type along the flow path due to replacement of  $Na^+$  by  $Ca^{2+}$  (i.e. reverse ion exchange).

Schumacher (1999) investigated the groundwater quality in the Lower Manawatu Valley. He examined major ion content, their temporal fluctuations, spatial distributions, ratios and oxygen–isotope composition. His trend analysis indicates no significant change in groundwater quality since the onset of groundwater quality monitoring in 1969. He also noticed that seasonal groundwater quality variability is insignificant. His study reveals that  $Cl^-$  concentration near the Tararua Ranges is low (<12 ppm) and increases with depth, whereas in the Pohangina area it is relatively high (>45 ppm) and decreases with depth. Schumacher (1999) believed that anthropogenic activities (irrigation and use of fertilisers) are responsible for the relatively elevated  $Cl^-$  concentrations at shallow depths in the Pohangina area,

---

<sup>6</sup> mbgl: metre below ground level.

where agriculture is extensive. He found that salinity (expressed as *TDS*) in the Lower Manawatu Valley area is generally low and that calcium–magnesium–bicarbonate ( $Ca^{2+} - Mg^{2+} - HCO_3^-$ ) is the dominant water type, which in his opinion is typical of local flow system settings where flow paths are short and flow velocities are high (low residence time). He theorised that  $Na^+ - HCO_3^-$  facies results from upwelling of deeper groundwater along fracture zones in the greywacke basement whereas  $Ca^{2+} - Mg^{2+} - Cl^- - SO_4^{2-}$  facies possibly reflects leachate from fertiliser application.

Schumacher (1999) looked at oxygen isotopes in groundwater in the Lower Manawatu Valley. He found that delta oxygen–18 ( $\delta^{18}O$ )<sup>7</sup> is laterally and vertically variable with no systematic distribution, which in his opinion indicates mixing of different recharge waters. He noted that there is no isotopic evidence of groundwater recharge from the Manawatu River to the groundwater system in his study area. He concluded that hydrogeochemical data support hydraulic evidence that recharge at the Pohangina anticline superimposes a local groundwater flow system over the regional groundwater flow system that is controlled by the Tararua Ranges.

Martley (2001) studied groundwater quality in the Feilding area in the Oroua Catchment. She believed that hydrogeochemical typifying in the Feilding area indicates the existence of a shallow local unconfined aquifer exemplified by  $Mg^{2+} - Cl^- / Mg^{2+} - HCO_3^-$  water type, which is superimposed on deep confined aquifers that constitute a regional groundwater flow regime in which  $Ca^{2+} - HCO_3^-$  water type predominates.

Primarily based on isotope evidence ( $^{18}O$ ,  $^3H$ ,  $^{13}C$  and  $^{14}C$ ), Taylor *et al.* (2001) defined two confined aquifers underneath an unconfined aquifer in the Palmerston North area. They named the shallower unit the Pohangina aquifer, which they assumed to be recharged on the foothills of the Ruahine Ranges, with groundwater flow in a northeast–southwest direction. They named the deeper confined unit the

---

<sup>7</sup> Delta oxygen–18 ( $\delta^{18}O$ ) is the ratio of oxygen–18 ( $^{18}O$ ) to oxygen–16 ( $^{16}O$ ).

Tararua aquifer, hypothesising that it is recharged on the Tararua Range and that groundwater flows in it in a southeast–northwest direction. They noted that both aquifers are essentially tritium–free (submodern groundwater, recharged prior to 1950s), but only a few of their samples showed conclusive evidence of significant ageing on the  $^{14}\text{C}$  timescale.

Based on covert quality parameters, Begg *et al.* (2005) drew a map for the Manawatu–Horowhenua districts that proposes areas of river aquifer recharge, areas of rainfall recharge and areas likely to have unconfined aquifers. The map suggests that in the LMC unconfined groundwater conditions occur in the majority of the area covered with Last Glacial and Holocene material. Begg *et al.* (2005) believed that there is no simple relationship between geology and water quality in their study area.

McCarron and Zarour (2005) noted the existence of very saline,  $\text{Na}^+ - \text{Cl}^-$  water type in a Well 352271, which is drilled in greywacke basement rock in the Poroutawhao area near the groundwater divide between the Manawatu and the Horowhenua areas. They also noted that  $\text{Ca}^{2+} - \text{Mg}^{2+} - \text{HCO}_3^-$  groundwater type prevails in the area, with  $\text{Ca}^{2+} - \text{Mg}^{2+} - \text{Cl}^- - \text{SO}_4^{2-}$  in limited locations. They believed that groundwater quality in the area reflects heterogeneity and anisotropy of the aquifer system more than expressing hydrogeological relationships and characteristics. They noted that they found no evidence on seawater invasion in the coastal area.

Zarour (2008) reported that only about 30% of the hydrochemical data in the regional groundwater database has acceptable cation–anion balance (see Section 7.5). He maintained that long–term hydrogeochemical monitoring data do not exhibit noteworthy seasonal variability or long–term trends. Zarour (2008) confirmed that  $\text{Ca}^{2+} - \text{Mg}^{2+} - \text{HCO}_3^-$  water type predominates in the area. He did not see distinct hydrochemical facies distribution and he considered that to be an indication of the absence of discrete separate aquifers. Zarour (2008) noted that mineral dissolution and ion exchange are the dominant processes controlling

groundwater quality evolution in the area. He found no indication of mixing of fresh groundwater with saline seawater in the coastal section of the study area. Zarour (2008) believed that the area's groundwater generally meets potable standards and that it is generally suitable for irrigation, with low to medium salinity hazard and low sodium hazard.

Daughney *et al.* (2009) undertook statistical analysis of available hydrochemical data in the Horizons region. They employed Hierarchical Cluster Analysis (HCA) techniques to define distinct groundwater quality 'categories' and partition monitoring sites amongst them. They found that available data allow for a high level of hydrogeochemical interpretation but noted that limitations in the length and continuity of data for most monitoring sites make it difficult to assess trends in groundwater quality in the area. For the few sites that they found to have sufficient data, they perceived that groundwater quality is not changing substantially over time. They found no evidence of seawater intrusion into the coastal aquifer and only very few wells that have  $NO_3^-$  concentrations that exceed the expected natural background. Hence, Daughney *et al.* (2009) concluded that there is not much detectable influence of human activities on the area's groundwater. They contended that spatial groundwater quality variations across the area reflect differences in the origin and type of materials comprising the various aquifers. They highlight that most of the area's groundwater is oxygen-poor due to natural chemical and biological reactions that take place as water flows under the ground. They explain that these processes result in accumulation of dissolved *Fe*, *Mn* and ammonium ( $NH_4^+$ ), alongside the depletion of  $NO_3^-$  and, sometimes,  $SO_4^{2-}$  in the groundwater, a pattern that they observed across much of the Wanganui Basin. They suspected that naturally occurring high levels of *Fe*, *Mn*,  $NH_4^+$ , hardness and *pH* may slightly impair groundwater usability for human consumption and irrigation.

Zarour *et al.* (2011) reported on Horizons Regional Council's groundwater monitoring activities, including groundwater quality. Their report clarifies that the main purpose of Horizons groundwater quality monitoring is meeting their statutory responsibilities. The report provides a clear account of what parameters and sites

are being monitored. The report does not deal with non-programme groundwater quality monitoring, but this thesis utilises data from both non-programme and one-off sources to provide the maximum possible spatial coverage for hydrochemical interpolation purposes.

PDP (2013a) undertook a review of Horizons Regional Council's groundwater quality data and monitoring network. They noticed a gap in the data between late 2002 and 2005 as only few parameters from few wells have been recorded during that period. PDP (2013a) confirmed that  $Ca^{2+} - HCO_3^-$  water quality type dominates the groundwater system in the area and that reduced conditions prevail. They argue that salinity increases with depth in the region, but the data they present do not support that opinion, which is contrary to all previous work. They maintained that salinity as indicated by electrical conductivity ( $EC$ ) increases near the coastal area to the north of the Manawatu River due to longer flow paths. They also noticed high  $EC$  in a well near the confluence of the Manawatu River with the Pohangina River and relatively high  $Cl^-$  in a well in the coastal area and two wells in the Pohangina Catchment. The shallow well with high  $Cl^-$  near the Manawatu River–Pohangina River confluence also had elevated *E. coli*, possibly a reflection of contamination from nearby land use activities.

PDP (2013b) undertook a review of the seawater intrusion monitoring network in the Manawatu–Wanganui region. There are no seawater intrusion monitoring wells in the LMC. However, seawater intrusion is monitored in Well 332009 (25 m deep) located about 10 km to the north of the LMC in the Rangitikei plains and Well 352312 (86 m deep) located about 5 km to the south of the LMC in the Horowhenua plains. The construction details, including screen length and position are unknown for both wells. PDP (2013b) review of the seawater intrusion monitoring network revealed that there is no evidence of seawater invasion into the aquifers in the coastal area in the Manawatu–Wanganui region and assessed the risk of seawater intrusion in that area to be low. The review indicated that groundwater quality at the coast is not significantly different to that seen inland, especially in terms of ion ratios. The study showed that  $EC$  and  $Cl^-$  concentration in the two monitored wells near the

study area are relatively low (c. 550  $\mu\text{S}/\text{cm}$  and c. 20–40 mg/L, respectively). PDP (2013b) also found no obvious trend of increasing  $\text{Cl}^-$  or  $\text{EC}$  with depth in coastal monitoring bores. They noted that salinity can increase or decrease during pumping. In their opinion, an increase in salinity with pumping can mean drawing saltier water towards the pumped well whereas salinity reduction with pumping can mean inducing flow of fresher water towards the well because of pumping or that water in the well was stagnant and the well water's salinity is reduced with the removal of stagnant, relatively more saline water.

Overall, the following general characteristics of the LMC groundwater system can be deduced from previous hydrochemical investigations:

1. ion-ratios in groundwater and surface water are similar, but content concentrations are higher in groundwater
2. groundwater quality is generally good in the LMC, making it suitable for many beneficial purposes
3. groundwater quality has not changed much since the start of monitoring in 1969, and possibly over the last 120 years since the study by Marchbanks in 1898
4. groundwater quality seasonal variability is very small
5. there is no evidence of anthropogenic influence over groundwater quality in the area, including salinity levels and nitrate concentrations
6. there is no indication of seawater invasion into the coastal part of the groundwater system
7. discharge settings dominate in the lower part of the LMC, i.e. groundwater provides baseflow in low surface water flow conditions and gains no water from surface waterways in the area
8. groundwater salinity and major ion content increase along flow direction from northeast to southwest and decrease with depth
9. there is no evidence of distinct aquifers or special areal groundwater quality domains within the groundwater flow system in the LMC

10. there is need for additional isotope and age determination investigations to help understand recharge and flow mechanisms.

## 1.7 Thesis organisation

This chapter presents an introduction to the thesis, portraying the importance of groundwater in the study area, outlines the research problem and objectives, new contribution to knowledge and science, and describes the research methodology and material. It provides a general description of the LMC and critically reviews literature relevant to its groundwater resource. Chapter 2 presents methodological background for groundwater flow modelling and clarifies the basis for selecting the adopted approach, code and software for modelling the LMC groundwater system. Chapter 3 describes the physiography, soil and geology of the area, providing a general framework for further lithological interpretation. Chapter 4 discusses the area's climate and presents a soil moisture balance model to calculate various components of the hydrological cycle, including groundwater recharge. Chapter 5 summarises the area's hydrology to help recognise the relationships between surface water and groundwater in the area. Chapter 6 draws the hydrogeological scene, including identification of hydrolithostratigraphical units as basis for hydrogeological conceptualisation, discusses aquifer properties and sets out the groundwater flow system picture including variability of hydraulic head in space and time, flow directions, and hydraulic gradients. To complement hydrogeological characterisation, Chapter 7 extracts evidence from groundwater quality data, depicting processes controlling groundwater quality and clarifying groundwater quality issues relating to various uses. Chapter 8 is dedicated to presenting the modelling process and results. Chapter 9 presents the investigation's conclusions, discusses the main findings and makes recommendations for further work. Cited references are listed at the end of the thesis followed by appendices that contain selected used datasets and model calculation results.

## Chapter 2 Groundwater modelling methodology

### 2.1 Introduction

Characteristics and historical behaviour of groundwater systems can be deduced through investigations and examination of past records, where 'real' data can be analysed to decipher how static and changing natural and anthropogenic influences resulted in the current hydrogeological situation. However, assessing future behaviour of aquifers under various resource management scenarios and/or changing natural conditions requires subjecting the aquifer to the anticipated stresses and allowing time for the aquifer to react, which is virtually unattainable. Realistically, the only practical option is to simulate the groundwater system and study its response to anticipated conditions to advise resource management planning and decision making (Thangarajan, 2007). To achieve this, an operational groundwater model is needed (Mercer & Faust, 1980).

#### 2.1.1 Fitness for purpose

In general terms, a model is a representation of an object, a subject or a system. Models emulate fundamental characteristics of items or themes but ignore insignificant traits. Similarly, simulations embody only essential aspects of real-life conditions and omit trivial factors. Models are useful to understand things we cannot see, find out how things work, find solutions to confounding problems, and expressing and communicating thoughts. They can be presented in the form of physical objects, words, equations, images, schematic diagrams, animated multi-media, or any combination of the above depending on the nature of the modelled subject, purpose of the model, the target recipients, available technology, time and resources.

Box and Draper (1987) theorise that because models are approximations, essentially, they all '*are wrong, but some are useful.*' However, they also argue that the fact that although the polynomial is an approximation does not necessarily detract from its usefulness. So, they articulate that '*... the practical question is how*

*wrong do they [models] have to be to not be useful?* Posters in the Boston Museum of Science seen by the author in September 2012 advocate that models must be assessed only for how they fit their purposes and that whether a model is good or bad entirely depends on how well it serves its intended use. Hence, the foremost and most important step in any modelling work is to determine clearly the model objectives so that its fitness for purpose can be objectively assessed (e.g. Anderson & Woessner, 2002; Barnett *et al.*, 2012; Younger, 2007).

### 2.1.2 Understanding through modelling

Most commonly, groundwater modelling objectives are focused on the quantitative assessment of the response of heads, flows or solute concentrations to future stresses on the groundwater system. However, important modelling objectives include gaining insight into the processes that are important under certain conditions (i.e. analysing sensitivities), identification of knowledge gaps and informing where additional effort should be focused to gather further information (Barnett *et al.*, 2012).

Quantitative groundwater modelling has become an essential tool in hydrogeological investigations and assessments. It is now widely accepted that modelling is a useful reality check to test our understanding of hydrogeological systems. Lichtner (1996) upholds that '*Quantitative models force the investigator to validate or invalidate ideas by putting real numbers into an often vague hypothesis and thereby starting the thought process along a path that may result in acceptance, rejection, or modification of the original hypothesis.*' Therefore, many conferences and special journal issues have been focused on the theme of understanding groundwater systems through modelling (Zheng *et al.*, 2006).

### 2.1.3 Limitations and challenges

Non-uniqueness in models presents a particularly important challenge. It means that many different combinations of model inputs produce results that match measured data. Consequently, there will always be more than one possible reasonable model (Anderson *et al.*, 2015). Non-uniqueness of groundwater

models is particularly noteworthy in inverse modelling, the process during which the model is attempted to be calibrated to real-life observations. Inverse modelling may, at times, result in meaningless solutions (Carrera & Neuman, 1986), so sensibility and reality checks are needed. Yeh *et al.* (2015) believe that inherent inverse modelling shortcomings can be mitigated through increased model parameterisation. In reality, it is impossible to produce a unique representative model of a groundwater system. In addition, every model is based on data and assumptions that contain some degree of uncertainty (Merry *et al.*, 2003). Uncertainty in groundwater models arises from a number of factors related to representing groundwater processes. During various stages of modelling, the modeller makes subjective choices (code to use, important processes, datasets trustworthiness, etc.) that honour or discount various attributes of the modelled system to various degrees. Ignorance of one or more important parameters represents another dimension of uncertainty (Hunt & Welter, 2010). Obviously, the unknowns can only be left out of models. Overall, modelling uncertainty can only be reduced, never eliminated (Anderson *et al.*, 2015).

Modelling limitations such as simplifying assumptions, field-data quality, non-uniqueness and uncertainties must be recognised and acknowledged in all groundwater models (e.g. Anderson & Woessner, 2002; Doherty & Hunt, 2010; Hill & Tiedeman, 2007; Mercer & Faust, 1980; PDP, 2002; Sreekanth *et al.*, 2015). Typically, these issues are addressed by evaluating the sensitivity of model predictions to changes in model conceptualisation or input. Failing to assess and communicate model limitations is considered modelling misuse. This is commonly unintentional, stemming from the modeller's lack of knowledge. However, it could also be deliberate.

## 2.2 Flow in porous media

The aquifer system in the LMC consists predominantly of loose to poorly-cemented Quaternary clastic sediments. Groundwater flows in such material mostly through pores. Groundwater flow through porous media is quantitatively described by Darcy's law.

### 2.2.1 Darcy's law

In 1856, Henry Darcy developed an empirical equation to describe flow of fluid through porous media from extensive work on the flow of water through sand filter beds (e.g. Bennett, 1989; Fetter, 2013; Freeze & Cherry, 1979; Kruseman & de Ridder, 1991). Figure 2–1 schematically represents Darcy's experimental apparatus.

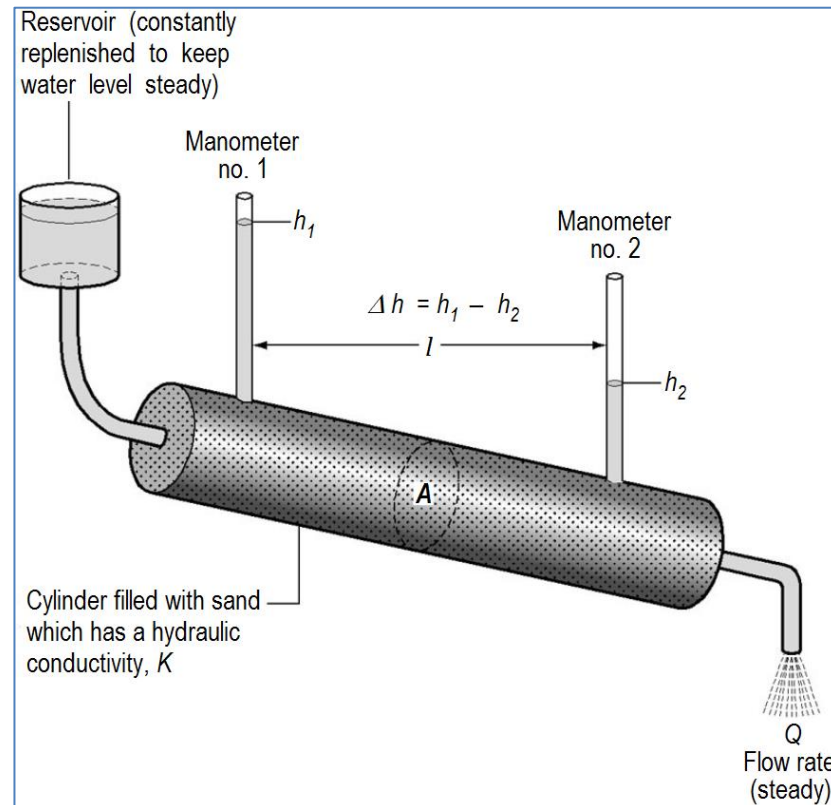


Figure 2–1. Schematic represent of Darcy's experimental apparatus illustrating the terms in Darcy's Law (after Younger, 2007).

Darcy noticed that steady flow per unit area ( $q$ ), termed specific discharge or Darcy flux, is directly proportional to the hydraulic gradient over the flow distance, i.e.

$$q = \frac{Q}{A} \propto \frac{\Delta h}{l} \quad 2-1$$

where  $Q$  represents the volumetric flow rate of the fluid downward through the cylindrical sand pack of cross-sectional area  $A$  and length  $l$ , and  $\Delta h$  is the difference between the hydraulic head above the standard datum of the water in the manometers located at the input and output ports ( $h_1$  and  $h_2$ , respectively).

Conveniently, hydraulic gradient ( $i$ ) is defined as  $\Delta h / l$ . Hence, Equation 2–1 can be written as:

$$\frac{Q}{A} \propto i \quad 2-2$$

Darcy assigned a proportionality constant ( $K$ ), which represents the ability of the porous media to allow flow through it. In general terms,  $K$  is a ‘coefficient of permeability’. In the case of water,  $K$  is termed ‘hydraulic conductivity’. In contemporary format, using a particular sign convention, Darcy's equation (law) is usually written as:

$$Q = K i A \quad 2-3$$

### 2.2.2 Reynolds number

Kruseman and de Ridder (1991) clarify that Darcy’s law (Equation 2–3) is valid for laminar flow, but not for turbulent flow, as the case may be in cavernous or fractured rocks. Reynolds number ( $N_R$ ) is a criterion to distinguish between laminar and turbulent flow. It is expressed as:

$$N_R = \rho \frac{qd}{\mu} \quad 2-4$$

where  $\rho$  is the fluid density,  $q$  is the specific discharge,  $\mu$  is the viscosity of the fluid, and  $d$  is a representative length dimension of the porous medium, usually taken as effective grain–size diameter ( $D_{10}$ ), or mean pore diameter. Theoretically, Darcy’s law is valid for  $N_R < 1$  but in reality no serious errors are created up to  $N_R = 10$ . Fortunately, most groundwater flow occurs with  $N_R < 1$ , so that Darcy’s law applies (Kruseman & de Ridder, 1991). Kruseman and de Ridder (1991) indicate that the relation between  $q$  and the hydraulic gradient ( $i$ ) is not linear for low  $i$  values, invalidating Darcy’s law. Such circumstances could be encountered for example in compact clays. However, they note that it is impossible to give a unique lower limit to the hydraulic gradients at which Darcy’s law is still valid because the

values of  $i$  vary with the type and structure of the clay, while the mineral content of the water also plays a role.

### 2.3 Groundwater flow governing equations

Using a cubical representative fixed control volume element (RFCVE) as shown in Figure 2-2, a mass balance can be established as:

$$Q_{in} - Q_{out} = \frac{\Delta M}{\Delta t} \quad 2-5$$

where  $Q_{in}$  is total inflow,  $Q_{out}$  is total outflow,  $\Delta M$  is change in mass over a specific time period ( $\Delta t$ ).

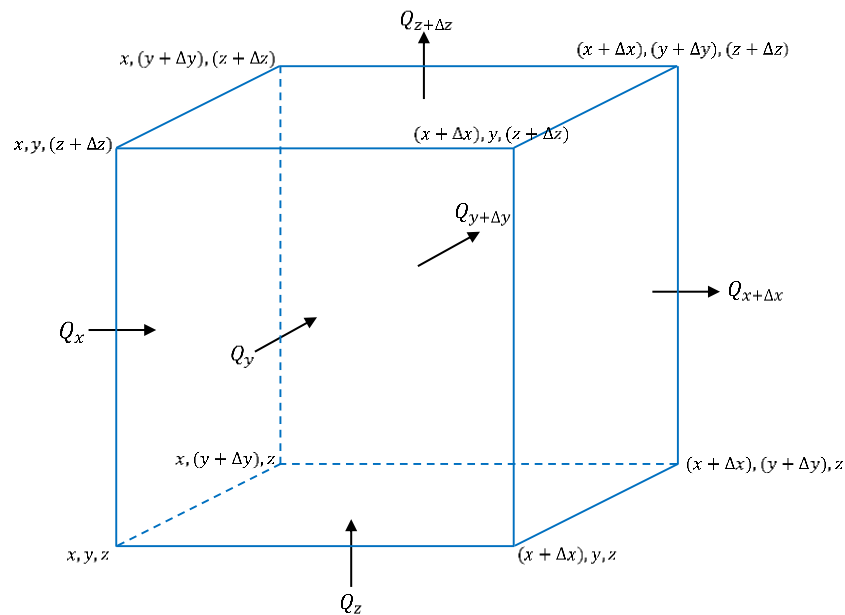


Figure 2-2. Schematic illustration of mass balance for a representative fixed control volume element (RFCVE).

Darcy's law is a phenomenological law or constitutive equation. Hence, it can be combined with the conservation equation to provide 3D mass balance. Using Figure 2-2 notation, Equation 2-5 can be written as:

$$[Q_x - Q_{x+\Delta x}] + [Q_y - Q_{y+\Delta y}] + [Q_z - Q_{z+\Delta z}] = S_s \frac{\Delta h}{\Delta t} \quad 2-6$$

where  $S_s$  is the specific storage coefficient, defined as the volume of water released from storage ( $\Delta V_w$ ) per unit change in head per unit volume, i.e.

$$S_s = \frac{\Delta V_w}{\Delta h \Delta x \Delta y \Delta z} \quad 2-7$$

Axes for the RFCVE (Figure 2-2) are selected in the principal directions of permeability (directions of maximum and minimum permeabilities for the  $x$  and  $z$  directions, respectively).

Using Darcy's law terms (Equation 2-3) and making  $\Delta t$  very small, Equation 2-6 can be written as:

$$\frac{\partial}{\partial x} \left( K_x \frac{\partial h}{\partial x} \right) + \frac{\partial}{\partial y} \left( K_y \frac{\partial h}{\partial y} \right) + \frac{\partial}{\partial z} \left( K_z \frac{\partial h}{\partial z} \right) = S_s \frac{\partial h}{\partial t} - R^* \quad 2-8$$

Equation 2-8 is the governing equation of groundwater flow in 3D. It includes a general source/sink term ( $R^*$ ) that can be used to represent additional inputs (e.g. recharge) and outputs (e.g. pumping).  $R^*$  is a positive value for inputs and negative for outputs.

Application of the governing equations to real-life situations requires the definition of boundary and initial conditions (Igboekwe & Achi, 2011).

### 2.3.1 Laplace equation

Under isotropic ( $K_x = K_y = K_z$ ), homogeneous ( $K_1 = K_2 = \dots = K_n$ ) aquifer conditions and steady-state flow conditions<sup>8</sup>, Equation 2-8 can be reduced to Equation 2-9, which is a Laplace equation.

$$\frac{\partial^2 h}{\partial x^2} + \frac{\partial^2 h}{\partial y^2} + \frac{\partial^2 h}{\partial z^2} = 0 \quad 2-9$$

<sup>8</sup> Steady-state flow is flow in which all conditions (velocity, pressure, etc.) remain constant with respect to time.

### 2.3.2 Unconfined aquifers

For unconfined aquifer conditions (Dupuit–Forchheimer assumption; horizontal flow that is proportional to the saturated aquifer thickness), it is standard practice to assume that  $T_x = K_x h$  and  $T_y = K_y h$  where  $h$  is assumed to be equal to  $b$ , the aquifer saturated thickness (Anderson & Woessner, 2002). Under these conditions, the groundwater flow governing equation takes the following form (the Boussinesq equation):

$$\frac{\partial}{\partial x} \left( K_x h \frac{\partial h}{\partial x} \right) + \frac{\partial}{\partial y} \left( K_y h \frac{\partial h}{\partial y} \right) = S_y \frac{\partial h}{\partial t} - R^* \quad 2-10$$

where  $S_y$  is the specific yield. By realising that

$$\frac{\partial h^2}{\partial x} = 2h \frac{\partial h}{\partial x} \quad 2-11$$

$$\frac{\partial h^2}{\partial y} = 2h \frac{\partial h}{\partial y} \quad 2-12$$

Equation 2-10 can be rewritten as:

$$\frac{\partial}{\partial x} \left( K_x \frac{\partial h^2}{\partial x} \right) + \frac{\partial}{\partial y} \left( K_y \frac{\partial h^2}{\partial y} \right) = 2S_y \frac{\partial h}{\partial t} - 2R^* \quad 2-13$$

## 2.4 Analytical solutions

Analytical solutions, also known as closed form solutions, use symbolic manipulation techniques to solve mathematical problems and evaluate the unknown variable. The famous Thiem (1906) equation (Eq. 2-14) and the Theis (1935) equation (Eq. 2-15) for flow in homogeneous, isotropic, confined aquifers under steady-state and unsteady-state conditions, respectively, are examples of analytical solutions.

$$Q = \frac{2\pi T(s_{m1} - s_{m2})}{2.30 \log(r_2/r_1)} \quad 2-14$$

where  $Q$  is the well discharge,  $T$  is the aquifer transmissivity ( $T = Kb$ ),  $r_1$  and  $r_2$  are the respective distances of the piezometers from the pumped well,  $s_{m1}$  and  $s_{m2}$  are the respective steady-state drawdowns in the piezometers.

$$s = \frac{Q}{4\pi T} \int_u^\infty \frac{e^{-y}}{y} dy = \frac{Q}{4\pi T} W(u) \quad 2-15$$

Where  $s$  is the drawdown in a piezometer at a distance  $r$  from the pumped well,  $Q$  is the well discharge,  $T$  is the transmissivity of the aquifer,  $u = r^2 S / 4Tt$ ,  $S$  is the dimensionless storativity of the aquifer,  $t$  is time since pumping started, and the well function of  $u$  is defined as:

$$W(u) = -0.5772 - \ln u + u - \frac{u^2}{2.2!} + \frac{u^3}{3.3!} + \frac{u^4}{4.4!} + \dots \quad 2-16$$

According to Perina (2010), the governing formula for the Theis equation (Eq. 2-15) is:

$$\frac{\partial^2 s}{\partial r^2} + \frac{1}{r} \frac{\partial s}{\partial r} = \frac{S}{T} \frac{\partial s}{\partial t} \quad 2-17$$

The boundary conditions are:

$$s \rightarrow 0 \text{ for } r \rightarrow \infty, t \geq 0 \quad 2-18$$

and

$$-2\pi r T \frac{\partial s}{\partial r} = Q \text{ for } r \rightarrow \infty, t \geq 0 \quad 2-19$$

and the initial condition is:

$$s = 0 \text{ for } t = 0 \qquad 2-20$$

where  $s(r, t)$  is the drawdown,  $r$  is the radial distance from the pumping well,  $t$  is the time since pumping started,  $Q$  is the constant extraction rate,  $T$  is transmissivity, and  $S$  is storativity.

Analytical methods use simplifying assumptions to provide an exact solution for every point in space and/or time uniformly over the model domain. For example, given abstraction rate and transmissivity, we can use the Thiem (1906) equation (Eq. 2-14) to calculate drawdown at various distances from a pumped well in a homogeneous, isotropic, confined aquifer under steady-state flow conditions. We can also evaluate transmissivity given abstraction rate, distances to observation points and drawdown at them (e.g. to evaluate  $T$  from pumping test data).

Analytical solutions are well suited for simplified problems. To a certain degree, real-life complexity can be dealt with analytical solutions through the application of the principle of superposition to scalar potentials and velocity vectors (Reilly *et al.*, 1984), introducing terms to represent processes such as recharge and/or manipulating boundary conditions. Nevertheless, it is impossible to use analytical methods to account for variations in field conditions that occur with time and space because of their inherent simplicity. For situations where it is important to account for spatial and temporal variations in hydraulic properties and conditions, the assumptions to be made to obtain an analytical solution will not be realistic. Approximation using numerical solution techniques is obligatory in such situations to solve the governing equation satisfactorily under the given boundary, initial and operational conditions.

## 2.5 Numerical solutions

Numerical methods are not intended to calculate an exact solution for the groundwater flow governing partial differential equation (PDE; Eq. 2-8), but they

are formulated to obtain a reasonable approximate solution (Anderson *et al.*, 2015; Thangarajan, 2007). Unlike analytical solutions, numerical solutions are not continuous in space or time. They calculate head at discrete points (nodes) in space and for specified values of time (stress periods and time steps within them). This allows numerical models to be used in full transient, 3D simulations of heterogeneous, anisotropic aquifers under complex boundary and initial conditions.

Finite difference (FD) and finite element (FE) methods are the most commonly used approximation methods to solve the PDE. It has been shown that both FD and FE formulations of the Laplace equation (Eq. 2-9) and even more complex versions of the PDE produce the same set of algebraic equations and the same results if nodal spacing is sufficiently small (e.g. Pinder & Gray, 1976; H. F. Wang & Anderson, 1977, 1982).

### 2.5.1 Finite difference methods

By introducing transmissivity ( $T = Kb$ ) and storativity ( $S = S_s b$ ) to the general groundwater flow governing equation (Eq. 2-8), one-dimensional (1D) flow in isotropic media can be expressed as follows:

$$\frac{\delta^2 h}{\delta x^2} T = S \frac{\delta h}{\delta t} - R^* \quad 2-21$$

Because  $h$  appears to the second power on the left-hand side of the equation and to the first power on its right-hand side, Eq. 2-21 is nonlinear (Figure 2-3). However, it can be effectively linearised in a numerical model by using the current (known) value of the saturated thickness ( $b$ ), which is the approach used in many modelling packages, including MODFLOW (Anderson & Woessner, 2002).

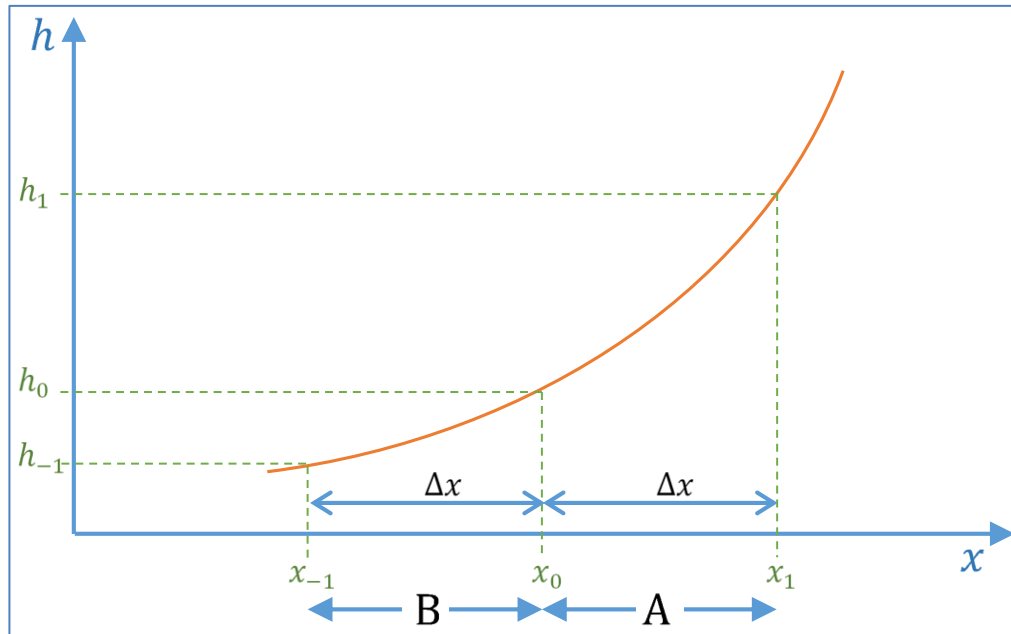


Figure 2-3. Graphical illustration of approximation used to linearise Eq. 2-21.

Solving Eq. 2-21 requires approximation of the term  $\frac{\delta^2 h}{\delta x^2}$ . If we divide space in the  $x$  direction into equal segments ( $\Delta x$ ) as illustrated in Figure 2-3, the change in hydraulic head for segments A and B can be expressed as follows:

$$\left(\frac{dh}{dx}\right)_A = \frac{h_1 - h_0}{\Delta x} \quad 2-22$$

and

$$\left(\frac{dh}{dx}\right)_B = \frac{h_0 - h_{-1}}{\Delta x} \quad 2-23$$

The difference in hydraulic gradient over segments A and B can be written as:

$$\frac{d}{dx} \left(\frac{dh}{dx}\right) = \frac{\left(\frac{dh}{dx}\right)_A - \left(\frac{dh}{dx}\right)_B}{\Delta x} \quad 2-24$$

By substituting equations 2-22 and 2-23 into Eq. 2-24 and simplifying, we get:

$$\frac{\delta^2 h}{\delta x^2} = \frac{h_1 - 2h_0 + h_{-1}}{\Delta x^2} \quad 2-25$$

So, we can write the differential equation for steady-state as:

$$h_1 - 2h_0 + h_{-1} = \frac{-R^* \Delta x^2}{T} \quad 2-26$$

The same approach can be followed to produce differential equations in the  $y$  and  $z$  directions. Given initial conditions and boundary conditions, equations like Eq. 2-26 can be solved numerically. This approach is known as the finite difference (FD) method.

In the FD method, a continuous medium is subdivided into cuboidal RFCVEs similar to the one shown in Figure 2-2 and relevant hydrogeological parameters are assigned to nodes positioned at RFCVE centres (Figure 2-4). Relative positions of nodes within the grid are assigned using  $i$ ,  $j$ ,  $k$  indices representing column, row and layer, respectively<sup>9</sup>. Difference operators defining the spatial-temporal relationships between various parameters replace the partial derivatives, giving a set of finite difference equations, one for each node. Solving the finite difference equations starts with the initial distribution of heads to compute heads at later time instants. Heads are defined and calculated only at nodes and the head at a node represents the average head in the FD cell. Fast converging iterative algorithms have been developed to solve the set of algebraic equations obtained through discretisation of the PDE (Thangarajan, 2007).

<sup>9</sup> Sometimes a different indexing convention is used. For example, in MODFLOW  $i$  = rows and  $j$  = columns.

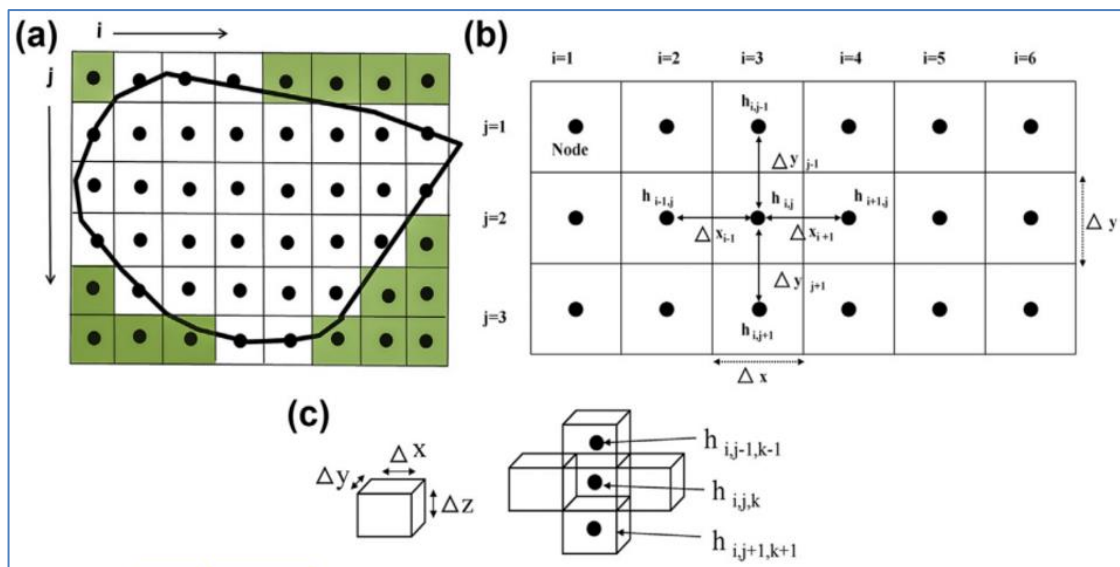


Figure 2-4. Finite-difference (FD) grid and notation (after Anderson *et al.*, 2015).

(a) 2D horizontal FD grid with uniform nodal spacing;  $i =$  columns and  $j =$  rows<sup>9</sup>. The cells are block-centred; the heavy dark line represents the problem domain. Inactive cells (those outside the boundary of the problem domain) are shaded.

(b) 2D horizontal FD grid with notation for the group of five nodes comprising the FD computational module (star) centred around node  $(i, j)$ .

(c) 3D notation where  $\Delta z$  represents the vertical distance between nodes and  $k$  is the vertical index. The group of blocks at the right is shown in 2D space (the two blocks perpendicular to the page along the  $y$ -axis are not shown). The group of seven nodes including node  $(i, j, k)$  comprise the FD computational module in three dimensions.

### 2.5.2 Finite element methods

In the FE method, the continuous flow field is discretised into a number of elements, which are used for interpolation of the field parameters such as the head and hydraulic conductivity (Figure 2-5). The locations of elements are designated using spatial coordinates  $(x, y, z)$  in a two dimensional (2D) or 3D mesh. The mesh consists of a triangulated irregular network (TIN) representing the modelled space. The basic idea is to transform the governing equations into integral form and evaluate flow rate by carrying out piecewise integration over small-volume elements in space and time. The FE method starts by mathematically defining the potential surface over any small region of interest and then evaluates the gradient in any given direction by evaluating derivatives in that direction (Thangarajan, 2007).

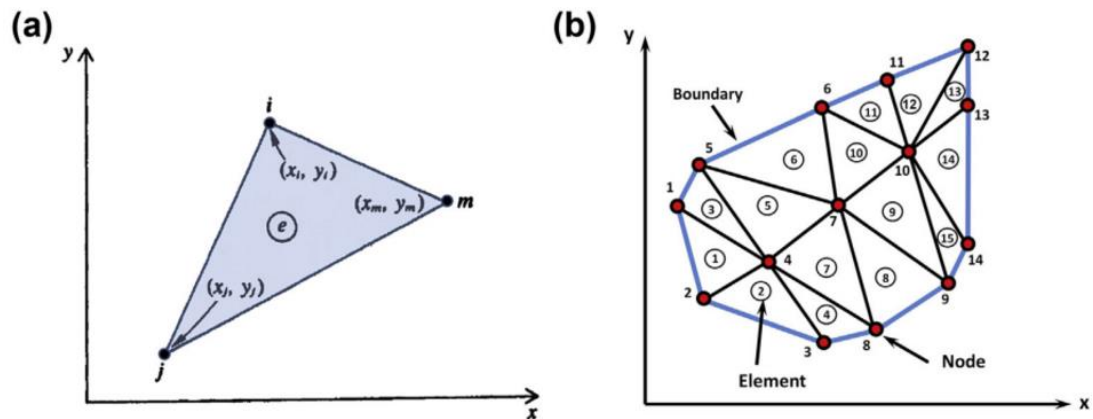


Figure 2-5. Two-dimensional (2D) horizontal finite-element mesh with triangular elements and notation (after Anderson *et al.*, 2015).

(a) A representative triangular element with nodes  $i$ ,  $j$ , and  $m$ , labelled in counter clockwise order, with spatial coordinates  $(x, y)$ .

(b) Triangular elements, with element numbers inside circles, are defined by numbered nodes. The elements are fitted to the boundary of the problem domain.

The FE equations are generated by introducing a trial solution of head within the element by interpolation functions, usually called basis functions, that relate head at the nodes to head within the element. Linear interpolation function is commonly used but more complex functions like the inverse distance weighted (IDW) and Kriging may be necessary. In addition, many of the more sophisticated interpolation techniques include options that could be used to refine the solution.

## 2.6 Modelling method and code selection

There are other additional mathematical groundwater modelling methods to the ones discussed above. These methods are either analytical (too many to list), numerical (e.g. the control volume finite difference; CVFD), or hybrid (e.g. the analytical element method; AEM). Because of their high calculations demand, all numerical and analytical element models require the use of digital computers. So, various computer codes have been written to implement these methods.

Different groundwater modelling codes implement modelling methods differently, and many of them allow the use of various numerical iteration techniques (solvers) to solve groundwater flow problems. For example, the United States Geological Survey (USGS) modular FD code (MODFLOW) allows the use of a number of

numerical solvers to execute calculations, including the Strongly Implicit Procedure (SIP), Conjugate-Gradient (PCG) and the Direct Solver (DE4), to name some. In addition, many public-domain, shareware and proprietary software have been developed to provide convenient graphical user interfaces (GUI) for various codes (e.g. Visual MODFLOW Flex by Waterloo Hydrogeologic for MODFLOW and GMS by Aquaveo for MODFLOW, FEMWATER, MODAEM and other codes). GUIs enable convenient pre-processing of data for input in the appropriate format to the selected modelling code, running the code seamlessly with easy viewing and manipulating of the modelling results (post-processing). Alternatively, general mathematical software packages such as MATLAB and COMSOL can be used to solve the general groundwater flow PDE (Eq. 2-8) (Anderson *et al.*, 2015).

The complexity of the LMC groundwater system renders analytical and analytical element solutions unsuitable to simulate it. So, the choice is realistically limited to numerical models that are based on FD, FE and CVFD methods, such as MODFLOW, FEFLOW and MODFLOW-USG, respectively. FE and CVFD methods are more difficult to use than FD methods and there are no clear gains from using them to model the LMC groundwater system.

On face value, the MODFLOW code seems to be the most plausible choice for modelling the LMC groundwater system but there are numerous other modelling codes that could also be used. Anderson *et al.* (2015) list four important criteria for groundwater modelling code selection: (1) code verification (2) water budget computation ability and accuracy, (3) proven track record, and (4) availability and capabilities of GUIs. In addition, the possibility of using automated calibration tools is an important criterion that should be considered during mathematical modelling code selection. The following sections briefly assess how MODFLOW measures against each of the above criteria.

### 2.6.1 Code verification

Numerical modelling codes are verified by comparing their results to the results of analytical solutions and other numerical codes. The principle objective of code verification is to ensure it has been appropriately programmed.

Since the original release of MODFLOW (McDonald & Harbaugh, 1984), it has been the most widely used code to solve groundwater flow problems (Anderson *et al.*, 2015). The first release was followed by MODFLOW 2000 (Harbaugh *et al.*, 2000) and MODFLOW 2005 (Harbaugh, 2005). The code's modular design was particularly advantageous as proven by the code's wide use and the large number of enhancement and additions to the original code (McDonald & Harbaugh, 2003). Recently, the ability to use an unstructured grid has been added to the software (Panday *et al.*, 2013) and was implemented in many GUIs such as Aquaveo's GMS and Groundwater Vistas by Environmental Simulations, Inc. (ESI).

Because of its effectiveness and wide use, MODFLOW has become an industry standard. It is globally used to verify nearly all analytical and numerical models, old and new. Thereby, MODFLOW itself has become the most verified code in the groundwater modelling arena. This gives confidence in its ability to simulate the LMC groundwater system efficiently.

### 2.6.2 Water budget calculations

Water budget calculations are an essential component in hydrogeological studies. Accordingly, they have become standard features of most codes. Comparison of field observations-based water budget calculations that normally form part of conceptual models (e.g. Table 5-3) to numerical model computations provide a means to assess the accuracy of the numerical solution. Numerical models water budgets itemise flows across boundaries, to and from sources and sinks, user specified zones, and in transient simulations to and from storage.

It is important to notice that the governing equation for groundwater flow is derived from combining Darcy's law with conservation of mass (Section 2.3). Hence,

numerical solutions of the governing equation should conserve mass, which the FE method has reportedly failed to achieve locally (Berger & Howington, 2002). Anderson *et al.* (2015) argue that this is due to flawed methodology in early FE solutions and not inherent to the FE method. They indicate that modern FE codes include procedures that compute numerically accurate water budgets. Difference in model calculated inputs and outputs represent a water budget balance error. According to Konikow (1978), that is ideally less than 0.1%, but it would still be acceptable up to around 0.5%. High water budget balance error may be due to conceptualisation deficiencies, unreasonably high solution converged closure criteria, or low maximum number of iterations allowed. It could also reflect errors in input and/or model design, or it could be an artefact of how the code simulates head-dependent boundaries.

Both the FD method and all versions of the MODFLOW code are well-known for their ability to maintain highly accurate water budgets. Consequently, no serious water budget errors are expected from the use of MODFLOW to model groundwater in the LMC.

### 2.6.3 Proven track record

MODFLOW is the most widely used groundwater code in the world and the standard for litigation purposes in many countries, including and led by the United States (Anderson *et al.*, 2015). It has been applied to numerous and diverse field problems and is the focus of a wide range of international conferences. This history of successful use and testing provide an unmatched track record to any modelling code. The code's extensive use over more than 30 years in academic and professional settings enabled errors to be discovered and corrected, new modules (packages and processes) to be developed and a variety of GUIs to become available. A main advantage of MODFLOW over other codes is that it is supported by the USGS who put it in the public domain free of charge to users. This encouraged users and GUI developers alike to use it and contribute to its development, particularly because MODFLOW is an open source code.

With such a track record, there is no risk arising from utilisation of MODFLOW code in modelling the LMC groundwater system.

#### 2.6.4 Availability and capabilities of GUIs

Most modelling codes require data input in specific tabular text format and output results in the form of numerical tables, both of which are not particularly user friendly. Therefore, an interface between the modeller and the code is needed to facilitate data preparation, code runs and manipulation of results. User interfaces are software designed to serve as intermediary between the modeller and the code, most often providing the modeller with a visual (graphical) working environment. They facilitate model design, data input and enable easy visualisation, inspection and analysis of outputs. GUIs help designing grids and meshes as applicable to the code and boundaries. GUIs also assist in the exchange of data between various computer applications, especially with mapping, GIS and database packages. GUIs enable modellers to focus on the actual model build rather than data entry and visualisation of input and model results. Anderson *et al.* (2015) see that due to the complexity of most numerical modelling projects, a GUI is an indispensable tool for groundwater modelling.

MODFLOW code does not include an embedded GUI but a range of GUIs have been developed for it. The USGS has put ModelMuse MODFLOW GUI in the public domain (Winston, 2009) and ModelMate for parameter estimation using UCODE with MODFLOW (Banta, 2011). Freeware MODFLOW GUIs like Processing MODFLOW for Windows (PMWIN) and commercial packages like Groundwater Vistas, Visual MODFLOW-flex and the Groundwater Modelling System (GMS) are also available.

Often, MODFLOW GUIs handle several versions of the code (e.g. MODFLOW-SURFACT, MODHMS, MODFLOW-USG) and many enable conjunct or consequential use of automated parameter estimation codes (e.g. PEST) and other useful software such as particle tracking codes (e.g. MODPATH) and solute transport codes (e.g. PATH3D, MT3DMS, SEAWAT).

The availability of GUIs and other compatible modelling packages for parameter estimation and transport modelling makes MODFLOW a good choice for modelling the LMC groundwater system.

## 2.7 Modelling software package selection

As noted above, MODFLOW GUIs are by no means in short supply. However, prudent selection of the modelling software package will definitely maximise benefits and minimise risk and cost in terms of money, time, effort and quality of output. Criteria similar to those used for code selection apply to GUI selection. Most popular packages tick all the selection criteria but the United States Department of Defense (DoD) Groundwater Modeling System (GMS) stands out as a capable, user-friendly, flexible, intuitive GUI.

GMS was initially developed at Brigham Young University (BYU), then commercialised through EMS-I, a BYU commercial enterprise. In 2007, GMS software development was moved to a private enterprise, Aquaveo, LLC. Due to US government support, GMS is available at no cost to the US DoD, the Environmental Protection Agency (EPA), the Department of Energy (DoE), the Nuclear Regulatory Commission (NRC), the National Aeronautics and Space Administration (NASA) and onsite contractors to these agencies. The software is available through Aquaveo commercially to professionals and at a discounted rate for academic users.

GMS provides an integrated graphical system for modelling the subsurface environment, including stratigraphy, flow, contaminant transport and fate. The software possesses remarkable 2D and 3D geostatistical capabilities (e.g. Kriging, IDW and Natural Neighbour) and seamlessly utilises and integrates ESRI's ArcGIS technology.

In GMS, stratigraphy can be modelled deterministically using horizons and solids or stochastically through T-PROGS. Groundwater flow modelling can be undertaken using a variety of methods including analytical element (MODAEM), FD

(MODFLOW), and FE (FEMWATER). GMS supports all MODFLOW versions (88, 96, 2000, 2005, NWT, LGR<sup>10</sup> and USG<sup>11</sup>) and most existing packages (Table 2-1). Both steady-state and transient modelling are possible with the GUI supporting real date/time format and interpolation of transient data. Modelling of contaminant transport is possible through MODPATH, MT3DMS, PHT3D, SEAWAT, RT3D, and SEAM3D. Stochastic groundwater modelling is possible through Monte Carlo, Latin Hypercube and Gaussian Field. GMS has built in ZONEBDGT code and supports the Model-Independent Parameter Estimation and Uncertainty Analysis (PEST) software by Doherty (2015), which could be used for model calibration and sensitivity analysis. The software also supports Parallel PEST, Monte Carlo simulations, calibration targets, plots and charts.

GMS has excellent visualisation capabilities which enable easy interaction with models in 2D and 3D. The software is capable of producing high quality contour maps, cross-sections, fence diagrams and block diagrams for stratigraphy and hydrology.

The most important feature in GMS is perhaps its conceptual modelling approach, which the software pioneered to then be followed by other major groundwater modelling packages. The conceptual approach enables constructing a high-level representation of the model using familiar GIS objects such as points, arcs and polygons and easy updating of the model as may be required.

Consequently, GMS appears to be very well suited for modelling the LMC groundwater system using MODFLOW codes and other supported software needed to achieve this research's objectives.

---

<sup>10</sup> LGR: local grid refinement.

<sup>11</sup> USG: unstructured grid.

Table 2–1. GMS supported MODFLOW packages (modules).

Package	Description
BAS6	Basic Package
BCF6	Block Centered Flow Package
CHD1	Time Variant Specified Head Package
DE4	Direct Solver
DRN1	Drain Package
DRT1	Drain Return Package
EVT1	Evapotranspiration Package
ETS1	Evapotranspiration Segments Package
GAGE	Gage Package
GHB1	General Head Boundary Package
GMG	Geometric Multi-Grid
HFB1	Horizontal Flow Barrier Package
HUF	Hydrogeologic Unit Flow Package
LAK3	Lake Package
LPF	Layer Property Flow Package
MNW1	Multi-Node Well 1 Package
MNW2	Multi-Node Well 2 Package
NWT	Newton Solver
OUT1	Output Control
PCG2	Preconditioned Conjugate Gradient Method
PCGN	Preconditioned Conjugate Gradient Solver with Improved Nonlinear Control
RCH1	Recharge Package
RIV1	River Package
SAMG	Algebraic MultiGrid for Systems Solver
SFR2	Streamflow-Routing Package
SIP	Strongly Implicit Procedure
SOR	Slice-Successive Overrelaxation Method
SUB	Subsidence Package
STR1	Stream-Routing Package
WEL1	Well Package
UPW	Upstream Weighting Flow Package
UZF1	Unsaturated-Zone Flow Package

## 2.8 Modelling approach

Groundwater modelling is an exigent undertaking, which needs to be carefully managed to produce a satisfactory output. Every groundwater system is unique and, therefore, the modelling approach must be tailored to the specific circumstances of the project. Principally, objectives of modelling vary, data availability differs, time, technical and financial resources are not the same for all models, and subjective choices are inevitable. In addition, groundwater modelling is an active field of research and developments are driven by the need for better

hydrogeological process expressions, newly encountered management issues and expanding mathematical and computing capabilities. Consequently, attempts to prescribe an orchestrated and repeatable hydrogeological modelling protocol proved to be unviable. Instead, modelling and model auditing guidelines have been developed (e.g. Barnett *et al.*, 2012; PDP, 2002; Wels *et al.*, 2012). Such guidelines attempt to represent what is considered good practice in groundwater modelling, based on historical and current literature and the experience of practitioners involved in the guidelines development. Development of guidelines must be reviewed and updated continually to keep up with the changing questions being asked of modelling, mathematical and software developments and transformations in modelling approaches.

It is noticed that successful groundwater models are developed through a phased approach that incorporates what could be considered common typical steps. Comparable modelling workflows have been proposed by various investigators (e.g. Anderson *et al.*, 2015; Barnett *et al.*, 2012; Kumar, 2004; PDP, 2002; Wels *et al.*, 2012; Younger, 2007). Figure 2–6 presents a flow chart illustrating the typical sequence of steps involved in groundwater modelling.

The modelling approach in this thesis generally follows the Younger (2007) workflow presented in Figure 2–6 and the Australian groundwater modelling guidelines (Barnett *et al.*, 2012). Following such best–practice methodology facilitates the modelling process and results in a robust modelling outcome.

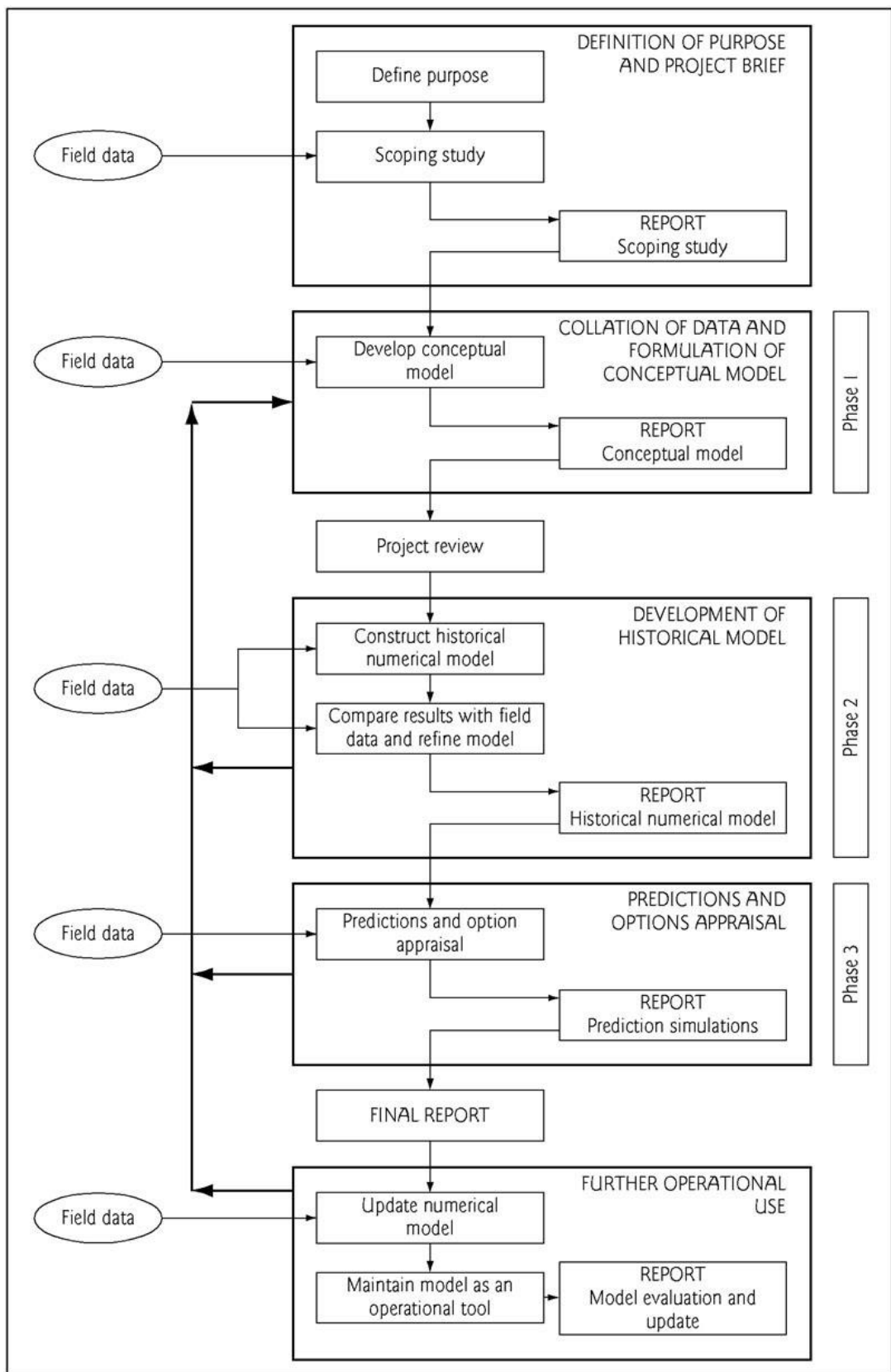


Figure 2-6. Flow chart illustrating the typical sequence of steps involved in groundwater modelling (after Younger, 2007).

## 2.9 Calibration

Model calibration implicates adjusting independent variables (parameters and fluxes) within sensible ranges to achieve the best fit between measured and model calculated groundwater heads and water balance components like flow exchanges (gains and losses) with surface water features. Hence, it is a form of inverse analysis or modelling. It is an iterative trial and error process of systematic parameter adjustment until a set calibration target is achieved. It can be undertaken manually but this a tedious and subjective process. Because of their higher level of complexity, it is more difficult to manually calibrate transient models than steady-state models. Manual calibration is greatly beneficial as it enables the modeller to examine the conceptual model and have a sense of the sensitivity of the model output to changes in input parameters. Commonly, manual calibration is followed by automated inverse parameter estimation, which reduces subjectivity inherent in the manual data matching process and enables quantification of parameter sensitivity.

Groundwater models are subject to non-uniqueness, where more than one set of parameters can produce the same model results. For example, recharge and hydraulic conductivity are highly correlated in groundwater flow models and, therefore, various combinations of these two parameters can produce the same result. Therefore, a calibrated model does not imply that it is the only feasible representation of the modelled system. While there is always just one reality, there are infinite possibilities to represent it.

Remarkably, not all models need to be calibrated to be useful. The Australian groundwater modelling guidelines recognises that in some cases model calibration is not necessary, such as when using a model to test a conceptual model (Barnett *et al.*, 2012). Furthermore, in some cases numerical modelling itself may not be needed. Younger (2007) notes that conceptual models do not necessarily have to be followed by mathematical modelling as they '*are largely ends in themselves.*'

### 2.9.1 Targets

When calibrating a model using automated parameter estimation (inverse modelling), a target measurement Objective Function ( $\Phi$ ) defining an acceptable level of model to measurement misfit is defined as

$$\Phi = \sum (w_i r_i)^2 \quad 2-27$$

where  $r_i = (h_{\text{calculated}} - h_{\text{observed}})$  and  $w_i$  is a weighting factor assigned to each observation. Inverse modelling aims at minimising the Objective Function ( $h_{\text{calculated}}$  and  $h_{\text{observed}}$  are the calculated and observed heads, respectively). Flux can also be incorporated in equation 2-27.

The weight assigned to each of the observations points is a function of the standard deviation. It is calculated as

$$W = \frac{1}{\sigma^2 * GW} \quad 2-28$$

where  $W$  is the weight of the observation point,  $\sigma$  is the standard deviation for the observation and  $GW$  is the observation points group weight. The observation point weight is multiplied by the residual for the observation in the objective function. Obviously, the smaller the standard deviation of an observation point the greater it will influence the objective function.

Often, the standard deviation is not known, but an error interval and level of confidence can be assigned to an observation that is desired to be used in model calibration, e.g. a head measurement with  $\pm 1$  m acceptable/expected error and 95% level of confidence in the measurement within that range. These data can be converted into standard deviation and used in inverse modelling. In practical terms, specifying an interval (or standard deviation) and confidence is an indication of how much error is believed to be associated with the observed value.

GMS GUI allows entry of observation data with standard deviation or confidence interval. It also facilitates model calibration by graphical presentation of calibration

targets on a map of the model in the form shown in Figure 2–7. The error bar is colour coded to indicate the goodness of the match between observed and calculated values. Green means the calculated value falls within the calibration target, yellow means that the calculated value is outside the target range but the error is no more than 200%, and red denotes that the error is greater than 200%.

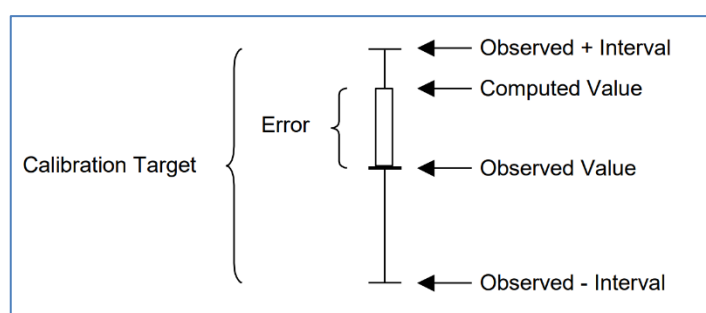


Figure 2–7. Model calibration target.

### 2.9.2 Calibration goodness circumstantial and statistical assessment

Assessing the quality of calibration of a groundwater flow model involves comparing the calibrated model results to anecdotes (e.g. unquantified field observations, piezometric maps and analytical flow estimates) and statistical evaluation of the fitness of computed values to actual measurements. Important and commonly used statistical metrics include:

#### 1. Calculated–observed data agreement

A scatter plot of calculated against observed values provides a useful visual means to assess the goodness of the model calibration. Clearly, the closer the points to the 1:1 ratio, the better the match between observed and calculated data. Data points plotting above the 1:1 line indicates model overestimation (positive residual) and data points falling under the line represent negative residual. Therefore, it is useful to draw lines to represent certain disagreement intervals in such graphs, e.g.  $\pm 10$  m as implemented in Section 8.10 (Figure 8–12).

#### 2. R-squared ( $R^2$ )

R-squared ( $R^2$ ), the coefficient of determination, is a statistical measure of how close the data are to the fitted regression line. It represents the percentage of the

response variable variation that is explained by a linear model. The lowest possible value (0%) indicates that the model explains none of the variability of the response data around its mean and the maximum possible value (100%) indicates that the model explains all the variability of the response data around its mean. The higher the  $R^2$  the better the model fits the data.

### 3. Mean residual

The calibration residual ( $R_i$ ) is defined as the difference between the calculated results ( $X_{cal}$ ) and the observed results ( $X_{obs}$ ) at data points  $i \rightarrow n$ . The mean residual ( $\bar{R}$ ) is a measure of the average residual value:

$$\bar{R} = \frac{1}{n} \sum_{i=1}^n R_i \quad 2-29$$

There may be cases where over and under calculated values will negate each other, producing mean residual ( $\bar{R}$ ) value close to zero, which can lead to false interpretation of the model calibration. Therefore,  $\bar{R}$  should never be used by itself as a measure of fitness between simulated results and observed data.

### 4. Mean absolute residual

The mean absolute residual ( $|\bar{R}|$ ) is a measure of the average magnitude of the residuals and, therefore, provides a better indication of calibration than  $\bar{R}$ .

$$|\bar{R}| = \frac{1}{n} \sum_{i=1}^n |R_i| \quad 2-30$$

### 5. Root mean squared residual

The root mean squared residual ( $RMS$ ) is calculated by taking the average of the square of the errors for the observations and then taking its square root. It tends to give more weight to cases where a few extreme error values exist.

$$RMS = \sqrt{\frac{1}{n} \sum_{i=1}^n R_i^2} \quad 2-31$$

## Chapter 3 Geology and soil

### 3.1 Introduction

Stratigraphy and geological structure determine the extent and configuration of hydrogeological systems and lithology determines their hydraulic properties. Stratigraphy describes the geometrical and relative age of various strata in layered sedimentary and volcanic systems. Structural geology describes the 3D distribution of geological units with respect to their deformational histories, including folding and faulting. Lithology is a description of the physical makeup of the sediments or rocks, including mineral composition, grain-size, sorting and packing, all of which control the ability of geological material to store and bear water. On the other hand, the potential for groundwater reserves to be replenished is chiefly determined by land cover (soil and vegetation) and physiographical setting (landforms). Often, physiography is confused and/or used interchangeably with geomorphology. In this thesis, physiography is used to denote the classification of landforms and geomorphology is used to indicate studying the processes involved in the development of landforms.

### 3.2 Geological and conceptual uncertainty

Given the degree to which geology determines the nature of groundwater systems, sound geological conceptualisation and modelling is considered prerequisite to reliable conceptual and mathematical hydrogeological models. Refsgaarda *et al.* (2012) elucidate that groundwater models are affected by two main sources of uncertainty relating to geology: (a) geological structures, and (b) hydraulic parameter values within these structures. Hydraulic parameters are commonly heterogeneous and anisotropic. Heterogeneity occurs at various scales. Heterogeneity and anisotropy can be accounted for in groundwater models, but they are often neglected in the assessments of model uncertainty.

There are a variety of methods for assessing hydrogeological modelling uncertainty related to geological uncertainty. Such methods include multiple modelling, Monte Carlo analysis, regression analysis and moment equation approach (Refsgaard *et al.*, 2012). Ye *et al.* (2010) explored how alternative conceptual models can be evaluated to give insight into conceptual uncertainty. They found out that overall model uncertainty is greatly more susceptible to conceptual uncertainty rather than parametric uncertainty. Furthermore, they found that uncertainty in geological interpretations had a more significant effect on model uncertainty than changes in recharge estimates. These findings are important because groundwater system conceptualisation and modelling depend on geological conceptualisation and, hence, they automatically inherit geological uncertainty. Understanding the regional geological setting and geological history forms the basis for geological conceptualisation.

### 3.3 Data sources

The geological understanding presented in this thesis is developed from synthesising information from accessible literature and databases. Accessed databases include digital maps and models. Limited field reconnaissance has been undertaken to validate information from literature and to achieve better understanding of the study area's geological setting.

#### 3.3.1 Ground elevation data

Land surface elevation data was obtained from the digital elevation model (DEM) created by the Otago University School of Surveying through interpolating Land Information New Zealand (LINZ) topographical vector data (Columbus *et al.*, 2011). The DEM known as NZSoSDEM v1.0 covers the whole of New Zealand at a spatial resolution of 15 m. It consists of a series of 30 maps that correspond exactly with the extent of the LINZ Topo250 topographical map series. DEM files are available from [koordinates.com](http://koordinates.com) under Creative Commons Public License (CCPL). The study area spans four DEM maps, namely:

1. Map 08 – New Plymouth
2. Map 10 – Napier

3. Map 14 – Palmerston North
4. Map 15 – Dannevirke.

The above-listed four NZSoSDEM maps have been combined to form a single DEM for the study area using ArcGIS 10.4 for Desktop (ArcGIS)<sup>12</sup>. These maps are supposed to fit together seamlessly. However, upon inspection, it was found that they contain some topological imperfections (slivers and overlaps). ArcGIS was used to check and correct topology problems in the amalgamated DEM. Attempts to extend the DEM coverage offshore using New Zealand 250 m Bathymetry Grid (2008) obtained from [koordinates.com](http://koordinates.com) under CCPL proved unsatisfactory as the resolutions of the two datasets are quite different. The final DEM for the LMC and vicinity is presented in Figure 3-1. It is used in physiographical and geomorphological analyses, to estimate the elevation of wells that have not been surveyed, to obtain outcrop elevations for lithostratigraphical modelling and to determine the elevations of hydrogeological model layers.

### 3.3.2 Geological maps

Published 1:250 000 geological map sheets and associated reports are amongst the most important sources of information for this study. The quarter million geological map (QMAP) sheets and associated reports by GNS Science provide information about surface geology and some structural data, which can be interpreted through cross-sections for example to obtain an approximate knowledge of the subsurface geology. The study area is covered by four QMAP sheets, namely:

1. Taranaki – QMAP Sheet 7 (Townsend *et al.*, 2008)
2. Hawke's Bay – QMAP Sheet 8 (Lee *et al.*, 2011)
3. Wellington – QMAP Sheet 10 (Begg & Johnston, 2000)
4. Wairarapa – QMAP Sheet 11 (Lee & Begg, 2000).

---

<sup>12</sup> © Copyright 2015 Environmental Systems Research Institute, Inc. (ESRI).

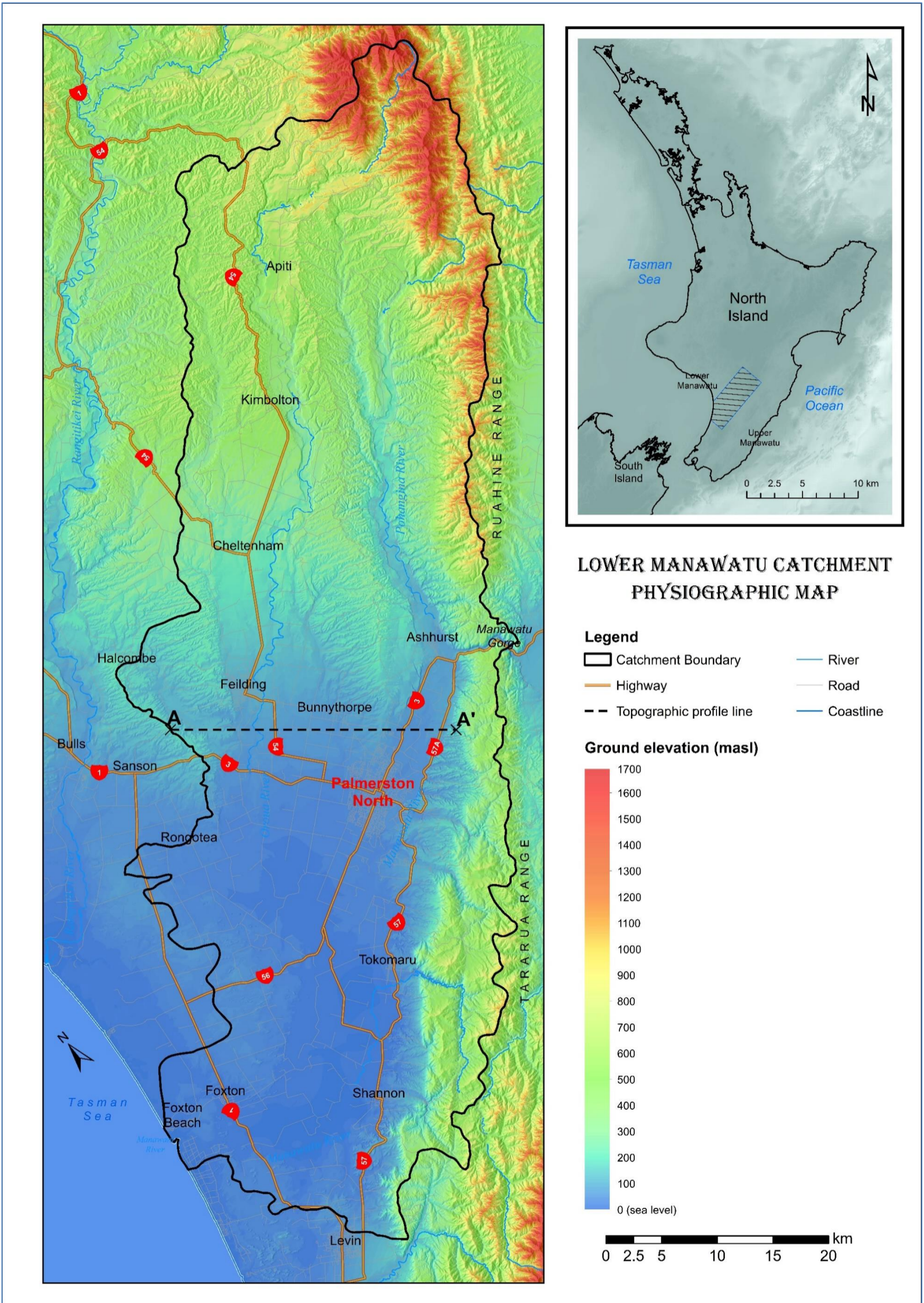


Figure 3-1. Physiographical map sourced from digital elevation model data.  
For topographical profile, see Figure 3-10.

The fact that the study area extends over four QMAP sheets complicates geological assessments. The maps were drawn at different times, using different data sets, coding and symbology systems. Therefore, geological units and boundaries at the edges of the above-listed four geological map sheets do not always match. In many cases, it was noticed that disagreement of geological unit codes is due to better data/standards being used in newer map sheets.

Heron (2014) amalgamated all QMAP geological map sheets in a single ArcGIS project. This map is free of topological errors. Nonetheless, it has not unified geological unit codes across the different QMAP sheets. To enable catchment-scale geological analysis, the amalgamated geological map has been checked and a single stratigraphical unit coding system has been developed (Table 3-1). The final geological map for the study area is presented in Figure 3-2. Colours and symbols used in this report may differ slightly from those used in published GNS Science QMAP sheets.

Geological chronology in this thesis is based on New Zealand Geological Timescale v. 2015/1 (Figure 3-3).

### 3.3.3 Horizons Regional Council groundwater database

Zarour *et al.* (2011) portrays the groundwater monitoring programme in the Manawatu-Wanganui (Horizons) region, in which the LMC is situated. Horizons Regional Council has a corresponding database to store and manage groundwater information. Most of the hydrological and hydrogeological data used for this study had been obtained from Horizons groundwater database, including data on well locations, drillers' well logs, groundwater levels and groundwater quality parameters.

Table 3-1. Geological units and map codes.

Rock group	Age <sup>13</sup>	Map code <sup>14</sup>	General characteristics
Holocene	OIS1	Q1dm	Windblown loose sand in active unvegetated or sparsely vegetated dune fields and deflation zones.
		Q1ds	Windblown inactive undifferentiated dunes and associated facies.
		Q1f	Poorly sorted, poorly consolidated alluvial, colluvial and scree fan deposits consisting of angular to sub-rounded boulders, cobbles, pebbles, gravel, sand and clay.
		Q1l	Earthflow hill slope deposits containing poorly sorted clasts up to boulder size in a clay matrix.
		Q1a	Poorly consolidated (loose), well sorted alluvial gravel, sand, silt and clay with local peat in modern floodplains and low terraces.
Late Quaternary	OIS2	Q2f	Poorly sorted, weakly consolidated alluvial and colluvial steep fan gravel deposits consisting gravel, sand, silt and clay.
		Q2a	Poorly to moderately sorted alluvial gravel with minor sand and silt underlying terraces.
	OIS3	Q3f	Alluvial and colluvial fan deposits consisting of poorly sorted, weakly consolidated gravel, sand, silt and clay.
		Q3a	Moderately weathered, poorly to moderately sorted alluvial gravel with minor sand and silt underlying loess-covered, commonly eroded aggradational surfaces.
	OIS4	Q4f	Moderately weathered alluvial and colluvial fan deposits underlying eroded terraces consisting of poorly to moderately sorted, weakly consolidated gravel, sand, silt and clay.
		Q4a	Weathered, poorly to moderately sorted alluvial gravel with sand and silt.
	OIS5	Q5b	Rapanui, Hauriri and Inaha terrace beach and shallow marine covered deposits consisting of conglomerate, shellbeds, dune sands and peat commonly underlying loess and fan deposits.
	OIS5-2	IQf	Undifferentiated moderately weathered poorly sorted alluvial gravel, sand, silt and clay.
		IQl	Landslide deposits ranging from coherent shattered masses of rock to unsorted fragments in a fine-grained matrix.
		IQa	Undifferentiated moderately weathered poorly sorted loess-covered alluvial gravel deposits.
Middle Quaternary	OIS6	Q6f	Very weathered alluvial and colluvial steep fan deposits consisting of poorly sorted, weakly consolidated gravel, sand, silt and clay.
	OIS7	Q6a	Very weathered, poorly to moderately sorted gravel with minor sand and silt underlying eroded terraces.
	OIS8	Q8a	Weathered, poorly to moderately sorted alluvial gravel underlying loess-covered, commonly eroded aggradational surfaces.
	OIS9	Q9b	Braemore and Brunswick terrace coverbeds comprising beach and shallow marine conglomerate, shellbeds, dune sands, mud and peat.
	OIS10	Q10a	Weathered, poorly to moderately sorted gravel with minor sand and silt underlying eroded terraces loess covered.

<sup>13</sup> OIS: Oxygen Isotope Stage (also known as Marine Isotope Stage: MIS) or geological time unit name.

<sup>14</sup> Symbols require QMAP Text true type font.

Rock group	Age <sup>13</sup>	Map code <sup>14</sup>	General characteristics
Early Quaternary	Castlecliffian	Q11b	Gravel, sand and mud.
		eQa	Weathered, poorly sorted loess-covered alluvial and fan gravel, pumiceous sand and lacustrine silt deposits.
		eQp	Lacustrine and shoreline fluvial sediments.
		e-mQs	Sandstone, siltstone, bioclastic limestone and conglomerate, including OIS 15–9 marine terrace deposits. Sandstone, siltstone, bioclastic limestone and conglomerate, including OIS 15–9 marine terrace deposits. Early Pleistocene – Middle Pleistocene sedimentary rocks.
		eQk	Coarse pumice grit, tephra, sand, silt, shellbeds and conglomerate. Sandstone, siltstone, bioclastic limestone, conglomerate and pumiceous sand. Early Pleistocene sedimentary rocks.
		eQo	Sandstone, siltstone, conglomerate and shell beds. Early Pleistocene sedimentary rocks.
Neogene	Pliocene–Pleistocene	Pep	Limestone.
		Pea	Massive, poorly bedded deeper water mudstone and sandy mudstone with minor alternating limestone, siltstone, sandstone and shallow water conglomerate.
		Pi	Sandstone, concretionary sandstone, mudstone, limestone and conglomerate.
		Pm	Pumiceous and non-pumiceous sandstone, mudstone, conglomerate, carbonaceous siltstone, lignite and shell beds.
		Pio	Alternating limestone, sandstone and siltstone.
		Pik	Alternating siltstone, sandstone and limestone.
		Pim	Weakly bedded, cross-bedded, bioturbated sandstone, siltstone and conglomerate.
		Pp	Thin pebbly shell beds and massive, well sorted sandstone in the west, and massive silty mudstone, concretionary sandstone; limestone and conglomerate in the east.
		Puo	Conglomeratic limestone and sandstone.
		Pu	Muddy, very fine sandstone, concretionary sandstone and sandy mudstone.
		Pit	Massive mudstone interbedded with well sorted, fine to medium, micaceous sandstone.
Mesozoic (Eastern Province Basement)	Triassic–Early Cretaceous	Ktw	Well-bedded alternating sandstone and mudstone.
		Ktp	Alternating sandstone and mudstone, massive mudstone and concretionary mudstone. Well bedded sandstone and mudstone.
		Kep	Sandstone blocks and packets of thin-bedded sandstone and mudstone in a sheared mudstone matrix. Basement (Eastern Province) melange.
		Tev	Small to large blocks of basalt within melange zones. Basement (Eastern Province) igneous rocks.
		Te	Sandstone and mudstone in a sheared argillite matrix with broken formation and melange.
		Jtk	Massive sandstone to alternating sandstone and argillite.
		Ttt	Alternating sandstone and mudstone, poorly bedded sandstone with minor coloured mudstone, conglomerate, basalt and chert.

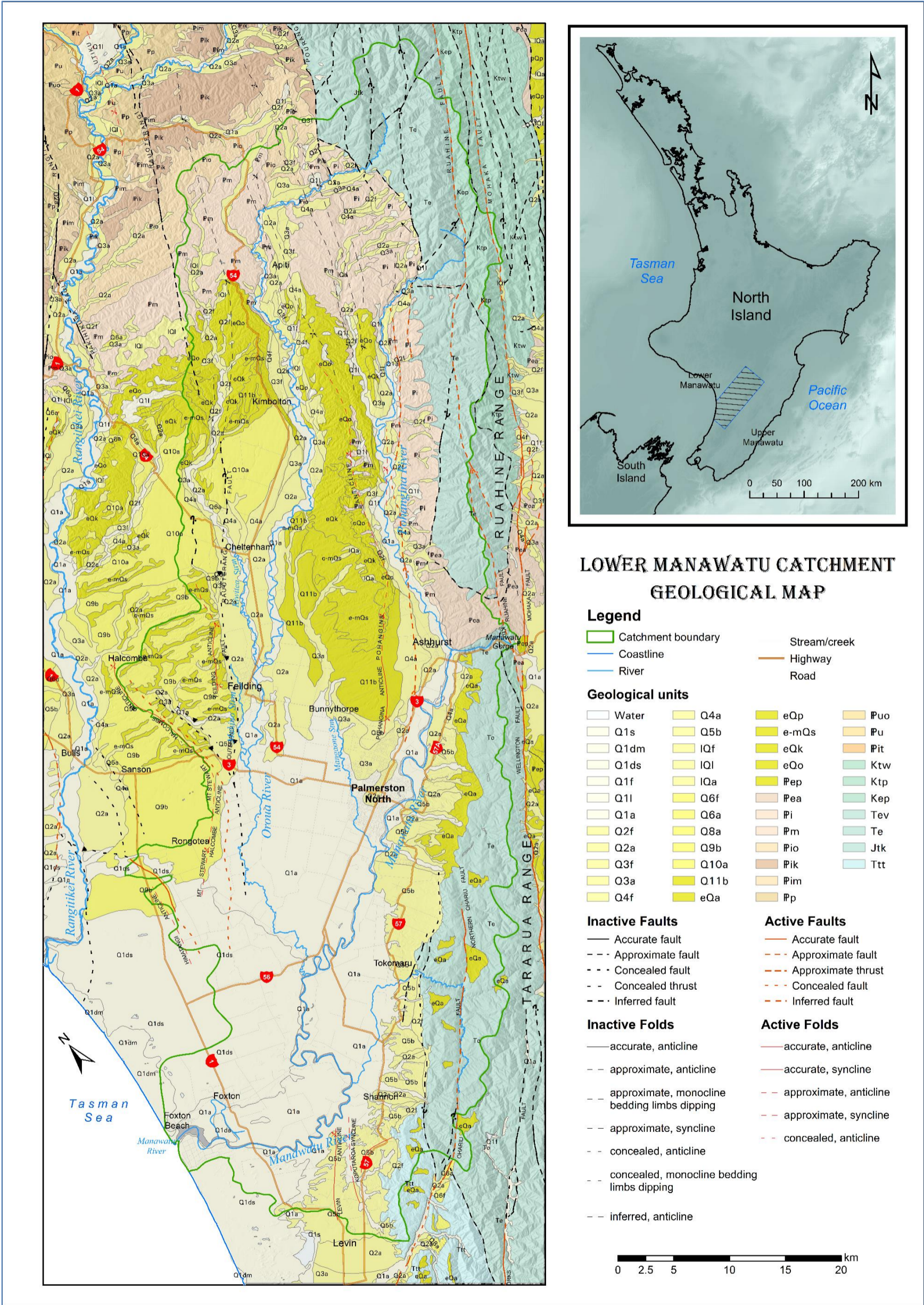


Figure 3-2. Geological map based on digital QMAP data (Heron, 2014).

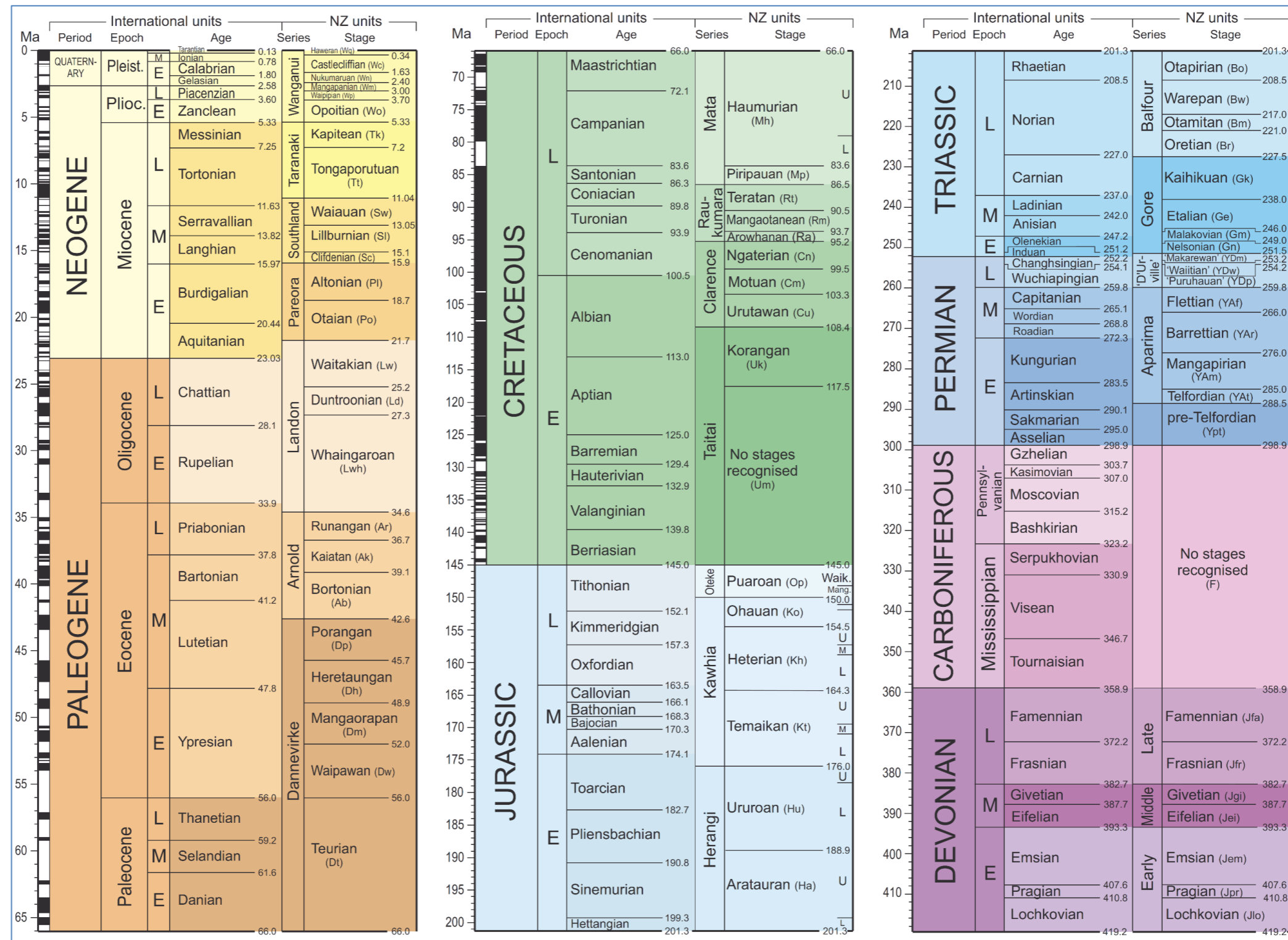


Figure 3-3. New Zealand and international geological timescales (Extracted from GNS Science, 2015).

### 3.3.4 Soil data

Soil data for this research were obtained from the New Zealand Soils Portal<sup>15</sup>, which provides access to information on New Zealand's soils held by Landcare Research. Landcare is undertaking national-scale soil mapping, the S-map. The S-map is the most recent digital soil spatial information system for New Zealand. It is intended to provide consistent and comprehensive national soil data layers to support applications at local, and regional to national-scales. However, there is not yet S-map coverage for the study area. Therefore, this research uses Landcare's Fundamental Soil Layers (FSLs) data, which predate and are being replaced by the S-map.

The FSLs contain spatial information for 16 key soil attributes. Each attribute is measurable (i.e. given a numerical value rather than being assigned to a descriptive class or category) and is recorded in appropriate units of measure. Because FSLs attributes have measurable values, the FSLs are particularly useful in computer modelling and GIS analyses. The 16 key soil attributes generally fall into three groups: (1) soil fertility/toxicity, (2) soil physical properties particularly those related to soil moisture, and (3) topography and climate. Parameters include slope, potential rooting depth, topsoil gravel content, proportion of rock outcrop, pH, salinity, cation exchange capacity, total carbon, phosphorus retention, flood interval, soil temperature, total profile available water, profile readily available water, drainage, and macro-pores (shallow and deep). The attributes are described in detail in the New Zealand Soil Classification (NZSC) by Hewitt (2010). LMC soils are described in Section 3.13 of this thesis.

## 3.4 Regional geological setting

The LMC is situated in the Pliocene–Pleistocene (Plio–Pleistocene) Wanganui Basin in the Lower North Island of New Zealand, approximately 200 km northwest of the Hikurangi Trough at the southern end of the Tonga–Kermadec subduction zone, which forms the boundary between the Australian and Pacific crustal plates (Figure

---

<sup>15</sup> <https://iris.scinfo.org.nz>

3–4). The two plates move relative to one another on the earth's surface, and are converging at a rate of about 40–50 mm/y (Begg & Johnston, 2000). As a result, the thicker, lighter continental Australian Plate overrides the thinner, denser oceanic Pacific Plate in the New Zealand region (Figure 3–5). Much of the strain associated with the collision is transferred to the leading edge of the Australian Plate, the landmass of the North Island. This strain produces the crumpled physiography of the sea floor to the east of the North Island, in the landmass itself, and in the sea floor to the west of the North Island (Begg *et al.*, 2005) (Figure 3–6).

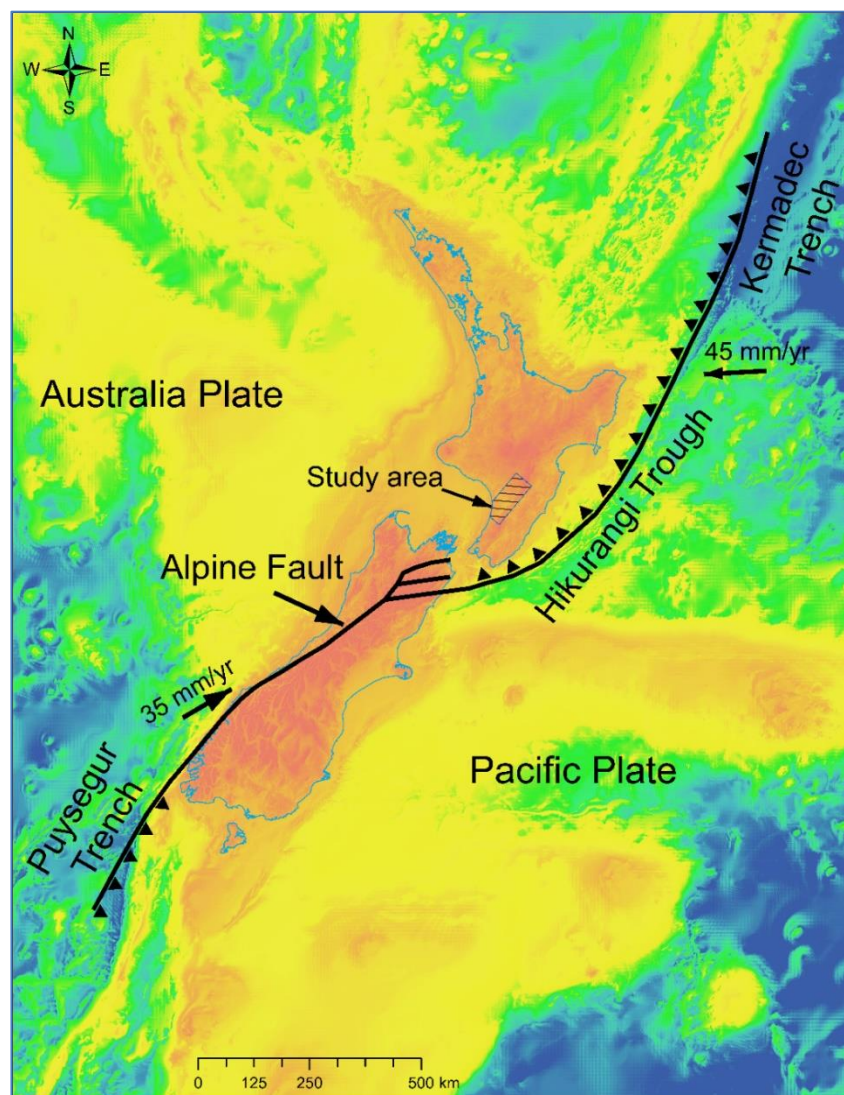


Figure 3–4. Tectonic setting of New Zealand.

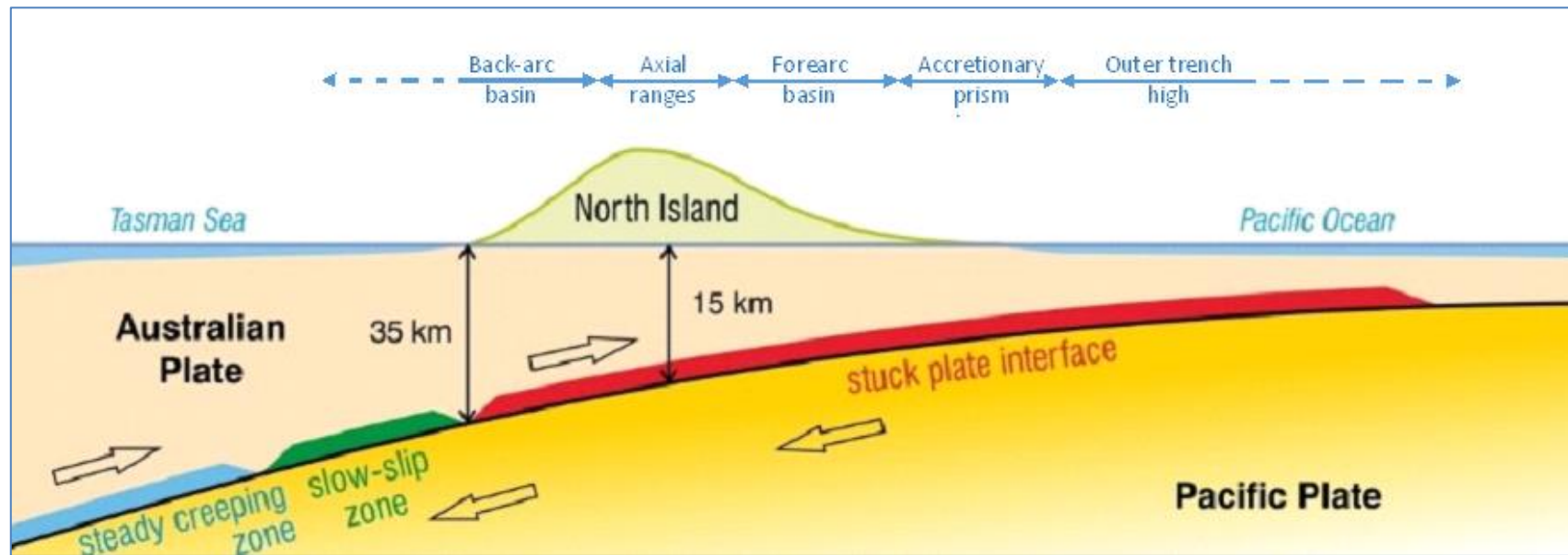


Figure 3–5. Schematic of plate interface beneath southern North Island viewed from Cook Strait (modified after Little, 2013).

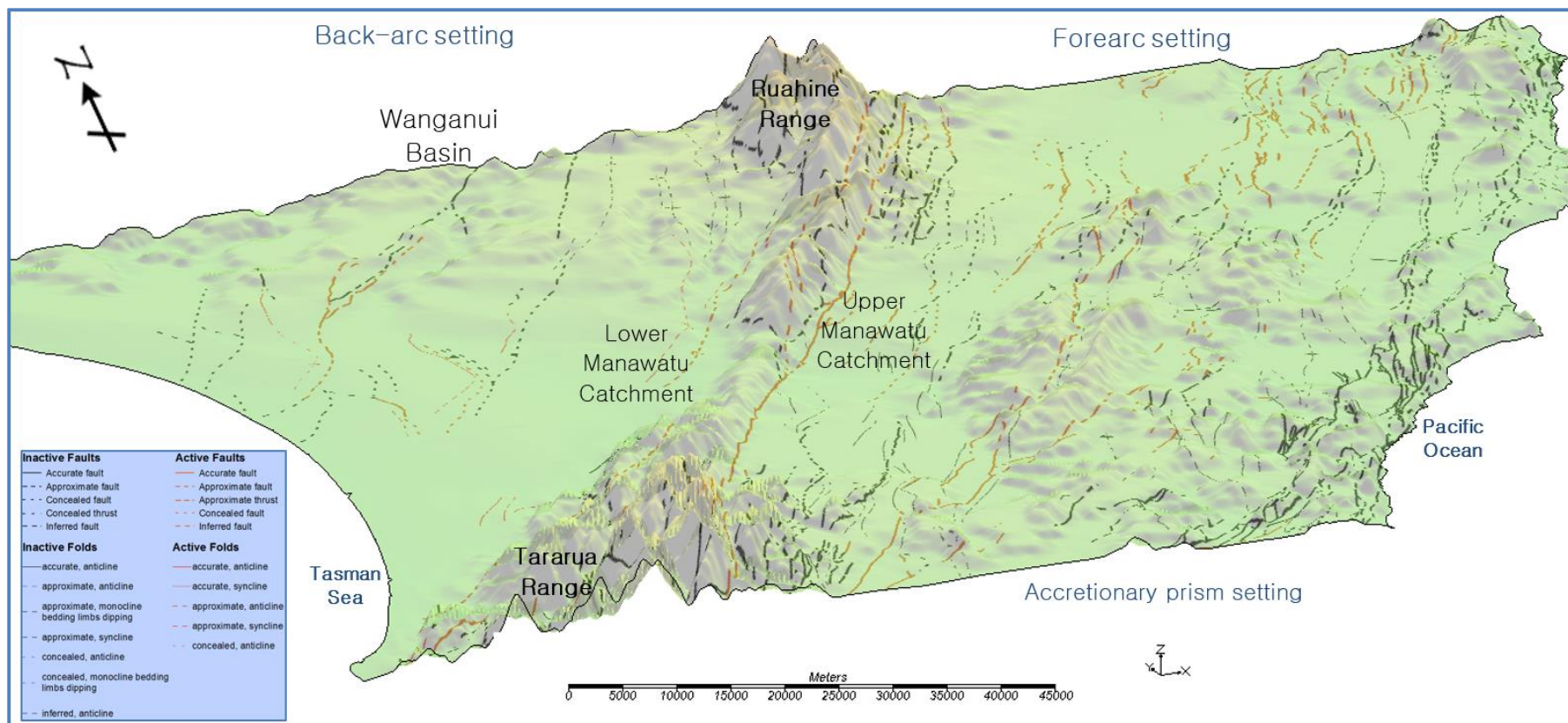


Figure 3–6. Three–dimensional impression of the southern North Island showing effect of tectonic setting on structural geological setting.

The top of the overridden Pacific Plate dips ever deeper northwest of the Hikurangi Trough, and can be found at depth beneath the landscape of the North Island (c. 30 km beneath the Manawatu River mouth). Strain associated with the plate boundary is transferred up through the overriding Australian Plate to the ground surface in the form of active folds and faults (Figure 3–2 through Figure 3–7). This deformation, both the broad regional strain and the more local deformation associated with faults and folds significantly influences the hydrogeological environment (Begg *et al.*, 2005).

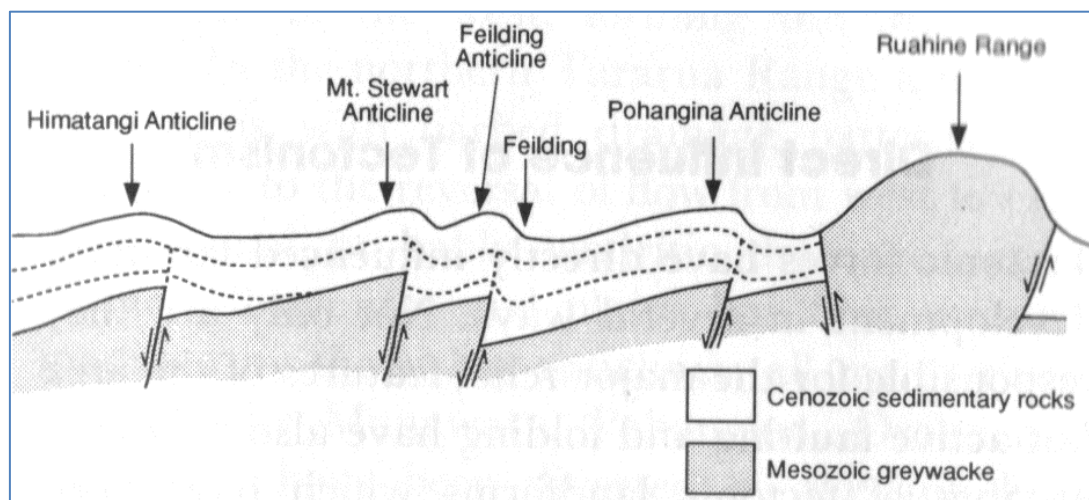


Figure 3–7. Sketch section between Tangimoana and the Ruahine Ranges showing the relationship between structure and relief (after Heerdegen & Shepherd, 1992).

Active reverse faults in the study area are bounded by asymmetrical growing folds (Figure 3–7). Progressive growth of these folds elevated their crests above major rivers valley floors, isolating them from alluvial deposition. Consequently, areas underlying active folds in the Wanganui Basin form interfluvial, channelling the major river catchments down the fault zones and synclinal axes between anticlines. Cool climate aggradational alluvial gravels were deposited in these loci, forming highly productive aquifer zones (Begg *et al.*, 2005).

### 3.5 Structure

The Wanganui Basin is affected by regional and local-scale tectonic deformation relating to its back-arc setting (Pillans, 1994) within the transition zone between the convergent Tonga-Kermadec subduction system to the northeast and the Alpine Fault continent-continent transform to the southeast (Figure 3-4) atop the subducting Pacific Plate (Brackley, 1999) (Figure 3-5). Regional tectonics is responsible for deep marine deposition in the Wanganui Basin during the early Pliocene and its subsequent uplift in the Late Pliocene and Pleistocene. The cause of this regional uplift (and eversion of the Wanganui Basin) is uncertain, but may be associated with processes at the southern end of the Taupo Volcanic Zone, and/or with deeper crustal processes associated with the subduction interface (Begg *et al.*, 2005).

In addition to regional-scale tectonic uplift, smaller scale shallower deformation has profoundly influenced young deposits in the Wanganui Basin. These structures are probably rooted near the subduction interface. They form a series of northeast to north-northeast striking faults through the area (Figure 3-8). Seismic reflection work indicates that these reverse faults associated with folding (Anderton, 1981; Lamarche *et al.*, 2005; Melhuish *et al.*, 1996). Some of these faults dip westward and some dip eastward. Where they fail to penetrate to the land surface, their presence may be signalled by asymmetrical folds (Figure 3-7). These folds generally have sigmoidal axes, gently dipping northwest flanks and more steeply dipping eastern flanks (Figure 3-7). Displacement on these faults was initiated at least as long ago as earliest Pleistocene. The major ones are still active. They have greatly influenced Middle and Late Quaternary deposition in the area. Not only has fold development progressively lifted their crests above the influence of fluvial action, but they also have confined river channels to the synclines.

The following sections provide an account of the main structural features in the study area based mainly on the description of Begg *et al.* (2005).

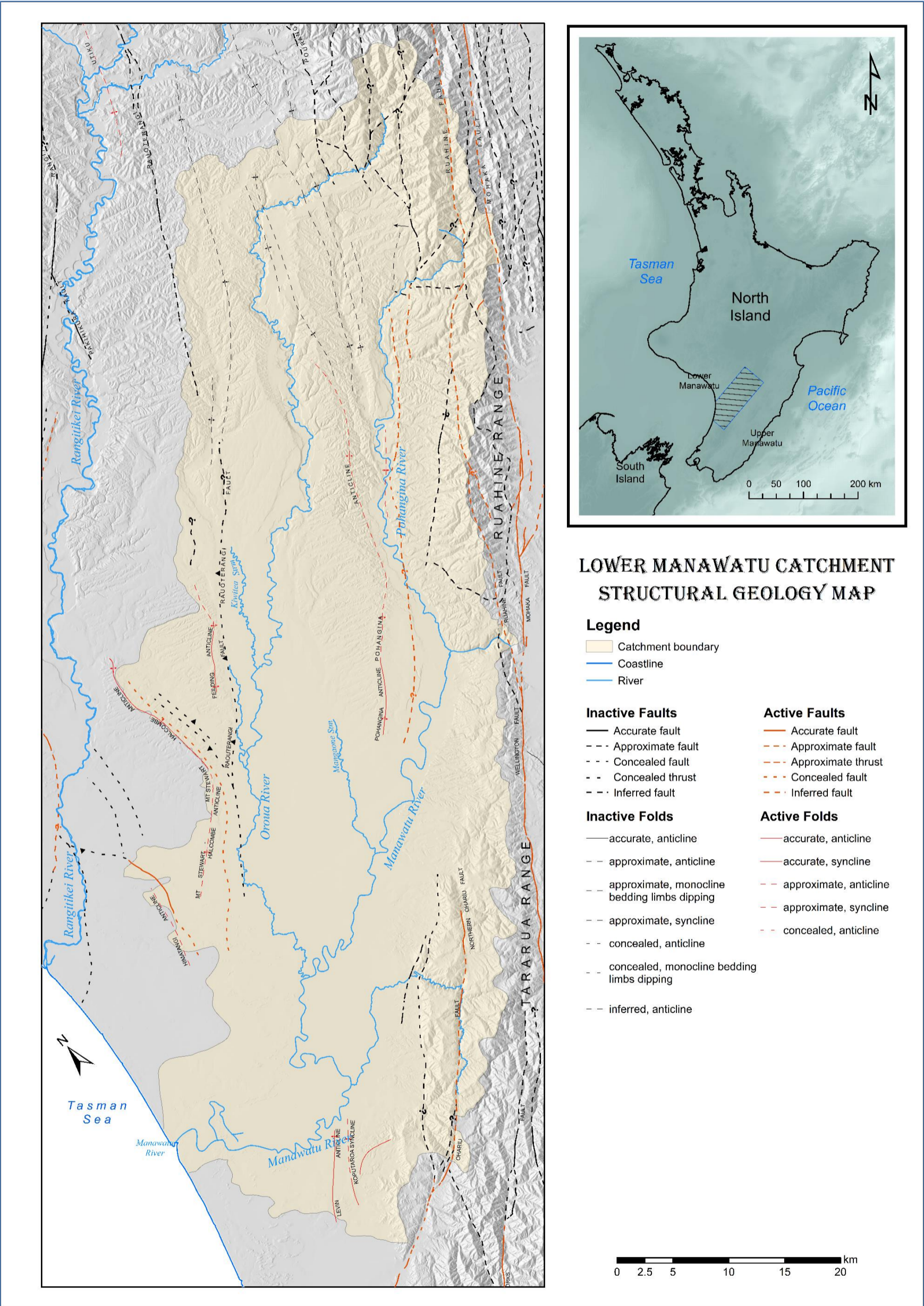


Figure 3–8. Structural geological map for LMC and surrounds based on digital QMAP data (Heron, 2014).

### 3.5.1 Subduction interface

The shallowly west–northwest–dipping fault that separates the Pacific and Australian plates at depth lies about 15 km beneath the Wairarapa coast and 25–30 km beneath Palmerston North (Figure 3–5). Deposits on top of the Pacific Plate to the east are being scraped off on the leading edge of the Australian Plate, and underplated beneath the east coast of the Wairarapa. While the plates slide easily, one across the other to the east of the Wairarapa coast, they are locked from beneath the Wairarapa coast to beneath the western side of the ranges. Strain associated with the relative motion of the two plates accumulates in the locked portion of the subduction fault and is released periodically as large earthquakes. Deformation at the surface associated with plate convergence over a long period of time has resulted in broad (long wavelength) patterns of deformation at the earth’s surface, notably uplift of the Wairarapa coastal ranges, development of the Wairarapa–Pahiatua basins, uplift of the Tararua and Rimutaka ranges, and perhaps development and eversion of the Wanganui Basin.

During the Middle–Late Quaternary period, uplift rates within the axial ranges accelerated exceeding 1 mm/y (Kamp, 1992; Pillans, 1986) but rates vary spatially owing to broad warping and tilting and varying deformation histories of individual fault blocks (Heerdegen & Shepherd, 1992).

### 3.5.2 Faults and Folds

There are many active upper plate structural features within the study area (Figure 3–8). Figure 3–9 shows the style of deformation that might be expected near faults and folds in the LMC area.

Te Punga (1957) described the Wanganui Basin anticlines in detail. He considered them young features with high uplift rates, in the order of 8 mm/y. He hypothesised that folding could not have begun until after deposition of Haweran sediments. Melhuish *et al.* (1996) argues that this is incorrect, as folding has been going on for at least three million years.

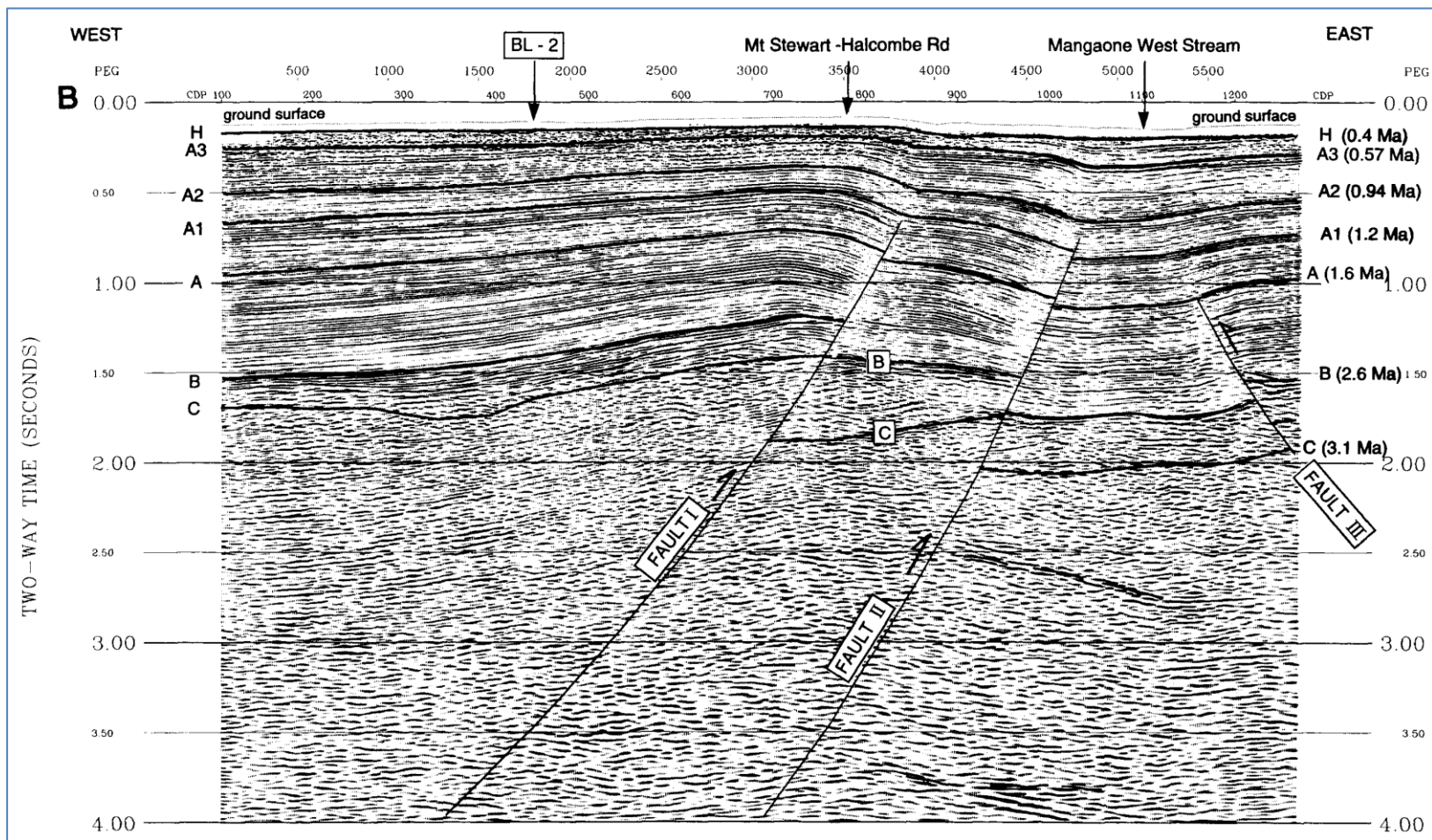


Figure 3–9. Interpreted seismic line from Melhuish *et al.* (1996) across the Mt Stewart–Halcombe Anticline and associated faults indicating the style of deformation that might be expected near at least some of the other faults and folds in the LMC area.

### *Wellington Fault*

The Wellington Fault is one of the major dextral strike–slip faults in the North Island. Its location is known to the south of the south Wellington coast, and it traverses all the way to the Bay of Plenty, changing only in name and reducing slightly in long–term slip rate. The vertical component of slip on the Wellington Fault is largely responsible for the development of the Tararua and Ruahine ranges during the last c. 1–1.5 Ma<sup>16</sup>. Near the ground surface, the fault plane dips steeply but dip probably decreases at depth (listric), dipping to the west. The fault plane probably extends right through the upper (Australian) plate and bottoms out on the subduction interface.

### *Ruahine Fault*

The Ruahine Fault is a western splay of the Wellington Fault, and as such is likely to be largely dextral strike–slip in character. The fault splays from the Wellington Fault near the Manawatu Gorge and traverses north through the middle of the Ruahine Range.

### *Northern Ohariu Fault*

Another of the large, active dextral strike–slip faults of the North Island Fault Belt, the Northern Ohariu Fault is believed to be a northern extension of the Ohariu Fault in the Wellington area. It enters the Tararua Range at the Ohau River near Levin and can be mapped through the upper Tokomaru catchment to the top of Kahutarawa Road. Its location, if present, is unknown to the northeast.

### *Pohangina structure/Pohangina Anticline*

There is good evidence for a fault and series of folds down the Pohangina River on the eastern side of the Pohangina Anticline (Begg *et al.*, 2005). Based on geological reconnaissance and seismic data, a fault has been marked down the Pohangina River (exposed in the river near Pohangina) (Anderton, 1981; Carter,

---

<sup>16</sup> Ma: million years.

1972; Feldmeyer *et al.*, 1943). The nature of the fault is poorly understood, although associated folding strongly suggests that it is active (Begg *et al.*, 2005).

#### *Mt Stewart–Halcombe fault/Anticline*

Melhuish *et al.* (1996) reported on a seismic reflection profile across the Mt Stewart–Halcombe Anticline clearly showing the relationship between west-dipping reverse faults and the folds of the Manawatu area (Figure 3–9). The profile imaged three faults, two associated with the Mt Stewart–Halcombe Anticline, and took in the west flank of the Feilding Anticline as well. The faults associated with the folds sometimes penetrate to the surface, but in many places are only indicated by the location of the fold axis. The anticline and its associated fault may be related to the fault named Rauoterangi Fault by Feldmeyer *et al.* (1943) and Anderton (1981) (see also Journeaux *et al.*, 1996; Lamarche *et al.*, 2005; Naish & Kamp, 1995). According to Melhuish *et al.* (1996), Mt Stewart–Halcombe Anticline is at least 25 km in length.

#### *Feilding fault/Feilding Anticline*

The Feilding Fault is a splay of the fault associated with the Mt Stewart–Halcombe Anticline, and the Feilding Anticline may be similarly related to the Rauoterangi Fault.

### 3.6 Physiographical setting

The geology and geomorphology in the LMC are products of tectonic–climatic interplay (Heerdegen & Shepherd, 1992). On the periphery of the Manawatu coastal plain, the long-term uplift rate of the Last Interglacial Tokomaru Marine Terrace over the past 120,000 years is estimated at 0.35 mm/y (Hesp & Shepherd, 1978). However, the terrace is tilted along its length and laterally towards the Manawatu coastal plain, implying lower rates of uplift on the plain than at the rear of the terrace, which onlaps against the Tararua Range (Clement, 2011). According to Clement (2011), research suggests that the rates of uplift near the LMC coastline ranges between of 0–0.06 mm/y since the Last Interglacial whereas the average uplift rate over the past 18,000 years has been about 0.5 mm/y further inland in the

Manawatu Valley area. The Manawatu coastal plain lies in a zone of subsidence albeit a zero rate of tectonic movement is suggested for the Manawatu through the Late Quaternary (Gibb, 1983; Pillans, 1986; Villiaxns, 1991).

The LMC plunges in a south-westerly direction. The upper part of the catchment comprises interfluves and river valleys whereas the lower part consists of nearly flat and flat plains. Figure 3-10 portrays a cross-sectional profile through the lower part of the interfluves-river valleys area in the LMC. The figure shows the restriction of river valleys between local active folds and is helpful for identifying potential groundwater recharge and discharge areas.

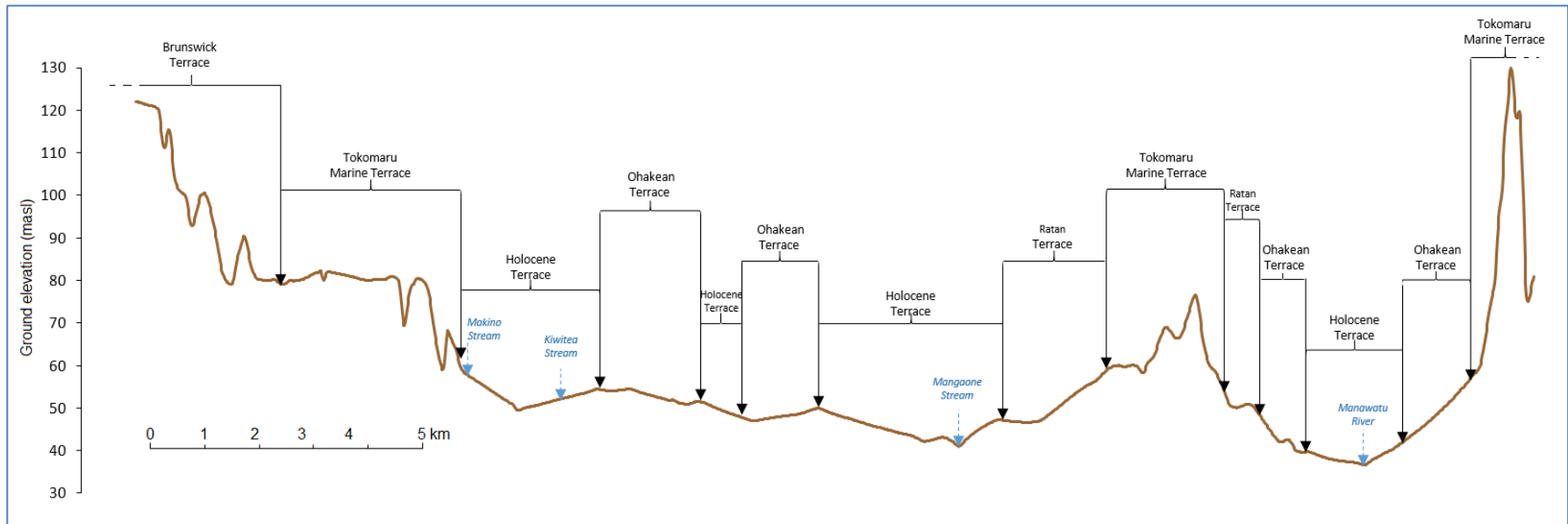


Figure 3-10. Cross-sectional profile through the lower part of the interfluvies-river valleys area in the LMC. For location, see Figure 3-1.

### 3.7 Landforms

Physiographical setting manifested as landforms influences the potential of geological material to host groundwater. In particular, slope strongly affects the apportionment of precipitation water into surface runoff and groundwater recharge. The steeper the land the higher the proportion of precipitation water that turns into runoff at the expense of groundwater recharge. In addition, relative elevation of land defines its hydrogeological setting. Typically, elevated land marks potential recharge areas and low-lying land coincides with groundwater discharge zones.

The landforms of the Manawatu have been investigated by a number of researchers, e.g. Cotton (1918), Rich (1959), Fair (1968), Hesp (1975), Heerdegen (1982), Clark (1989), Heerdegen and Shepherd (1992), Kenny and Hayward (1993 & 1996), Sloss (2006), N. S. Wang and Grapes (2008) and Clement *et al.* (2009). Nonetheless, a systematic, quantitative landforms classification method would suit the purposes of this study better than classifications presented in previous studies. Therefore, the methodology developed by Hammond (1954 & 1964) was adopted in this thesis to categorise the study area's landforms. Hammond (1954 & 1964) method is based on the examination of relative elevation of land, specifically slope, local relief, tableland setting and profile. These terms are explained in the method implementation description below.

Hammond (1954 & 1964) method is widely used for local and regional-scale landform classification, with or without modifications, manually and GIS/computer assisted (e.g. Barka *et al.*, 2011; L. Brabyn, 2006; L. K. Brabyn, 1996; Dikau *et al.*, 1991; Naydenova & Stamenov, 2013). Wallace (1955) classified New Zealand landforms manually using a 1:1 000 000 base map and the Hammond (1954 & 1964) method with few modifications. To date, that work remains the only morphological classification of landforms for the entire of New Zealand despite computer hardware and software advances and the availability of better elevation data, including LiDAR coverage of many areas through the country. Influenced by the work of Dikau *et al.* (1991), L. K. Brabyn (1996) automated and slightly modified his method to

classify landforms in a land area of approximately 37,000 km<sup>2</sup>, extending from shore to shore across the middle of the South Island.

### 3.8 Landform classification

The original Hammond (1954 & 1964) method depends on manual interrogation of topographical maps and uses a moving window of 9.6 km for physiographical analysis. In this thesis, the analysis was undertaken digitally using ArcGIS, NZSoSDEM v1 (Columbus *et al.*, 2011) and a 900 m diameter moving circle. The relatively small moving window is necessary to pick up catchment-scale changes in the landforms. Using 900 m diameter moving circle in the landform analysis does not provide enough high resolution for the characterisation of some local-scale features. For example, most of the narrow valleys with Holocene alluvial deposits are not characterised in their most suitable local-scale landform classes. This limitation in the used methodology may well extend to other small-scale features but is inevitable in catchment-scale studies such as this research. A description of the analysis parameters and steps is provided below.

#### *Slope*

Slope is the percentage of area occupied by gentle slope within 900 m radius around the cell. Hammond (1954 & 1964) specified 8% as the threshold for gentle slope. Slope is used to define how flat or steep the terrain is according to the criteria outlined in Table 3-2. It was calculated through:

1. Loading the 15-m resolution digital elevation model [*DEM\_study\_area*]
2. Calculating slope in percent rise for each pixel [*Slope\_percent\_rise*]
3. Reclassifying cells into gentle slope (code = 0) and steep slope (code = 1) [*Slope\_steep*]
4. Reclassifying DEM\_study\_area to 1 value (code = 1) to enable counting them [*Cells\_total*]
5. Counting the steep sloping cells (slope > 8%) within 900 m radius around each cell [*Cell\_steep\_slope\_count\_900m*]

Table 3–2. Land slope classes (adapted after Dikau *et al.*, 1991).

Percent of neighbourhood over 8% of slope	Slope Class
0 – 20%	400
21% – 50%	300
51% – 80%	200
>81%	100

Table 3–3. Land relief classes (adapted after Dikau *et al.*, 1991).

Change in elevation	Relief Class
0 – 30 metres	10
31 – 90 metres	20
91 – 150 metres	30
151 – 300 metres	40
301 – 900 metres	50
>900 metres <sup>17</sup>	60

6. Counting all the cells within 900 m radius around each cell  
[Cell\_all\_count\_900m]
7. Calculating percentage of steep slope within 900 m radius around each cell  
[Slope\_steep\_percent\_900m =  $100 \times \text{Cell\_steep\_slope\_count\_900m} \div \text{Cell\_all\_count\_900m}$ ]
8. Classifying slope for each pixel according to the criteria outlined in Table 3–2 [Slope\_classes]

Figure 3–11a presents a map of the calculated slope for the LMC.

### Local relief

Local relief is the difference between the maximum and minimum elevation within 900 m neighbourhood around the cell. It is used to define terrain ruggedness (i.e. the complexity of its texture). Local relief was classified according to the criteria outlined in Table 3–3. It was calculated through:

1. Finding the maximum elevation in 900 m radius around each pixel  
[Elevation\_max\_900m]
2. Finding the minimum elevation in 900 m radius around each pixel  
[Elevation\_min\_900m]

<sup>17</sup> Class inexistent in study area.

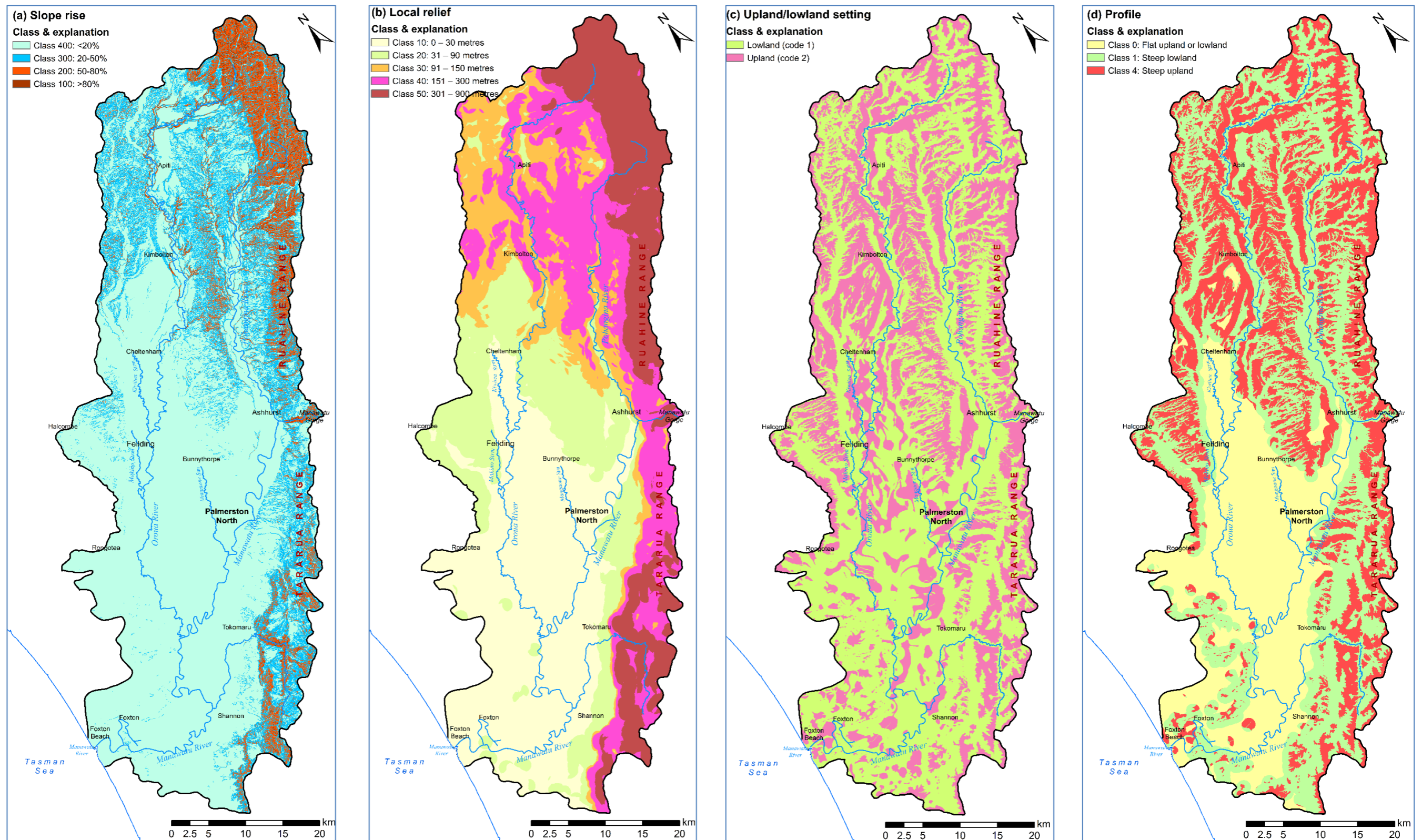


Figure 3–11. Slope rise, local relief, upland/lowland setting and profile calculations in 900 m radial moving window calculated from 15x15 m digital elevation model to enable landform classification using a modification of the Hammond (1954 & 1964) approach to suit local conditions and study objectives.

3. Calculating the local relief in metres [ $Relief\_in\_metres = Elevation\_max\_900m - Elevation\_min\_900m$ ]
4. Classify local relief for each pixel according to the criteria outlined in Table 3-3 [ $Relief\_classes$ ]

Figure 3-11b presents a map of the calculated slope for the LMC.

### *Tableland setting*

Tableland (upland/lowland) setting is determined by the difference between average local relief and elevation as outlined in Table 3-4. The cell is classified as upland if the difference between its elevation and the maximum elevation within 900 m radius around it is less than half of the local relief. Otherwise, the cell is classified as lowland. It was calculated through:

1. Calculating upland or lowland parameter [ $Low\_up\_parameter = \text{if}(\text{abs}(\text{Elevation\_Max\_900m} - \text{DEM})) < (0.5 \times \text{Relief\_in\_metres}), \text{then } 2, \text{ else } 1)$ ]

Figure 3-11c presents a map of the calculated slope for the LMC.

Table 3-4. Upland/lowland classification (adapted after Dikau *et al.*, 1991).

Criteria	Classification
maximum elevation – cell elevation $\geq$ 1/2 local relief	Lowland (code 1)
maximum elevation – cell elevation $<$ 1/2 local relief	Upland (code 2)

### *Profile*

Profile is used to determine tableland areas. It is a calculation of the percent area of gently sloping terrain within upland and lowland areas within 900 m radius according to the criteria outlined in Table 3-5 [ $profile\_class$ ]. Figure 3-11d presents a map of the calculated slope for the LMC.

Table 3–5. Land profile classes (adapted after Dikau *et al.*, 1991).

% of neighbourhood over 8% slope	Class if in lowland area	Class if in upland area
50%<	0	0
50%–75%	2	3
>75%	1	4

According to the criteria presented in Figure 3–12, landform classes were determined in the LMC using the above noted parameter values (Figure 3–13). This exercise resulted in too many landform classes, which makes it unsuitable for hydrogeological purposes. Accordingly, similar landforms were grouped together and the LMC has been categorised into five landform types, namely: (1) high hills and low mountains, (2) open and moderate hills, (3) irregular plains, (4) plains with some relief, and (5) nearly flat plains (Figure 3–14). The landform classification proposed in this thesis is compatible to that of (Wallace, 1955) and (L. K. Brabyn, 1996).



Figure 3–12. Hammond (1954 & 1964) landform classification method criteria.

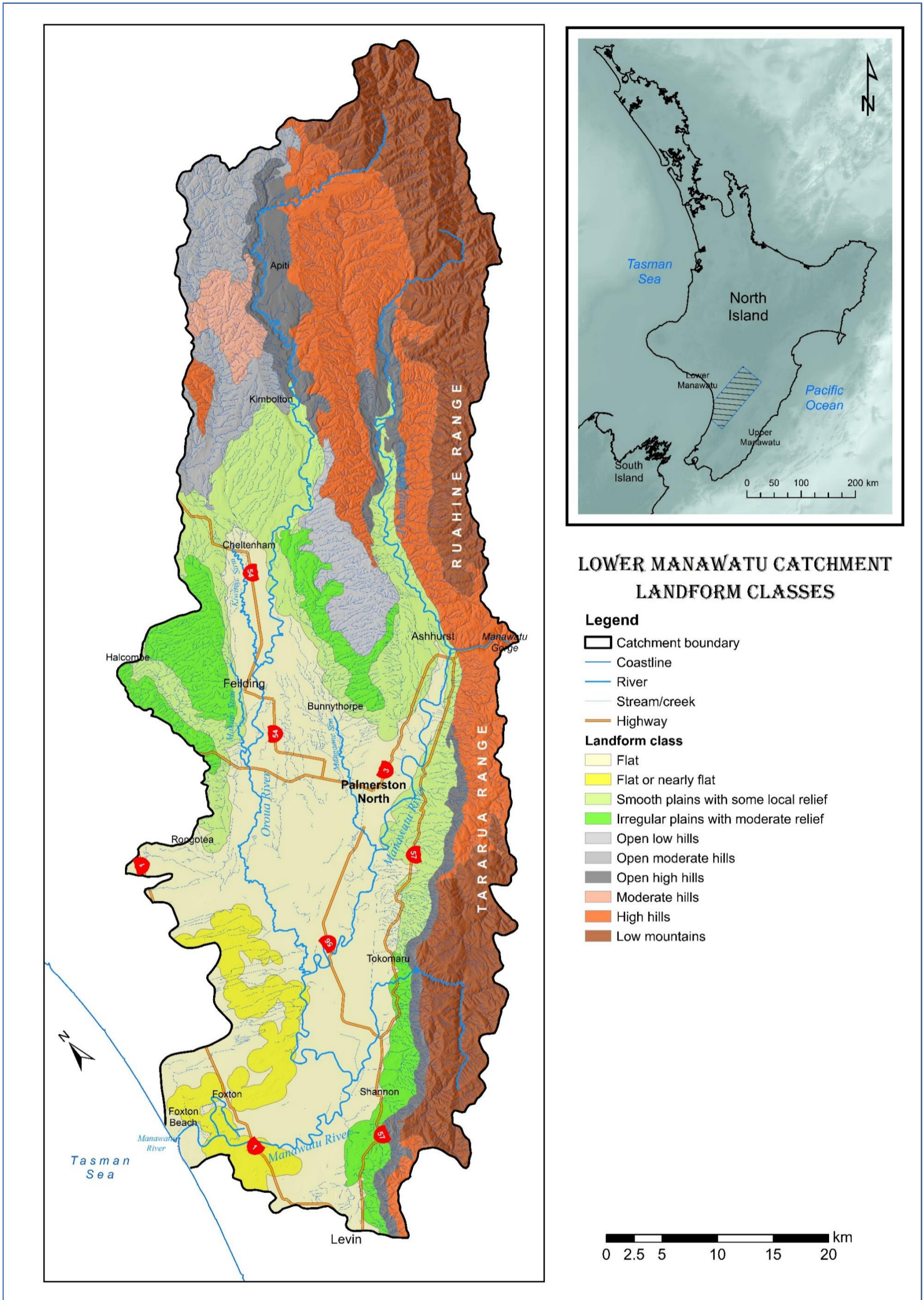
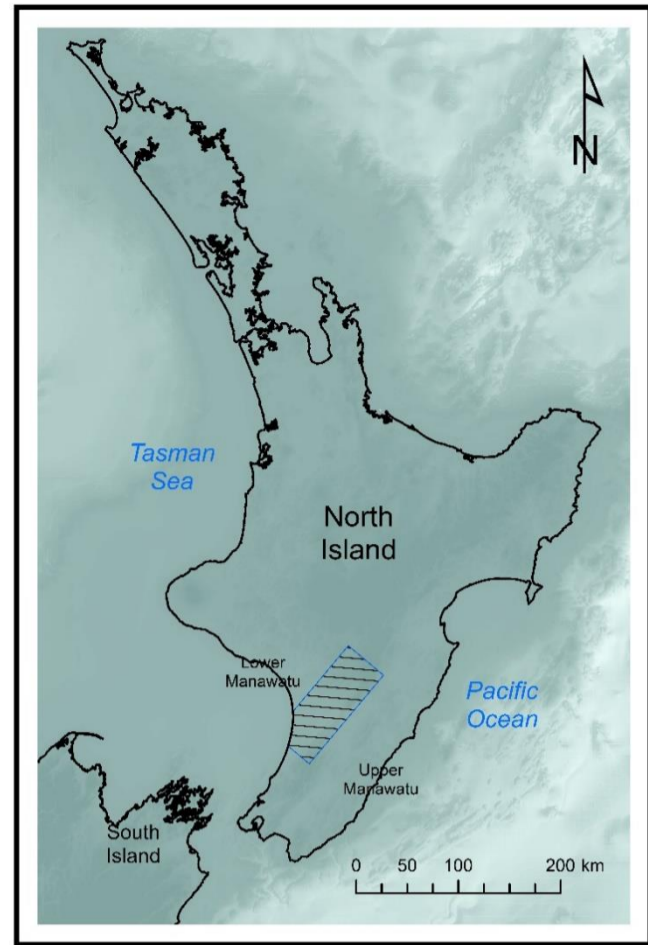
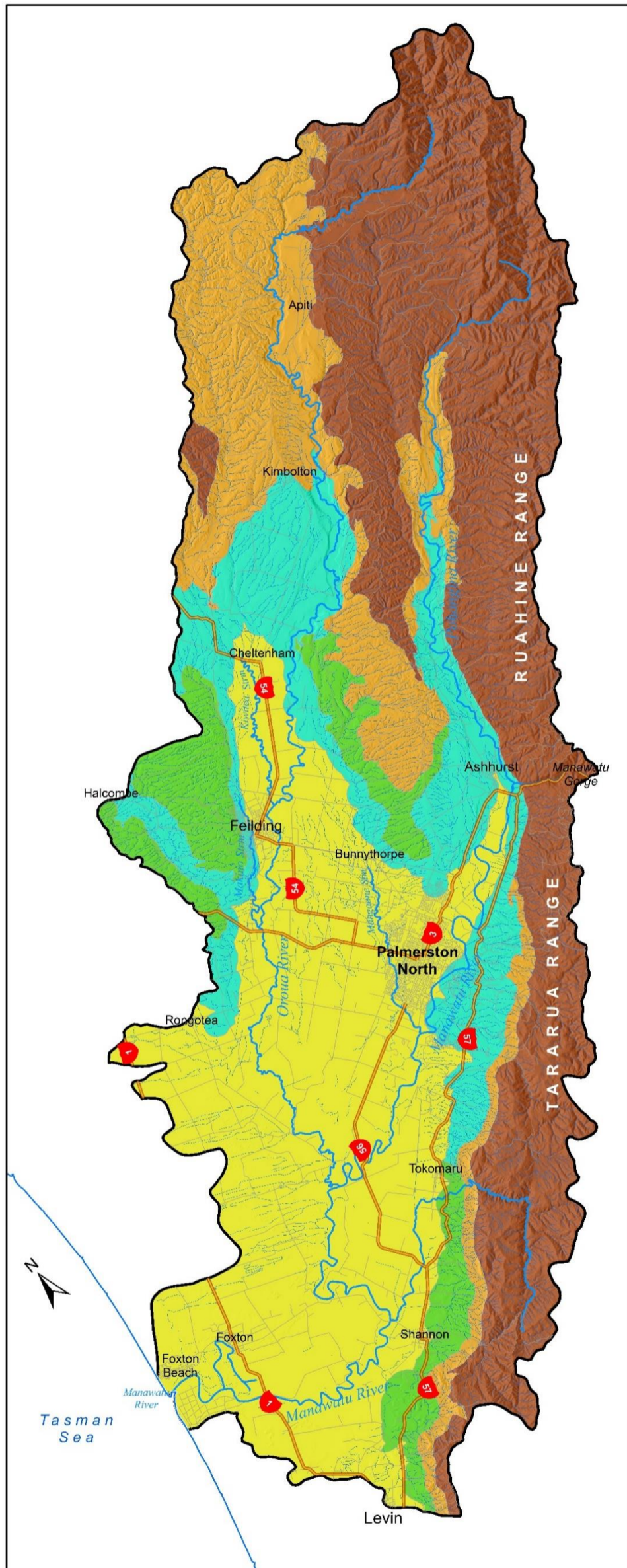


Figure 3-13. Landform classes calculated using the Hammond (1954 & 1964) method with modifications to suit local conditions.



### LOWER MANAWATU CATCHMENT LANDFORM TYPES

#### Legend

- |                    |              |
|--------------------|--------------|
| Catchment boundary | Stream/creek |
| Coastline          | Highway      |
| River              | Road         |

#### Landform type

- Flat plains (including sand dunes)
- Weakly dissected terraces
- Dissected terraces
- Strongly dissected terrace remnants and moderate hills
- Mountains and steep land

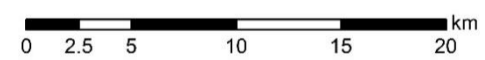


Figure 3-14. Landform types in the LMC.

### 3.9 Landform types

Begg *et al.* (2005) note that landforms in the LMC are exclusively geologically young, the entire area, from the coast to the top of the axial range at the Manawatu Gorge, having emerged from the sea in less than the last million and a half years.

#### 3.9.1 Mountains and steep land

≈ 883 km<sup>2</sup>; 33% of LMC area ≈

This landform type combines the low mountains, high hills and moderate hills landform classes delineated in Figure 3–13. It is situated in a structurally complex region, traversed by a multitude of folds and faults (Figure 3–14). Northeast–southwest trending mountains and steep land that form part of the North Island’s axial ranges dominate the eastern landscape of the LMC (Figure 3–14). The mountains include the Tararua and Ruahine ranges which define the LMC’s south–eastern boundary. The mountains are mainly underlain by Torlesse greywacke basement rock (Figure 3–2). In the upper part of the LMC, high, steep hills abut the mountains and extend in the north–eastern area of the catchment. There, the steep hills are mainly underlain by Plio–Pleistocene rocks.

The Manawatu River is an antecedent drainage feature that has maintained its original course through the uplifting of the axial ranges over the last million and a half years. It has incised its gorge through the high hills, separating the Ruahine Range to the north from the Tararua Range to the south. Steep greywacke bluffs enclose the gorge on either side.

In the north–eastern part of the catchment, the mountains achieve a maximum elevation of just under 1,700 metres above sea level (masl). The elevation of the basement rock drops in the area between the Ruahine and Tararua ranges where they are classified as high hills in Figure 3–13, but mountains and steep land in Figure 3–14. An increasingly intact remnant of an ancient erosion surface is preserved as land elevation descends from the high part of the crests of the Tararua and Ruahine ranges toward the Manawatu Gorge. Begg *et al.* (2005) describe it as

a gently folded surface (fold axis aligned northeast–southwest) of gentle relief, with relatively steep north–western and south–eastern flanks. They note that the basement rock underlying this surface is deeply weathered to about 10 m depth in places, and is overlain by loess and soil covered bed sequences. They also note that in the Saddle Road area on the northern side of the Manawatu Gorge, the surface is capped by marine and non–marine deposits less than 1.5 million years old.

The mountains and steep land region are dominated by an extensive dendritic drainage pattern (Figure 3–14). In dendritic drainage patterns, tributaries meet at low angles and branch in a random, tree–like pattern. They form on sloping land of erodable impervious or non–porous rocks or sediment, forming V–shaped valleys. They normally form on homogeneous rock masses with equal resistance to erosion in all directions, i.e. rock that contains no relatively weak layers (Zarour, 2017). In the low mountains area, the main streams and gullies are aligned nearly perpendicular to the structural grain whereas they run parallel, or sub–parallel, to it in the high hills area. Rivers in the eroded part of the ranges are typically steep and the landscape is deeply dissected.

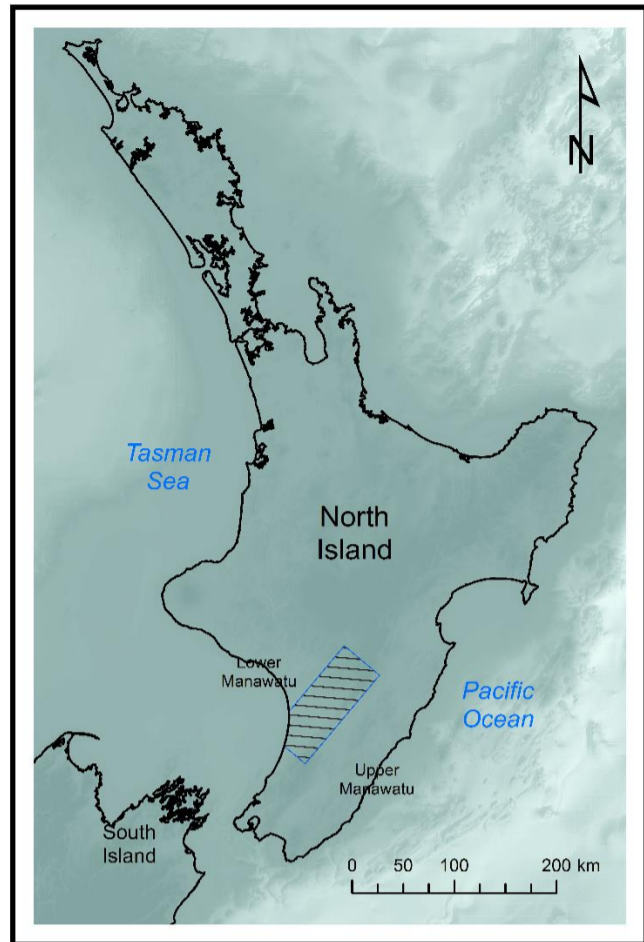
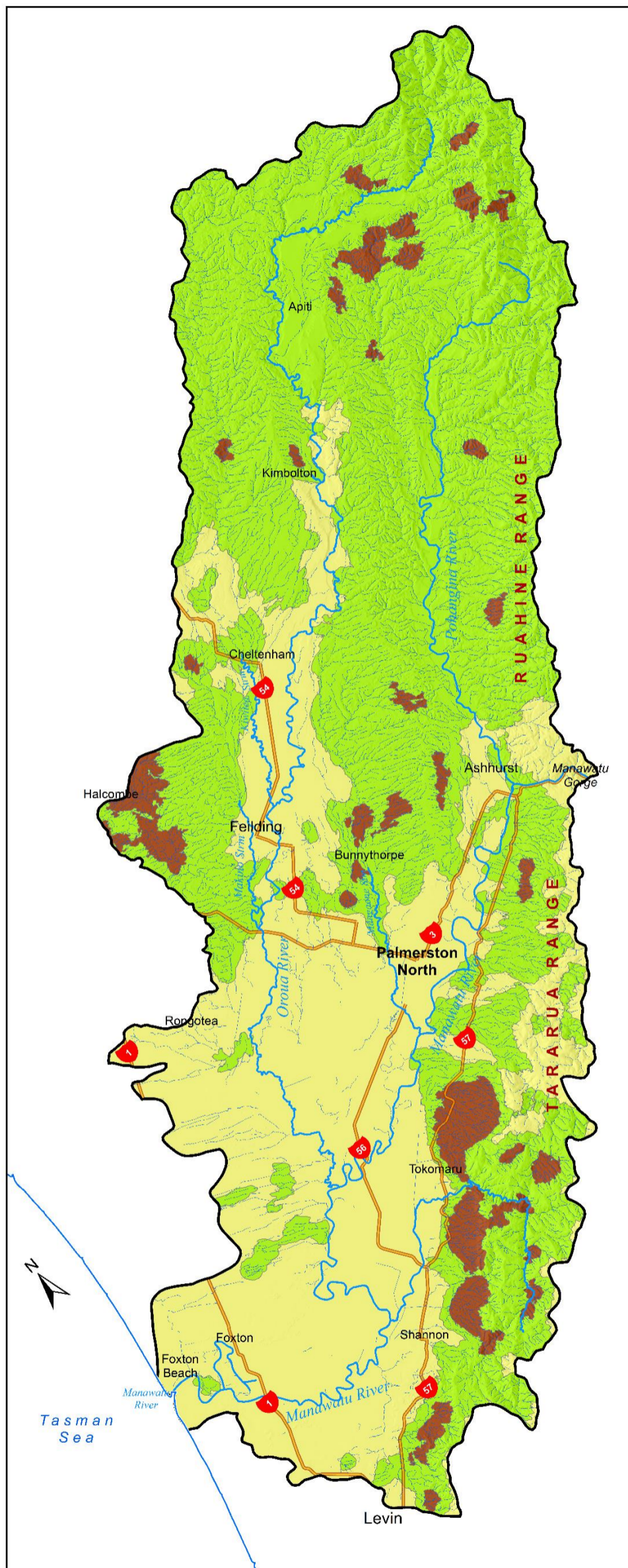
The low mountains and the high hills landform classes are grouped together as a single landform type due to their similar surface water drainage patterns and geological structure characteristics (Figure 3–14). Geomorphological and geological settings of this part of the LMC do not indicate it contains important aquifers.

### 3.9.2 Strongly dissected terrace remnants and moderate hills

≈ 402 km<sup>2</sup>; 15% of LMC area ≈

Strongly dissected terrace remnants and moderate hills landform type comprises the open high hills, open moderate hills and open low hills. Although strongly deformed, the area of this landform type is much less structurally complex than the mountains and steep land (Figure 3–14).

This landform type is characterised by dendritic drainage patterns developed on Plio–Pleistocene marine sediments that were deposited in the Wanganui Basin, which have subsequently been faulted, folded, tilted and uplifted. Overall, relief and dissection increase inland, and valley profiles are V-shaped. In some places, more resistant sand beds, shellbeds or landslide-prone mudstone within the siltstone and sandstone marine deposits result in lines of steep V-shaped gorges or gently undulating belts traversing the landscape (Begg *et al.*, 2005). The area of this landform type has abundant colluvial sediment. Late Last Glacial fan deposits (Q2f) cover a strip of this landform type to the south and Early Quaternary alluvial deposits (eQa) bury this landform type land to the north (Figure 3–14 and Figure 3–2). Last Glacial and Holocene alluvial sediment in this area is limited in extent to narrow river valleys and is thin, not exceeding a few metres in thickness. Geomorphology and geology suggest that exploitable aquifers are unlikely to be present in areas of this landform. Most importantly, surface water drainage density in the area is classified as high to very high (Figure 3–15). Nonetheless, visual inspection of the Mangapikopiko Stream floodplain area near Apiti that is situated on Last Glacial terraces shows relatively low local surface water drainage density. The underlying geology and the relatively low surface drainage network density in the Mangapikopiko Stream floodplain area denote good local groundwater resource potential.



**LOWER MANAWATU CATCHMENT  
DRAINAGE DENSITY**

**Legend**

- Catchment boundary
  - Coastline
  - River
  - Stream/creek
  - Highway
- Drainage density classes**
- Low (<3%)
  - High (3-6%)
  - Very high (>6%)

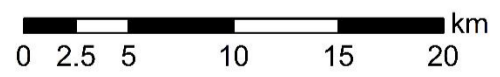


Figure 3-15. Surface drainage density in the LMC.

### 3.9.3 Dissected terraces

≈ 180 km<sup>2</sup>; 7% of LMC area ≈

The dissected terraces landform type delineated in Figure 3–14 corresponds to the irregular plains with moderate relief landform class in Figure 3–13. Its area nearly exclusively consists of elevated Quaternary interglacial marine terraces (Q11b, Q9b, and Q5b; Figure 3–14 and Figure 3–2). These terraces cover areas that are folded and tilted, with gently dipping to rolling topography. Generally, such sediments in the Wanganui Basin form the toes of interfluves that separate the valleys of the southwest–flowing major rivers, e.g. the upper part of the Oroua River system from the Pohangina River to the east and the Rangitikei River to the west. The crests of the interfluves are marked by anticlines.

The dominant lithology in the sediments forming these terraces is sand. Gravely horizons are present in them, reflecting stadial periods and beach environment deposition. The fine–grained lithology of the sediment or sediment matrix significantly reduces their hydraulic conductivity. In addition, these terraces are characterised by high local relief (Figure 3–11b), which favours surface water runoff over groundwater recharge. This is reflected in very high to high density dendritic surface water drainage, which signals low groundwater recharge. These sediments are expected to have low groundwater resource potential.

### 3.9.4 Weakly dissected terraces

≈ 356 km<sup>2</sup>; 13% of LMC area ≈

A flight of weakly dissected terraces skirts the LMC flat plains from the northeast (Figure 3–14). This landform type corresponds to the irregular plains with moderate relief and the smooth plains with some local relief landform classes in Figure 3–13. These terraces mainly consist of glacial periods alluvial deposits (Q10a, Q4a, Q3a, and Q2a) with some relatively low–lying Last Interglacial deposits (Q5b) forming marine terraces and Holocene age alluvial gravel in current river valleys.

Like all the above-mentioned landform types, dendritic drainage patterns characterise this landform type areas (Figure 3-14). However, this landform encompasses areas of high and low drainage density (Figure 3-15).

Last glacial alluvial sediment forming these terraces are fairly permeable and the terraces geomorphology is not as strongly biased towards surface water runoff as the previous landform types. Hence, these sediments can receive recharge from rainwater percolation and they can transmit sufficient water to allow them to be classified as aquifers. If hydraulic conditions permit, these sediments can also receive recharge from surface waterways. Therefore, they have good groundwater resource potential.

### 3.9.5 Flat plains

≈ 858 km<sup>2</sup>; 32% of LMC area ≈

An area of flat plains dominates the lower part of the LMC (Figure 3-14). This landform type consists mainly of the Oroua and Manawatu rivers floodplain. It also includes the area between Poroutawhao and the coastline, and both flanks of the Himatangi Anticline, which are covered by sand dunes (units Q1dm and Q1ds in Figure 3-2). Inactive sand dunes (Q1ds) are found closer to the shoreline. Sand dunes in the area reach a maximum elevation of 30 masl. They are mostly classified as flat or nearly flat landform in Figure 3-13.

The area is characterised generally by non-existent to low density surface water drainage network (Figure 3-14 and Figure 3-15). However, very high and high surface water drainage network density can be found in places within this landform type. Dendritic drainage is limited within this landform type to areas underlain by Last Interglacial and Last Glacial deposits. Holocene sediment covered areas are characterised by trellis drainage patterns. In trellis drainage, short tributaries meet long trunk streams at near right angles. The trunks are notably unconnected. In the trellis drainage patterned areas, consequent streams follow the dips and subsequent streams are parallel to strikes. Thus, short juvenile streams flow

towards the longitudinal centre of the LMC and join longer secondary streams and rivers that flow towards the coastline.

Trellis drainage pattern forms where surficial sediments overlie faulted and folded strata (Zarour, 2017). Hence, trellis drainage patterns on areas mantled by sand dunes possibly indicate that Holocene sand unconformably overlay structurally deformed sediment, probably Q5b or Q9b interglacial periods deposits. According to Begg *et al.* (2005), they are underlain by river silt, sand and minor alluvial gravel and incorporate inter-dune swamps.

Dune morphology varies from longitudinal dunes, barchan-style dunes to shore-parallel mounds, their shape probably influenced by topography and consequently, wind velocity (Begg *et al.*, 2005).

The sand dunes merge smoothly with the Manawatu River system alluvial plains. Begg *et al.* (2005) note that the Manawatu River floodplain is very low-lying, with the river meandering greatly in its course to the sea; the 20 m contour crosses the river bed almost 70 km upstream from the sea. As a result, all gravel in the Manawatu River bedload is lost well before it reaches its mouth. This is an important characteristic of the area because of its possible hydrogeological implications.

Strata underlying the flat plains are permeable and the area's surface water drainage pattern generally does not indicate that surface runoff is favoured over recharge. There is also evidence on groundwater-surface water interaction in this area. Hence, strata underlying this area have the potential to bear groundwater and serve as a resource for the environment and other purposes. This is proven by the area's well yields that are used for domestic and economical productive supplies.

### 3.10 Stratigraphy

In unconsolidated strata like the aquifer system in the LMC, stratigraphy and lithology are the most important geological controls on groundwater occurrence

and flow (Hiscock, 2009). Hence, a clear stratigraphical understanding is essential to this research.

The geological sequence in the Region can broadly be divided into three main divisions as suggested by Rich (1959):

1. well indurated and deformed rocks of early Mesozoic and perhaps late Paleozoic age
2. poorly consolidated, predominantly marine sediments of Plio–Pleistocene age with interbeds of glacial times alluvial deposits
3. Recent (Holocene) unconsolidated non–marine surficial deposits.

Rocks of the first division constitute an undermass that is separated by a regional extent major unconformity from the overlaying sedimentary cover, which comprise sediment of the other two divisions. This two–fold concept of undermass and cover is well established in New Zealand geological literature and is especially useful in structural and geomorphological interpretation. Rich’s (1959) classification is well–suited to hydrogeological analysis purposes. Begg *et al.* (2005) and Zarour (2008) adopted a similar general stratigraphical classification approaches.

Figure 3–16 presents a simplified geological map for the LMC, in which the area’s stratigraphy has been classified into seven units based on the information presented in Table 3–1. These stratigraphical units can be aggregated into the following four main stratigraphical groups, which are described in Sections 3.10.1 through 3.10.4:

1. Greywacke basement rocks
2. Plio–Pleistocene marine rocks
3. Middle–Late Quaternary glacial terraces and interglacial benches
4. Holocene alluvium and dune sands.

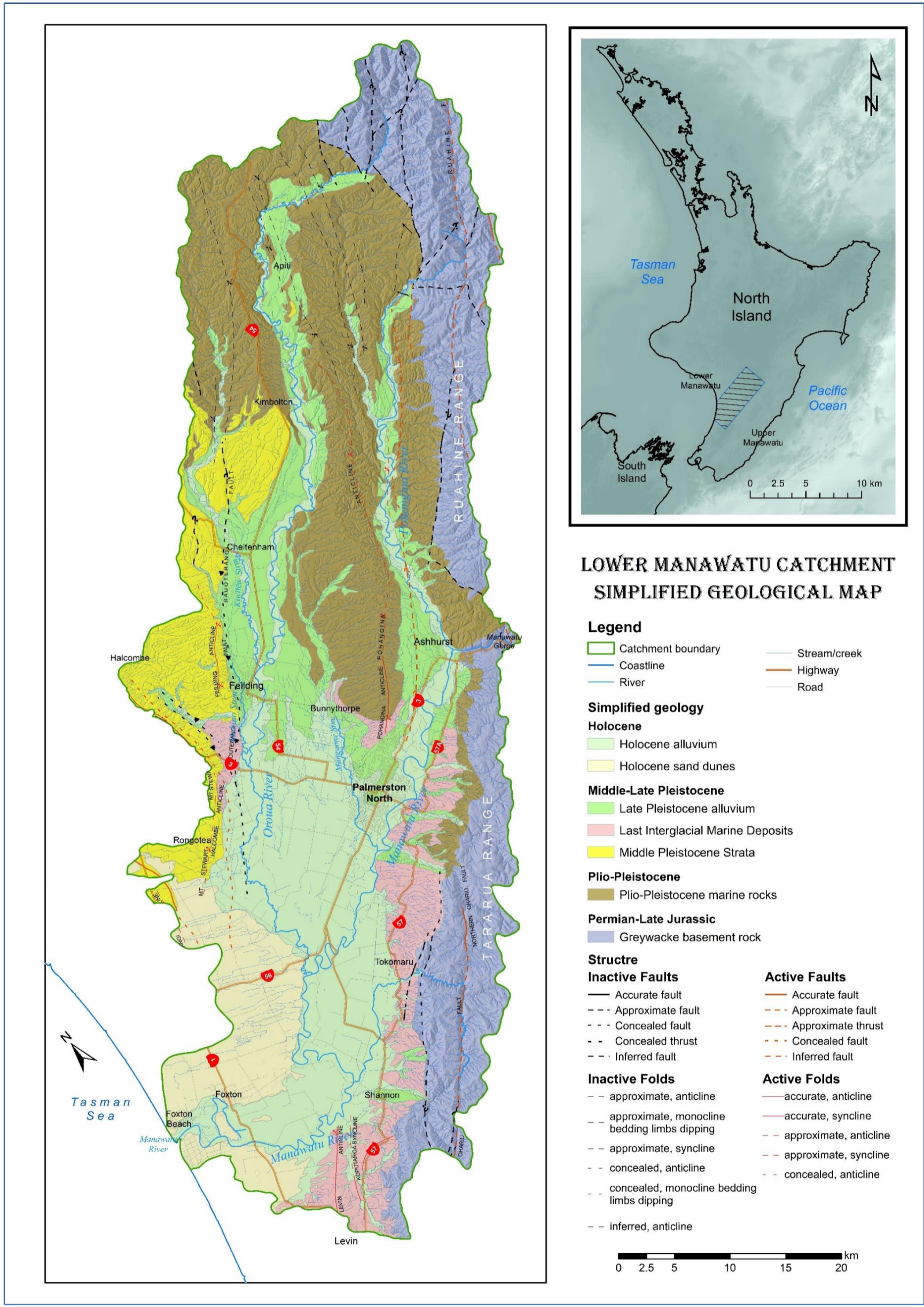


Figure 3-16. Simplified geological map for the LMC.

### 3.10.1 Greywacke basement rocks

Units **Ttt, Jtk, Te, Tev, Kep, Ktp, Ktw** in Table 3–1 and Figure 3–2.

Contemporary literature refers to this rock unit as the Torlesse Composite Terrane greywacke basement rather than undermass. Greywacke basement rocks undoubtedly underlay the North Island central ranges and all younger deposits in the LMC (Begg *et al.*, 2005). In the study area, exposures of these rocks are limited to the Ruahine and Tararua axial ranges and are best displayed in the Manawatu Gorge (Rich, 1959). These rocks occur at shallow depth in parts of the Horowhenua, at about 15 mbgl approximately midway between the foothills and the coastline, and they crop out offshore of Kapiti coast, forming the Kapiti Island (Zarour, 2008).

The thickness of the basement rock unit is unknown. It predominantly consists of unfossiliferous indurated quartzofeldspathic sandstone and interbedded mudstone. It also contains argillite with associated spilite and chert. Rare fossil occurrences within these rocks suggest they range in age from Permian to perhaps as young as Early Cretaceous, although they are mostly Triassic in age.

Rocks of this unit are commonly deformed, often showing several generations of folding and faulting (including bedding plane shear) and are now usually steeply dipping. Some rocks in this unit have been so thoroughly disrupted by ancient shearing that they consist of mixtures of blocks floating within a sheared mudstone matrix. These are known as melange and they commonly contain blocks of other rock types including basalt, chert and limestone.

Basement rocks commonly have mineralised cement. Therefore, they are impervious and impermeable. Consequently, they are not able to hold or transmit water except where they are weathered. Basement rock weathering generally ranges between low to moderate, but it can be extensive in places, possibly reaching up to around 10 mbgl.

### 3.10.2 Plio–Pleistocene marine rocks

Units coded **Pep**, **Pea**, **Pi**, **Pm**, **Pio**, **Pik**, **Pim**, **Pp**, **Puo**, **Pu**, **Pit**, **eQo**, **eQk**, **e-mQs**, **eQp**, **eQa**, **Q11b** in Table 3–1 and Figure 3–2.

The Wanganui Basin involves c. 4–5 km of Pliocene–Holocene sedimentary cover, which lies unconformably on basement rock. For the purposes of this thesis, a Plio–Pleistocene rock group is defined as rocks ranging in age from the Pliocene to the Castlecliffian Stage (OIS11).

Plio–Pleistocene rocks principally consist of marine deposits – mostly mudstone, siltstone, sandstone, pumiceous sand and minor limestone and conglomerate. Fine-grained strata in this rock unit are commonly described as papa by local drillers.

Plio–Pleistocene strata dip relatively gently south and southwest around the southern side of the Taranaki coastline. These rocks immediately underlie most of the land that is not designated as nearly flat and flat plains in the previous section (Figure 3–14). In places, northeast–southwest orientated faults cut the sequence (e.g. Kamp *et al.*, 2004; Naish & Kamp, 1995) (Figure 3–16).

These deposits are generally of continental shelf origin. A number of lithostratigraphical groups are incorporated within this unit. They include the Paparangi, Okiwa, Nukumarū, Maxwell, Okehu, Kai-iwi and Shakespeare groups. Paparangi, Okiwa and Nukumarū groups comprise principally marine mudstone and siltstone, with minor sandstone and limestone. The Maxwell Group is largely of non-marine origin, with lithologies ranging from shallow marine sand and estuarine silt to non-marine lignite and clay. The Okehu Group consists of siltstone and pumiceous sand (the Potaka pumice sand). The Kai-iwi Group consists of marine silts and sands, and the Kaimatira pumice sand. Marine fossils are common within

most of these units and indicate Late Pliocene to mid–Castlecliffian depositional age (c. 3.7 – 0.7 Ma BP<sup>18</sup>).

Due to sea level change during the Pliocene and Pleistocene times, few unconformities of relatively short duration can be found in the Maxwell, Okehu, Kai-iwi and Shakespeare groups. Nonetheless, this sequence is broadly conformable. It is regarded as one of the best onshore predominantly marine sequences of rocks of this age in the world (Carter & Naish, 1998b). In the Pohangina River catchment, these strata are faulted against and rarely unconformably overlie rocks of Torlesse greywacke basement (Begg *et al.*, 2005).

Siltstone and mudstone have high intrinsic porosity and very low primary permeability, rendering such strata in this unit as aquitards or aquicludes. Sandstone and pumiceous sand formations within this unit have significant intergrain pore space and good permeability, conglomerate has lower but reasonable permeability and mature limestone can have high secondary permeability due to dissolution and dolomitisation. However, relatively young age, structure, interfingering with silt and mud beds and topography generally diminish the potential for all strata in this unit to yield good amounts of water through wells. In addition, loess cover over most of the area underlain by this unit greatly limits its ability to receive recharge from rain and surface water. Consequently, rocks in this unit generally do not host important aquifers except in the Wanganui District where the city and surrounds depend on deep highly productive wells tapping Middle Nukumaruan age strata for their water supply. Middle Quaternary age rocks crop out in Kai-iwi and occur at about 700 mbgl under Wanganui City at relatively short distance down-dip of Kai-iwi.

---

<sup>18</sup> Before present.

### 3.10.3 Middle–Late Quaternary strata (Hawera Series)

Units coded Q10a, Q9b, Q8a, Q6a, Q6f, IQa, IQl, IQf, Q5b, Q4a, Q4f, Q3a, Q3f, Q2a, Q2f in Table 3–1 and Figure 3–2.

Haweran Stage sediments in this research are coded according to the QMAP convention. In this system, Quaternary age is designated in stratigraphical unit codes by the letter Q. Where the OIS during which the unit was deposited is known, it is indicated by its number and a suffix to denote the depositional environment, e.g. Q2a to symbolise alluvial OIS2 deposits. Sediments deposited during even numbered OISs relate to cool climatic periods and those deposited during odd numbered OISs relate to warm climatic periods, except for OIS3, which represents a warmer phase between cooler periods of the last glacial period. Where an OIS cannot be reasonably allocated, a prefix is used to delineate Late (l), Middle (m) or Early (e) Pleistocene age, e.g. mQf to signify middle–Pleistocene fan deposits. In this thesis, Early Quaternary refers to strata older than OIS10, Mid–Quaternary refers to unites deposited during the period OIS10–OIS6, and Late Quaternary refers to unites deposited in the Last Interglacial and last Glacial (OIS5–OIS2).

A flight of Middle–Late Quaternary age (Haweran Series) terrestrial and marine terraces flank river valleys in the LMC (Figure 3–2). They gradually diminish as they extend into the Manawatu Plains. The terraces consist of sediment relating to the period OIS10–OIS2, inclusive (i.e. c. 360–10 ka BP according to Pillans (1990) and Suggate (1990) stratigraphical classifications). Haweran Series deposits separate Castlecliffian Stage sediment from that of the Holocene (Fleming, 1953). The base of the Haweran Series is marked by the Rangitawa Tephra (350 ka BP), which lay within the OIS10 glacial period deposits (Beu, 2001). LMC terraces were created by tectonic and global climate change processes (Fair, 1968). Figure 3–17 schematically presents the stages of terrace development in the LMC. Pleistocene terraces in the Wanganui Basin are commonly mantled by sheets of loess relating to subsequent glacial periods.

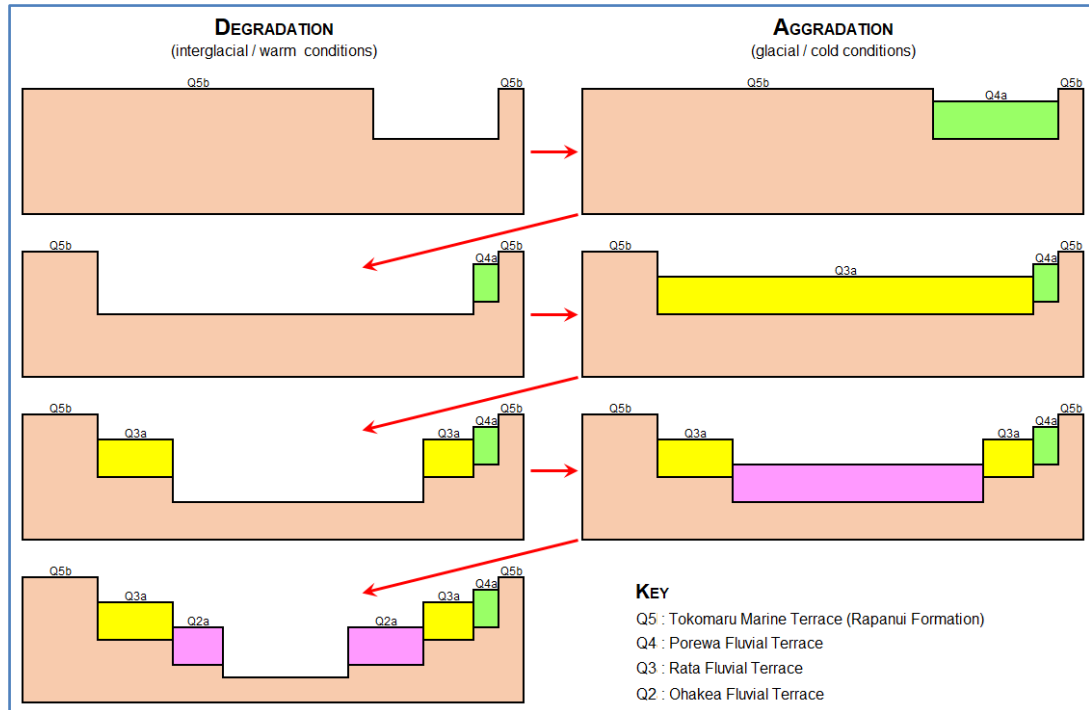


Figure 3–17. Schematic drawing illustrating the formation of terraces in the LMC (adapted after Fair, 1968).

Warm (interglacial) period deposits represent high sea level times during which marine deposition prevailed (e.g. Q9b and Q5b; Brunswick and Tokomaru marine benches, respectively). Now, these deposits constitute elevated marine terraces. Technically, where these sediments skirt the axial ranges, they form straths (bedrock terraces) rather than terraces because they are most probably eroded into greywacke basement rock. In contrast, terraces are elevated unconsolidated alluvium deposited by the same river that incised them.

Fluvial terraces are alluvial floodplain remnants formed as a result of river erosional downcutting, abandonment and lateral erosion of its former floodplains due to either changes in sea level, local or regional tectonic uplift; changes in local or regional climate, changes in sediment load, change in river flow, or a complex mixture of these and other factors. Alluvial terraces are remnants of cold climate period floodplains deposited when sea level (base level) was distant and lower. In the LMC, they relate to the Nemona Glacial period deposits (Q10a), Waimaunga Glacial period deposits (Q8a), Waimea Glacial period deposits (Q6a), and Otira Glacial period deposits (Q4a, Q3a, Q2a). During cold times, loose material

accumulated on steep slopes in the LMC due to aeolian, slopewash and downslope-creep deposition as colluvial deposits (e.g. **IQI** material). Alluvial fans (**Q6f**, **IQf**, **Q4f**, **Q3f**, **Q2f**) were built where small steep streams approached flattened surfaces and dump their bedload in fan-shaped deposits,

Alluvial terrace sediments of the Haweran Series generally consist of poorly to moderately sorted alluvial gravel with minor sand and silt. The older the sediment the more weathered it is. Quaternary terraces older than the Ohakea Terrace are commonly covered by loess. The loess cover is neither shown in the geological map (Figure 3-2) nor in Figure 3-17. Loess is discussed further in Section 3.13 because of the important role it plays in determining the ability of rainwater to percolate into underlying layers to replenish their groundwater reserves.

Steep alluvial and colluvial fan and landslide deposits are found in the LMC almost exclusively in areas classified as steep lowland (Figure 3-2 and Figure 3-11d). Fan deposits consist of very to moderately weathered, weakly consolidated, poorly sorted gravel, sand, silt and clay. Landslide deposits range from coherent shattered masses of rock to unsorted fragments in a fine-grained matrix. Fan and landslide deposits are characterised by low porosity and permeability due to their poor sorting. Their steepness and limited volume do not allow them to hold significant water.

Sediments underlying Brunswick and Tokomaru benches were deposited in shallow marine depositional environments. They consist of conglomerate, shellbeds, dune sand, silt and mud. These deposits are commonly mantled by loess and fan deposits. Loess cover restricts rainwater recharge to these layers, limiting their potential as water resources. In the Horowhenua, wells tapping **Q5b** sediment (the Otaki Sandstone<sup>19</sup>) can yield enough water for domestic supply purposes. Wells in the higher positioned Brunswick Terrace normally fail to produce useful amounts of water.

---

<sup>19</sup> Unit referred to as Rapanui Formation in other places.

Examination of drillers' well logs reveals common peat presence in interglacial deposits in the LMC. Peat is not normally deposited in shallow marine environments, although it can be deposited in marginal marine environments in special situations. The presence of peat has been critical in stratigraphical modelling undertaken in this research (Section 8.3.2).

#### 3.10.4 Holocene alluvium and dune sands

Units coded **Q1a**, **Q1l**, **Q1f**, **Q1ds**, **Q1dm** in Table 3–1 and Figure 3–2.

Various types of Holocene age sediment occur in the LMC, including alluvium (**Q1a**), dune sands (**Q1ds** and **Q1dm**), fan (**Q1f**) and landslide (**Q1l**) sediments.

Holocene alluvial deposits (**Q1a**) consist of loose, well-sorted, sub-rounded, sub-spherical alluvial gravel with some sand, silt and clay with local peat. They are found in river valleys and modern floodplains. According to Begg *et al.* (2005), degradational gravel surfaces that are of low elevation and are not overlain by loess units can be considered Holocene in age (Q1a).

Holocene alluvium is extremely permeable due to grain size, sorting, roundness, sphericity and lack of cementation and, from a groundwater perspective, is very productive, having high specific yield. Nevertheless, normally these deposits are not thick, limiting their potential as a water resource, particularly when associated rivers and streams are dry. Generally, groundwater in Holocene sediments in the LMC is present under unconfined hydraulic conditions. Wells in Holocene alluvium are commonly considered riparian as they either draw water from associated surface water systems or intercept groundwater that would otherwise have flown into them. Holocene gravel constitutes the main medium through which groundwater and surface water interact in the LMC area.

Holocene windblown loose sand in active unvegetated or sparsely vegetated dune fields and deflation zones (**Q1dm**) and windblown inactive dunes and associated facies (**Q1ds**) are porous and permeable, so they can store and transmit water. Dune sands are mapped in the lower part of the LMC, extending between Carnarvon

and Foxton Beach on the true right of the Manawatu River and Moutoa Floodway (Figure 3–2). They are also mapped at the southwestern most corner of the LMC on the Tasman Sea coastal area. The sand dunes can reach up to 30 m in elevation and they often embrace inter–dune swamps. Dune morphology varies from longitudinal dunes, barchan–style dunes to shore–parallel mounds, their shape probably influenced by topography and consequently, wind velocity.

Sand has good to moderate permeability and specific yield (e.g. Bear, 1972; Fetter, 2013; Freeze & Cherry, 1979). So, groundwater receives recharge and can be found in sand dune areas. Inter–dune swamps are indeed an outcrop of groundwater in sand covered areas in the LMC.

Holocene fan deposits (**Q1f**) are mapped only in a small area in the Pohangina Valley, near Awahou. These alluvial, colluvial and scree fan deposits consist of poorly sorted, poorly consolidated angular to sub–rounded boulders, cobbles, pebbles, gravel, sand and clay. They are not important from a hydrogeological point of view mainly due to their limited extent. Holocene earthflow hill slope deposits (**Q1I**) consist of poorly sorted clasts up to boulder size in a clay matrix. They are found in the LMC exclusively in areas classified as steep lowland (Figure 3–2 and Figure 3–11d). Their geomorphological setting and lithological properties make them unsuitable for storing and transmitting groundwater.

### 3.11 Interplay between alluvial deposition and sea level change

Wanganui Basin sediments are exclusively Pliocene and Quaternary in age, during which the region was characterised by dynamic interplay between sea level, tectonics, erosion and deposition. During the early stages of that period, the Wanganui Basin was a shelfal, subsiding depocentre. Then, it has been everted in the late part of that period and the present land has emerged from the influence of the sea (Begg *et al.*, 2005; Feldmeyer *et al.*, 1943; Fleming, 1953; Kamp *et al.*, 2004). Ongoing regional tectonic uplift is evidenced by the sequence of stranded marine benches. The Quaternary also witnessed smaller scale deformation, well–illustrated by the development of local folds and faults such as those at Mt Stewart–

Halcombe, Feilding and the Pohangina (Feldmeyer *et al.*, 1943; Fleming, 1953; Jackson *et al.*, 1998; Melhuish *et al.*, 1996). While regional-scale tectonic warping influenced the broader relative elevation of land and sea, local-scale tectonic features (faults and folds) progressively restricted the routes of the major rivers from the hinterland to the sea, particularly in the LMC. Subsequently, the Oroua and Pohangina rivers have broadly occupied the same courses throughout the Haweran until today, i.e. for the last 340 ka.

During the Pliocene and Quaternary, sea level has fluctuated on a cyclical basis, more recently by almost 125 m. This is particularly well documented for the last c. 1.8 Ma (Carter & Naish, 1998a; Imbrie *et al.*, 1984; Milankovitch, 1920). Cyclical sea level change has resulted in cyclicity in the deposition style in the Wanganui Basin, particularly in shallow marine environments. Interfingering non-marine beds and marine strata in the Maxwell Formation (late Nukumaruan age) is almost certainly due to sea level fluctuation.

As the Wanganui Basin landscape emerged from the sea during the Pliocene and Pleistocene, the shorelines were benched by marginal marine processes during high sea level stands. The elevated sea level during these periods resulted in lower river gradients behind the shorelines, changing the style of deposition to low energy, dominated by silt and sand. When the sea retreated from these high stands, rivers flowed across the marine benches to the sea, far beyond the present-day coastline, carrying gravel much further down their courses due to steeper gradients in this part of their catchments. Loess deposition was common during cold climatic conditions, because vegetation was reduced, and sediment supply increased (e.g. by frost heave, increased wind exposure, exposure of the plains between the high sea level coast and the low sea stand coast).

Analysis of lithological log data can help us define the paleogeographical changes related to sea level fluctuation and understand their likely impact on the deposits beneath the plains. For example, it can be assumed that the aggradational gravel units mapped at the surface as sequences of prominent terraces are likely to extend

down valley beneath the Holocene floodplain material. Begg *et al.* (2005) suggest that the gradient of the surface upslope from where the aggradational gravels disappear beneath Holocene alluvium can be extrapolated downslope to constrain the depth of burial of that surface.

The relative elevation of terraces is determined by the interplay between tectonic uplift and fluvial incision and deposition. The average rate of uplift and incision ( $r_x$ ) can be calculated as follows:

$$r_x = \frac{h_x}{t_x} \quad 3-1$$

where  $h_x$  is the height of the terrace and  $t_x$  is its age (Figure 3-18).

### 3.12 Geological history

The above geological data is synthesised to provide a geological history for the LMC and vicinity. Good appreciation of the area's geological history is instrumental for stratigraphical and hydrogeological conceptualisation.

During the Late Paleozoic to Early Cretaceous time, sand and mud forming the Torlesse Composite Terrane were deposited in deep marine basins along the eastern margin of Gondwanaland in a compressional or transpressional setting (Bradshaw, 1989). Active deformation of these strata (commonly involving bedding plane shear) commenced soon after they were deposited and continued until near the end of the Early Cretaceous. A major, abrupt tectonic event marks the termination of deep marine deposition around the Early Cretaceous, with significant and widespread tilting, folding and faulting. This period of intense deformation continued probably to the start of the Late Cretaceous. It marks the cessation (or near-cessation) of Mesozoic active margin compressional tectonics. It resulted in significant change in rock hardness, metamorphism and structural complexity. Begg and Johnston (2000) suggest that this event reflects the amalgamation of the various terranes of the Torlesse Composite Terrane when the Rakaia Terrane, the component of the Torlesse Composite Terrane that underlies the Tararua and Ruahine ranges, was amalgamated with terranes to the east, the Pahau and

Waioeka terranes. Begg *et al.* (2005) believe that the amalgamation event was probably the origin of at least some of the melange units found throughout the Torlesse Composite Terrane, including Esk Head Terrane.

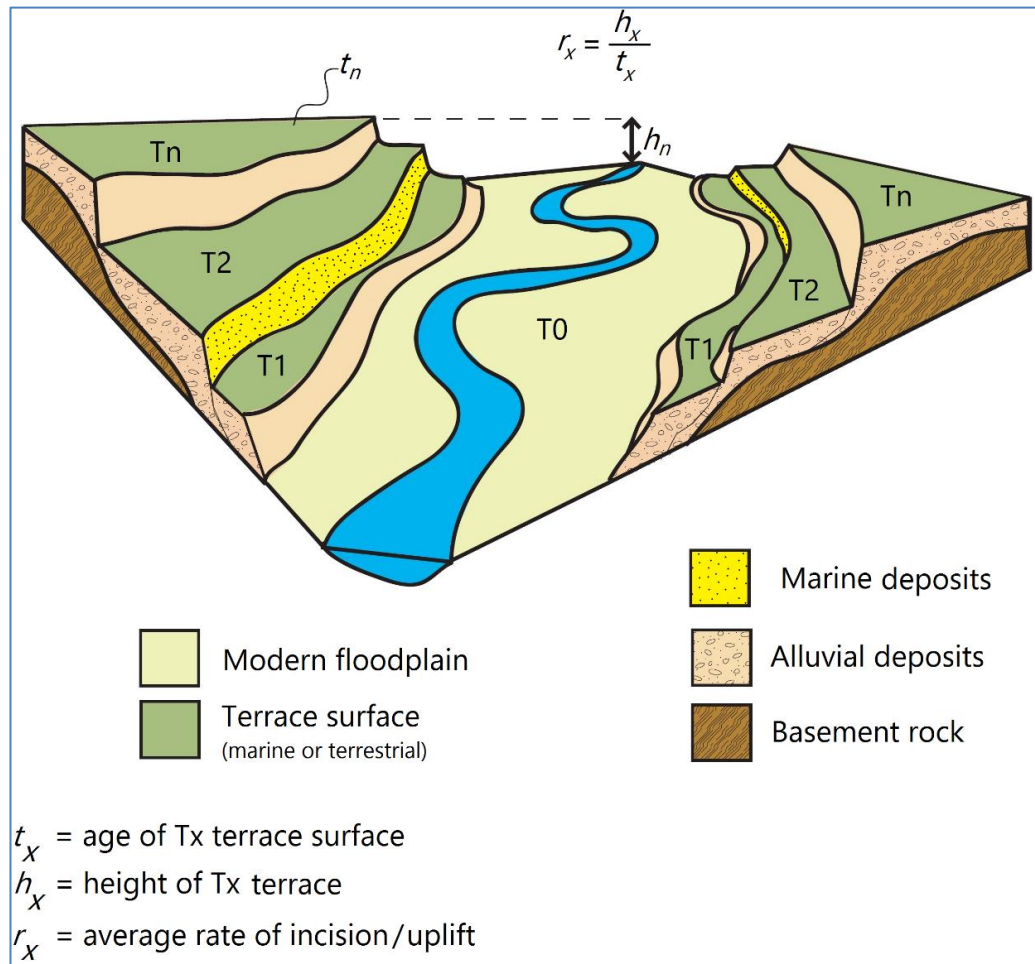


Figure 3–18. Method to calculate incision/uplift rates in deformed, terraced areas.

In the Wanganui Basin, the Paparangi Group (c. 3 Ma) lies uncomfortably on basement rock (Figure 3–19). This huge gap in the chronostratigraphical record reflects a long period of quiescence at the plate boundary extending from the cessation of transpressional activity at the plate boundary about 100 Ma ago until the inception of the Kaikoura Orogeny at the end of the Oligocene and Early Miocene (c. 25–20 Ma BP). This quiet period marks the opening of the Tasman Sea and the disintegration of the great Gondwanaland supercontinent. The transpressional activity that commenced at the start of the Kaikoura Orogeny at the plate boundary is continuing to the present day. Any deposition during that period

would subsequently have been eroded during the active period of the Kaikoura Orogeny. Hence, the earliest deposits found are 3 Ma, while the Kaikoura Orogeny started c. 25 Ma BP.

Possibly due to the mantle-driven crustal downwarping associated with renewed subduction at the plate margin 18 Ma ago, a marine basin developed in the Taranaki–Wanganui area (e.g. Kamp *et al.*, 2004). It was the locus of thick deposition, mostly siltstone and mudstone with minor sandstone interbeds, until it emerged from the sea within the last 700 ka (Begg *et al.*, 2005). Gradually, the centre of the basin migrated from the northwest to the southeast, again, possibly reflecting the onset and migration of subduction at the plate margin. South-eastward migration of the depocentre resulted in onlap of the basinal sequence to basement rocks at a progressively younger age from northwest to southeast. Deposition in the basin commenced in earnest in the Rangitikei area about 4–5 Ma ago. Basin eversion followed the migration of the depocentre, so the south-eastern part of the basin was last to emerge. Basinal deposits in the Manawatu and Horowhenua area represent the final gasp of onshore Wanganui Basin deposition (Begg *et al.*, 2005).

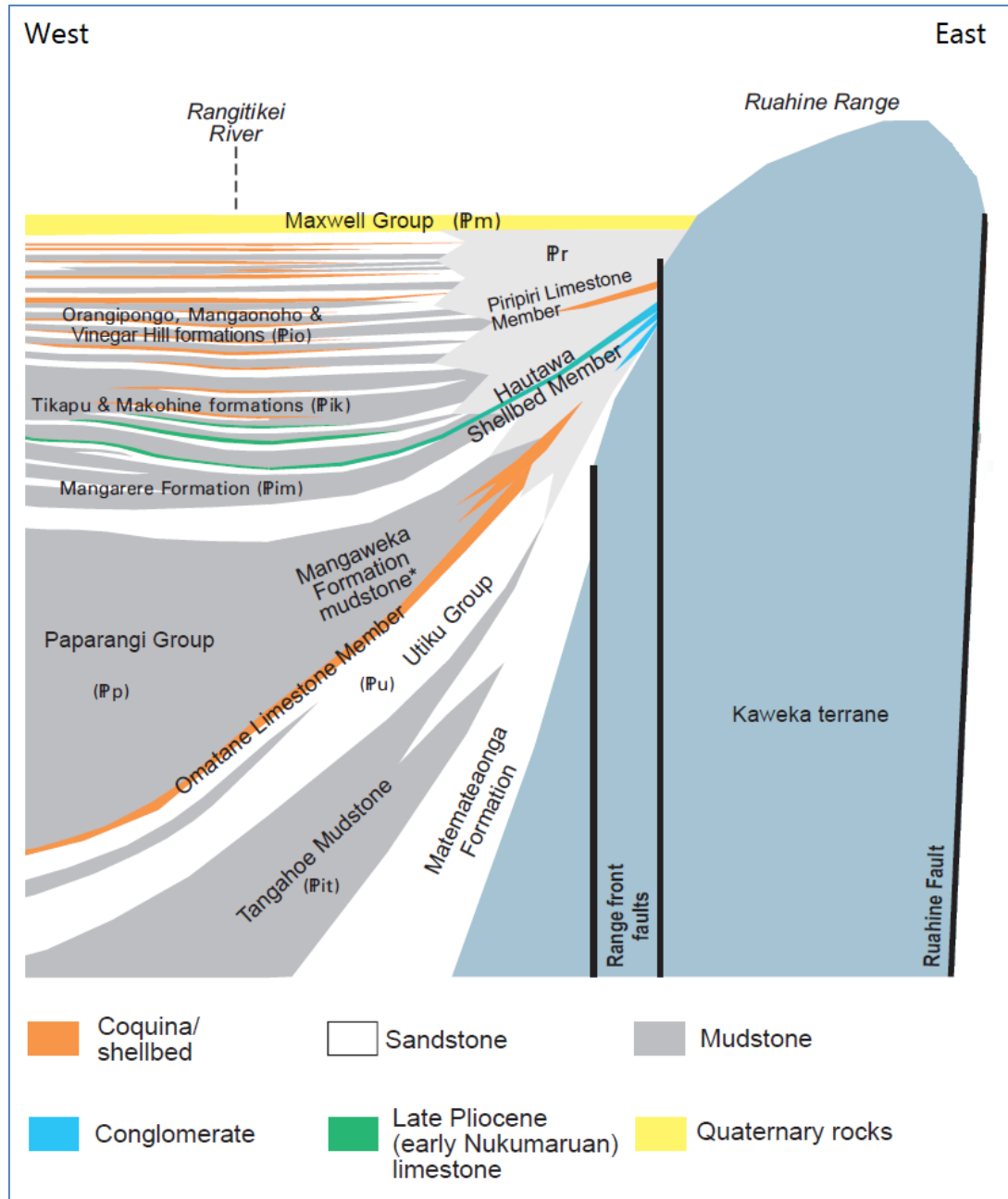


Figure 3–19. Schematic cross-section showing the relation between the Plio–Pleistocene sequence and basement rocks in the Wanganui Basin (after Lee *et al.*, 2011).

The LMC emerged from the sea before the start of the active reverse and strike-slip faulting on the large regional faults of the present day (e.g. the Wellington and Northern Ohariu faults), and also the faults and their associated folds of the Manawatu area. Commencement of uplift of the Tararua and Ruahine ranges was associated with the initiation of displacement on the Wellington Fault c. 1–1.5 Ma BP, and it seems likely that the Northern Ohariu Fault developed at

about the same time (Begg *et al.*, 2005). Uplift of the ranges and hills resulted in a large and increasing supply of greywacke cobbles from the developing catchment systems. There must have been a significant river system flowing from the northern and eastern hinterland to the residual Wanganui Basin prior to the commencement of uplift of the Tararua and Ruahine ranges to account for subsequent development of the Manawatu Gorge. The catchment size and volume of the water provided the power needed to incise into the growing range at a rate that could keep pace with its development. Quaternary age fluvial sediments sourced from the ranges were deposited in valleys and on the plains. Slow uplift and deformation have raised flights of marine and river terraces. Windblown river silt was deposited as loess on older deposits, particularly on older terraces and slopes. The Oroua and Pohangina catchments developed through the uplifted and tilted deposits of the Wanganui Basin, deeply dissecting the sediments through which their rivers flow. Evidence suggests that, at least in the east, stream capture is continuing.

Except for the remnant of the erosion surface above the Manawatu Gorge, the entire landscape of the region post-dates uplift from the sea <1–1.5 Ma BP. Younger Quaternary sequences have been deformed progressively by the processes associated with basinal uplift and active faulting since deposition (Begg *et al.*, 2005).

### 3.13 Soil

Although soil is merely a thin skin covering the land, it plays a very important role in the hydrological cycle. Largely, its physical and biological properties and moisture content determines the proportions of natural precipitation and irrigation waters that turn to evapotranspiration, surface runoff or groundwater recharge. Soils physical composition and properties also influence groundwater quality, directly and indirectly. Therefore, it needs to be included in this study.

Floodplain land in the LMC is amongst the most fertile areas in the south-western North Island of New Zealand. It forms a triangle of about 1,000 km<sup>2</sup> of low-lying land that extends between the northern Horowhenua around Levin in the south to

Marton in the north, to the Manawatu Gorge inland. Soils in this area are generally productive, and their fertility can be further enhanced with irrigation and fertilising (Zarour, 2008). Soil Orders and Groups in the LMC are mapped in Figure 3–20 and Figure 3–21, respectively using Fundamental Soil Layers (FSLs) digital data by Landcare Research (Hewitt, 2010). Table 3–6 summarises LMC soil properties based on the New Zealand Soil Classification (NZSC).

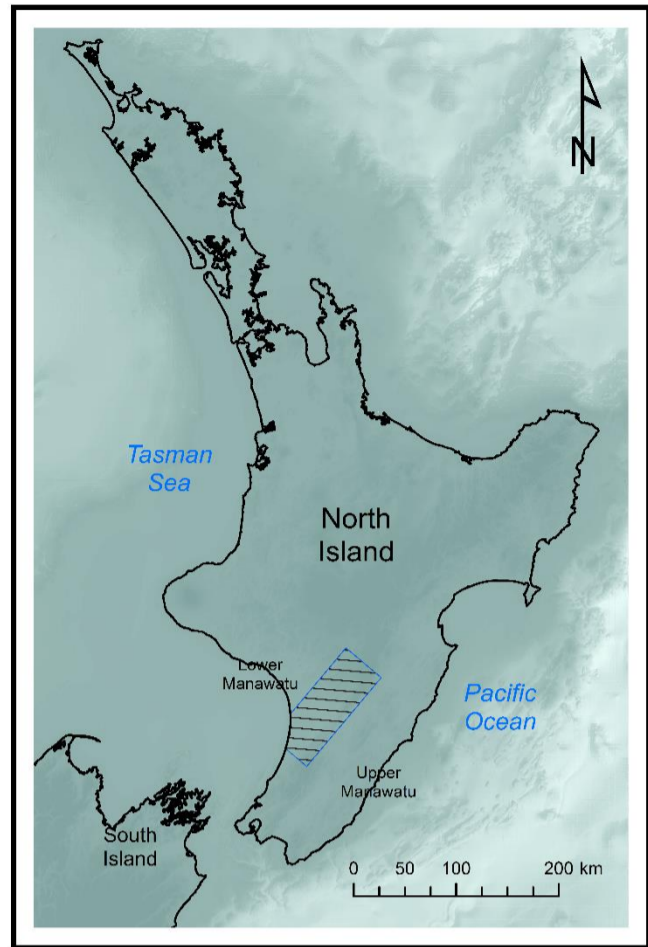
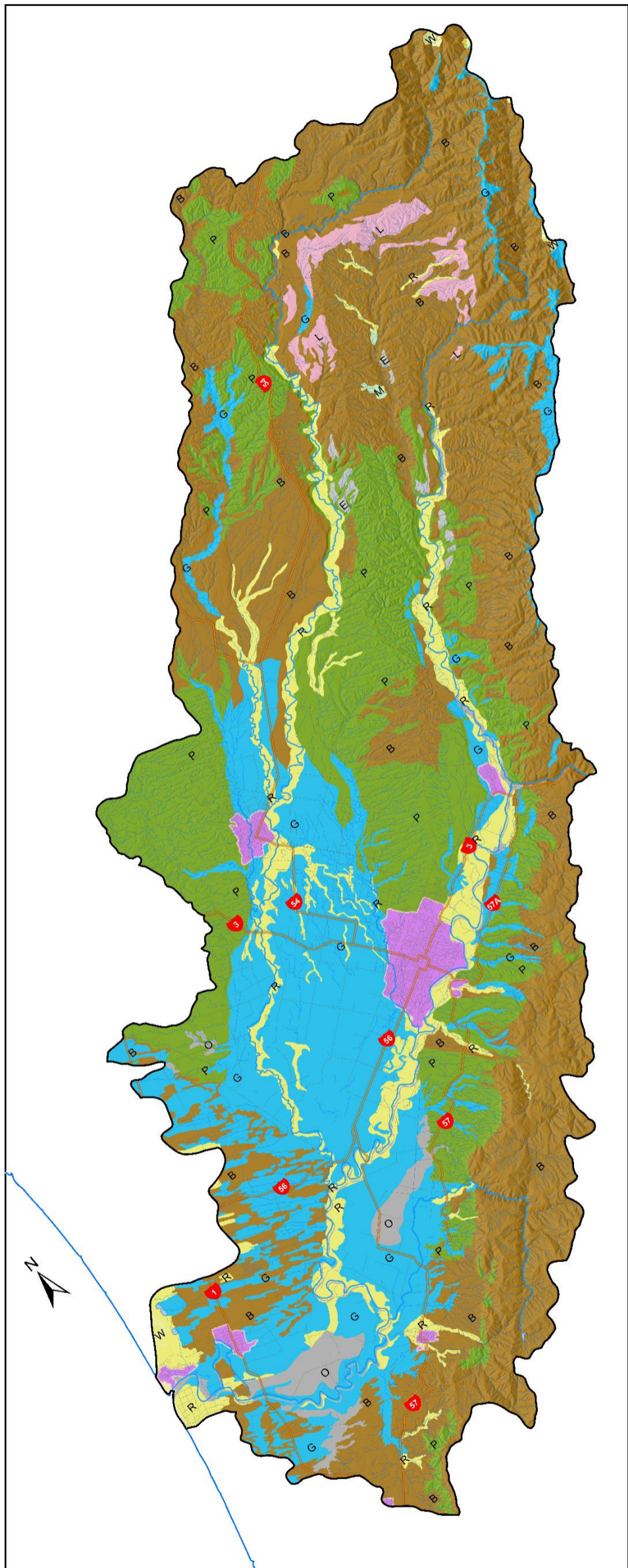
The LMC is covered by sandy soils and swampy hollows around the coast with river flats and loess-covered terraces farther inland. River flats and swamp areas contain fertile alluvial and organic soils (Recent and Gley soils, respectively). The floodplains also contain areas covered by Organic Soils. Areas covered by Gley and Recent soils have low surface water drainage network density reflecting their high permeability (Figure 3–15 and Figure 3–21). Brown soils covering sand dunes have lower permeability and, consequently, higher surface water drainage network density. The flat fertile soils suit intensive cropping, dairy and sheep farming while the hill country favours only sheep and beef farming. The characteristic pale straw (yellow–grey) coloured subsoils of Pallic Soils predominate on the drier terraces inland. These soils have hard, brittle fragipans that form where annual rainfall is between 500 and 1,000 mm. Multiple loess sheets cover these terraces (Table 3–7), greatly reducing their infiltration capacity (Table 3–8). Fragipan in loessial soils severely restricts land–surface recharge and the depth of plant rooting (Poulsen, 2013).

Pallic Soils are normally dry for part of the growing season, especially summer to mid–autumn and have limited uses (mostly sheep grazing) because the subsoil is dense. Roots cannot penetrate to deeply buried moisture, so the soil becomes even drier. Some younger Pallic soils are not so dense and have a range of agricultural uses. Although dry in summer, the soil can be wet in winter or spring. When saturated, they instigate high rates of surface runoff.

Brown Soils cover 43.65% of LMC area, nearly the same proportion as the national coverage. They occur in places where summer drought is uncommon and that are

not waterlogged in winter. They are found mainly in elevated rugged areas in the LMC (Figure 3–14 and Figure 3–20), which normally receive more than 1,000 mm of precipitation per year. These soils are often well drained (Houlbrooke & Monaghan, 2009).

Areas close to the volcanic plateau consist largely of Allophanic Soils, which lack some essential trace elements.



**LOWER MANAWATU CATCHMENT  
FUNDAMENTAL SOIL LAYERS  
NEW ZEALAND  
SOIL CLASSIFICATION ORDERS**

**Legend**

- |                    |              |
|--------------------|--------------|
| Catchment boundary | Stream/creek |
| Coastline          | Highway      |
| River              | Road         |
| Lake               | Town         |

**NZSC Order**

- Allophanic Soils [L]
- Brown Soils [B]
- Gley Soils [G]
- Melanic Soils [E]
- Organic Soils [O]
- Pallic Soils [P]
- Pumice Soils [M]
- Raw Soils [W]
- Recent Soils [R]

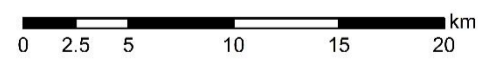


Figure 3–20. Soil classification orders in the LMC drawn using Fundamental Soil Layers (FSLs) digital data by Landcare Research (Hewitt, 2010).

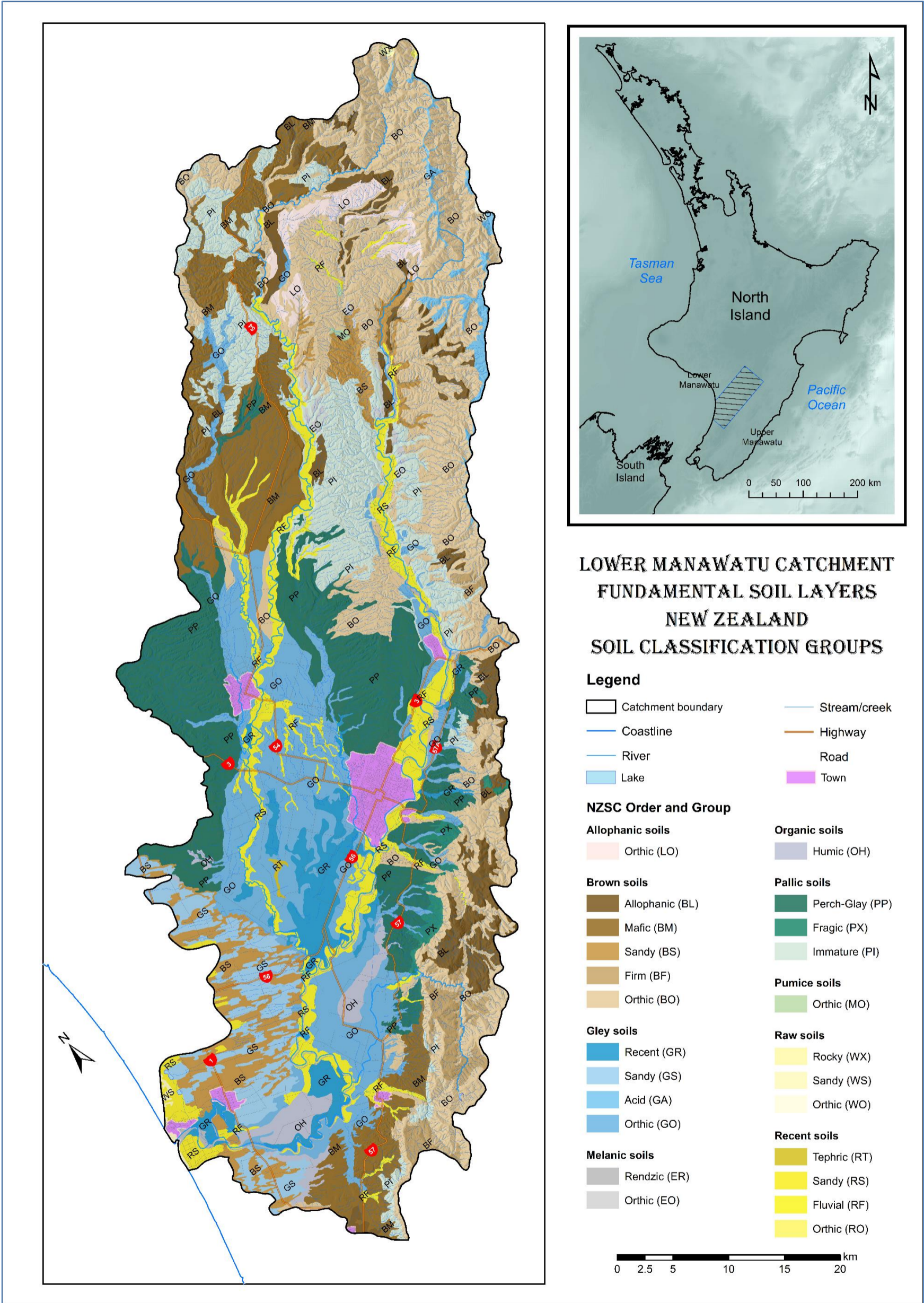


Figure 3-21. Soil classification groups in the LMC drawn using Fundamental Soil Layers (FSLs) digital data by Landcare Research (Hewitt, 2010).

Table 3-6. Soil Orders and Groups in the LMC.

Soil Order	General description	Characteristics	Soil Groups in LMC
<b>Allophanic Soils [L]</b> 37.45 km <sup>2</sup> 1.40% of LMC area	<p>Occur predominantly in the North Island volcanic ash, and in the weathering products of other volcanic rocks.</p> <p>Dominated by allophane with imogolite or ferrihydrite. These stiff, jelly-like minerals coat the sand and silt grains and maintain porous, low density structure with weak strength.</p> <p>Identified by a distinctly greasy feel when moistened and rubbed firmly between the fingers. Easy to dig and samples crumble easily when crushed in the hand.</p>	<p>Little resistance to root growth due to low bulk density. Topsoils are stable and resist the impact of machinery or grazing animals in wet weather. Erosion rates are generally low except on steep slopes or exposed sites.</p> <p>Low natural fertility. The ability to retain phosphorous is high – up to 30 tonnes/ha of phosphorous may be locked away in intensively farmed topsoils.</p> <p>Contain large populations of soil organisms, particularly in A horizons.</p>	<b>Orthic Allophanic [LO]:</b> other Allophanic Soils.
<b>Brown Soils [B]</b> 1,169.10 km <sup>2</sup> 43.65% of LMC area	<p>New Zealand's most extensive soils, covering 43% of the country. Occur in places where summer drought is uncommon and that are not waterlogged in winter.</p> <p>Have a brown or yellow-brown subsoil below a dark grey-brown topsoil. The brown colour is caused by thin coatings of iron oxides weathered from the parent material.</p>	<p>Relatively stable topsoils with well-developed polyhedral or spheroidal structure.</p> <p>Have low to moderate base saturation. Clay minerals are dominantly mica/illite and vermiculite, with allophane in Allophanic Brown Soils.</p> <p>Contain large, active populations of soil organisms, particularly earthworms.</p>	<p><b>Allophanic Brown [BL]:</b> have a horizon with soil properties dominated by allophanic material.</p> <p><b>Mafic Brown [BM]:</b> in materials from dark igneous rocks or sediments.</p> <p><b>Sandy Brown [BS]:</b> dominated by sand or loamy sand to depth.</p> <p><b>Firm Brown [BF]:</b> strong, apedal subsurface horizon.</p> <p><b>Orthic Brown [BO]:</b> other Brown Soils.</p>
<b>Gley Soils [G]</b> 560.86 km <sup>2</sup> 20.94% of LMC area	<p>Occur in low parts of the landscape where the water table is high or where there are seepages. Together with Organic Soils, they represent the original extent of New Zealand wetlands, which have been greatly restricted in area by artificially drainage to form productive agricultural land.</p> <p>Gley Soils are strongly affected by waterlogging and have been chemically reduced. They have light grey subsoils, usually with reddish brown or brown mottles. The grey colours usually extend to more than 90 cm depth. Waterlogging occurs in winter and spring, and some soils remain wet all year.</p>	<p>These soils have high water tables, shallow potential rooting depth and relatively high bulk density. Trafficability is limited when soils are wet. Drainage is necessary for most agricultural development.</p> <p>Have common segregated iron and manganese oxide mottles, concretions or nodules. Organic matter content is usually high.</p> <p>Many soil organisms are restricted because of anaerobic conditions.</p>	<p><b>Recent Gley [GR]:</b> on young land surfaces, mainly alluvial or estuarine.</p> <p><b>Sandy Gley [GS]:</b> dominated by sand or loamy sand to depth.</p> <p><b>Acid Gley [GA]:</b> strongly or extremely acid.</p> <p><b>Orthic Gley [GO]:</b> other Grey Soils.</p>
<b>Melanic Soils [E]</b> 7.43 km <sup>2</sup> 0.28 % of LMC area	<p>Occupy scattered small areas, associated with lime-rich rocks or dark (basic) volcanic rocks. Arguably the most naturally fertile soils in New Zealand. They grow high quality pinot noir.</p> <p>Characterised by well-structured black or dark grey topsoils. The subsoil either contains lime, or has well-developed structure and is neutral or only slightly acid.</p>	<p>Topsoil structure is usually stable. The soils shrink on drying and swell on wetting.</p> <p>High natural fertility. High base saturation with high exchangeable calcium or magnesium. The clay fraction is usually dominated by swelling (smectite) clays.</p> <p>Biologically very active with high populations of soil organisms.</p>	<p><b>Rendzic Melanic [ER]:</b> limestone or lime rich rock at shallow depth.</p> <p><b>Orthic Melanic [EO]:</b> other Melanic Soils.</p>

Soil Order	General description	Characteristics	Soil Groups in LMC
<b>Organic Soils [O]</b> 39.36 km <sup>2</sup> 1.47% of LMC area	<p>Occur in wetlands or under forests that produce acid litter in areas with high precipitation. They are formed in the partly decomposed remains of wetland plants (peat) or forest litter. Some mineral material may be present but the soil is dominated by organic matter.</p> <p>They serving as giant sponges in the landscape with the ability to hold up to 20 times their weight in water.</p>	<p>Very low bulk densities, low bearing strength, high shrinkage potential when dried, very low thermal conductivity and high total available-water capacity.</p> <p>High cation exchange capacities. Usually strongly or extremely acidic and nutrient deficiencies are common.</p> <p>High carbon/nitrogen ratios indicate slow decomposition rates. Many soil organisms are restricted because of anaerobic conditions.</p>	<b>Humic Organic [OH]:</b> in peat that is strongly decomposed.
<b>Pallic Soils [P]</b> 587.82 km <sup>2</sup> 21.95% of LMC area	<p>Predominantly occur in the seasonally dry eastern part of the North and South Islands and in the Manawatu where annual precipitation usually between 500 and 1,000 mm and the climate is typically droughty in summer and moist or wet in winter.</p> <p>Parent materials are commonly loess derived from greywacke.</p> <p>Have pale coloured subsoils, due to low contents of iron oxides. Weak structure and high density in subsurface horizons. Dry in summer and wet in winter.</p>	<p>Slow permeability with limited rooting depth, and medium to high bulk density. A cubic metre of some subsoils can weigh more than 1.8 tonnes. They are susceptible to erosion because of high potential for slaking and dispersion.</p> <p>Medium to high nutrient content (except for sulphur), high base saturation, low concentrations of secondary oxides, and low organic matter contents.</p> <p>Strongly worm-mixed, at the boundary of the A and B horizons.</p>	<p><b>Perch-Gley Pallic [PP]:</b> periodic wetness caused by a perched water table.</p> <p><b>Fragic Pallic [PX]:</b> a compact pan in the subsoil.</p> <p><b>Immature Pallic [PI]:</b> weakly expressed pallic soil features.</p>
<b>Pumice Soils [M]</b> 1.55 km <sup>2</sup> 0.06% of LMC area	<p>Predominantly occur in the central North Island, particularly in the Volcanic Plateau. Mostly derived from one of the greatest volcanic eruptions ever known from the crater now occupied by Lake Taupo.</p> <p>Sandy or gravelly soils dominated by pumice, or pumice sand with high content of natural glass. Drainage of excess water is rapid but the soils are capable of storing large amounts of water for plants. They occur in tephra ranging from 700 to 3,500 years old.</p>	<p>Low clay contents, generally less than 10%. Low soil strengths, especially when disturbed. High macroporosity and deep rooting depth.</p> <p>Fresh or only moderately weathered pumice with low reserves of major nutrient elements. Trace elements are likely to be deficient. Clay minerals are dominated by allophane.</p> <p>Soil animal populations are low with most species concentrated in the topsoil. Earthworm populations are limited by droughtiness and coarse texture.</p>	<b>Orthic Pumice [MO]:</b> other Pumice Soils.

Soil Order	General description	Characteristics	Soil Groups in LMC
<p><b>Raw Soils [W]</b> 4.10 km<sup>2</sup> 0.15% of LMC area</p>	<p>Raw Soils are scattered throughout New Zealand, particularly in association with high mountains (alpine rock areas and active screes), braided rivers, beaches and tidal estuaries. They cover 3% of New Zealand.</p> <p>Infant soils that may never grow older because of active erosion or sedimentation.</p> <p>Raw Soils are very young soils. They lack distinct topsoil development or are fluid at a shallow depth. They occur in environments where the development of topsoils is prevented by rockiness, by active erosion, or deposition.</p>	<p><b>PHYSICAL PROPERTIES:</b> Raw Soils have no B horizon, and a topsoil is either absent or less than 5 cm thick. Most occur in environments with active erosion or deposition. Fluid soils have a continuously high water-table.</p> <p><b>CHEMICAL PROPERTIES:</b> Fertility is limited by lack of organic matter and nitrogen deficiency.</p> <p><b>BIOLOGICAL PROPERTIES:</b> Vegetation cover is sparse and often consists of ephemeral herbaceous plants, mosses, or lichens.</p>	<p><b>Rocky Raw [WX]:</b> rock at shallow depths. <b>Sandy Raw [WS]:</b> dominated by sand or loamy sand to depth. <b>Orthic Raw [WO]:</b> other Raw Soils.</p>
<p><b>Recent Soils [R]</b> 201.83 km<sup>2</sup> 7.54% of LMC area</p>	<p>Occur on young land surfaces, including alluvial floodplains, unstable steep slopes and slopes mantled by young volcanic ash. Age varies depending on the environment and soil materials, but most are less than 1,000 to 2,000 years old.</p> <p>Weakly developed, showing limited signs of soil-forming processes. A distinct topsoil is present but a B horizon is either absent or only weakly expressed.</p>	<p>Variable texture, with common stratification of contrasting materials and high spatial variability. Generally deep rooting and high plant-available water capacity.</p> <p>Natural fertility is usually high with high base saturation. Clay mineralogy usually dominated by illite.</p> <p>Normally well-established continuous cover of vascular plants.</p>	<p><b>Tephric Recent [RT]:</b> in sediments originating as volcanic ejecta. <b>Sandy Recent [RS]:</b> dominated by sand or loamy sand to depth. <b>Fluvial Recent [RF]:</b> in sediments deposited by flowing water. <b>Orthic Recent [RO]:</b> other Recent Soils.</p>

Table 3–7. Quaternary terraces ages, names and loess cover in the LMC (after Begg *et al.*, 2005).

OIS	Relative age	Absolute age (ka)	Terrace name	Number of loess sheets
1	Holocene	0–12	Unnamed	–
2	Late Otiran Glacial	12–25	Ohakea	–
3	Middle Otiran Glacial	25–60	Rata	1
4	Early Otiran Glacial	60–71	Porewa	2
5	Kaihinu Interglacial	71–128	Tokomaru	3
6	Waimea Glacial	128–186	Greatford/Marton	3
8	Waimaunga Glacial	245–303	Burnand	4
9	Brunswick/Braemore Interglacial	303–339	Brunswick/Braemore	5
10	Unnamed	339–362	Aldworth/Waituna	5
11	Ararata/Rangitatau Interglacial	362–423	Ararata/Rangitatau	6
13	Ball Interglacial	478–524	Ball	7
15	Piri Interglacial	565–620	Piri	8

Table 3–8. General order of magnitude for saturated hydraulic conductivity for soil horizons in loessial soils (after Poulsen, 2013).

Soil horizon	Saturated hydraulic conductivity (m/d)	
	infiltration tests	cores lab testing
A horizon	$10^0 - 10^{-1}$	
B horizon	$10^{-1} - 10^{-2}$	$10^{-4} - 10^{-5}$
Fragipan	$10^{-3} - 10^{-4}$	$10^{-5} - 10^{-6}$
Loess	similar to or slightly higher than fragipan	

## Chapter 4 Climate, soil moisture and groundwater recharge

### 4.1 Introduction

Water enters the LMC only in the form of atmospheric precipitation and surface flow through the Manawatu Gorge. This chapter is aimed at the conceptualisation and quantification of groundwater recharge from precipitation and irrigation returns. As a by-product, the calculations produced estimates of soil moisture content, actual evapotranspiration, irrigation water demand and surface runoff. Groundwater interaction with surface water in the LMC is discussed in Chapter 5.

### 4.2 Pathway of precipitation water

Water reaching the ground surface in the form of precipitation and/or irrigation is proportioned according to Eq. 4-1. Figure 4-1 schematically shows this part of the hydrological cycle and subsurface hydrological zones.

$$P + IR = R_o + ET + DP + \Delta S \quad 4-1$$

where  $P$  is precipitation,  $IR$  irrigation,  $R_o$  surface runoff,  $ET$  evapotranspiration,  $DP$  deep percolation and  $\Delta S$  change in soil water storage. Deep percolation of soil water below the root zone forms groundwater recharge ( $RCH$ ).

Eq. 4-1 and Figure 4-1 assume that  $DP$  water can freely drain from the soil profile into the underlying permeable geology to recharge groundwater. Where the underlying geology is impermeable, groundwater recharge is assumed not to be able to occur. In addition, it is assumed that there is no upward groundwater seepage into the soil zone, no preferential flow paths and no lateral soil water movement. Notwithstanding, rising water table has been noted in places in the LMC and there is potential for preferential and lateral soil moisture movement. However, these phenomena can generally be ignored in regional-scale hydrogeological assessments and models.

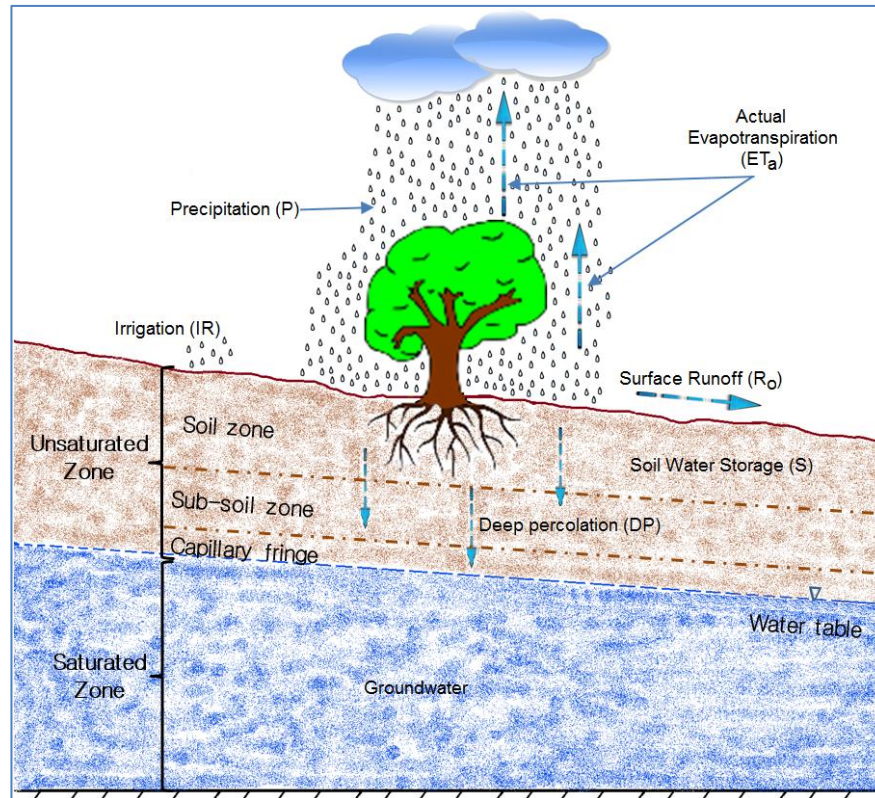


Figure 4-1. Schematic diagram showing the apportionment of precipitation and/or irrigation water reaching the ground surface.

According to Kim and Mohanty (2016), lateral moisture transfers are fairly marginal in regional-scale soil water budgets and, consequently, they are commonly ignored at the grid- and subgrid- scales, effectively resulting in modelling soil moisture exchanges as a 1D process. Hardie (2011) clarifies that preferential water flow in soil can take place due to the presence of: (1) continuous root channels, earthworm burrows, fissures or cracks within well-structured soils (macropores), (2) instabilities in the wetting front develop due to water repellence or air entrapment (unstable flow or fingering), (3) textural or lithographical boundaries resulting in lateral redirection or funnelling of infiltration via pathways of least resistance, bypassing the less permeable zones (funnel flow or heterogeneity-driven flow), (4) depression focused recharge, and (5) oscillatory flow. Preferential and lateral water flows in soil are ignored in this research as they occur at much finer scales than what can be analysed using the available low resolution soil and climate data (Sections 3.3.4 and 4.5, respectively) and their analysis requires much

higher resolution than that of the 500x500 m grid used in the numerical groundwater flow models (Section 8.5.2).

### 4.3 Soil moisture

#### 4.3.1 Conditions and definitions

The fate of precipitation water depends on climate conditions, soil saturation level and land use and cover, including plant types, rooting depth and growth level. Figure 4–2 schematically shows various possible soil moisture scenarios and corresponding plant and hydrological conditions.



Figure 4–2. Possible soil moisture conditions, corresponding plant and hydrological conditions.

Terminology used in Figure 4–2 and soil sciences literature in general includes:

- Field Capacity (FC), also known as ‘Full Point’, is the level of moisture in the soil after excess water has drained away. This implies that above FC, deep percolation (groundwater recharge) can take place.
- Permanent Wilting Point (PWP) is the minimal level of soil moisture the plant requires not to wilt. Below this point, plants wilt and cease to grow.
- Stress Point (SP), also known as ‘Refill Point’, is the soil moisture level at which plant roots cannot extract water at the rate they require, subjecting the plant to 'stress'. It occurs approximately half way between FC and PWP.
- Readily Available Water (RAW), otherwise known as ‘Growth Water’ and termed in New Zealand Profile Readily Available Water (PRAW), is soil water that is easily available for plants to use. It corresponds to the soil moisture range between FC and SP.
- Total Available Water (TAW), otherwise known as ‘Survival Water’ and termed in New Zealand Profile Available Water (PAW), is the soil moisture range between FC and PWP.
- Soil Moisture Deficit (SMD) is the amount of moisture required to return the soil moisture to FC.

Soil grain–size (texture) and particle arrangement (structure) play a vital role in determining soil hydraulic properties because soil TAW is determined by the capillary porosity. Soil stone, clay and organic matter content also affect its moisture storage ability. In addition, the amount of soil water available to plants depends on the depth of soil that roots can exploit (the root zone). The root zone for various plants is not the same. Figure 4–3 shows the relationship between soil texture and soil hydraulic properties.

#### 4.3.2 Influence over evapotranspiration

Evapotranspiration is possible as long as the soil moisture content (SMC) is above the PWP level. When soil moisture drops below the SP level, evapotranspiration occurs at depleted rates. A dimensionless water stress coefficient ( $K_s$ ) is defined to express evapotranspiration reduction depending on available soil water. Where SMC is at or above the SP level,  $K_s$  equals 1. It drops linearly from 1 to 0 between the SP and the PWP levels (Figure 4–4).

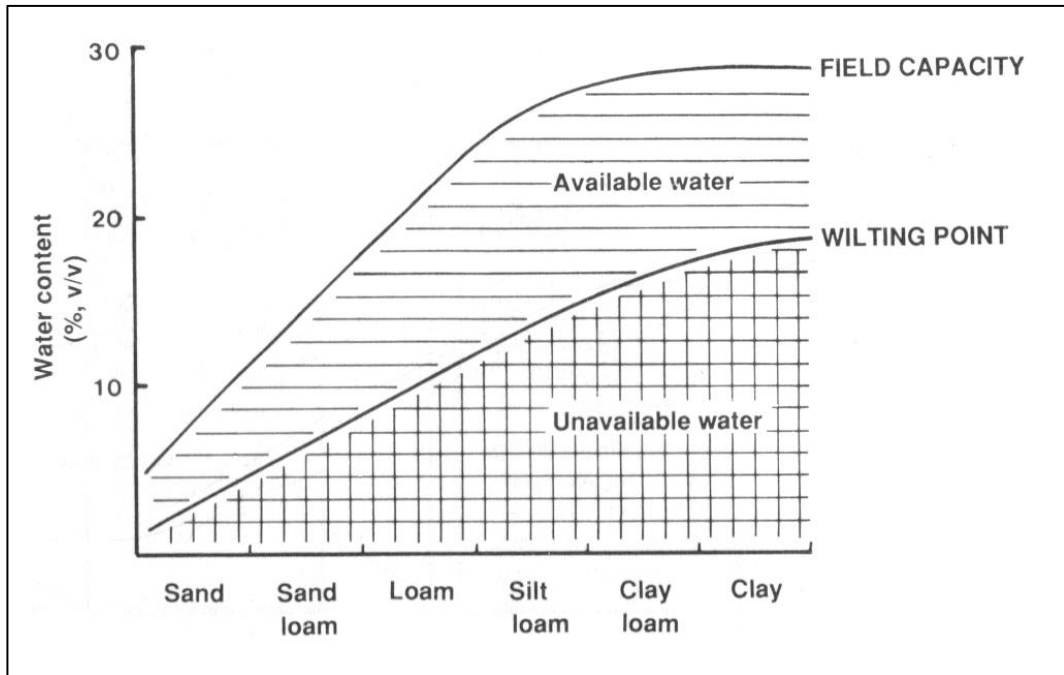


Figure 4-3. Schematic diagram showing relationship between soil texture, field capacity (FC), permanent wilting point (PWP) and total available water (TAW) (after McLaren & Cameron, 1996).

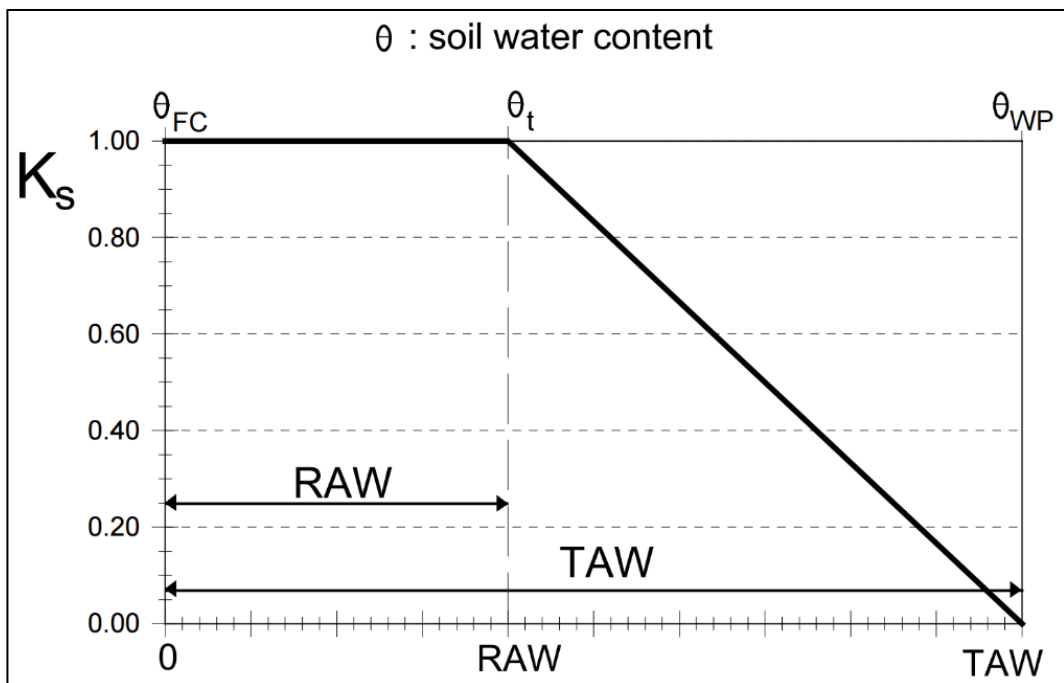


Figure 4-4. Water stress coefficient ( $K_s$ ) under various soil moisture conditions (after Allen *et al.*, 1998).

### 4.3.3 Influence over surface water runoff

Surface runoff ( $R_o$ ) is the portion of precipitation (rain and/or irrigation water) that appears as flowing water in the surface drainage network of a watershed during and following a rainfall event (Mekonnen *et al.*, 2016). It is determined by many factors including storm characteristics, antecedent SMC, watershed geography, soil physical properties (depth, thickness, texture, structure), land cover and land use. It only occurs when the water reaching the ground surface cannot infiltrate into the soil at a rate equal to or greater than rainfall intensity. Soil infiltration rate is controlled by three parameters:

- (1) Soil texture – infiltration rate is higher for coarse textured soils than for fine textured soils
- (2) Soil structure – water infiltrates faster in granular soils but very slowly into massive soils, especially clay-rich compact varieties
- (3) Soil moisture content – water infiltration rate is higher when the soil is dry than when it is wet, except for hydrophobic soils (e.g. peat and sand).

Despite their importance, soil texture and structure will not be considered explicitly in this research as factors controlling surface runoff. They are implicitly included in soils hydraulic characteristics, namely FC and WP.

Figure 4–2 assumes that runoff can only take place when the soil is fully saturated. Precipitation on impervious surfaces like greywacke basement outcrops and sealed built-up areas will also turn into surface runoff after satisfying evapotranspiration demand. In general, surface runoff will take place where the intensity of effective rainfall<sup>20</sup> exceeds the soil infiltration capacity. Rainfall intensity data are not available for the LMC, so infiltration rates and storm characteristics have not been included in runoff estimations.

---

<sup>20</sup> Effective rainfall is rainfall less evapotranspiration.

#### 4.3.4 Influence over groundwater recharge

Figure 4–2 assumes that deep drainage (groundwater recharge) occurs only when SMC exceeds soil FC. In reality, however, deep drainage can take place even when soil moisture content is below FC through bypass flow. This prospect is nearly impossible to specifically account for in regional–scale studies and is arguably more important in rocky aquifers than in unconsolidated aquifers like the system in the LMC. Hence, bypass groundwater recharge is disregarded in this thesis.

#### 4.3.5 Modelling

Soil moisture balance (SMB) models utilise the concepts presented in Eq. 4–1, Figure 4–1 and Figure 4–2 to represent the soil component of the hydrological cycle for a variety of purposes, including calculating crop water demand and estimating catchment water yield. SMB modelling has been regularly utilised to calculate groundwater recharge (e.g. Bekesi & McConchie, 1999; de Silva & Rushton, 2007; Rushton, 2003; Rushton *et al.*, 2006; Scott, 2004; Wilson & Lu, 2011). For groundwater recharge calculations, Eq. 4–1 can be rewritten as follow:

$$RCH = P + IR - ET - R_o + \Delta S \quad 4-2$$

Calculating groundwater recharge by SMB modelling requires knowledge on the soil moisture content (SMC) antecedent state, rain, potential evapotranspiration, land cover (including land use and crop type), soil hydraulic properties and irrigation practices. The soil water budget can be balanced at any term, e.g. daily, 10–daily, monthly, quarterly or yearly. The smaller the modelling time step the more ‘accurate’ the balance.

### 4.4 Potential and actual evapotranspiration

Water is lost from land and water surfaces to atmosphere through evaporation and transpiration, collectively termed evapotranspiration (*ET*) because they co–occur. Evaporation is the process where liquid water is converted to water vapour and removed from sources such as open water, soil surface, wet vegetation, pavement, etc. Transpiration consists of the vaporisation of liquid water within a plant and subsequent loss of water as vapour through leaf stomata.

Potential evapotranspiration ( $ET_p$ ) is a measure of the possibility for water to escape from earthy surfaces (soil, shallow water, plants, etc.) to the atmosphere through the processes of evaporation and transpiration under no water supply limitations. Actual evapotranspiration ( $ET_a$ ) is a measure of the quantity of water that is actually removed from the earth cover surfaces to the atmosphere due to evaporation and transpiration. Water availability for the processes of evapotranspiration determine how much of the  $ET_p$  is realised. Potential evapotranspiration is also known as crop reference evapotranspiration ( $ET_0$ ). It is an essential parameter to estimate crop water demand and defining drought and aridity. Clearly,  $ET_a$  cannot be greater than  $ET_p$ .

It is nearly impossible to directly measure evapotranspiration (Eagleman, 1967). Therefore, empirical methods and equations have been developed to estimate  $ET_p$  and  $ET_a$ .

There are many variations of the well-known Penman (1956) equation for the estimation of  $ET_p$ . Currently, the most used is the FAO Penman–Monteith equation (Allen *et al.*, 1998):

$$ET_p = \frac{0.408\Delta(R_n - G) + \gamma \frac{900}{T + 273} u_2 (e_s - e_a)}{\Delta + \gamma(1 + 0.34u_2)} \quad 4-3$$

where

- $ET_p$ : reference evapotranspiration [ $\text{mm day}^{-1}$ ]
- $R_n$ : net radiation at the crop surface [ $\text{MJ m}^{-2} \text{day}^{-1}$ ]
- $G$ : soil heat flux density [ $\text{MJ m}^{-2} \text{day}^{-1}$ ]
- $T$ : mean daily air temperature at 2 m height [ $^{\circ}\text{C}$ ]
- $u_2$ : wind speed at 2 m height [ $\text{m s}^{-1}$ ]
- $e_s$ : saturation vapour pressure [kPa]
- $e_a$ : actual vapour pressure [kPa]
- $e_s - e_a$ : saturation vapour pressure deficit [kPa]
- $\Delta$ : slope vapour pressure curve [ $\text{kPa } ^{\circ}\text{C}^{-1}$ ]
- $\gamma$ : psychrometric constant [ $\text{kPa } ^{\circ}\text{C}^{-1}$ ]

As can be deduced from Eq. 4-3, evapotranspiration processes depend on solar radiation, air temperature, relative humidity and wind speed (Zotarelli *et al.*, 2015). Energy received from the sun accounts for nearly 80% of the variation in potential

evapotranspiration. The second most important factor influencing potential evapotranspiration is wind, which enables the removal of water molecules from the earth cover surface into the atmosphere.

$ET_p$  provides a standard to which evapotranspiration at different periods and/or areas can be compared and a reference value from which evapotranspiration of various crops can be calculated as it represents grass  $ET_o$ . Crop evapotranspiration ( $ET_c$ ) is calculated by multiplying  $ET_p$  by a suitable crop coefficient ( $K_c$ ). Variations of  $K_c$  account for various cropping conditions including type, growth, soil moisture and management practices.

## 4.5 Climatic data availability

### 4.5.1 Monitoring network

Long-term climatological records are available for Palmerston North city from two stations: (1) Palmerston North Aws which was discontinued after 31/05/2001, and (2) Palmerston North Ews which was commissioned on 1/04/2001. NIWA numbers and location information for these two climatic stations are provided in (Table 4–1). The new Station is located c. 6.35 km to the south east of the old station (Figure 4–5).

Table 4–1. Palmerston North climatic stations.

Name	Agent number	Network number	Latitude (dec.deg)	Longitude (dec.deg)	Height (masl)
Palmerston North Aws	3243	E05368	-40.325	175.611	39
Palmerston North Ews	21963	E0536D	-40.38195	175.60915	21

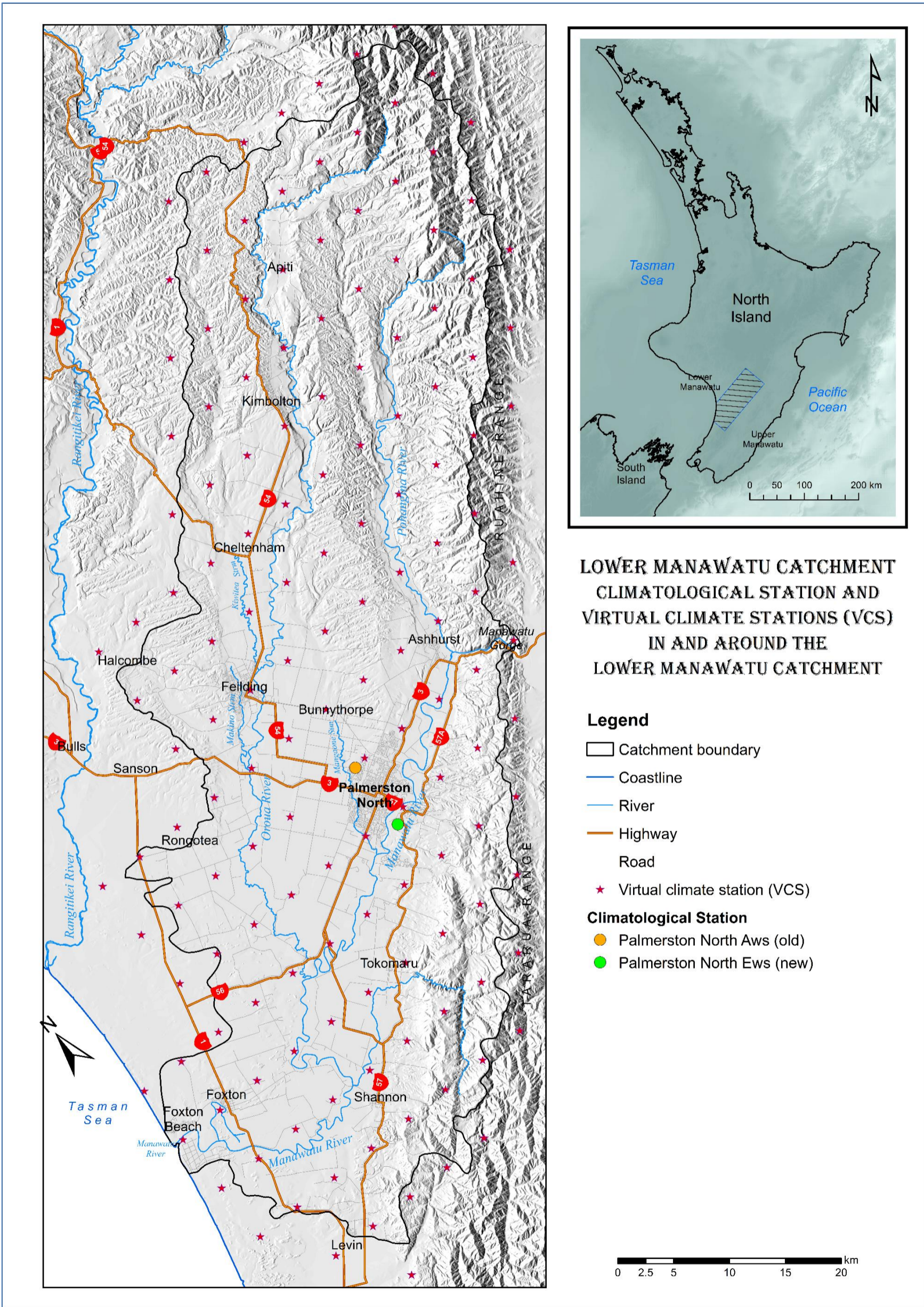


Figure 4-5. Climatic and virtual climatic stations in and near the LMC.

Palmerston North Aws and Ews climatic stations coincided for two months (April – May 2001). During the overlap period, daily rainfall reported for the two stations slightly differs (Table 4–2). The old station recorded 6.5 mm of rain less than the new station, which is mostly related to rain on 12/04/2001. In May 2001, however, the old station recorded 11.9 mm of rain more than the new station. The old station recorded 5.4 mm of rain more than the new station over the overlap period. On 22/05/2001, both stations recorded the same amount of rainfall, 1.2 mm.

Table 4–2. Reported daily rainfall for stations Palmerston North Aws (old) and Palmerston North Ews (new) during their co-operating period.

Date	New	Old	Dif.
2/04/2001	5.6	6.7	-1.1
10/04/2001	0.1	0.0	0.1
12/04/2001	22.7	12.2	10.5
13/04/2001	14.2	15.3	-1.1
20/04/2001	0.4	1.5	-1.1
21/04/2001	9.4	10.2	-0.8
2/05/2001	22.2	23.2	-1.0
3/05/2001	0.0	0.3	-0.3
4/05/2001	0.0	0.1	-0.1

Date	New	Old	Dif.
5/05/2001	0.4	0.7	-0.3
6/05/2001	1.2	1.8	-0.6
7/05/2001	2.0	2.6	-0.6
8/05/2001	0.4	0.5	-0.1
10/05/2001	2.8	3.1	-0.3
12/05/2001	0.0	0.3	-0.3
13/05/2001	4.6	5.2	-0.6
14/05/2001	3.8	4.4	-0.6
15/05/2001	0.2	0.1	0.1

Date	New	Old	Dif.
17/05/2001	1.0	1.6	-0.6
18/05/2001	31.8	35.5	-3.7
19/05/2001	3.2	2.0	1.2
20/05/2001	22.2	24.3	-2.1
21/05/2001	1.6	1.9	-0.3
23/05/2001	7.2	7.5	-0.3
24/05/2001	18.0	18.7	-0.7
25/05/2001	14.6	15.5	-0.9
27/05/2001	0.2	0.0	0.2

#### 4.5.2 Virtual climate stations

NIWA calculates estimates of daily rainfall, potential evapotranspiration, air and vapour pressure, maximum and minimum air temperature, soil temperature, relative humidity, solar radiation, wind speed and soil moisture on a regular (c. 5 km) grid covering the whole of New Zealand. The estimates are based on spatial interpolation of actual data observations made at climate stations distributed around the country. The centroids of the grid cells represent a network of virtual climate stations (VCSs). VCSs in and around the LMC are shown in (Figure 4–5). In the LMC, synthetic VCS data largely agree with actual measurements from physical climate stations.

VCS data consist of two unique station identifiers – the ‘agent’ and the ‘network’, date, barometric pressure reduced to mean sea level in hPa, Penman potential evapotranspiration depth in mm, rainfall depth in mm, relative humidity in percent, earth temperature at 10 cm depth in °C, amount of accumulated global solar

radiation in Mega Joules per square metre, maximum air temperature in °C, minimum air temperature in °C, vapour pressure in hPa, mean wind speed in m/s at 10 m above ground level, and soil moisture deficit (SMD) depth in mm calculated from rainfall and evapotranspiration. The base value is 150 mm SMD (hypothetical unified permanent wilting point) based on soil store capacity. SMD value of 0 indicates the soil is at field capacity. SMD value less than zero indicates deep percolation, i.e. groundwater recharge (Section 4.3.4).

NIWA made LMC VCS data available for this thesis. VCS rain data are available from 1/01/1960, wind speed data from 1/01/1997, and all other variables from 1/01/1972. However, only VCS rain, potential evapotranspiration and soil moisture data were analysed in this research for the period 1/01/1985–31/12/2015, inclusive (31 years). The period 1985–2015 has been selected for analysis in this thesis because useful groundwater level data extend from 1990 to the present. Starting climatological analysis five years earlier enables comfortable accounting of the time lag between rainfall and groundwater level response.

## 4.6 LMC climate

### 4.6.1 General setting

The LMC location between latitudes 39° 52' 30" and 40° 39' 00" South gives it temperate climate. In general, the area enjoys a mild climate with moderate seasonal variations.

The National Institute of Water and Atmospheric Research (NIWA) subdivides New Zealand land into broad climate zones and the LMC falls within the South–West North Island zone, which includes Taranaki, Manawatu–Wanganui and Wellington regions. This zone is exposed to disturbed weather systems from the Tasman Sea and although it is relatively windy, climatic extremes are rare and limited. The inland parts of the zone, with greater orographic influence, are more prone to climatic extremes. The most settled weather in the zone occurs during summer and early autumn, with winter normally the most unsettled time of the year.

North–westerly airflows prevail over the area. Sea breezes occasionally occur along the coast during summer. Frost occurs inland in winter during clear calm conditions. In average, air temperature exceeds 25°C in Palmerston North 25 days per year and drops below zero centigrade 16 days per year (Chappell, 2015). Table 4–3 presents mean climatological characteristics for Palmerston North, which is situated nearly in the centre of the LMC.

#### 4.6.2 Precipitation

Rainfall is the dominant type of precipitation in the LMC, snow being very rare on most of the area, particularly the plains. The area does not experience the severity of droughts that affect some other parts of New Zealand.

Tait and Sturman (2008) prepared mean and median annual rainfall maps for the Horizons region for the two overlapping 30–year periods of 1971–2000 and 1978–2007 at 500 m spatial resolution using all data archived at the time in NIWA’s National Climate Database (CliFlo) and additional data supplied by Horizons. Extracts for the LMC area from these four maps are reproduced in Appendix A and Figure 4–6 presents mean annual rainfall isohyetal map for the period 1971–2000 based on their work. Tait and Sturman (2008) chose the period 1971–2000 because it is the latest climate ‘normal’ period at the time. But since that period does not include more recent years that include some anomalously high or low rainfalls, they also analysed and prepared rain maps for the ‘most recent’ 30–year period at the time, being 1978–2007.

Tait and Sturman (2008) rain maps were prepared using the thin plate smoothing spline model in the ANUSPLIN software package. The maps which are reproduced in Appendix A show that the mean annual rainfall over the LMC ranges between around 810 mm/y in the Bunnythorpe and Awahuri area, to more than 3,000 mm/y in the in the Ruahine Range to the northeast of LMC.

Table 4–3. Long-term mean climatic parameter values for Palmerston North (mainly compiled from Chappell, 2015)<sup>21</sup>.

Climatic Parameter	Units	Jul	Aug	Sep	Oct	Nov	Dec	Jan	Feb	Mar	Apr	May	Jun	Year
Mean number of wet days <sup>22</sup>	days	12	13	12	12	10	11	7	7	8	8	10	12	122
Mean rainfall	mm	85	69	85	84	75	96	55	71	55	60	74	92	900
Daily minimum air temperature	°C	<i>4.6</i>	<i>5.0</i>	<i>6.6</i>	<i>8.1</i>	<i>9.3</i>	<i>11.5</i>	<i>12.5</i>	<i>13.0</i>	<i>11.2</i>	<i>8.6</i>	<i>6.9</i>	<i>4.9</i>	<i>4.6</i>
Daily maximum air temperature	°C	<i>12.7</i>	<i>13.5</i>	<i>15.3</i>	<i>16.7</i>	<i>18.3</i>	<i>20.9</i>	<i>23.0</i>	<i>23.5</i>	<i>21.5</i>	<i>18.6</i>	<i>15.8</i>	<i>13.3</i>	<i>23.5</i>
Mean air temperature	°C	8.3	8.5	8.5	8.6	9.1	9.4	10.3	10.3	10.2	9.9	8.9	8.2	9.1
Monthly earth temperature <sup>23</sup>	°C	7.1	7.8	10.0	12.5	14.7	16.9	18.2	18.1	16.1	13.2	10.6	8.4	12.8
Ground frost occurrence	days	10.3	9.2	4.1	2.3	0.7	0.2	0.1	0.0	0.2	1.5	4.8	8.0	41.4
Mean relative humidity <sup>24</sup>	%	86.8	84.6	79.7	80.5	76.7	76.0	75.7	77.7	79.4	81.2	85.8	86.8	80.9
Monthly total sunshine	Hours	<i>103.8</i>	<i>119.9</i>	<i>124.2</i>	<i>142.6</i>	<i>165.3</i>	<i>176.7</i>	<i>212.4</i>	<i>191.0</i>	<i>173.5</i>	<i>145.6</i>	<i>109.3</i>	<i>79.1</i>	<i>1,743.5</i>
Daily global radiation	Mj/m <sup>2</sup> /d	6.1	8.7	12.3	15.7	19.8	21.1	22.4	19.9	15.4	10.6	7.0	5.3	13.7
Wind speed	Km/hr	13.9	14.2	15.6	17.0	17.8	16.1	15.8	15.6	15.3	12.9	13.7	13.7	15.1
Min potential evapotranspiration <sup>25</sup>	mm	17.8	30.3	46.2	77.4	95.2	98.3	120.7	103.1	74.3	38.7	22.8	13.6	163.2
Max potential evapotranspiration <sup>25</sup>	mm	34.0	45.0	66.6	98.0	138.7	174.2	178.0	141.3	119.1	64.9	41.1	25.9	2,136
Mean potential evapotranspiration	Mm	22.8	36.4	58.3	87.4	113.5	135.4	148.1	122.6	97.6	52.2	29.7	19.2	922.8

<sup>21</sup> Italic type font indicates data compiled from NIWA's National Climate Database (CliFlo).

<sup>22</sup> Days with 1 mm or more of rain. Mean annual number of days with 0.1 mm or more of rain = 171.

<sup>23</sup> Measured at 10 cm depth.

<sup>24</sup> Measured at 9.00 am.

<sup>25</sup> Yearly minimum, maximum and mean potential evapotranspiration values are not calculated from monthly data, but for actual annual totals.

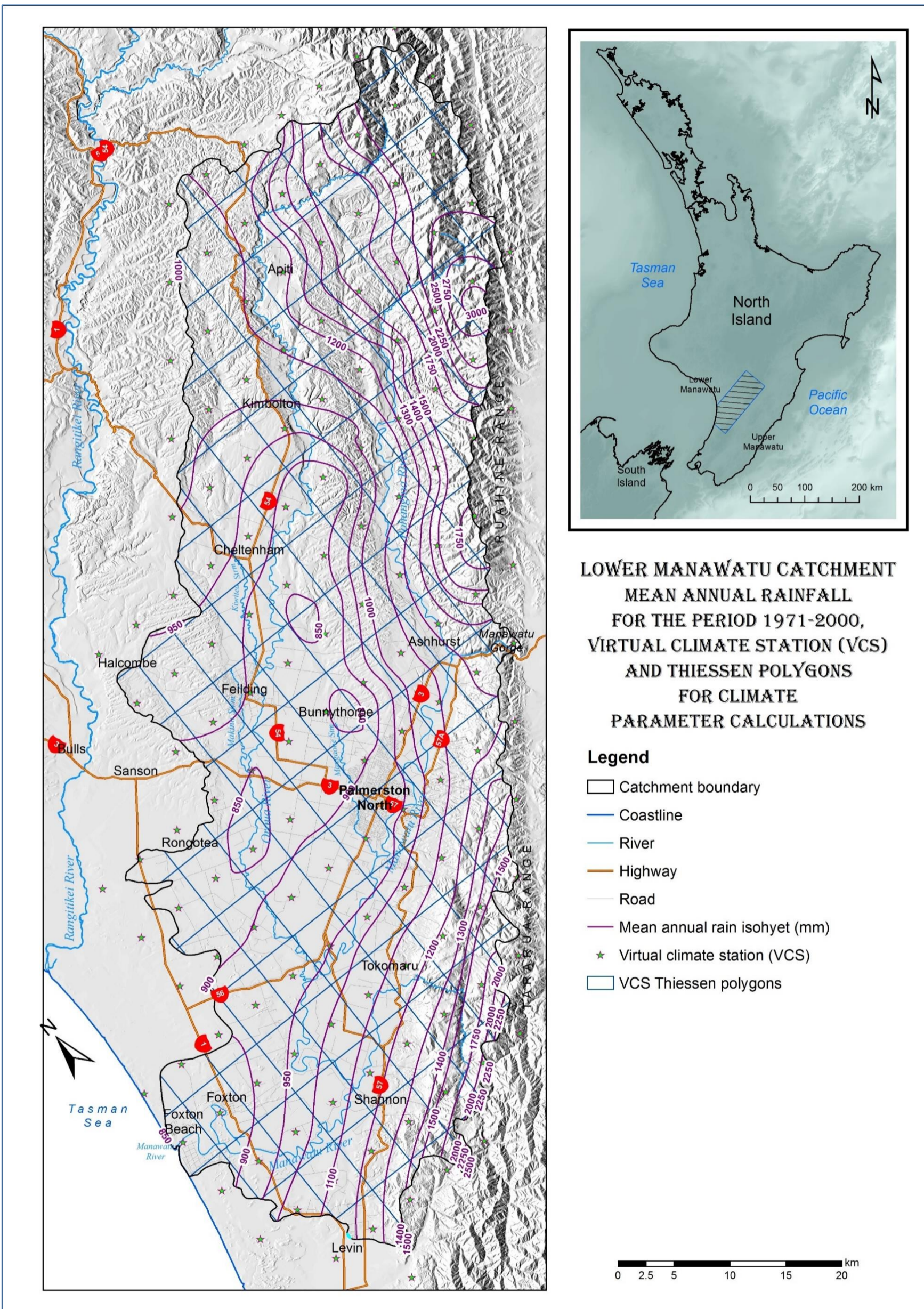


Figure 4-6. Virtual climate stations (VCS), Thiessen polygons for climatic parameter calculations and mean annual rainfall isohyetal map for the period 1971-2000 (based on digital map by Tait & Sturman, 2008).

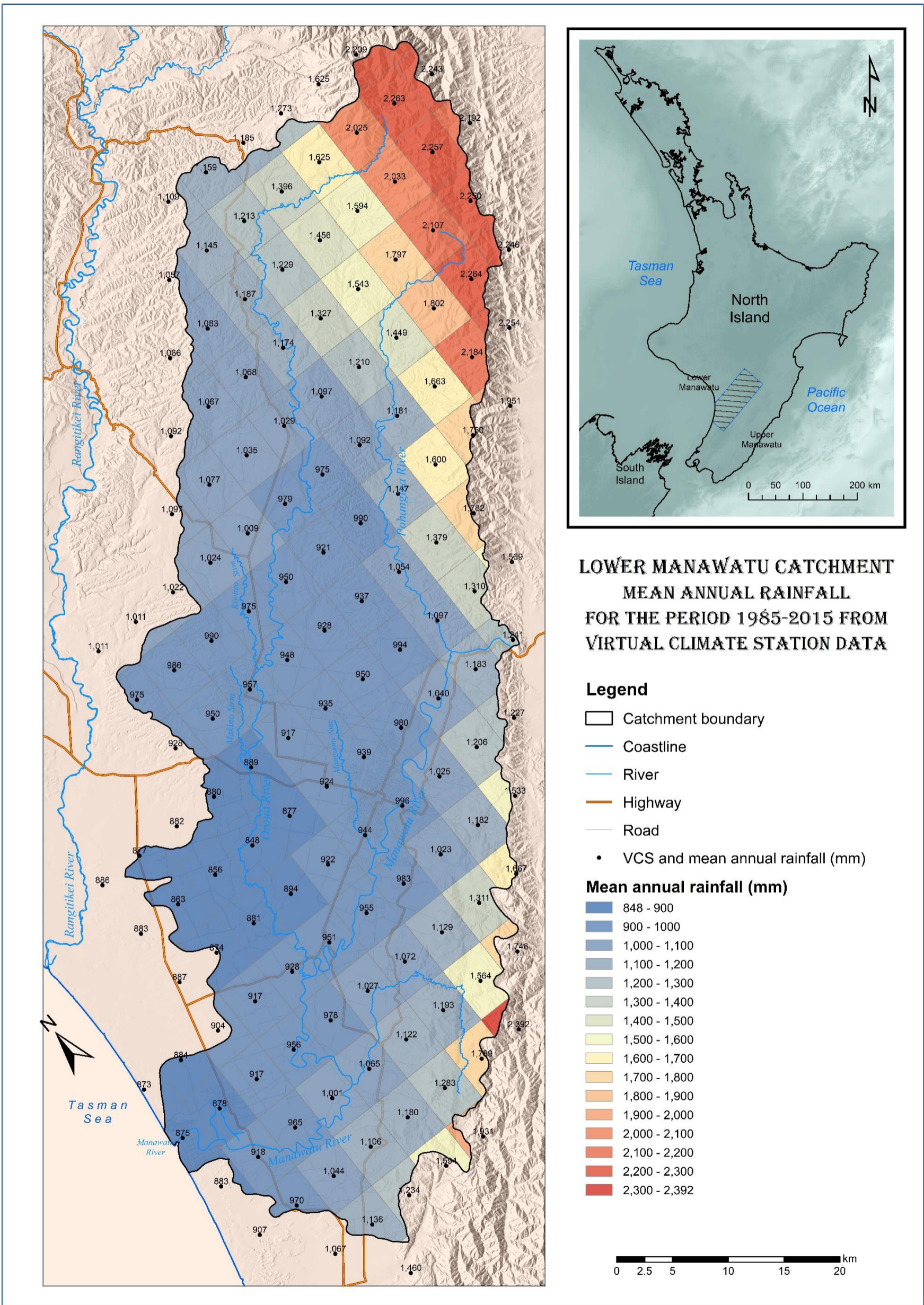


Figure 4-7. Mean annual rainfall calculated from VCS data for the period 1985 – 2015.

NIWA statistics indicate that rain falls on Palmerston North approximately 5% of the time and that, on average, the city enjoys 200 rain free days per year.

To estimate mean annual rain over the LMC area, Thiessen polygons were drawn around VCSs to identify the area of representation for each of them (Figure 4–6). The results are summarised in Table 4–4 and presented graphically in Figure 4–7.

Table 4–4. Annual mean rain rates and volumes over the LMC area for the periods 1985–2015 calculated from VCS data.

Catchment	Area (m <sup>2</sup> ) <sup>26</sup>	Rain	
		Mean (mm)	Total (mcm <sup>27</sup> )
Pohangina	547,828,093	1,567.37	858.65
Oroua	910,284,347	1,150.26	1,047.06
Manawatu–Lower	1,206,437,484	1,052.30	1,269.54
Overall (LMC)	2,664,549,924	1,191.66 <sup>28</sup>	3,175.25

Mean annual rainfall over Palmerston North calculated using VCS data ranges between c. 925 mm and c. 995 mm, decreasing from southeast to northwest (Figure 4–7). Mean annual rainfall volumes and rates calculated for the LMC over the period 1985–2015 from VCS data (Table 4–4) slightly differ from estimates extracted from Tait and Sturman (2008) rain maps (Table 4–5), with the difference being around 1.5%.

Table 4–5. Mean and median rain rates and volumes over the LMC area for the periods 1971–2000 and 1978–2007 (estimated from digital maps by Tait & Sturman, 2008).

LMC annual rain	1971–2000		1978–2007	
	mean	median	mean	median
Total Volume (mcm/y)	3,242	3,248	3,233	3,210
Depth (mm/y)	1,210	1,212	1,207	1,198

Figure 4–8 presents monthly rain recorded for Palmerston North over the period 1985–2015, which averages to c. 80 mm/month compared to c. 76 mm/month over the period 1971–2007 as calculated by Tait and Sturman (2008).

<sup>26</sup> This estimation is smaller than the LMC area estimation in other parts of the thesis due to discounting some of the area covered by rivers, particularly the Manawatu River.

<sup>27</sup> mcm: million cubic metre.

<sup>28</sup> Geographic weighted mean, calculated by dividing total rain volume by area.

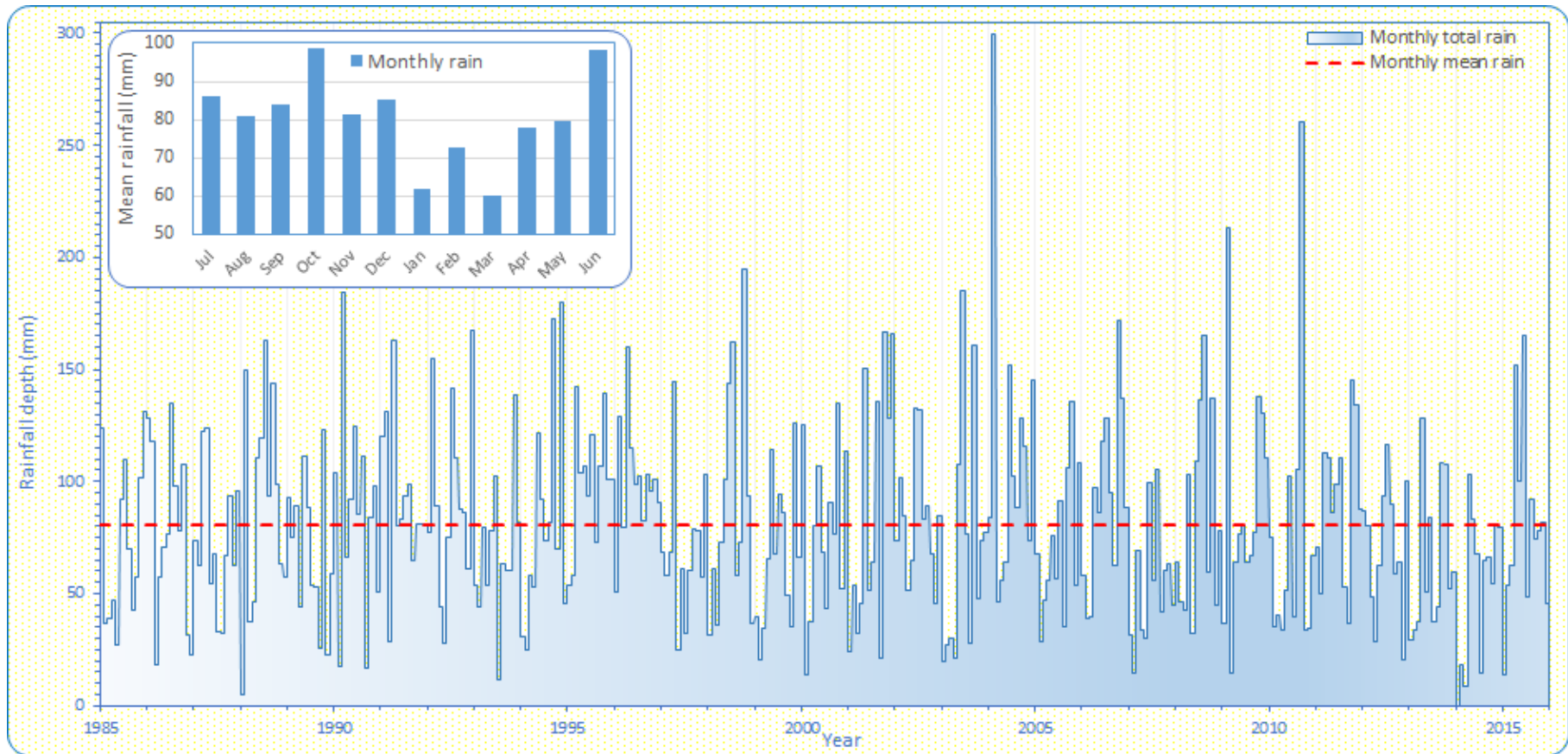


Figure 4–8. Monthly rainfall at Palmerston North for the period 1985–2015.

Inset presents long-term mean monthly rainfall for the same period. Data for the period 1/01/1985–31/05/2001 from Palmerston North Aws Station (NIWA agent number 3243). Data for the period 1/06/2001–31/12/2015 from Palmerston North Ews Station (NIWA agent number 21963). Inset presents monthly average rainfall for the same period.

The data presented in Figure 4–8 suggest a greatly variable, unpredictable rainfall pattern in the LMC. During the period 1985–2015, the highest annual rainfall (c. 1,355 mm) was recorded in 2004 and the lowest (641 mm) in 2014 (Figure 4–9 Top). The inset plot in Figure 4–8 indicates that the driest months in the year in average are the summer months January–March. Noticeably, the maximum monthly rainfall (c. 300 mm) was recorded in summer, in February 2004 (Figure 4–8).

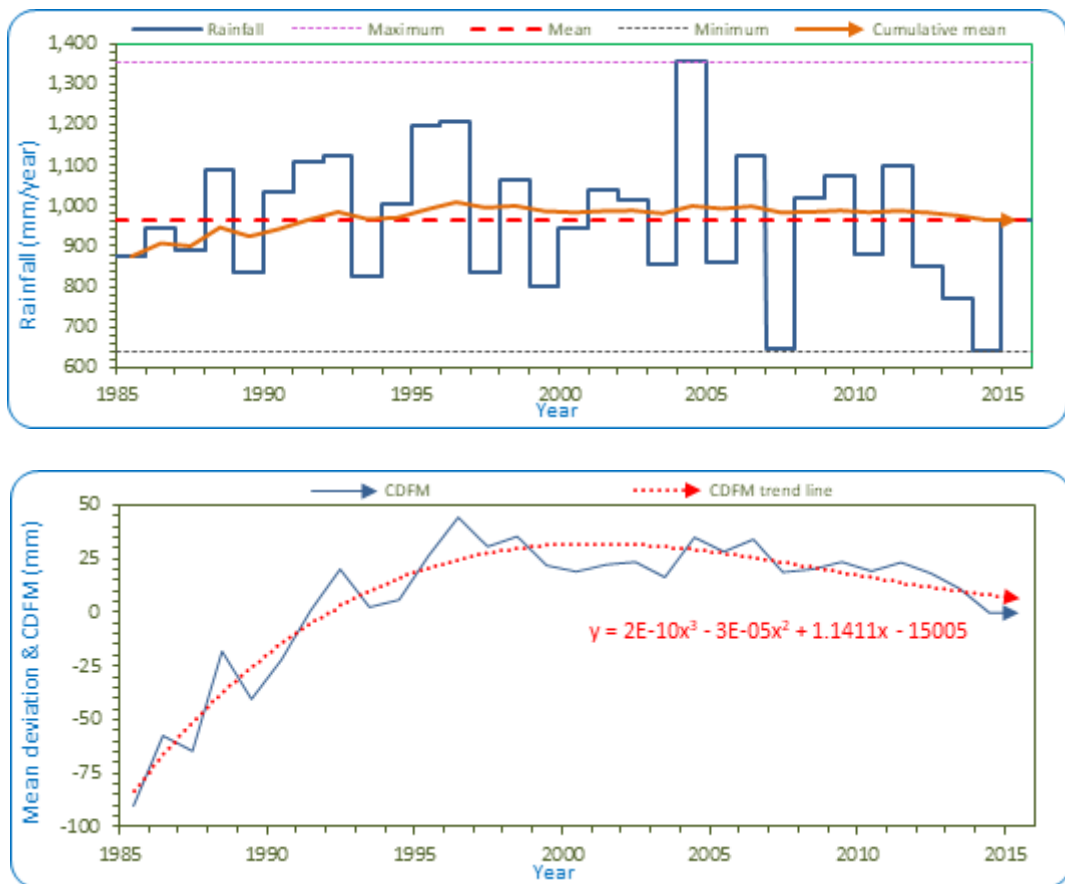


Figure 4–9. Yearly rainfall at Palmerston North.

**Top:** yearly total, maximum, mean, minimum and cumulative mean.

**Bottom:** Annual cumulative deviation from mean (CDFM), showing increasing rainfall until 1996, relative stability during the period 1996–2007, followed by a slight decrease until end of 2015.

Figure 4–9 (bottom) shows monthly rainfall cumulative deviation from mean (CDFM) at Palmerston North for the period 1985–2015 and Figure 4–10 shows monthly rainfall CDFM for the same period. The plots suggest that rainfall over Palmerston North has been trending upwards from 1988 until 2006. From 2006–2012, rainfall

has been constant, but dropped after that to a record low in 2014. The trend noticed in Palmerston North rainfall seems to exemplify rainfall over the entire LMC area. Correspondingly, groundwater levels over the period 1988–2012 in the LMC are expected to be higher than their long-term averages.

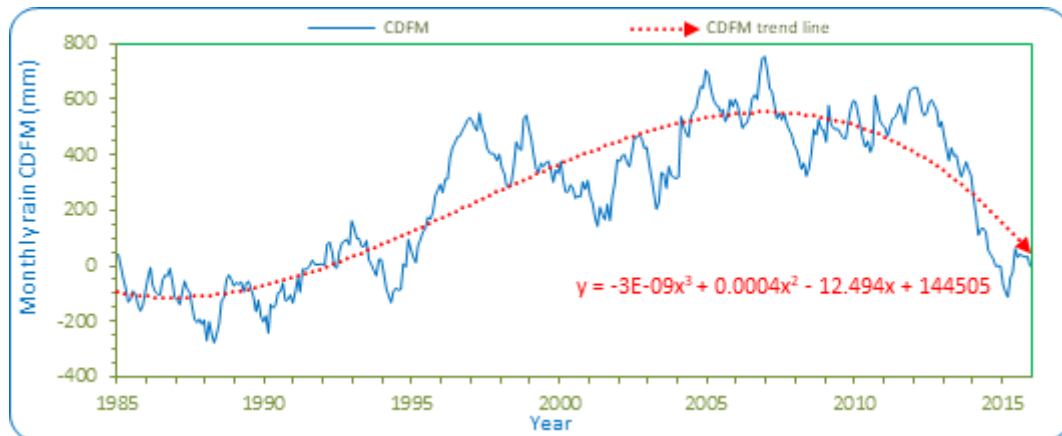


Figure 4–10. Monthly rain cumulative deviation from mean (CDFM) at Palmerston North for the period 1985–2015.

#### 4.6.3 Evapotranspiration

The coastal area of the LMC has an average of about 2,000 sunshine hours a year but Palmerston North is defined as cloudy with an average of only 1,725 sunshine hours a year. In 1992, Palmerston North claimed the national low record of only 1,357 sunshine hours.

Summer in the LMC is warm, with a maximum mid-summer daily average air temperature of around 20–23 °C. The minimum mid-winter daily average temperature for the coastal area is a cool 4–8 °C, while inland areas are considerably colder.

Westerly breeze prevails in the area. It can be stronger in spring but rarely reaches gale force. The mountains that bound the catchment from two sides arguably provide the most consistent wind in New Zealand, especially in spring.

Palmerston North meteorological stations do not measure pan evaporation and NIWA's CliFlo database does not include  $ET_p$  data. However, NIWA calculates  $ET_p$

as part of their VCS network climatological modelling (Section 4.5.2). Figure 4–11 shows the spatial distribution of potential evapotranspiration across the LMC. Generally speaking,  $ET_p$  is highest in the LMC in areas classified as open low hills landform type and gentler topography as delineated in Section 3.9.

Chappell (2015) calculated minimum, mean and maximum monthly  $ET_p$  for Palmerston North (Table 4–3). Figure 4–12 shows that potential evapotranspiration normally exceeds rainfall in Palmerston North during the period from October to March, which indicate a need to irrigate crops during that period. During most of this season (November–March), mean monthly rain is even less than the mean monthly minimum potential evapotranspiration. Albeit, Palmerston North has an overall average rain surplus of 86.4 mm/y as calculated from values presented in Table 4–3.

Figure 4–13 shows the mean annual difference between rainfall and potential evapotranspiration calculated from VCS data for the period 1985–2015. A general deficit can be seen in a relatively small area around the Halcombe Anticline between Bunnythorpe and Rongotea, indicating little to no possibility for groundwater recharge in that area.

VCS data calculations (Table 4–4) suggest that mean annual rain in the LMC is generally higher than mean annual potential evapotranspiration by c. 360 mm, the equivalent to c. 965 million cubic metre per year (mcm/y) over the catchment area. In reality, however, the surplus is greater because actual evapotranspiration is less than potential evapotranspiration during nearly half of the year. Soil water balance modelling results presented in Section 4.7.2 imply that over the LMC area rainfall exceeds actual evapotranspiration ( $ET_p$ ) by c. 590 mm/y, the equivalent to c. 1,580 mcm/y. This surplus water is available for runoff and groundwater recharge.

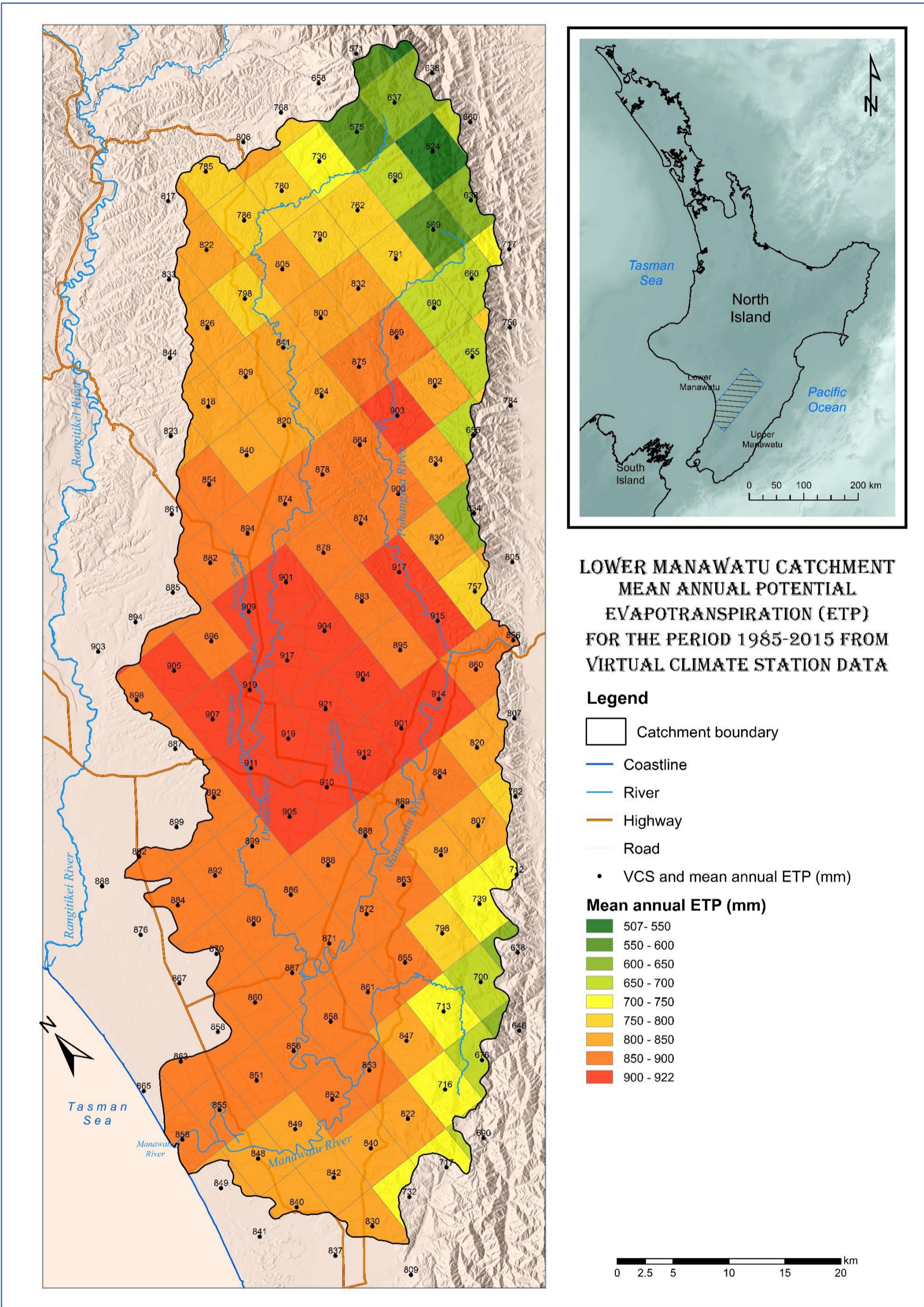


Figure 4-11. Mean annual potential evapotranspiration calculated from VCS data for the period 1985 – 2015.

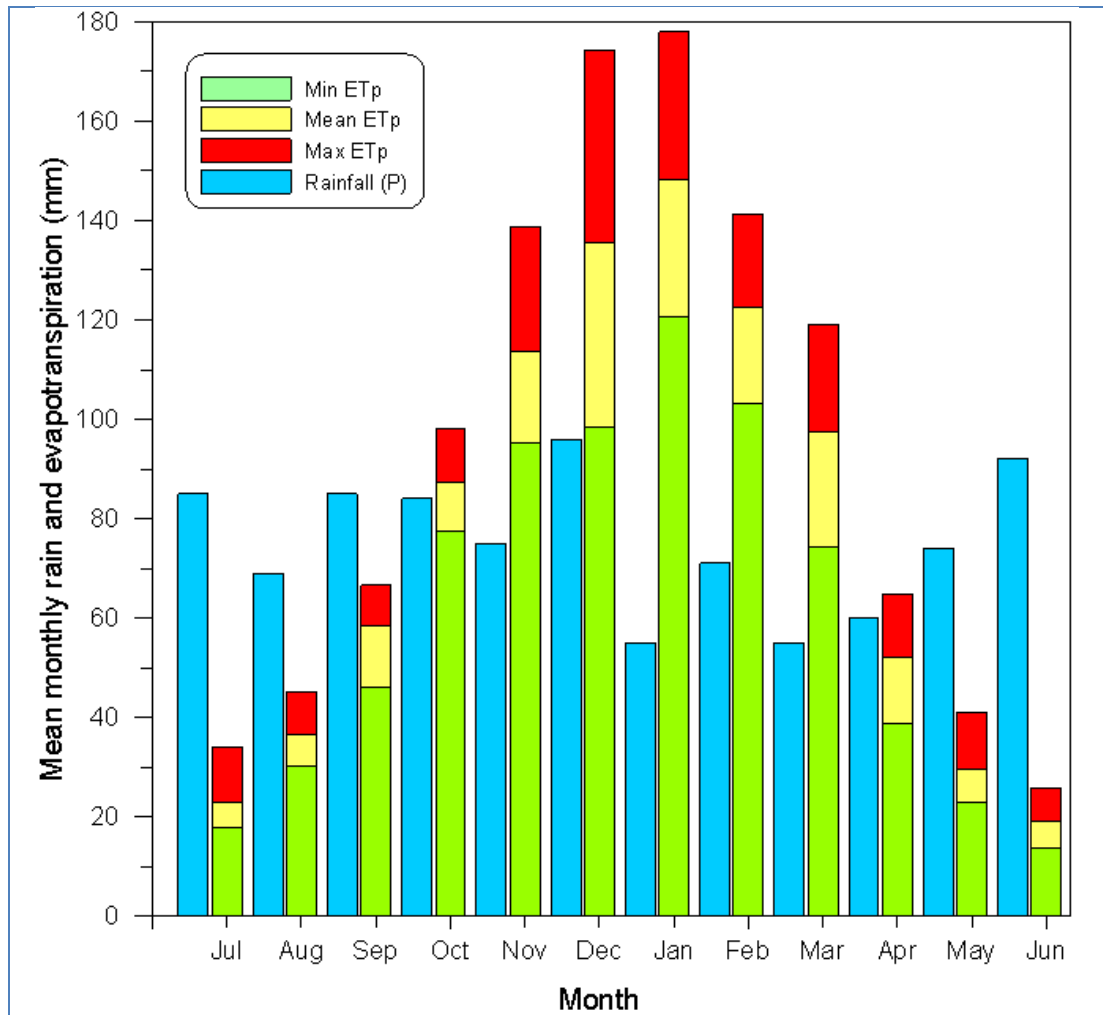


Figure 4–12. Mean rainfall ( $P$ ) compared to calculated maximum, mean and minimum monthly potential evapotranspiration ( $ET_p$ ) at Palmerston North Aws station (data sourced from Chappell, 2015).

Differences between mean monthly rainfall data presented here and those presented in the inset in Figure 4–8 may be due to differences in the analysed periods.

#### 4.6.4 Hydrological year

The graph in Figure 4–12 suggests that a hydrological year in the LMC can be defined from 1 July to 30 June. This agrees with the NIWA recommended water year for the North Island of New Zealand. The calendar year is not suitable for hydrological calculations because significant droughts often begin in December and extend over summer, which can lead to double counting of droughts (Henderson & Dietrich, 2007).

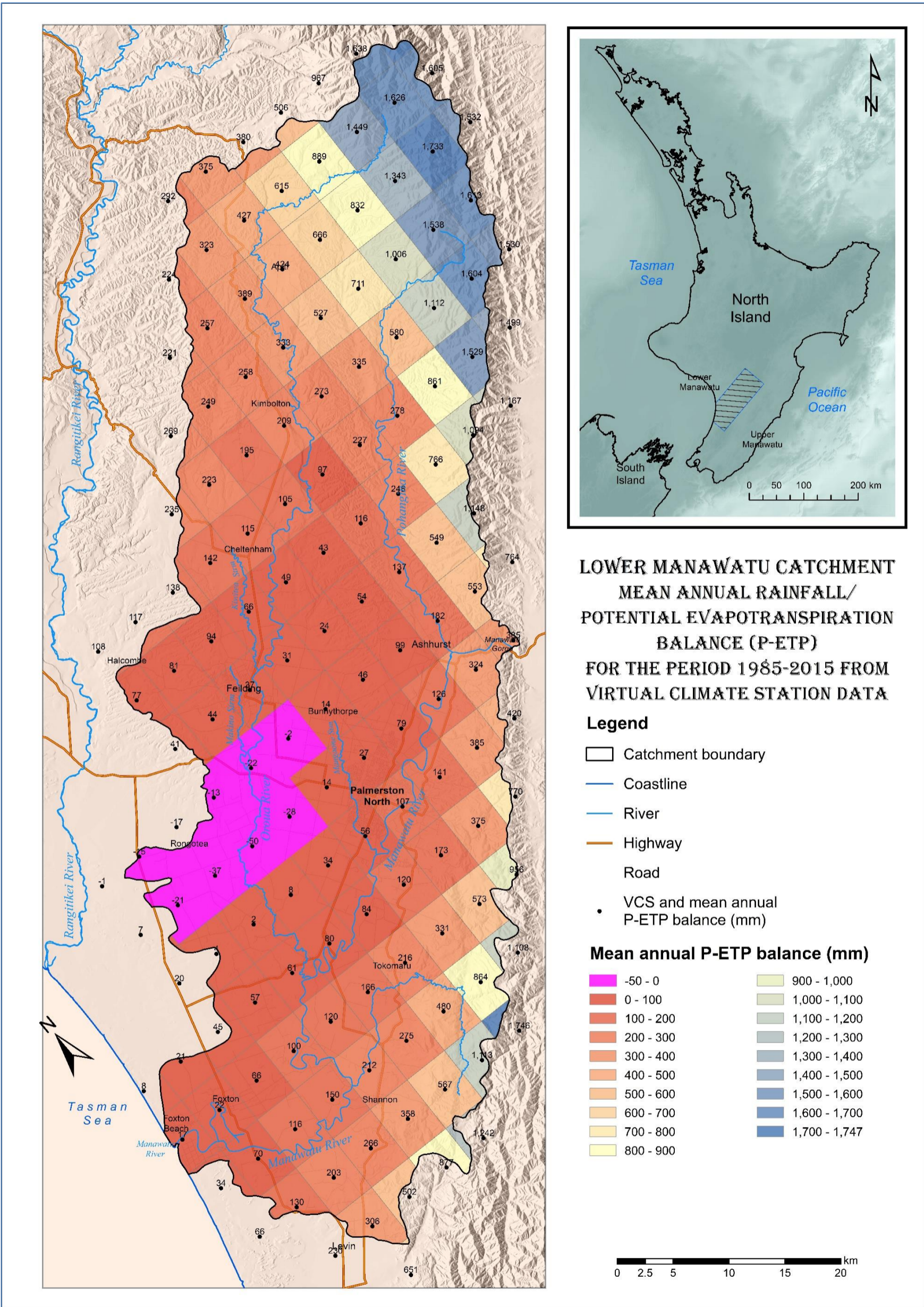


Figure 4-13. Mean annual difference between rainfall and potential evapotranspiration calculated from VCS data for the period 1985-2015.

## 4.7 LMC soil moisture balance modelling

### 4.7.1 Set up

A purpose-built Microsoft® Access™ 2016 application<sup>29</sup> (Figure 4-14) has been prepared using Visual Basic for Applications (VBA) to undertake SMB modelling for the LMC over the period 1/01/1985 – 31/12/2015.

The LMC SMB model utilises synthetic daily rain and evapotranspiration data from NIWA's VCS network. Thiessen polygons have been drawn to delineate the area represented by each VCS (Figure 4-5). Soil hydraulic properties have been set by classifying soil in the area according to the United States Department of Agriculture (USDA) Soil Texture Classification (STC) based on their Fundamental Soil Layer (FSL) classification (Table 4-6). To represent sealed areas, 'built-up area' and 'basement rock' soil types have been added to the USDA-STC. These areas have been delineated based on data from the geological map (Figure 3-16) and from the 2012 Ministry for the Environment (MfE) land use map (Figure 4-15). Unclassified soils in the FSL in the coastal area to the south of the Manawatu River have been typified as sand in the USDA-STC. Unclassified soils in the FSL in the Tararua Range area were typified as silt loam in the USDA-STC. However, this later assumption may have no real bearing on the modelling results because much of the area covered unclassified soils in the Tararua Range has been considered basement rock area where only evapotranspiration and surface runoff can take place, rendering soil properties irrelevant to the calculations.

The 2012 Ministry for the Environment land use map (Figure 4-15) implies that most of the LMC excluding built-up and basement rock area is grassland with some cropland patches. This enables SMB modelling simplification whereby all soil-covered land can safely be considered grassland.

---

<sup>29</sup> Copyright 2016 © All rights reserved by author.

Soil Moisture Balance Modelling Utility

VCS\_Id      Soil

27122	1 Sand
27137	2 Loamy sand
27148	3 Sandy loam
27149	4 Loam
27155	5 Silt loam
27180	6 Silt clay loam
27181	7 Built up area
27182	8 Basement rock

Soil: Sand    FC: 120.00    IT: 101.25    SP: 82.50    WP: 45.00    Land surface: Soil

Irrigation on:  No     Yes    IR % of FC-SMC = 80%

From: 23/07/2016    To: 23/07/2016

Buttons: Refresh, Calculate, Delete existing records, Hide results, Exit

Input data

VCS_Id	Date	P	ETp	SMD
27122	01/01/1985	0.0	4.3	-126.2
27122	02/01/1985	1.1	1.9	-126.0
27122	03/01/1985	0.0	3.6	-126.1
27122	04/01/1985	6.4	2.1	-120.1
27122	05/01/1985	0.0	6.3	-123.0
27122	06/01/1985	0.0	4.8	-124.5
27122	07/01/1985	0.0	4.2	-125.7
27122	08/01/1985	0.0	4.2	-126.0
27122	09/01/1985	0.0	4.2	-127.3
27122	10/01/1985	2.9	4.2	-121.8
27122	11/01/1985	24.1	1.3	-104.3
27122	12/01/1985	5.2	4.1	-101.5
27122	13/01/1985	0.0	3.5	-102.3
27122	14/01/1985	0.0	4.9	-102.3
27122	15/01/1985	0.0	5.3	-102.3
27122	16/01/1985	0.0	2.0	-105.1
27122	17/01/1985	0.0	6.2	-107.7
27122	18/01/1985	0.0	5.7	-110.1
27122	19/01/1985	0.0	5.1	-115.0
27122	20/01/1985	0.0	5.1	-116.7
27122	21/01/1985	14.3	1.5	-106.0
27122	22/01/1985	29.5	2.8	-62.1
27122	23/01/1985	0.0	4.4	-64.9
27122	24/01/1985	3.0	3.4	-79.2

Model results

Soil	Irrigate	Polygon	Date	P	ETp	IR	ETa	Ro	RCH	SMC	SMD
Sandy loam	Yes	30361 Sandy loam Yes 31/03/1970 1/10/2001	01/01/1985	0.0	4.3	78.2	4.0	0.0	0.0	206.4	23.6
Sandy loam	Yes	30361 Sandy loam Yes 31/03/1970 1/10/2001	02/01/1985	7.3	2.3	0.0	2.3	0.0	0.0	211.4	18.6
Sandy loam	Yes	30361 Sandy loam Yes 31/03/1970 1/10/2001	03/01/1985	0.0	4.8	0.0	4.8	0.0	0.0	206.6	23.4
Sandy loam	Yes	30361 Sandy loam Yes 31/03/1970 1/10/2001	04/01/1985	5.9	5.0	0.0	5.0	0.0	0.0	207.5	22.5
Sandy loam	Yes	30361 Sandy loam Yes 31/03/1970 1/10/2001	05/01/1985	0.0	6.1	0.0	6.1	0.0	0.0	201.4	28.6
Sandy loam	Yes	30361 Sandy loam Yes 31/03/1970 1/10/2001	06/01/1985	0.0	5.4	0.0	5.4	0.0	0.0	196.0	34.0
Sandy loam	Yes	30361 Sandy loam Yes 31/03/1970 1/10/2001	07/01/1985	0.0	4.5	27.2	4.5	0.0	0.0	218.7	11.3
Sandy loam	Yes	30361 Sandy loam Yes 31/03/1970 1/10/2001	08/01/1985	0.0	4.3	0.0	4.3	0.0	0.0	214.4	15.6
Sandy loam	Yes	30361 Sandy loam Yes 31/03/1970 1/10/2001	09/01/1985	0.0	4.0	0.0	4.0	0.0	0.0	210.4	19.6
Sandy loam	Yes	30361 Sandy loam Yes 31/03/1970 1/10/2001	10/01/1985	0.0	4.2	0.0	4.2	0.0	0.0	206.2	23.8
Sandy loam	Yes	30361 Sandy loam Yes 31/03/1970 1/10/2001	11/01/1985	14.0	2.5	0.0	2.5	0.0	0.0	217.7	12.3
Sandy loam	Yes	30361 Sandy loam Yes 31/03/1970 1/10/2001	12/01/1985	10.1	3.9	0.0	3.9	0.0	0.0	223.9	6.1
Sandy loam	Yes	30361 Sandy loam Yes 31/03/1970 1/10/2001	13/01/1985	5.2	3.2	0.0	3.2	0.0	0.0	225.9	4.1
Sandy loam	Yes	30361 Sandy loam Yes 31/03/1970 1/10/2001	14/01/1985	1.6	3.8	0.0	3.8	0.0	0.0	223.7	6.3
Sandy loam	Yes	30361 Sandy loam Yes 31/03/1970 1/10/2001	15/01/1985	0.0	5.6	0.0	5.6	0.0	0.0	218.1	11.9
Sandy loam	Yes	30361 Sandy loam Yes 31/03/1970 1/10/2001	16/01/1985	0.0	3.2	0.0	3.2	0.0	0.0	214.9	15.1
Sandy loam	Yes	30361 Sandy loam Yes 31/03/1970 1/10/2001	17/01/1985	0.0	6.6	0.0	6.6	0.0	0.0	208.3	21.7
Sandy loam	Yes	30361 Sandy loam Yes 31/03/1970 1/10/2001	18/01/1985	0.0	6.4	0.0	6.4	0.0	0.0	201.9	28.1
Sandy loam	Yes	30361 Sandy loam Yes 31/03/1970 1/10/2001	19/01/1985	0.0	5.4	0.0	5.4	0.0	0.0	196.5	33.5
Sandy loam	Yes	30361 Sandy loam Yes 31/03/1970 1/10/2001	20/01/1985	0.0	4.3	26.8	4.3	0.0	0.0	219.0	11.0
Sandy loam	Yes	30361 Sandy loam Yes 31/03/1970 1/10/2001	21/01/1985	5.7	1.9	0.0	1.9	0.0	0.0	222.8	7.2
Sandy loam	Yes	30361 Sandy loam Yes 31/03/1970 1/10/2001	22/01/1985	9.6	3.5	0.0	3.5	0.0	0.0	228.9	1.1
Sandy loam	Yes	30361 Sandy loam Yes 31/03/1970 1/10/2001	23/01/1985	12.2	5.0	0.0	5.0	0.0	6.1	230.0	0.0
Sandy loam	Yes	30361 Sandy loam Yes 31/03/1970 1/10/2001	24/01/1985	18.1	3.2	0.0	3.2	0.0	14.9	230.0	0.0

Record: 1 of 11322    No Filter    Search

Record: 1 of 308672    No Filter    Search

Copyright © 2016 Hisham Zarour  
All rights reserved. No part of this software may be reproduced, distributed, or transmitted in any form or by any means, including all electronic and mechanical methods, without the prior written permission of the copyright holder.

Figure 4–14. Screenshot of the user interface for the LMC SMB model.

Table 4–6. Typical soil water characteristics for various USDA–STC<sup>30</sup> classes (after Allen *et al.*, 1998), correlated to LMC soils based on NZ FSL.

USDA STC Soil type	New Zealand Fundamental Soil Layer Soil Type	Soil water characteristics (m <sup>3</sup> /m <sup>3</sup> )		
		$\theta_{FC}^{31}$	$\theta_{WP}$	$TAW^{32}$
Sand	Black sand, sand, sand & stony gravel, weakly mottled sand	0.07 – 0.17	0.02 – 0.07	0.05 – 0.11
Loamy sand	Brown loamy sand, loamy sand, loamy sand & sandy loam	0.11 – 0.19	0.03 – 0.10	0.06 – 0.12
Sandy loam	Black sandy loam, brown sandy loam, fine sandy loam, mottled fine sandy loam, mottled sandy loam, sandy loam, sandy loam and silt loam, stony loam	0.18 – 0.28	0.06 – 0.16	0.11 – 0.15
Loam	Loam	0.20 – 0.30	0.07 – 0.17	0.13 – 0.18
Silt loam	black silt loam, heavy silt loam, mottled silt loam, peaty silt loam, sandy loam and silt loam, silt loam, silt loam and clay loam, silt loam on sand, stony silt loam, strongly mottled silt loam	0.22 – 0.36	0.09 – 0.21	0.13 – 0.19
Silt clay loam	Loamy peat, peaty loam	0.30 – 0.37	0.17 – 0.24	0.13 – 0.18
Built-up area <sup>33</sup>	Town	—	—	—
Basement rock <sup>33</sup>	Rock	—	—	—

<sup>30</sup> USDA–STC: United States Department of Agriculture Soil Texture Classification.<sup>31</sup>  $\theta$ : Content (%).<sup>32</sup>  $TAW = \theta_{FC} - \theta_{WP}$ .<sup>33</sup> Not in original USA–STC.

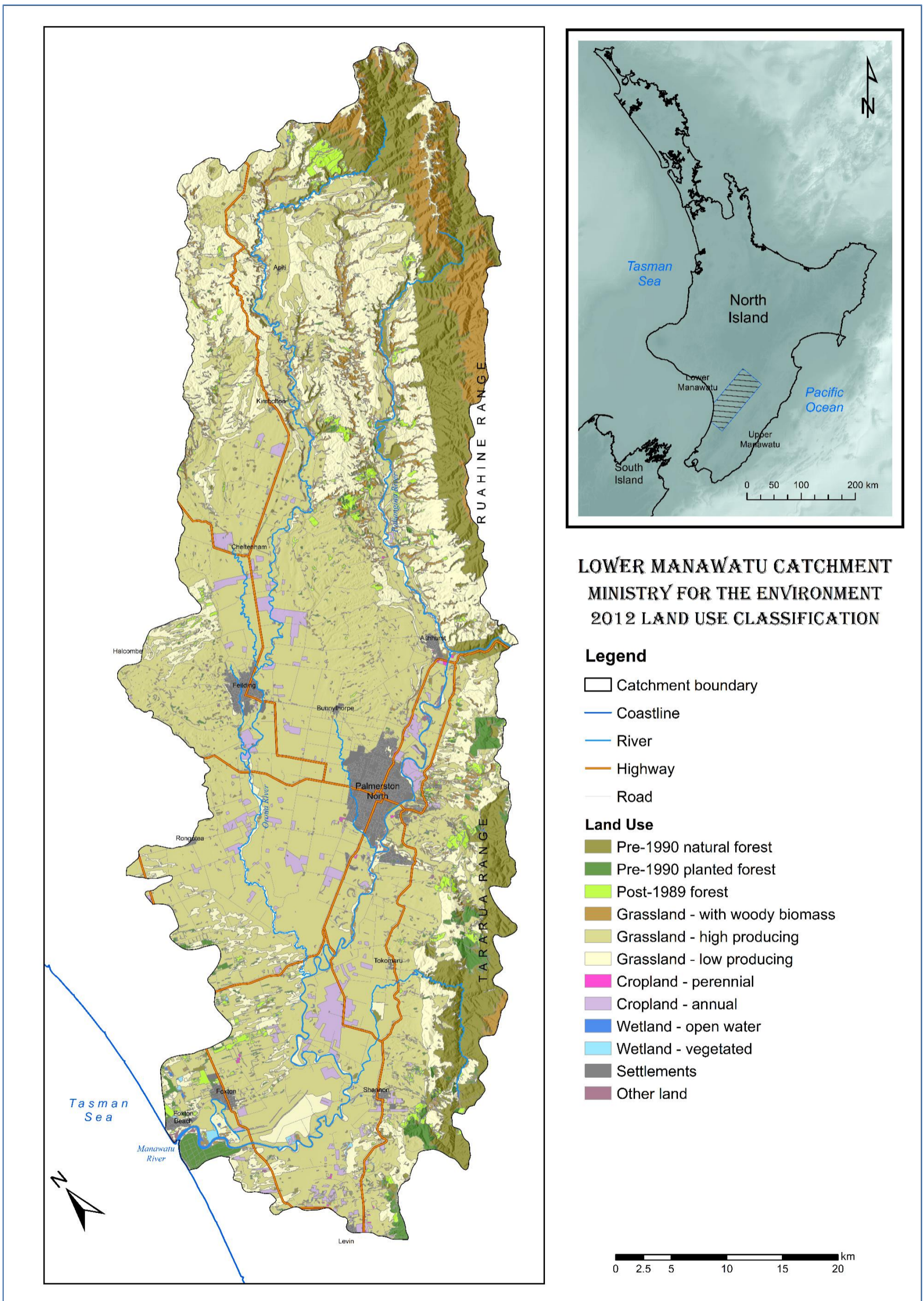


Figure 4-15. Ministry for the Environment 2012 land use map.

The LMC SMB model makes the following assumptions:

- (1) Rainfall and irrigation are the only forms of precipitation, i.e. no snow or dew
- (2) Daily time step
- (3) 1 m soil profile
- (4) Grass grown everywhere except in built-up and basement rock areas, i.e.  $K_c = 1$
- (5) Irrigation is only practiced with a resource consent and only over the term of the consent (data sourced from Horizons consents database to identify irrigated areas)
- (6) Irrigation is only practiced during the irrigation season (October–March, inclusive)
- (7) Water is available for irrigation where and when needed
- (8) If  $SMC$  at the beginning of the day is below the midpoint between  $FC$  and  $SP$ , irrigation is applied to replenish soil moisture to 80% of  $PAW$
- (9) Water input into the soil is limited to  $P$  and  $IR$ , i.e. there is no upward or lateral seepage
- (10) Water available to meet  $ET_a$  on any day include initial  $SMC$ ,  $P$  and  $IR$
- (11) Evapotranspiration demand is met as follows
  - i. In built-up and basement rock areas, the smallest of  $P$  and  $ET_p$
  - ii. Elsewhere,  $ET_a$  is achieved at full potential where  $SMC \geq SP$  and at reduced rate ranging from 100% at  $SMC = SP$  to 0% where  $SMC \leq WP$
- (12) After  $ET_a$ ,  $R_o$  occurs when  $SMC > 100\%$ , i.e. soil is saturated
- (13)  $RCH$  does not take place in built-up and basement rock areas
- (14) After  $ET_a$  and  $R_o$ ,  $RCH$  occurs while  $SMC > FC$
- (15)  $RCH$  can drain freely into a permeable subsurface medium (e.g. aquifer)
- (16)  $R_o$  does not turn into  $RCH$
- (17) End of day  $SMC$  is calculated as the balance of all input and output terms in Eq. 4-1
- (18) End of day  $SMC$  is carried over to the following day as initial  $SMC$ .

To account for spatial variability in the LMC SMB model, the area was divided into 1,686 polygons by overlaying GIS polygon layers representing VCS Thiessen polygons, soil types, farming practices (irrigated or dry land farming), and terms of irrigation consents where applicable. For each resultant polygon, the LMC SMB model calculated daily values of  $P$ ,  $ET_p$ ,  $IR$ ,  $ET_a$ ,  $R_o$  and  $RCH$  as depth in mm.

Corresponding volumes were calculated by multiplying depths by polygon areas. Mean annual volumes over the LMC three sub-catchments were thereafter summed and averaged (Table 4-7).

#### 4.7.2 Results

The LMC SMB model indicates that  $ET_p$  demand is least met in the built-up and basement rock area (Figure 4-16). This is understandable because the model assumes no soil moisture storage capacity in these two land categories, which means water is available to fully or partially meet  $ET_p$  demand only on rainy days.

Figure 4-17 and Figure 4-18 show the model calculated long-term mean annual  $R_0$  mean annual  $RCH$ , respectively. The LMC SMB model estimates the long-term mean annual recharge to be 23.43% of precipitation (Table 4-8). This is noticeably agreeable with the estimation of 22.43% by Zarour (2008).

A SMB model scenario was also run assuming no irrigation in the area (Table 4-9). On catchment-wide scale, the differences in SMB modelling results with and without irrigation are negligible.

Table 4–7. SMB model calculated mean annual rain, potential evapotranspiration, irrigation, actual evapotranspiration, surface runoff and groundwater recharge over the periods 1985–2015.

Catchment	Area (m <sup>2</sup> )	Units	$P$	$ET_p$	$IR$	$ET_a$	$R_o$	$RCH$
Pohangina	547,828,093	Total (m <sup>3</sup> /y)	858,649,654	428,272,718	387,512	297,363,041	359,613,393	202,216,455
		Average (mm/y)	1,567	782	1	543	656	369
Oroua	910,284,347	Total (m <sup>3</sup> /y)	1,047,059,491	757,346,263	2,054,980	598,999,238	167,451,207	283,044,638
		Average (mm/y)	1,150	832	2	658	184	311
Manawatu	1,206,437,484	Total (m <sup>3</sup> /y)	1,269,537,314	1,025,078,075	6,897,946	706,602,987	311,492,325	258,818,225
		Average (mm/y)	1,052	850	6	586	258	215
Overall	2,664,549,924	Total (m <sup>3</sup> /y)	3,175,246,459	2,210,697,055	9,340,438	1,602,965,266	838,556,926	744,079,318
		Average (mm/y)	1,192	830	4	602	315	279

Table 4–8. Ratios between SMB model calculated mean annual hydrological parameters over the periods 1985–2015.

Catchment	$ET_a/ET_p$ (%)	$ET_a/P$ (%)	$IR/P$ (%)	$R_o/P$ (%)	$RCH/P$ (%)
Pohangina	69.43%	34.63%	0.05%	41.88%	23.55%
Oroua	79.09%	57.21%	0.20%	15.99%	27.03%
Manawatu	68.93%	55.66%	0.54%	24.54%	20.39%
Overall	72.51%	50.48%	0.29%	26.41%	23.43%

Table 4–9. Overall LMC SMB model results for the periods 1985–2015 assuming only dry land farming conditions.

Overall	$P$	$ET_p$	$ET_a$	$R_o$	$RCH$
Total (m <sup>3</sup> /y)	3,188,796,059	2,222,813,333	1,607,098,127	838,554,481	744,287,404
Average (mm/y)	1,191	830	600	313	278

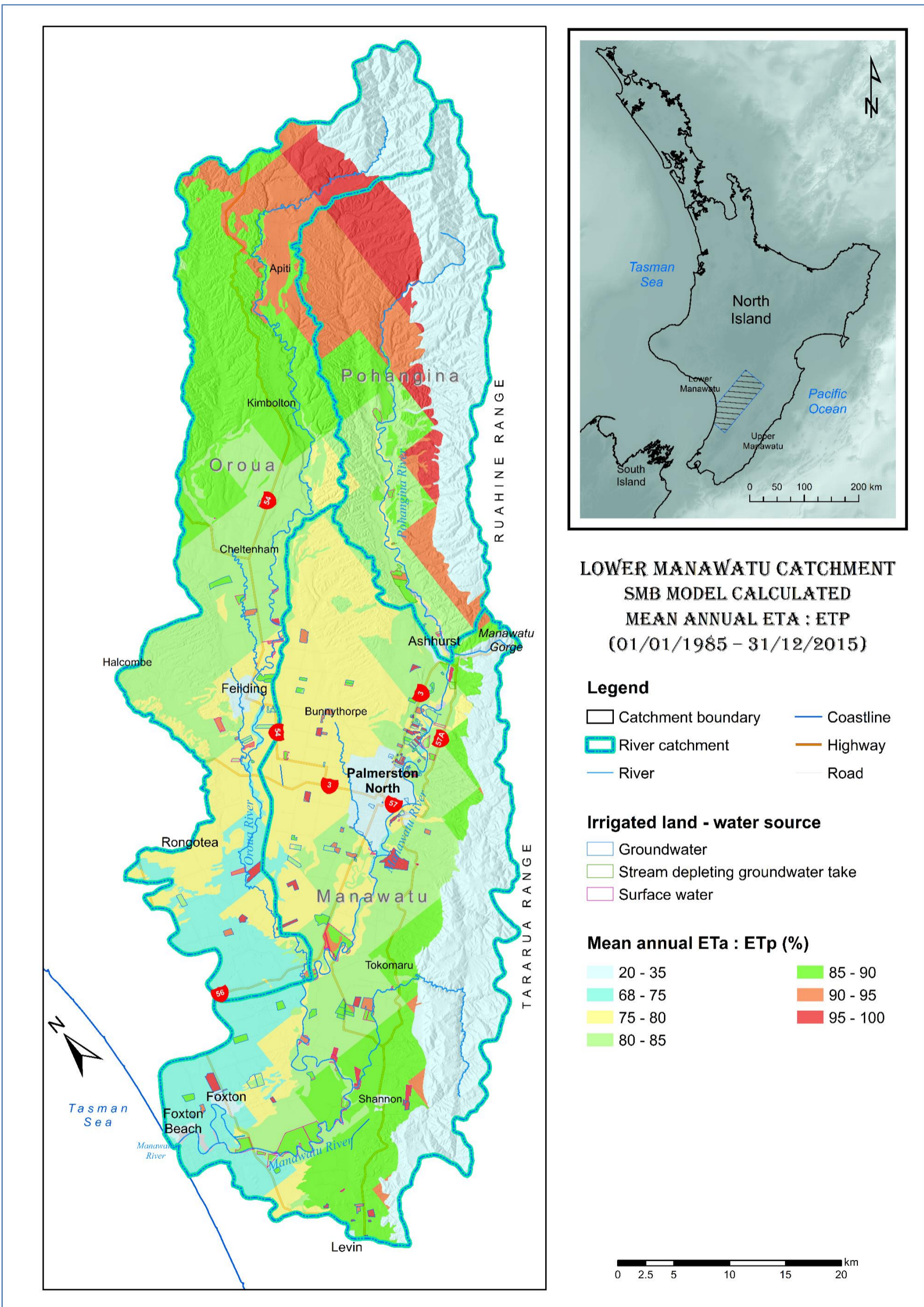


Figure 4-16. Long-term mean annual actual to potential evapotranspiration ratio.

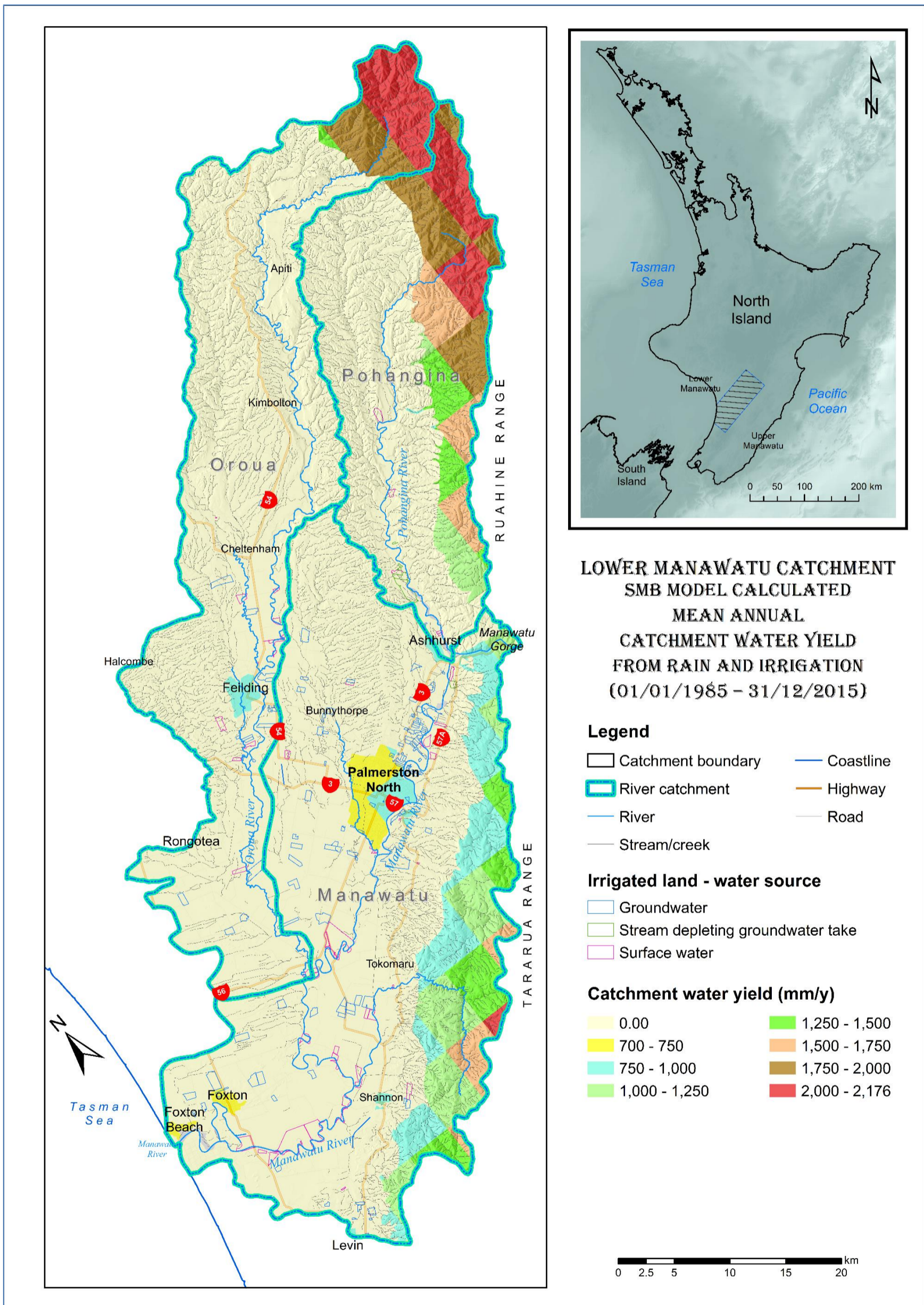


Figure 4-17. Long-term mean annual surface runoff depth.

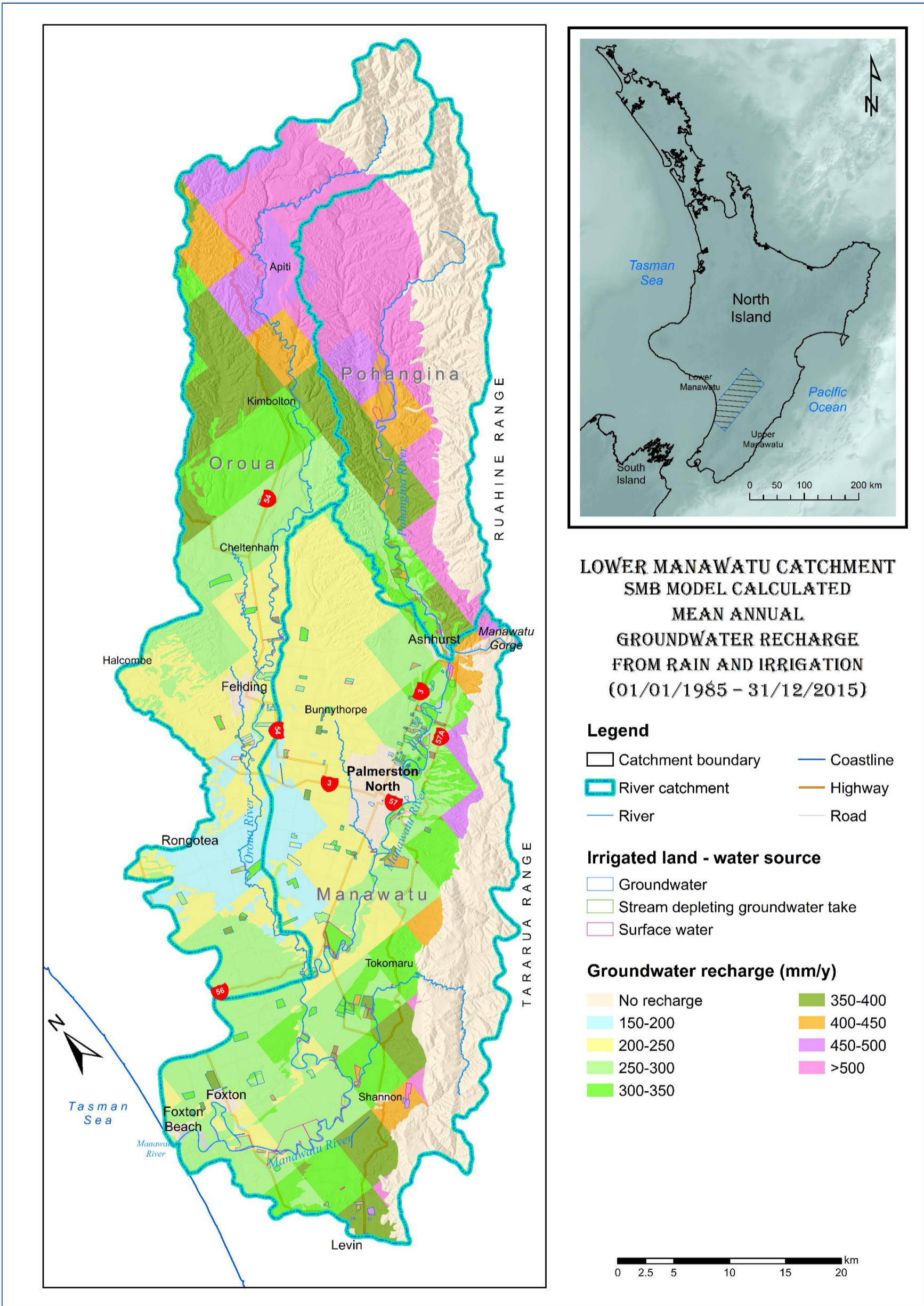


Figure 4-18. Long-term mean annual groundwater recharge depth.

### 4.7.3 Limitations

Like all models, the SMB model presented in this chapter simplifies reality. In doing so, conceptual and computational approximations had to be made.

The LMC SMB model is focused on assessing direct groundwater recharge from atmospheric precipitation. It also estimates actual evapotranspiration, reference crop irrigation demand, surface water runoff, soil moisture content and soil moisture deficit. Recharge from urban runoff and losses from water and wastewater networks and storage facilities is out of scope for this specific component of the research. Notwithstanding, applied and academic research shows that urbanisation affects groundwater recharge from precipitation, distorting its natural areal distribution, timing and rates (Barrett *et al.*, 1997; Foster *et al.*, 2005; Hughes & Mansour, 2005; Lerner, 2000, 2002). However, urban water balance is a matter that is better dealt with separately from SMB modelling. Direct recharge from precipitation is only one aspect of urban hydrology and SMB modelling can be useful in dealing with it.

Urban recharge has not been included in the LMC numerical models presented in Chapter 8, which is a limitation discussed there. Since the study area is largely unurbanised, the effect of considering the built-up areas to be totally sealed to groundwater recharge in the LMC SMB model could be insignificant to the groundwater flow models presented in this thesis. In numerical groundwater flow models, adjusting hydraulic conductivity values in underlying model cells can compensate for errors in groundwater recharge estimates. It may be argued that this can result in unrealistic estimation of both groundwater recharge and hydraulic conductivity, but they both can be maintained within realistic bounds and the overall model would continue to reasonably represent the modelled system.

This research is focused on groundwater. So, the effects of assuming that the built-up areas are completely impervious and do not allow the infiltration of precipitation water on the LMC SMB model estimates of surface runoff have not been investigated. Estimation errors in surface water flows and stage elevations

are thought to be negligible in regional-scale, steady-state groundwater assessments and flow models.

The LMC SMB model does not incorporate lateral or preferential soil moisture flow or the possibility of flow interception. Lateral and preferential soil water flows and interception occur at the grid- and subgrid- scales. They are thought to be marginal in regional or catchment-scale water models and, hence, could be ignored without greatly affecting the reliability of the modelling outcomes (Section 4.2).

The above noted limitations of the SMB modelling exercise undertaken in this research must be acknowledged and are recommended to be considered in subsequent work. There is also scope to enhance the LMC SMB model through the incorporation of flow interception and lateral and preferential soil moisture flow components, which will particularly be useful in more site-specific and/or transient assessments and modelling work. The sensitivity of regional-scale SMB and numerical groundwater flow model solutions to assumptions relating to lateral, preferential and intercepted soil water flow is an area that merits further research.

#### 4.7.4 Verification

The methodology adopted for SMB modelling in the LMC is consistent with research in New Zealand (e.g. Scott, 2004; Wilson & Lu, 2011; Woodward *et al.*, 2010) and internationally (e.g. Allen *et al.*, 1998; Dastane, 1978; de Silva & Rushton, 2007; Jensen *et al.*, 1997; Rushton *et al.*, 2006). The model-calculated actual evapotranspiration, irrigation demand and groundwater recharge values have been limitedly verified through comparison with previous work (e.g. Bekesi, 1998; Bekesi & McConchie, 1999; Zarour, 2008). The average results of the model are in general agreement with estimates reported in previous work, particularly with regards to the LMC SMB evapotranspiration estimates as compared to the results of the irrigation component of the Soil Plant Atmosphere System Model (SPASMO-IR) described in Green *et al.* (2004), White *et al.* (2010) and Green (2011).

The LMC SMB model-calculated surface water runoff values have not been validated against previous work or monitoring records. However, it can be said that the above noted basic verification of the other calculated parameters, namely, evapotranspiration and groundwater recharge, provides enough confidence that the model runoff estimates are overall reasonable.

Additional verification leading to possible enhancement of the model is recommended for future research. This can include calibration of the model against surface runoff measurements both on large and small-scales, calibration against actual measurements of soil moisture and water deep percolation, and comparison with outputs of other methods and software packages.

## Chapter 5 Hydrology

### 5.1 Introduction

Groundwater and surface water are a single resource (e.g. White *et al.*, 2001; Winter *et al.*, 1998). Therefore, hydrogeological investigations and modelling must account for surface water bodies that interact with the investigated groundwater resource.

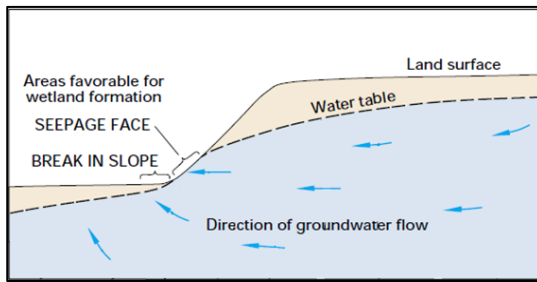
The interaction between groundwater and surface water can take different forms, change in time and from one place to another. Figure 5-1 shows possible relationships between groundwater and stagnant surface water bodies such as lakes and wetlands. Figure 5-2 illustrates possible relationships between groundwater and running surface waterways like rivers and streams. Figure 5-3 presents a method for determining stream-groundwater relationship using groundwater level contour maps.

Groundwater abstraction affects natural groundwater-surface water hydraulic balance. It can result in depleting surface water by pulling water from it through the tapped aquifer or by intercepting groundwater that otherwise would have flowed into the connected surface water body.

### 5.2 Springs, seeps, lakes and wetlands

There are seeps in the LMC, but they are not mapped and there are no distinct springs. The area contains a few small lakes and wetlands (Figure 5-4). Nevertheless, none is particularly important from a hydrological perspective. Where directly connected to groundwater, such features can help with water table mapping, hydrogeological conceptualisation and numerical model set up and calibration.

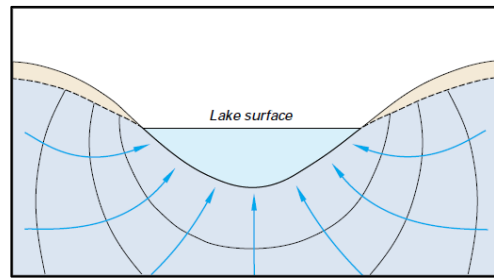
**Wetlands**



**(a) Fens**

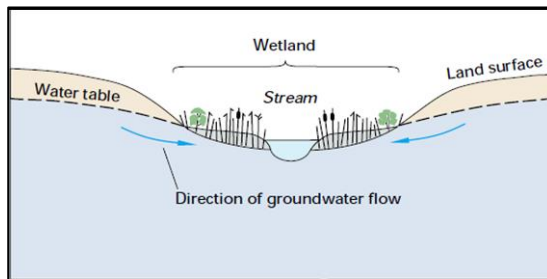
Fens are wetlands that commonly receive groundwater discharge; therefore, they receive a continuous supply of chemical constituents dissolved in the groundwater.

**Lakes**



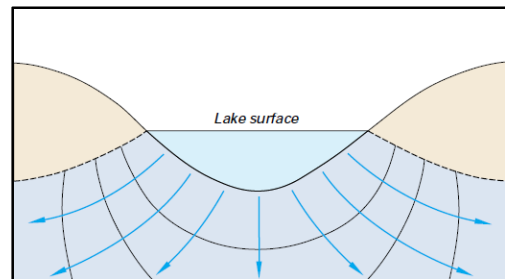
**(d) Gaining lake**

Groundwater level is higher than the lake water level. Hence, water moves from the aquifer into the lake.



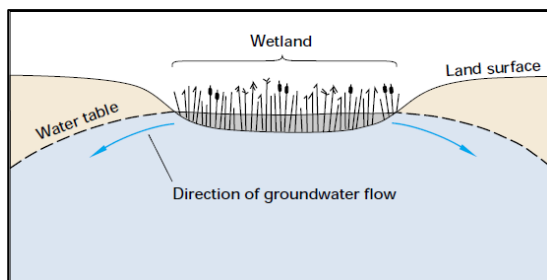
**(b) Riverine wetlands**

Many wetlands are present along streams, especially slow-moving streams. Although these riverine wetlands commonly receive groundwater discharge, they are dependent primarily on the stream for their water supply.



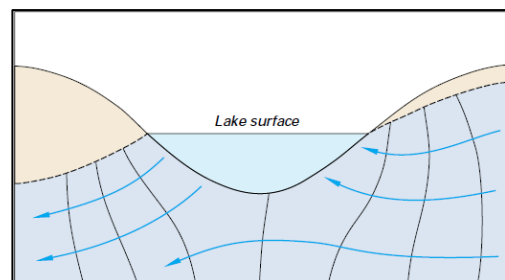
**(e) Losing lake**

Groundwater level is lower than the lake water level. Hence, water moves from the lake into the aquifer.



**(c) Bogs**

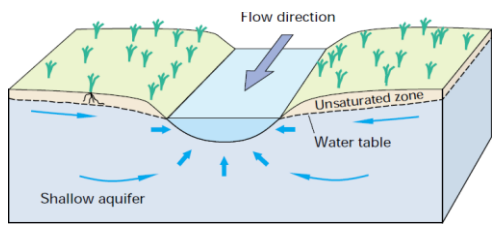
Bogs are wetlands that occupy uplands or extensive flat areas. They receive much of their water and chemical constituents from precipitation. They have the potential to affect groundwater quality.



**(f) Groundwater flow through lake**

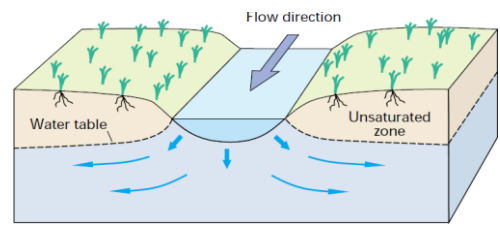
Groundwater level is higher than the lake water level in one side and lower in the other side. Hence, part of the groundwater moves in the aquifer from one side to the other through the lake.

Figure 5–1. Possible relationships between groundwater, wetlands and lakes (after Winter *et al.*, 1998).



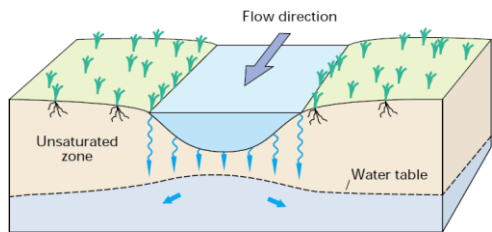
**(a) Gaining stream**

Gaining streams receive water from the groundwater system.



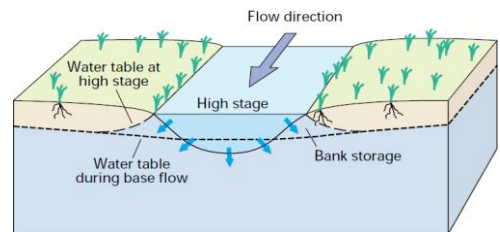
**(b) Losing stream**

Losing streams lose water to the groundwater system.



**(c) Disconnected stream**

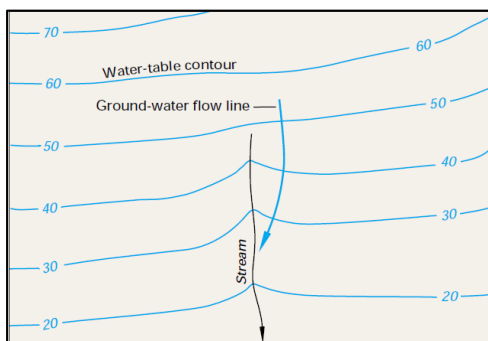
Disconnected streams are separated from the groundwater system by an unsaturated zone.



**(d) Stream bank storage**

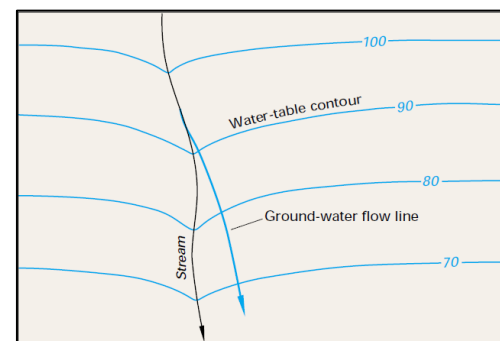
If stream levels rise higher than adjacent groundwater levels, stream water moves into the stream banks as bank storage.

Figure 5–2. Possible relationships between groundwater, rivers and streams (after Winter *et al.*, 1998).



**(a) Gaining stream**

Gaining streams (e.g. Figure 5–2a). The contour lines point in the upstream direction where they cross the stream.



**(b) Losing stream**

Losing streams (e.g. Figure 5–2b). The contour lines point in the downstream direction where they cross the stream.

Figure 5–3. Method for determining stream–groundwater relationship using groundwater level contour maps (after Winter *et al.*, 1998).

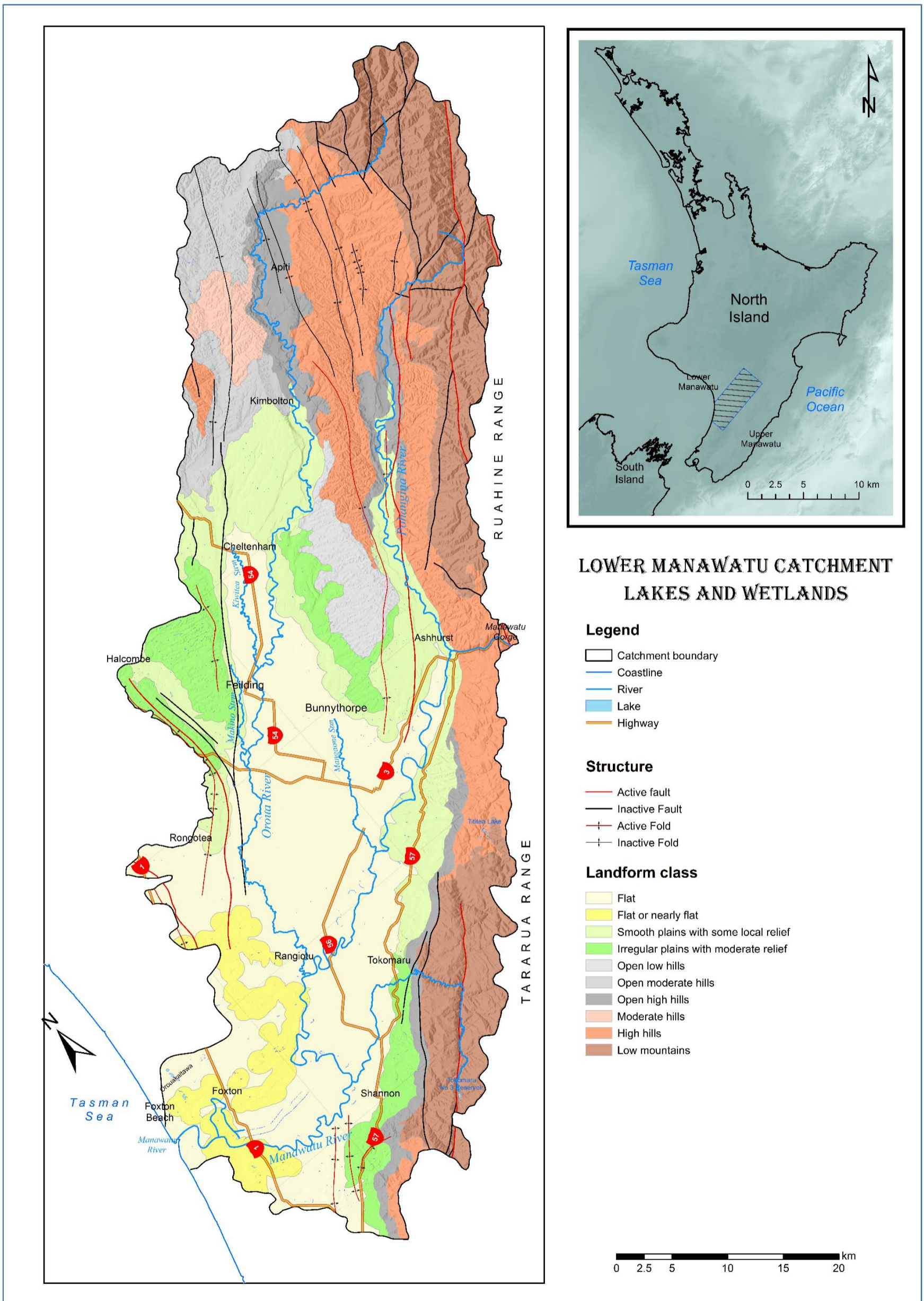


Figure 5-4. Lake distribution in relation to landforms and geological structure.

Lakes and wetlands in the LMC are small. Only 22 mapped lakes are larger than 2 ha in area. The dammed Turitea Lake is the largest in the LMC at about 11.5 ha. It is the main water source for Palmerston North. Tokomaru No 3 Reservoir (9.5 ha) is another relatively large dammed lake in the ranges. In the coastal area between Foxton Beach and Orouakaitawa, there is a north/south oriented line of relatively large wetlands/lakes (c. 5 – 10 ha) with smaller wetlands in between. The highest concentration of lakes coincides with anticlinal structures on the ‘irregular plains with moderate relief’ and to a lesser extent the ‘smooth plains with some local relief’ landforms identified in Section 3.9.4.

### 5.3 Rivers and streams

Figure 5–5 shows surface waterways in the LMC area that are in the order of 7 to 4 according to the New Zealand River Environment Classification (REC) system developed by the Ministry for the Environment. The REC system groups rivers of similar character across New Zealand according to factors such as climate, source of flow for the river water, topography, geology and catchment land cover.

### 5.4 Surface water monitoring and surveys

River flows monitoring in the study area started in the 1920s (Table 5–1). It has been carried out by Horizons Regional Council and its predecessors. In addition, flows and levels of some surface waterways in the LMC are monitored by NIWA and consent holders for compliance with their consent conditions (Roygard *et al.*, 2011). Figure 5–5 shows the monitoring sites in the area and Table 5–1 presents basic information and statistics for them.

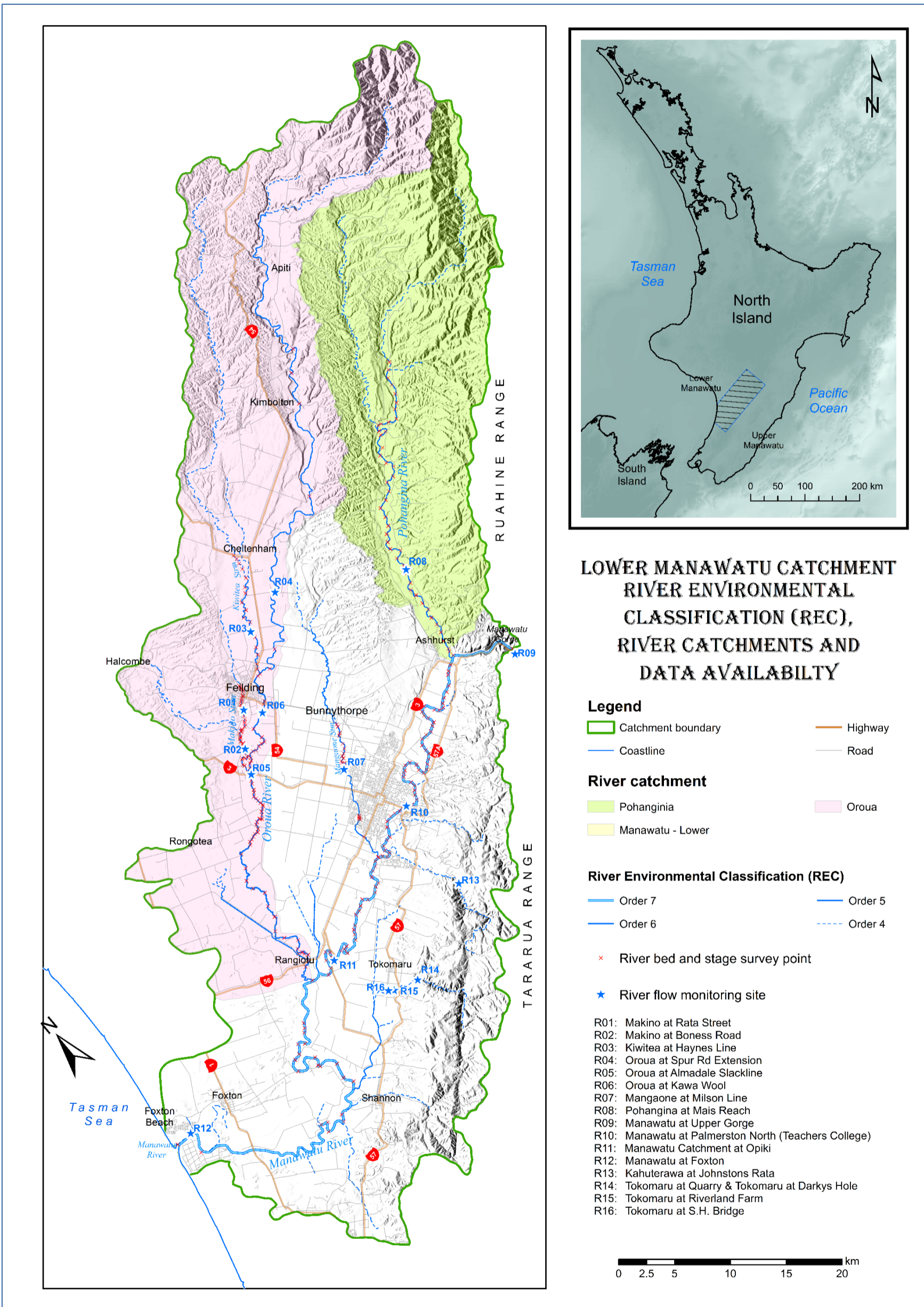


Figure 5-5. Environmental river classification (REC), river catchments and surface water data availability in the LMC.

Horizons Regional Council have also undertaken intermittent surveys of river bottom and stage elevation for main surface waterways in the LMC area over the period from 1/03/1990 to 21/12/2010 (Figure 5–5). The surveys have been undertaken in different seasons and under varying hydrometeorological conditions. Nevertheless, they can still be used to provide a general representation of the main surface waterways in the LMC for catchment–scale groundwater numerical modelling purposes.

## 5.5 Units and conventions

Commonly, surface water statistics are expressed in litres per second (L/s) or cubic metre per second ( $\text{m}^3/\text{s}$  or cumecs). Other units are also used to suit different purposes, e.g. Mega Litre per day (ML/day) are often used in water supply work and cumec–days (CMD) in the hydropower industry. In groundwater studies, however, units of metre (m), cubic metre ( $\text{m}^3$ ) and million cubic metre (mcm) per day (d) or year (y) are conventional for flow, and millimetre (mm) or metre per day or year are common place to express parameters like recharge and groundwater level fluctuation, which are usually expressed as depth. For the purpose of comparison of river flow to other catchment wide variables such as rainfall, evapotranspiration and groundwater recharge, it is more convenient to use depth of runoff – the mean flow divided by the catchment area upstream of the flow recording site in mm/time interval unit.

Table 5–1. Continuous river level and flow monitoring sites operated by Horizons and basic flow statistics<sup>34</sup>.  
(compiled from Horizons Regional Council data: Henderson & Dietrich, 2007; McArthur & Clark, 2007; Roygard *et al.*, 2011; Walter, 1990).

Label <sup>35</sup>	Site name	NZMG <sup>36</sup>		extent <sup>37</sup>			Mean			STDEV <sup>38</sup> (m <sup>3</sup> /s)	MALF <sup>39</sup> (m <sup>3</sup> /s)	MAF <sup>40</sup> (m <sup>3</sup> /s)	Median (m <sup>3</sup> /s)	½ Median (m <sup>3</sup> /s)	3x Median (m <sup>3</sup> /s)
		Easting	Northing	From	To	Years	(mcm/y) <sup>41</sup>	(m <sup>3</sup> /d)	(m <sup>3</sup> /s)						
R01	Makino at Rata Street	2727584	6105069	25/12/1986	31/12/2014	28	14.652	40,089	0.464	1.532	N/R <sup>42</sup>	N/R	0.113	0.056	0.339
R02	Makino at Boness Road	2725442	6102306	21/12/1991	31/12/2014	23	28.517	77,987	0.903	2.397	0.083	38.928	0.254	0.127	0.762
R03	Kiwiitea at Haynes Line	2732557	6110027	11/08/2005	18/06/2014	9	47.437	139,043	1.609	2.467	N/R	N/R	0.814	0.407	2.441
R04	Oroua at Spur Rd Extension	2736502	6111331	7/11/1976	22/10/1998	22	72.088	198,566	2.298	3.776	0.161	75.15	1.033	0.517	3.099
R05	Oroua at Almadale Slackline <sup>43</sup>	2724386	6100210	5/12/1947	31/12/2014	55	322.822	902,649	10.447	11.872	1.211	173.85	7.086	3.543	21.257
R06	Oroua at Kawa Wool	2728708	6103802	5/02/1967	11/03/2013	46	348.855	1,030,015	11.921	16.305	1.24	204.83	7.250	3.625	21.750
R07	Mangaone at Milson Line	2731033	6095220	15/04/1978	31/12/2014	37	28.445	77,741	0.900	2.940	N/R	N/R	0.192	0.096	0.577
R08	Pohangina at Mais Reach	2746789	6105350	12/06/1969	21/08/2014	45	533.088	1,473,686	17.057	24.633	2.315	489.99	10.320	5.160	30.960
R09	Manawatu at Upper Gorge	2749400	6093300	18/07/1979	31/12/2014	35	2,689.333	7,397,436	85.618	106.875	11.703	1237.2	53.340	26.670	160.020
R10	Manawatu at Palmerston North (Teachers College)	2733214	6089133	1/01/1926	31/12/2014	88	3,604.899	9,957,232	115.246	136.854	15.735	1518.9	73.690	36.845	221.070
R11	Manawatu Catchment at Opiki <sup>44</sup>	2719380	6082696	3/01/1980	31/12/2014	34	3,359.651	9,282,246	107.433	132.033	15.9	1508.4	68.770	34.385	206.310
R12	Manawatu at Foxton <sup>45</sup>	2699600	6079100	3/01/1980	31/12/2014	34	3,858.824	10,661,945	123.402	148.733	N/R	N/R	80.285	40.143	240.855
R13	Kahuterawa at Johnstons Rata	2732351	6080805	30/04/2005	31/12/2014	9	51.332	139,870	1.619	2.354	N/A	N/R	0.963	0.481	2.889
R14	Tokomaru at Quarry & Tokomaru at Darkys Hole <sup>46</sup>	2723992	6076569	15/12/1979	22/05/2004	25	72.815	204,885	2.371	3.354	0.247	98.882	1.330	0.665	3.990
R15	Tokomaru at Riverland Farm	2721769	6077190	6/08/2009	31/12/2014	5	69.560	201,267	2.329	3.276	N/R	N/R	1.339	0.670	4.017
R16	Tokomaru at S.H. Bridge	2721362	6077502	13/01/2005	11/01/2006	2	42.361	116,057	1.343	1.383	N/R	N/R	0.949	0.475	2.848

<sup>34</sup> Unnormalised (denormalised) flows.

<sup>35</sup> Site label in Figure 5–5.

<sup>36</sup> NZMG: New Zealand Map Grid coordinate system. Approximate position.

<sup>37</sup> Data obtained from Horizons Regional Council extend from start of record to the end of 2014.

<sup>38</sup> STDEV: Standard deviation.

<sup>39</sup> MALF: Mean annual low flow.

<sup>40</sup> MAF: Mean annual flood.

<sup>41</sup> Annual flow calculated as the sum of daily flows and thereafter averaged over record length.

<sup>42</sup> N/R: Not reported.

<sup>43</sup> Record discontinued between 31/01/1979 and 2/08/1992.

<sup>44</sup> Synthetic record.

<sup>45</sup> Synthetic data, discarding tide effects.

<sup>46</sup> Tokomaru at Quarry record from 15/12/1979 to 23/02/1998, Tokomaru at Darkys Hole record from 13/02/1998 to 22/05/2004.

## 5.6 Hydrological statistics

Henderson and Diettrich (2007) documented flow statistics for Horizons and NIWA sites that have continuous flow records with an emphasis on low flow parameters. They note that flow measurements are commonly recorded at a short time interval of the order of 15 minutes. They consider that at least 10 year, preferably 20-year, long record is needed to allow the compilation of reliable flow statistics for a site comparison to other sites. They suggest that hydrological time-series can be initially defined by a short list of useful statistics that seeks defining the flow magnitude, its variability, and uncertainty. The various parameters in Henderson and Diettrich (2007) short list of flow statistics are described in Sections 5.7– 5.9.

## 5.7 General flow statistics

### 5.7.1 Mean flow

Mean flow is arguably the most important and commonly used statistical descriptor of river flow. Graphically, it is the area under the river flow hydrograph divided by the length of the hydrograph. Appendix B graphically presents yearly and monthly total and average flows for the sites noted in Figure 5-5 and Table 5-1 that have sufficient record.

In average, the LMC receives about 2,689 mcm/y of water from the upper catchment through the Manawatu Gorge and discharges about 3,859 mcm/y of water into the Tasman Sea (Table 5-1). Hence, the overall depth of runoff over the LMC area can be estimated to be c. 437 mm/y, compared to 315 mm/y as calculated from SMB modelling (Table 4-7). The difference between the two estimates (327 mcm/y or 122 mm/y) could be related to one or a combination of the following possibilities:

1. Failure to account for soil infiltration and storm characteristics in SMB calculations due to lack of data
2. Exaggerated soil thickness (1 m) assumed in SMB calculations (Section 4.7), resulting in underestimation of runoff (Table 4-7)

3. Overestimation of river discharge to the sea in the synthetic data for the Manawatu at Foxton site (Table 5–1)
4. Gauging inaccuracies in estimating flows at the Manawatu Gorge
5. Mean flows are calculated for different periods
6. Surface waterways gains from groundwater (Sections 5.9.2 and 5.12)
7. Unaccounted for effects of interflow in the LMC SMB model
8. Exclusion of drains from the water balance and numerical model calculations due to lack of data and perceived insignificance in regional–scale analysis.

Both surface runoff estimates represent unnormalised flow as they do not account for abstraction. Total surface water abstraction in the LMC (Section 5.11) is very small compared to the overall amounts of water in the catchment. Hence, surface water abstraction can be ignored in catchment–scale water budget calculations.

### 5.7.2 Median flow

Henderson and Diettrich (2007) define median flow as the flow that is equalled or exceeded half the time over the period of analysis. It is different from mean flow because river flow is not a normally distributed quantity. Henderson and Diettrich (2007) note that rivers in the area spend only about 30% of the time above the mean (standard deviation 5%), but these flows can be very large. Flows below the mean are bounded by zero as a lower limit.

## 5.8 Flow variability

The LMC is situated on the western side of the North Island, where variability is expected to be low relative to areas on the eastern side of the island (Henderson & Diettrich, 2007).

### 5.8.1 Yearly variability

Year to year variability in flow can be captured by use of annual average flows and their spread measured by a statistic such as standard deviation or coefficient of variation (standard deviation divided by the mean). Yearly flow variability at monitoring sites in the LMC can be noticed in the figures in Appendix B. Figure

5–6 presents flow variability percentiles for selected surface waterways as reported by Henderson and Diettrich (2007).

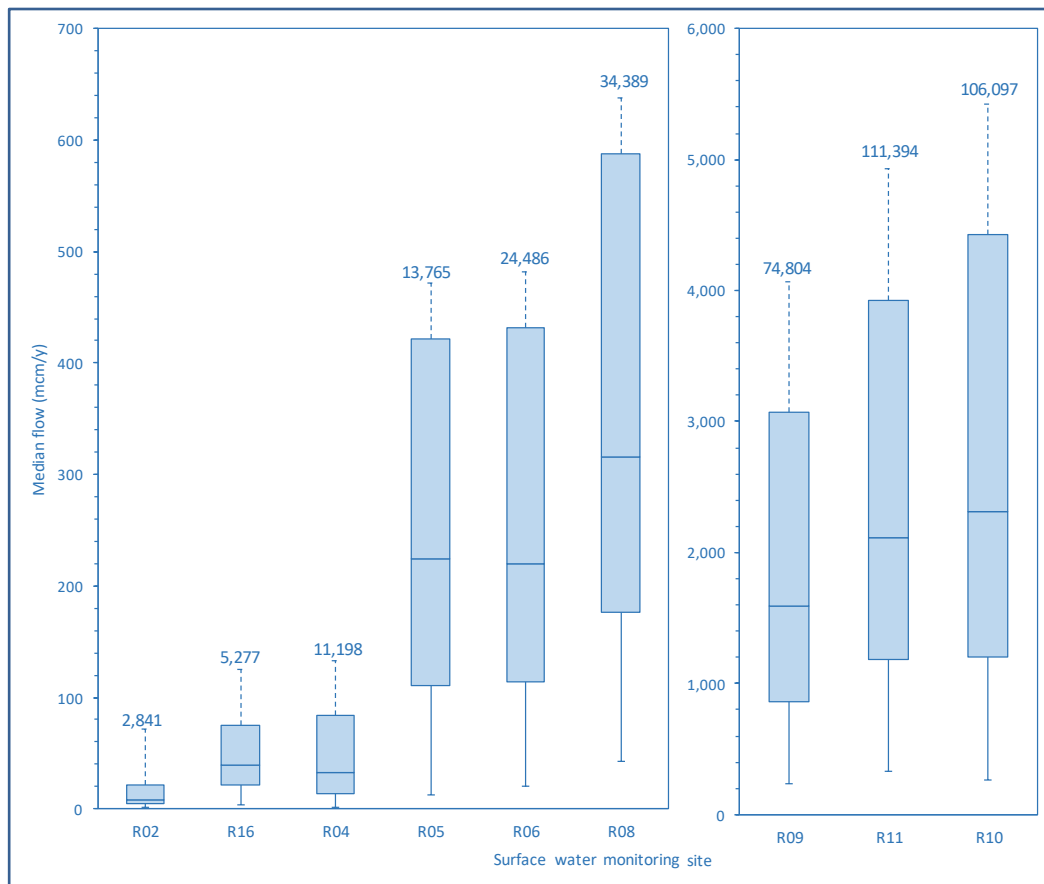


Figure 5–6. Flow variability percentiles for selected surface waterways (data from Henderson & Diettrich, 2007).

Surface water monitoring site locations are shown in Figure 5–5. Maximum flows are shown as numbers to enable showing other values in a reasonable scale. The low whisker extents show minimum flows. The tops and bottoms of the boxes represent the 75<sup>th</sup> and 25<sup>th</sup> percentiles, respectively. The lines in the middle of boxes represent medians

### 5.8.2 Seasonal variability

Graphical presentation of the distribution of monthly mean flows provides a measure of seasonal variability. Year to year variability of seasonal behaviour may be assessed by considering each month in turn, and calculating the quartiles, flow values that are equalled or exceeded one quarter and three quarters of the time (Henderson & Diettrich, 2007). Monthly flow variability at monitoring sites in the LMC can be noticed in the figures in Appendix B.

### 5.8.3 Flow distribution

Temporal flows distribution can be expressed as a range (maximum – minimum) or alternatively the inter–quartile range, which is less affected by extremes of floods and droughts. Flow distribution can also be used to examine seasonal flow variability on a monthly basis. A more detailed presentation of flow distribution is the flow duration curve (FDC). This curve plots each flow against the percentage of time that that flow is equalled or exceeded in the time period being analysed (e.g. Figure 5–7).

## 5.9 Flow extremes

High flows and low flows could be characterised in several ways; by the top and bottom 5%–10% of the FDC, by some multiple or fraction of the mean flow or median, or by use of extreme value sampling (low flows and floods).

### 5.9.1 Mean annual flood

Mean annual flood (MAF) is the average of the highest instantaneous flow measurement from each year. In New Zealand, the definition of a water year (Section 4.6.4) is generally not as important for floods as it is for the mean annual low flow calculations (Henderson & Diettrich, 2007). The magnitude of disturbance can be expressed as the ratio of MAF to mean and low flow. These ratios allow comparison between sites, and relate to the gradient of river environment from benign (low ratios) to harsh (high ratios). Mean annual flood values adopted in Table 5–1 from Henderson and Diettrich (2007) were calculated on a calendar year rather than a water year.

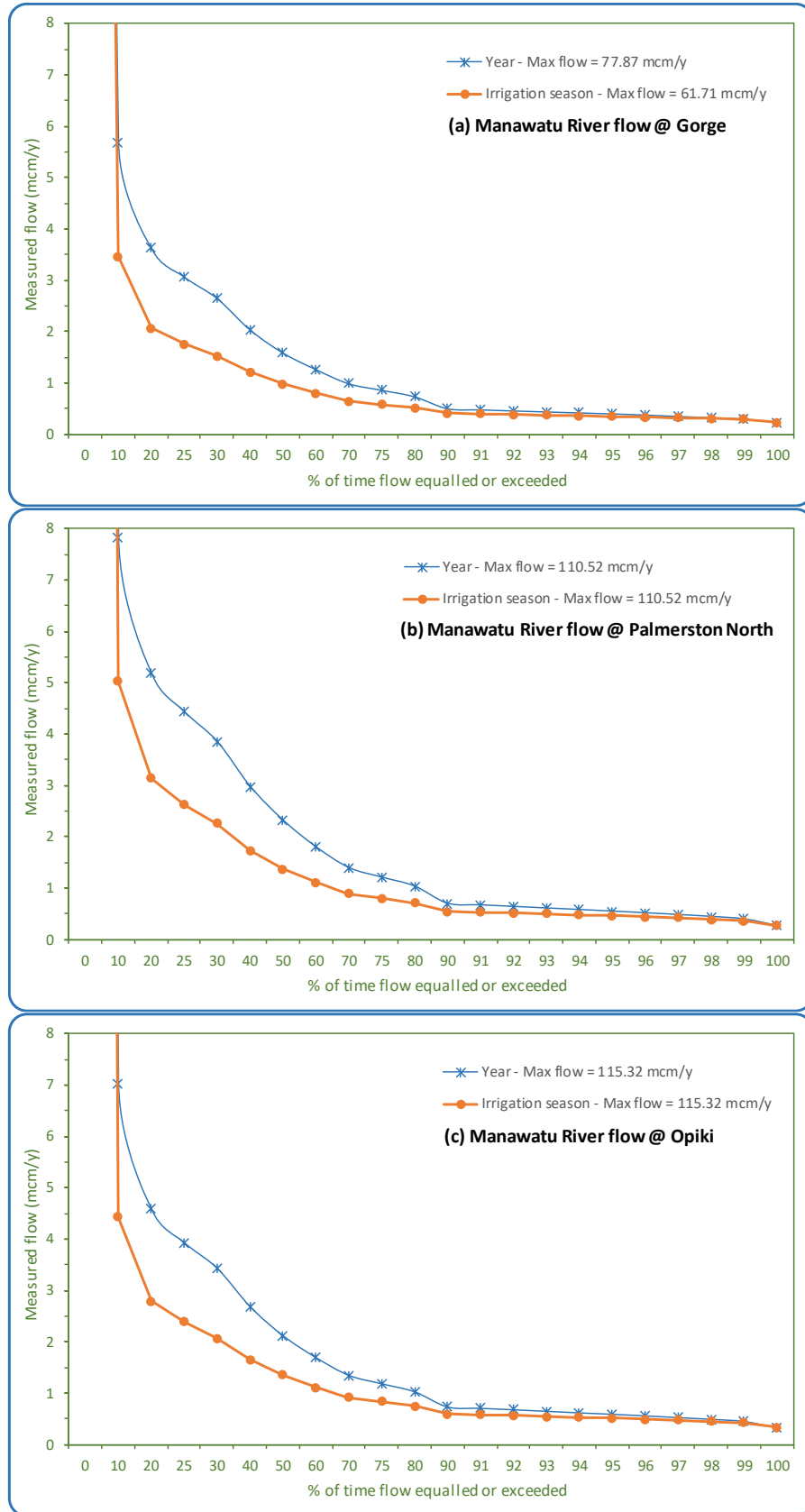


Figure 5–7. Flow duration curve (FDC) for the Manawatu River at three locations in the LMC showing percentage of time flows are equalled or exceeded (data from Henderson & Diettrich, 2007).

### 5.9.2 Mean annual low flow

Mean annual low flow (MALF) is the average of the lowest flow measured in each year of record. MALF values adopted in Table 5–1 from Henderson and Diettrich (2007) were calculated on water year (Section 4.6.4) to avoid the possibility of biasing the sample by summer time low flows, which can span two calendar years. Low flows can be taken as instantaneous flows or as moving means over a range of averaging intervals. Henderson and Diettrich (2007) low flow calculations use a one-day interval for reasons relating to surface water consents and abstractions.

### 5.10 Surface water–groundwater interaction

There are no concurrent surface water gauging data to enable identification of losses and gains from rivers and streams in the LMC. Regional-scale average groundwater level contour maps by Bekesi (2001) and Zarour (2008) suggest that most of the area's rivers and streams gain from groundwater. This is consistent with the conceptualisation by Russell (1989) of the area as a regional groundwater discharge zone. Figure 5–8 conceptually presents the main elements of the surface water network in the area using mean annual flows. From the figure, the following can be deduced:

1. Makino Stream is a gaining waterway.
2. Oroua River gains flow until it is joined by the Makino Stream near Almadale Slackline (Site R05), where it starts losing flow but at a relatively small rate
3. The Manawatu River gains flow from groundwater between the Manawatu Gorge and its confluence with the Kahuterawa Stream. Then it loses water in the area where it meanders in the general Opiki area. A small distance downstream from the flood gates, the river returns to gaining flow from groundwater.
4. Tokomaru River loses water along its length.

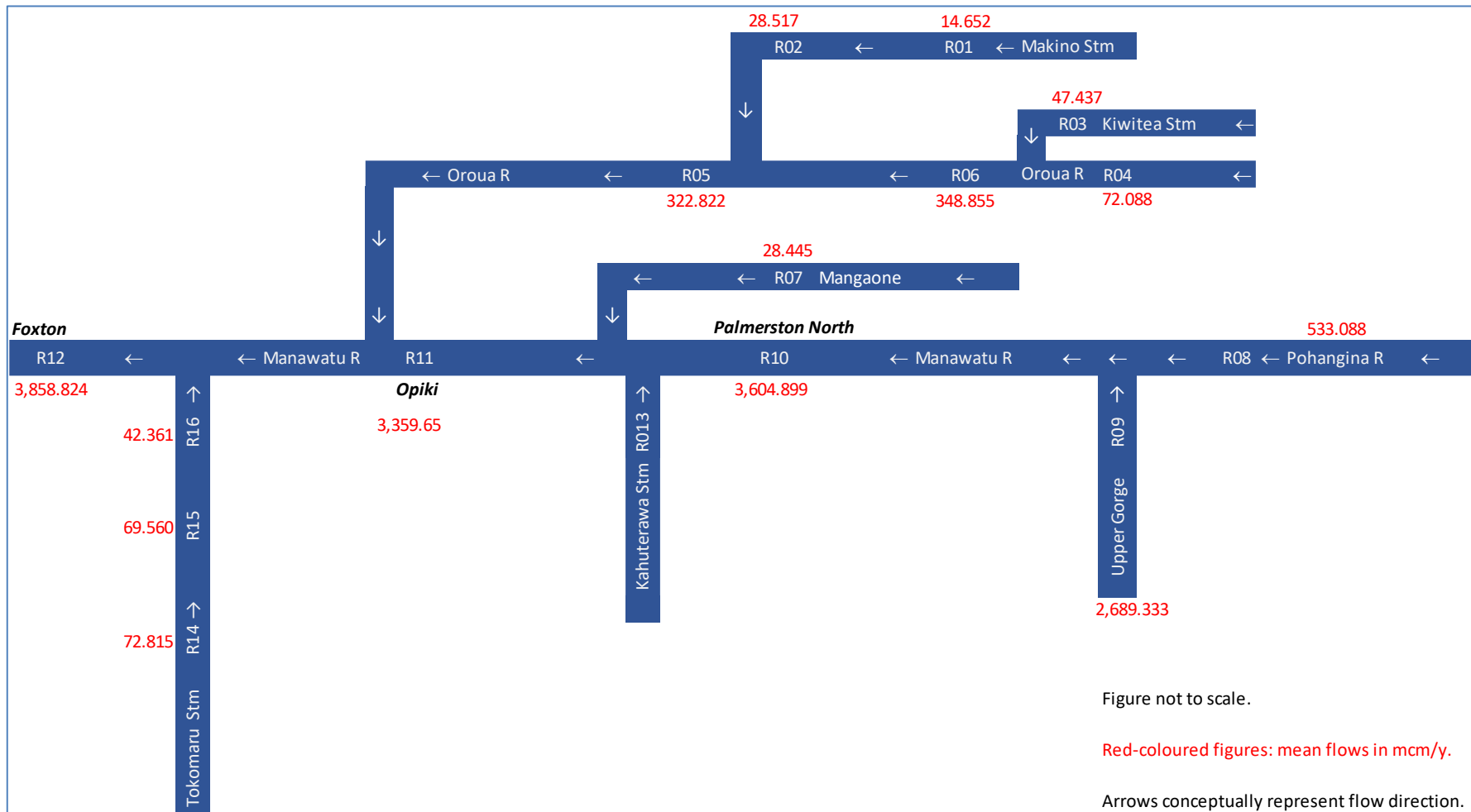


Figure 5–8. Conceptual presentation of main rivers and streams and their mean annual flows.

### 5.11 Surface water abstraction

Data to enable reliable and accurate assessment of surface water abstraction and use are lacking in the LMC. Water abstraction resource consents data were obtained from Horizons. This data set required tedious manual manipulation to structure it in a format that is usable to roughly estimate surface water takes. During the period 2010–2015, there were around 63 active surface water consents that allow the abstraction of up to 71 mcm of water per year (Table 5–2). In the absence of other data, it is assumed that all consented volumes are taken and that the period 2010–2015 represents long-term average conditions.

Table 5–2. Consented surface water takes active during the period 2010–2015.

Water use	Number of consents	Consented volume (m <sup>3</sup> /y)
Drinking	6	17,613,440
Stock	11	1,260,820
Industrial	8	3,188,645
Irrigation	38	48,931,071
<b>Total</b>	<b>63</b>	<b>70,993,976</b>

### 5.12 Catchment water budget

The Manawatu River is the only surface water feature in the LMC that discharges directly to the Tasman Sea. The river drains the Upper Manawatu Catchment (c. 3,205 km<sup>2</sup>) into the LMC (c. 2,678 km<sup>2</sup>) through the Manawatu Gorge at a mean rate of about 2,670 mcm/y (Table 5–1 and Figure 5–8). Along its course from the Gorge to the Tasman Sea, the Manawatu River is joined to the southeast of Ashhurst by the Pohangina River which in average adds 533 mcm/y of flow to the Manawatu River. The Oroua River joins the Manawatu River to the south of Rangiotu, adding in average 323 mcm/y to the Manawatu River flow. The Manawatu, Pohangina and Oroua rivers are joined by a number of smaller surface waterways, the most important of which are Mangaone, Makino and Kiwitea streams.

In general terms, the LMC water budget can be expressed as follows:

$$\Delta S = P + G_{in} + Q_{in} - ET - G_{out} - Q_{out} - A_g - A_s \quad 5-1$$

where  $\Delta S$  is the change in storage,  $P$  is precipitation,  $G_{in}$  is groundwater inflow,  $Q_{in}$  is surface water inflow,  $ET$  is evapotranspiration,  $G_{out}$  is groundwater outflow,  $Q_{out}$  is surface water outflow,  $A_g$  is groundwater abstraction and  $A_s$  is surface water abstraction.

To solve Eq. 5-1 for long-term average conditions, we assume steady-state. Under steady-state conditions, storage does not change, i.e.  $\Delta S = 0$ . There is no groundwater inflow into the LMC, i.e.  $G_{in} = 0$  and all other terms in Eq. 5-1 except groundwater discharge to the sea ( $G_{out}$ ) can be reasonably estimated. Hence, we can use Eq. 5-1 to estimate  $G_{out}$  as shown in Table 5-3.

Table 5-3. LMC water balance parameters.

Parameter	value (m <sup>3</sup> /y)	source
Precipitation ( $P$ )	3,175,246,459	Table 4-7
Flow through the Manawatu Gorge ( $Q_{in}$ )	2,700,064,140	Table 5-1
Evapotranspiration ( $ET$ )	1,602,965,266	Table 4-7
River discharge to the Tasman Sea ( $Q_{out}$ )	3,891,609,925	Table 5-1
Groundwater abstraction ( $A_g$ )	53,019,173	Zarour (2008)
Surface water abstraction ( $A_s$ )	70,993,976	Section 5.11
Groundwater discharge to the Tasman Sea ( $G_{out}$ )	256,722,259	Calculated
Groundwater contribution to surface water flow	434,337,886	$RCH - A_g - G_{out}$

While Table 4-7 estimates groundwater recharge at about 744 mcm/y, Table 5-3 estimates total groundwater outputs at about 257 mcm/y. The difference between groundwater inputs ( $RCH$ ) and outputs ( $A_g + G_{out}$ ) represents the overall groundwater contribution to surface water flow (base flow) throughout the LMC area, estimated at about 434 mcm/y (Table 4-7). So, baseflow accounts for about 11% of the total surface water discharge to the Tasman Sea, which is the equivalent to about 58% of the total groundwater recharge in the LMC.

## Chapter 6 Hydrogeology

### 6.1 Introduction

This chapter utilises information presented in the previous chapters and new data to draw a picture of groundwater in the LMC in terms of its occurrence and movement, the hydraulic characteristics of the host geological material, groundwater flow pattern, and groundwater interaction with other components of the hydrological cycle.

### 6.2 Hydrogeological classification of geological material

The ability of earth material to absorb and allow the movement of water has long been regarded as the most important aspect in hydrogeological studies. Accordingly, geological units are classically classified in terms that reflect their competence as water-bearing media. Literature defines an ‘aquifer’ as a saturated permeable geological unit that is capable of transmitting significant quantities of water under ordinary hydraulic gradients (e.g. Fetter, 2013; Freeze & Cherry, 1979). Contrastingly, an ‘aquifuge’ is an unsaturated impermeable geological unit which neither absorbs nor transmits water. An ‘aquiclude’ is a term used to describe a saturated geological unit that cannot transmit significant quantities of water under ordinary hydraulic gradients. The term ‘aquitard’ is used to describe the less-permeable zones in a stratigraphical sequence where strata may not be permeable enough to provide water to wells screened within them but still can transmit water in quantities that are significant in the long-term and/or at large-scale. Geological material that qualify to be described as aquifuge are normally considered hydrogeological basement or flow barrier (e.g. the bulk of the Torlesse greywacke basement rock throughout New Zealand). Most other geological strata are classified as either aquifers or aquitards and only very few units fit the strict definition of an aquiclude. As a result, there is a trend toward the use of the first two of these terms at the expense of the third (Freeze & Cherry, 1979). As the terms aquifer and aquitard are imprecise with respect to hydraulic conductivity,

these terms could be used in a relative sense. For example, silt strata in an interlayered sand–silt sequence may be considered aquitards, whereas we may consider them locally important aquifers in a silt–clay system. Table 6–1 presents typical ranges of hydraulic conductivity for the most common rocks and sediments in the world.

Table 6–1. Typical Hydraulic conductivity values for selected rocks and sediments (compiled from Bear, 1972; Heath, 1983; Younger, 2007).

$K$ (m/d)	$10^5$	$10^4$	$10^3$	$10^2$	10	1	$10^{-1}$	$10^{-2}$	$10^{-3}$	$10^{-4}$	$10^{-5}$	$10^{-6}$	$10^{-7}$
Relative permeability	Pervious				Semi-pervious			Impervious					
Aquifer potential	Good				Poor			None					
Unconsolidated sand & gravel	Well sorted gravel		Well sorted sand or sand & gravel		Very fine sand, silt, loess, loam				Local loess				
Unconsolidated clay and organic					Peat		Layered clay		Fat/unweathered clay				
Consolidated rocks	Highly fractured rocks, karstic rocks and rocks with caves				Conglomerate, sandstone			Fresh limestone, dolomite		Greywacke, fresh granite			

### 6.3 Hydrolithostratigraphical setting

Building on the account of stratigraphy presented in Section 3.10, four main hydrolithostratigraphical units can be defined in the LMC:

1. Basement rocks: Permian–Early Cretaceous (mostly Triassic) indurated impervious rocks
2. Plio–Pleistocene marine rocks: poorly consolidated, predominantly marine sediments
3. Middle–Late Pleistocene unconsolidated terrestrial and marine deposits
4. Holocene alluvium and sands.

#### 6.3.1 Greywacke basement rocks

This unit of commonly deformed, indurated sandstone with mudstone and other material interbeds lacks intrinsic and secondary permeability (aquifuge), except perhaps the weathered top few metres. Water in the weathered part of these rocks will evaporate and/or run into the nearest surface water drainage feature. These rocks constitute the hydrogeological basement for the LMC groundwater system and form its true left side boundary.

### 6.3.2 Plio–Pleistocene marine rocks

The Wanganui Basin in which the LMC lies is filled with up to more than 4 km of Plio–Pleistocene sediments. These strata dip to the southeast and are predominantly marine, but the Pleistocene Epoch part of the unit is characterised by alternating terrestrial and marine sequence corresponding to deposition during cold and warm periods, respectively.

The Plio–Pleistocene sequence in the LMC comprises interbeds of limestones, massive and sandy mudstones, carbonaceous and non-carbonaceous siltstones, pumiceous and non-pumiceous sandstones, and shallow water conglomerate with some lignite and shell beds. Castlecliffian stage strata of the Wanganui epoch represent the topmost part of this hydrogeological unit, which crops out in the upper part of the LMC where the unit is incised by the Oroua and Pohangina rivers, splitting them into three northeast–southwest aligned elongated chunks. These outcrop batches are longest near the ranges at the real left of the catchment, but they become shorter in the middle of the catchment and at its true right edge. In the lower part of the LMC, younger Quaternary deposits overlie the Plio–Pleistocene sequence. Overall, Plio–Pleistocene marine sediments are characterised by low to very low permeability that renders them as aquitard or aquiclude strata. However, they form an important regional recharge area for the LMC groundwater flow system (Figure 3–16 and Figure 4–18).

### 6.3.3 Middle–Late Pleistocene strata

Late Pleistocene (c. 340–12 ka BP) sediments in the LMC incorporate three main types of lithologies:

- (1) alluvium: gravelly river alluvium deposited in cold periods, moderately sorted, extensive areal coverage, up to 10s of metres thickness, gentle dip, high to very high hydraulic conductivity
- (2) beach sand: marginal marine sediment deposited in warm periods, extensive areal coverage, up to 10s of metres thickness, gentle dip, moderate hydraulic conductivity

- (3) fan and landslide deposits: thin, poorly sorted, angular alluvial and colluvial deposits on steep slopes, limited areal coverage, low hydraulic conductivity, deposited in cold periods.

The terraced setting of the Middle–Late Pleistocene terrestrial and marine sediments in the LMC can affect groundwater flow in the area (Figure 6–1). In addition, many of these terraces are overlain by loess of variable thickness, potentially limiting their ability to receive recharge from rain.

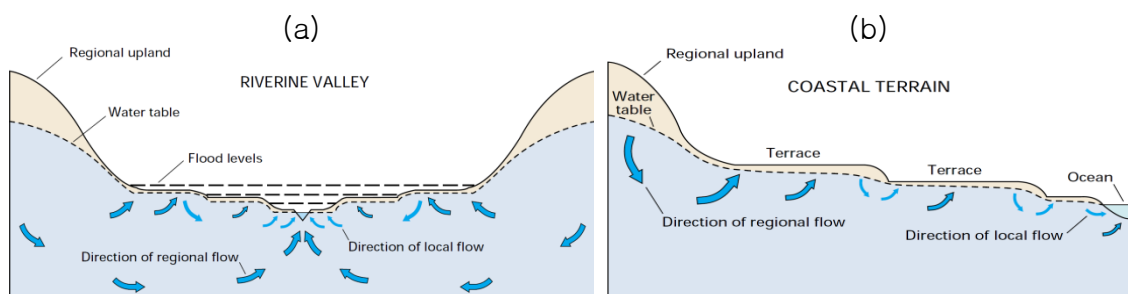


Figure 6–1. Effect of terraces on groundwater flow (after Winter *et al.*, 1998).

- (a) In broad river valleys, small local groundwater flow systems associated with terraces overlie more regional groundwater flow systems. Recharge from flood waters superimposed on these groundwater flow systems further complicates the hydrology of river.
- (b) In coastal terrain, small local groundwater flow cells associated with terraces overlie more regional groundwater flow systems. In the tidal zone, saline and brackish surface water mixes with fresh groundwater from local and regional flow systems.

#### 6.3.4 Holocene alluvium and sands

Various types of Holocene age sediment occur in the LMC, including alluvium (Q1a), dune sands (Q1ds and Q1dm), alluvium fan (Q1f), and colluvium sediments (Q1l). The latter two lithologies are both limited in extent and thickness (Figure 3–2 and Table 3–1). Hence, they can be ignored in catchment–scale hydrogeological assessments.

The Holocene alluvium is characterised by high to very high permeability and occupy the lowest areas in the LMC. Hence, they are expected to exhibit unconfined aquifer conditions and a high level of groundwater–surface water

interaction. However, their limited thickness may constrain their usability as an aquifer.

Loose, windblown Holocene sands in active and inactive dunes in the lower part of the LMC enjoy moderate to high permeability (Table 6–1). Inter–dune swamps in this area would most probably represent the water table.

## 6.4 Aquifer properties

In hydrogeology, geological materials are characterised by their hydraulic conductivity ( $K$ ) and specific yield ( $S_y$ ). Aquifers however are characterised by transmissivity ( $T$ ) and Storativity ( $S$ ). Transmissivity is a measure of the amount of water that can be transmitted horizontally by a full saturated thickness of aquifer. It is calculated as the product of the hydraulic conductivity by the aquifer thickness ( $T = Kb$ ) and conveniently expressed in  $m^2/d$  units. Storativity is a measure of the volume of water that a permeable unit will absorb or expel from storage per unit surface area per unit change in hydraulic head (dimensionless,  $<1$ ). In confined aquifers, storativity is termed storage coefficient and typically ranges between  $5 \times 10^{-5}$  and  $5 \times 10^{-3}$ . Storativity of unconfined aquifers is defined as the specific yield ( $S_y$ ) and typically ranges between 0.01 and 0.3 (Kruseman & de Ridder, 1991).

There are several methods to evaluate aquifer properties including laboratory measurements, pumping and slug tests, geophysical methods and lithological analysis. Aquifer properties data sources in the LMC are limited to grain–size distribution and pumping test records.

### 6.4.1 Grain–size distribution analysis

Svensson (2014) studied methods for the estimation of hydraulic conductivity from grain–size analysis and compared them to laboratory and in–situ methods. She found little difference in results obtained from various hydraulic conductivity estimation methods from grain–size data when applied to well–sorted soils. However, the differences reach several orders of magnitude when dealing with poorly–sorted samples, i.e. soils with large uniformity coefficient ( $C_U$ ). Uniformity

coefficient is calculated as  $D_{60}/D_{10}$ , where  $D_{60}$  is the particle size for which 60% of the material is finer and  $D_{10}$  is the particle size for which 10% of the material is finer, in consistent units. Material with  $C_U$  less than 3 is considered well sorted (uniform),  $C_U$  values between 3 to 5 indicate nonuniform material and  $C_U$  greater than 5 is indicative to highly nonuniform material.

Cooper (1999) reports on grain-size distribution analysis for 15 samples believed to be from the Last Interglacial marginal marine sand unit (Q5b) between Palmerston North to the Manawatu Gorge. Grain-size distribution plots in Cooper (1999) have been used to evaluate hydraulic conductivity using the Hazen and Gustafson methods (Table 6-2). According to Svensson (2014), the Hazen equation can be written as:

$$K = C_H D_{10}^2 \quad 6-1$$

where  $K$  = hydraulic conductivity [m/s],  $C_H$  = empirical constant set to 0.01157 in Svensson (2014), and  $D_{10}$  = the particle size for which 10% of the material is finer [mm].

Svensson (2014) presents the Gustafson equation in the form:

$$K = E(C_U) \left( \frac{D_{10}}{1000} \right)^2 \quad 6-2$$

Table 6–2. Hydraulic conductivity calculations based on grain–size distribution data reported in Cooper (1999).

Cooper (1999) description			Grain–size distribution data			Hazen $K$ (m/d)	Gustafson				Hazen: Gustafson
Sample	Mean Size	Sorting	$D_{10}$	$D_{60}$	$C_u$		$g(CU)$	$E$	$E(CU)$	$K$ (m/d)	
1. Dairy 1	Fine sand	Extremely poorly sorted	0.100	0.180	1.80	9.9965	3.96	0.23	6,760.99	5.8415	1.71
2. Dairy 3	Fine sand	Very poorly sorted	0.100	0.200	2.00	9.9965	3.72	0.24	8,579.71	7.4129	1.35
3. Dairy 5	Coarse silt	Extremely poorly sorted	0.001	0.060	60.00	0.0010	1.66	0.10	3,127.34	0.0003	3.70
4. ANZAC 1	Coarse silt	Extremely poorly sorted	?	0.025	?	?	?	?	?	?	?
5. ANZAC 4	Fine sand	Extremely poorly sorted	0.080	0.150	1.88	6.3977	3.86	0.24	7,511.22	4.1534	1.54
6. ANZAC 8	Fine sand	Very poorly sorted	0.020	0.230	11.50	0.3999	1.98	0.16	8,548.40	0.2954	1.35
7. ANZAC 9	Fine sand	Very poorly sorted	0.030	0.230	7.67	0.8997	2.17	0.18	10,539.28	0.8195	1.10
8. ANZAC 11	Medium sand	Moderately sorted	0.300	0.650	2.17	89.9683	3.56	0.25	9,708.65	75.4945	1.19
9. Burgess 1	Fine sand	Extremely poorly sorted	0.030	0.160	5.33	0.8997	2.41	0.20	12,115.65	0.9421	0.95
10. Burgess 3	Fine sand	Very poorly sorted	0.080	0.160	2.00	6.3977	3.72	0.24	8,579.71	4.7442	1.35
11. Forest Hill 1	Medium sand	Extremely poorly sorted	0.001	0.850	850.00	0.0010	1.71	0.06	686.51	0.0001	16.85
12. Forest Hill 4	Fine sand	Extremely poorly sorted	0.010	0.100	10.00	0.1000	2.04	0.16	9,228.19	0.0797	1.25
13. Tuapaka 4	Fine sand	Extremely poorly sorted	0.050	0.180	3.60	2.4991	2.79	0.23	12,785.03	2.7616	0.90
14. Tuapaka 10	Fine sand	Very poorly sorted	0.001	0.160	160.00	0.0010	1.63	0.08	1,745.10	0.0002	6.63
15. Tuapaka 3	Medium sand	Extremely poorly sorted	0.010	0.180	18.00	0.1000	1.84	0.14	6,568.98	0.0568	1.76

According to Svensson (2014), the function  $E(C_U)$  is expressed through the following connections:

$$E(C_U) = 10.2 \times 10^6 \left( \frac{E^3}{1 + E} \right) \left( \frac{1}{g(C_U)^2} \right) \quad 6-3$$

$$E = 0.8 \left( \frac{1}{2 \ln(C_U)} \right) - \left( \frac{1}{C_U^2 - 1} \right) \quad 6-4$$

$$g(C_U) = \left( \frac{1.3}{\log_{10} C_U} \right) \left( \frac{C_U^2 - 1}{C_U^{1.8}} \right) \quad 6-5$$

Hydraulic conductivity estimates from grain-size distribution data using the Hazen and Gustafson equations presented in Table 6-2 fall within the expected range for sand and poorly sorted sand with gravel as depicted in Table 6-1. However, the results presented in Table 6-2 show that the difference between the Hazen and Gustafson equations hydraulic conductivity estimates are proportionally related to uniformity coefficients. Since poor sorting reduces effective porosity and permeability, Gustafson equation results may provide more realistic results for the tested samples.

#### 6.4.2 Pumping tests

Pumping test data are useful for aquifer typifying and evaluation of aquifer parameters, particularly transmissivity ( $T$ ) and storativity ( $S$ ). There are records of quite a few pumping tests in the LMC. The tests are a mix of constant discharge rate and step-drawdown types, and some have recovery data.

It has been chosen not to use aquifer test data in this research for the following reasons:

1. Pumping test data are not readily available from Horizons Regional Council.
2. Most pumping test records at Horizons are saved in digital format that require dated proprietary software that is not available to the author of this thesis.

3. From the author's experience, having worked at Horizons Regional Council from 2004 to 2011, most pumping tests undertaken in the LMC severely breach pumping test analysis methods assumptions, making them unreliable as a source of aquifer parameter data.
4. Many tests are short to a level that does not allow reliable aquifer typifying and, consequently, the selection of a suitable analysis method.
5. Most available records are for single-well pumping tests, which cannot be used to estimate storativity.
6. As a rule, the aquifer thickness is unknown and, in most cases, well construction data are not available, which does not enable calculation of hydraulic conductivity values from transmissivity estimates.
7. Many pumping tests failed to use reliable methods to measure discharge rates during the tests, which introduces a major source of uncertainty in the tests and their results.
8. Most of the constant rate tests failed to maintain constant discharge rate throughout their durations.
9. Available specific capacity ( $Q/s$ ) data are largely consistent with pumping test data, but neither can be used to calculate hydraulic conductivity with confidence.

Despite the above, the following can be deduced from pumping tests in the LMC based on the author's experience in the area having audited few reasonably good quality pumping tests and from limited published work:

1. Time-drawdown curves suggest unconfined aquifer conditions, including many relatively deep wells, e.g. the 40 m deep Well 336093 (Figure 6-2).
2. Step-drawdown tests indicate low efficiency for many wells, possibly due to lack of gravel pack and unmethodological well screen design. It is normal in the LMC to see declining well efficiencies due to siltation. For example, the efficiency of a public water supply well in Foxton Beach dropped to a level that necessitated its replacement.

3. Hydraulic conductivity for most screened material in the LMC falls in the clean sand–clean gravel range ( $\geq 1$  m/d) (Figure 6–3).
4. Although there are no pumping test data to support this assumption, hydraulic conductivity for non–gravelly material in the LMC are expected to be within the sand–silt range, i.e. 1–0.0001 m/d, as suggested in Table 6–1, and Table 6–2.

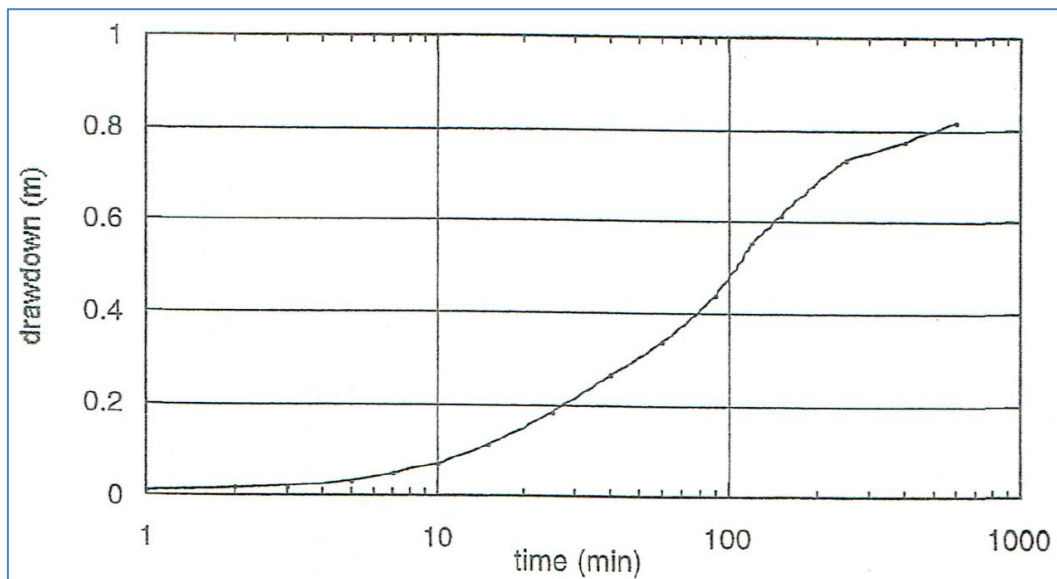


Figure 6–2. Constant rate pumping test time–drawdown semi–log plot for Well 336093 (40 m deep) in Aokautere, east of Palmerston North. The S–shaped time–drawdown curve is typical of unconfined aquifer with delayed yield (figure sourced from Schumacher, 1999).

## 6.5 Groundwater piezometry

Hydraulic or piezometric head is a measurement of liquid pressure above a geodetic datum (Chanson, 2004; Mulley, 2004). For groundwater, it is also termed groundwater level and is useful for determining the aquifer ‘fullness’ and flow direction. Groundwater level data are essential for calibrating groundwater models.

Groundwater level data in the LMC are collected by Horizons Regional Council and available in digital format from their groundwater database. Table C–1 in Appendix C summarises groundwater level data availability in the LMC.

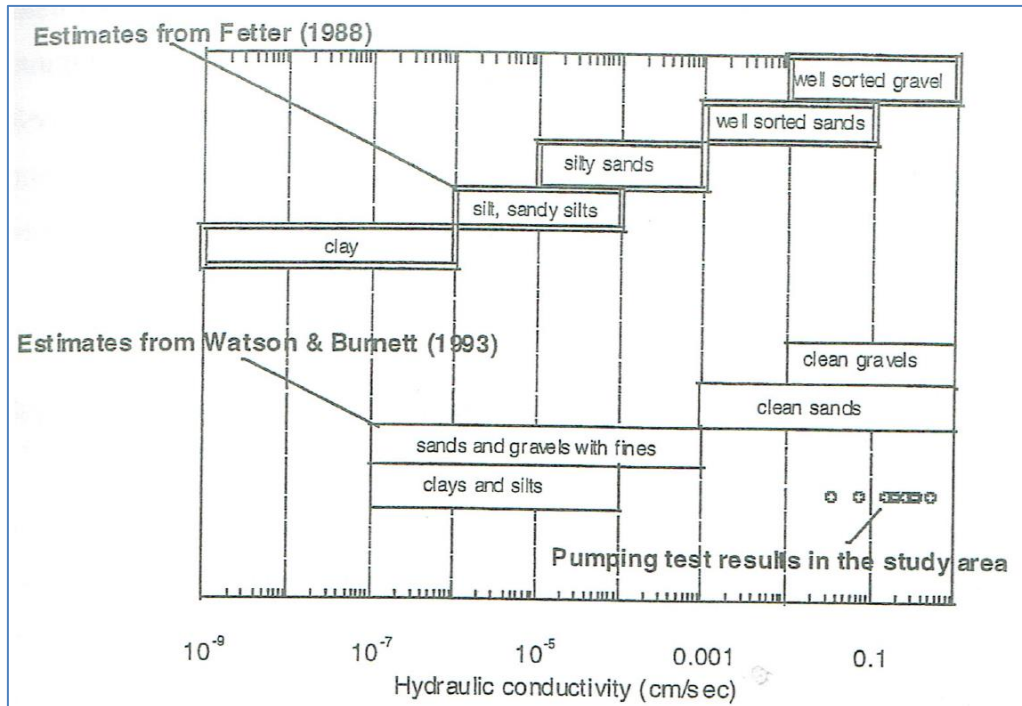


Figure 6–3. Comparison of hydraulic conductivity values obtained from pumping tests in the LMC to literature values (figure sourced from Schumacher, 1999). Screen length is used in the calculations as a proxy to aquifer thickness.

### 6.5.1 Groundwater level variability in time

Figures C–1 through C–84 in Appendix C present groundwater level hydrographs for monitoring wells in the LMC. They also show long-term mean, yearly mean, cumulative mean, deviation from the mean (mean deviation), and cumulative deviation from the mean (CDFM). The figures include information on the land elevation at the well site, screen extent, mean groundwater level and groundwater level standard deviation (STDEV).

The groundwater level hydrographs have been visually inspected for trend and classified into three categories: (1) declining, (2) steady, and (3) rising. Rising groundwater levels are indicated by CDFM curves concaving underneath the mean deviation curve, and rising cumulative mean curves (e.g. Figure 6–4). The opposite curve configuration implies dropping groundwater levels. The shape of the yearly mean curve also helps in the interpretation. The map presented in Figure 6–5 depicts groundwater trends in the LMC.

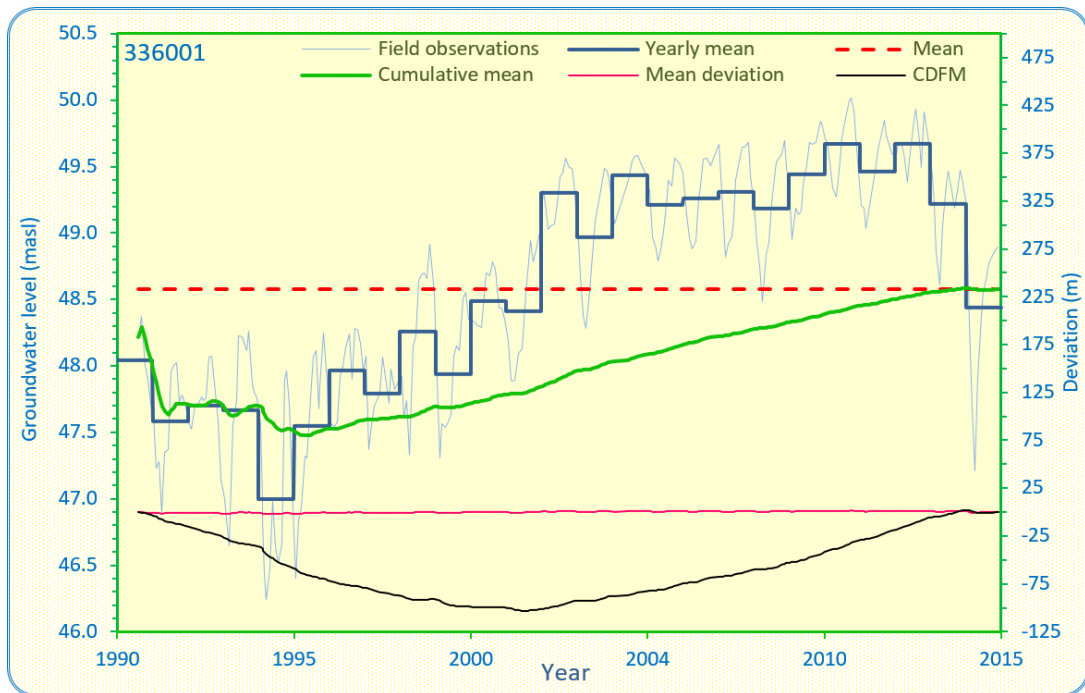


Figure 6-4. Example of groundwater level hydrograph plots presented in Appendix C.

Groundwater level records for four wells have been excluded because they were found to be old and/or too short to be relevant and/or useful in the groundwater level trend analysis presented here (wells 325009, 333035, 336017 and 354003 presented in Figures D-6, D-24, D-40 and D-82, respectively).

Visual inspection of groundwater level hydrographs is subjective, but useful when the data is plotted in a variety of forms and supported by basic statistics like standard deviation. Examination of such groundwater level hydrographs in the LMC reveals that the effects of the highest recorded rainfall in the area in 2004 has been very short-lived. However, the low rainfall in 2014 has noticeably affected groundwater levels in the catchment.

Overall, inspection of groundwater data reveals no extreme trends and the magnitude of groundwater level fluctuations seems to be generally small, mostly less than 1 m and very seldom above 2 m from the long-term average.

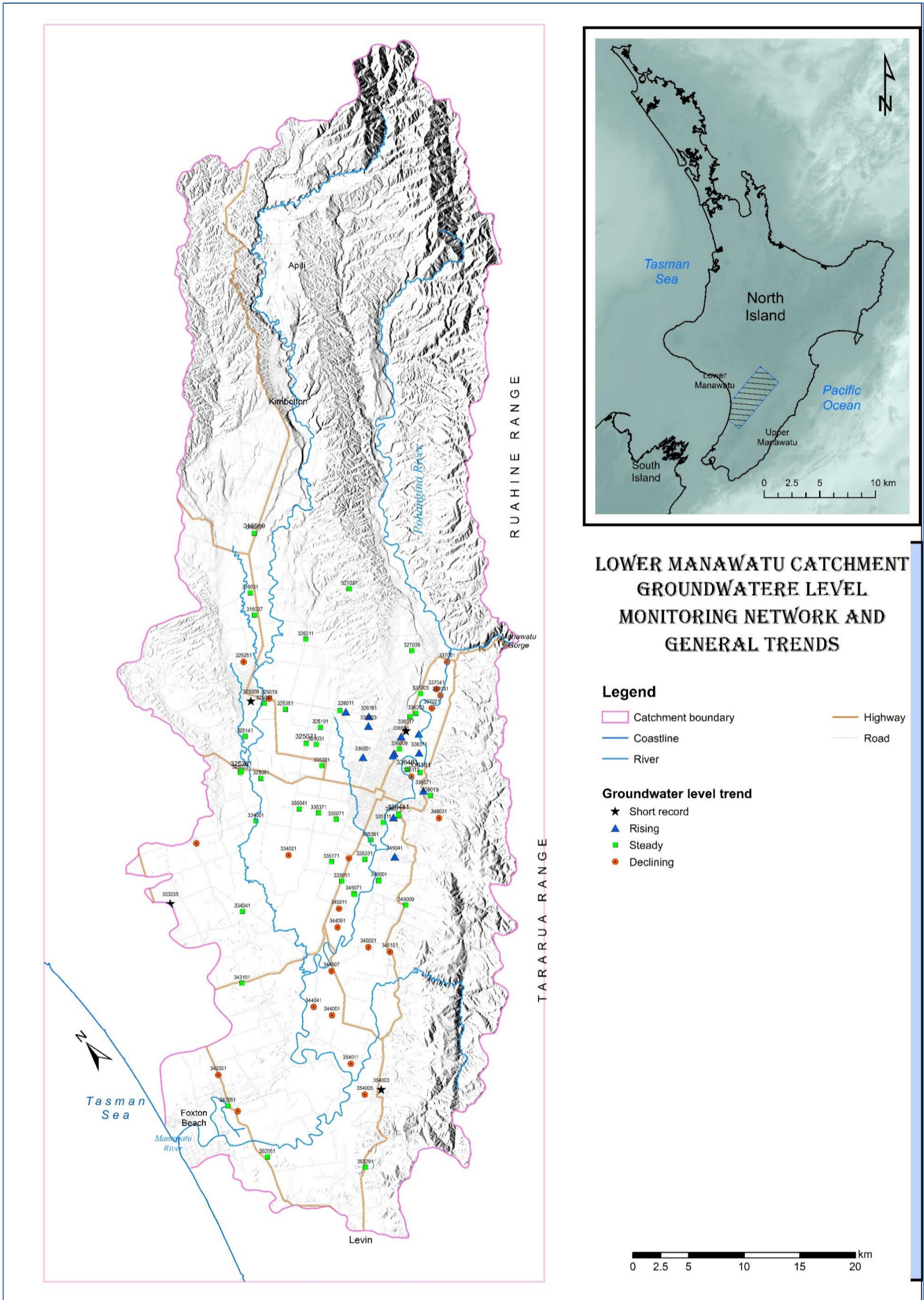


Figure 6-5. Groundwater level trends in the LMC.

There seems to be no correlation between well depths and groundwater level trends. However, a spatial pattern in groundwater level trends can be seen in the map presented in Figure 6–5. Groundwater levels seem to have been persistently rising at the eastern and southern outskirts of Palmerston North. This may be due to irrigation returns from prolonged market garden irrigation in the area.

Slightly, but persistently declining groundwater levels can be noticed in the low-lying area between Opiki, Shannon, Tokemaru and Tiakitahuna. Elsewhere, groundwater levels have been steady with only few outliers.

Most examined groundwater level hydrographs exhibit a seasonal pattern. In general, groundwater levels are highest just before the start of the irrigation season and lowest around its end.

### 6.5.2 Groundwater level change with depth

Schumacher (1999) constructed hydrogeological cross-sections and fence diagrams to depict the change in head with depth in the LMC. His diagrams denote decreasing head with depth in recharge zone settings locations such as the Pohangina Anticline, and upward hydraulic head gradients in groundwater discharge zone setting areas such along the Manawatu River near Palmerston North. Zarour (2008) showed that the 1:5 upward hydraulic gradient exhibited by the Whakarongo multi-level piezometer setup is gradual (Figure 6–7), indicating groundwater discharge settings in a continued aquifer system rather than a sequence of aquifers and aquitards.

### 6.5.3 Piezometry and groundwater flow

Groundwater flows from higher to lower head positions. Groundwater head is a measure of energy per unit weight of water and is measured in units of length relative to datum, e.g. masl. Groundwater head is a combined expression of kinetic, gravitational and fluid pressure energies. Kinetic energy can be ignored in groundwater due to its normally slow flow velocities.

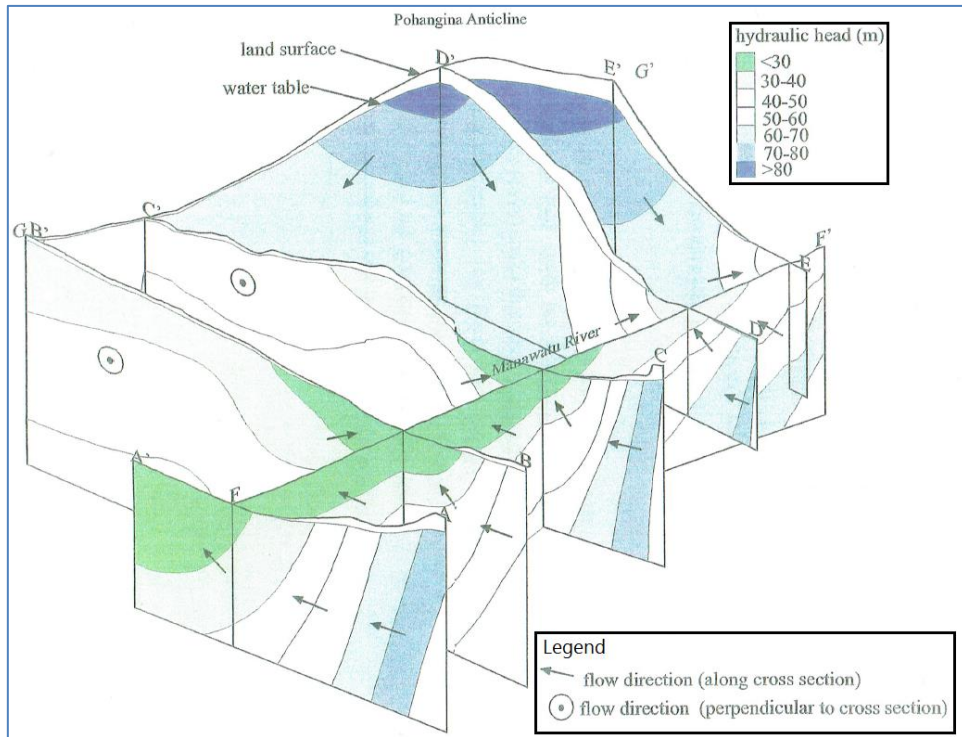


Figure 6-6. Hydrogeological fence diagram (after Schumacher, 1999).

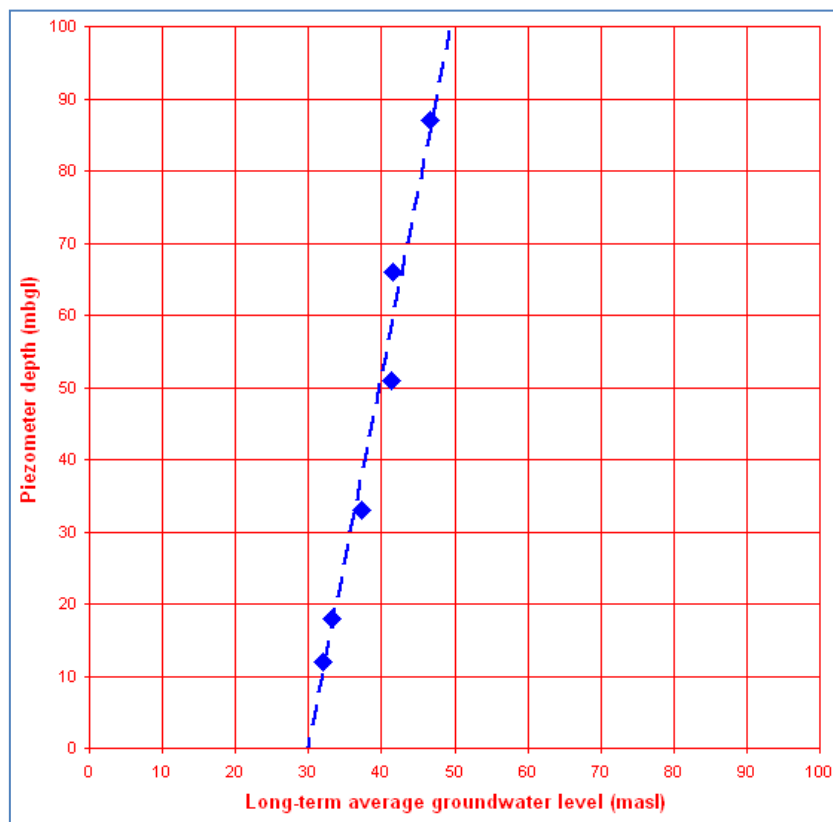


Figure 6-7. Relation between screen depth and head as observed in the Whakarongo multi-level piezometer setup (after Zarour, 2008).

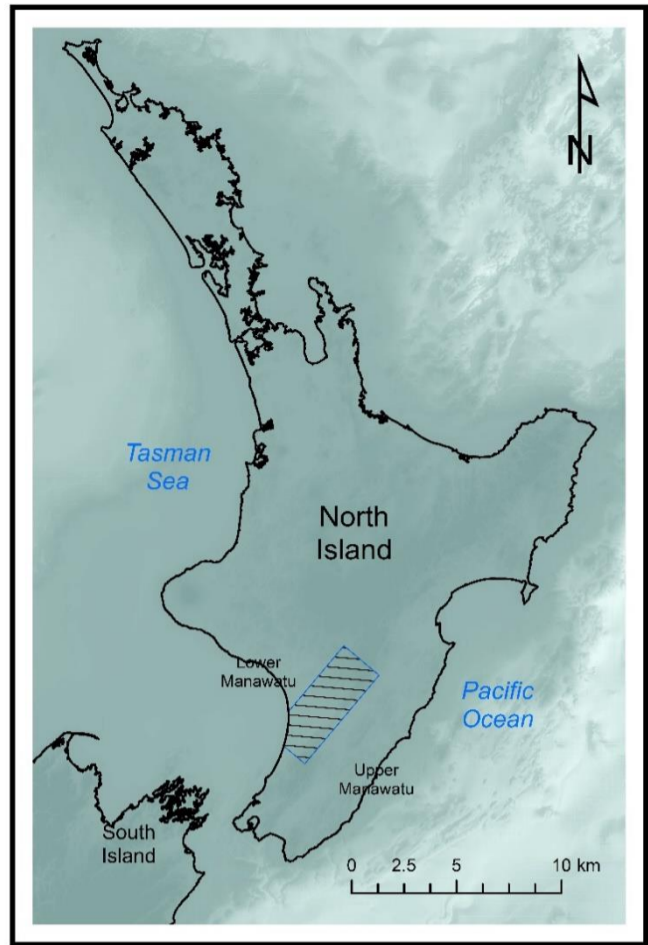
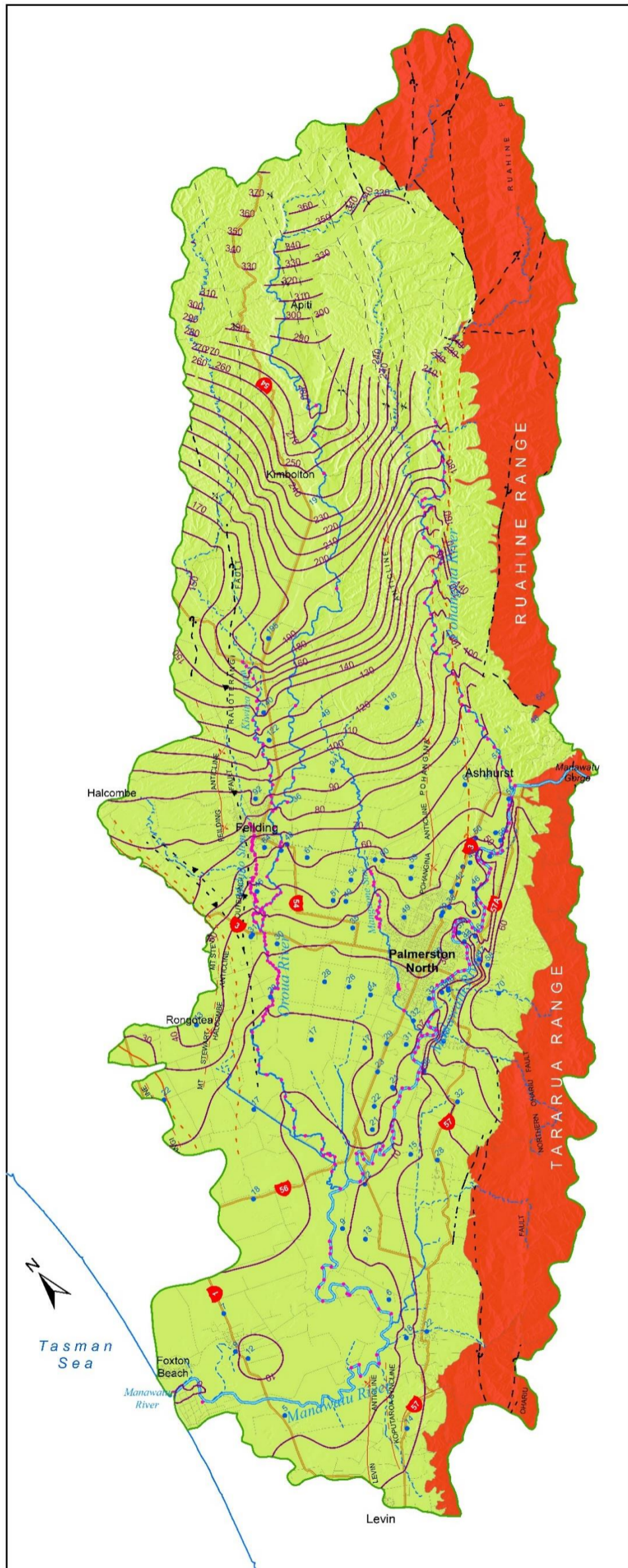
Contour maps are commonly used to represent the spatial distribution in groundwater head. Known as piezometric maps, they provide a means to assess flow directions, which are perpendicular to groundwater level contour lines. Since there is no evidence of disconnect between surface water and groundwater in the LMC, surface water elevations can be incorporated in piezometric maps.

Figure 6–8 presents a piezometric map for the LMC drawn using long–term average groundwater level and surface water height (stage) monitoring. The piezometric map indicates that groundwater flow is generally from northeast to southwest, aligned to the dip of the geological strata.

The relatively dense contours in the upper part of the LMC indicate low transmissivity whereas the flatter hydraulic gradients between Palmerston North and the ocean indicate relatively high transmissivity.

The piezometric map presented in Figure 6–8 provides a basic picture of average surface water–groundwater interaction conditions in the LMC. Bending piezometric contour lines with tips pointing upstream indicate groundwater discharge zone settings (Figure 5–3a). An example on such settings is found in the Pohangina Valley. Conversely, the V–shaped piezometric contours along most of the Oroua River upstream of Feilding indicate losing river condition, where surface water recharges the underlying aquifer. Below Feilding and Palmerston North, the Oroua and Manawatu rivers predominantly gain flow from groundwater. The Mangaone Stream seems to be largely dependent on groundwater, acting as a drain along nearly its entire length.

Understanding groundwater–surface water interaction and flow directions is important for efficient allocation of both resources. It is essential to determining surface water and groundwater environments that could be affected by various land use and waste disposal activities. Numerical modelling could be a useful tool for improving this understanding.



### LOWER MANAWATU CATCHMENT PIEZOMETRIC MAP

#### Legend

- |                    |         |
|--------------------|---------|
| Catchment boundary | Highway |
| Basement rock      | Road    |
| Coastline          |         |
- Rivers**
- |         |         |
|---------|---------|
| Order 7 | Order 5 |
| Order 6 | Order 4 |
- Groundwater level data**
- Monitoring well (with average gwl in masl)
  - River bed & stage survey point
  - Average groundwater level contour line in masl

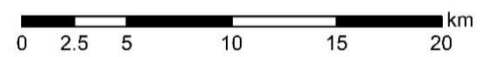


Figure 6–8. Piezometric map for the LMC drawn using long-term average groundwater level and surface water stage monitoring data.

The effect of the Pohangina Anticline on piezometry is prominent in the outcrop area of the Last Interglacial beach deposits in the middle of the catchment, to the northeast of Palmerston North (near Stoney Creek Lane). The topographical high on the marine terraces apparently coincides with a groundwater divide, separating flow towards the Manawatu River from flow towards the Mangaone Stream, then separating flow towards the Manawatu River from flow towards the Oroua River.

The area's topographical, geological and hydrological settings favour the development of topography-controlled groundwater flow system like the system presented in Figure 6-9. The groundwater flow system in the LMC is most probably multi-scaled like the system shown in Figure 6-10.

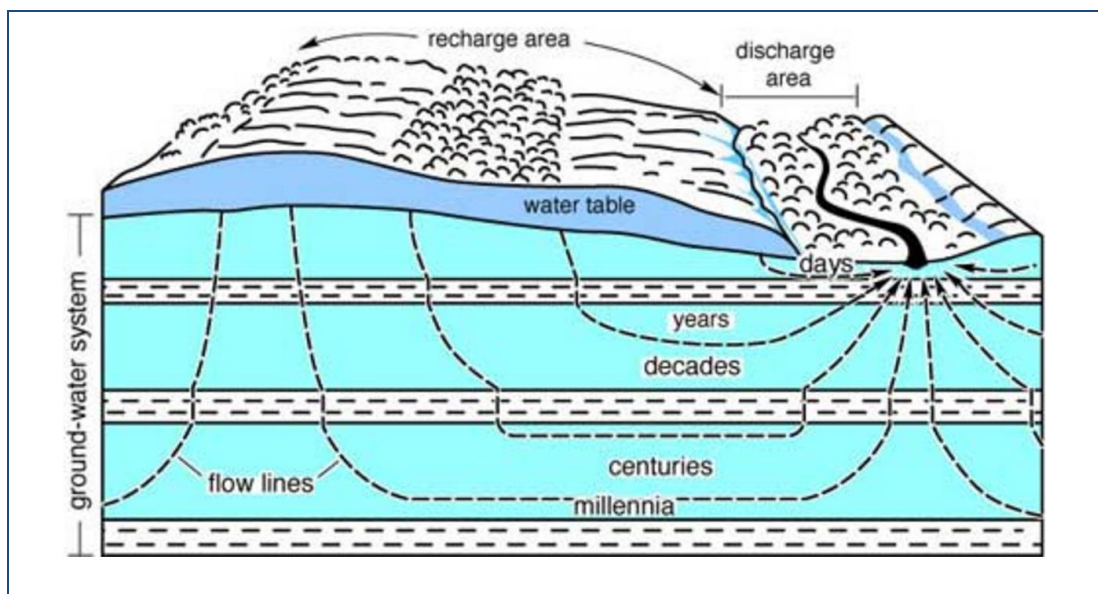


Figure 6-9. Schematic diagram for a topographically controlled groundwater system and flow times (after Buchanan & Buddemeier, 2005).

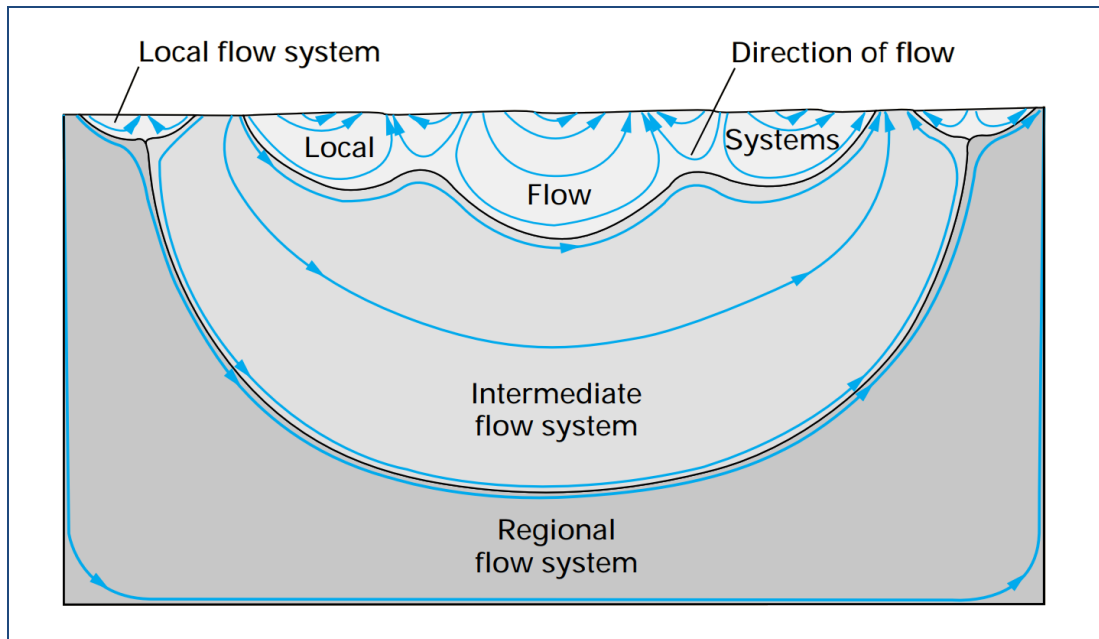


Figure 6-10. Schematic diagram showing multi-scale flow system (after Winter *et al.*, 1998).

## Chapter 7 Hydrochemistry

### 7.1 Introduction

The aptness of water for various purposes is determined by its quality. Hence, early hydrogeochemical studies were mainly aimed at determining groundwater fitness for municipal and agricultural purposes (Domenico & Schwartz, 1990). In the 1940s, researchers started developing hydrogeochemical techniques to decipher the processes that control groundwater quality evolution along flow paths with the aim to complement and enhance hydrogeological investigation methods. Groundwater quality is also studied to gauge the effect of land and water resource management practices and interventions on the environment.

### 7.2 Processes controlling groundwater quality

Water is branded as the universal solvent because it can dissolve more substances than any other material (Brezonik & Arnold, 2011). Most inorganic substances are electrolytes, dissolving in water to form ions. Organic substances can also dissolve in water but they are usually nonelectrolytes and, therefore, they mostly dissolve in water as nonionic molecules (Domenico & Schwartz, 1990).

During its flow through geological materials under the ground, groundwater interacts with minerals and it is affected by the subsurface environment in a manner that changes its composition. Groundwater quality can change due to one or any combination of the following processes (e.g. Appelo & Postma, 2005; Fetter, 2013; Freeze & Cherry, 1979; Hem, 1985; Lloyd & Heathcote, 1985; Winter *et al.*, 1998):

1. **Mixing, dilution and concentration** can change groundwater composition. For example, evapotranspiration condenses chemicals in precipitation and recharge waters. The extent of condensation can be estimated by studying the change in concentration of conservative ions such as chloride ( $Cl^-$ ).

Groundwater can also mix with surface water or seawater, and it can become polluted due to mixing with leachate from various anthropogenic activities.

2. **Acid–base reactions** involve the transfer of hydrogen ions ( $H^+$ ) among solutes dissolved in water, which affects the effective concentrations of dissolved chemicals.  $pH$  is a notation for  $H^+$  concentration (activity) that equals the negative logarithmic–scale of the  $H^+$  concentration. It ranges from 0 to 14, with the middle point ( $pH$  7) being neutral (neither acidic nor basic). Lower  $pH$  values represent larger  $H^+$  concentrations (acidic solutions), and higher  $pH$  values represent smaller  $H^+$  concentrations (basic or alkaline solutions). Many metals stay dissolved when  $pH$  values are low, but they precipitate from solution when  $pH$  increases.
3. **Mineral dissolution–precipitation reactions:** Mineral solubility and kinetics determine the release of cations into groundwater. Dissolution of carbonate and silicate minerals is largely driven by the action of carbon dioxide ( $CO_2$ ), which dissolves in rainwater in the atmosphere to produce diluted carbonic acid ( $H_2CO_3$ ) (Eq. 7–1).  $CO_2$  is also produced within the soil zone by biochemical processes like the decay of organic matter (e.g. Eq. 7–2).  $H_2CO_3$  affects the solubility of minerals as it increases its acidity (lowers water  $pH$ ) in the process of creating bicarbonate ions ( $HCO_3^-$ ) (Eq. 7–3) and then, if conditions permit carbonate ions ( $CO_3^{2-}$ ) (Eq. 7–4).



Dissolution of carbonate–bearing rocks aided by  $H_2CO_3$  is responsible for the existence of calcium ( $Ca^{2+}$ ) and magnesium ( $Mg^{2+}$ ) in groundwater. Weathering of silicate rock minerals (e.g. feldspar and biotite) releases solutes into groundwater and forms clays. Weathering of cation–rich clays

forms cation-poor clays. All these reactions consume  $CO_2$  and, consequently, change groundwater's  $pH$ . During recharge, the percolating water remains in contact with the atmosphere and soil  $CO_2$  (open system) up to a certain depth. However, below that level, diffusive groundwater interaction with the soil and atmosphere become negligible and groundwater quality evolution proceeds with a fixed quantity of atmospheric  $CO_2$  (closed system). Therefore, the prevalence of open or closed system conditions with respect to  $CO_2$  is important during the early evolution of groundwater chemical composition.

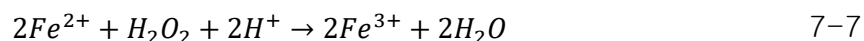
According to Palmer and Cherry (1984), a groundwater system may be described as being 'open' with respect to  $CO_2$  if its pores contain sufficient mass of  $CO_2$  such that the soil gas partial pressure ( $pCO_2$ ) in this space does not significantly change as the pore water equilibrates with it, or if the rate of  $CO_2$  production in the soil is comparable to the rate at which it is lost to the aqueous phase within the pore space. Below the capillary fringe, the pores are filled with water and there is little or no replenishment of gaseous  $CO_2$  to the water from the atmosphere, in which case the system is considered as being 'closed' with respect to  $CO_2$ . Initial mineral dissolution may occur under either open or closed conditions with respect to  $CO_2$ , depending on the soil conditions and the availability of the mineral phase.

Dissolution of minerals can take place as long as the groundwater is under saturated with respect to these minerals. Precipitation of minerals take place when their concentrations exceed their saturation indices ( $SI$ ) resulting in minerals forming from ions dissolved in water. For example, iron hydroxide ( $Fe(OH)_3$ ) will form when iron dissolved in groundwater encounters oxygen ( $O_2$ ) dissolved in surface water, which is common in areas of groundwater seeps and springs. However, precipitation of minerals is not a prompt process and, therefore, groundwater may become supersaturated with respect to certain minerals.

4. **Sorption and ion exchange:** Sorption (or adsorption) is a process in which solutes (ions or molecules dissolved in liquid) become attached to the surfaces (or near-surface parts) of solid materials, either temporarily or permanently. Thus, solutes in groundwater can be sorbed (adsorbed) either to the aquifer material or to particles suspended in the groundwater. Release of sorbed chemicals to water is termed desorption. When ions attached to the surface of a solid are replaced by ions that were in water, the process is known as ion exchange. For example,  $Ca^{2+}$  and  $Mg^{2+}$  ions in groundwater can be exchanged for sodium ions ( $Na^+$ ) on the surface of the aquifer material, resulting in a decline in the amount of  $Ca^{2+}$  and  $Mg^{2+}$  in the groundwater and increase in the amount of  $Na^+$  in it. The opposite can take place when saltwater enters an aquifer, where some of the sodium in the saltwater is exchanged for calcium sorbed to the solid material of the aquifer (reverse ion exchange). The exchangeability of cations between aqueous and solid phases is governed by the strength of ions bond to the solid phase. Divalent ions bond more strongly to the solid phase than monovalent ions and, therefore are more difficult to exchange. The order of exchangeability of the major cations can be described as  $Na^+ > K^+ > Mg^{2+} > Ca^{2+}$ .
5. **Oxidation–reduction (redox) reactions** control the concentrations of nitrate ( $NO_3^-$ ), manganese ( $Mn^{4+}$ ), iron ( $Fe^{3+}$ ) and sulphate ( $SO_4^{2-}$ ) in groundwater. Redox reactions happen when electrons ( $e^-$ ) are exchanged among solutes. They involve loss of electrons of certain elements (oxidation) which is associated with gain of electrons of other elements (reduction). For example, when iron dissolved in water that does not contain dissolved oxygen ( $DO$ ) mixes with water that contains  $DO$ , the iron and oxygen interact by oxidation and reduction reactions. The result of such reactions is that the dissolved iron loses electrons (i.e. the iron is oxidised, Eq. 7–5) and the oxygen gains electrons (i.e. the oxygen is reduced, Eq. 7–6). The overall reaction is presented in Eq. 7–7. In this case, the iron is an electron donor and the oxygen is an electron acceptor.



Overall equation:



Oxidation of iron will result in its precipitation because  $Fe^{3+}$  is much less soluble than  $Fe^{2+}$ . Iron occurs as  $Fe^{3+}$  in groundwater that contains *DO* of more than 1 mg/L, but it occurs as  $Fe^{2+}$  at lower *DO* concentrations. Iron (and manganese) dissolve more readily in oxygen-poor groundwater, especially if the groundwater is acidic (*pH* on the low side; <7).

Bacteria can use energy gained from redox reactions as they decompose organic material. This reduction process involves a sequence of electron acceptors consisting of  $O_2$ ,  $NO_3^{-}$ ,  $Mn^{4+}$ ,  $Fe^{3+}$ ,  $SO_4^{2-}$ ,  $CO_2$  and then methane ( $CH_4$ ) fermentation products. This sequence is reversed during oxidation. So, the presence of products of redox reactions in groundwater can be used to identify the dominant type of such reactions in the aquifer. For example, the bacterial reduction of  $SO_4^{2-}$  to sulphide ( $HS^{-}$ ) can result from oxidation of organic matter to  $CO_2$ . According to Edmunds and Shand (2008), a sequence of redox changes may be recognised along flow paths in aquifers. Hence, understanding redox conditions in a groundwater flow system can aid with hydrogeological conceptualisation and can provide additional evidence to help with the study of the system's hydrodynamics.

### 7.3 Material and methods

In this thesis, groundwater quality is investigated in order to supplement the understanding of the LMC groundwater system that is achieved from studying the area's geology, hydrology and hydrogeology. This undertaking involved reviewing previous hydrogeochemical studies (Section 1.6.2) and synthesis of water quality data available from Horizons Regional Council. Horizons collect groundwater quality data primarily to fulfil their State of the Environment (SoE) monitoring

responsibilities. However, the data they collect are also suitable for hydrochemical investigation purposes.

Hydrochemical interpretations undertaken in this research attempt to mine available data to reveal the processes that control the groundwater quality in the study area. Hence, the study is focused on the major inorganic constituents. Davis and DeWiest (1966) classified groundwater quality constituents based on their global average ranges as follows:

1. major constituents (1–1,000 mg/L)
2. secondary constituents (0.01–10 mg/L)
3. minor constituents (0.0001–0.1 mg/L)
4. trace constituents (<0.001 mg/L).

The study of major constituents and their ratios in groundwater enables identification of different water types (hydrogeochemical facies or groundwater masses). Interpolation of the spatial distribution of the concentrations of various parameters and hydrogeochemical facies can provide information on groundwater recharge and discharge areas, flow paths, aquifer conditions and the dynamics of groundwater quality evolution. Hydrochemical interpretations in this study have been mainly undertaken using maps and classical graphical methods.

Zarour *et al.* (2011) and PDP (2013a) list the groundwater quality parameters that Horizons monitor. They include:

1. Physiochemical field measurements: temperature, electrical conductivity (*EC*), *pH*, redox potential (*Eh*), dissolved oxygen (*DO*)
2. Major cations: calcium (*Ca*), magnesium (*Mg*), sodium (*Na*), potassium (*K*)
3. Major anions: alkalinity or bicarbonate (*HCO<sub>3</sub>*), sulphate (*SO<sub>4</sub>*), chloride (*Cl*)
4. Nutrients: nitrate (*NO<sub>3</sub>*), nitrite (*NO<sub>2</sub>*), ammonium (*NH<sub>4</sub>*), phosphate (*PO<sub>4</sub>*);
5. Parameters that often affect water supply quality: iron (*Fe*), manganese (*Mn*), arsenic (*As*)

6. Other indicative parameters: silica ( $SiO_2$ ), fluoride ( $F$ ), boron ( $B$ ), bromide ( $Br$ )
7. Bacterial contamination indicator: *Escherichia coli* (*E. coli*).

#### 7.4 Data availability

Data collected from the start of groundwater quality monitoring in the LMC until the end of 2007 had been obtained from Horizons Regional Council for this research. These data include 1,584 records relating to 631 wells in the LMC and within 2 km around it (Figure 7-1). The distribution of sampled wells shown in Figure 7-1 indicates reasonably good spatial coverage. However, there are no data from areas topographically higher than 160 masl. Sampled wells encompass a useful range of depth into the groundwater system (Figure 7-1 and Figure 7-2).

Post 2007 groundwater quality data are not readily available in useable form from Horizons Regional Council. For this reason and given the lack of trend noticed by previous studies and the abundance of pre-2007 data, this research has not attempted to use data collected after 2007.

Accurate sample collection data are missing. Anecdotes indicate that all samples are collected from non-dedicated, privately owned, operational bores. Monitored bores vary in design and the construction detail of some are not known. Samples are generally thought to have been collected after purging the bores of standing water by pumping the equivalent to three bore water volumes. It is believed that field measurements are only taken after monitoring of purged water shows they have stabilised.

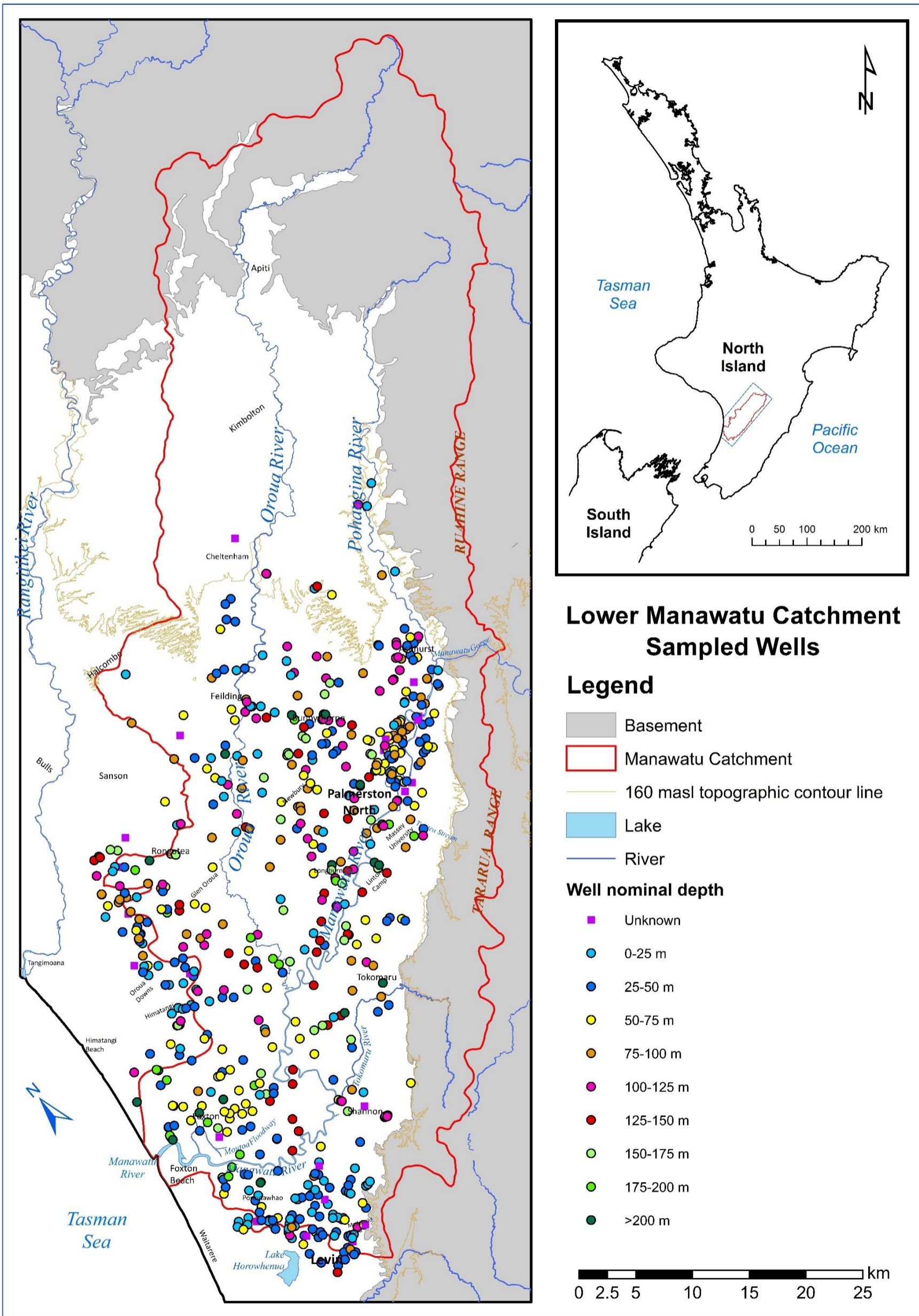


Figure 7-1. Location map showing groundwater quality sampling sites and depths in the LMC until the end of 2007.

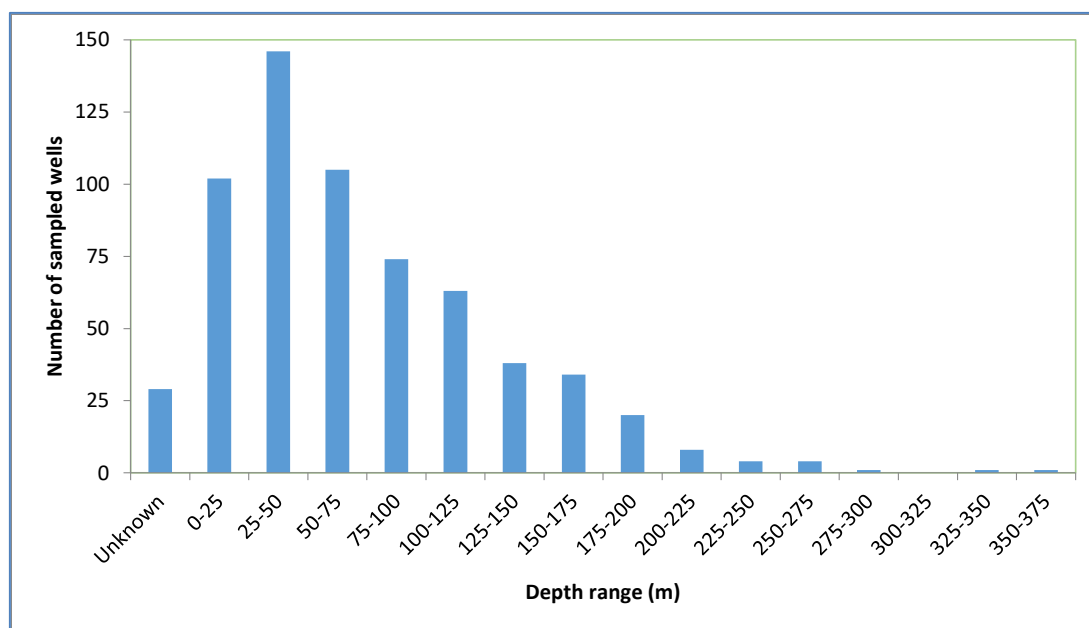


Figure 7–2. Depth range of sampled wells in the LMC.

All groundwater quality samples are thought to have been collected in three bottles, one for unprocessed water, another for filtered water, and the third for filtered and acid treated water. Information recorded during sampling include pre-sampling water level, site and weather conditions. Samples are stored in cooler boxes and couriered to laboratory overnight. Laboratory analyses are thought to be carried out according to the current edition at the time of analysis of the Standard Methods Examination of Water and Wastewater by the American Public Health Association and American Water Works Association and Water Environment Federation.

### 7.5 Data reliability

The relative abundance of hydrogeochemical data in the LMC enables interpretation to help understand the processes that control groundwater quality in the area and groundwater hydraulic conditions. However, the reliability of the data and their representativeness must also be examined before attempting any spatial interpolation of available hydrochemistry records.

### 7.5.1 Quality control (QC)

Water is electrically neutral, i.e. positive and negative charges in it are equal. Hence, laboratory analysis results are expected to present a balanced sum of cations and anions calculated in milliequivalent/litre (meq/L). Checking the cation–anion balance (*CAB*) in hydrogeochemical data is considered the first and foremost important quality control (QC) check of the goodness of the data. The United Nations Environment Programme (UNEP) and the World Health Organization (WHO) regard the ionic balance check as one of the basic tests of the quality of groundwater quality data, and recommend an upper acceptable limit of 5% to enable qualified interpretation of the data (Bartram & Ballance, 1996). However, *CAB* is perhaps one of the most confusingly defined parameters in groundwater sciences. Some workers define *CAB* as the ratio of the difference between the cations and anions to either sum (*CAB*<sub>1</sub> in Eq. 7–8) whereas others define it as the ratio of the difference between the cations and anions to their mean (*CAB*<sub>2</sub> in Eq. 7–9). In both Eq. 7–8 and Eq. 7–9, the sum of cations ( $\sum \text{Cations}$ ) and sum of anions ( $\sum \text{Anions}$ ) are taken as absolute values, i.e. neither negative nor positive. Comparing Eq. 7–8 and Eq. 7–9 provides that *CAB*<sub>2</sub> is double *CAB*<sub>1</sub>. Noticeably, users of both equations implicitly agree on acceptable *CAB* limits for groundwater quality analysis data. Users of Eq. 7–8 normally set the acceptable *CAB* value range between –5% and 5% and users of Eq. 7–9 set the acceptable *CAB* value range between –10% and 10%. The two error limits are clearly identical. Anyway, one should be very careful with the way *CAB* is defined when dealing with data from various sources because, for example, accepting chemical analyses that have *CAB* up to 10% that is calculated using Eq. 7–8 will introduce serious interpretation errors.

$$CAB_1 = \left[ \frac{\sum \text{Cations} - \sum \text{Anions}}{\sum \text{Cations} + \sum \text{Anions}} \right] \times 100\% \quad 7-8$$

$$CAB_2 = \left[ \frac{\sum \text{Cations} - \sum \text{Anions}}{(\sum \text{Cations} + \sum \text{Anions})/2} \right] \times 100\% \quad 7-9$$

To avoid confusion in this thesis, Eq. 7-8 is adopted to calculate the cation–anion balance, which is simply termed *CAB* from this point onwards. Acceptable analysis in this thesis must have *CAB* values in the range of –5% and 5%.

Only major constituents are normally used in *CAB* calculations, namely calcium ( $Ca^{2+}$ ), magnesium ( $Mg^{2+}$ ), sodium ( $Na^+$ ), bicarbonates or alkalinity ( $HCO_3^-$ ), sulphate ( $SO_4^{2-}$ ), and chloride ( $Cl^-$ ). Occasionally, investigators consider potassium ( $K^+$ ) to be a major cation and include it in *CAB* calculations.

A positive *CAB* value indicates missing anions and a negative *CAB* value implies missing cations. Zarour (2008) explains that large *CAB* is indicative of a laboratory error and/or overlooking analysis of one or more important constituents in the water sample. In both situations, the trustworthiness of the reported groundwater quality results is compromised. Accordingly, *CAB* can be used to check on the reliability of a chemical analysis.

### 7.5.2 Quality assurance (QA)

Zarour (2008) examined all groundwater quality data available in Horizons Regional Council database. He found that nearly half of the records are for incomplete analyses that do not include all major constituents, so the reliability of their laboratory analysis results cannot be assessed. He also found that around 30% of the samples pass the 5% *CAB* threshold whereas the remaining samples (20%) do not.

Table 7-1 summarises the *CAB* status of available hydrochemical data in the LMC until 2007. It shows that 28% of the available records are considered complete and pass the *CAB* test. These 446 records relate to 268 wells that are well distributed in the LMC below the 160 masl topographical contour line (Figure 7-3).

Table 7-1. Status of available groundwater quality records in and within 2 km of the Lower Manawatu Catchment until the end of 2007.

Analysis status	No. of samples	Percentage of total
Incomplete	1,093	69.00
Acceptable error	446	28.16
Unacceptable error	45	2.84
<b>Total</b>	<b>1,584</b>	<b>100.00</b>

The number of samples with unacceptable *CAB* amount to nearly 10% of the number of samples with acceptable *CAB*. This indicates that the laboratory results are generally good, which allows cautious use of data from incomplete analyses for hydrogeochemical interpolation purposes. Most of the incomplete analyses relate to samples that have been collected for a specific reason that did not require the analysis of all other constituents, e.g. nitrate monitoring. Overall, the available hydrogeochemical data represent a wealth of information that can be used effectively to enhance hydrogeological knowledge of the LMC groundwater system.

Table D-1 in Appendix D presents a list of all wells in the LMC that have complete, acceptable groundwater quality data up to the end of 2007, with brief data availability statistics. Table D-2 in the same appendix presents all groundwater quality records that were obtained from Horizons and found to be complete and acceptable for the purposes of this thesis.

Acceptable samples cover the area fairly well (Figure 7-3). The depth range coverage of these samples is also relatively satisfactory (Figure 7-4). Figure 7-5 presents a histogram of *CAB* values for samples analysed for all major constituents in the area. The histogram shows that it is more likely that anions exceed cations in samples. This may be related to laboratory accuracy, sample collection and handling methodology, or not analysing for certain cations.

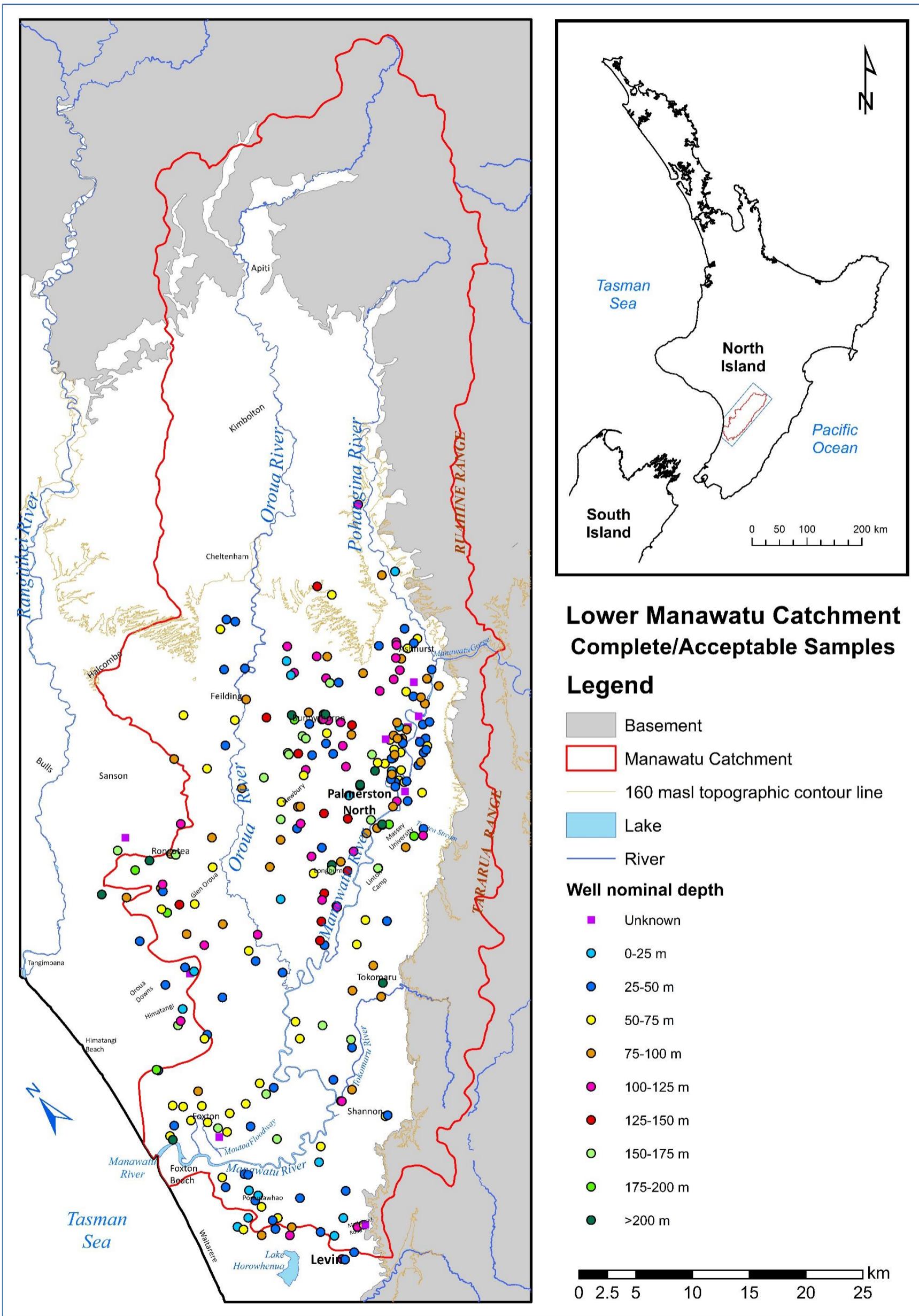


Figure 7-3. Map showing location and depth of wells with complete, acceptable groundwater quality samples in the LMC until the end of 2007.

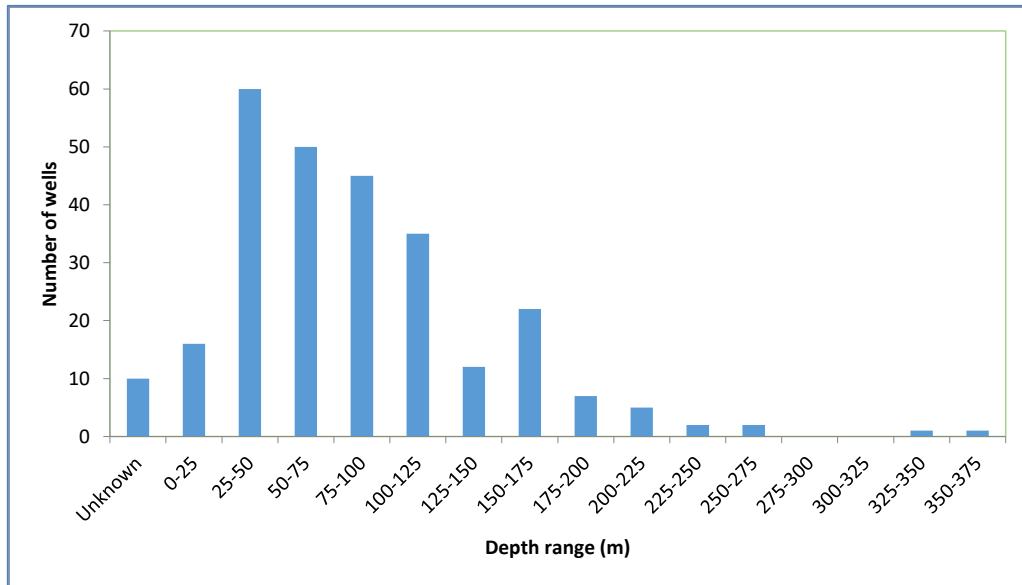


Figure 7-4. Depth range of wells with acceptable samples in the LMC.

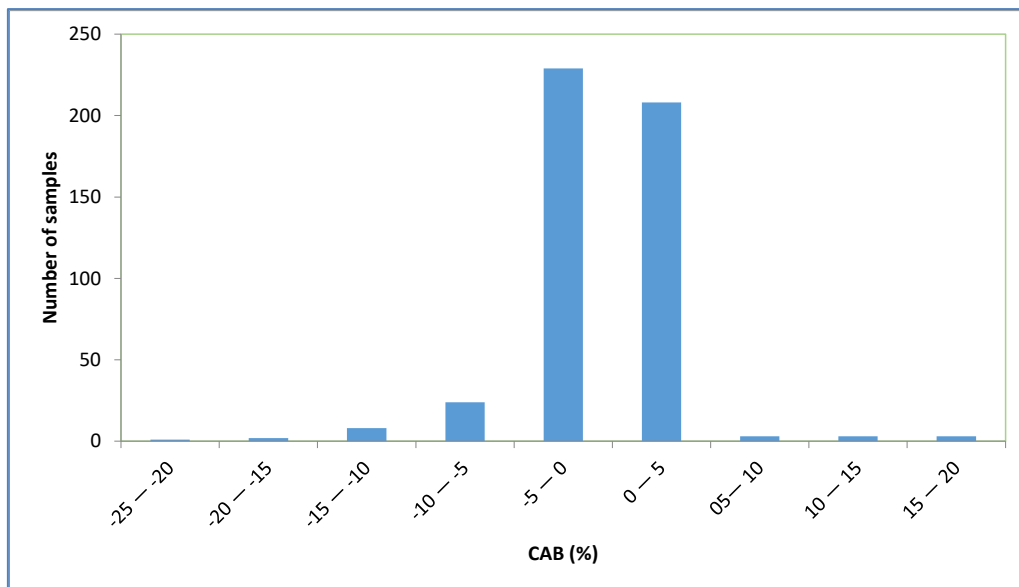


Figure 7-5. Frequency plot of CAB values for samples from LMC until the end of 2007.

## 7.6 Groundwater quality temporal variability

Seven wells in the LMC have reasonably long-term groundwater quality monitoring records until the end of 2007 (Appendix D). Table 7-2 lists such wells and presents information on their available groundwater quality records. Figure 7-6 shows the locations of these seven wells and Figure 7-7 through Figure 7-13 present groundwater quality time-series plots for them.

Table 7–2. Status of available groundwater quality records in and within 2 km of the Lower Manawatu Catchment until the end of 2007

Well	NZMG		Elevation (masl)	Well Nominal Depth (m)	Well Screens			All Samples			Acceptable Samples		
	Easting	Northing			Number	From	To	Number	From	To	Number	From	To
316037	2733577	6110663	129.64	26.50	1	24.40	26.50	23	11/04/1983	31/07/2007	20	08/11/1994	16/06/2005
336113	2735033	6090471	34.49	34.00	1	32.00	34.00	62	15/06/1992	25/03/2008	45	15/06/1992	28/06/2004
336114	2735675	6091722	36.83	12.30	1	11.80	12.30	26	28/09/1994	08/08/2007	20	08/11/1994	26/01/2004
337005	2743665	6094800	51.08	83.00	1	77.00	83.00	39	05/12/1990	17/08/2004	25	13/12/1990	17/08/2004
352271	2700615	6067756	14.30	93.20				38	09/08/1984	18/08/2004	8	10/09/1987	01/04/1997
353015	2708625	6069442	14.71	22.30	1	17.30	22.30	58	21/06/1995	19/11/2007	17	02/10/1995	16/08/2004
354011	2714255	6074187	5.05	36.50	1	33.50	36.50	65	01/05/1989	25/03/2008	13	08/06/1993	04/03/1997

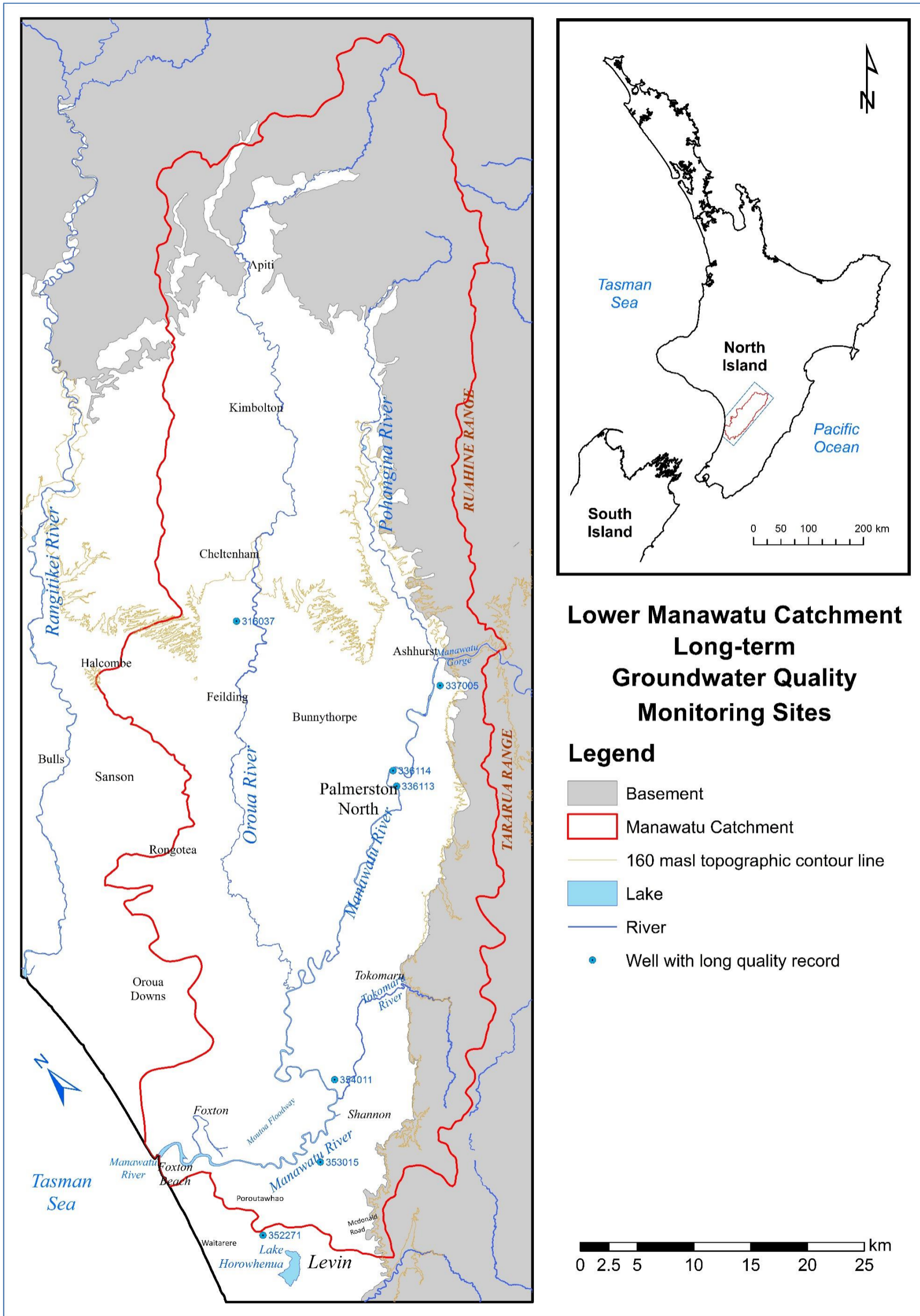


Figure 7-6. Location map showing wells with long-term groundwater quality record until the end of 2007 in the LMC.

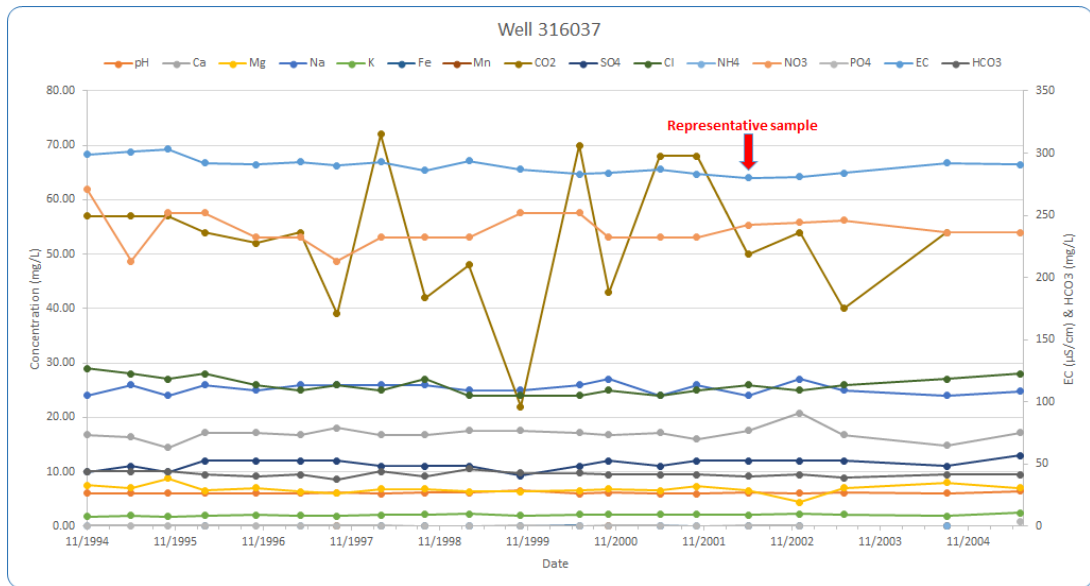


Figure 7-7. Groundwater chemistry hydrograph for Well 316037. Representative sample date (28/05/2002) indicated by red arrow.

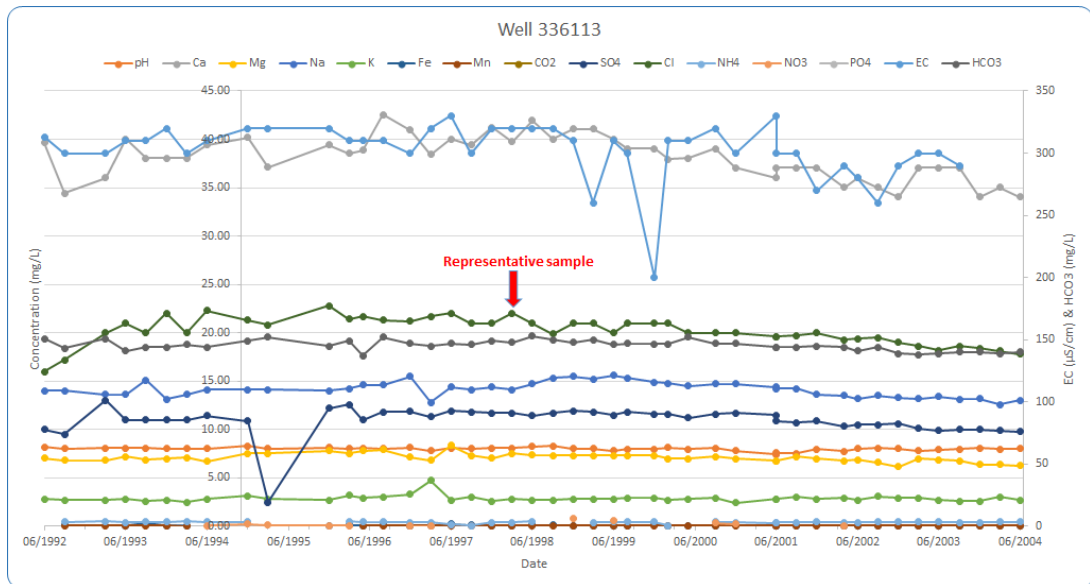


Figure 7-8. Groundwater chemistry hydrograph for Well 336113. Representative sample date (4/03/1998) indicated by red arrow.

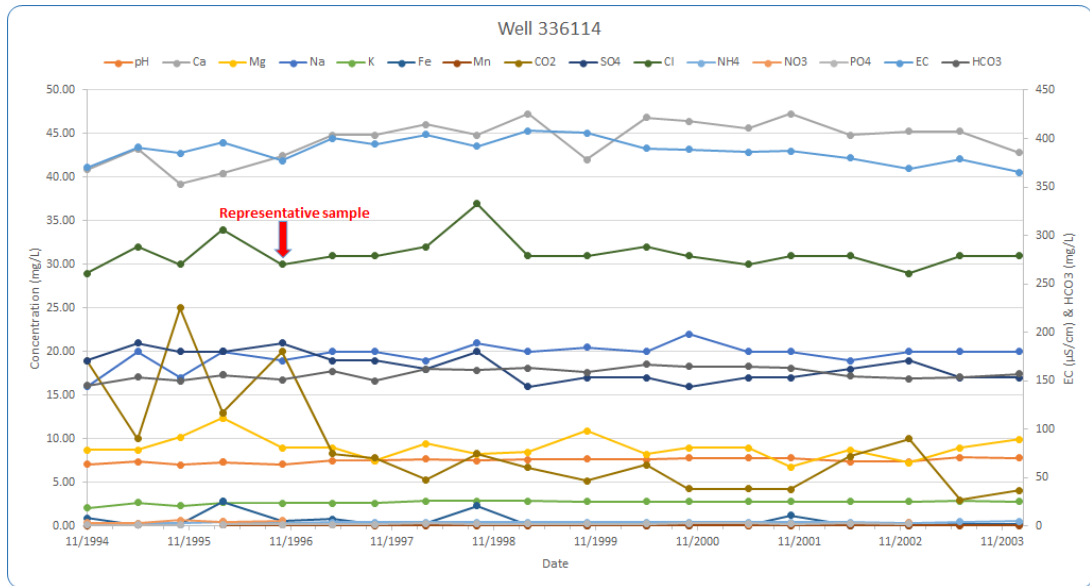


Figure 7-9. Groundwater chemistry hydrograph for Well 336114. Representative sample date (30/10/1996) indicated by red arrow.

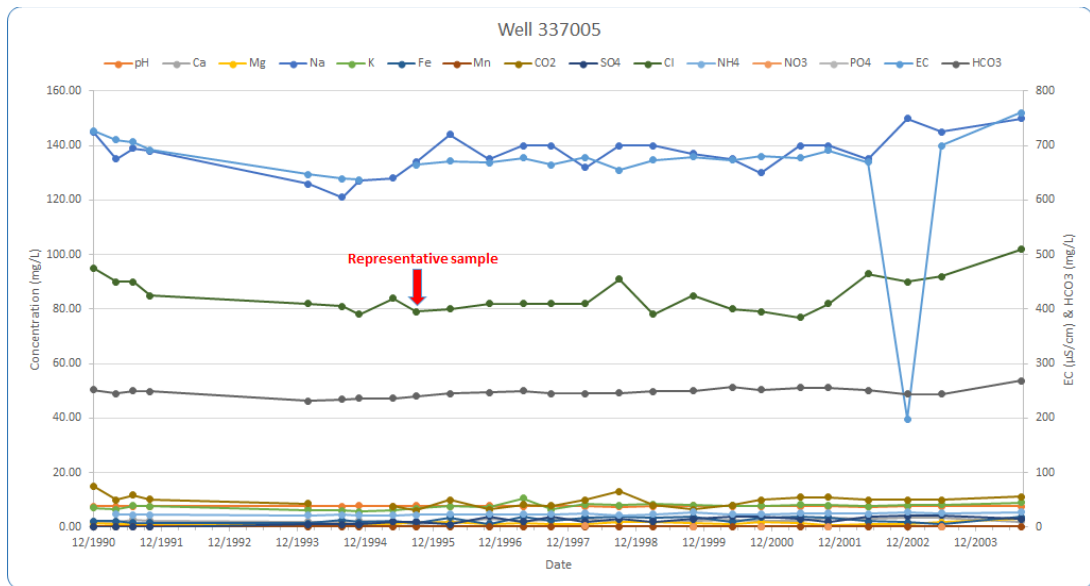


Figure 7-10. Groundwater chemistry hydrograph for Well 337005. Representative sample date (29/09/1995) indicated by red arrow.

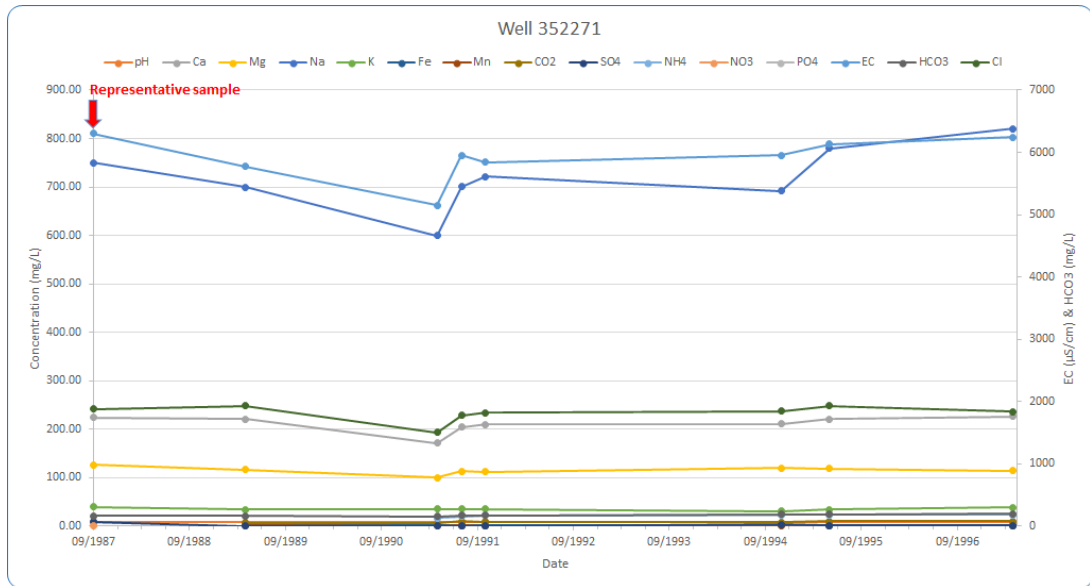


Figure 7-11. Groundwater chemistry hydrograph for Well 352271. Representative sample date (10/09/1987) indicated by red arrow.

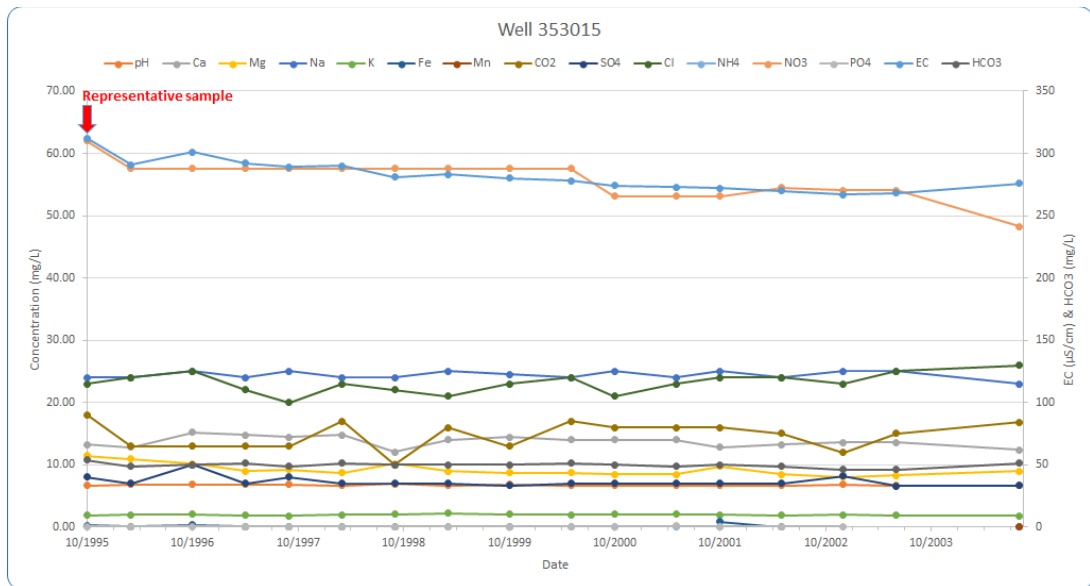


Figure 7-12. Groundwater chemistry hydrograph for Well 353015. Representative sample date (2/10/1995) indicated by red arrow.

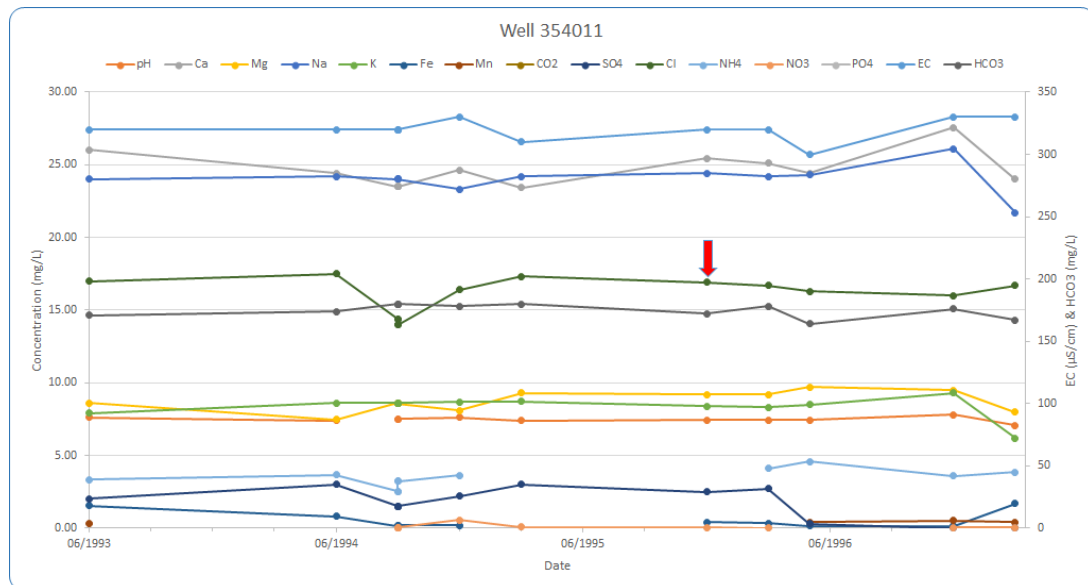


Figure 7–13. Groundwater chemistry hydrograph for Well 354011. Representative sample date (18/12/1995) indicated by red arrow.

The groundwater quality hydrographs (Figure 7–7 through Figure 7–13) support the interpretation of previous investigators who all agree that groundwater quality in the LMC neither exhibits strong seasonal variability nor entails noticeable temporal trends. Absence of significant trend in groundwater quality data is not only characteristic to the LMC, but is rather a commonplace phenomenon throughout New Zealand. Daughney and Wall (2007) statistically analysed groundwater quality data from 119 National Groundwater Monitoring Programme (NGMP) sites and 871 SoE monitoring sites throughout New Zealand. They reported that they did not detect any perceptible long-term trend in the country’s groundwater quality. Two of the NGMP wells studied by Daughney and Wall (2007) are the LMC Wells 336113 and 354011 (Table 7–2, Figure 7–6, Figure 7–8 and Figure 7–13).

## 7.7 Representative samples

To maximise the possibilities for hydrogeochemical interpretation, representative samples for the largest possible number of wells are needed to provide greatest areal and depth range coverage. The well-established lack of notable seasonal and temporal variability in the area’s groundwater quality means that it is feasible to use data collected from different wells at different times for catchment-scale

interpretation. If a well has only one complete/acceptable sample, that sample is considered representative to that well unless proven an outlier during further data synthesis. If a well has more than one complete/acceptable sample, the sample with the smallest *CAB* value is taken to represent it unless proven an outlier by subsequent processing. Hence, a representative sample has been assigned to each of the 268 wells shown in Figure 7–3. Table D–2 in Appendix D specifies which samples are considered representative to the area’s wells. The date of the representative sample for each of the wells that have long–term groundwater quality record is shown on the groundwater quality hydrograph for that well (Figure 7–7 through Figure 7–13).

## 7.8 Hydrogeochemical facies (multi–ion ratios and water types)

The notion of hydrogeochemical facies was developed in analogy with the concept of geological facies (Schumacher, 1999). It is a diagnostic method to determine the chemical character of water in hydrogeological systems based on the ratios between major dissolved ions. Hence, it provides a convenient means to subdivide water masses based on their major constituents into special categories that reflect the hydrogeochemical processes and controls in the groundwater system (Nwankwoala & Udom, 2011). Graphical methods have been conveniently used for hydrogeochemical facies classification (e.g. Durov, 1948; Piper, 1944). Ion ratios and hydrogeochemical facies plots require concentrations to be expressed in milliequivalent per litre (meq/L) units.

More recently, researchers have been increasingly utilising Hierarchical Cluster Analysis (HCA) in hydrogeochemical assessments (e.g. Daughney *et al.*, 2009). However, hydrogeochemical facies methods are preferred to HCA as the latter does not consider hydrogeochemical processes and conditions, but rather depends on fuzzy logic to relate water quality statistics to hydrogeology.

A number of previous groundwater studies in the LMC utilised ion ratio plots and the well–known Piper and Durov diagrams (e.g. Mark–Brown, 1978; Schumacher, 1999; Zarour, 2008). According to Younger (2007), the Durov diagram is similar to

the Piper Diagram (Figure 1–3) but it produces clearer output that is especially well-suited to deducing the processes contributing to the chemical evolution of groundwaters in a given flow system. The Piper Diagram has a diamond-shaped centre area and requires the calculation of the percentages of individual ions to be determined as percentages of the separate totals of cations and anions. The Durov Diagram has a squared centre area and the percentages of individual ions used in it are calculated as percentages of total ions. Both diagrams are well-suited for fresh groundwater hydrogeochemical interpretation (Younger, 2007). An Expanded Durov Diagram was introduced by Burdon and Mazloun (1958) and Lloyd (1965). It has the advantage of being able to classify groundwater into very distinct fields that correspond to specific hydrogeochemical conditions. The procedure for plotting the Expanded Durov Diagram is illustrated in (Figure 7–14). Lloyd and Heathcote (1985) and Younger (2007) describe how to interpret data using the Expanded Durov Diagram (Figure 7–15).

Plotting trilinear diagrams is a tedious process, which has been facilitated by software packages that enable easy production of the Piper and Durov diagrams. There has not been a package to produce the much more laborious Expanded Durov Diagram until Al-Bassam *et al.* (1997) presented DurovPlot©. However, it was difficult to obtain this DOS-based programme and it was not possible to run it on computers operating on modern versions of Microsoft Windows©. Therefore, the method has not been widely used. Al-Bassam and Khalil (2012) released DurovPwin©, which can plot up to 100 samples on the Expanded Durov Diagrams at a time. Aided with DurovPwin©, this thesis utilises the Expanded Durov Diagram in hydrogeochemical facies classification.

Because DurovPwin© has a 100-sample limit which, representative groundwater samples were plotted on the Expanded Durov Diagram in three continued drawings (Figure 7–16, p 209–211). Figure 7–17 shows the areal distribution of various groundwater facies across the LMC.

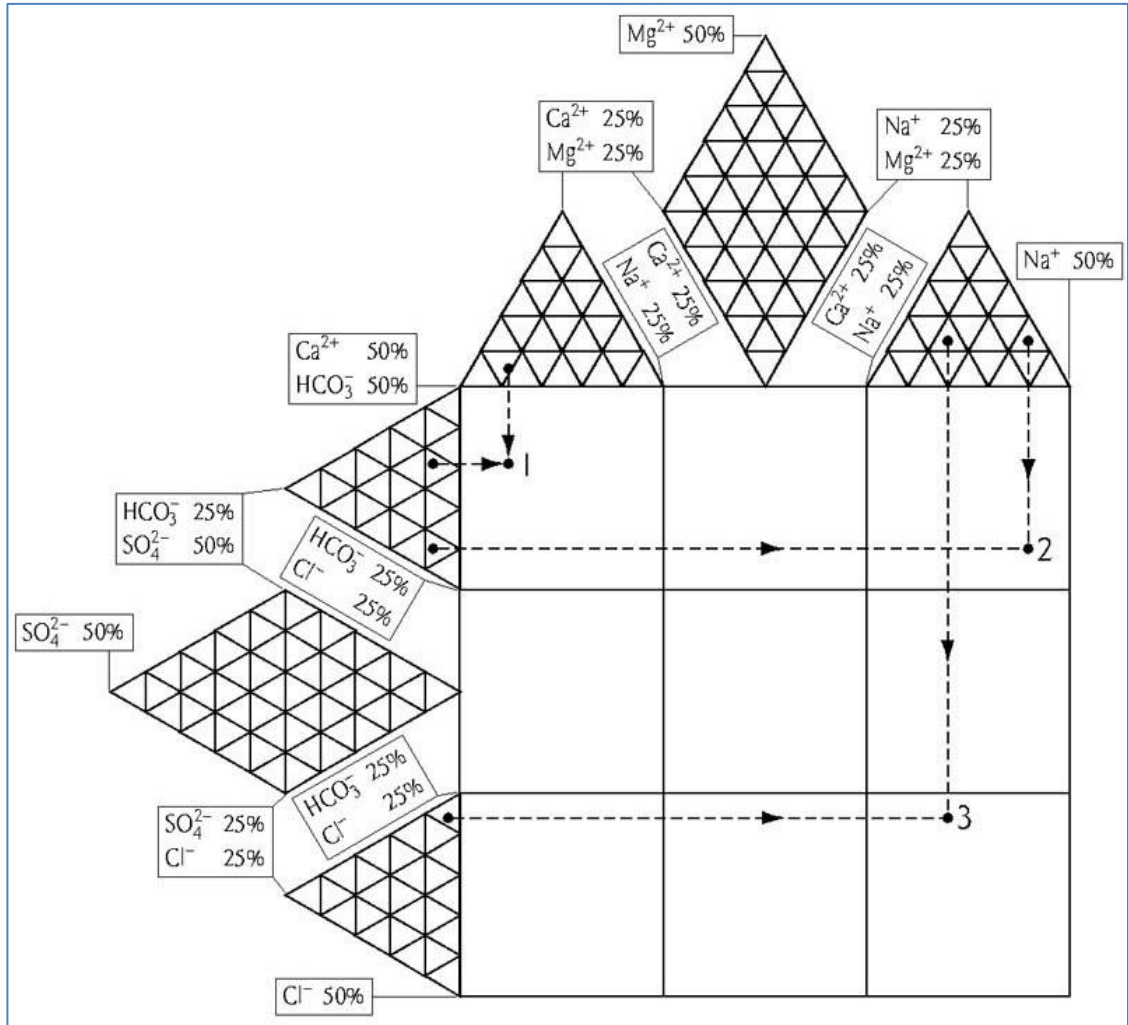


Figure 7-14. Procedure to plot samples on the Expanded Durov Diagram (adapted after Younger, 2007).

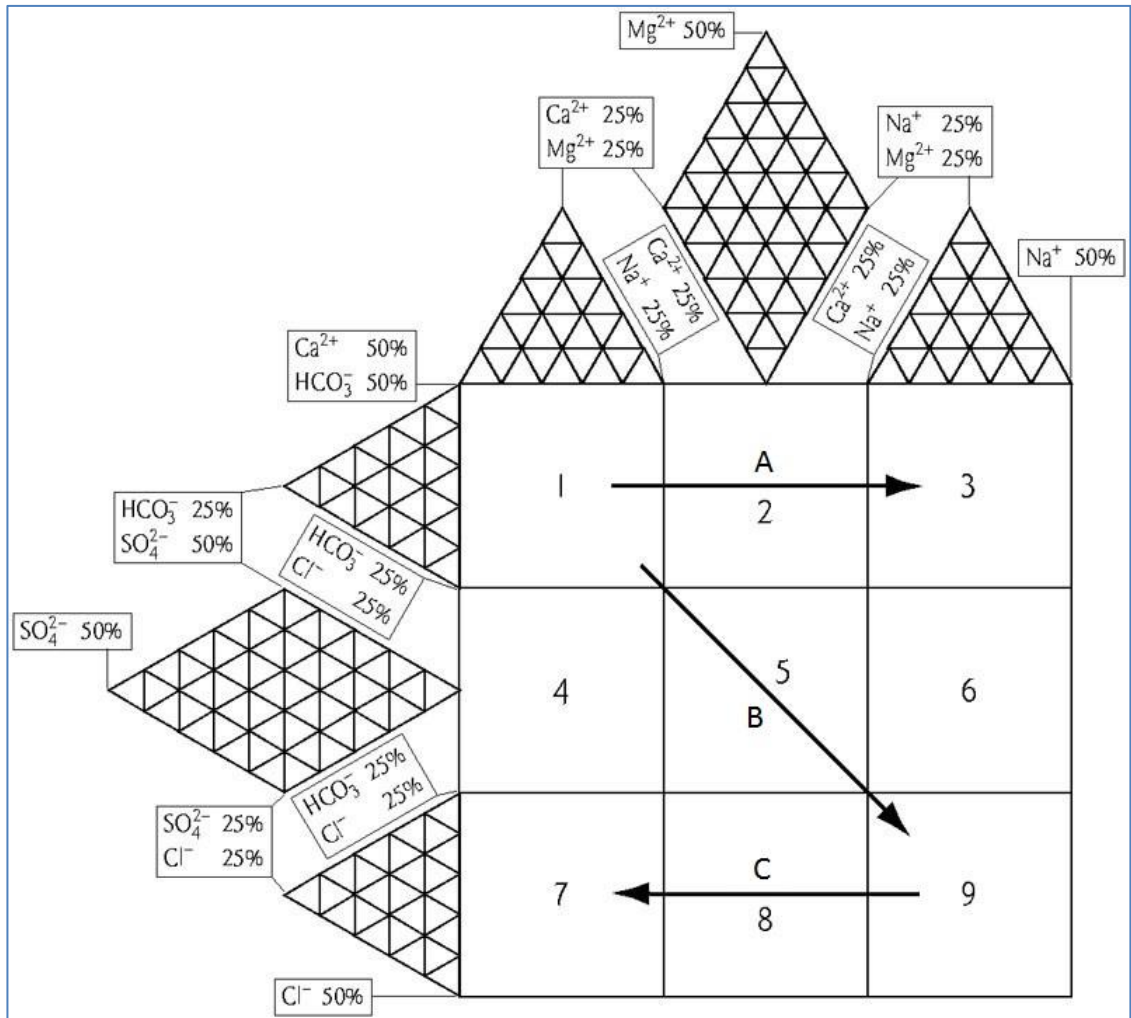


Figure 7-15. Interpolation of the Expanded Durov Diagram (Modified after Younger, 2007).

Field numbers can be used to typify the water and labelled arrows indicate evaluation processes for samples on the same flow path (A: ion exchange, B: dissolution and/or mixing, C: reverse ion exchange).

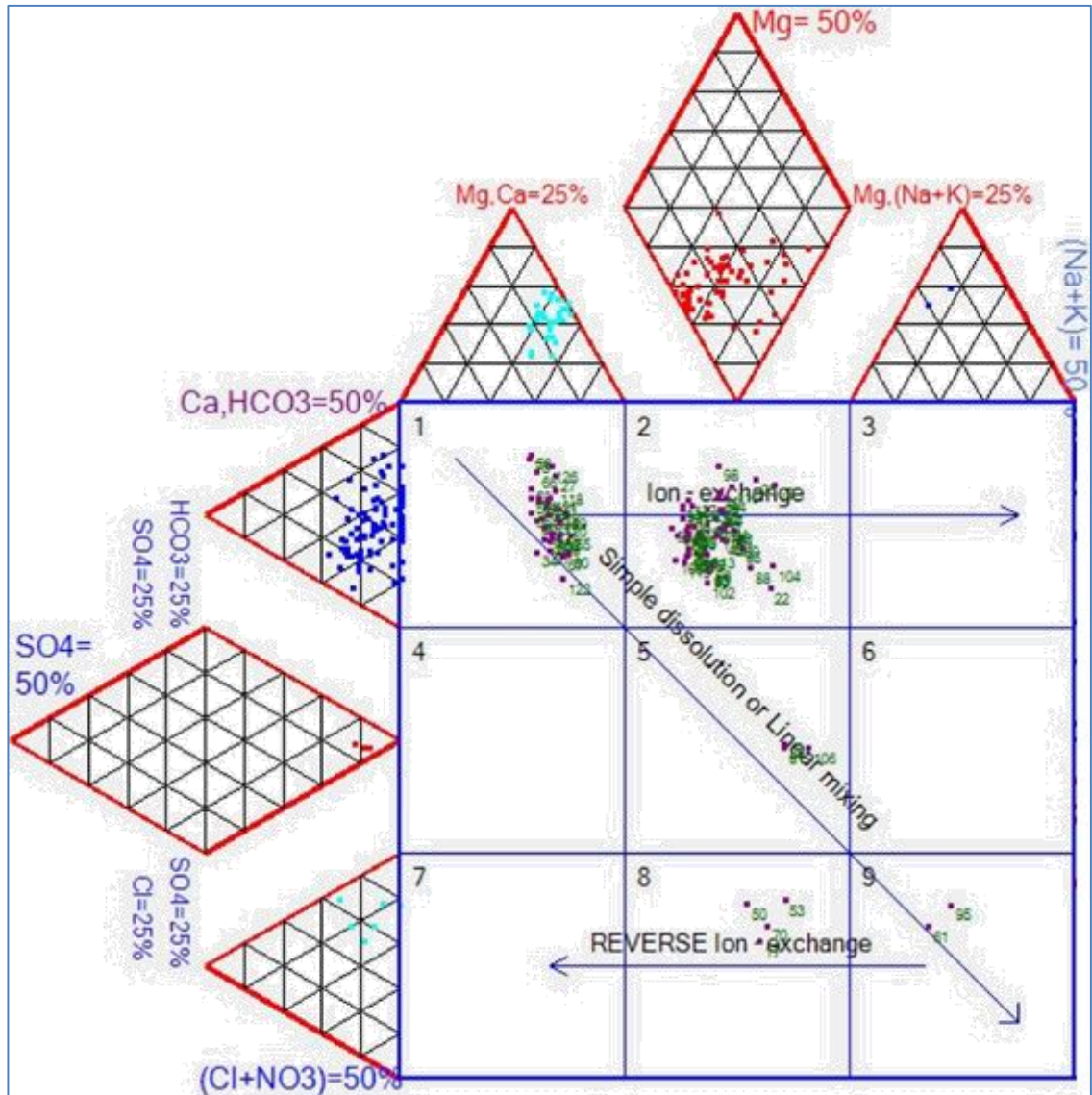


Figure 7-16. Expanded Durov plot of samples from the LMC (continued overleaf).

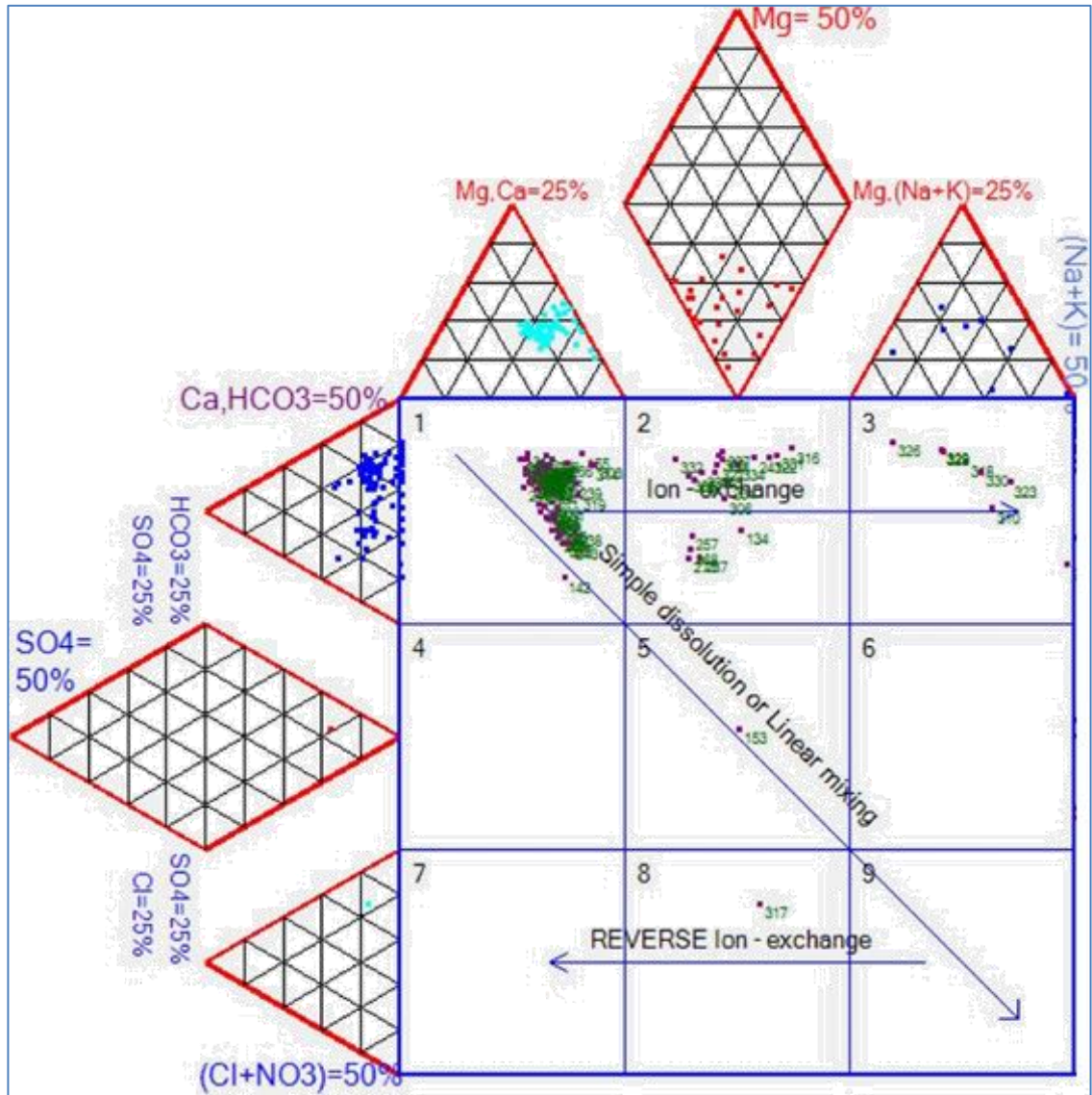


Figure 7-16 (cont.). Expanded Durov plot of samples from the LMC (continued overleaf).

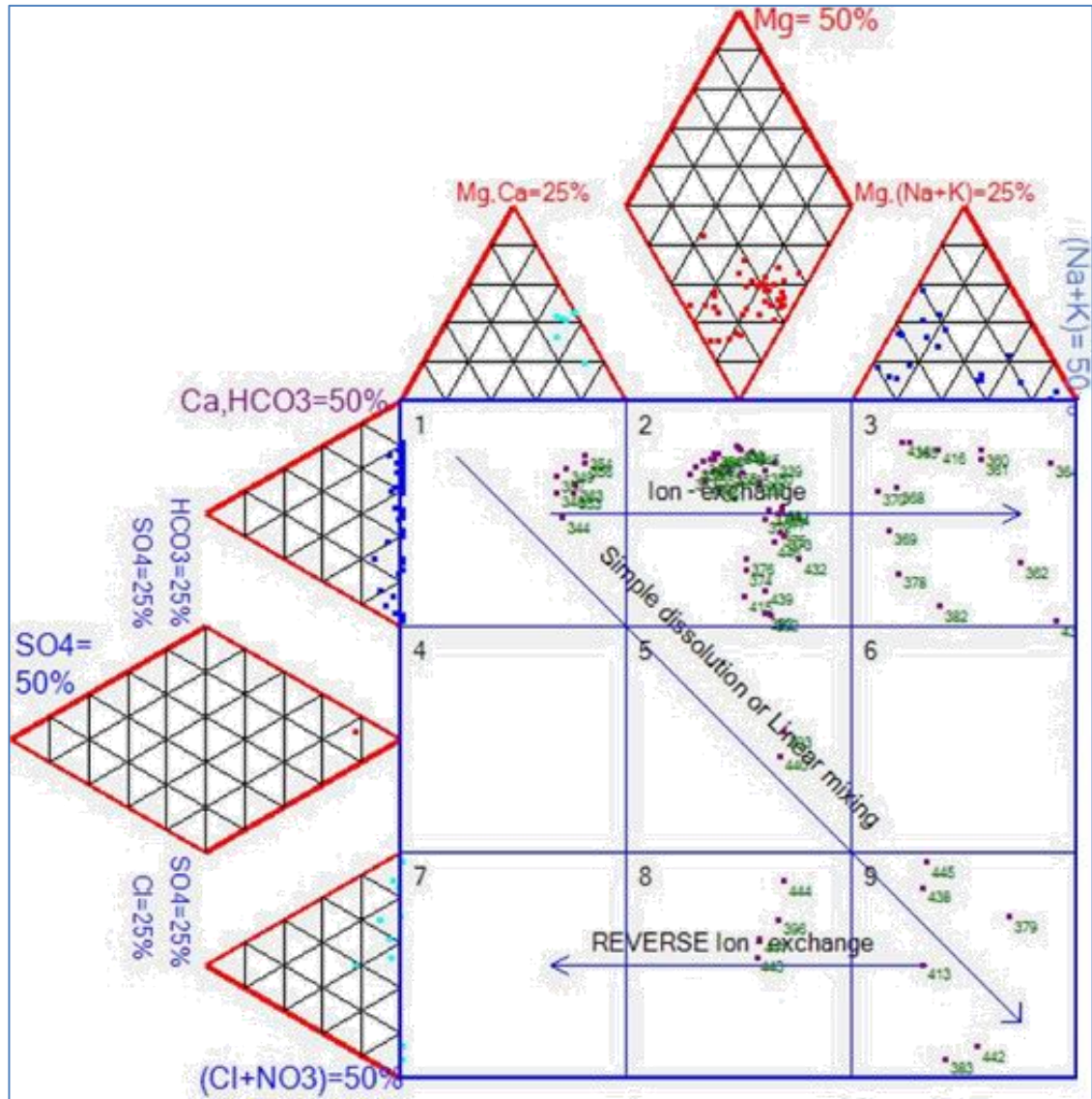


Figure 7-16 (cont.). Expanded Durov plot of samples from the LMC.

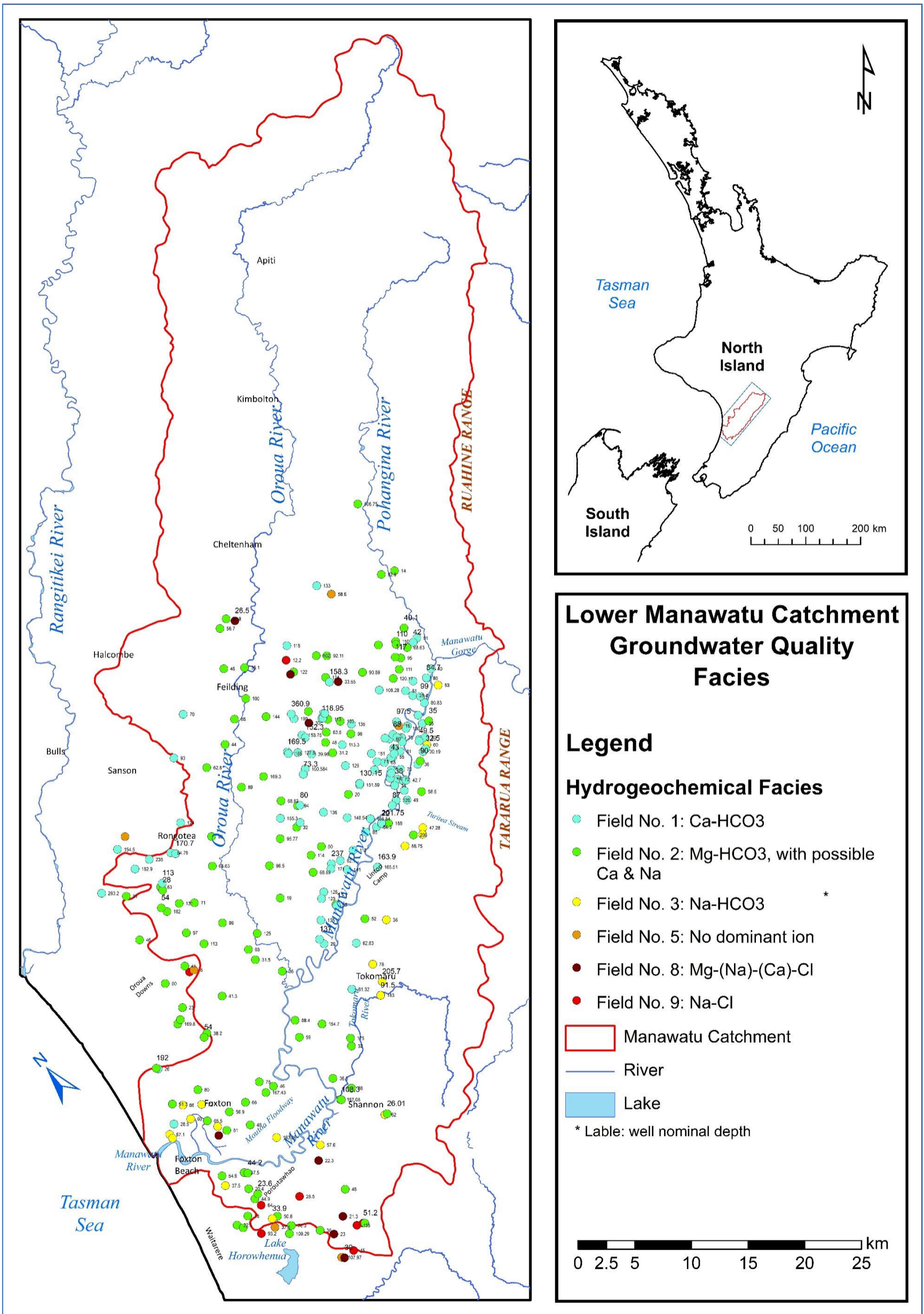


Figure 7-17. Groundwater quality types in the LMC.

The main characteristics and possible interpretation of the groundwater facies identified using the Expanded Durov Diagram are summarised in Table 7–3.

Table 7–3. Classification of LMC representative samples using the Expanded Durov Diagram hydrogeochemical facies typifying.

*Interpretation is based on Lloyd and Heathcote (1985) and Younger (2007).*

Field number	Predominant facies <sup>47</sup>	Possible interpretation	Number of samples
1	$Ca - HCO_3$	Fresh groundwater in recharge area.	111
2	$Mg - HCO_3$	Important proportions of $Ca^{2+}$ and $Na^+$ indicative of ion exchange.	113
3	$Na - HCO_3$	Unconfined aquifer or shallower portion of a regional-scale confined aquifer. $HCO_3^-$ possibly resulting from dissolution of $CO_2$ generated at depth. $Na^+$ is dominant due to ion exchange, dissolution of plagioclase or dilution of mineralised geothermal groundwater.	21
5	<i>No clear facies</i>	Normally the result of mixing of two or more different facies or indicative of waters exhibiting simple dissolution	6
8	$Mg - (Na) - (Ca) - Cl$	Mixing of fresh and saline waters. Possible influence of reverse ion exchange.	9
9	$Na - Cl$	Influence of seawater, ancient saline groundwaters, or dissolution of halite ( $NaCl$ ) <sup>48</sup> frequently indicating end-point waters (e.g. seawater).	8

Figure 7–17 indicates that Expanded Durov diagram Field No. 1  $Ca - HCO_3$  facies is dominantly characteristic of groundwater in the Lower Manawatu Valley, from Ashhurst to the confluence of the Manawatu River with Oroua River (Figure 7–17). It reflects dominance of alkali earth and weak acids in the groundwater and may indicate local recharge from rain and/or river water. This hydrogeochemical facies is also found in the area between Taonui Stream and Manawatu River, to the southwest of Bunnythorpe and in the groundwater divide area associated with the Mt Stewart–Halcombe anticlinal structure. Coincidence of  $Ca - HCO_3$  water with topographical highs and groundwater divides commonly signifies recharge area settings.

<sup>47</sup> It may be necessary to refer to the raw data to determine the precise facies in some cases.

<sup>48</sup> Discrimination between these various alternatives requires further analysis, such as plotting a Hounslow diagram.

Expanded Durov diagram Field No. 2  $Mg - HCO_3$  water facies is widespread across the LMC (Figure 7-17). It represents recharge water that had the chance to evolve further than Field No. 1 water masses. Important proportions of  $Ca^{2+}$  and  $Na^+$  in these waters indicate noticeable ion exchange. In coastal settings, this water type is generally typical of the 'leading-edge' of seawater intrusion into a shallow unconfined aquifer. However, this is not the case in the LMC as groundwater of this type is not excessively saline and the water type is fresh in the coastal area.

Expanded Durov diagram Field No. 3  $Na - HCO_3$  water type seems to be associated with Last Interglacial deposits, but also is found in the Foxton area (Figure 7-17).  $Na - HCO_3$  facies possibly indicates ion exchange resulting from slower flow rates and longer interaction between groundwater and the aquifer material. According to Herczeg *et al.* (1991), the release of  $Na^+$  into dilute waters nearer the recharge areas may be accomplished by: (a) dissolution of  $Na^+$ -bearing minerals (e.g. plagioclase or orthoclase), (b) cation exchange that releases  $Na^+$  from clay minerals, (c) conversion of a  $Na^+$ -smectite to kaolinite. Incongruent dissolution of albite releases  $Na^+$  and  $HCO_3^-$  into solution in an approximately 1:1 ratio, which clearly is not the case in the LMC (Figure 7-18).  $Na - HCO_3$  water type may also indicate the generation of  $CO_2$  at depth in a  $Na^+$  dominated environment (Chadha, 1999). Dominant  $Na^+$  can result from the dissolution of plagioclase in greywacke and greywacke-derived sediments and the dilution of mineralised geothermal groundwater. The warmest groundwater in the LMC (c. 20°C) is tapped by the nearly 200 m deep Wells 336233 and 336442 located at Massey University Turitea Campus. There is also anecdotal evidence that deep wells at Linton Military produce even warmer water. At such depths, it is unlikely that the groundwater temperature is a result of thermal pollution to the aquifer from the university or the army camp. It is more likely to be related to mineralised geothermal water emerging from the nearby basement rock, which mixes with groundwater affecting its physical and hydrogeochemical properties.

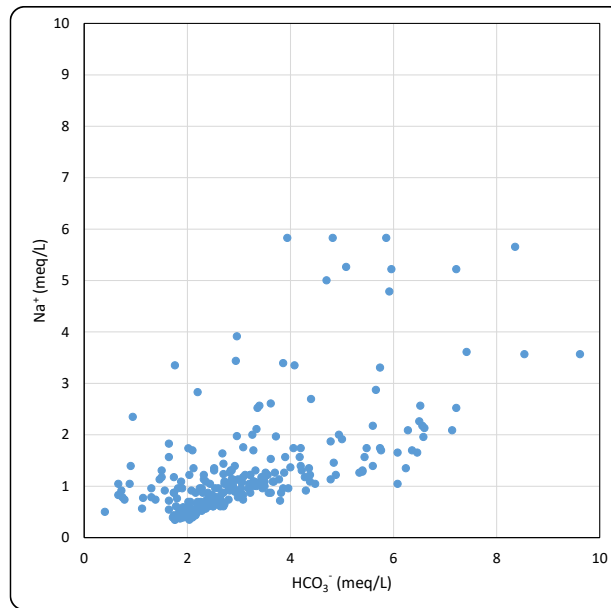


Figure 7–18.  $HCO_3^-:Na^+$  relationship for LMC groundwater.

Field No. 3 water type is also found in the Foxton area, near the terminus of the Manawatu River and LMC groundwater system into the Tasman Sea (Figure 7–17). In the absence of elevated  $Cl^-$  levels, the source of  $Na^+$  in that area is likely to be ion exchange rather than seawater invasion or sea spray. In some cases where ion exchange is a predominant process, high  $Na^+$  can remain in groundwater after the flushing of  $Cl^-$ .

There are only few samples representing Expanded Durov diagram Field No. 5 water type, mainly located at marginal settings, e.g. very close to the groundwater divide (Figure 7–17). The sample of this type found near Te Matai Road could also be considered  $Ca - HCO_3$  water facies (Field No. 1), despite technically falling in Field No. 5 on the Expanded Durov diagram. There is also a Field No. 5 sample that relates to a nearly 56 m deep well on the crest of the Pohangina Anticline. This sample has high proportions of  $Na^+$ ,  $Mg^{2+}$  and  $Cl^-$ , which may reflect effects of local land use practices on the groundwater resource. However, this effect is not widespread as evidenced by data from neighbouring wells.

Expanded Durov diagram Field No. 8  $Mg - (Na) - (Ca) - Cl$  water type and Field No. 9  $Na - Cl$  water type are found preliminarily in the Poroutawhao Basement High

area, close to the southwestern boundary of the LMC (Figure 7–17). These water types are also found in the Bunnythorpe area and the area north of it. Field No. 8 water type is probably a mix of fresh groundwater and greywacke connate water that has undergone reverse ion exchange. Field No. 9 groundwater is believed to be connate waters from the greywacke basement high and overlying deposits like the Plio–Pleistocene marine rocks in the Bunnythorpe area and the Last Interglacial strata near Levin.

### 7.9 Alkalinity and hardness

Groundwater in the LMC generally has low–moderate salinity ( $TDS < 1,000$  mg/L) and is mostly slightly alkaline ( $7.0 < pH < 8.5$ ). In waters with  $pH$  not exceeding 9, alkalinity mostly consists of  $HCO_3^-$ . The areal distribution of  $pH$  values unsurprisingly suggests that acidic waters are present in recharge areas and alkaline waters are found in discharge zone settings (Figure 7–19).

$Ca^{2+}$  and  $Mg^{2+}$  are the dominant cations in groundwater in the LMC (Figure 7–16 and Figure 7–17).  $Ca^{2+}$  and  $Mg^{2+}$  are mostly sourced from carbonate minerals. Miller (1952) clarifies that the solubility of  $CaCO_3$  (e.g. calcite and aragonite) in water depends on the presence of  $CO_2$ , the concentration of which is a function of temperature and  $CO_2$  pressure in equilibrium with the water. At fixed temperature, the solubility of  $CaCO_3$  increases as  $CO_2$  pressure increases. At constant  $CO_2$  pressure,  $CaCO_3$  solubility increases with decreasing temperature.  $CO_2$  pressure is conveniently expressed as  $CO_2$  partial pressure ( $pCO_2$ ). Macpherson (2009) developed equation 7–10 to calculate partial pressure of  $CO_2$  ( $pCO_2$ ) from alkalinity ( $HCO_3^-$ ) and  $pH$ .

$$\log_{10}(pCO_2) = \log_{10}(HCO_3^-) - pH + 7.749 \quad 7-10$$

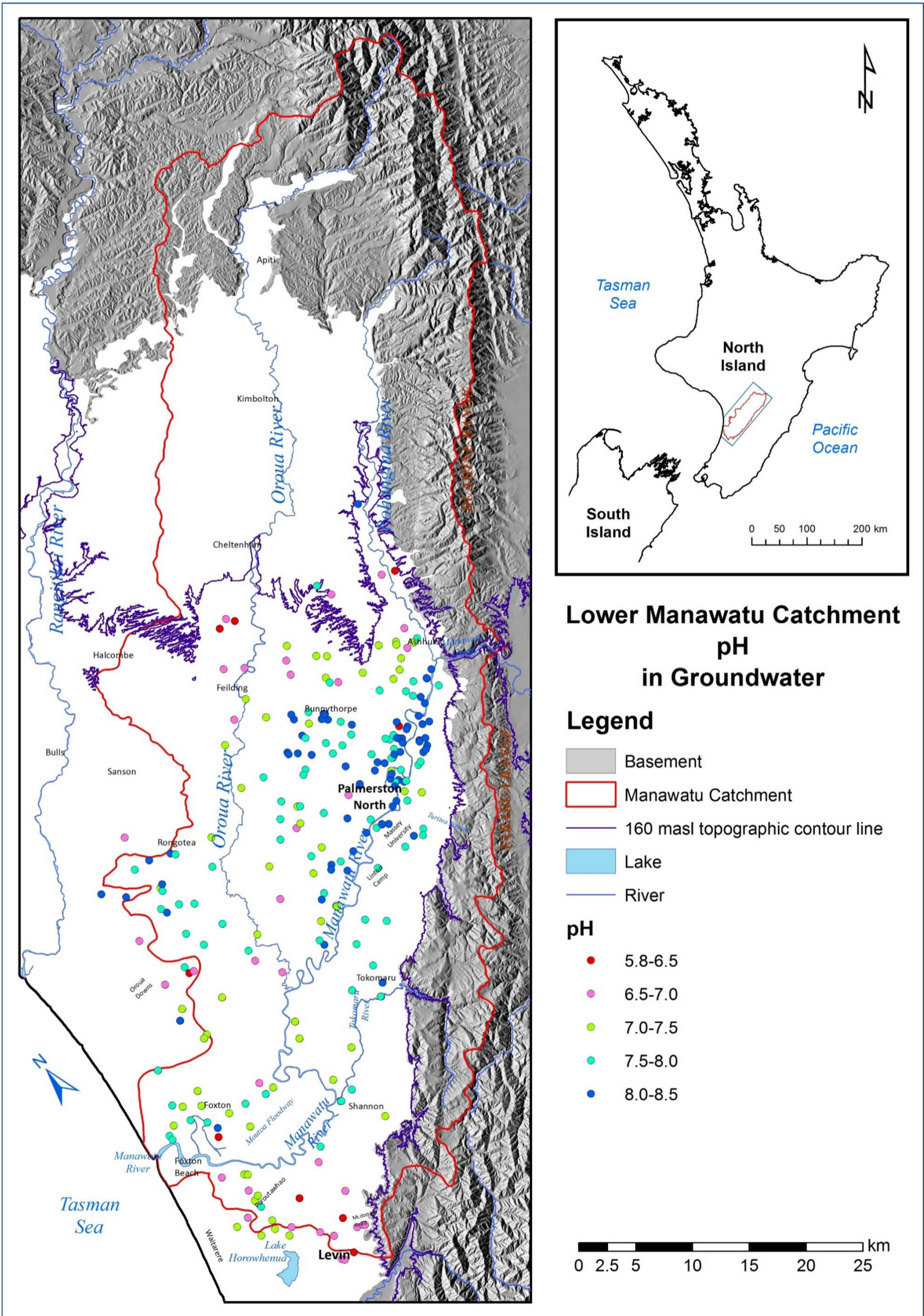


Figure 7-19. pH values for representative groundwater samples in LMC.

Equation 7–10 was used to calculate  $pCO_2$  for representative samples from the LMC (Table D–3 in Appendix D). Global average for  $pCO_2$  in the atmosphere is approximately  $3.95 \times 10^{-4}$  atm<sup>49</sup> (Atkins *et al.*, 2013). Table D–3 in Appendix D shows that  $pCO_2$  in LMC groundwaters ranges between  $3.96 \times 10^{-3}$  and  $8.23 \times 10^{-1}$  atm, which is much higher than atmospheric values. This indicates that LMC groundwater is  $CO_2$ -enriched, which is consistent with drillers' anecdotal observation of 'gas' release occasionally noticed during drilling in the LMC. Irrigation with  $CO_2$ -enriched water such as the LMC groundwater may also result in  $CO_2$  degassing, but this is not easily quantifiable (Macpherson, 2009). To check on the applicability of equation 7–10 to LMC conditions, calculated  $pCO_2$  values have been plotted against measured  $CO_2$  values (Figure 7–20). The linear relationship shown in Figure 7–20 gives confidence in both  $pCO_2$  calculations and  $CO_2$  laboratory results. The good correlation also suggests that the parameters used in  $pCO_2$  calculations are reliable, namely  $HCO_3^-$  and  $pH$ .

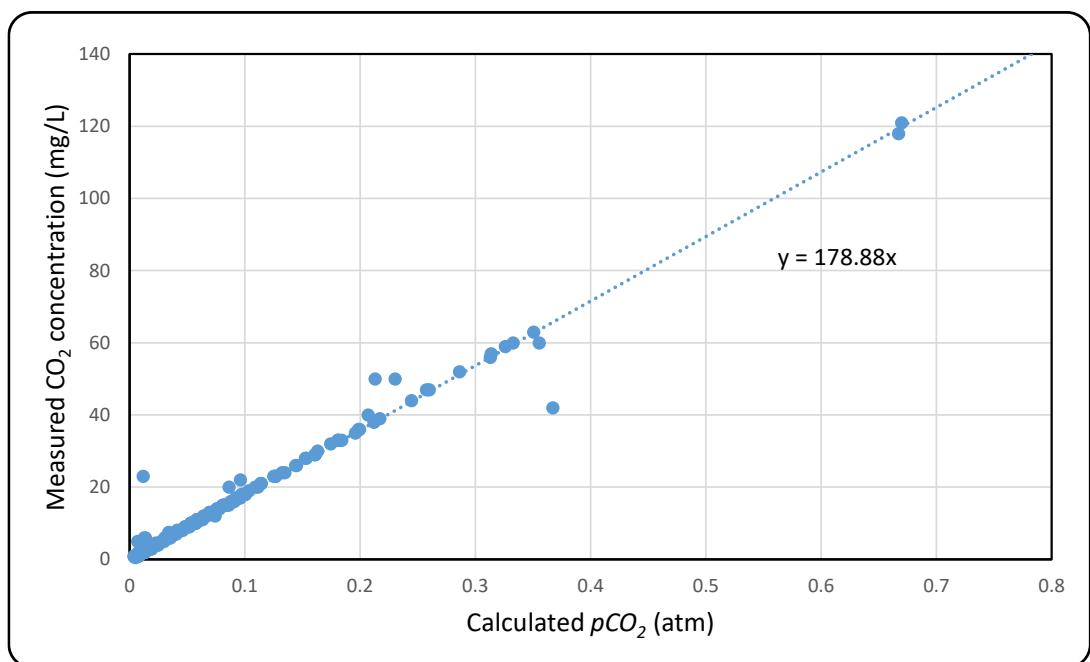


Figure 7–20. Relationship between calculated  $pCO_2$  and measured  $CO_2$  values in LMC groundwaters.

<sup>49</sup> 1 atm = 101.325 kPa

Co-existence of alkalinity ( $\text{HCO}_3^-$ ) and bivalent cations such as  $\text{Ca}^{2+}$  and  $\text{Mg}^{2+}$  results in hardness, which is a cationic phenomenon. Hardness is a water use nuisance. It is normally expressed in units of mg/L as  $\text{CaCO}_3$ . When total hardness is less than alkalinity, all the hardness is due to carbonate. When total hardness exceeds carbonate hardness, the balance is non-carbonate hardness. Total, carbonate and non-carbonate hardness values for representative samples from the LMC have been calculated using USGS<sup>50</sup> PHREEQC© geochemical speciation and thermodynamics modelling code (Parkhurst & Appelo, 2013), which is incorporated in AquaChem© software (Table D-3 in Appendix D).

From the above data, it is clear that high  $\text{CO}_2$  content and pressure in the LMC aquifer system is responsible for making  $\text{HCO}_3^-$ ,  $\text{Ca}^{2+}$  and  $\text{Mg}^{2+}$  dominant in the area's groundwater.  $\text{CO}_2$ -enriched groundwater environments comprise shallow unconfined aquifers that are in contact with the high  $\text{CO}_2$  soil zone and deep groundwater that is supplied with  $\text{CO}_2$  from decomposition of organic matter such as peat.

### 7.10 Redox conditions and nitrate concentrations

Redox potential ( $Eh$ ) is a measure of the tendency of a chemical species to accept electrons, i.e. to be reduced. It is expressed in volt (V) or millivolt (mV) units. Every species has its own intrinsic reduction potential. The more positive the species intrinsic reduction potential, the greater its affinity for electrons and tendency to be reduced. Positive  $Eh$  values indicate environments that favour oxidation reaction (e.g. free oxygen-rich systems) and negative  $Eh$  values characterise reducing environments (e.g. free metals-rich systems). Groundwater redox status is determined by the aquifer material composition, the relative rates of introduction of oxidants (e.g.  $\text{O}_2$ ,  $\text{CO}_2$  and  $\text{NO}_3^-$ ) and the consumption of these oxidants by bacterially catalysed decomposition of organic matter (Rissmann, 2011).

---

<sup>50</sup> USGS: United States Geological Survey.

No  $Eh$  data are available to enable depiction of the redox status for the LMC groundwater system. Only very few measurements are available for dissolved oxygen ( $DO$ ), iron and manganese species ( $Fe^{2+}$ ,  $Fe^{3+}$ ,  $Mn^{4+}$ ,  $Mn^{3+}$ ) to assist with standard quantitative analysis. Nevertheless, the system's redox situation can be assessed using other available hydrogeochemical data.

Examination of the redox category of the 268 representative groundwater samples using AquaChem© software reveals that only 18 wells tap 'weakly oxidised' groundwater, being water containing nitrate and sulphate, but no or very little oxygen and iron. All the remaining samples represent groundwater that is characterised by a 'redox conflict' as they contain strongly reduced and highly oxidised constituents. This is rather dissimilar to the opinion of previous investigators who believed that reduced conditions prevail in the LMC aquifers. Table D-3 in Appendix D shows that both 'weakly oxidised' and 'redox conflict' water types can occur at any depth in the LMC. However, 'weakly oxidised' groundwaters are more likely to be found at the southwestern boundary of the LMC, where Plio-Pleistocene strata may be thinner near the Poroutawhao Basement High (Figure 7-21).

Peat is abundant in the stratigraphy of the LMC (Figure 7-22). Its release of  $CO_2$  is responsible for the LMC being dominated by  $HCO_3^-$ ,  $Ca^{2+}$  and  $Mg^{2+}$ .  $CO_2$  is released from the organic material (peat) in the aquifer stratigraphy into groundwater through fermentation of organic matter (see Section 7.9 for equations), which only occurs when all external electron acceptors have been used in accordance with the redox ladder or sequence (Figure 7-23). This process, which is known as methanogenesis involves production of methane ( $CH_4$ ) as well as production and consumption of  $CO_2$ .

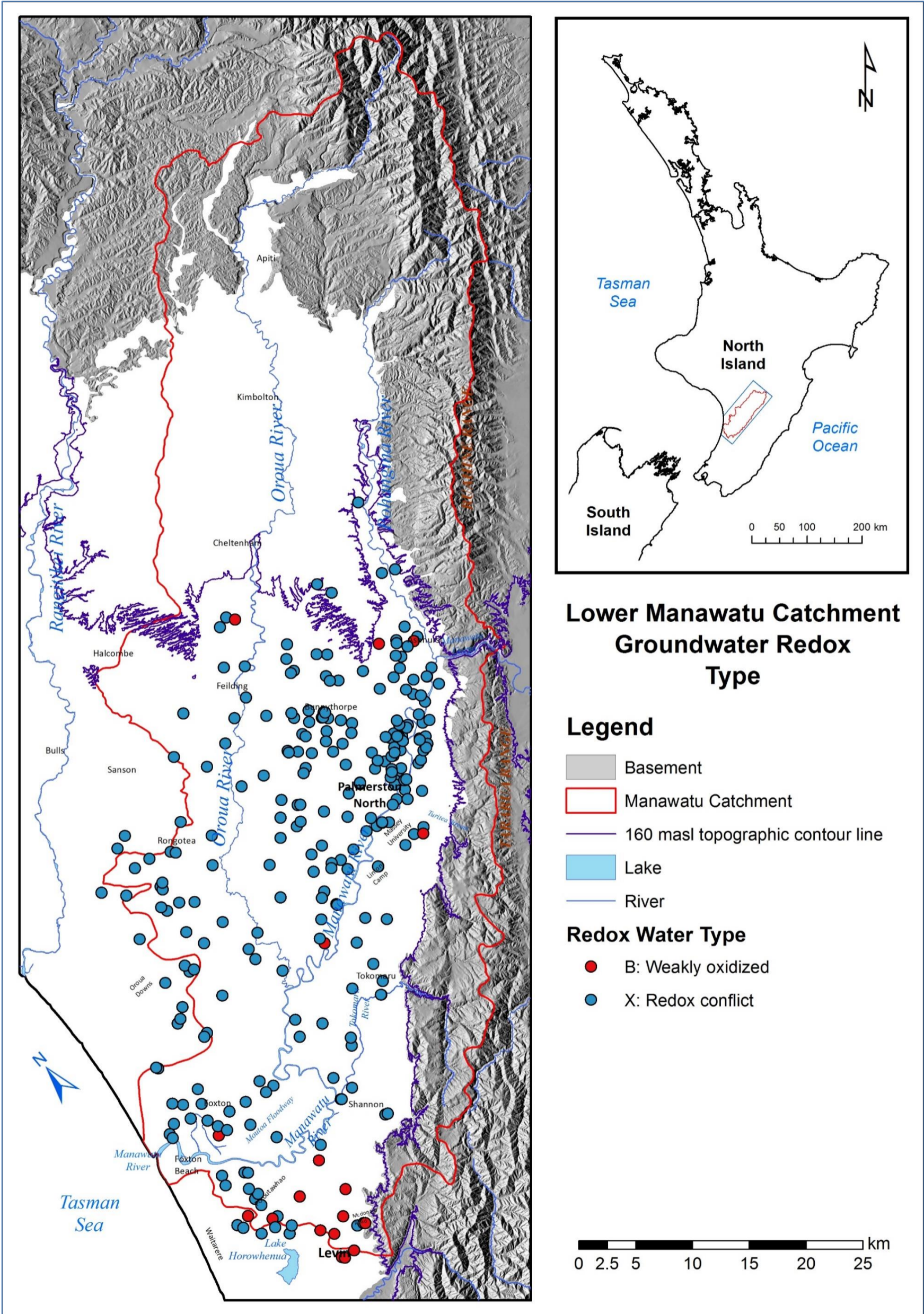


Figure 7-21. Redox groundwater types in the LMC.

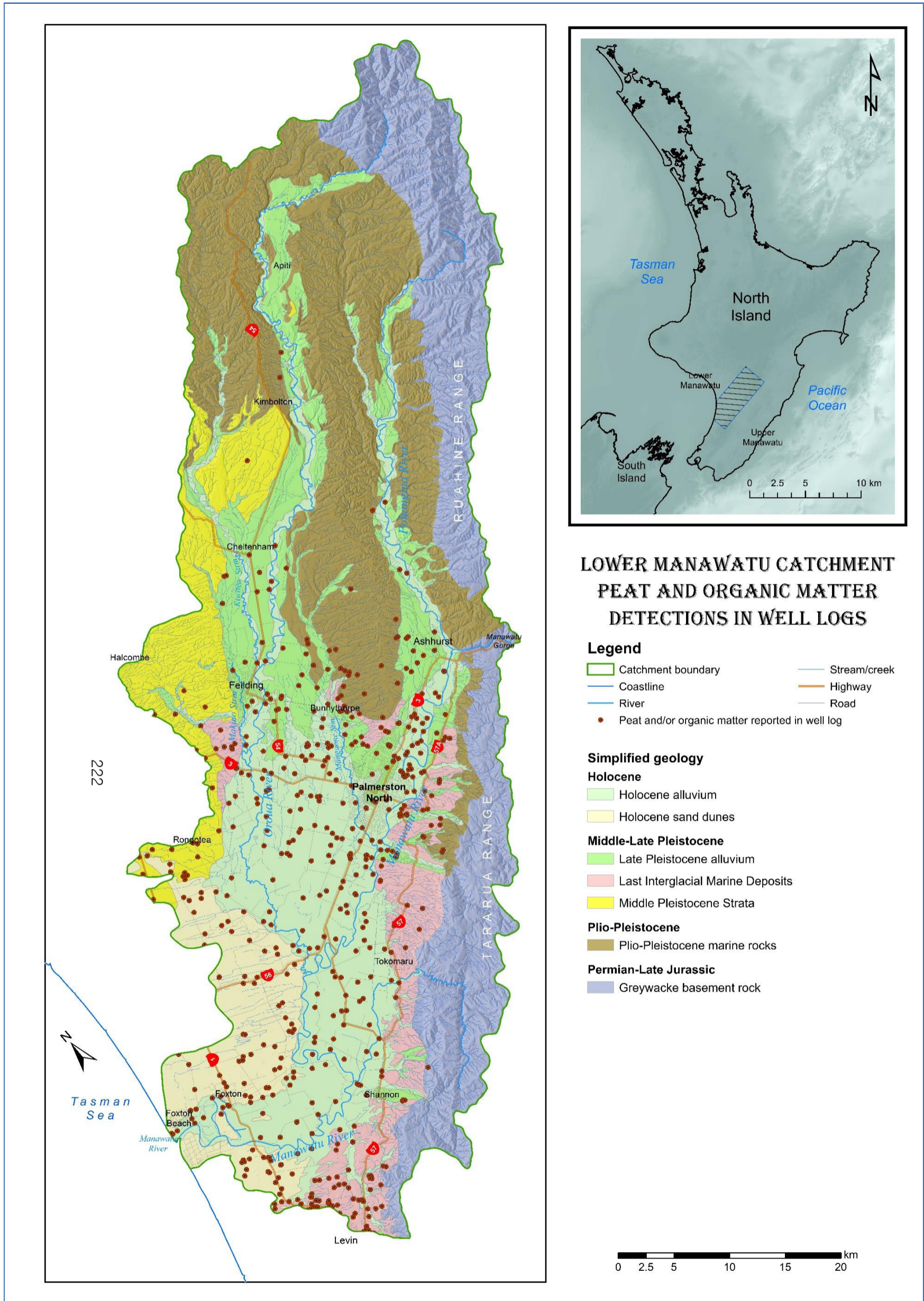


Figure 7-22. Location map showing detections of peat/organic matter reported in drillers' well logs.

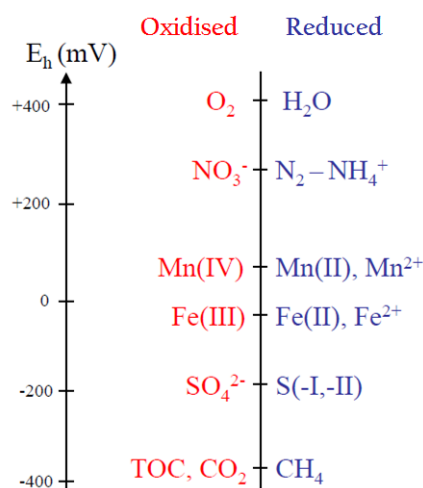


Figure 7–23. Redox ladder: electron acceptors and donors.

Aquifers with abundant electron donors tend to rapidly consume oxygen and progress quickly through the redox sequence, making water increasingly reduced. Accordingly, organic matter is the most common electron donor in groundwater. The rate of progression down the redox ladder depends on many factors including the aquifer material composition, sediment size and groundwater temperature (Rissmann, 2011).

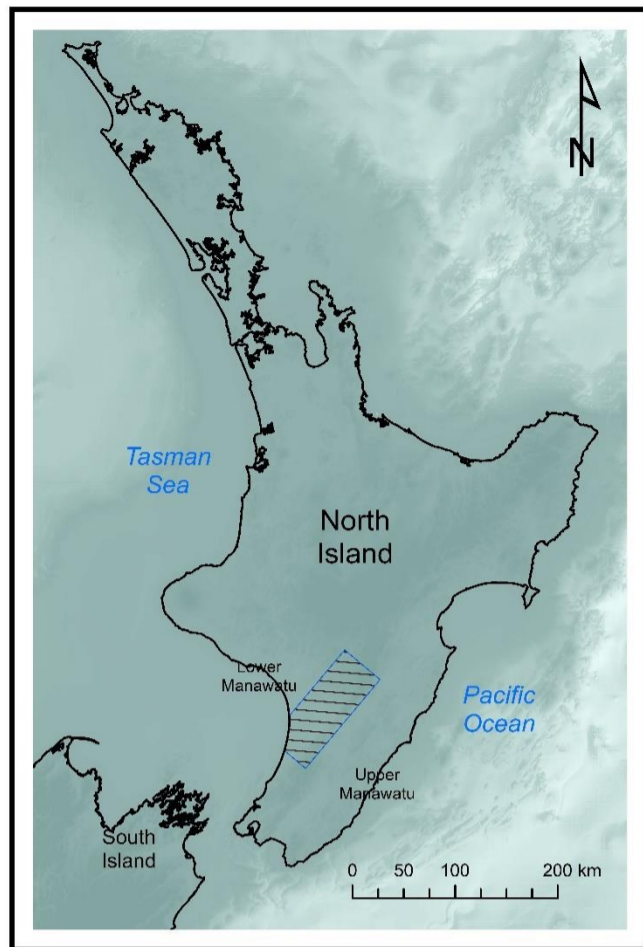
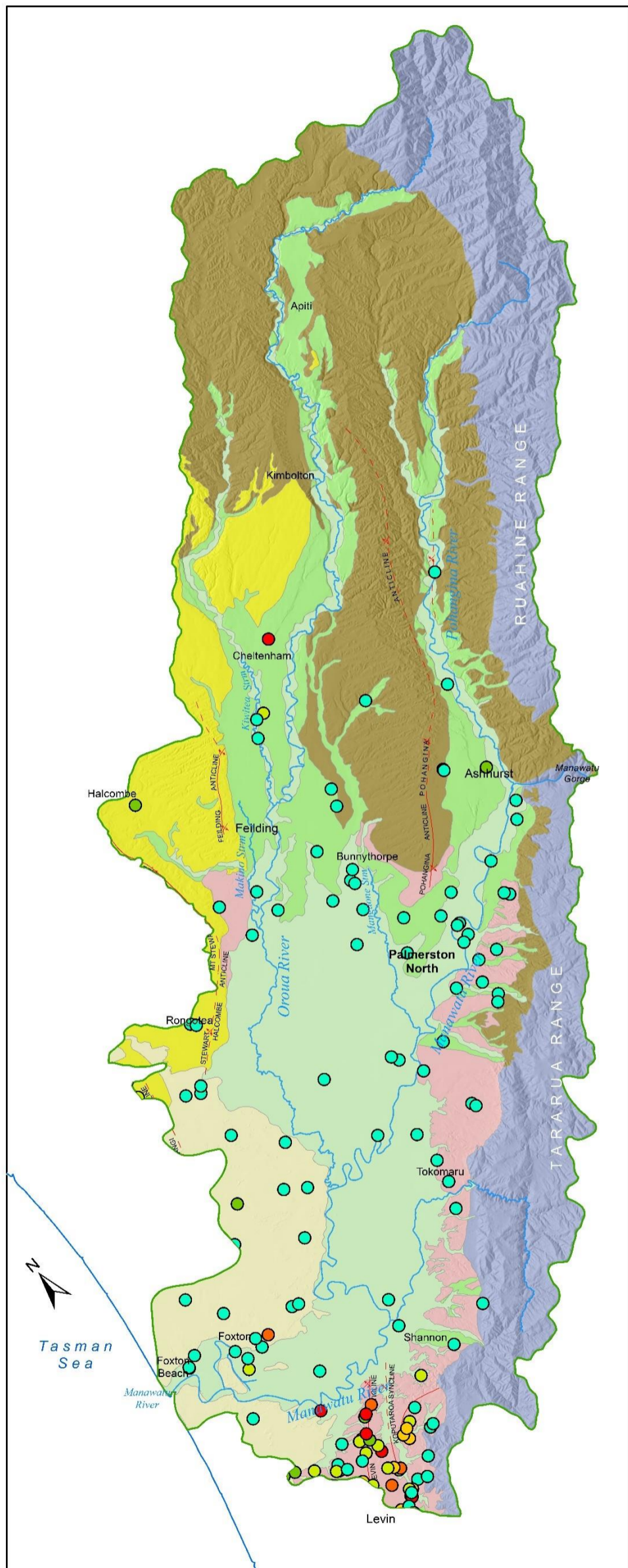
Prevalence of non-oxidised conditions, specifically ‘redox conflict’ in the LMC groundwater regime greatly reduces its sensitivity to pollution by nitrate from agricultural activities. Abundant  $CO_2$  and high  $pCO_2$  reflect strong reducing conditions in the LMC groundwater system. If an energetically more favourable electron acceptor such as  $NO_3^-$  is introduced to such water, bacteria in the system will quickly switch to using that compound to obtain the energy it needs to decompose the available organic matter. In the process,  $NO_3^-$  will be reduced to nitrogen gas ( $N_2$ ) or gaseous nitrous oxides ( $NO_x$ ). Both products are poorly soluble in water and tend to float up the groundwater system as bubbles that ultimately escapes the groundwater system to the atmosphere, resulting in a net loss of nitrogen from the groundwater. This process is known as denitrification. It effectively removes nitrate from groundwater, lessening the possibility of its accumulation. Denitrification requires anoxic conditions in the groundwater marked with  $DO$  below 2 mg/L. Reduced water is normally associated with relatively high

concentrations of *Fe*, *Mn*, and  $NH_4^+$ . Oxidised groundwater conditions in New Zealand are typically characterised by nitrate concentrations greater than 1 mg/L  $NO_3^- - N$ , the equivalent to 4.43 mg/L  $NO_3^-$  (Daughney & Reeves, 2005).

Nitrate concentrations in groundwater in the LMC are generally low (Figure 7–24), indicating reduced groundwater conditions according to the measure suggested by Daughney and Reeves (2005) and is well below the short-term maximum allowable value (MAV) of 50 mg/L  $NO_3$  (11.3 mg/L  $NO_3-N$ ) set by the Ministry of Health (2005) in the Drinking water standards for New Zealand (DWSNZ). The nitrate MAV is intended to safeguard against methaemoglobinaemia in foetus and infants (the blue baby syndrome).

Nitrate concentrations exceed MAV only in the Levin Anticline–Koputaroa Syncline area east of Levin (Figure 7–24). The area's geology is not much different than the rest of the LMC. The area is not lacking in terms of organic material in the aquifer material (Figure 7–22). Local structure affecting Last Interglacial strata may be responsible for the noticed elevated nitrate concentrations through creating low velocity groundwater flow conditions that limit dilution of nitrate contamination from local land use activities. In addition, there are a couple of outlier high nitrate concentrations that are believed to be related to anthropogenic activities in the immediate vicinity of the affected wells, one in Cheltenham and the other in Foxton.

Nitrate concentrations in the LMC do not exceed the guidelines set by the Australian and New Zealand Environment and Conservation Council, which specify a nitrate trigger value (TV) of 400 mg/L of  $NO_3$  as a measure for fitness of water for livestock consumption (ANZECC & ARMICANZ, 2000). The same guidelines set maximum recommended average for irrigation water of 22 mg/L of  $NO_3$  over periods of up to 100 years (long-term) and 110–550 mg/L of  $NO_3$  over periods of up to 20 years (short-term) to minimise nitrogen leaching into aquifers and surface water bodies.



### LOWER MANAWATU CATCHMENT NITRATE CONCENTRATION (MG/L) IN GROUNDWATER

#### Legend

- Catchment boundary
- River
- Coastline

#### Simplified geology

##### Holocene

- Holocene alluvium
- Holocene sand dunes

##### Middle-Late Pleistocene

- Late Pleistocene alluvium
- Last Interglacial Marine Deposits
- Middle Pleistocene Strata

##### Plio-Pleistocene

- Plio-Pleistocene marine rocks

##### Permian-Late Jurassic

- Greywacke basement rock

#### Active Folds

- accurate, anticline
- accurate, syncline
- approximate, anticline
- approximate, syncline
- concealed, anticline

#### NO<sub>3</sub> concentration

- <5 mg/L
- 5-10 mg/L
- 10-25 mg/L
- 25-50 mg/L
- 50-75 mg/L
- 75-120 mg/L



Figure 7-24. Nitrate concentration in mg/L  $NO_3^-$  in the LMC.

### 7.11 Groundwater quality variability with depth

Groundwater quality evolves along flow paths, which takes place in three-dimensions. Hence, the study of groundwater quality variance with depth can reveal important information about the subsurface flow system.

On a catchment-scale, there seems to be little relationship between sampled depth and salinity (Figure 7-25 and Figure 7-26). The groundwater quality-depth plots suggest that fresh and saline water can be found at any depth, shallow and deep. However, it seems more likely to encounter fresher water at greater depths, especially below 200 m below sea level. Any groundwater salinity-depth relationship may be indiscernible on the regional-scale because of the common areal change in groundwater salinity. Therefore, local-scale scrutiny is needed to adequately check the groundwater quality-depth relationship.

There are no multi-level groundwater quality monitoring wells in the LMC. To compensate for that, eight clusters of wells screened at different depths have been selected to check on the relationship between hydrochemistry and depth using representative samples. Table D-4 in Appendix D lists the wells in these clusters and Figure 7-27 shows their locations.

Figure 7-28 (p 229-232) shows changes in the main groundwater parameters with sampling depth expressed as the elevation of the bottom levels of sampled wells at the selected eight sites. Overall, groundwater quality-depth plots presented in Figure 7-28 suggest that salinity and concentrations of major constituents generally decrease with depth. This observation is consistent with the findings of previous investigators (e.g. Lieffering, 1990; Russell, 1989; Schumacher, 1999). In contrast, *pH* tends to increase with depth.

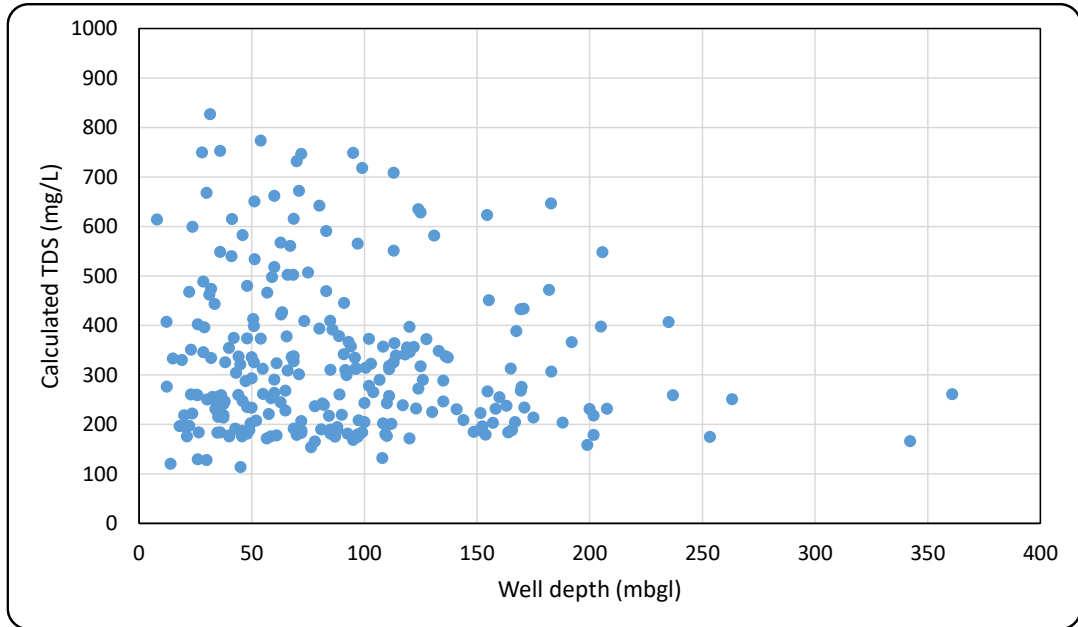


Figure 7–25. Plot of calculated total dissolved solids (TDS) against well nominal depth<sup>51</sup>.

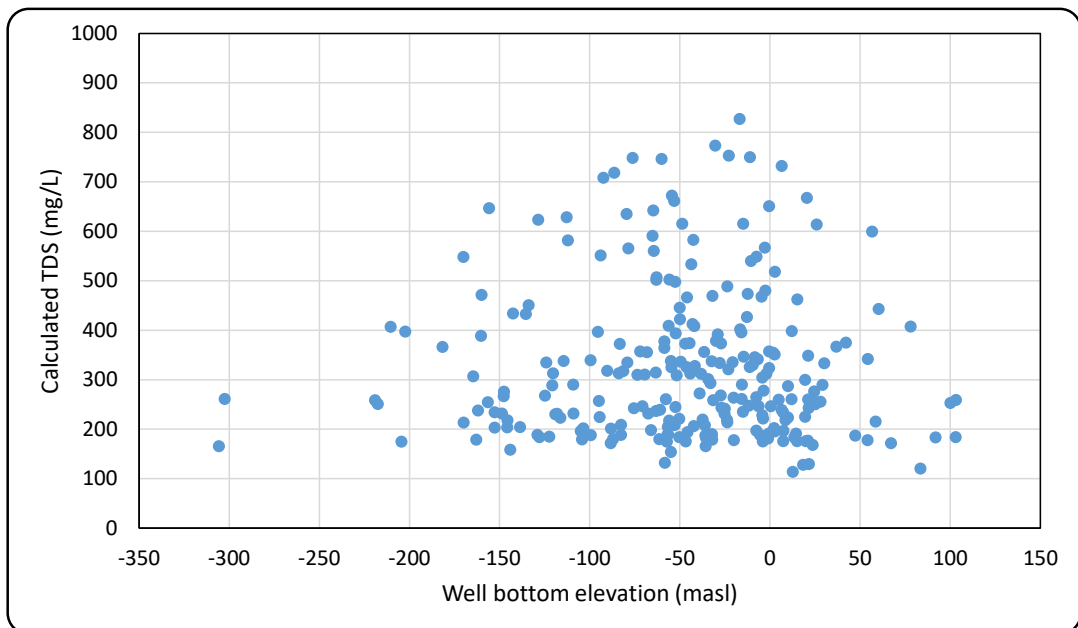


Figure 7–26. Plot of calculated total dissolved solids (TDS) against elevation of well nominal bottom<sup>51</sup>.

<sup>51</sup> For clarity, the plot is limited to maximum TDS < 1,000.

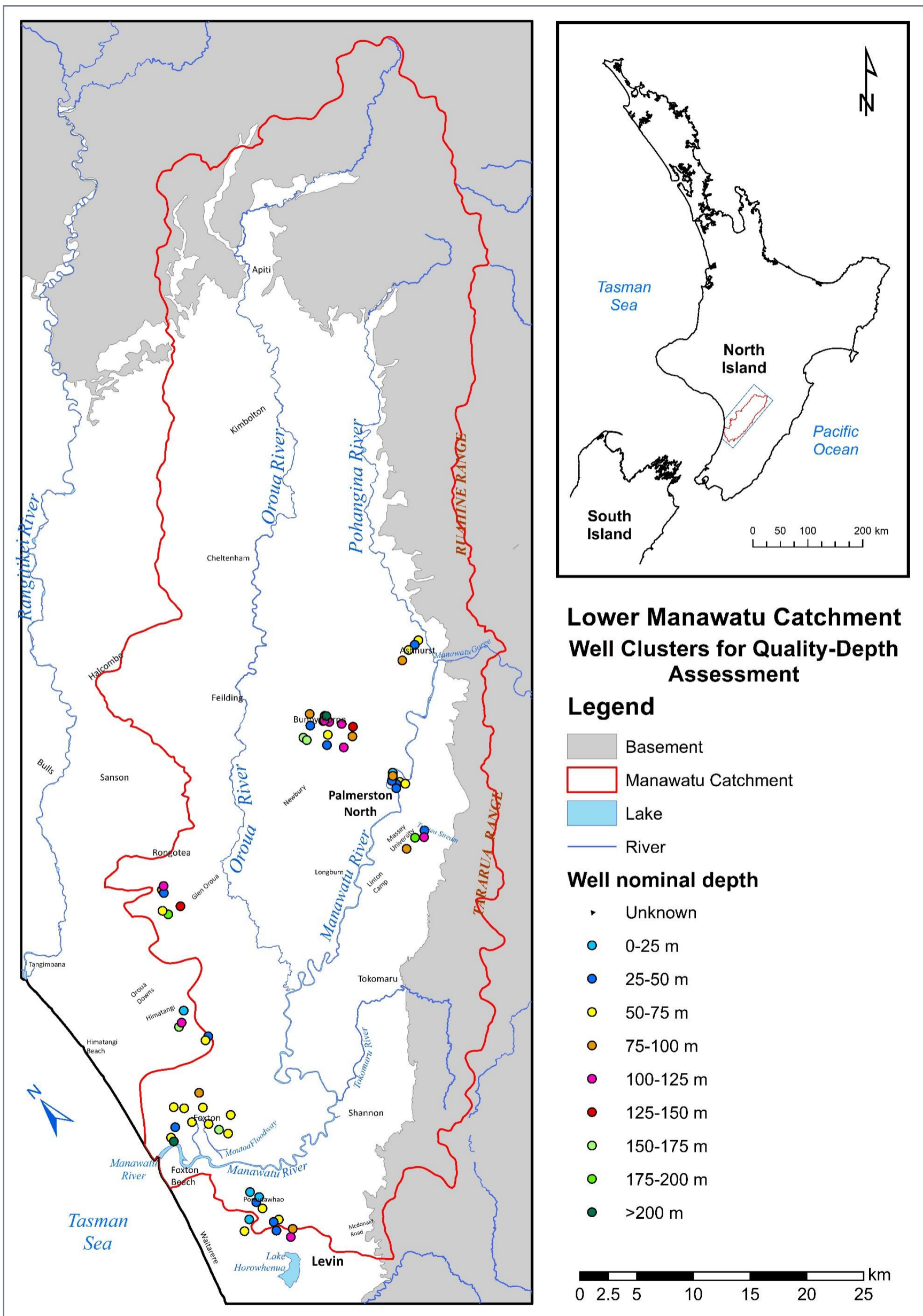
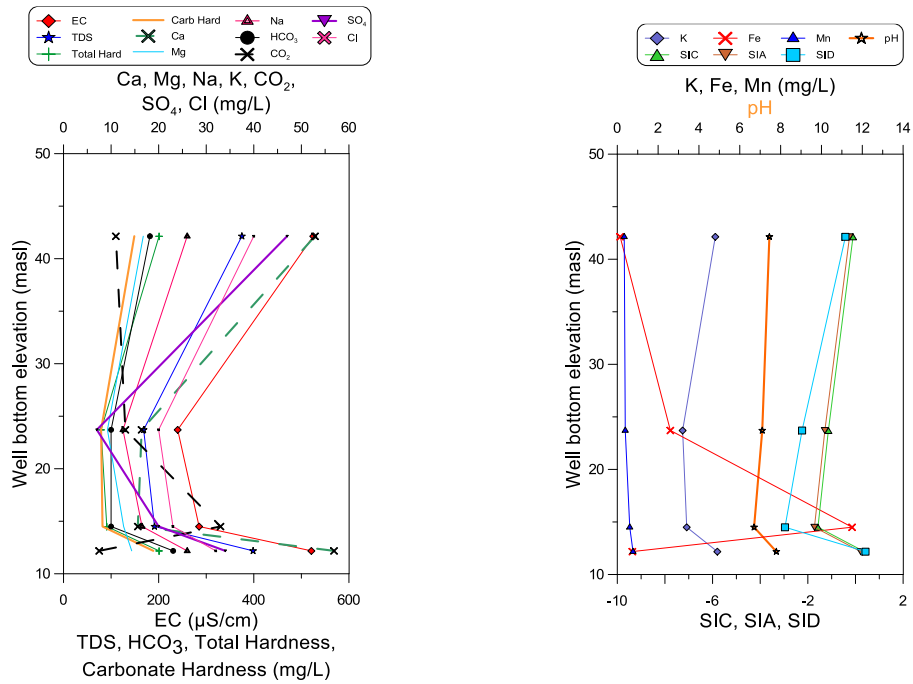


Figure 7-27. Location map showing well clusters used to investigate groundwater quality–depth relationship.

(a) Ashhurst well cluster



(b) Bunnythorpe well cluster

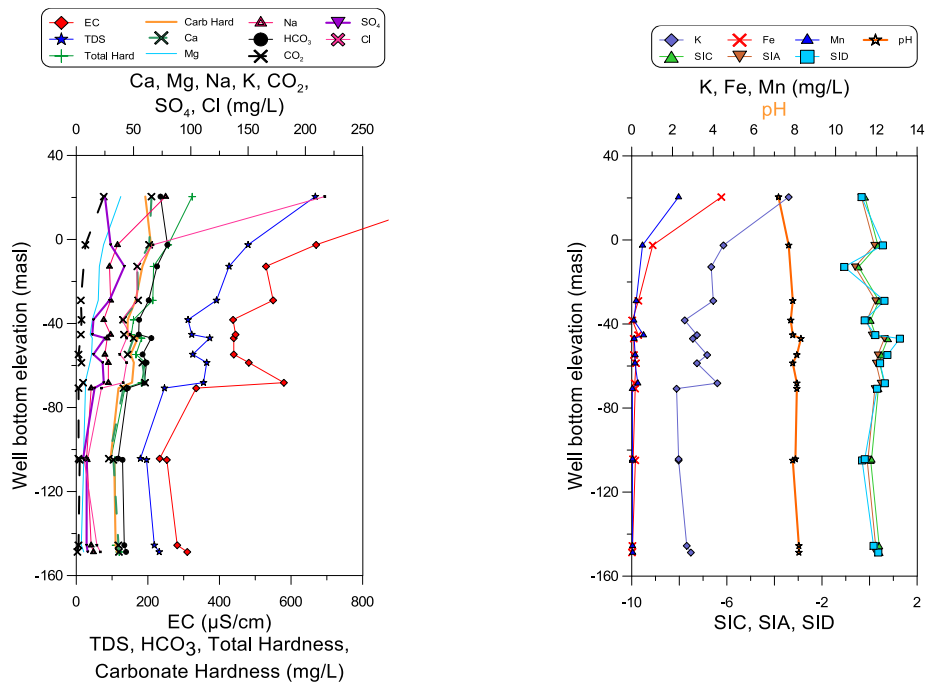
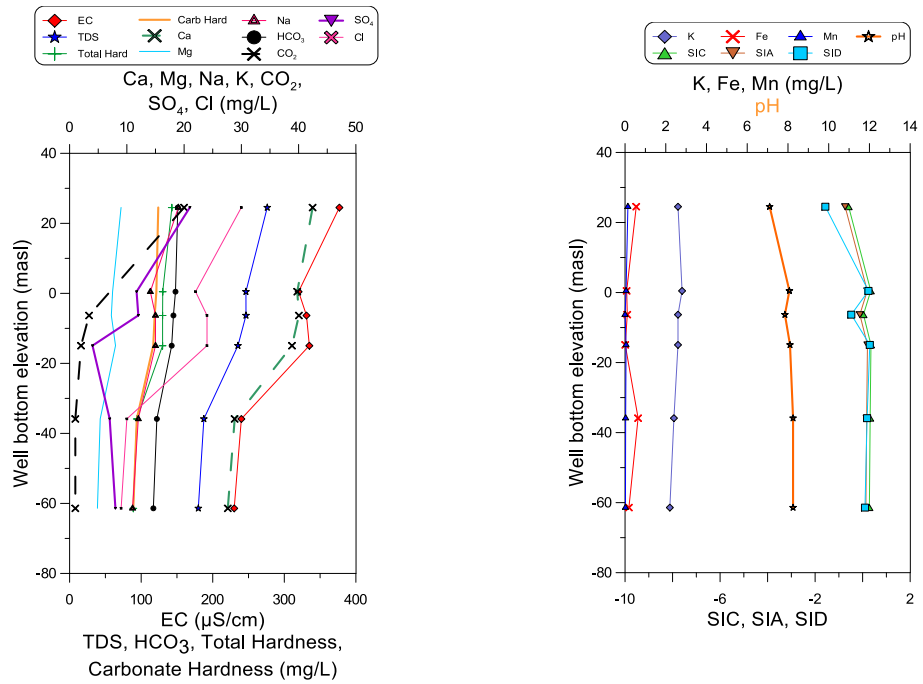


Figure 7–28. Change in hydrogeochemical parameters<sup>52</sup> with depth in selected areas across the LMC (continued overleaf).

<sup>52</sup> SIC: saturation index of calcite, SIA: saturation index of argonite, SID: saturation index of dolomite.

(c) Stages Road/Pinfold Road well cluster



(d) Massey University well cluster

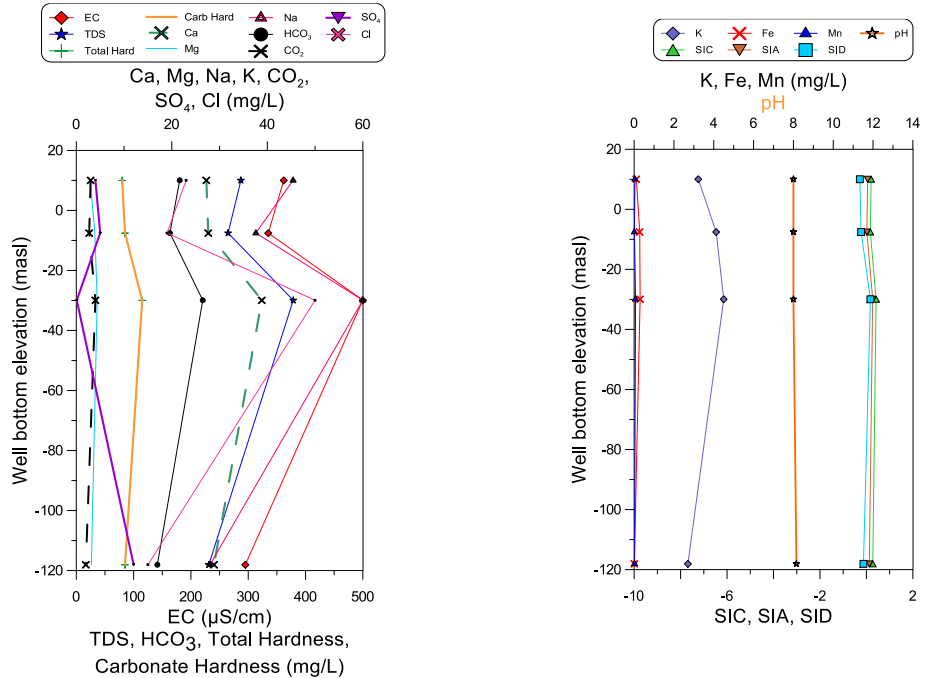
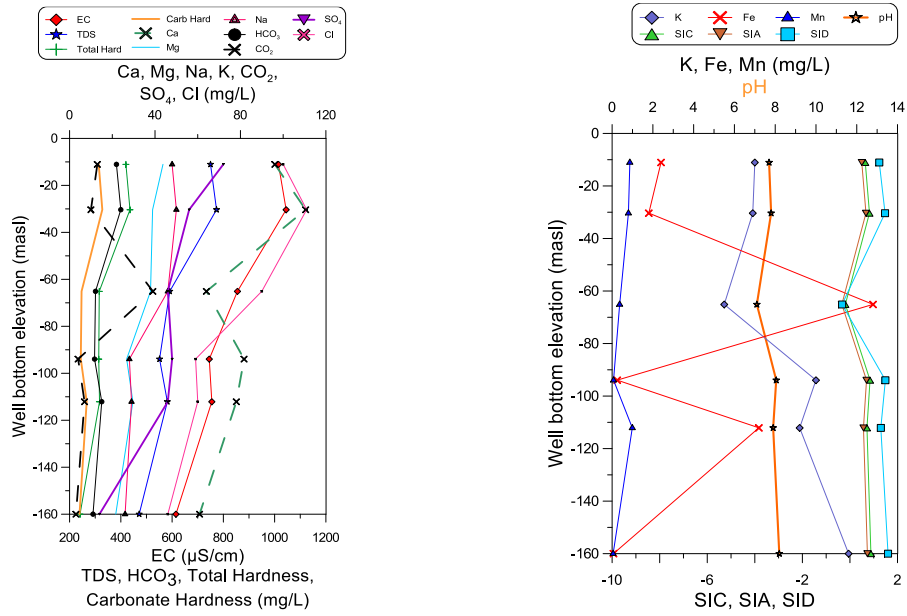


Figure 7-28 (cont.). Change in hydrogeochemical parameters with depth in selected areas across the LMC (continued overleaf).

(e) Glen Oroua well cluster



(f) Himatangi well cluster

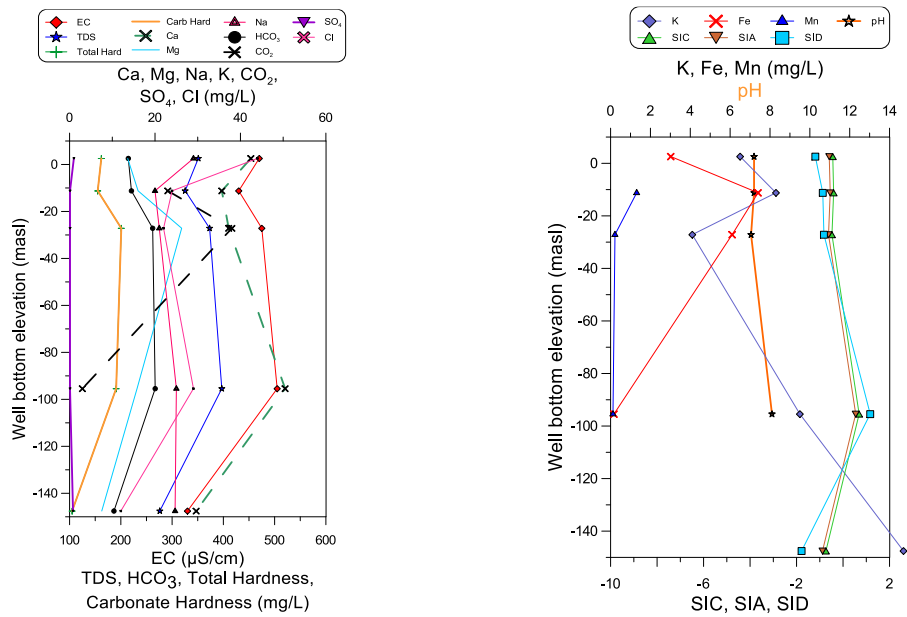
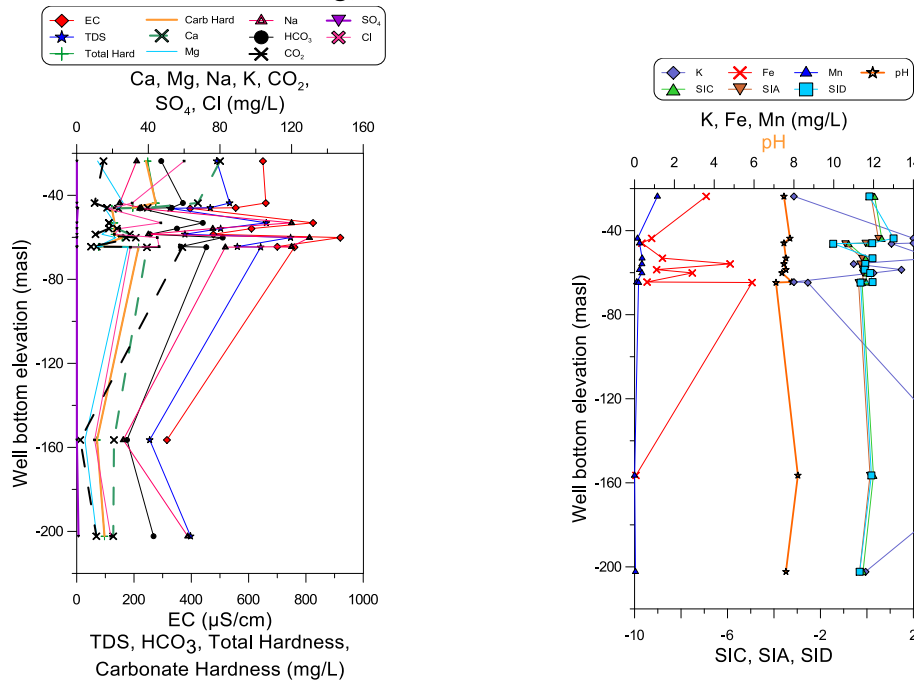


Figure 7-28 (cont.). Change in hydrogeochemical parameters with depth in selected areas across the LMC (continued overleaf).

(g) Foxton well cluster



(h) Poroutawhao well cluster

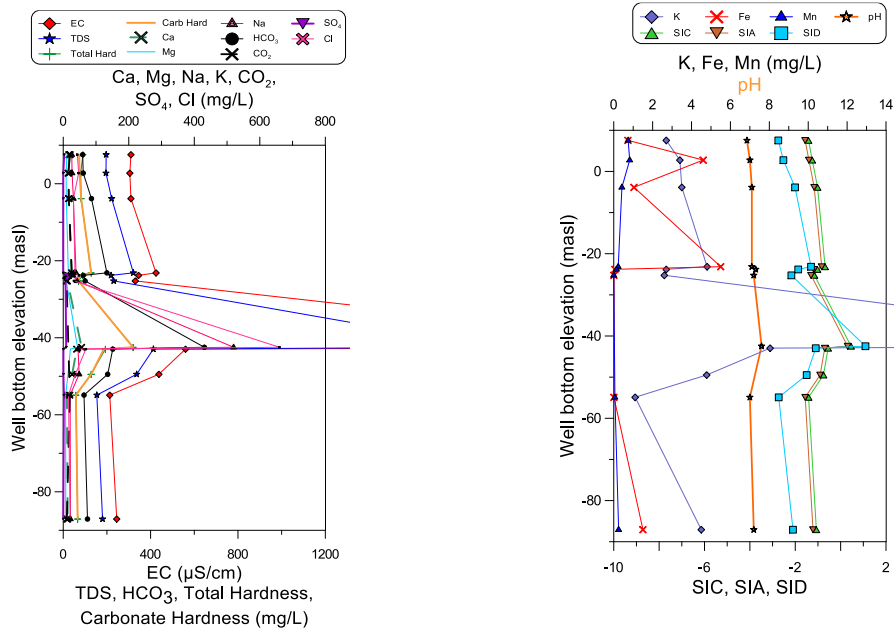


Figure 7-28 (cont.). Change in hydrogeochemical parameters with depth in selected areas across the LMC.

The groundwater-quality-depth plots presented in Figure 7-28 imply that groundwater quality in the LMC is sensitive to *pH*, which is dependent on  $HCO_3^-$

concentration. Higher water acidity at shallow depths result in greater dissolution of minerals and, hence, higher salinity. Alkaline groundwater at depth is fresher and is saturated with respect to carbonate minerals such as calcite, aragonite and dolomite as indicated by their saturation indices (SIC, SIA and SID, respectively).

### 7.12 Groundwater suitability for various uses

To assess groundwater suitability for human consumption, groundwater quality parameters in representative samples have been compared to the Drinking water standards for New Zealand (DWSNZ 2005). To assess suitability of the water for irrigation and livestock supply, representative samples were tested against the Australian and New Zealand Environment and Conservation Council, which specify a nitrate trigger values (ANZECC 2000). Daughney *et al.* (2009) summarised the most important water quality guideline values in the DWSNZ 2005 and ANZECC 2000 (Table 7-4). Table D-5 in Appendix D summarises exceedances of DWSNZ 2005 MAVs and GVs.

Acidity higher than MAV and GV is common place in groundwater in the LMC and the oxidised conditions generally do not exist. As a result, high metal content is common place as exemplified by 160 exceedances of *Mn* GV, including 96 exceedances of *Mn* MAV, and 149 exceedances of *Fe* GV. The redox conflict status of groundwater is exemplified by samples showing elevated  $NO_3$  together with high  $NH_4$ , *Fe* and *Mn*. The pattern of groundwater quality exceedance of DWSNZ 2005 does not display any clear relationship with location, depth, geology, connectedness with surface water or land use.

Table 7–4. important water quality guideline values in the DWSNZ and ANZECC 2000 (after Daughney *et al.*, 2009)

Parameter	Units	DWSNZ 2005		ANZECC 2000	
		MAV <sup>53</sup>	GV <sup>54</sup>	Irrigation TV <sup>55</sup>	Livestock TV <sup>55</sup>
<i>EC</i>	µS/cm	-	-	600-12,800 <sup>56</sup>	-
<i>TDS</i>	mg/L	-	1,000	-	2,000-5,000
<i>pH</i>	pH units	-	7.0-8.5	6-8.5	-
<i>Turbidity</i>	NTU	-	2.5	-	-
<i>Ca</i>	mg/L	-	see Hardness	-	1,000
<i>Mg</i>	mg/L	-	see Hardness	-	-
<i>Hardness</i>	mg/L CaCO <sub>3</sub>	-	200	>60 and <350 <sup>57</sup>	-
<i>Na</i>	mg/L	-	200	<115 to >460 <sup>58</sup>	-
<i>Cl</i>	mg/L	-	250	<175 to >700 <sup>58</sup>	-
<i>Fe</i>	mg/L	-	0.2	10	not sufficiently toxic
<i>Mn</i>	mg/L	0.4	0.04	10	not sufficiently toxic
<i>B</i>	mg/L	1.4	-	<0.5-15	5
<i>SO<sub>4</sub></i>	mg/L	-	250	-	1,000
<i>F</i>	mg/L	1.5 <sup>59</sup>	-	2	2
<i>NH<sub>4</sub></i>	mg/L	-	-	-	-
<i>NO<sub>2</sub></i>	mg/L	3 <sup>60</sup>	-	22 or 110-550 <sup>61</sup>	30
<i>NO<sub>3</sub></i>	mg/L	50 <sup>62</sup>	-	-	400
<i>PO<sub>4</sub> – P</i>	mg/L	-	-	0.05 or 0.8-12 <sup>63</sup>	-
<i>SAR</i>					
<i>Extremely sensitive</i>	-	-	-	<2-8	-
<i>sensitive</i>	-	-	-	<8-18	-
<i>medium</i>	-	-	-	<18-46	-
<i>high</i>	-	-	-	<46-102	-

Some groundwater in the LMC exceed ANZECC 2000 irrigation and livestock trigger values, but groundwater in the LMC is generally suitable for agricultural activities.

<sup>53</sup> Maximum Allowable Value (MAV) for parameters of significance to human health.

<sup>54</sup> Guideline Value (GV) for parameters of aesthetic significance.

<sup>55</sup> Trigger Values (TVs) are for short term exposure, and a range of higher values may be tolerated depending on the type of crop/livestock.

<sup>56</sup> General guide for EC of irrigation water at the threshold level for a range of plants and soil types: for sensitive crops in poorly draining soil, EC should be less than 600 µS/cm, whereas more tolerant crop types in well-drained soil may withstand EC above 12,000 µS/cm.

<sup>57</sup> Hardness <60 mg/L CaCO<sub>3</sub> has an increased corrosion potential, >350 mg/L CaCO<sub>3</sub> has an increased fouling potential. DWSNZ 2005 does not specify a health-related MAV for hardness.

<sup>58</sup> Concentration causing foliar injury depending on crops sensitivity: <115 mg/L Na and <175 mg/L Cl for sensitive crops, up to >460 mg/L Na and >700 mg/L Cl for tolerant crops. High levels of chloride in irrigation water trigger the risk of increasing cadmium concentrations in crops: <350 mg/L risk is low.

<sup>59</sup> For oral health reasons, the Ministry of Health recommends that the fluoride content for drinking-water in New Zealand be in the range of 0.7–1.0 mg/l; this is not a MAV.

<sup>60</sup> A GV of 1.5 mg/L is specified as an odour threshold, and in addition, NH<sub>4</sub> concentration should be less than 0.3 mg/L in cases where treatment for use as drinking water requires addition of chlorine.

<sup>61</sup> Now short-term only. The short-term exposure MAVs for nitrate and nitrite have been established to protect against methaemoglobinaemia in infants.

<sup>62</sup> TVs are set for minimisation of nitrogen leaching into aquifers and surface water bodies: long-term TV (maximum recommended average over periods of up to 100 years) is 22 mg/L for NO<sub>3</sub> as a generic guide, whereas short-term TV (maximum recommended average over periods of up to 20 years) is between 110 and 550 mg/L and is site-specific and considers the crop being grown.

<sup>63</sup> The long-term TV (maximum recommended average over periods of up to 100 years) is 0.05 mg/L for PO<sub>4</sub>-P is set to minimise algal growth in irrigation water. The short-term TV (maximum recommended average over periods of up to 20 years) is 0.8 to 12 mg/L PO<sub>4</sub>-P to minimise phosphorus leaching to aquifers and surface waters, and is site-specific depending on fertiliser input and the fraction of phosphorus taken up by plants and soils.

The Wilcox plot presented in Figure 7–29 suggests that groundwater salinity hazard is acceptable ( $EC < 1000 \mu\text{S}/\text{cm}$ ) and only five samples record higher than S1 level sodium hazard, rendering LMC groundwater generally suitable for irrigation.

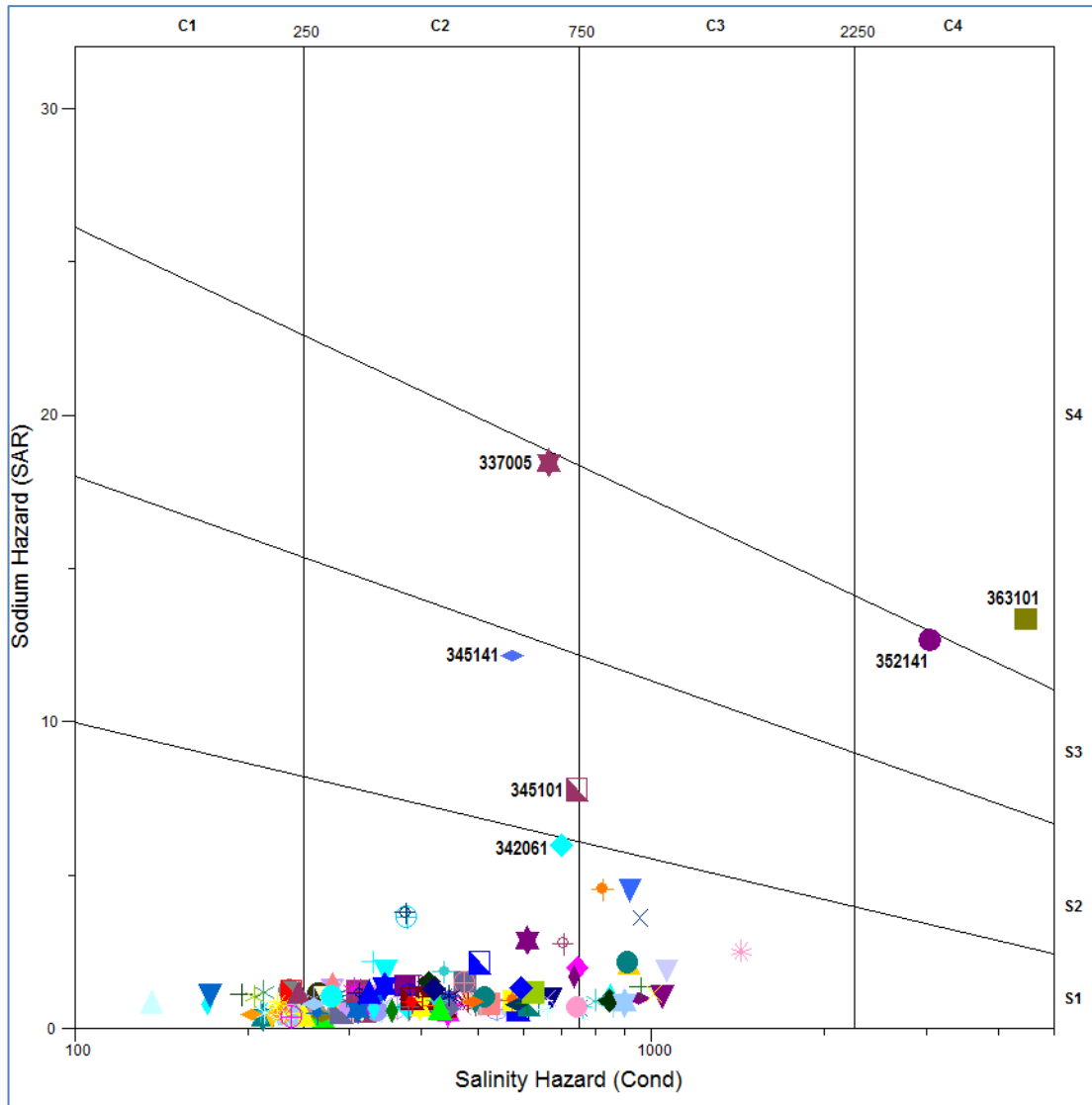


Figure 7–29. Wilcox plot for representative groundwater samples from the LMC.

### 7.13 Summary

Data collected from the start of groundwater quality monitoring in the LMC until the end of 2007 are a useful resource for hydrochemical analysis. They include 1,584 records relating to 631 wells in and around the LMC. Noticeably, there are no data from areas topographically higher than 160 masl.

Representative samples for 268 wells have been used in the analysis presented in this thesis. They satisfactorily cover the LMC below 160 masl and represent various depths. However, available groundwater quality data cannot be used to determine flow paths, recharge and discharge zones, or the relationship between groundwater and surface water features in the area.

Like previous investigations, this research has not detected seasonal variability or long-term trends in groundwater quality records in the LMC. In terms of groundwater quality variability with depth, this research confirms the findings of previous investigators that groundwater salinity improves with depth, probably due to the prevalence of reduced conditions and higher *pH* that result in lower solubility of alkaline minerals.

Groundwater quality in the LMC is dominated by fresh groundwater recharge water facies (*Ca – HCO<sub>3</sub>* and *Ca – Mg – HCO<sub>3</sub>* water types). However, there seems to be areas of ion exchange that result in relatively elevated *Na<sup>+</sup>* concentrations along the Tararua Range foothills and in the Levin Anticline and Poroutawhao Basement High areas, resulting in the existence of *Na – HCO<sub>3</sub>* to *Na – Cl* water facies. The Levin Anticline area is also characterised by high nitrate concentrations that are believed to relate to local sources and low groundwater flow velocities. Away from the Levin Anticline area, human impacts on groundwater quality are not evident. This is believed to be related to the lack of oxidised groundwater conditions due to the presence of organic matter in the stratigraphy, mainly reported in drillers' well logs as peat.

Overall, groundwater in the LMC is suitable for human consumption, irrigation and livestock, with exceptions relating principally to natural conditions across the general LMC area and anthropogenic influences in the Levin Anticline area. Natural limitations mainly include elevated *Mn* and *Fe*, and low *pH* (acidity). Elevated nitrate concentrations in the Levin Anticline area pose a health risk to unborn babies and infants. There is no indication of seawater invasion into the aquifer in the coastal area.

## Chapter 8 LMC groundwater flow model

### 8.1 Introduction

Mathematical modelling has revolutionised earth sciences, particularly by enabling us to understand physical processes that occur over prolonged times (Ellis *et al.*, 2008). Hydrogeological processes may look short-lived in comparison to other geological phenomena, but mathematical modelling is still very useful when it comes to understanding groundwater flow dynamics and aspects that control them. Mathematical modelling is also a powerful tool for exploring matters that cannot be directly seen like groundwater and helps communicating our conceptualisations on them. In this thesis, mathematical modelling is intended to provide an overarching analytical framework for multidisciplinary data synthesis and hydrogeological analysis.

### 8.2 Objectives and strategy

The foremost step in any modelling exercise is to set up its objective (e.g. Anderson *et al.*, 2015; Barnett *et al.*, 2012; PDP, 2002; Reilly & Harbaugh, 2004; Wels *et al.*, 2012; Younger, 2007). The main objective of the groundwater flow modelling work completed in this research is to validate the characteristics of the LMC groundwater flow system presented in the previous chapters and explore the fundamental constituents and processes that affect the area's hydrogeology. The numerical modelling component of this research is also intended to:

- (1) help communicate the findings of the research
- (2) provide a useful tool for stakeholders to enable assessment of land and water use management options and help them with decision making
- (3) provide basis for further work.

In conformity with the principle of parsimony, also known as the Ockham's razor<sup>64</sup>, '*Entia non sunt multiplicanda praeter necessitatem*'<sup>65</sup>, both the conceptual and numerical models developed for the LMC groundwater system have been kept as simple as possible and as complex as needed. In dealing with various components of the models, the level of complexity has been stepped up only when that has been unavoidable and only to the degree that is necessary.

### 8.3 Hydrolithostratigraphical framework

Bona fide understanding of the groundwater system's hydrolithostratigraphical setting and characteristics is a prerequisite to reliable hydrogeological conceptualisation. There have been a few attempts to construct stratigraphical models for parts of the LMC, some are published (e.g. Martley, 2001; Schumacher, 1999) and some are found in Horizons Regional Council's old database, unpublished drawings and internal reports. Previous work mainly focused on interpolation between gravelly stratigraphical horizons reported in drillers' well logs, attempting to define aquifers. In this research, stratigraphical interpolation is not intended to define aquifers, but to depict a hydrolithostratigraphical framework that can be used in conceptual and numerical hydrogeological modelling.

#### 8.3.1 Data sources, limitations and uncertainty

GNS Science QMAP sheets are the most obvious and reliable source of stratigraphical information. Drillers' well logs in Horizons database can help understand the subsurface geology. Published work like the seismic data interpretation by Melhuish *et al.* (1996) can also aid the process.

Different types of data from various sources have been synthesised to create the stratigraphical model presented below. The data used included the DEM and the geological map described in sections 3.3.1 and 3.3.2, respectively. The scale and accuracy of the used topographical and geological data are not suited for local-

---

<sup>64</sup> Also spelt Occam's razor.

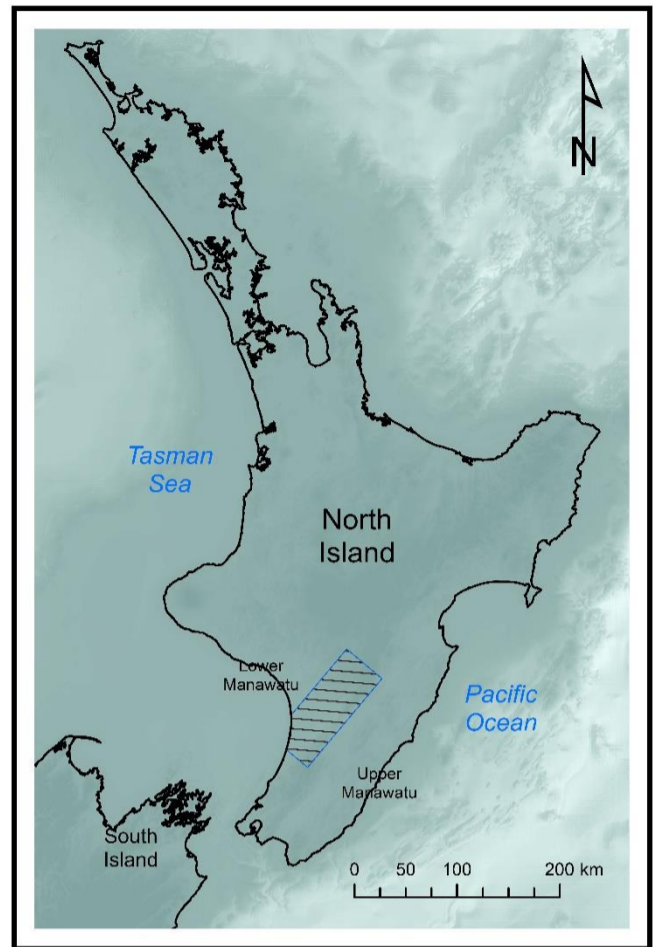
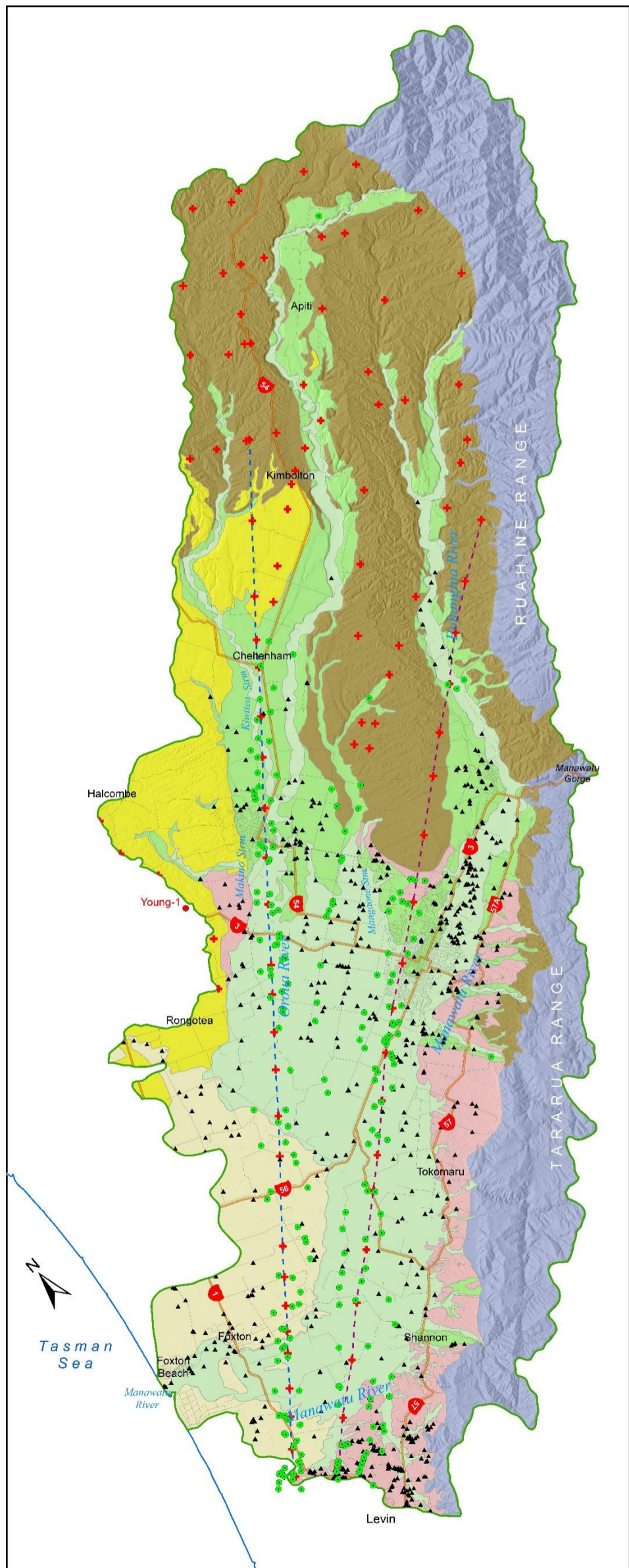
<sup>65</sup> Roughly meaning: more things should not be used than are necessary.

scale interpolation, but they are considered sufficient for the purposes of this catchment-scale groundwater study.

Drillers' well logs have been heavily utilised in this research. They were obtained in digital format from Horizons Regional Council. This dataset is a computerised version of the manually recorded lithological descriptions by drillers. Drillers' well logs are very useful but they are subject to limitations that introduce various levels of uncertainty that must be acknowledged and considered when utilising such data in geological and hydrogeological investigations. The LMC area is not evenly covered by well log data, and not all well logs have been used in the construction of the stratigraphical model presented in this thesis for practicality reasons and data quality considerations. Figure 8-1 shows the locations of wells with drillers' description in the LMC, real and imaginary wells and cross-sections (Section 8.3.2, p 246) used in stratigraphical modelling in this research. Drillers' well logs are considered the most imprecise and uncertain data used in this research. These data are subject to the following five main areas of limitation and error:

#### 1. Well position and level

Wells with drillers' lithological descriptions can have estimated or precise positions. Well position estimates have traditionally been obtained from topographical maps, aerial photographs, and starting from 2006 using handheld global positioning system (HGPS) devices. Wells precisely positioned have been traditionally surveyed with theodolite, but recently using differentially corrected global positioning system (DGPS) technology. Surveyed wells have accurate easting, northing and elevation data. Elevations of non-surveyed wells have been traditionally estimated from topographical maps and more recently using DEMs. Such estimates are more uncertain than values obtained from surveying. Some of the wells that have drillers' logs have been surveyed for elevation using optical levelling techniques, but their locations are estimated. It goes without saying that if the location data are inexact, elevation data will be doubtful at best.



### LOWER MANAWATU CATCHMENT LITHOLOGICAL WELL LOG DATA

#### Legend

- Catchment boundary
- Coastline
- River
- Highway
- Road
- Stream/creek

#### Lithological well log

- Driller's well log used in stratigraphical modelling
- Young-1 exploration well
- ▲ Driller's well log not used in stratigraphical modelling
- + Imaginary wells used in stratigraphical modelling
- Imaginary borehole section 1
- Imaginary borehole section 2

#### Simplified geology

##### Holocene

- Holocene alluvium
- Holocene sand dunes

##### Middle-Late Pleistocene

- Late Pleistocene alluvium
- Last Interglacial Marine Deposits
- Middle Pleistocene Strata

##### Plio-Pleistocene

- Plio-Pleistocene marine rocks

##### Permian-Late Jurassic

- Greywacke basement rock

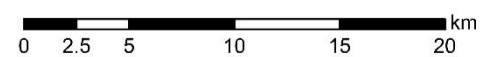


Figure 8-1. Location map showing wells with drillers' description in the LMC, real and imaginary wells and cross-sections used in the construction of the stratigraphical model presented in Section 8.3.3.

## 2. Sample depth representativeness

All available drillers' lithological records have been obtained from ordinary water production wells rather than exploration boreholes. These wells have been drilled with a variety of methods and lithological sampling was not critical or a priority in the process. Hence, there is a considerable degree of uncertainty associated with lithological sample depths despite some drillers' records suggesting millimetre precision.

## 3. Lithological description

Available lithological data from wells in the LMC come from drillers' descriptions, not from geologists' logging. Noticeably, the level of detail and used terminology in available lithological records are highly variable. They clearly vary from one drilling company to another, but also amongst operators in the same company. Even geologists may have inconsistencies in describing material from drilling returns.

Schumacher (1999) developed an approach to relate drillers' descriptions to usable lithological classes (Table 8-1). This classification is particularly useful when combined with the general characterisation of lithological units by Begg *et al.* (2005) presented in Table 8-2.

## 4. Level of detail and description usefulness

Some drillers' well log records are lacking on detail, whereas some provide too much information that is not all relevant. For example, a record in a well log may simply provide a colour (e.g. grey) or a relative descriptor (e.g. better than above) to characterise a lithological facies in the well log. Some descriptions are also impossible to be obtained from well logs, e.g. clay lens. In addition, the only mention of fossils in drillers' well logs is through the occasional recording of shells or pieces of temper, without further clarification. There is no mention in all reviewed well logs to tephra, which would have been very helpful as a stratigraphical marker in well log interpolation and correlation.

Table 8–1. Commonly used drillers' descriptions of rock and soil units in well logs and their most likely lithological interpretation (adapted after Schumacher, 1999).

Drillers' description	<b>Interpretation – based on the Unified Soil Classification System (USSC)</b> (American Society for Testing and Materials, 1985) <i>K</i> = Hydraulic conductivity values from (Watson & Burnett, 1993, except for peat)		
<ul style="list-style-type: none"> <li>• Gravel</li> <li>• Gravel &amp; sand</li> <li>• Metal</li> <li>• Fine gravel &amp; sand</li> <li>• Metal &amp; sand</li> </ul>	Clean gravels (Little or no fines) $K > 10^1$	Gravel and gravelly soils	Coarse grained soils
<ul style="list-style-type: none"> <li>• Gravel, sand &amp; silt</li> <li>• Metal &amp; brown silt</li> <li>• Gravel &amp; sandy clay bound</li> <li>• Gravel clay bound</li> <li>• Gravels, sands &amp; some clay</li> </ul>	Gravels with fines (appreciable amount of fines) $K > 10^{-4} - 10^0$		
<ul style="list-style-type: none"> <li>• Sand</li> <li>• Sand &amp; gravel</li> <li>• Gravelly sands</li> <li>• Fine sand &amp; small gravel</li> <li>• Sands &amp; shell</li> </ul>	Clean sand $K > 10^0$	Sands and sandy Soils	
<ul style="list-style-type: none"> <li>• Sand &amp; layers of silt</li> <li>• Silty sand</li> <li>• Sand, some peat</li> <li>• Sand &amp; lenses of clay</li> <li>• Clay sands</li> </ul>	Sands with fines $K > 10^{-4} - 10^0$		
<ul style="list-style-type: none"> <li>• Sandy silt</li> <li>• Silt &amp; sand</li> <li>• Silt &amp; gravel</li> <li>• Silt, sand &amp; some small gravel</li> <li>• Silts, some brown peat</li> <li>• Silts</li> </ul>	Silts and clays $K > 10^{-4} - 10^{-1}$		Fine grained soils
<ul style="list-style-type: none"> <li>• Clay</li> <li>• Clay &amp; sand</li> <li>• Clay &amp; gravel</li> <li>• Sandy clay</li> <li>• Clay, sand and some gravel</li> <li>• Silty clay</li> </ul>	Clays and silts $K > 10^{-5} - 10^{-1}$		
<ul style="list-style-type: none"> <li>• Peat</li> </ul>	Highly organic soils $K = 10^0 - 10^1$ (from Table 6–1)		

Table 8–2. Upper Wanganui Series and Haweran Series stratigraphical units (adapted after Begg *et al.*, 2005).

QMAP code	Relative age	Material	Name	Depositional environment	Sea level	Age (ka)
Q1	Holocene (Aranuian)	Mud, silt & peat; gravel & sand		Estuarine, lacustrine, dunes, alluvial	High	0–12
Q2a	Late Otiran	Gravel & sand	Ohakea	Alluvial	Low	12–25
Q3a	Middle Otiran	Gravel & sand; 1 loess	Rata	Alluvial	Low–moderate	25–60
Q4a	Early Otiran	Gravel & sand; 2 loesses	Porewa	Alluvial	Low–moderate	60–71
Q5m	Kaihinu (Oturian) Interglacial	Sand, silt, & minor gravel; 3 loesses	Rapanui (Tokomaru, Otaki Sst)	Marginal marine to marine	High	71–128
Q6a	Waimea Glacial	Gravel & sand; 3 loesses	Greatford, Marton	Alluvial	Low	128–186
Q7	Karoro Interglacial	Sand, silt, 4 loesses, tephra	Rapanui	Marginal marine to marine	High	186–245
Q8	Waimaunga Glacial	Gravel & sand; 4 loesses	Burnand	Alluvial	Low	245–303
Q9	‘Brunswick’, Braemore Interglacial	Sand, silt, 5 loesses, tephra	‘Brunswick’, Braemore	Marginal marine to marine	High	303–339
Q10	Nemona Glacial*	Gravel & sand; 5 loesses	Aldworth, Waituna	Alluvial	Low	339–362
Q11	Ararata, Rangitatau Interglacial	Sand, silt, 6 loesses, tephra	Ararata, Rangitatau	Marginal marine to marine	High	362–423
Q13	‘Ball’ Interglacial	Sand, silt, 7 loesses, tephra	Ball	Marginal marine to marine	High	478–524
Q15	Piri Interglacial	Sand, silt, 8 loesses, tephra	Piri	Marginal marine to marine	High	565–620

---

\* Unnamed in Begg *et al.* (2005)

## 5. Typographical errors and terminology inconsistency













Typographical errors have been noticed in both original drillers' paper records and Horizons digital groundwater database. Most of the paper record errors transpire into the digital record. In addition, there is noticeable terminology inconsistency in well logs. For example, gravel is variably referred to as conglomerate, metal, shingle and, of course, gravel. Correcting typographical errors and terminology standardisation will be required if drillers' well log records are to be digitally queried, which has not been the case in this research.

### 8.3.2 Stratigraphical modelling methodology

The LMC hydrolithostratigraphical system is conceptualised as a sequence of predominantly marine Plio–Pleistocene rocks overlapped by alternating marine and terrestrial Middle–Late Pleistocene poorly consolidated strata, with Holocene alluvium filling the valleys and covering the floodplains and Holocene dune sands mantling the coastal area (Section 6.3). To enable digital synthesis and representation of the stratigraphical system, geological information from literature and the QMAP has been used to classify the LMC's stratigraphy into the units shown in Table 8–3. Each unit has been designated a hydrogeological unit code (HGUCode) to uniquely identify it and a Horizon ID to denote its top (contact with overlying unit, where applicable). Horizon IDs are assigned to units in order of deposition, from older to younger. HGU coding and Horizon ID numbering can include gaps, e.g. there are no HGUCode 7 and Horizon ID 9 in Table 8–3. Initial hydraulic conductivity values and ranges have been determined based on the perceived lithology of various units from QMAP data (Table 3–1), Begg *et al.* (2005) lithological descriptions (Table 8–2), drillers' lithological descriptions, and textbook values (Table 6–1, Table 6–2, Figure 6–3 and Table 8–1).

Interpretation of well logs entail identification of stratigraphical units, marking their upper contacts and assigning Horizon IDs to the identified contacts. Correlation between well logs can then be made through linking the contacts identified at wells. Stratigraphical Horizon IDs can also be assigned to stratigraphical outcrops, enabling correlating subsurface units to outcrops.

Table 8–3. LMC stratigraphical model units.

HGUCode	Horizon ID	Symbol colour	Code	Description	General lithology	Initial K value (m/d)	Expected K range (m/d)
1	15		Q1s	Holocene sands	Sand	0.15	0.1–1
2	14		Q1a	Holocene alluvium	Gravel	100.00	1–1,000
4	12		Q4–2a	Last Glacial alluvium	Gravel, sand	10.00	0.1–50
6	10		Q5b	Last Interglacial beach deposits	Sand, silt, minor gravel	20.00	1–100
8	8		Q6a	Marton alluvium	Gravel, sand	10.00	0.1–50
9	7		Q7	Rapanui marginal marine deposits	Sand, silt	1.00	0.1–50
10	6		Q8a	Burnand alluvium	Gravel & sand	10.00	1–50
11	5		Q9b	Brunswick marginal marine deposits	Sand, silt	1.00	0.1–50
12	4		Q10a	Waituna alluvium	Gravel, sand	2.00	0.1–50
13	3		Cc	Castlecliffian strata ( $\geq$ OIS 11)	Sand, silt	2.00	0.1–50
14	2		PP	Plio–Pleistocene strata	Silt, sand, limestone, mainly consolidated	2.00	0.1–10
15	1		Bs	Basement rock	Indurated rock	—	—

Initially, lithostratigraphical correlation and modelling have been attempted following the workflow shown in Figure 8–2. However, direct lithostratigraphical correlation proved to be prohibitively difficult and incapable of providing a complete picture of the area’s lithostratigraphy. Subsequently, it has been decided to construct the needed 3D stratigraphical model based on modelled cross–sections, imaginary wells and selected interpreted drillers’ well logs. Figure 8–1 shows the two strategically aligned cross–sections lines used in the process and various types of well logs used in the process. All imaginary wells have been extended from the land surface to 350 m below mean sea level and all stratigraphical units thought to exist in each imaginary well site have been marked from the ground level to the bottom of the imaginary well. Thereafter, stratigraphical units at the imaginary wells have been correlated and extrapolated between the imaginary wells to create the cross–sections presented in Figure 8–3.

Stratigraphical analysis and correlation have been an iterative process. Imaginary wells have been placed in areas with relatively abundant drillers’ well log records and/or surficial contacts between stratigraphical units. Drillers’ well log records around each imaginary well have been examined to estimate stratigraphical contacts at each actual well, comparing the initial stratigraphical interpretation to nearby wells and outcrops, then assign stratigraphical Horizon ID to unit contacts on the imaginary wells and, where feasible, on the real wells. Key information that helped in lithostratigraphical interpolation included grain–size descriptors (e.g. gravel, sand, silt) and the presence of peat/organic matter. Peat and organic matter are repeatedly reported in well logs (Figure 7–22) and have been noticed to be associated in the LMC mainly with interglacial shallow/marginal marine deposits (e.g. Q5b and Q7b). Interpretation of drillers’ descriptions also depended on the location of the well. For example, sand reported in a driller’s log as the top most layer in Q1a outcrop area is considered part of the Q1a alluvial unit. Thickness has been considered in the interpolation so that thin layers have been ignored and considered part of the larger surrounding sequence. For example, gravelly units only few centimetres thick that fall in a few metres thick sequence of sands and peat have been commonly ignored in the stratigraphical interpretation. Change in

stratigraphical facies has been allowed for in the interpretation. For example, the Q5b unit become sandier between Opiki and the coastline.

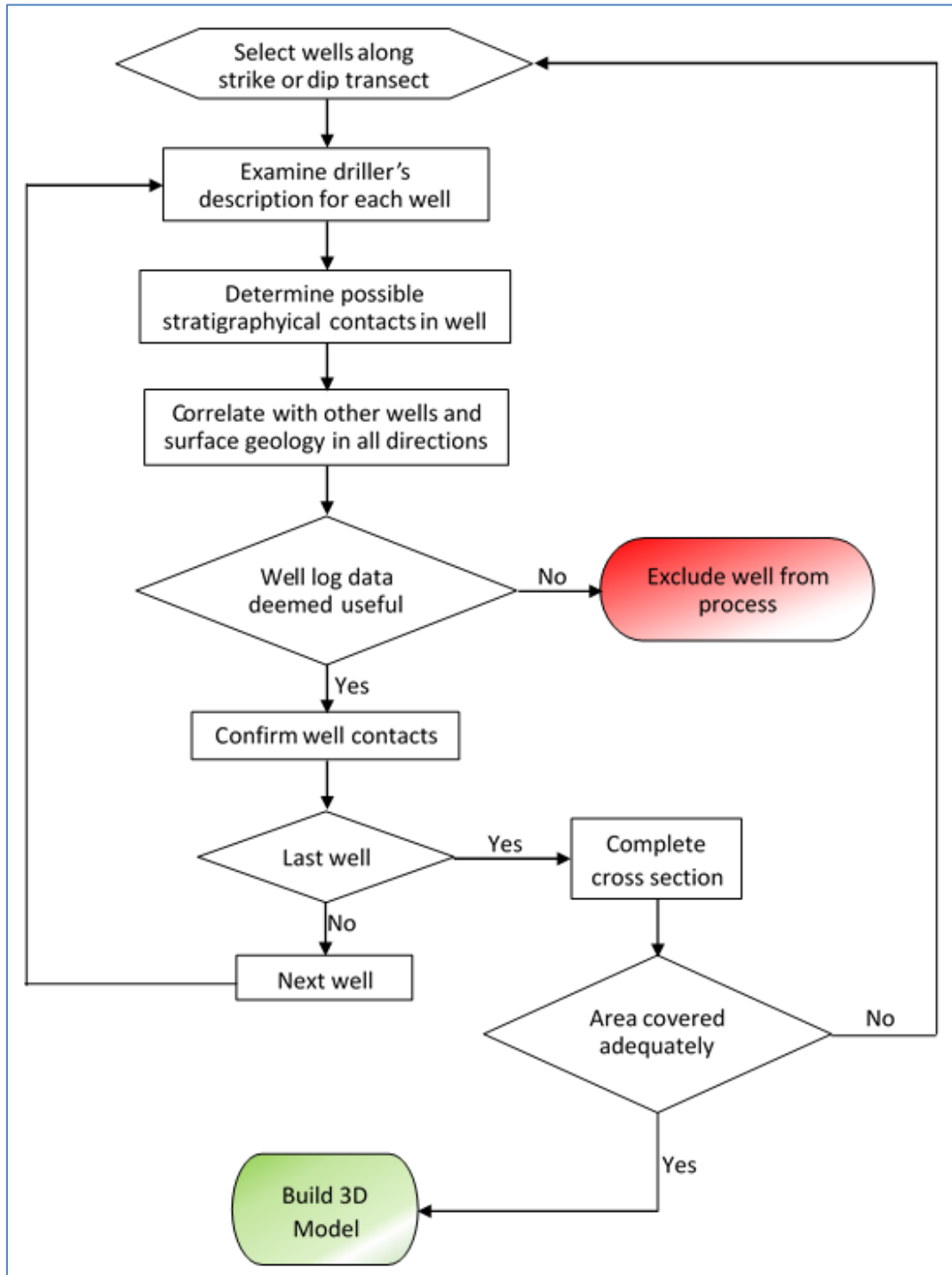


Figure 8-2: Flow chart illustrating attempted and abandoned stratigraphical model construction methodology.

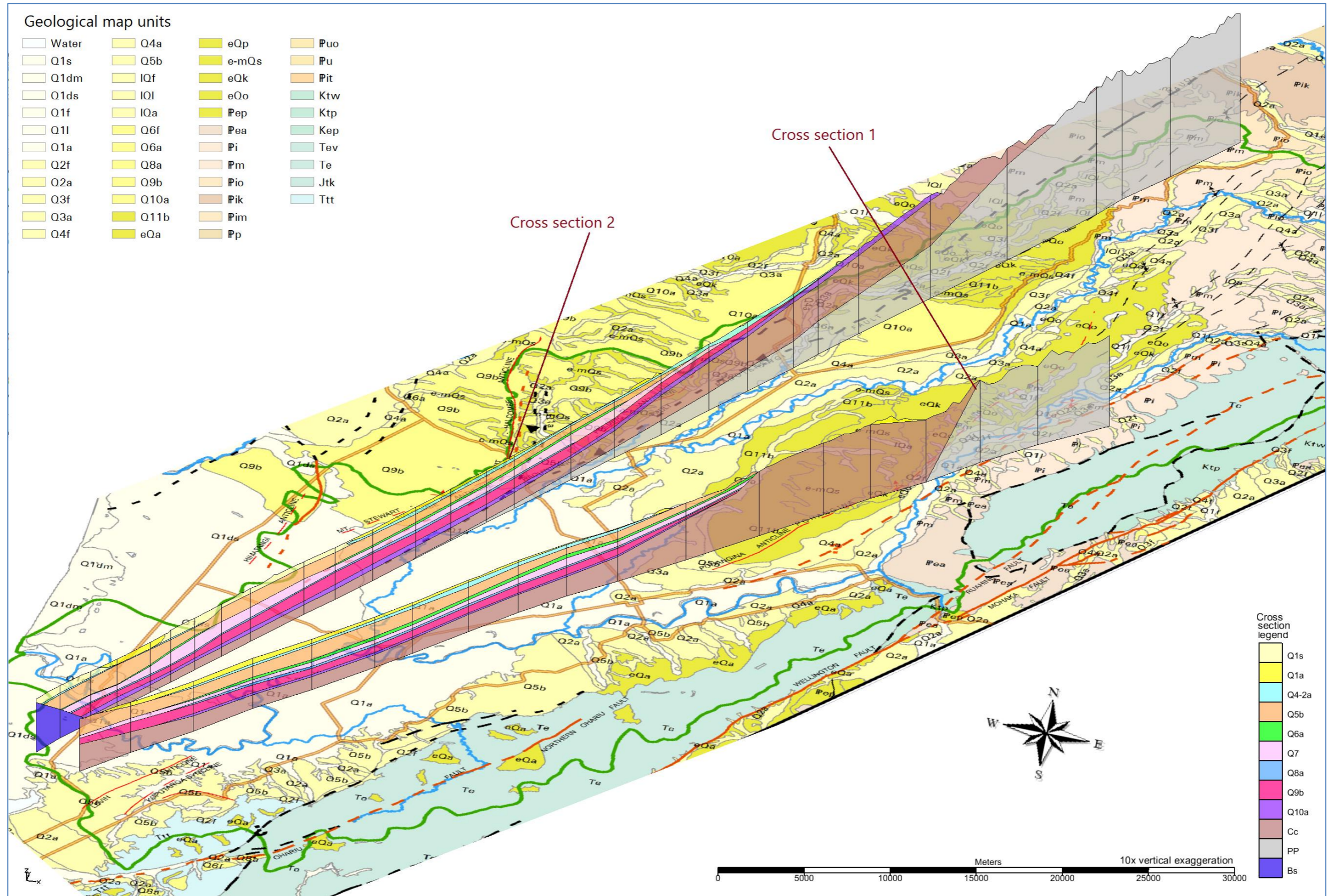


Figure 8-3. Stratigraphical cross-sections extrapolated between imaginary wells to help with 3D stratigraphical modelling.

Basement greywacke rock (Bs) has been identified in a few wells in the Poroutawhao Basement High area. This rock is easy to distinguish in well logs and is normally described by drillers as hard rock. However, all other borehole log units had to be recognised by considering the reported lithology and figuring out possible depositional environment, mainly marginal/shallow marine, aeolian terrestrial, or fluvial terrestrial to enable matching them to model layers.

As can be seen in Figure 8-1, there is a dearth of well log data in the upper part of the LMC. Therefore, imaginary wells have been placed in that area to model its stratigraphy based on published layer thickness and structure information (strike and dip). Melhuish *et al.* (1996) analysis has been particularly enlightening of the subsurface geology in this area of the LMC. Their seismic interpolation incorporated lithological data from three oil exploration wells, the Mount Stewart-Halcombe Anticline Young-1 and the Marton Anticline Stantiall-1 wells drilled in 1942 and the Santoft 1A well drilled in 1964 near the coast, west of Bulls. The Young-1 well is situated c. 5 km to the west of Feilding, less than c. 500 m to the west of the LMC boundary. All three wells reached the Torlesse greywacke basement. According to Melhuish *et al.* (1996), Nukumaruan sediments lie on basement, which is found at 1,100 m depth in the Young-1 well, the bottom of the Castlecliffian Series lies at c. 550 m depth, c. 40 m of Haweran sediments were deposited across the entire Mount Stewart area before continuing regional uplift combined with folding created the present-day topography, and the depth to basement is fairly uniform along the entire crest of the Mount Stewart-Halcombe Anticline. Melhuish *et al.* (1996) clarify that the sedimentary sequence is folded into a broad, gently asymmetric anticline whose eastern limb dips more steeply than the western limb (c. 22° and c. 6°, respectively). This information has been used to estimate the contacts of various stratigraphical units in imaginary wells in the upper parts of the LMC.

Figure 8-3 shows that the stratigraphical units listed in Table 8-3 do not cover the entire LMC stratigraphical model domain. Subsequently, the extent of spatial interpolation and extrapolation of the model's various different units had to be

identified in the modelling process (Figure 8–4). The determination of the possible spatial extent of most unit is based on surface geological information except for the antepenultimate and penultimate glacial periods deposits (Q8a and Q6a, respectively) and the basement rock unit (Bs), which do not crop out in the LMC groundwater system model area. Stratigraphical unit extents were delineated assuming that marine units cannot extend beyond the extents of the underlying units in the up-dip direction and terrestrial areas are limited to their river courses and floodplains. Structural geology and well log data have been considered in drawing the unit extent maps shown in Figure 8–4. The boundary delineating the area of occurrence of a stratigraphical unit can either be an inside or outside line. Inside boundary lines define contacts between units, e.g. Q1a and Q4–2a, whereas an outside boundary demarks an external model boundary, which does not mean that the stratigraphical unit stops at that boundary but the model ends. The watershed line between the Manawatu and Rangitikei catchments is an example of an outside boundary for some model units that extend across it, e.g. Q9b.

GMS software has been used in storing and visualising stratigraphical well log data, interpreted well logs and cross-sections, constructing the 3D stratigraphical model and incorporating it into a flow model. Figure 8–5 presents the developed LMC stratigraphical model as a block diagram and Figure 8–6 presents it as a fence diagram.

### 8.3.3 LMC stratigraphical model

Figure 8–3, Figure 8–5 and Figure 8–6 show that structure has a profound influence over the area's stratigraphy. The system configuration is largely determined by faults and folds like the Northern Ohariu Fault, Pohangina Anticline, Wellington Fault, Ruahine Fault, Rauoterangi Fault, Feilding Anticline, Mt Stewart–Halcombe Anticline, Himatangi Anticline, Levin Anticline, Koputaroa Syncline, and Shannon Anticline. These structures both determine the extent of the groundwater flow system and the extent of hydrolithostratigraphical units within it.

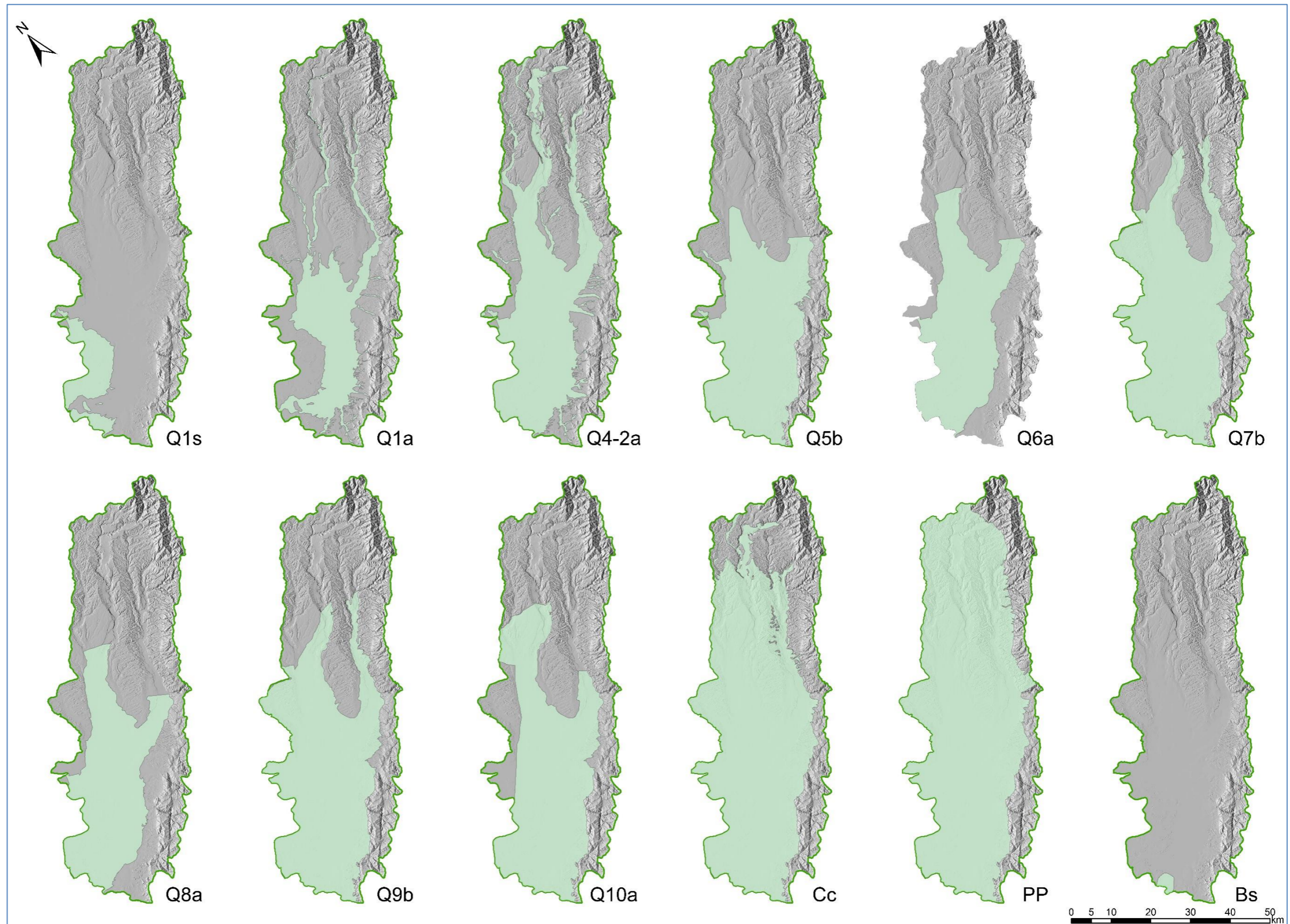


Figure 8-4. Perceived possible extent of stratigraphical units.

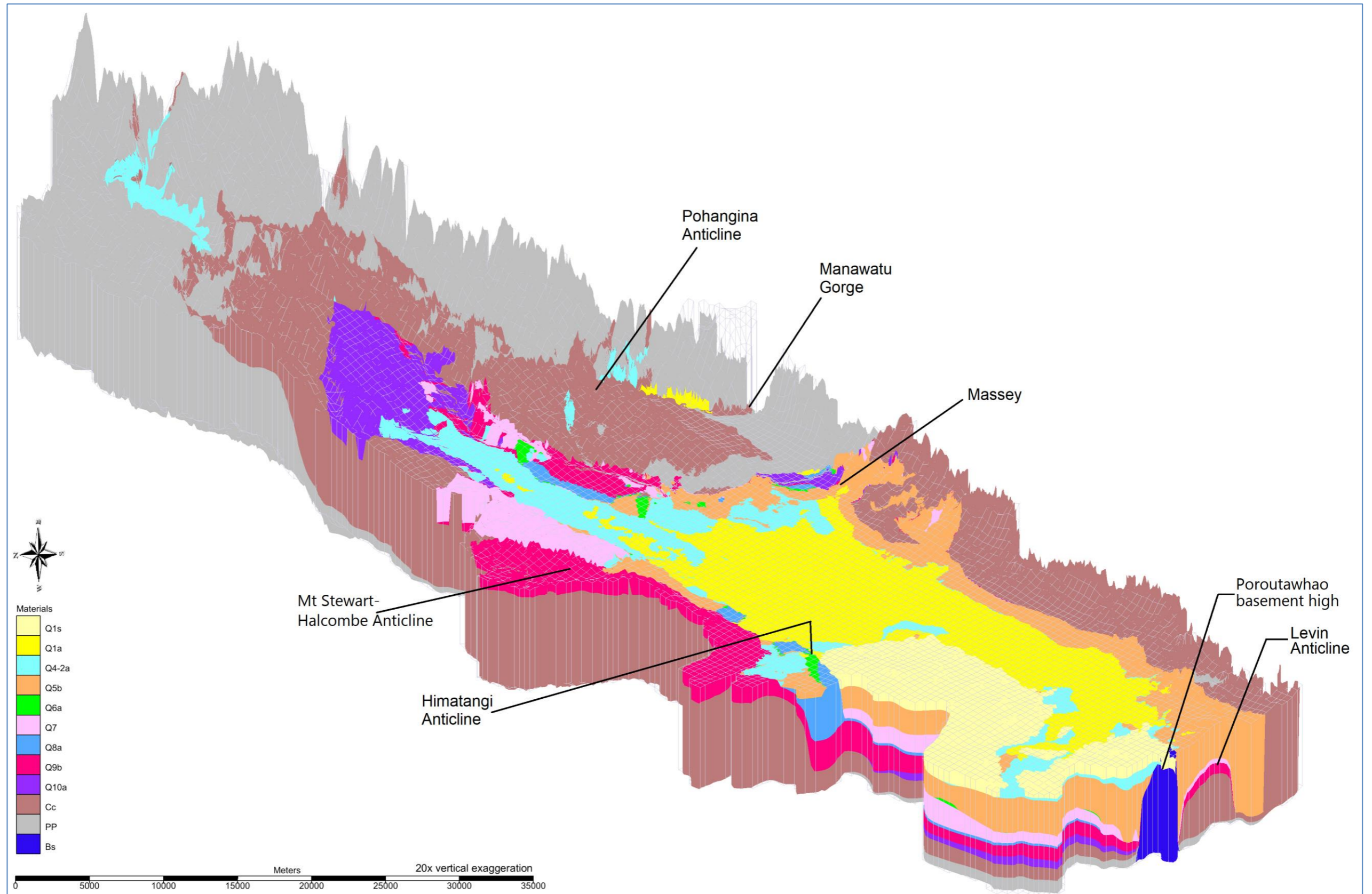


Figure 8-5. Block diagram presenting the stratigraphical framework in the LMC.

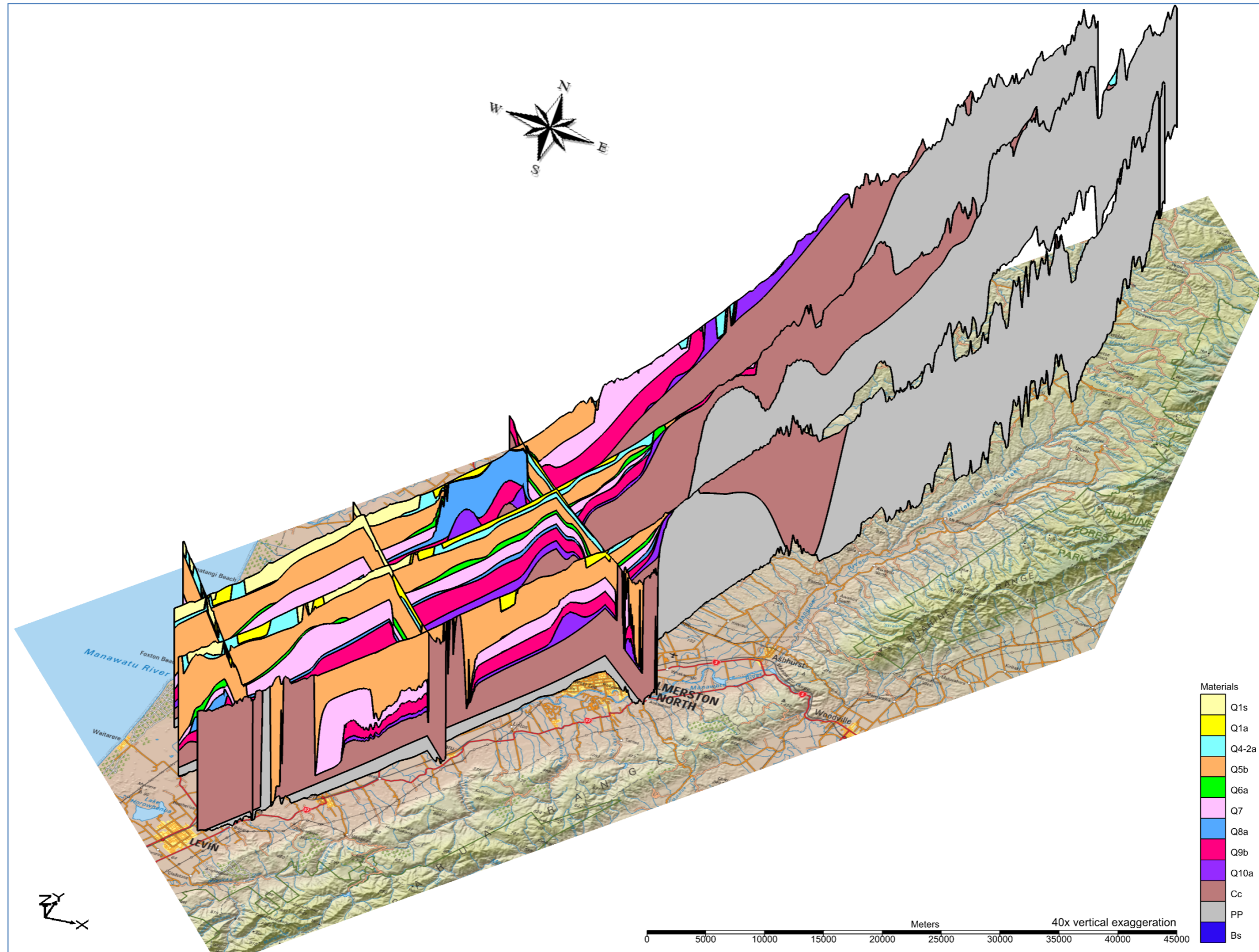


Figure 8-6. Fence diagram presenting the stratigraphical framework in the LMC.

Structure has been critical in controlling river courses through previous cold weather periods, certainly from the Waimaunga Glacial period (OIS8) but possibly also starting from the Nemona Glacial (OIS10). Begg *et al.* (2005) note that folding and faulting in the Wanganui Basin through the Late Castlecliffian to middle Quaternary period (700–128 ka; OIS17–OIS5) have restricted river courses to areas between anticlinal crests for much of that period, and alluvial gravels relating to that period lap against older elevated deposits around the anticline axes. Because of this local deformation, the Pohangina and Oroua rivers have broadly occupied the same courses as today from about OIS10. The stratigraphical model developed in this thesis clearly supports this hypothesis.

## 8.4 LMC conceptual hydrogeological model

Model conceptualisation entails making simplifying assumptions that reduce the complexity of the modelled system to an appropriate level to enable it to be efficiently simulated. Groundwater conceptual models are commonly presented as a description, graphical presentation or a combination of both. In this thesis, it has been chosen to present the groundwater system conceptualisation through clarifying its main assumptions and highlighting principal uncertainties and limitations.

### 8.4.1 Assumptions

The LMC groundwater flow system model presented in this thesis is based on the following conceptual assumptions:

1. The groundwater flow system comprises a hydraulically continued sequence of Pliocene–Quaternary deposits, with no mappable aquitards.
2. The lithostratigraphy determines the system's hydraulic properties and structure controls the system's boundaries.
3. Greywacke rocks cropping out in the ranges and underlying cover bed strata represent an impervious hydrogeological basement.
4. Groundwater divides coinciding with hydrological divides separate the hydrogeological system in the LMC area from the hydrogeological systems

in the Rangitikei catchment to the north and the Horowhenua area to the south. No groundwater flow is considered possible through these vertical boundaries.

5. Groundwater flow below 350 mbgl is predominantly horizontal and/or very slow (stagnant), which enables defining the model bottom at that level as a no-flow boundary.
6. Surface water features in the LMC area are hydraulically connected to the underlying groundwater system, with no perching, allowing exchange of water between the hydrological and hydrogeological systems subject to relative hydraulic head conditions and bed material conductance.
7. A regional water table bounds the groundwater flow system from above.
8. The groundwater system is replenished by rainfall and irrigation returns percolating to the water table.
9. The water table does not lose water to the atmosphere directly through evapotranspiration.
10. There is no need to include the unsaturated flow component of the hydrogeological system in the groundwater flow model. Rain recharge and irrigation return inputs into the groundwater system are best obtained from soil moisture calculations (Section 4.7.2).
11. Surface water and groundwater in the LMC ultimately discharge into the Tasman Sea.
12. There is no indication of seawater incursion into the groundwater system, i.e. there is a hydrodynamic balance between fresh groundwater flowing into the Tasman Sea and the saline seawater.
13. Gravity and topography are the main controls on the groundwater flow, which takes place in a general northeast-southwest down catchment direction.
14. The river valleys and plains in the LMC represent a regional groundwater discharge zone.
15. There are no significant seasonal, annual or longer-term changes in the hydraulic head or groundwater quality, which allow for representing the system using long-term average conditions (steady-state).

16. Groundwater flow occurs in porous media equivalent system, to which Darcy's law applies.
17. Literature reported values can be used as initial estimates of aquifer properties for various lithologies.
18. Anthropogenic interferences have little influence on the groundwater flow regime and quality in the area, but abstraction from permitted and consented wells must be considered in hydrogeological analysis and modelling for completeness.

#### 8.4.2 Uncertainty and limitations

The main uncertainty in the above presented conceptual model relates to the assumed no-flow conditions across the vertical projection of the surface water divides between the LMC and the Rangitikei groundwater system to the north and the LMC and the Horowhenua groundwater system to the south. The occurrence of the Poroutawhao Basement High to the south enhances the feasibility of selecting the surface water divide as a southern model boundary. The northern model boundary is more uncertain, however, especially that it can theoretically move with pumping and variation in recharge rates and distribution pattern. Nevertheless, there is no evidence that this has happened in the past and it is believed that it is unlikely to happen in the future.

The adopted conceptual model assumes hydraulic properties heterogeneity across the identified hydrolithostratigraphical units. However, this limitation has been overcome through calibrating the model using pilot point sets specified for individual hydrolithostratigraphical units (Section 8.10.3).

The configuration of the 'solids' that represent the hydrolithostratigraphy is based on Inverse Distance Weighted (IDW), which is one of the most commonly used techniques for geospatial interpolation of point data. The results of this method could be compared in future work with other interpolation methods like Kriging and Natural Neighbour to investigate the most appropriate algorithms for stratigraphical modelling in the LMC area.

Uncertainty relating to observation and production wells screen positions influences the reliability of the calibrated model. To overcome this limitation, additional data on wells should be gathered and incorporated in any future fine tuning of the model presented in this study.

## 8.5 Groundwater numerical model implementation

Groundwater flow models are described in terms of their spatial and temporal coverage. They can be 1D, 2D or 3D, transient or steady-state. Numerical modelling requires representing or approximating the continuous bulk and series using discrete quantities and periods, respectively. This approach is known as discretisation. Model grids or meshes discretise the continuous natural system into segments (cells, elements or blocks) that allow numerical solutions to be calculated. In transient simulations, the flow equations are discretised through time by steps. Model run times are proportional to the number of spatial segments and time-steps. This aspect becomes particularly critical in model calibration runs where the model needs to be run repeatedly to estimate the most appropriate parameters. Therefore, spatial and temporal discretisation should be fine enough to define the problem adequately but not too small to maintain practical computational requirements.

### 8.5.1 Temporal discretisation

An important decision that had to be made in the early stages of this research is related to whether a transient model is needed or a steady-state model is fit for purpose (Section 2.1.1). Under steady-state flow conditions, the hydraulic head does not change with time whereas it does under transient flow conditions. Steady-state flow conditions are assumed to be achieved when the hydraulic head and, hence, the magnitude and direction of flow are constant with time throughout the model domain. Transient flow conditions are realised when the magnitude and direction of the flow change with time.

Based on the information presented in Section 6.5.1, it can be assumed that in the long-term the LMC groundwater flow system features steady-state conditions.

Therefore, it has been decided that a steady-state model is adequate to represent average long-term groundwater flow conditions in the LMC.

Assuming steady-state flow conditions is advantageous in groundwater flow modelling as it significantly simplifies the groundwater flow governing equation (Section 2.3). Under steady-state groundwater flow conditions, time is no longer an independent variable and, therefore, the storage term in the groundwater flow equation disappears because there is no change in the amount of water within the model domain. Eliminating the storage term from the groundwater flow governing equation is useful in terms of not just reducing computational time, but also data requirements and associated uncertainty.

Although real steady-state conditions do not exist in nature, steady-state models are used widely (Reilly & Harbaugh, 2004). The LMC hydrological system does not experience significant climatic seasonal, annual, decadal or longer-term variations (Section 4.6.1) and the objectives of this research do not require high-resolution information on the time it takes for the system to respond to new stresses or the behaviour of the system between periods of relative equilibrium. So, it can be safely assumed that the LMC groundwater flow system can be represented by a state of dynamic equilibrium or an approximate equilibrium condition, i.e. a steady-state simulation.

According to Franke *et al.* (1987), steady-state simulations are useful in analysing pre-development (natural) and new equilibrium conditions, and calibration of steady-state models provides information on hydraulic conductivity and transmissivity. Franke *et al.* (1987) argue that because storage effects are not involved in steady-state modelling, its calibration results are often less ambiguous than transient state calibrations.

### 8.5.2 Spatial discretisation

Reilly and Harbaugh (2004) clarify that simplification of the model domain to one or two dimensions in plan-view or cross-section is commonly undertaken to save

on modelling time and effort. However, such simplification should not compromise the modelling objectives and there should be no or negligible flow orthogonal to the line or plane of the one- or two-dimensional representation of the system. Given the geological and hydrological complexity of the LMC hydrogeological system, 3D (multi-layer) modelling has been decided to be necessary.

The LMC groundwater model domain is defined on hydrological and geological basis. It covers the entire lower Manawatu hydrological catchment except basement rocks outcrop areas. The top of the model domain is defined by the land surface and the bottom of the model domain is defined at 350 mbgl or the basement rock contact, whichever is shallower. The model is based on a 500x500 m finite difference grid, originating from 2,712,000 m Easting and 6,050,000 m Northing on the New Zealand Map Grid, rotated 45° to the north to align it with the principal groundwater flow direction. The model domain covers an area of 112x41 km (4,592 km<sup>2</sup>), divided into 224 columns and 82 rows. Vertically, the model thickness has been divided into seven layers. Model cells that fall outside the area and/or depth of interest have been inactivated. The LMC groundwater flow model comprises a total of 128,576 cells (56,722 active cells and 71,854 inactive cells).

3D geological models (e.g. Figure 8-5) can be transposed on finite element grid in different ways, including (1) boundary matching, (2) grid overlay, and (3) grid overlay with equivalent hydraulic conductivity ( $K_{eq}$ ) (Figure 8-7).

Aquaveo (2017) explains that in boundary matching approach, the top and bottom of the grid are deformed to match the tops and bottoms of the stratigraphical model and the interior grid layers are deformed to match stratigraphical boundaries. The grid cell properties are set to match the stratigraphical material coinciding with the grid cell centre. This approach requires determining which grid layers should be associated with which stratigraphical unit. boundary matching produces a close fit between the grid and the stratigraphy, but can result in thin cells that can cause stability or dry cell problems in MODFLOW simulations.

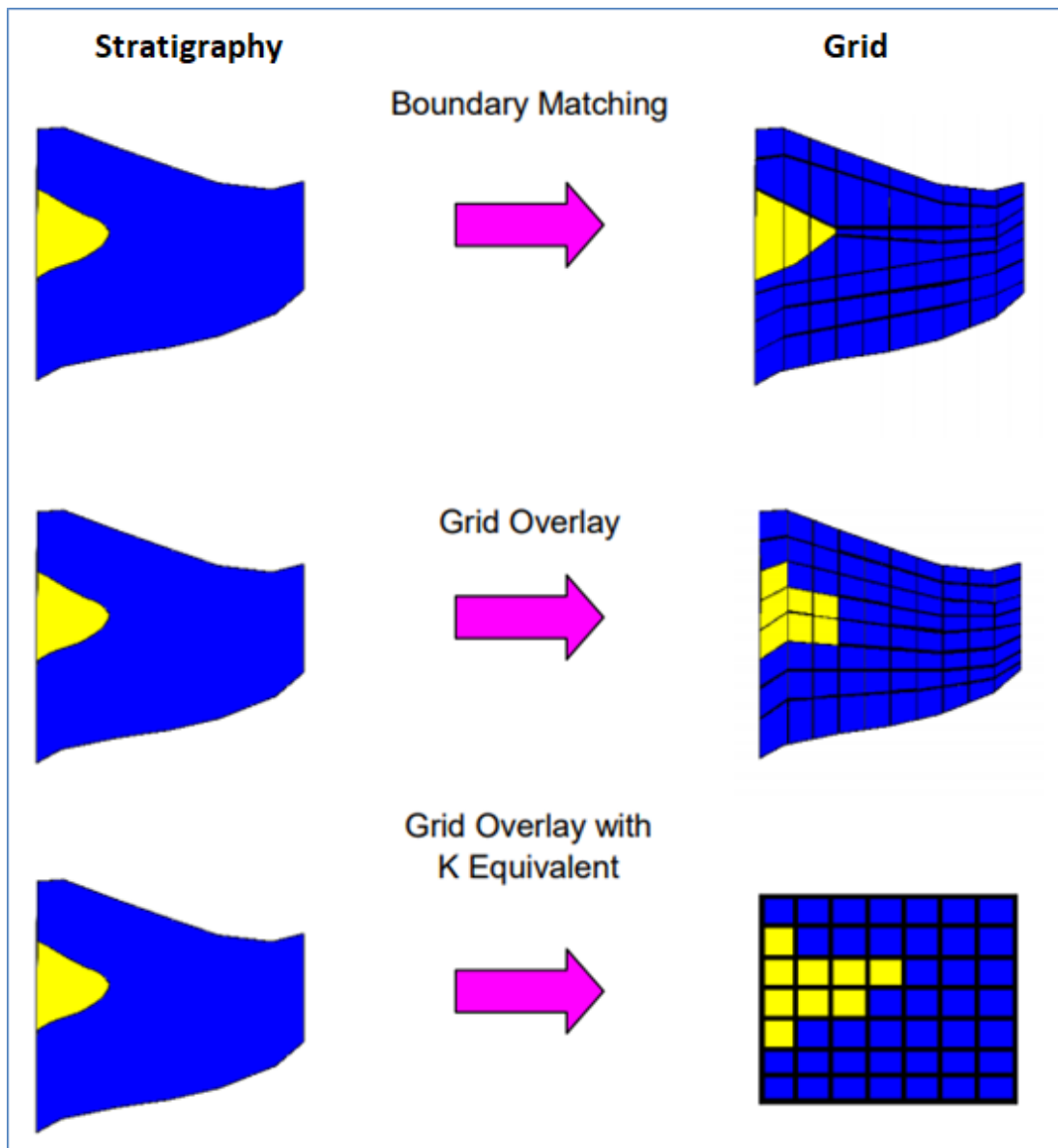


Figure 8–7. Approaches for superimposing stratigraphical models on finite difference grid (after Aquaveo, 2017).

With the grid overlay approach, the top and bottom of the grid is deformed to match the top and bottom of the stratigraphical model and the interior grid layer boundaries are deformed to be evenly spaced between the top and bottom of the grid using a simple linear interpolation without matching stratigraphical boundaries. As with the boundary matching method, the grid cell properties are set to match the properties of the stratigraphical unit at the grid cell centre. This method does not result in as close a fit between the grid and the stratigraphy as the boundary matching method, but it may avoid thin cell problems associated with the boundary

matching approach. The grid overlay option does not require assigning grid layer ranges to each stratigraphical unit.

One of the problems with the grid overlay approach is that if there is a relatively thin layer in the stratigraphical model which does not encompass any cell centres or only few cell centres, the layer will be under-represented in the finite difference grid. This becomes particularly important if the layer is meant to represent a low permeability layer. For such cases, the grid overlay with *K* Equivalent (*Keq*) option may give superior results. The grid overlay with *Keq* method is identical to the grid overlay method in terms of how the elevations of the grid cells are defined but rather than simply assigning cell properties based on the stratigraphy at cell centres, it computes custom horizontal and vertical hydraulic conductivity (*K<sub>h</sub>* and *K<sub>v</sub>*, respectively) values for each cell based on the thickness of each stratigraphical unit in it and computes equivalent *K<sub>h</sub>*, *K<sub>v</sub>* and storage coefficient for the cell. Thus, the effect of a thin seam in a cell would be included in the cell properties.

The LMC groundwater flow models presented in this thesis have been parametrised using the grid overlay approach, through which the stratigraphical model 11 variable thickness units have been superimposed on the seven numerical model layers of unified thickness of 50 m each (Section 8.8).

### 8.5.3 Model code and software

Based on the discussion presented in Sections 2.6 and 2.7, the LMC has been implemented using MODFLOW 2000 numerical model engine (Harbaugh *et al.*, 2000) and GMS 10.3 graphical user interface for pre- and post-processing of model input data and results. Microsoft Access™ 2016, Microsoft Excel™ 2016 and ArcGIS for Desktop™ 10.4 have been extensively used in data preparation for input in the modelling and in the manipulation of the modelling results.

The LMC model is a steady-state cell centred model. It uses the Layer-Property Flow (LPF) package to specify properties controlling flow between cells. By using this package, the top and bottom elevations, horizontal and vertical hydraulic

conductivity are defined for each layer and MODFLOW computes the cell by cell conductances using the layer geometry and hydraulic conductivity values. The preconditioned conjugate–gradient (PCG) method is used to solve linear and nonlinear flow conditions equations for hydraulic head in the finite difference equations in each step of a MODFLOW stress period.

## 8.6 Boundary conditions

Hydraulic head and/or hydraulic head gradient must be defined at the periphery of groundwater flow models (Barnett *et al.*, 2012). There are three types of groundwater flow model boundary conditions, specified head, specified flux, and mixed (Table 8–4).

Table 8–4. Groundwater boundary conditions (Barnett *et al.*, 2012; Franke *et al.*, 1987).

Boundary type & general name	Formal name (Bear, 1979)	Mathematical Designation
Type 1 – specified head	Dirichlet	$h = \text{constant}$
Type 2 – specified flux	Neumann	$\frac{dh}{dn} = \text{constant}$ , where $n$ is the time level.
Type 3 – mixed boundary condition	Cauchy	$\frac{dh}{dn} + ch = \text{constant}$ , where $c$ is also a constant

For specified head boundary condition (Type 1), the head of a boundary cell or node is specified. When the head is specified along a section of the model boundary, the model calculates the flow across this boundary section. For specified head–gradient boundary condition (Type 2), the gradient of the hydraulic head is specified at the boundary, which implies that the flow rate across the boundary is specified. For specified head and gradient boundary condition (Type 3), both the head and the head gradient are specified. This type of boundary condition in groundwater flow models is implemented indirectly by specifying a head and a hydraulic conductance or resistance, both representing effects of features that are located outside the model domain. Examples of such boundary conditions include lakes and rivers overlying confined aquifers where the flow between the aquifer and the lake can be represented by specifying the lake level

and a conductance value related to the bed of the lake or river. The LMC groundwater flow model have been assigned boundary conditions as described below.

### 8.6.1 The coastline

The LMC groundwater system is in contact with and discharges into the Tasman Sea. There are many ways to represent aquifer coastal boundary conditions, including setting a specified head boundary in all model layers along the coastline, setting a specified head boundary at the topmost layer along the coastline and no-flow boundary in the underlying layers, or extending the modelled aquifer into the sea. In this research, it has been decided to set a specified head boundary along the coastline only in the topmost model layer and no-flow boundary at the perceived groundwater-seawater interface in the other model layers using the Ghyben-Herzberg relation, which describes the position of the interface between the fresh groundwater and the saline seawater in coastal settings. According to Todd and Mays (2005), the Ghyben-Herzberg relation can be written for typical groundwater-seawater<sup>66</sup> interface situation as:

$$z = 40h_f \quad 8-1$$

where  $z$  is the depth to the groundwater-seawater interface below the datum (mean sea level) and  $h_f$  is the groundwater level above the datum as illustrated in Figure 8-8.

Table D-3 in Appendix D shows that groundwater density in the LMC varies from 1,000.065 kg/m<sup>3</sup> to 1,002.409 kg/m<sup>3</sup>. The highest groundwater densities in the LMC and surrounds are found in the Poroutawhao Basement High/Levin Anticline area, not in the coastal area. So, it is safe to assume that Eq. 8-1 can be used to delineate the groundwater-seawater relationship in the LMC near the coastline and approximating the contact between freshwater and seawater as a sharp interface.

---

<sup>66</sup> Typical density of freshwater ( $\rho_f$ ) is 1,000 kg/m<sup>3</sup> and typical density of seawater ( $\rho_s$ ) is 1,025 kg/m<sup>3</sup>.

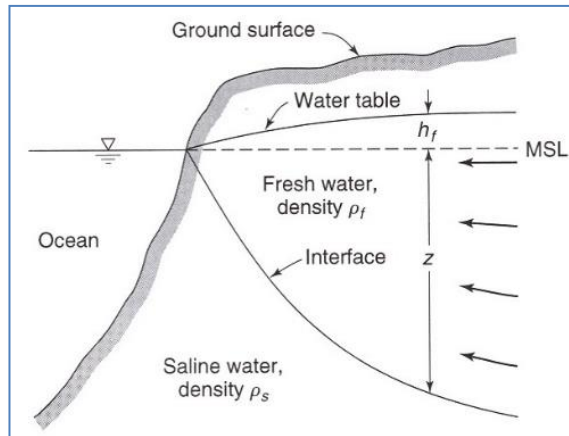


Figure 8–8. Idealised sketch of the relationship between fresh groundwater and seawater in an unconfined coastal aquifer (after Todd and Mays, 2005).

The flow across the groundwater–seawater interface is considered negligible. So, no–flow boundaries have been applied to model layers 2 through 7 at the saltwater interface. The location of the interface in these layers have been approximated using the Ghyben–Herzberg relation and the piezometric map presented in Figure 6–8. Model domain cells seawards of the interface have been inactivated. MODFLOW 2000 ‘CHD1 – Time–Variant Specified Head’ package has been used to simulate the coastline boundary in the model’s topmost layer.

### 8.6.2 Water divides and basement rocks

A no–flow boundary condition implies that the component of flux in the direction normal to the boundary is zero, i.e. the head gradient normal to the boundary is zero ( $\partial h / \partial n = 0$ ). A no–flow boundary condition has been defined at the bottom of the model as delineated in Section 8.5.2 and along the contact between the Pliocene–Quaternary deposits and the greywacke basement rocks of the axial ranges. The groundwater divide that is assumed to coincide with the surface water divide has also been set as no–flow boundary.

### 8.6.3 The water table

The top boundary for the LMC groundwater flow model is defined by the water table, which is conceptualised as a free surface recharge boundary that is not subject to losses by evaporation and transpiration. Recharge to the water table is specified as calculated in Section 4.7.2 (Figure 4–18). MODFLOW 2000 ‘RCH1 – Recharge’ package has been used to simulate the influx into the water table.

#### 8.6.4 Surface water features

Surface water features are not only important as groundwater flow model boundaries, but their flow data can also be useful in model calibration. The LMC comprises rivers, streams, drains, wetlands, lagoons and lakes. In a catchment-scale model such as that presented in this thesis, not all such features need to be incorporated. Commonly, Type 3 mixed boundary condition settings are used to represent surface water features in groundwater flow models. MODFLOW 2000 ‘RIV1 – River’ package has been used to simulate rivers and streams in the model and the ‘DRN1 – Drain’ package has been used to simulate the coastal lakes.

Bed conductance ( $C$ ) is an important parameter in the ‘RIV1 – River’ and ‘DRN1 – Drain’ packages. It is expressed in units of  $L^2/T$  and defined as

$$C = \frac{k}{t}lw \quad 8-2$$

where  $k$  is the hydraulic conductivity [ $L/T$ ],  $t$  is the thickness of the material in the direction of flow [ $L$ ], and  $lw$  is the cross-sectional area perpendicular to the flow direction [ $L^2$ ]. Conductance can be calculated for linear and areal features such as streams and lakes, respectively.

The modelling graphical user interface used (GMS) automatically calculates the lengths of arcs (linear features) and areas of polygons (areal features).

Therefore, conductance for rivers and streams for input into the model through the GMS GUI is required to be in terms of conductance per unit length

$$C_{\text{arc}} = \frac{k}{t}w \quad 8-3$$

where  $C_{\text{arc}}$  is conductance per unit length [ $L/T$ ],  $t$  is the thickness of the material [ $L$ ], and  $w$  is the width of the material along the length of the arc [ $L$ ].

Conductance for lakes for input into the model through the GMS GUI is required to be in terms of conductance per unit area

$$C_{\text{poly}} = \frac{k}{t}$$

8-4

where  $C_{\text{poly}}$  is conductance per unit area [ $1/T$ ] and  $t$  is the thickness of the material [L].

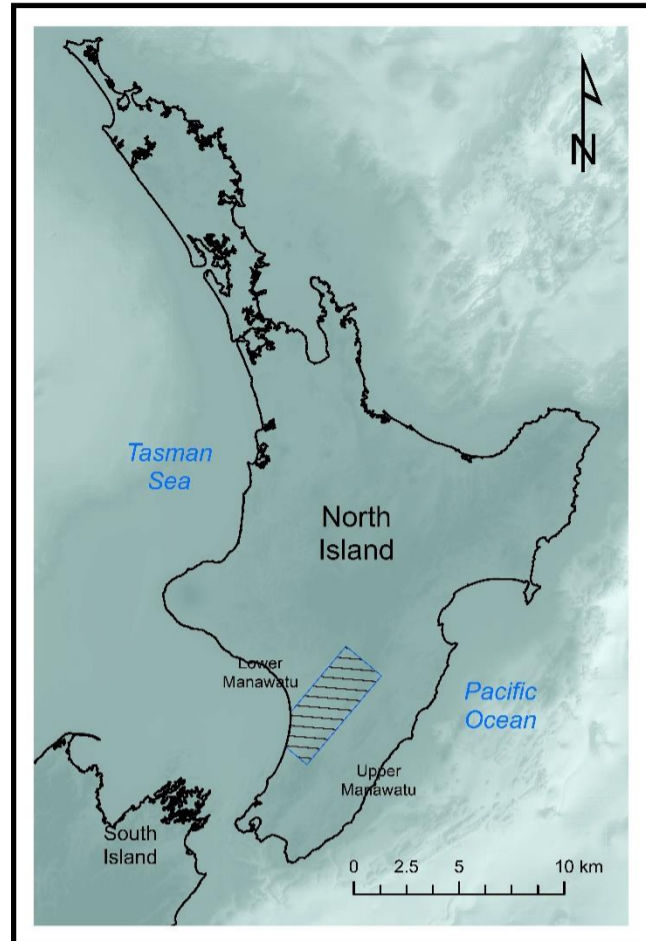
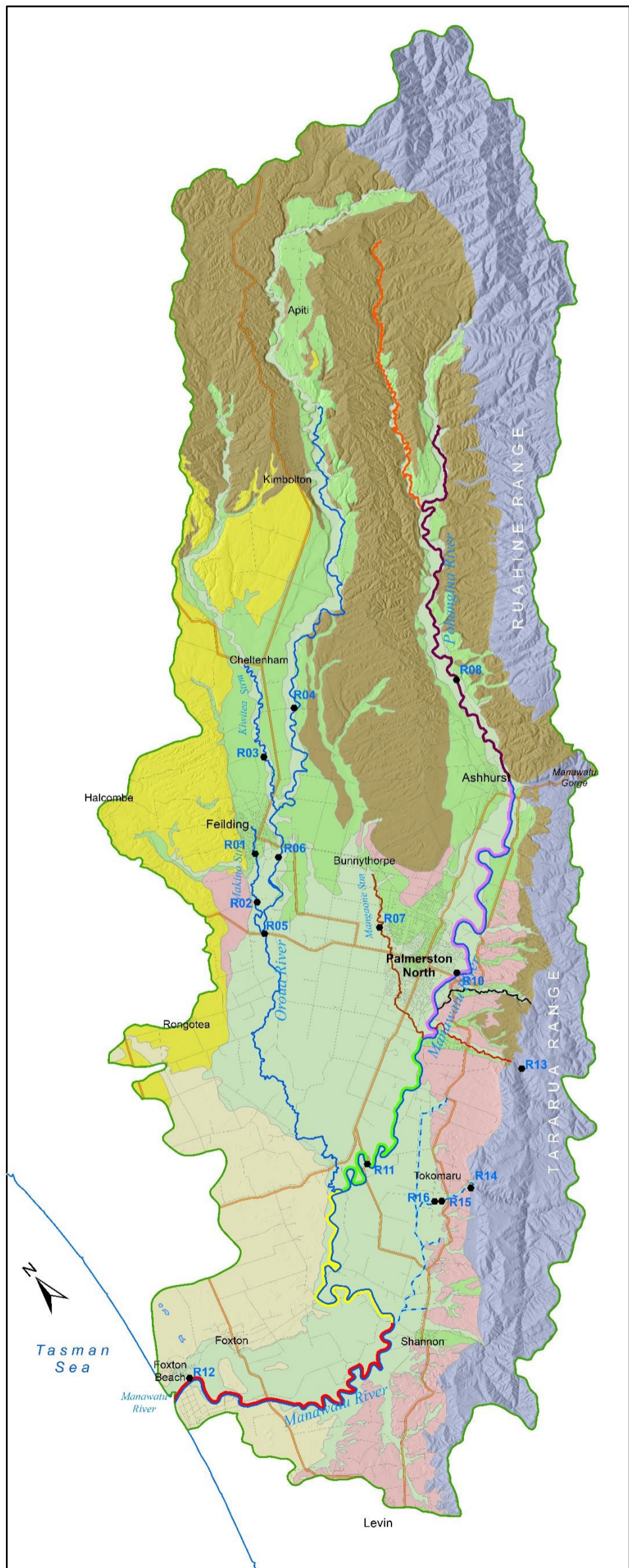
Initial conductance values have been estimated for modelled surface water features (Figure 8–9), but they have been refined during model calibration (Section 2.9).

## 8.7 Groundwater abstraction

Information on groundwater abstraction rates and the position of wells is needed for the groundwater flow model. In the LMC, it is permitted to take up to 50 m<sup>3</sup>/d of groundwater without resource consents (licence) from wells not deemed connected to surface water providing they meet conditions set in the regional plan. Wells considered connected to surface water are allowed to abstract up to 15 m<sup>3</sup>/d without resource consent. In 2016, there were records of c. 4,600 wells in the LMC, of which c. 260 well had resource consents to abstract water (Figure 8–10). Groundwater abstraction has been incorporated in the LMC groundwater flow model using the MODFLOW 2000 ‘WELL1– Well’ package and screen extent data.

### 8.7.1 Well depths and screen lengths

Within the LMC groundwater flow model domain, the depth of c. 3,530 production wells is known but screen length is known for only c. 690 wells. Well depth and screen extent information needs to be estimated for the groundwater flow model. For wells with known depth, the average depth is 48.75 m and the median depth is 30 m. For wells with screen data, the average screen length 4.5 m and the median screen length is 3 m. Therefore, wells that have no depth information have been assumed to be 30 m deep and a screen length of 3 m has been assumed for wells that do not have that data. There are c. 70 wells that are shallower than 3 m. They have been excluded from the model.



### LOWER MANAWATU CATCHMENT MODELLED SURFACE WATER FEATURES

#### Legend

- Catchment boundary
- River flow monitoring site
- Lake (initial conductance =  $5 \text{ d}^{-1}$ )
- Coastline
- Highway
- Road

#### Rivers/streams

- Oroua River System (initial conductance = 250 m/d)
- Manawatu Opiki to Moutoa (initial conductance = 500 m/d)
- Manawatu below Moutoa (initial conductance = 500 m/d)
- Makiekie (Coal) Creek (initial conductance = 625 m/d)
- Pohangina (initial conductance = 1,875 m/d)
- Manawatu Ashhurst to Linton (initial conductance = 600 m/d)
- Turitea Stream (initial conductance = 120 m/d)
- Kahuterawa Stream (initial conductance = 120 m/d)
- Mangaone Stream (initial conductance = 100 m/d)
- Manawatu Linton to Opiki (initial conductance = 2,250 m/d)
- Tokomaru River (initial conductance = 325 m/d)

#### Estimated values for bed conductance calculations

Feature/s	$k$ (m/d)	$t$ (m)	$w$ (m)
Coastal lakes	10	2	N/A
Oroua River System	50	2	10
Manawatu Opiki to Moutoa	10	2	100
Manawatu below Moutoa	10	2	100
Makiekie (Coal) Creek	50	2	25
Pohangina River	50	2	75
Manawatu Ashhurst to Linton	20	2	60
Turitea Stream	20	1	6
Kahuterawa Stream	20	1	6
Mangaone Stream	20	1	5
Manawatu Linton to Opiki	50	2	50
Tokomaru River	50	2	13

See Figure 2-16 for geological units symbols.

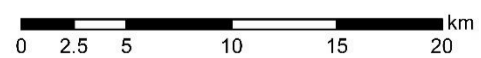
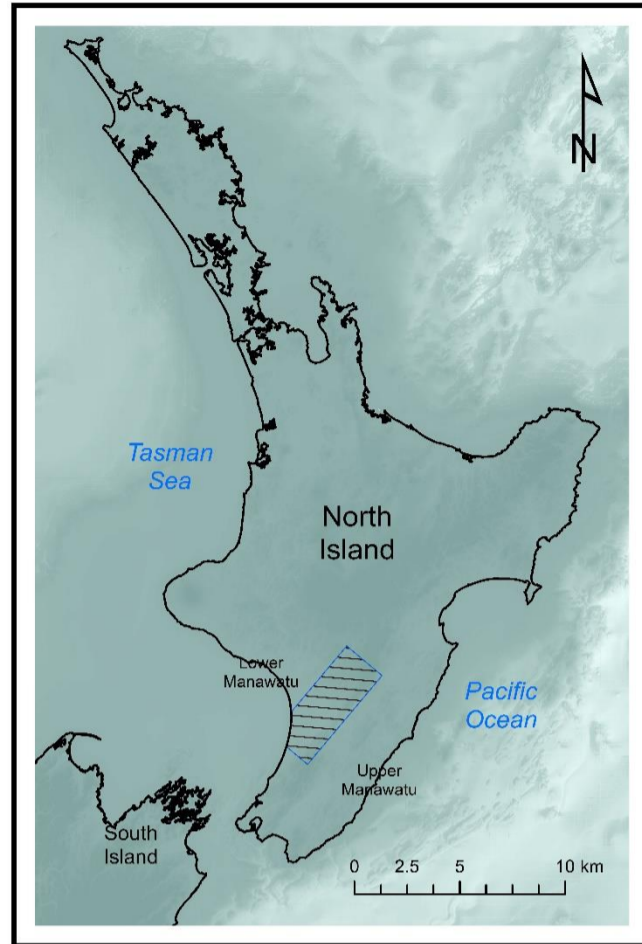
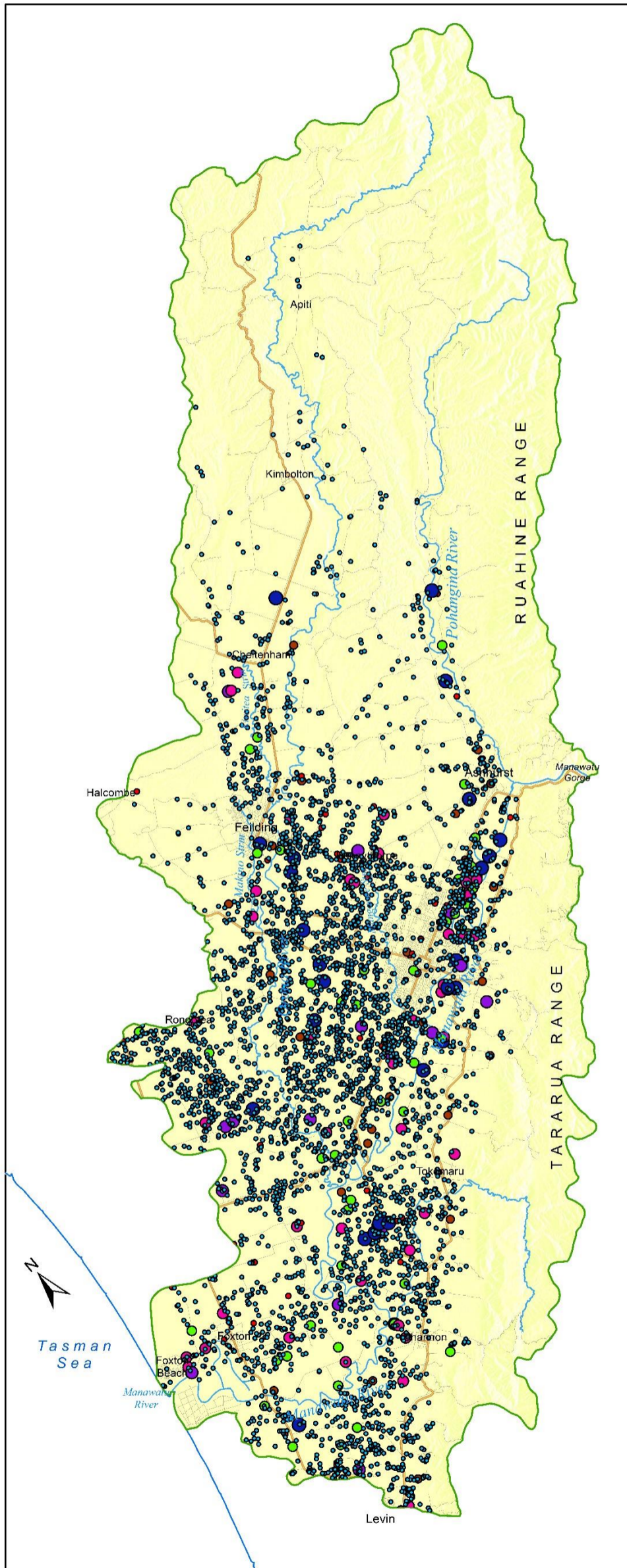


Figure 8-9. Surface water features and monitoring data incorporated in the LMC groundwater flow model.



### LOWER MANAWATU CATCHMENT GROUNDWATER ABSTRACTION

#### Legend

- Catchment boundary
- Coastline
- River
- Highway
- Road
- Stream/creek

#### Estimated groundwater abstraction rate

- Permitted well (15 m<sup>3</sup> per day)

#### Consented well

- ≤ 25 m<sup>3</sup> per day
- 25 - 50 m<sup>3</sup> per day
- 50 - 100 m<sup>3</sup> per day
- 100 - 300 m<sup>3</sup> per day
- 300 - 500 m<sup>3</sup> per day
- 500 - 967 m<sup>3</sup> per day

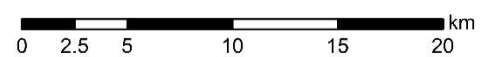


Figure 8-10. Average groundwater abstraction rates included in the groundwater flow model.

### 8.7.2 Pumping rates

There are no data on groundwater abstraction in the LMC. Zarour (2008) developed a method to estimate abstraction in the Manawatu–Wanganui region assuming that on average permitted wells take 15 m<sup>3</sup> per day throughout the year, and consented wells are pumped 100 days per year at 80% of their maximum consented daily take volume. This approach has been adopted to estimate groundwater abstraction in the LMC numerical groundwater model.

## 8.8 Model parametrisation

Groundwater flow models use hydraulic conditions and properties in head computations. Initial best estimates need to be input in the model, which can later be adjusted to better suit field observations. There are various methods to assign hydraulic properties to model cells. Hydraulic conditions and properties can be assigned unvaryingly to the entire model domain, to zones within it, or to individual cells. Over-parametrisation is often tempting, but should be avoided as much as practically possible just like the case with over-discretisation.

Due to the heterogeneous nature of most geological material, determination of parameter distribution in a groundwater flow system is one of the most difficult aspects in hydrogeological modelling. In approaching this question, the modeller should maintain the mindset that the objective is to represent the main features in the modelled system rather than replicating it. In this context, upscaling is obligatory and equivalent parameters need to be found to represent the modelled system and enable reproducing its behaviour.

The hydrolithostratigraphical model presented in Section 8.3.3 has been overlaid on the model domain described in Section 8.5.2, deforming the top and bottom of the grid to match the tops and bottoms of the solids that represent the various units in the hydrolithostratigraphical model and the interior grid layer boundaries have been deformed to be evenly spaced between the top and bottom of the grid. The interior grid layers have not been changed to match the stratigraphical boundaries. The grid cells have been assigned material from the hydrolithostratigraphical model

and parametrised with hydraulic properties of the material that coincide with their centres. Horizontal hydraulic conductivity for the model material have been initially assigned according to Table 8–3. The model materials have been assumed to be horizontally isotropic ( $K_x/K_y = 1$ ) but vertically anisotropic ( $K_h/K_v = 10$ ).

In addition to populating initial horizontal and vertical hydraulic conductivities, initial bed conductance values have been assigned to river and drain model cells based on the estimates presented in Figure 8–9. Initial estimates of horizontal and vertical hydraulic conductivities and conductance values have been changed during the model calibration stage.

### 8.9 Initial conditions

In addition to having to define hydraulic head and/or hydraulic head gradient conditions along the flow domain periphery, solving the groundwater flow governing equation using the finite difference method requires defining initial head values at each grid cell in the finite difference grid. Initial conditions refer to the distribution of hydraulic head at the beginning of the simulation and, thus, represent boundary conditions in time. In time-independent steady-state modelling, initial conditions do not affect the outcome of the simulation. However, good choice of initial head conditions reduces the number of required iterations for model convergence. In transient models, initial conditions strongly affect the outcome of the models. Transient models commonly use calibrated steady-state model results to provide them with their initial conditions. Initial model heads have been set at the model grid top elevations.

### 8.10 Set up and calibration

In this research, three steady-state numerical groundwater flow model versions have been produced for the LMC, specifically:

1. Manually calibrated model assuming homogeneous geological strata (Section 8.10.1)

2. Automatically calibrated model assuming homogeneous geological material (Section 8.10.2)
3. Automatically calibrated model assuming heterogeneous geological material (Section 8.10.3).

The three versions of the LMC model represent stepped-up appreciation of the catchment's actual hydrogeological characteristics.

Only hydraulic properties relevant to steady-state conditions have been manipulated in the LMC groundwater flow model calibration, namely, horizontal hydraulic conductivity, horizontal hydraulic conductivity, vertical anisotropy and river and drain bed conductance. It has been assumed that the recharge estimates presented in Section 4.7.2 are reasonably trustworthy and should not be changed during model calibration. So, no flux adjustments have been attempted in the model calibration.

Observations used in model calibration included average groundwater level data presented in Appendix C and surface water losses and gains reported in Section 5.10 and summarised in Table 8-5. Positive groundwater flux values in Table 8-5 indicate groundwater gains and negative values indicate groundwater losses.

Table 8-5. Surface water calibration targets<sup>67,68</sup>.

Calibration target code	System/description	Input point/s	Output point/s	Total input	Total output	Groundwater Flux <sup>69</sup>
TK1	Tokomaru River	R14	R15	204,885	201,267	3,618
TK2	Tokomaru River	R15	R16	201,267	116,057	85,210
MK	Makino Stream	R01	R02	40,089	77,987	-37,898
K-O	Kiwitea & Oroua above Kawa Wool	R03, R04	R06	276,553	1,030,015	-753,462
M-O	Makino & Oroua above Rangitau	R02, R06	R05	1,108,002	902,649	205,353
M-M	Mangaone Stream & Manawatu River above Opiki	R07, R10	R11	10,034,973	9,282,246	752,727

<sup>67</sup> All units in mcm/y.

<sup>68</sup> See Figure 8-9 for input and output point locations.

<sup>69</sup> Positive values indicate surface water loss, negative values indicate surface water gain.

For model calibration purposes, groundwater level standard deviation values have been calculated and directly input in GMS. For surface water, 10% of the flux values has been specified as the calibration target interval and GMS calculated the corresponding standard deviations.

Where available, well screen data have been used in model calibration against groundwater head targets. Where that information has not been available, screen extents and positions have been estimated following the method described in Section 8.7.1.

Accurate top of well elevation data are available from surveys for all the groundwater level monitoring wells used in the model as calibration targets, but some of these wells lack screen and/or depth data. Subsequently, confidence levels have been assigned to groundwater level observations as follows:

1. 95% for groundwater level observations from wells with screen data
2. 75% for groundwater level observations from wells without screen data but with known depth
3. 50% for groundwater level observations from wells without screen or depth data.

The confidence interval for flux calibration targets taken from Table 8–5 has been set to 75%.

#### **8.10.1 Initial parametrisation and manual calibration**

The LMC groundwater flow model calibration targeted reproducing average groundwater heads and groundwater–surface water interaction conditions within the observed standard deviations at various sites across the catchment.

The LMC groundwater flow model incorporates 11 hydrolithostratigraphical units (Table 8–3). Assuming hydraulic properties homogeneity within each of these units, the model has been parameterised using initial hydraulic conductivity values

presented in Table 8–3 and conductance values presented in Figure 8–9. Manual calibration of the model has been undertaken to refine the initial parameter estimates. The adopted hydraulic conductivity values and ranges presented in Table 8–3 are conformable with those assigned to similar units in the Kapiti Coast groundwater model (Gyopari *et al.*, 2014). The manually calibrated model produced acceptable results (Figure 8–11), largely matching the general piezometric pattern presented in Figure 6–8 and mostly exhibiting surface water–groundwater interaction conditions in line with the picture presented in Section 5.10.

The fit between calculated and observed groundwater heads presented in Figure 8–12 shows extraordinarily reasonable fitness for a manually calibrated, catchment–scale model.

The model fitting statistics and water budget elements presented in Table 8–6 suggest that the manually calibrated model reasonably represents the groundwater system. The simulation shows areas in the upper model layers that are dry (head below bottom of cells) or flooded (head above top of cells) (Figure 8–11). Dry cells in the model coincide with topographically elevated areas like the crests of the Feilding Anticline and Pohangina Anticline where the water table is deepest. So, dry cells are found where they are expected and reflect actual conditions. Flooded cells occur in river valleys and low–lying areas, which is understandable and expected. It must be noted, however, that dry and flooded cells marked by GIS analysis are not only subject to model performance, but they are also related to the resolution and accuracy of the used DEM, model discretisation, the accuracy of land elevation and groundwater head spatial interpolation, and the model resolution.

Initial manual synthesis of the model involved adjusting some cell bottom elevations to allow them to accommodate river boundary conditions, making sure that both the stage and bottom of the river cells are above the cell bottom elevation. Manipulation of the manually parametrised and calibrated model provided important information for the following stages of automated parameter estimation and model

calibration, including the setup of initial head conditions and initial values and ranges for the model parameters.

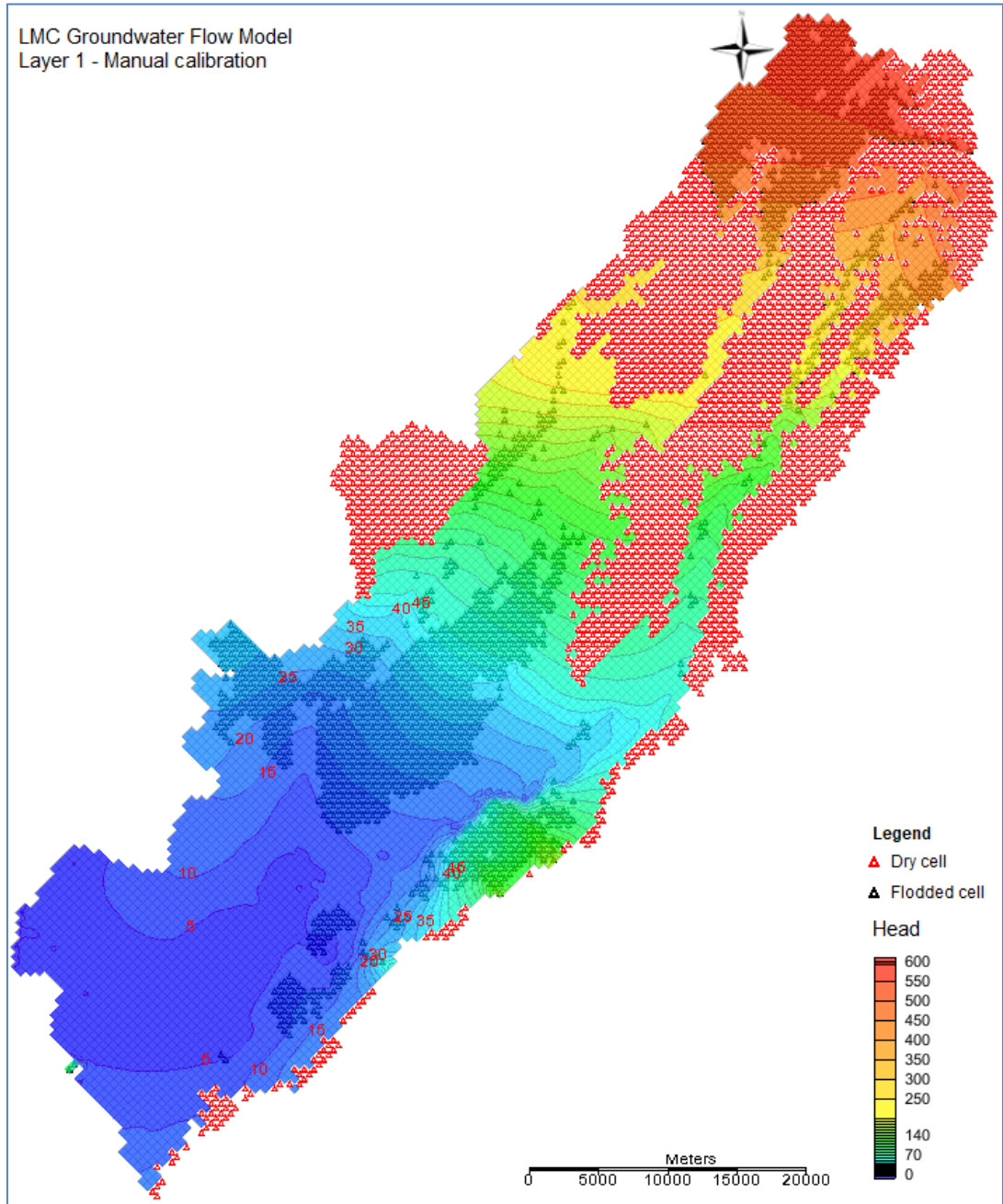


Figure 8–11. Model calculated head distribution (in masl) for the topmost layer from manual calibration.

Used hydraulic conductivity values are presented in Table 8–3 and conductance values are presented in Figure 8–9.

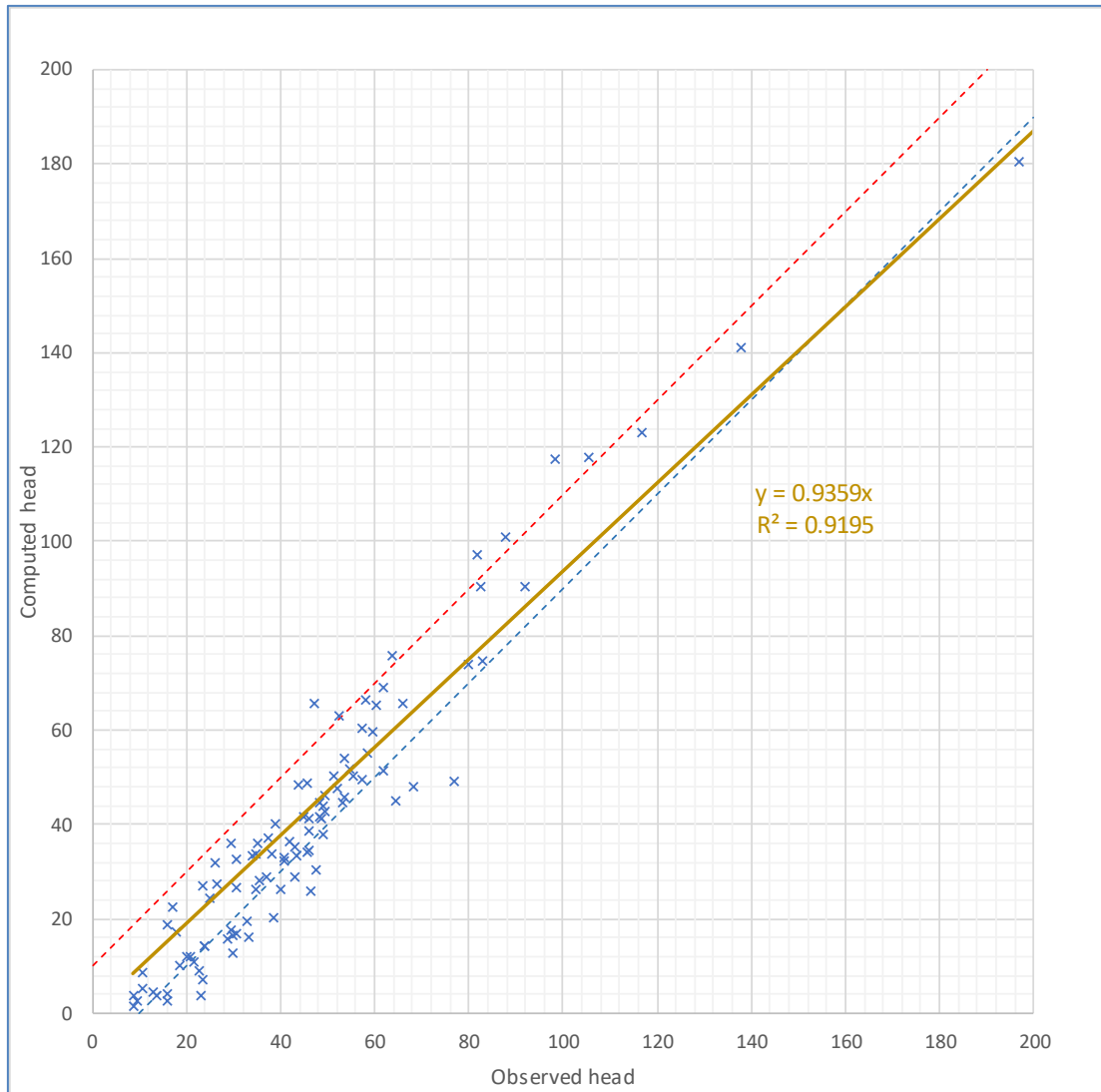


Figure 8–12. Scatter plot of measured heads against manually calibrated model calculated heads using initial estimates of hydraulic conductivity values presented in Table 8–3 and river/stream bed conductance values presented in Figure 8–9.

The brown solid line represents the data linear trend, the red dashed line represents 10 m model overestimation, and the blue dashed line represents 10 m model underestimation. The trend line equation and linear regression goodness-of-fit ( $R^2$ ) are shown on the graph.

Table 8–6. Manually calibrated model main results and basic calibration metrics.

Measure	Value	Units
Groundwater recharge	1,991,586.40	m <sup>3</sup> /d
Groundwater abstraction	-99,633.76	m <sup>3</sup> /d
Net groundwater exchange with rivers	-1,876,529.93	m <sup>3</sup> /d
Flow into the coastal lakes	-14,818.51	m <sup>3</sup> /d
Flow into the ocean	-826.75	m <sup>3</sup> /d
R-squared (Head)	0.92	—
Mean Residual (Head)	5.02	m
Mean Absolute Residual (Head)	8.52	m
Root Mean Squared Residual (Head)	10.31	m
Mean Residual (Flow)	176,212.18	m <sup>3</sup> /d
Absolute Residual (Flow)	281,428.48	m <sup>3</sup> /d
Root Mean Squared Residual (Flow)	518,864.51	m <sup>3</sup> /d

### 8.10.2 Homogeneous layers calibration and parameter sensitivity

The initial manually calibrated model was followed by automated parameter estimation using PEST 14.0 software (Doherty, 2015) through the GMS GUI. This has been intended to mathematically enhance the initial estimates of hydraulic properties and evaluate model parameter sensitivity. In this process, PEST was run to estimate a ‘representative bulk equivalent’ hydraulic conductivity value for each of the hydrolithostratigraphical units identified in Table 8–3. Overlaying the stratigraphical model presented in Section 8.3.3 on the groundwater flow model finite difference grid resulted in zonation of the grid cells (Figure 8–13). A reasonable agreement has been achieved between observed and calculated heads from this stage of modelling (Figure E–1 in Appendix E). Model parameters estimated using PEST for this set up are presented in Table 8–7. Maps showing the automated estimates of hydraulic conductivity for the various model layers are presented in Appendix E (Figures E–2 through E–8). Table 8–8 presents the water budget components calculated from this stage of modelling and model calibration metrics.

During the zonal model calibration process, the quality of observation data proved to be challenging, hindering PEST’s runs, especially in terms of apparently inaccurate screen extent information. Problematic observation wells have been identified and their data have been excluded from the automated model calibration.

The wells used in automated parameter estimation are listed in Table E-1 in Appendix E.

The automated parameter estimation code PEST enables the evaluation of the sensitivity of the model to input parameters, which is important to assess whether the conceptual model needs revision and/or initial conditions and parameter estimates need adjustment. Sensitivity analysis also helps the users of the model to understand the uncertainties inherent in the model calibration.

Figure 8-14 graphically represents parameter sensitivities obtained from the PEST optimisation process assuming homogeneous geological strata. As explained by Gyopari *et al.* (2014), following the calculation of the Jacobian matrix for each iteration PEST calculates the composite sensitivities for the parameters, then multiplies the composite value for each parameter by the magnitude of the log of its value to obtain relative sensitivity for each parameter. Evaluation of the relative sensitivities enables comparing the effects of different parameters of different magnitude on the results of the model calibration. Figure 8-14 suggests that in the zonal (homogeneous) model calibration process, riverbed conductance parameters have not been relatively sensitive ( $<0.1$ ), whereas hydraulic conductivities of interglacial times material are relatively moderately sensitive ( $>0.1$ ) and the hydraulic conductivities for the Plio-Pleistocene and Castlecliffian strata are most relatively sensitive ( $>0.4$ ). This could be due to the fact that Plio-Pleistocene, Castlecliffian and interglacial times material comprise the bulk of the model volume and, therefore, they have the potential to exert huge influence on the model results.

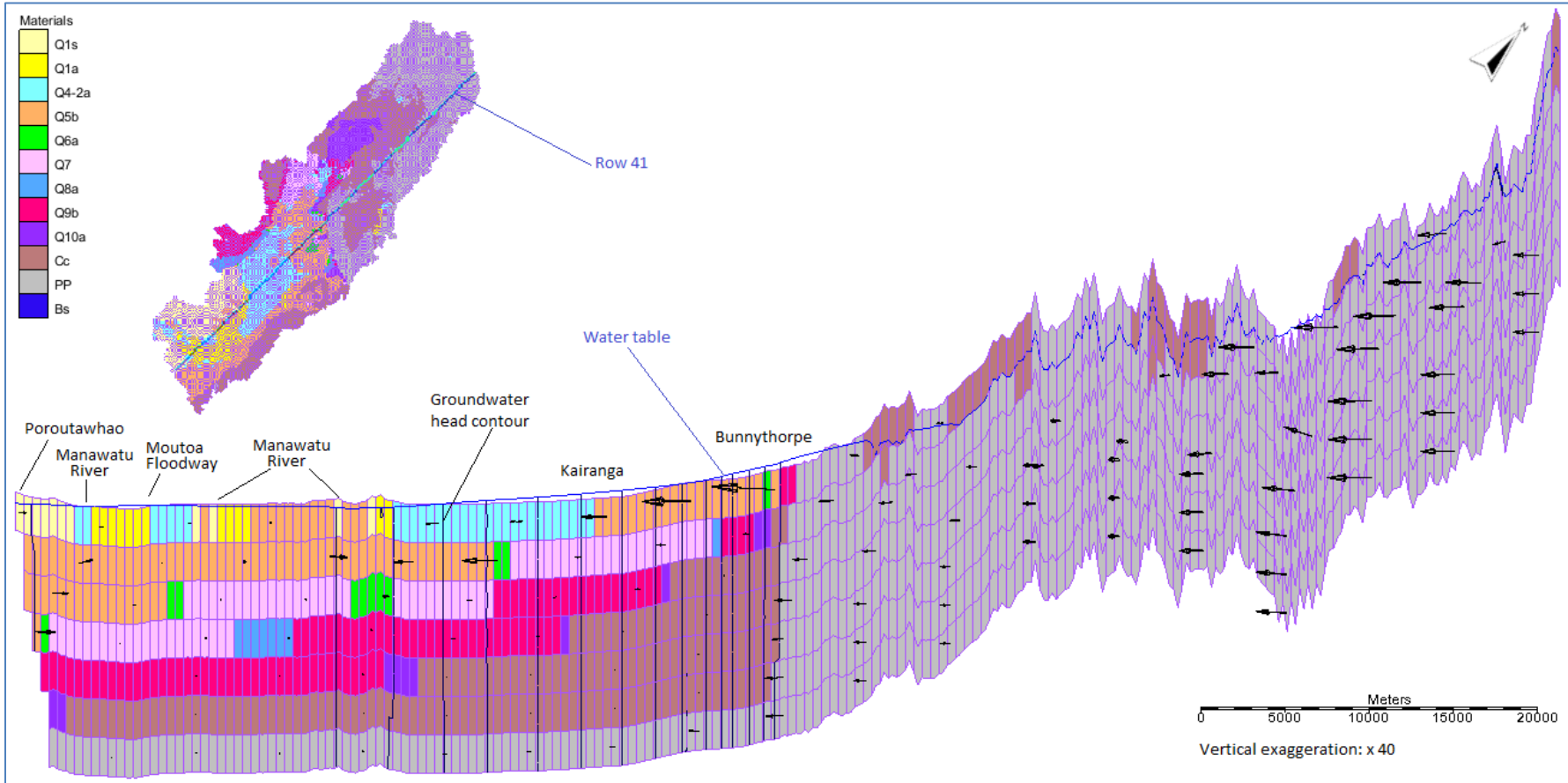


Figure 8–13. Cross-section through row 41 in the homogeneous stratigraphical strata model showing the overlay of geology on the groundwater flow model finite difference grid, flow velocity vectors (black arrows) and the water table (Blue line).

Table 8–7. Automated estimates of hydraulic conductivity and riverbed conductance assuming homogeneity in geological strata.

Parameter	Description	Value	Units
HK_1010	Hydraulic conductivity – Holocene sands (Q1s)	0.01	m/d
HK_1020	Hydraulic conductivity – Holocene alluvium (Q1a)	50.24	m/d
HK_1030	Hydraulic conductivity – Last Glacial alluvium (Q4–2a)	8.57	m/d
HK_1040	Hydraulic conductivity – Last Interglacial beach deposits (Q5b)	15.14	m/d
HK_1050	Hydraulic conductivity – Marton alluvium (Q6a)	66.94	m/d
HK_1060	Hydraulic conductivity – Rapanui marginal marine deposits (Q7b)	3.88	m/d
HK_1070	Hydraulic conductivity – Burnand alluvium (Q8a)	15.37	m/d
HK_1080	Hydraulic conductivity – Brunswick marginal marine deposits (Q9b)	2.58	m/d
HK_1090	Hydraulic conductivity – Waituna alluvium (Q10a)	0.38	m/d
HK_1100	Hydraulic conductivity – Castlecliffian strata (Cc)	0.42	m/d
HK_1110	Hydraulic conductivity – Plio–Pliocene strata (PP)	2.99	m/d
RIV_2020	Bed conductance – Oroua River System	4,667.20	m/d
RIV_2030	Bed conductance – Manawatu Opiki to Moutoa	93.85	m/d
RIV_2040	Bed conductance – Manawatu below Moutoa	95.79	m/d
RIV_2050	Bed conductance – Makiekie (Coal) Creek	3,111.90	m/d
RIV_2060	Bed conductance – Pohangina River	50,000.0	m/d
RIV_2070	Bed conductance – Manawatu Ashhurst to Linton	99.09	m/d
RIV_2080	Bed conductance – Turitea Stream	22.66	m/d
RIV_2090	Bed conductance – Kahuterawa Stream	16.24	m/d
RIV_2100	Bed conductance – Mangaone Stream	487.23	m/d
RIV_2110	Bed conductance – Manawatu Linton to Opiki	3.82	m/d
RIV_2120	Bed conductance – Tokomaru River	13.59	m/d
DRN_5000	Bed conductance – Coastal lakes	0.012	1/d

Table 8–8. Main results and basic calibration metrics for the automated parameter estimation model assuming hydraulic conductivity homogeneity in each hydrolythostratigraphical unit.

Measure	Value	Units
Groundwater recharge	1,991,083.51	m <sup>3</sup> /d
Groundwater abstraction	–99,561.93	m <sup>3</sup> /d
Net groundwater exchange with rivers	–1,883,939.62	m <sup>3</sup> /d
Flow into the coastal lakes	–7,974.42	m <sup>3</sup> /d
Flow into the ocean	–1,177.01	m <sup>3</sup> /d
R-squared (Head)	0.92	—
Mean Residual (Head)	3.40	m
Mean Absolute Residual (Head)	7.95	m
Root Mean Squared Residual (Head)	10.82	m
Mean Residual (Flow)	127,676.73	m <sup>3</sup> /d
Absolute Residual (Flow)	230,428.04	m <sup>3</sup> /d
Root Mean Squared Residual (Flow)	410,214.82	m <sup>3</sup> /d

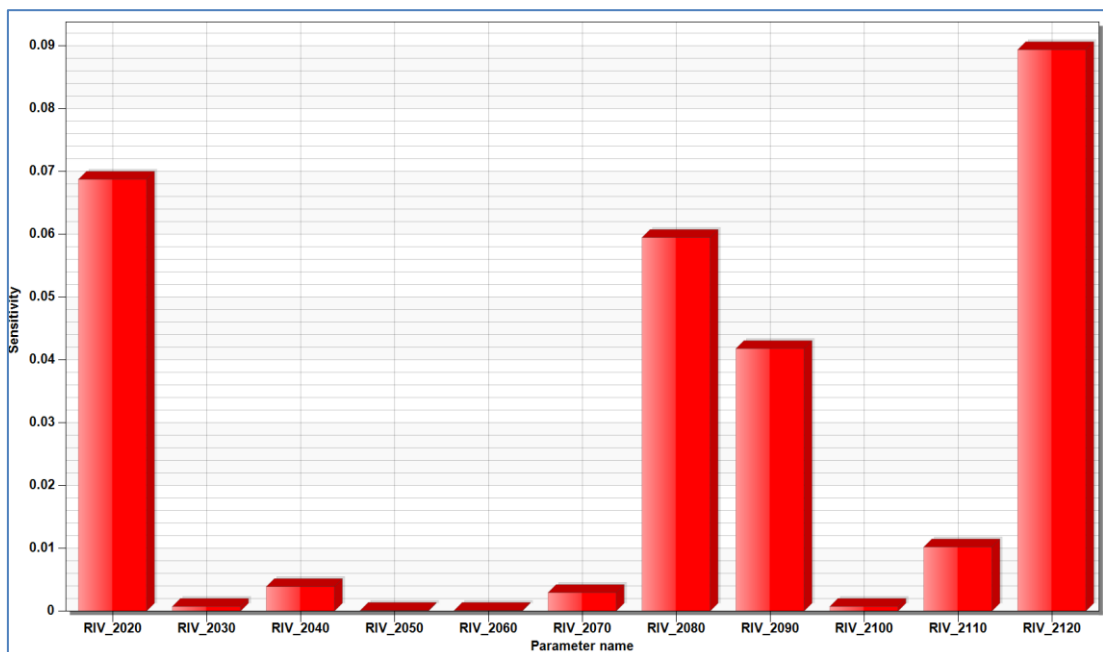
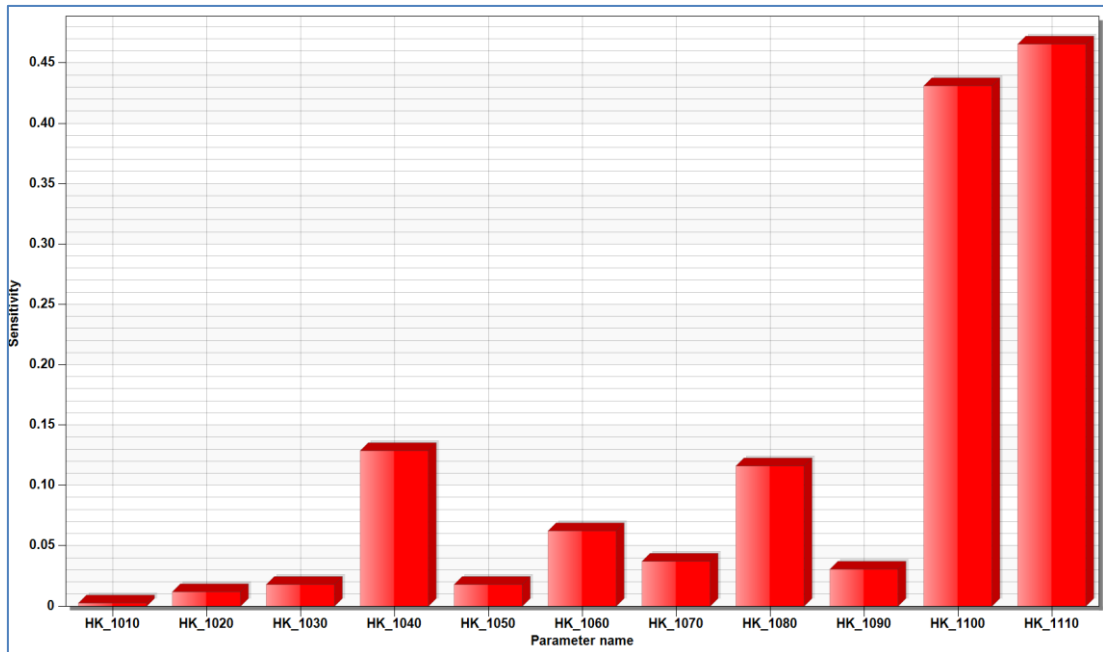


Figure 8–14. Sensitivity evaluation of hydraulic conductivity (top) and bed conductance (bottom) values obtained from automated parameter estimation assuming homogeneity of geological strata.

### 8.10.3 Heterogeneous layers calibration and parameter sensitivity

Knowledge of the lithology of the stratigraphical sequence in the LMC from outcrops and well logs indicates that the strata are heterogeneous. For example, an alluvial unit can in locations comprise coarse sand and gravel with hydraulic conductivity

in the order of 250–500 m/d, but in other places it could consist of clay-bound gravel and sand, characterised by hydraulic conductivity in the order of 1–20 m/d. Consequently, it has been decided to incorporate heterogeneity in automated parameter estimation for the various hydrolithostratigraphical units recognised in the LMC area utilising the pilot points calibration technique in specified zones corresponding to identified lithostratigraphical units. The concept adopted simply allows for spatial variability of hydraulic properties within set limits through each of the hydrolithostratigraphical units overlaid onto the finite difference grid rather than assigning constant parameter values for each of these units. This approach respects both the broad differences between geological distinct units (e.g. Q4–2a versus Q5b) and the variability within individual units. To implement this solution, initial estimates and acceptable ranges of hydraulic conductivity have been set for each hydrolithostratigraphical unit at 25 pilot points across the LMC area (Figure E–9 in Appendix E) based on the first stage of automated parameter estimation and PEST has been used to estimate hydraulic properties at these points and between them for every hydrolithostratigraphical unit as it occurs across the groundwater flow finite difference grid. This approach resulted in good fit between calculated and observed heads (Figure 8–15 and Figure D–9 in Appendix D). Table 8–9 presents the hydraulic conductivity ranges estimated for various hydrolithostratigraphical units in the LMC using zoned pilot point calibration and Table 8–10 presents the calculated elements of the water budget and model metrics from the zoned pilot points calibration. The model suggests that hydraulic conductivity ranges from less than 0.01 m/d to 115.7 m/d through the simulated stratigraphical sequence. Figures E–10 through E–16 in Appendix E portray the estimated hydraulic conductivity values for the LMC groundwater flow model layers and the heads calculated in them.

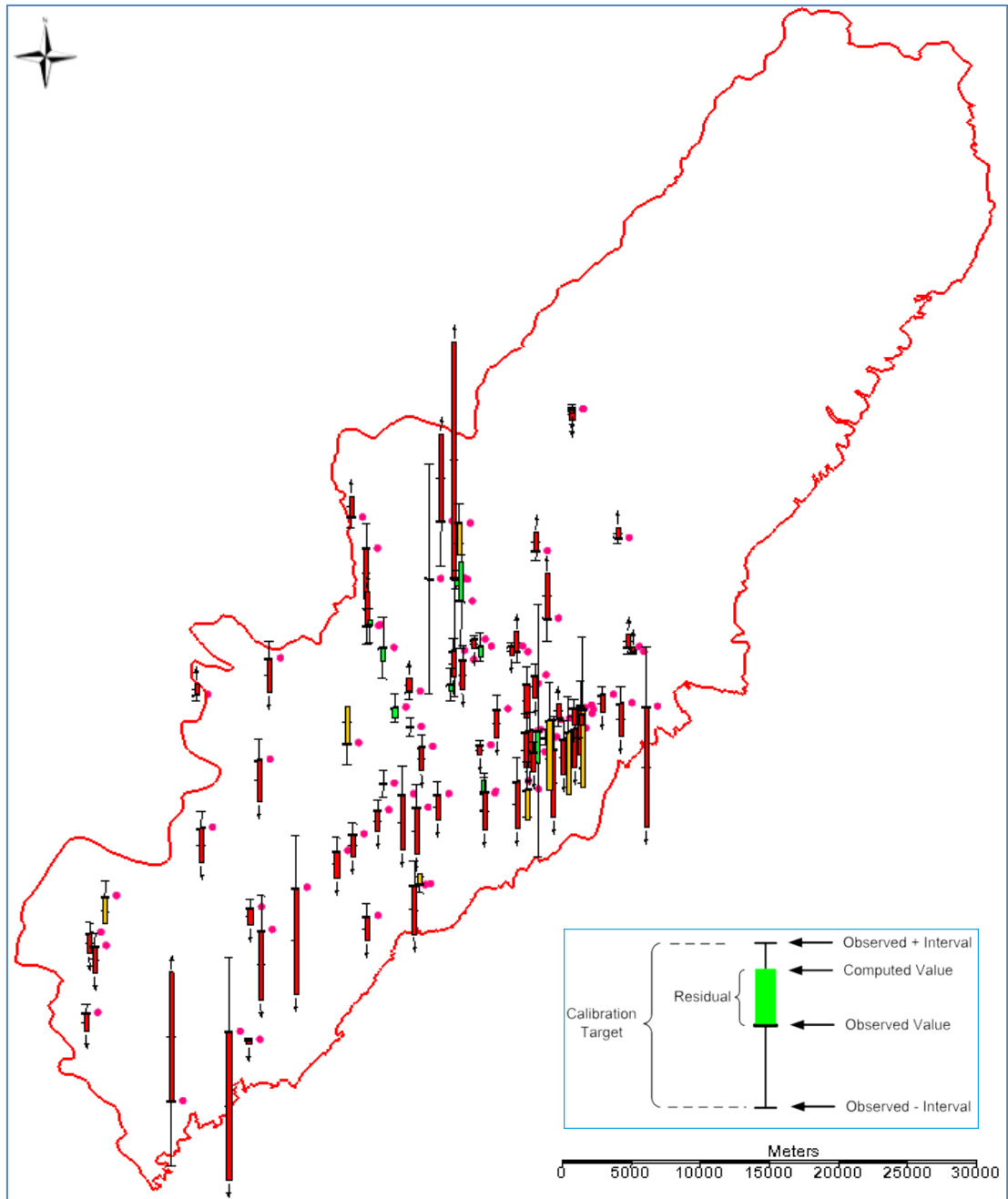


Figure 8–15. Error bars at observation points showing the degree of fitness between calculated and observed heads from automated parameter estimation assuming heterogeneity of hydrolythostratigraphical units within the LMC model area.

Green colour code means the calculated value falls within the calibration target, yellow means that the calculated value is outside the target range but the error is less than 200%, and red denotes that the error is greater than 200%.

Table 8–9. Hydraulic conductivity ranges estimated for hydroliothostratigraphical units in the LMC using zoned pilot point calibration.

Parameter	Description	Set range		Model values	
		min	max	min	max
HK_1010	Hydraulic conductivity–Q1s	0.010	100.0	0.89	6.860
HK_1020	Hydraulic conductivity–Q1a	0.010	100.0	0.54	50.000
HK_1030	Hydraulic conductivity–Q4–2a	0.010	500.0	0.88	115.700
HK_1040	Hydraulic conductivity–Q5b	0.010	200.0	0.38	83.480
HK_1050	Hydraulic conductivity–Q6a	0.010	200.0	0.64	29.800
HK_1060	Hydraulic conductivity–Q7b	0.010	200.0	0.15	11.020
HK_1070	Hydraulic conductivity–Q8a	0.010	200.0	1.08	93.660
HK_1080	Hydraulic conductivity–Q9b	0.010	200.0	0.02	9.450
HK_1090	Hydraulic conductivity–Q10a	0.010	10.0	0.08	8.920
HK_1100	Hydraulic conductivity–Cc	0.001	200.0	0.01	4.950
HK_1110	Hydraulic conductivity–PP	0.010	200.0	0.06	9.940
RIV_2020	Riverbed conductance–Oroua River System	1,000.000	25,000.0	4,677.28	
RIV_2030	Riverbed conductance–Manawatu Opiki to Moutoa	100.000	2,500.0	100.00	
RIV_2040	Riverbed conductance–Manawatu below Moutoa	100.000	2,500.0	100.00	
RIV_2050	Riverbed conductance–Makiekie (Coal) Creek	125.000	3,125.0	605.11	
RIV_2060	Riverbed conductance–Pohangina River	750.000	18,750.0	18,750.00	
RIV_2070	Riverbed conductance–Manawatu Ashhurst to Linton	120.000	3,000.0	120.00	
RIV_2080	Riverbed conductance–Turitea Stream	24.000	600.0	24.00	
RIV_2090	Riverbed conductance–Kahuterawa Stream	24.000	600.0	24.00	
RIV_2100	Riverbed conductance–Mangaone Stream	5.000	125.0	125.00	
RIV_2110	Riverbed conductance–Manawatu Linton to Opiki	50.000	1,250.0	50.00	
RIV_2120	Riverbed conductance–Tokomaru River	13.000	325.0	13.00	
DRN_5000	Drain bottom conductance–Coastal lakes	0.060	1.5	0.06	

Table 8–10. Main results and basic calibration metrics for the automated parameter estimation model assuming hydraulic conductivity heterogeneity in hydroliothostratigraphical material.

Measure	Value	Units
Groundwater recharge	1,991,083.51	m <sup>3</sup> /d
Groundwater abstraction	–99,546.93	m <sup>3</sup> /d
Net groundwater exchange with rivers	–1,866,841.82	m <sup>3</sup> /d
Flow into the coastal lakes	–20,724.30	m <sup>3</sup> /d
Flow into the ocean	–3,632.20	m <sup>3</sup> /d
R–squared (Head)	0.94	—
Mean Residual (Head)	4.09	m
Mean Absolute Residual (Head)	6.50	m
Root Mean Squared Residual (Head)	8.46	m
Mean Residual (Flow)	136,396.22	m <sup>3</sup> /d
Absolute Residual (Flow)	248,031.17	m <sup>3</sup> /d
Root Mean Squared Residual (Flow)	433,616.31	m <sup>3</sup> /d

Pilot point calibration is extremely demanding in terms of computing resources even for steady–state simulations. So, to keep model run times practical, Singular Value Decomposition (SVD) and SVD–Assist PEST functionalities have been utilised in the zoned pilot point calibration of the LMC groundwater flow model. The SVD process analyses the parameters that are part of a parameter estimation process and

removes parameters that are not helping to solve the problem. SVD-Assist is particularly advantageous for models that have a large number of parameters, e.g. models using pilot points. SVD-Assist helps shorten run times. When using it, PEST runs MODFLOW once for every parameter to compute a matrix and uses that information to create super parameters that are combinations of the parameters originally specified and create a new PEST control file that enables the software to use significantly fewer MODFLOW runs for each of the needed iterations, commonly reducing the number of runs required for each PEST iteration by an order of magnitude.

Simulation of heterogeneity in hydrolithostratigraphical units has been controlled through the application of the Tikhonov regularisation, which provides prior information equations for pilot points to PEST. Tikhonov preferred homogeneous regularisation imposes a homogeneity constraint on the pilot points so that in absence of other information pilot points that are near to one another are set to about the same value. Tikhonov preferred value regularisation was also used to include prior information equations that constrain the pilot points near their starting values. The starting values were assigned to pilot points based on the hydraulic conductivity estimates provided in Table 8-3 and PEST was set to only change those values to calibrate the model if necessary.

Parameter sensitivity plots presented in Figure 8-16 suggest relatively large uncertainty in the assessment of hydraulic conductivity of the Castlecliffian and Plio-Pliocene units in the Pohangina Anticline area, which is understandable given the lack of knowledge about the hydraulic properties of these geological units, particularly in that area, in addition to structural complexities that may affect their hydrogeological parameters. The model seems not to be very sensitive to river bed conductance parameters, possibly due to the scale of the simulation.

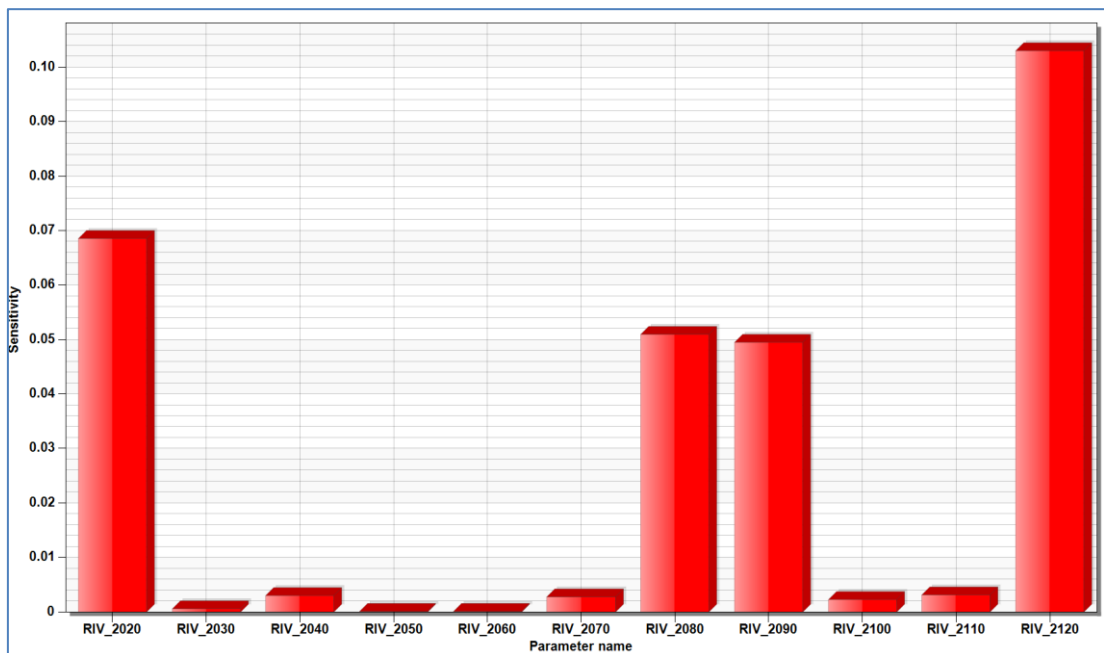
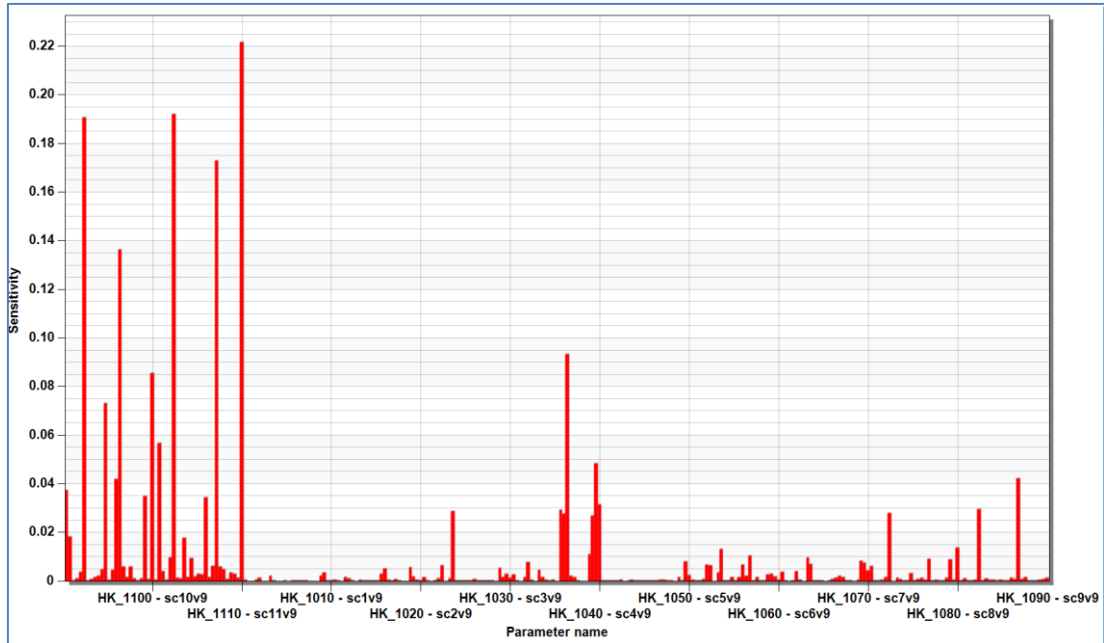


Figure 8–16. Sensitivity evaluation of hydraulic conductivity (top) and bed conductance (bottom) values obtained from automated parameter estimation assuming heterogeneity of geological strata.

### 8.11 Usability and confidence level

No model can be claimed to be a unique representation of the simulated object or subject or answer all possible questions on it. The steady–state models presented in this thesis are intended to represent long–term average conditions of the

groundwater flow system on a catchment-scale and, therefore, are not expected to be able to directly and precisely help with local-scale questions (e.g. effects of abstraction from a particular well on a nearby stream) or what would be the consequences of global sea level rise on the groundwater resource. The models presented here serve well their objectives, which are centred around characterising the LMC groundwater flow system and validating the presented catchment-scale conceptual model.

The Australian groundwater modelling guidelines provide a method to establish confidence level for groundwater models based on semi-quantitative assessment of the available data on which model is based, the manner in which the numerical model is implemented and calibrated, and how the predictions are formulated (Barnett *et al.*, 2012). The guidelines define three classes, 1–3, with Class 3 being the highest level of model confidence. The guidelines clarify key indicators and provide examples of model applications for each model confidence tier. The main features of the LMC groundwater flow models with regards to the Australian groundwater modelling guidelines confidence classification system are as follows:

### 1. Data

- Rainfall and evaporation data are available (Class 3)
- Reliable land-use and soil-mapping data available (Class 3, commensurate with the model scale)
- Good quality and adequate spatial coverage of digital elevation model to define ground surface elevation (Class 3)
- Groundwater head observations and bore logs are available but do not provide adequate coverage throughout the model domain (Class 2)
- Streamflow data and baseflow estimates available at a few points (Class 2).

### 2. Calibration

- Model is calibrated to heads and fluxes (Class 3, suitable for catchment-scale modelling)

- Acceptable calibration metrics (Class 2)
- Reasonable water budget figures (Class 2)
- Calibration statistics are generally reasonable (Class 2).

### 3. Temporal performance

- The LMC is not transient so measures relating to temporal performance do not apply in assessing its level of confidence class.

### 4. Prediction

- The LMC model has not been intended to be used in predictions, so this aspect is not relevant in determining its confidence level class.

### 5. Key indicators

- Key calibration statistics are acceptable and meet set targets (Class 3)
- Mass balance closure error is less than 0.5% of total (Class 3)
- Model parameters consistent with conceptualisation (Class 3)
- Appropriate computational methods used with appropriate spatial discretisation to model the problem (Class 3).

Accordingly, the LMC models can be designated Class 2 level of confidence, with many Class 3 level of confidence criteria met. The presented models are particularly useful as catchment management tools. They also provide reliable basis for subsequent higher confidence class models and provide basis for systematic data collection planning.

## 8.12 Uncertainty and limitations

The LMC groundwater flow models presented in this thesis are based on two other models, the soil moisture balance model presented in Sections 4.7 and the lithostratigraphical model presented in Section 8.3.3. Both models are uncertain and their uncertainties naturally transpire into the groundwater flow models that are

based on them. In particular, the SMB model used to calculate groundwater recharge sets that quantity at zero in urban and suburban areas (sections 4.7.1 and 4.7.3). Specialised investigations are needed to assess urban groundwater recharge in the LMC.

Assuming groundwater recharge to be zero in built-up areas is considered a limitation rather than an uncertainty in the models presented here. In general, across many studies throughout the world, urban recharge has been found to be greater than pre-urbanisation (e.g. Barrett *et al.*, 1997; Cook *et al.*, 2001; Foster *et al.*, 2005; Hughes & Mansour, 2005; Lerner, 2000, 2002). Nevertheless, there is very little research on the effects of urbanisation on groundwater recharge in New Zealand and it is regularly either trivialised or ignored altogether. For example, commenting on the estimation of groundwater recharge by Hadfield (2001), Toews and Moreau (2014) argue that groundwater recharge over the residential area of Matamata (c. 3.7 km<sup>2</sup>) is expected to be reduced due to runoff diversion to stormwater drainage from paved surfaces. Singh *et al.* (2018) contemplate that urban settlements and mountainous areas with steep slopes, hard rocks and thin soil layers have a low potential to contribute to groundwater recharge. There is a clear need for further study of urban groundwater recharge in New Zealand.

The LMC groundwater flow models are subject to uncertainties relating to the flow and head data used to calibrate them and the use of average values to represent long-term steady-state conditions is also a source of uncertainty. Simplifying assumptions unavoidable in any modelling work also introduce uncertainty in the LMC groundwater flow models, e.g. the inclusion of anisotropy in bulk hydraulic property values. The lack of good data on groundwater abstraction and screens for both production and monitoring wells contributes to the models' uncertainty.

The discussion of parameter sensitivities in Sections 8.10.2 and 8.10.3 provides a general feel of the models' level of uncertainty. The general agreement between the initial manually calibrated model and the homogeneous and heterogeneous automated calibrations of the model provide a reasonably good level of certainty in

the correctness of the conceptual model and the appropriateness of the numerical model implementations, particularly with regards to the stipulated boundary conditions. During the modelling exercise, the model sensitivity for the location of the no-flow boundary that coincide with the assumed surface water divide in the area between Sanson and the coastline has been anecdotally assessed, but neither quantified nor documented. The current location of the no-flow has been considered more appropriate than the groundwater divide in the same area assumed by Zarour (2008). In the models presented here, an 'unnamed' catchment has been removed from the model domain and considered to be part of the Rangitikei system rather than the LMC system. This assumption has been reached after examining the perceived groundwater flow paths in the area from different model setups.

It must be noted that any more advanced modelling will be subject to a higher level of uncertainty. For example, storativity is not used in the LMC model because they are steady-state simulations. Transient simulations require this parameter and will be affected by the uncertainty associated with it. Particle tracking, transient, solute transport and smaller scale models will all be subject to further sources of uncertainty.

### 8.13 Key findings

The numerical models presented in this thesis indicate that groundwater flow in the LMC is generally from the northeast to the southwest, largely aligned to geological structure and rivers (Figure 8-17). The sedimentary stratigraphical sequence is hydraulically continued without distinct aquifers and aquitards. Explicitly, this means that sandy material in the LMC are an integral part of the aquifer system and should not be discarded in any analysis. It may be convenient to screen wells in gravelly sections where higher yields are expected, but the groundwater taken from wells come from storage and movement throughout the entire aquifer system.

The models indicate that the hydraulic conductivity of the aquifer material ranges between less than 0.01 m/d and c. 120 m/d. the aquifer and rivers are highly

hydraulically connected, with the rivers mainly gaining from groundwater (Figure 8–17). There are places with prominent upwards hydraulic gradients which give rise to strong artesian head in their wells, e.g. the Manawatu Golf Course area (Figure 8–18).

Although calibrated using different methods, similar results have been obtained from the manually and automatically calibrated models that assume geological material homogeneity and the automatedly calibrated model that assumes geological material heterogeneously. In all three models, computed heads in the higher parts of the catchment are higher than the observed heads, and vice versa in the lower catchment. This may be due to underestimating the hydraulic conductivity of the Castlecliffian and older strata (> OIS 10) that prevail in the upper part of the catchment, or overestimating groundwater recharge in that area. However, it has not been possible to obtain better calibration of the models using lower hydraulic conductivity values and recharge values obtained from soil moisture modelling have not been altered during the calibration of the three models. This pattern of calculated–observed values relationship could also be related to the above–average rainfall noticed over the period 1985–1995 (Section 4.6.2). The current steady–state models cannot account for such a change, which may have happened at varying rates across the catchment.

The noticeable agreement between manual and automated model calibrations assuming aquifer material homogeneity and heterogeneity supports the opinion of Ye *et al.* (2010) noted in Section 3.2 that overall model uncertainty is greatly more susceptible to conceptual uncertainty rather than parametric uncertainty.

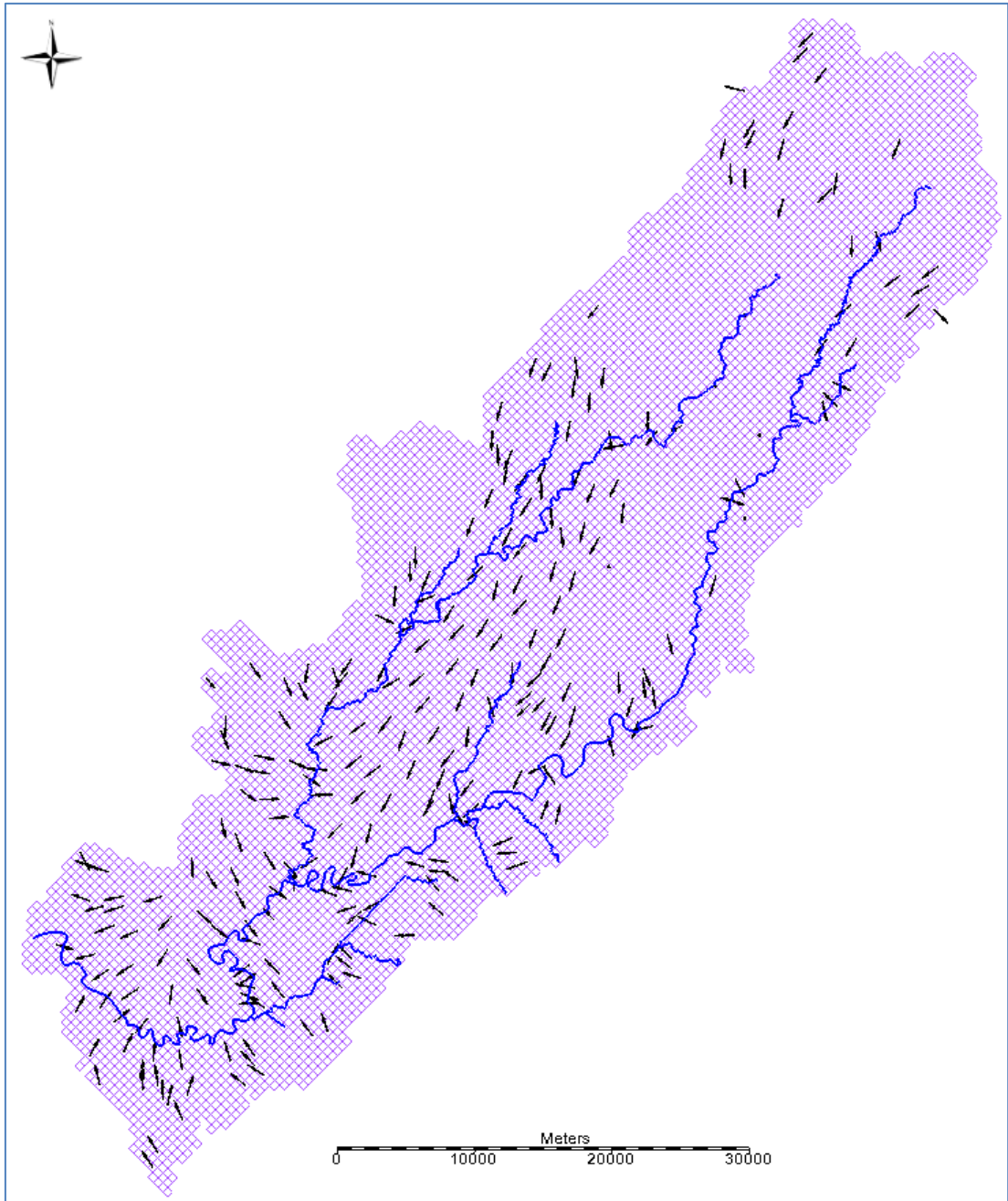


Figure 8-17. Flow velocity vectors showing groundwater flowing mainly towards rivers in Layer 1 of the LMC model.

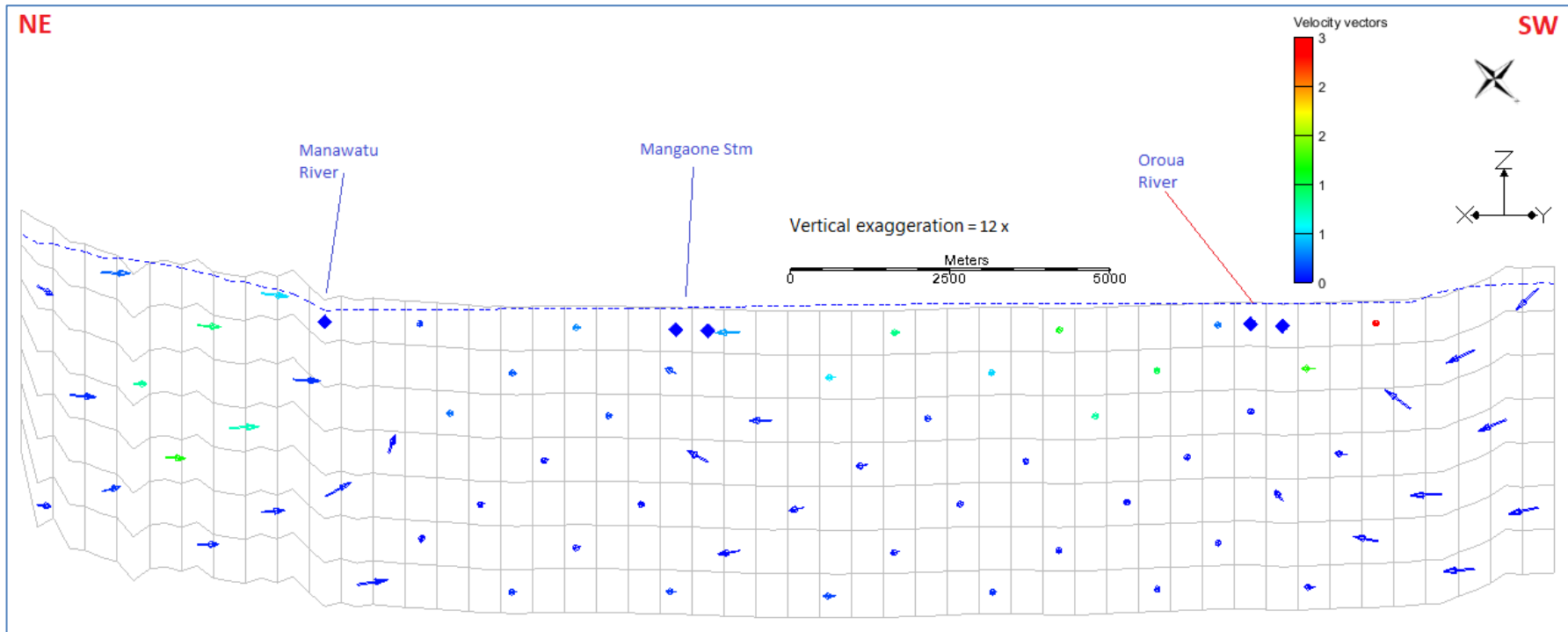


Figure 8-18. Cross-section through the Square at the centre of Palmerston North, showing vertical groundwater flow components.

The LMC models suggest that groundwater abstraction in the catchment has been generally within sustainable limits. Table 8–11 shows that groundwater abstraction may have been reducing overall flow in rivers by around 5%. However, the models' scales and levels of calibration do not allow making any assessments of the effects of certain abstractions on particular rivers or streams and being steady–state, the LMC models cannot be used in making seasonal assessments or predictions of surface water depletion due to groundwater abstraction.

Table 8–11. Heterogeneous hydrolithostratigraphical units model calculations of overall average effects of groundwater abstraction on main river flows and other elements of the water budget.

Water budget component	Groundwater abstraction scenario			
	None	Permitted wells only	Consented Wells only	All wells
Groundwater recharge (m <sup>3</sup> /d)	1,991,083.51	1,991,083.51	1,991,083.51	1,991,083.51
Groundwater abstraction	–	62,346.08	37,200.85	99,546.93
Net groundwater discharge into rivers (m <sup>3</sup> /d)	1,966,385.60	1,905,165.99	1,929,773.79	1,868,553.33
Reduction in river flow due to groundwater abstraction (m <sup>3</sup> /d)	–	61,219.61	36,611.81	97,832.27
Reduction in river flow due to groundwater abstraction (mcm/y)	–	22.35	13.36	35.71
Reduction in river flow due to groundwater abstraction (%)	–	0.03	0.02	0.05
Flow into the coastal lakes (m <sup>3</sup> /d)	21,699.84	20,914.24	21,184.46	20,398.55
Flow into the ocean (m <sup>3</sup> /d)	2,327.12	2,279.04	2,275.38	2,227.30

## Chapter 9 Conclusion and recommendations

### 9.1 Introduction

Groundwater in the LMC is an important resource for sustaining human and animal life and for the social, economic and environmental wellbeing of the catchment and its communities. Reliable, relevant, realistic and useful understanding of the hydrogeology is fundamental for managing the resource beneficially and sustainably.

Numerical modelling provides an integrated analytical framework to develop a robust understanding of groundwater resources and is a useful tool that can help with resource planning and management through allowing the exploration, testing and comparison of alternatives. This thesis updates knowledge of the LMC hydrogeological system and presents defensible conceptual and numerical models developed to represent it. The information and tools presented herein can enhance the ways by which stakeholders in the catchment communicate, collaborate, develop policies, prepare plans and make decisions regarding the protection and sustainable management of land and water resources and the larger environment. The approach followed in this research and the developed new modelling techniques can be adopted to other areas in New Zealand and internationally, particularly to simulate stratified heterogeneous aquifer systems.

### 9.2 The modelling process and techniques

Development of the LMC groundwater conceptual model was achieved through the synthesis of a huge amount of data on the geology, soil, climate, surface water, land use, land cover, and information sourced from boreholes about the tapped lithology, groundwater level, quality and abstraction. Numerical model implementation was obstructed by the lack of important information such as groundwater recharge estimates and the maldistribution of some data, particularly

and arguably most importantly lithological well logs. Incorporating heterogeneity in the numerical groundwater flow model was deemed necessary to enhance the model representativeness of the simulated system.

To understand the influence of geomorphology on the groundwater system, topographical data were analysed and a landform model was specially developed. Geomorphological investigation indicates that the groundwater system is largely controlled by gravity, including the co-existence of various scale (local, intermediate and regional) flow systems.

A soil moisture balance modelling code was developed to provide the required groundwater recharge estimates for general water balance calculations and numerical groundwater flow modelling purposes. The developed SMB model is based on the United Nations Food and Agriculture (FAO) Penman–Monteith equation (Allen *et al.*, 1998) and compensates for the lack of readily useable soil data by transforming available New Zealand Fundamental Soil Layer (FSL) data into a United States Department of Agriculture (USDA) Soil Texture Classification (STC) proxy classification. Lack of climate data was overcome through the utilisation of virtual climate stations (VCS) data obtained from NIWA. The developed SMB model accounts for the depletion of evapotranspiration below the stress point as prescribed in the FAO Irrigation and Drainage Paper 56 (Allen *et al.*, 1998), providing a more realistic representation of the soil moisture fate than models that do not account for this phenomenon. The developed SMB model provides a simple but yet an effective tool to evaluate actual evapotranspiration for various purposes including crop water demand assessment, surface runoff for catchment yield studies, and groundwater recharge for hydrogeological investigations and modelling. The produced SMB modelling utility can be easily accustomed to other locations in New Zealand and internationally. It has been satisfactorily used to assess groundwater recharge in Nelson (Zarour *et al.*, 2017). The model code could be enhanced by adding contaminant load calculation capabilities, e.g. to assess nutrient loads and concentrations from various historical and planned land

use scenarios. It can also be enhanced by adding components to represent urban hydrology elements, preferential, lateral and intercepted soil water flow.

The groundwater flow model configuration, parametrisation, boundary and initial conditions were set up on geological and hydrogeological basis. Developing an appropriate geological model on which the numerical groundwater flow model can be based was complicated by the quality of the well drilling cuttings lithological descriptions and inadequate spatial coverage of this dataset. Based on the developed understanding of the geological history and depositional environments for different lithostratigraphical units, a systematic approach was devised to define stratigraphical unit contacts at wells. To enable lithostratigraphical correlation and extrapolation across the catchment in areas and at depths that have no or inadequate well log coverage, a method was developed to represent the geology in such areas by imaginary wells and cross-sections. By supplementing real surface and subsurface geological data with virtual geological data, it was possible to build a realistic 3D geological model for the catchment that was used in the groundwater flow models. The produced model correctly predicts marine incursion in interglacial periods (MOI 5, 7, and 9) and the extent of fluvial aggradation (mostly gravels) in glacial periods (MOI 2–4, 6, 8, and 10). It also predicts that alluvial deposition becomes progressively confined inland by uplift and growing geological structures (anticlines) and faults as theorised by Begg *et al.* (2005). A multitude of additional data types can be incorporated into the developed geological modelling approach including surface and subsurface geophysical data, structural geology measurements and remote sensing. The new geological modelling technique has global applications and can facilitate the construction of geological models for various purposes, especially in New Zealand where Quaternary age sediments are particularly important.

To enhance the preventiveness of the main characteristics of the LMC aquifer system, it was deemed necessary to incorporate geological stratification and material heterogeneity in the numerical groundwater flow models. Zonal and pilot point numerical model parameterisation and automated calibration techniques were

hybridised to represent hydraulically heterogeneous strata. The new zoned pilot points technique can be used universally to more realistically simulate stratified heterogeneous aquifer systems, enhancing model representativeness and, subsequently, confidence and acceptability levels.

### 9.3 Main results

The work undertaken produced a comprehensive defensible conceptual model of the LMC hydrogeological system with in-depth analysis of various relevant components like the geology, climate, interconnectedness with surface water, the main characteristics of the groundwater flow system and groundwater quality. A soil moisture balance modelling tool has been developed and used in a water balance context to establish and evaluate the relationships between rainfall, surface runoff, groundwater recharge and groundwater-surface water interaction. The developed soil moisture balance modelling utility can be used in the LMC for surface water and groundwater resources and irrigation management and can be adopted elsewhere in New Zealand and globally.

This research produced the first realistic stratigraphical model for the LMC. The stratigraphical modelling strategy developed in this research through the utilisation of imaginary wells can be further enhanced and the stratigraphical model presented can be refined to help with other geological research, particularly stratigraphy and structural geology.

The data generated from analytical calculations and the newly achieved understanding of the hydrogeological system have been incorporated in a numerical model for the area that confirms the aptness of the work and its findings. A novel approach has been developed and applied to account for heterogeneity in the stratigraphical sequence through pilot point interpolation in each stratigraphical unit. Overlaying the stratigraphical units on the groundwater flow model finite difference grid enabled realistic representation of the groundwater system and its general characteristics and behaviour. The presented numerical groundwater flow model can be maintained by stakeholders like Horizons Regional Council as a tool

to help them in their statutory functions. The systematic stratigraphical and numerical groundwater flow modelling approaches can be copied elsewhere in New Zealand and universally.

This research has proven that the groundwater resource in the LMC is best represented by a continuous flow system rather than a set of distinct aquifers and aquitards. The importance of the fine-grained, interglacial times deposits in the stratigraphical sequence is evident and these strata cannot be overlooked in hydrogeological assessments by considering them aquitards. Successful manual and automated calibration of the numerical models presented in this work gives confidence in the validity of the proposed conceptual model and its components, including stratigraphical characterisation, aquifer properties and groundwater-surface water interaction.

It is acknowledged that the calibration residuals from the numerical models are not very small. Nevertheless, they are totally suitable for the objectives, scale and resolution of the developed models and commensurate with the quality of the available data. In all cases, this model and in fact all other possible models should never be considered as the only representation of reality. They are useful tools, but not exclusive representations of real-world systems.

Overall, it seems that anthropogenic influence over the LMC groundwater system has been limited. Groundwater quality has not changed much since monitoring started about 50 years ago or perhaps even since the first hydrogeological study was undertaken in the catchment about 120 years ago.

#### 9.4 Further work

This thesis represents a one stop shop for information on groundwater in the LMC. The knowledge generated through the completed research and the presented conceptual and numerical models provide solid basis for further geological and hydrological work in the catchment. The developed techniques for modelling soil moisture, aquifer system stratification and heterogeneity can be applied in other

areas in New Zealand and internationally and can be further enhanced to provide more advanced modelling capabilities. The following actions and further research are recommended to capitalise on the findings of this research and maximise benefits from it to the studied catchment, other areas in New Zealand and hydrogeological research in general.

**(1) Water resource planning and management**

- Utilisation of the findings of this research and the developed conceptual and numerical groundwater flow models to meet National Policy Statement for Freshwater Management (NPSFM) requirements including the definition of freshwater management units and enforceable surface water and groundwater quality and quantity limits based on best available information and scientific and socio-economic knowledge as described by Gaz (2017).
- Adopting the developed groundwater flow models as formal tools to estimate the consequences of alternative water and land use scenarios to help with resource planning and management efforts. This can include deciding on resource consent applications for groundwater takes in which the developed models can be used to assess effects on the environment and other users of the resource.
- Utilising the developed SMB model to estimate actual evapotranspiration, irrigation demand, surface runoff and groundwater recharge and surface water catchment yield across all freshwater management units in the Manawatu–Wanganui region to help with regulatory and operational decision-making by the council and land and water resources users (e.g. irrigators, interest groups). Assessment of groundwater recharge in all groundwater management zones in the Manawatu–Wanganui region is particularly important because the NPSFM requires regional councils to set enforceable quality and quantity limits for surface water and groundwater based on best available information and scientific and socio-economic knowledge (Gaz, 2017).

**(2) Hydrological monitoring, databasing and investigations**

- Initiation of a comprehensive review of the regional land and water resources data gathering networks and programmes, purposefully targeting the collection of data for the development of useful surface water and groundwater quantity and quality models that can be used to meet SoE responsibilities and help with resource management duties. The review can be LMC-specific or Manawatu-Wanganui region-wide.
- Embark on a programme of concurrent surface water gauging to enable better conceptualisation, quantification and numerical modelling of surface water-groundwater interaction in the LMC and the Horizons region.
- Commission water level measurement and hydrochemical sampling programme aimed at mapping the groundwater-seawater interface in the coastal area. The collected data will enable better design of the seawater intrusion monitoring network and enhance groundwater modelling resources.
- Collaborate with drillers, universities, Crown Research Institutions, consulting firms and professional syndicates like the New Zealand Hydrological Society and Geoscience Society of New Zealand to enhance and standardise lithological borehole sampling and cutting description skills to enable efficient lithostratigraphical interpretation and modelling.
- Review database lithological records, correct typographical errors and standardise terminology to enable computerised processing of the data.
- Launch an environmental isotope programme to collect groundwater recharge source and age determination data.
- Review and update groundwater and related environmental databasing systems to make sure data are readily available for research and studies.
- Enhance metadata collection and documentation to support future research, e.g. field sampling and laboratory analysis methods for groundwater quality data.
- Lobbying for the completion of S-map for the LMC to provide better soil data for soil moisture modelling and other purposes.

- Develop and implement a plan to streamline and enhance lithological description capabilities in regional and national well drilling service providers to enable effective geological and hydrogeological modelling.
- Arranging professional lithological logging for deep wells that will be drilled in the catchment to provide high quality, high resolution data to refine geological models. This will require collaborating with drillers and well owners and may involve lithological description of samples by qualified geologists, grain-size testing, microfossil analysis, geochemical analysis of sediment and water samples.
- Install strategically-positioned multilevel groundwater level and quality monitoring setups to gather data on vertical changes in groundwater to enable reliable assessment of the impacts of land and water use practices and help with future modelling.
- Update surface water flow statistics undertaken by Henderson and Diettrich (2007). This is particularly relevant because there were no long data records at the time of the original study and there has been an extreme even of low rainfall in 2014 as revealed in Section 4.6.2.
- Update the rainfall maps and statistical analyses by Tait and Sturman (2008) and attempt making future predictions for rainfall in the LMC and wider region. This is particularly important following the extreme even of low rainfall in 2014 presented in Section 4.6.2.
- Launch a programme to enhance borehole data availability through surveying locations and elevations, measuring depth to water and obtain missing well construction detail (screen and open intervals) using downhole cameras.
- Pull out pumping test data from various digital and paper sources and organise them in a serviceable database to help with environmental effect assessments and future groundwater investigations and modelling.
- Organise a programme of well designed, performed and analysed step-drawdown and constant discharge rate pumping tests followed by adequate groundwater level recovery monitoring at strategically selected locations to

obtain better data on aquifer hydraulic conditions (confinement and boundary conditions) and properties (transmissivity, storativity and leakage). The data will be useful to assessment of environmental effects of various activities and will provide much needed data for hydrogeological modelling. This programme can be also used to educate drillers and consultants on best practices in well performance and aquifer tests.

- Commissioning stratigraphical, structural geology, geophysical and remote sensing investigations to provide additional data for geological models that can be used for various environmental resource and natural hazard management purposes.
- Update the spatial and temporal variations and trends in groundwater quality assessment undertaken by Daughney *et al.* (2009), including using different analytical techniques.
- Commission an investigation on the effect of organic material in the geological sequence (normally reported as peat in drillers' lithological descriptions) on nitrate attenuation capacity. This aspect may have important resource management policy implications. This investigation must comprise sampling and chemical analysis of water and geological material, field experimentation and simulation (particle tracking, contaminant transport and/or thermodynamics modelling).
- Commission a project to understand the effects of urbanisation on groundwater recharge, including modification of the characteristics of the land surface and losses from water and wastewater storage and distribution systems.

### **(3) Modelling**

- Verifying the LMC SMB model to determine its conceptual and parametric sensitivity, uncertainty, confidence levels and usability in resource and environmental management.

- Develop a methodology to calibrate the developed SMB model using surface water, soil moisture and groundwater recharge observations, which may be particularly useful to estimate catchment yield and help in flood-forecasting.
- Improving the LMC SMB model code through the addition of preferential, lateral and intercepted flow options to enable more complete and more realistic representation of the soil zone hydrology in any modelled system across in the country and the world.
- Adding contaminant load calculation capabilities to the developed SMB model to help with land use management efforts in New Zealand and internationally.
- Extending SMB modelling to the rest of the Manawatu-Wanganui region to help with natural resource and environmental hazard planning and management.
- Refining the LMC geological model by incorporating all lithological well logs not included in the model presented in this thesis to enhance its quality and representativeness of the LMC geological model and make it more useful for resource management, environmental hazard planning and response (e.g. flood protection and liquefaction studies), locating water wells and determining their depths, and civil engineering projects.
- Investigating the adequacy of available data for geological modelling in other groundwater management zones in the Manawatu-Wanganui region, and where feasible, constructing geological models for hydrogeological and other environmental and natural resources modelling and research purposes.
- Upgrade the LMC finite difference MODFLOW groundwater flow models to the latest version of the USGS MODFLOW-USG modelling code to enable greater flexibility in the representation of geological and hydrogeological traits and enhance its overall ability to simulate land and water management scenarios.

- Converting the steady-state groundwater flow models presented in this thesis to pseudo-steady-state models to estimate aquifer storativity ( $S_y$  and  $S_s$ ) and assess the models' sensitivity to these parameters.
- Using the presented models to provide regional-scale boundary and initial conditions in future finer-scale and/or transient groundwater flow and contaminant transport models, including delineation of capture zones through particle tracking or other techniques.
- Assessing the uncertainty in the presented models in relation to the location of the assumed no-flow boundaries to validate the extents of the LMC, Rangitikei and Horowhenua groundwater management zones. The NPSFM requires regional councils to define freshwater management units (Gaz, 2017).
- Developing the stratified heterogeneous steady-state groundwater flow model into a calibrated and verified transient model to explore the effect of the noticed change in rainfall pattern on the groundwater resource in the LMC and make predictions in respect to various possible natural and anthropogenic changes that can affect the groundwater and surface water resources quantity and quality in the LMC.
- Verifying and updating the models presented in this thesis in five years' time using new data to account for natural and anthropogenic changes (e.g. climate, land use, etc.).

## References

- Al-Bassam, A. M., Awad, H. S., & Al-Alawi, J. A. (1997). DurovPlot: a computer program for processing and plotting hydrochemical data. *Ground Water*, 35(2), 362–367.
- Al-Bassam, A. M., & Khalil, A. R. (2012). DurovPwin: A new version to plot the expanded Durov diagram for hydro-chemical data analysis. *Computers & Geosciences*, 42, 1–6.
- Allen, R. G., Pereira, L. S., Raes, D., & Smith, M. (1998). *Crop evapotranspiration – Guidelines for computing crop water requirements – FAO Irrigation and Drainage Paper 56*. Rome: FAO – Food and Agriculture Organization of the United Nations.
- American Society for Testing and Materials. (1985). *Classification of soils for engineering purposes: annual book of ASTM standards, D 2487–83, 04.08*.
- Anderson, M. P., & Woessner, W. W. (2002). *Applied groundwater modeling: simulation of flow and advective transport* San Diego, California: Academic Press.
- Anderson, M. P., Woessner, W. W., & Hunt, R. J. (2015). *Applied groundwater modeling: simulation of flow and advective transport* (Second Edition ed.): Academic Press.
- Anderton, P. W. (1981). Structure and evolution of the South Wanganui Basin, New Zealand. *New Zealand Journal of Geology & Geophysics*, 24, 39–63.
- ANZECC & ARMCANZ. (2000). *Australian and New Zealand guidelines for fresh and marine water quality* (Vol. National Water Quality Management Strategy Paper No 4). Canberra, Australia: Australian and New Zealand Environment and Conservation Council & Agriculture and Resource Management Council of Australia and New Zealand.
- Appelo, C. A. J., & Postma, D. (2005). *Geochemistry, groundwater and pollution*: (Vol. 2d edition). Rotterdam, the Netherlands: A.A. Balkema Publishers.
- Aquaveo. (2017). *GMS 10.3 Tutorial. MODFLOW – Generating data from solids. Using solid models to represent complex stratigraphy with MODFLOW*.

- Atkins, M. L., Santos, I. R., Ruiz-Halpern, S., & Maher, D. T. (2013). Carbon dioxide dynamics driven by groundwater discharge in a coastal floodplain creek. *Journal of Hydrology*, 493, 30–42.
- Banta, E. R. (2011). *ModelMate—a graphical user interface for model analysis*. U.S. Geological Survey techniques and methods 6–E4: U.S. Geological Survey.
- Barka, I., Vladovič, J., & Máliš, F. (2011). *Landform classification and its application in predictive mapping of soil and forest units*. Paper presented at the GIS Ostrava 2011, Ostrava, Czech Republic.
- Barnett, B., Townley, L. R., Post, V., Evans, R. E., Hunt, R. J., Peeters, L., . . . Boronkay, A. (2012). *Australian groundwater modelling guidelines*. Canberra: National Water Commission.
- Barrett, M. H., Yang, Y., Lerner, D. N., French, M. J., & Tellam, J. H. (1997). *The impact of cities on the quantity and quality of their underlying groundwater. Final Report, University of Bradford (unpublished)*.
- Bartram, J., & Ballance, R. (Eds.). (1996). *Water quality monitoring – a practical guide to the design and implementation of freshwater quality studies and monitoring programmes*: Published on behalf of United Nations Environment Programme and the World Health Organization.
- Bear, J. (1972). *Dynamics of fluids in porous media*: American Elsevier.
- Bear, J. (1979). *Hydraulics of groundwater*. New York: McGrawHill.
- Begg, J. G., & Johnston, M. R. (2000). *Geology of the Wellington area. Institute of Geological & Nuclear Sciences 1:250,000 geological map 10*. Retrieved from Lower Hutt:
- Begg, J. G., Palmer, A., & Gyopari, M. (2005). *Geological synopsis of the Manawatu–Horowhenua area for a review of the region's hydrogeology. Report prepared for Horizons Manawatu Regional Council* (Client report 2005/172, Project Number: 440W1159). Retrieved from
- Bekesi, G. (1991). *Underground water in the Lower Manawatu Valley* (External Report No 25. Council Report No. 96/EXT/243). Retrieved from Palmerston North, New Zealand:
- Bekesi, G. (1998). *The development of an aquifer vulnerability assessment methodology with application to the Manawatu area of New Zealand*. (PhD Unpublished PhD), Victoria University of Wellington, Wellington. New Zealand.
- Bekesi, G. (2001). Manawatu–Wanganui. In M. R. Rosen & P. A. White (Eds.), *Groundwaters of New Zealand* (pp. 387–396). Wellington, New Zealand: New Zealand Hydrological Society Inc. & the Caxton Press.

- Bekesi, G., & McConchie, J. (1999). Groundwater recharge modelling using the Monte Carlo technique, Manawatu region, New Zealand. *Journal of Hydrology*, 244, 137–148.
- Bennett, G. D. (1989). *Introduction to ground-water hydraulics: a programed text for self-instruction. Chapter B2. Book 3. Applications of hydraulics. Techniques of water-resources investigations of the United States Geological Survey.*: Department of the Interior, U.S. Geological Survey.
- Berger, R. C., & Howington, S. E. (2002). Discrete fluxes and mass balance in finite elements. *Journal of Hydraulic Engineering*, 128(1), 87–92.
- Beu, A. G. (2001). Local stages to be used for the Wanganui Series (Pliocene–Pleistocene), and their means of definition. *New Zealand Journal of Geology and Geophysics*, 44, 113–125.
- Box, G. E. P., & Draper, N. R. (1987). *Empirical model-building and response surfaces*
- Brabyn, L. (2006). *New Zealand landscape classification. Version II. A classification of visual landscape character.* Hamilton: Department of Geography, Tourism and Environmental Planning, University of Waikato.
- Brabyn, L. K. (1996). *Landscape classification using GIS and national digital databases.* (A thesis submitted in fulfilment of the requirements for the degree of Doctor of Philosophy), University of Canterbury.
- Brackley, H. (1999). *The stratigraphy and environments of deposition of early–mid Pleistocene sediments of the Pohangina Region, eastern Wanganui Basin, New Zealand.* (Master of Science with Honour in Quaternary Science Unpublished MSc), Massey University, Palmerston North, New Zealand.
- Bradshaw, J. D. (1989). Cretaceous geotectonic patterns in the New Zealand region. *Tectonics*, 8, 803–820.
- Brezonik, P. L., & Arnold, W. A. (2011). *Water chemistry: an introduction to the chemistry of natural and engineered aquatic systems:* Oxford University Press, Inc.
- Buchanan, R., & Buddemeier, R. W. (2005). *Kansas Ground Water – an introduction to the state's water quantity, quality and management issues. KGS Educational Series 10. Web version. Original publication 1993:* Kansas Geological Survey, Kansas Ground Water.
- Burdon, D. J., & Mazloun, S. (1958). *Some chemical types of groundwater from Syria.* Paper presented at the Proceedings of the UNESCO Symposium, Teheran.

- Carrera, J., & Neuman, S. P. (1986). Estimation of aquifer parameters under transient and steady state conditions: 2. Uniqueness, stability, and solution algorithms. *Water Resources Research*, 22(2), 211–227.
- Carter, R. M. (1972). Wanganui strata of Komako District, Pohangina Valley, Ruahine Range, Manawatu. *Journal of the Royal Society of New Zealand*, 2, 293–324.
- Carter, R. M., & Naish, T. R. (1998a). Have local stages outlived their usefulness for the New Zealand Plio–Pleistocene? *New Zealand Journal of Geology & Geophysics*, 41, 271–279.
- Carter, R. M., & Naish, T. R. (1998b). A review of Wanganui Basin, New Zealand: global reference section for shallow marine, Plio–Pleistocene (2.5–0 ma cyclostratigraphy). *Sedimentary Geology*, 122, 37–52.
- Catuneanu, O. (2006). *Principles of sequence stratigraphy*. Italy: Elsevier B.V.
- Chadha, D. K. (1999). A proposed new diagram for geochemical classification of natural waters and interpretation of chemical data. *Hydrogeology Journal*, 7, 431–439.
- Chanson, H. (2004). *Hydraulics of open channel flow: an introduction*: Butterworth–Heinemann.
- Chappell, P. R. (2015). *The climate and weather of Manawatu–Wanganui* (2nd ed.): NIWA.
- Clark, R. H. (1989). *New Zealand from the road, landforms of the North Island*: Heinemann Reed, a division of Octopus Publishing Group Ltd, 39 Rawene Road, Birkenhead, Auckland.
- Clement, A. J. H. (2011). *Holocene sea-level change in the New Zealand archipelago and the geomorphic evolution of a Holocene coastal plain incised–valley system: the Lower Manawatu Valley, North Island, New Zealand*. (Doctor of Philosophy in Geography Unpublished PhD thesis), Massey University, Palmerston North, New Zealand.
- Clement, A. J. H., Sloss, C. R., & Fuller, I. C. (2009). Late Quaternary geomorphology of the Manawatu coastal plain, North Island, New Zealand. *Quaternary International*.
- Columbus, J., Sirguey, P., & Tenzer, R. (2011). A free fully assessed 15 metre digital elevation model for New Zealand. *Survey Quarterly*, 66, 16–19.
- Cook, P. G., Stauffacherl, M., Therrien, R., Halihan, T., Richardson, P., Williams, R. M., & Bradford, A. (2001). *Groundwater recharge and discharge in a saline, urban catchment: wagga wagga, New South*

- Wales. CSIRO Land and Water Technical Report 39/01. October 2001.*  
Australia: CSIRO.
- Cooper, B. J. (1999). *Stratigraphy and Palaeoenvironmental analysis of Castlecliffian and Haweran sediments from Palmerston North to the Manawatu Gorge.* (BSc Honours), Massey University, Palmerston North, New Zealand.
- Cotton, C. A. (1918). The geomorphology of the coastal district of southwestern Wellington. *Transactions of the New Zealand Institute.*, 50, 212–221.
- Dastane, N. G. (1978). *Effective rainfall in irrigated agriculture. FAO irrigation and drainage paper 25.* Rome, Italy: Food and Agriculture Organization of the United Nations (FAO).
- Daughney, C., Meilhac, C., & Zarour, H. (2009). *Spatial and temporal variations and trends in groundwater quality in the Manawatu–Wanganui Region* (GNS Science Report 2009/02). Retrieved from Lower Hutt, New Zealand:
- Daughney, C., & Reeves, R. R. (2005). Definition of hydrochemical facies in the New Zealand National Groundwater Monitoring Programme. *J. Hydrol. (NZ)*, 44, 105–130.
- Daughney, C., & Wall, M. (2007). *State and trends of groundwater quality in New Zealand (1995–2006) (1st draft)* (Vol. GNS Science Consultancy Report 2007/23). Lower Hutt, New Zealand: GNS Science.
- Davis, S. N., & DeWiest, R. J. M. (1966). *Hydrogeology.* New York: John Wiley & Sons.
- de Silva, C. S., & Rushton, K. R. (2007). Groundwater recharge estimation using improved soil moisture balance methodology for a tropical climate with distinct dry seasons. *Hydrological Sciences Journal*, 52(5), 1051–1106.
- Dikau, R., Brabb, E. E., & Mark, R. M. (1991). *Landform classification of New Mexico by Computer.* Retrieved from
- Doherty, J. (2015). *Calibration and uncertainty analysis for complex environmental models:* Blurb, Incorporated.
- Doherty, J., & Hunt, R. J. (2010). *Approaches to highly parameterized inversion – a guide to using PEST for groundwater–model calibration. Scientific Investigations Report 2010–5169.* Reston, Virginia: U.S. Geological Survey.
- Domenico, P. A., & Schwartz, F. W. (1990). *Physical and chemical hydrogeology:* John Wiley & Sons, Inc.

- Durov, S. A. (1948). Natural waters and graphic representation of their composition. *Akademiya Nauk SSSR Doklady*, 59, 87–90.
- Eagleman, J. R. (1967). Pan evaporation, potential and actual evapotranspiration. *Journal of Applied Meteorology*, 6, 482–488.
- Edmunds, W. M., & Shand, P. (Eds.). (2008). *Natural groundwater quality*. Malden, MA: Blackwell publishing Ltd.
- Ellis, S., Benites, R., & Robinson, R. (2008). Geoscience supermodels. In I. J. Graham (Ed.), *A continent on the move—New Zealand geo-science into the 21st century* (Vol. 124). Wellington: The Geological Society of New Zealand in association with GNS Science.
- Fair, E. E. (1968). *Structural, tectonic and climatic control of the fluvial geomorphology of the Manawatu River west of Manawatu Gorge, North Island, New Zealand*. (Master of Science in Geography), Massey University, Palmerston North, New Zealand.
- Feldmeyer, A. E., Jones, B. C., Firth, C. W., & Knight, J. R. (1943). *Geology of the Palmerston–Wanganui Basin, "West Side", North Island, New Zealand*. Retrieved from Wellington:
- Fetter, C. W. (2013). *Applied Hydrogeology: Pearson New International Edition*: Pearson Education Limited.
- Fleming, C. A. (1953). *The geology of Wanganui subdivision*. Retrieved from Wellington, New Zealand:
- Foster, S., Garduño, H., Tuinhof, A., Kemper, K., & Nanni, M. (2005). *Urban wastewater as groundwater recharge – evaluating and managing the risks and benefits. GW Mate briefing note series* (Vol. 12). Washington, DC: The World Bank.
- Franke, O. L., Reilly, T. E., & Bennett, G. D. (1987). Definition of boundary and initial conditions in the analysis of saturated ground–water flow systems—an introduction. Chapter B5 *Techniques of water–resources investigations of the United States Geological Survey. Book 3. Applications of hydraulics*. United States Government Printing Office. Washington: U.S. Geological Survey. Department of the Interior.
- Freeze, R. A., & Cherry, J. A. (1979). *Groundwater*. Englewood Cliffs, New Jersey: Prentice–Hall, Inc.
- Gaz. (2017). LN 79. National Policy Statement for Freshwater Management Amendment Order 2017. *New Zealand Gazette*.
- Gibb, J. G. (1983). Sea levels during the past 10,000 years BP from the New Zealand region–South Pacific Ocean *Abstracts of International Symposium on Coastal Evolution in the Holocene, August 29–31*

- Tokyo, Japan* (pp. 28–31). Tokyo: Japan Society for the Promotion of Science.
- GNS Science. (2015). *New Zealand Geological Timescale v. 2015/1*. Retrieved from
- Green, S. (2011). *The SPASMO–IR tool to determine reasonable water use for the Bay of Plenty region. A report prepared for Bay of Plenty Regional Council, SPTS No. 5908, August 2011*. Retrieved from
- Green, S., Laurenson, M. L., van den Dijssel, C., & Clothier, B. E. (2004). *Expansion of SPASMO for determining reasonable water use for irrigation in the Wanganui–Manawatu region. HortResearch Client Report 13472/2005*. Retrieved from Palmerston North, New Zealand:
- Gyopari, M. (2005). *Assessment of the seawater intrusion hazard in the Manawatu coastal aquifers and monitoring action plan. Report prepared for Horizons Regional Council*. Retrieved from Wellington, New Zealand:
- Gyopari, M., Mzila, D., & Hughes, B. (2014). *Kapiti Coast groundwater resource investigation – catchment hydrogeology and modelling report*. Wellington: Greater Wellington Regional Council.
- Hadfield, J. (2001). Waikato. In M. R. Rosen & P. A. White (Eds.), *Groundwaters of New Zealand* (pp. 315–326). Wellington, New Zealand: New Zealand Hydrological Society Inc. & the Caxton Press.
- Hammond, E. H. (1954). Small scale continental landform maps. *Annals of Association of American Geographers*, 44, 32–42.
- Hammond, E. H. (1964). Analysis of properties in landform geography: An application to broadscale landform mapping. *Annals of Association of American Geographers*, 54, 11–19.
- Harbaugh, A. W. (2005). *MODFLOW–2005, the U.S. Geological Survey modular ground–water model–the ground–water flow process. Chapter 16 of Book 6. Modeling techniques, Section A. Ground water* U.S. Geological Survey
- Harbaugh, A. W., Banta, E. R., Hill, M. C., & McDonald, M. G. (2000). *MODFLOW–2000, the U.S. Geological Survey modular ground–water model–user guide to modularization concepts and the ground–water flow process*. Reston, Virginia: U.S. Geological Survey.
- Hardie, M. (2011). *Effect of antecedent soil moisture on infiltration and preferential flow in texture contrast soils. PhD thesis*. The University of Tasmania.
- Heath, R. C. (1983). *Basic ground–water hydrology. U.S. Geological Survey Water–Supply Paper 2220*.

- Heerdegen, R. G. (1982). Landforms of the Manawatu. In J. M. Soons & M. J. Selby (Eds.), *Landforms of New Zealand*. Auckland, New Zealand.: Longman Paul.
- Heerdegen, R. G., & Shepherd, M. J. (1992). Manawatu landforms – product of tectonism, climate change and process. In J. M. Soons & M. J. Selby (Eds.), *Landforms of New Zealand* (Second Edition ed., pp. 308–343). Auckland: Longmans Paul Ltd.
- Hem, J. D. (1985). *Study and interpretation of the chemical characteristics of natural water. U.S Geological Survey Water–Supply Paper 2254* (Third edition ed.). Alexandria, VA: U.S. Geological Survey.
- Henderson, R., & Diettrich, J. (2007). *Statistical analysis of river flow data in the Horizons Region*. Retrieved from
- Herczeg, A. L., Torgersen, T., Chivas, A. R., & Habermehl, M. A. (1991). Geochemistry of ground waters from the Great Artesian Basin, Australia. *Journal of Hydrology*, 126, 225–245.
- Heron, D. W. (Cartographer). (2014). Geological Map of New Zealand 1:250 000. GNS Science Geological Map 1
- Hesp, P. A. (1975). *The late Quaternary geomorphology of the Lower Manawatu*. (Master of Arts in Geography), Massey University, Palmerston North, New Zealand.
- Hesp, P. A., & Shepherd, M. J. (1978). Some aspects of the Late Quaternary geomorphology of the Lower Manawatu Valley, New Zealand. *New Zealand Journal of Geology & Geophysics*(21), 403 – 412.
- Hewitt, A. E. (2010). *New Zealand Soil Classification* (3rd Edition ed.). New Zealand: Manaaki Whenua Press.
- Hill, M. C., & Tiedeman, C. R. (2007). *Effective groundwater model calibration: with analysis of data, sensitivities, predictions, and uncertainty*. Hoboken, New Jersey: Wiley.
- Hiscock, K. (2009). *Hydrogeology: principles and practice*: John Wiley & Sons.
- Horizons. (2007). *The proposed One Plan – the consolidated resource policy statement, regional plan & regional coastal policy for the Manawatu–Wanganui Region*. Retrieved from Palmerston North, New Zealand:
- Houlbrooke, D. J., & Monaghan, R. M. (2009). *The influence of soil drainage characteristics on contaminant leakage risk associated with the land application of farm dairy effluent*. Retrieved from
- Hughes, A. G., & Mansour, M. M. (2005). *Recharge modelling for the West Bank aquifers. Groundwater Systems and Water Quality Programme*.

- Commissioned Report CR/05/087N*. Keyworth, Nottingham: British Geological Survey.
- Hunt, R. J., & Welter, D. E. (2010). Taking account of “unknown unknowns”, 48: 477. doi:10.1111/j.1745-6584.2010.00681.x. *Ground Water*, 48(4), 477-477.
- Igboekwe, M. U., & Achi, N. J. (2011). Finite difference method of modelling groundwater flow. *Journal of Water Resource and Protection*, 3(3), 192-198.
- Imbrie, J., Hays, J. D., Martinson, D. G., McIntyre, A., Mix, A. C., Morley, J. J., . . . Shackleton, N. J. (1984, Nov. 30-Dec. 4, 1982). *The orbital theory of Pleistocene climate: support from a revised chronology of the marine  $\delta^{18}O$  record*. Paper presented at the Proceedings of the NATO Advanced Research Workshop on Milankovitch and Climate, Lamont-Doherty Laboratory, Palisades, New York.
- Jackson, J., van Dissen, R. J., & Berryman, K. R. (1998). Tilting of active folds and faults in the Manawatu region, New Zealand: evidence from surface drainage patterns. *New Zealand Journal of Geology & Geophysics*, 41, 377-386.
- Jensen, L. S., Mueller, T., Nielsen, N. E., Hansen, S., Crocker, G. J., Grace, P. R., . . . Poulton, P. R. (1997). Simulating trends in soil organic carbon in long-term experiments using the soil-plant-atmosphere model DAISY. *Geoderma*, 81(1-2), 5-28.
- Journeaux, T. D., Kamp, P. J. J., & Naish, T. (1996). Middle Pliocene cyclothem, Mangaweka region, Wanganui Basin, New Zealand: a lithostratigraphic framework. *New Zealand Journal of Geology and Geophysics*, 39(1), 135-149.
- Kamp, P. J. J. (1992). Tectonic architecture of New Zealand. In J. m. Soons & M. J. Selby (Eds.), *Landforms of New Zealand* (2 ed., pp. 1-30): Longman Paul Ltd.
- Kamp, P. J. J., Vonk, A. J., Bland, K. J., Hansen, R. J., Hendy, A. J. W., McIntyre, A. P., . . . Nelson, C. S. (2004). Neogene stratigraphic architecture and tectonic evolution of Wanganui, King Country and eastern Taranaki basins, New Zealand. *New Zealand Journal of Geology and Geophysics*, 47, 625-644.
- Kenny, J. A., & Hayward, B. W. (1993). *Inventory of important geological sites and landforms in the Manawatu and Wellington regions*. Retrieved from Lower Hutt, New Zealand:
- Kenny, J. A., & Hayward, B. W. (1996). *Inventory and maps of important geological sites and landforms in the Manawatu and Wellington regions*. Retrieved from Lower Hutt, New Zealand:

- Kim, J., & Mohanty, B. P. (2016). Influence of lateral subsurface flow and connectivity on soil water storage in land surface modeling *Journal of Geophysical Research: Atmospheres*, *121*, 704–721.
- Konikow, L. F. (1978). *Calibration of ground–water models*. Paper presented at the Verification of Mathematical and Physical Models in Hydraulic Engineering.
- Kruseman, G. P., & de Ridder, N. A. (1991). *Analysis and evaluation of pumping test data* (2 ed. Vol. (second edition)). Wageningen, The Netherlands: International Institute for Land Reclamation and Improvement.
- Kumar, C. P. (2004). *Groundwater flow models*. Retrieved from Roorkee – 247667 (Uttaranchal):
- Lamarche, G., Proust, J.–N., & Nodder, S. D. (2005). Long–term slip rates and fault interactions under low contractional strain, Wanganui Basin, New Zealand. *Tectonics*, *24*(4), TC4004.
- Lee, J. M., & Begg, J. G. (2000). *Geology of the Wairarapa area. Institute of Geological & Nuclear Sciences 1:250,000 geological map 11*. Retrieved from Lower Hutt:
- Lee, J. M., Townsend, D., Bland, K., & Kamp, P. J. J. (2011). *Geology of the Hawke’s Bay area. Institute of Geological & Nuclear Sciences 1:250,000 geological map 8*. Retrieved from Lower Hutt:
- Lerner, D. N. (2000). *Guidelines for estimating urban loads of nitrogen to groundwater. Prepared for the Ministry of Agriculture, Fisheries and Food. Project NT1845*.
- Lerner, D. N. (2002). Identifying and quantifying urban recharge: a review. *Hydrogeology Journal*, *10*(1), 143–152.
- Lichtner, P. C. (1996). Continuum formulation of multicomponent–multiphase reactive transport. In P. C. Lichtner, C. I. Steefel, & E. H. Oelkers (Eds.), *Reactive Transport in Porous Media* (Vol. 34, pp. 1–82). Washington, DC: Mineralogical Society of America.
- Lieffering, R. E. (1990). *Hydrogeological investigation of the Palmerston North region*. (Masters of Science with Honours in Earth Science), Massey University, Palmerston North, New Zealand.
- Little, C. (2013). M7 slow release earthquake under Wellington. Retrieved from <http://info.geonet.org.nz/download/attachments/5505041/North%20Island%20plate%20subduction.jpg?api=v2>
- Lloyd, J. W. (1965). The hydrochemistry of the aquifers of northeastern Jordan. *J Hydrol*, *3*, 319–330.

- Lloyd, J. W., & Heathcote, J. A. (1985). *Natural inorganic hydrochemistry in relation to groundwater, an introduction*. Oxford: Clarendon Press.
- Macpherson, G. L. (2009). CO<sub>2</sub> distribution in groundwater and the impact of groundwater extraction on the global C cycle. *Chemical Geology*, 264, 328–336.
- Marchbanks, J. (1898). On the artesian wells at Longburn. *Transactions and Proceedings of the Royal Society of New Zealand 1868–1961*, 31, 551–554.
- Mark-Brown, N. V. (1978). *The water resources of the Oroua Downs drainage area*. Retrieved from
- Martley, P. R. (2001). *Hydrogeology of the Feilding District, Manawatu*. (Masters of Science in Engineering Geology Unpublished MSc), University of Canterbury, Christchurch, New Zealand.
- McArthur, K., & Clark, M. (2007). *Nitrogen and phosphorus loads to rivers in the Manawatu–Wanganui Region: an analysis of low flow state. Technical report to support policy development*. Retrieved from Palmerston North:
- McCarron, C., & Zarour, H. (2005). *State of the environment of the Manawatu–Wanganui Region–2005. Technical report five–groundwater* (Report 2004/EXT/609). Retrieved from Palmerston North, New Zealand:
- McDonald, M. G., & Harbaugh, A. W. (1984). *A modular three– dimensional finite–difference ground–water flow model. Open–File Report 83–875*: U.S. Geological Survey.
- McDonald, M. G., & Harbaugh, A. W. (2003). The history of MODFLOW. *Ground Water*, 41(2), 280–283.
- McLaren, R. G., & Cameron, K. C. (1996). *Soil science: sustainable production and environmental protection*: Oxford University Press.
- Mekonnen, M., Melesse, A. M., & Keesstra, S. D. (2016). Spatial runoff estimation and mapping of potential water harvesting sites: a GIS and remote sensing perspective, northwest Ethiopia. In A. M. Melesse & W. Abtew (Eds.), *Landscape dynamics, soils and hydrological processes in varied climates* (pp. 565–584). Switzerland: Springer International Publishing Switzerland.
- Melhuish, A., van Dissen, R., & Berryman, K. (1996). Mount Stewart–Halcombe Anticline: a look inside a growing fold in the Manawatu Region, New Zealand. *New Zealand Journal of Geology and Geophysics*, 39, 123–133.

- Mercer, J. W., & Faust, C. R. (1980). Ground-water modelling: an overview. *Ground Water*, 18(2), 108–115.
- Merry, A. G., Martin, P. J., Meyer, P., & Harvey, D. J. M. (2003). Assessing the calibration and predictive sensitivity of model parameters. In K. Kovar & Z. Hrkal (Eds.), *Calibration and reliability in groundwater modelling: a few steps closer to reality. Proceedings of ModelCARE 2002, Prague, Czech Republic, 17–20 June 2002. IAHS Publ. no. 277, 2002* (pp. 233–238). Prague, Czech Republic: International Association of Hydrological Sciences.
- Milankovitch, M. (1920). Théorie mathématique des phénomènes thermiques produits par la radiation solaire. Gauthiers–Villars, Paris, 1941. *Royal Serbian Academie, Special Publication 133*, 1–633.
- Miller, J. P. (1952). A portion of the system calcium carbonate–carbon dioxide–water, with geological implications. *American Journal of Science*, 250, 161–203.
- Ministry of Health. (2005). *Drinking–water Standards for New Zealand 2005*. Wellington, New Zealand: Ministry of Health.
- Mulley, R. (2004). *Flow of industrial fluids: theory and equations*: CRC Press.
- Naish, T., & Kamp, P. J. J. (1995). Pliocene–Pleistocene marine cyclothem, Wanganui Basin, New Zealand; a lithostratigraphic framework. *New Zealand Journal of Geology & Geophysics*, 38, 223–243.
- Naydenova, V., & Stamenov, S. (2013). *Landform classification using Aster GDEM and optical high resolution satellite images of Sofia City district*. Retrieved from Sofia:
- Nwankwoala, H. O., & Udom, G. J. (2011). Hydrochemical facies and ionic ratios of groundwater in Port Harcourt, Southern Nigeria. *Research Journal of Chemical Sciences*, 1(3), 87–101.
- Ongley, M. (1945). Ground water resources of the Palmerston–Wanganui Basin. *new zealand journal of Science and Technology*, 26(4), 200–205.
- Palmer, C. D., & Cherry, J. A. (1984). Geochemical evolution of groundwater in sequences of sedimentary rocks. *Journal of Hydrology*, 75, 27–65.
- Panday, S., Langevin, C. D., Niswonger, R. G., Ibaraki, M., & Hughes, J. D. (2013). *MODFLOW–USG version 1: An unstructured grid version of MODFLOW for simulating groundwater flow and tightly coupled processes using a control volume finite–difference formulation (2328–7055)*. Retrieved from

- Parkhurst, D. L., & Appelo, C. A. J. (2013). Description of input and examples for PHREEQC version 3—A computer program for speciation, batch-reaction, one-dimensional transport, and inverse geochemical calculations *U.S. Geological Survey Techniques and Methods, book 6, chap. A43* (pp. 497). available only at <http://pubs.usgs.gov/tm/06/a43/>: U.S. Department of the Interior. U.S. Geological Survey.
- PDP. (2002). *Groundwater model audit guidelines*. Retrieved from Wellington, New Zealand:
- PDP. (2013a). *Report on Horizons groundwater quality monitoring network*. Retrieved from D:\Users\WHisham\PhD 2013\References\GW Network - Quality 2013.PDF
- PDP. (2013b). *Review of Horizons coastal groundwater monitoring network*. Retrieved from D:\Users\WHisham\PhD 2013\References\GW Network - Coastal 2013.PDF
- Penman, H. L. (1956). Estimating evaporation. *Transactions, American Geophysical Union, 37*(1), 43–50.
- Perina, T. (2010). Derivation of the Theis (1935) equation by substitution. *Ground Water, 48*(1), 6–7. doi:10.1111/j.1745-6584.2009.00610.x
- Petricevich, M. (1970). *Preliminary report on the water resources in the Manawatu Region*. Retrieved from
- Pillans, B. (1986). A late Quaternary uplift map for the North Island, New Zealand. *Royal Society of New Zealand, Bulletin 24*, 409–417.
- Pillans, B. (Cartographer). (1990). Late Quaternary marine terraces, south Taranaki–Wanganui (Sheet Q22 and part Sheets Q20, Q21, R21 and R22), 1 : 100,000. New Zealand Geological Survey Miscellaneous Series, Map 18
- Pillans, B. (1994). Direct marine–terrestrial correlations, Wanganui Basin, New Zealand: the last 1 million years. *Quaternary Science Reviews, 13*, 189–200.
- Pinder, G. F., & Gray, W. G. (1976). Is there a difference in the finite element method? *Water Resources Research, 12*(1), 105–107.
- Piper, A. M. (1944). A graphic procedure in the geochemical interpretation of water analyses. *American Geophysical Union Transactions, 25*, 914–923.
- Poulsen, D. (2013). *The hydrogeological significance of loess in Canterbury* (R13/60). Retrieved from Christchurch:

- Refsgaarda, J. C., Christensen, S., Sonnenborg, T. O., Seifert, D., Højberg, A. L., & Troldborg, L. (2012). Review of strategies for handling geological uncertainty in groundwater flow and transport modeling. *Advances in Water Resources*, *36*, 36–50.
- Reilly, T. E., Franke, O. L., & Bennett, G. D. (1984). *The principle of superposition and its application in ground-water hydraulics*. U.S. Geological Survey open-file report 84-459. U.S. Geological Survey.
- Reilly, T. E., & Harbaugh, A. W. (2004). *Guidelines for evaluating ground-water flow models*: Scientific Investigations Report 2004-5038. Office of Ground Water. US Geological Survey.
- Rich, C. C. (1959). *Late Cenozoic geology of the Lower Manawatu Valley, New Zealand*. (PhD), Harvard University, Cambridge, Massachusetts, USA.
- Rissmann, C. (2011). *Regional mapping of groundwater denitrification potential and aquifer sensitivity – technical report*. Publication No 2011-12. Retrieved from
- Roygard, J., Hurndell, R., Clark, M., & Nicholson, C. (2011). *Overview of Horizons' surface water monitoring programmes*. Report No: 2011/EXT/1134. Palmerston North: Horizons Regional Council.
- Rushton, K. R. (2003). *Groundwater Hydrology: Conceptual and Computational Models*. Chichester: John Wiley and Sons Ltd.
- Rushton, K. R., Eilers, V. H. M., & Carter, R. C. (2006). Improved soil moisture balance methodology for recharge estimation. *Journal of Hydrology*, *318*, 379–399.
- Russell, W. (1989). *Groundwater-Manawatu Plains*. Retrieved from Auckland, New Zealand:
- Schumacher, J. (1999). *Groundwater in the Lower Manawatu Valley (Palmerston North area), New Zealand*. (Master of Science in Earth Science Unpublished MSc), University of Waikato, Hamilton, New Zealand.
- Scott, D. (2004). *Groundwater allocation limits: land-based recharge estimates (U04/97)*. Retrieved from Christchurch, New Zealand:
- Singh, S. K., Zeddies, M., Shankar, U., & Griffiths, G. A. (2018). Potential groundwater recharge zones within New Zealand. *Geoscience Frontiers*.
- Sloss, C. (2006). The Late Quaternary geomorphology of the Manawatu coastal plain. In J. Lecointre, B. Stewart, & C. Wallace (Eds.), *Geosciences '06-our planet our future (Field trip guides)*: Geological Society of New Zealand Miscellaneous Publication 122 B.

- Sreekanth, J., Moore, C., & Wolf, L. (2015). Estimation of optimal groundwater substitution volumes using a distributed parameter groundwater model and prediction uncertainty analysis. *Water Resources Management*, 29(10), 3663–3679.
- Stewart, M., & Bidwell, V. (2008). Water, water everywhere. In I. J. Graham (Ed.), *A continent on the move—New Zealand geo-science into the 21st century* (Vol. 124, pp. 302–305). Wellington: The Geological Society of New Zealand in association with GNS Science.
- Suggate, R. P. (1990). Late Pliocene and Quaternary glaciations of New Zealand. *Quaternary Science Review*, 9, 175–197.
- Svensson, A. (2014). *Estimation of hydraulic conductivity from grain size analyses – a comparative study of different sampling and calculation methods focusing on Västlänken*. (Master of Science Thesis in the Master's Programme Geo and Water Engineering), Chalmers University of Technology, Göteborg, Sweden.
- Tait, A., & Sturman, J. (2008). *Annual rainfall maps for the Horizons—Manawatu Region* (WLG2008/69). Retrieved from Wellington, New Zealand:
- Taylor, C. B., Trompetter, V. J., Brown, L. J., & Bekesi, G. (2001). The Manawatu aquifers, North Island, New Zealand: clarification of hydrogeology using a multidisciplinary environmental tracer approach. *Hydrological processes*, 15(17), 3269–3286.
- Te Punga, M. T. (1957). Live anticlines in Western Wellington. *New Zealand Journal of Geology & Geophysics*, 38B(5), 433–446.
- Thangarajan, M. (2007). Groundwater models and their role in assessment and management of groundwater resources and pollution. In M. Thangarajan (Ed.), *Groundwater: resource evaluation, augmentation, contamination, restoration, modeling and management* (pp. 362): Springer Science & Business Media.
- Theis, C. V. (1935). The relation between the lowering of the piezometric surface and the rate and duration of discharge of a well using groundwater storage. *Am. Geophys. Union Trans.*, 2, 519–524.
- Thiem, G. (1906). *Hydrologische methoden*. Gebhardt, Leipzig.
- Todd, D. K., & Mays, L. W. (2005). *Groundwater hydrology* (3 ed.). Hoboken, NJ, USA: John Wiley & Sons, Inc.
- Toebe, C. (1972). The water balance of New Zealand. *J. Hydrol. (NZ)*, 11(2), 127–139.
- Toews, M. W., & Moreau, M. F. (2014). *Groundwater protection zone delineation of Matamata supply wells*. Waikato Regional Council

- 
- Technical Report 2014/63. GNS Science Consultancy Report 2014/125*: Waikato Regional Council & GNS Science.
- Tóth, J. (2009). *Gravitational systems of groundwater flow: theory, evaluation, utilization*: Cambridge University Press.
- Townsend, D., Vonk, A., & Kamp, P. J. J. (2008). *Geology of the Taranaki area Institute of Geological & Nuclear Sciences 1:250,000 geological map 7*. Retrieved from Lower Hutt:
- Villiaxns, P. W. (1991). Tectonic geomorphology, uplift rates and geomorphic response in New Zealand. *Catena*, 18, 439–452.
- Wallace, H. W. (1955). New Zealand landforms. *New Zealand Geographer*, 11(1), 17–27.
- Walter, K. M. (1990). *Index to hydrological recording sites in New Zealand, 1989. Publication No. 21*. Retrieved from Christchurch:
- Wang, H. F., & Anderson, M. P. (1977). Finite differences and finite elements as weighted residual solutions to Laplace's equation. In W. G. Gray & G. F. Pinder (Eds.), *Finite elements in water resources, Proceedings of the First International Conference on Finite Elements in Water Resources, Princeton University* (pp. 2.167–162.178). London: Pentech Press.
- Wang, H. F., & Anderson, M. P. (1982). *Introduction to groundwater modeling: finite difference and finite element methods*. San Diego, CA: Academic press.
- Wang, N. S., & Grapes, R. (2008). Infrared–stimulated luminescence dating of late Quaternary aggradation surfaces and their deformation along an active fault, southern North Island of New Zealand. *Geomorphology*, 96(1–2), 86–104.
- Watson, I., & Burnett, A. D. (1993). *Hydrology: an environmental approach* Cambridge, Ft. Lauderdale: Buchanan Books.
- Wels, C., Mackie, D., & Scibek, J. (2012). *Guidelines for groundwater modelling to assess impacts of proposed natural resource development activities*: British Columbia Ministry of Environment. Water Protection & Sustainability Branch
- White, P., Clausen, B., Hunt, B., Cameron, S., & Weir, J. J. (2001). Groundwater–surface water interaction. In M. R. Rosen & P. A. White (Eds.), *Groundwaters of New Zealand* (pp. 133–160). Wellington, New Zealand: New Zealand Hydrological Society Inc. & the Caxton Press.
- White, P., Raiber, M., Zarour, H., Meilhac, C., & Green, S. (2010). *Horowhenua water resources: water budget and groundwater–surface water interaction. GNS Science Consultancy Report 2010/22*.

- 
- Prepared for Horizons Regional Council. Horizons Regional Council Report 2010/Ext/1087.* Retrieved from Lower Hutt, New Zealand:
- White, P., & Rosen, M. R. (2001). Introduction. In M. R. Rosen & P. A. White (Eds.), *Groundwaters of New Zealand* (pp. 1–3). Wellington, New Zealand: New Zealand Hydrological Society Inc. & the Caxton Press.
- Wilson, S., & Lu, X. (2011). *Rainfall recharge assessment for Otago groundwater basins*. Dunedin: Otago Regional Council.
- Winston, R. B. (2009). *ModelMuse—a graphical user interface for MODFLOW-2005 and PHAST. Chapter 29 of Section A, Ground water—Book 6, Modeling techniques*: U.S. Geological Survey.
- Winter, T. C., Harvey, J. W., Franke, O. L., & Alley, W. M. (1998). *Groundwater and surface water a single resource. U.S. Geological Survey circular: 1139*. Denver, CO: U.S. Geological Survey.
- Woodward, S. J. R., Barker, D. J., & Zyskowski, R. F. (2010). A practical model for predicting soil water deficit in New Zealand pastures. *New Zealand Journal of Agricultural Research*, 44(1), 91–109.
- Ye, M., Pohlmann, K. F., Chapman, J. B., Pohl, G. M., & Reeves, D. M. (2010). A model-averaging method for assessing groundwater conceptual model uncertainty. *Groundwater*, 48(5), 716–728.
- Yeh, T.-c. J., Mao, D.-q., Zha, Y.-y., Wen, J.-c., Wan, L., Hsu, K.-c., & Lee, C.-h. (2015). Uniqueness, scale, and resolution issues in groundwater model parameter identification. *Water Science and Engineering*, 8(3), 175–194.
- Younger, P. L. (2007). *Groundwater in the environment – an introduction*. Oxford, UK: Blackwell Publishing.
- Zarour, H. (2008). *Groundwater resources in the Manawatu–Wanganui Region: technical report to support policy development (2008/EXT/948)*. Retrieved from Palmerston North, New Zealand:
- Zarour, H. (2017). *Lower Waitaki hydrogeology*. Retrieved from Christchurch, New Zealand:
- Zarour, H., Kaelin, N., & Zarour, D. (2017). *Nelson groundwater resources – management requirements for the Whakamahere Whakatū Nelson Plan*. Christchurch, New Zealand: Nelson City Council and Groundwater Services New Zealand (gH2Onz).
- Zarour, H., Roygard, J., Hurdell, R., & Clark, M. (2011). *Overview of Horizons’ groundwater monitoring programme. Report No: 2011/EXT/1143*. Palmerston North: Horizons Regional Council.

- Zheng, C., Poeter, E., Hill, M., & Doherty, J. (2006). Understanding through modeling. *Ground Water*, 44(6), 769–770.
- Zotarelli, L., Dukes, M. D., Romero, C. C., Migliaccio, K. W., & Morgans, K. T. (2015). Step by step calculation of the Penman–Monteith evapotranspiration (FAO–56 method). In U. o. F. U.S. Department of Agriculture and UF/IFAS Extension Service (Ed.). Gainesville, FL 32611: UF/IFAS Extension.

## Appendix A Rainfall maps

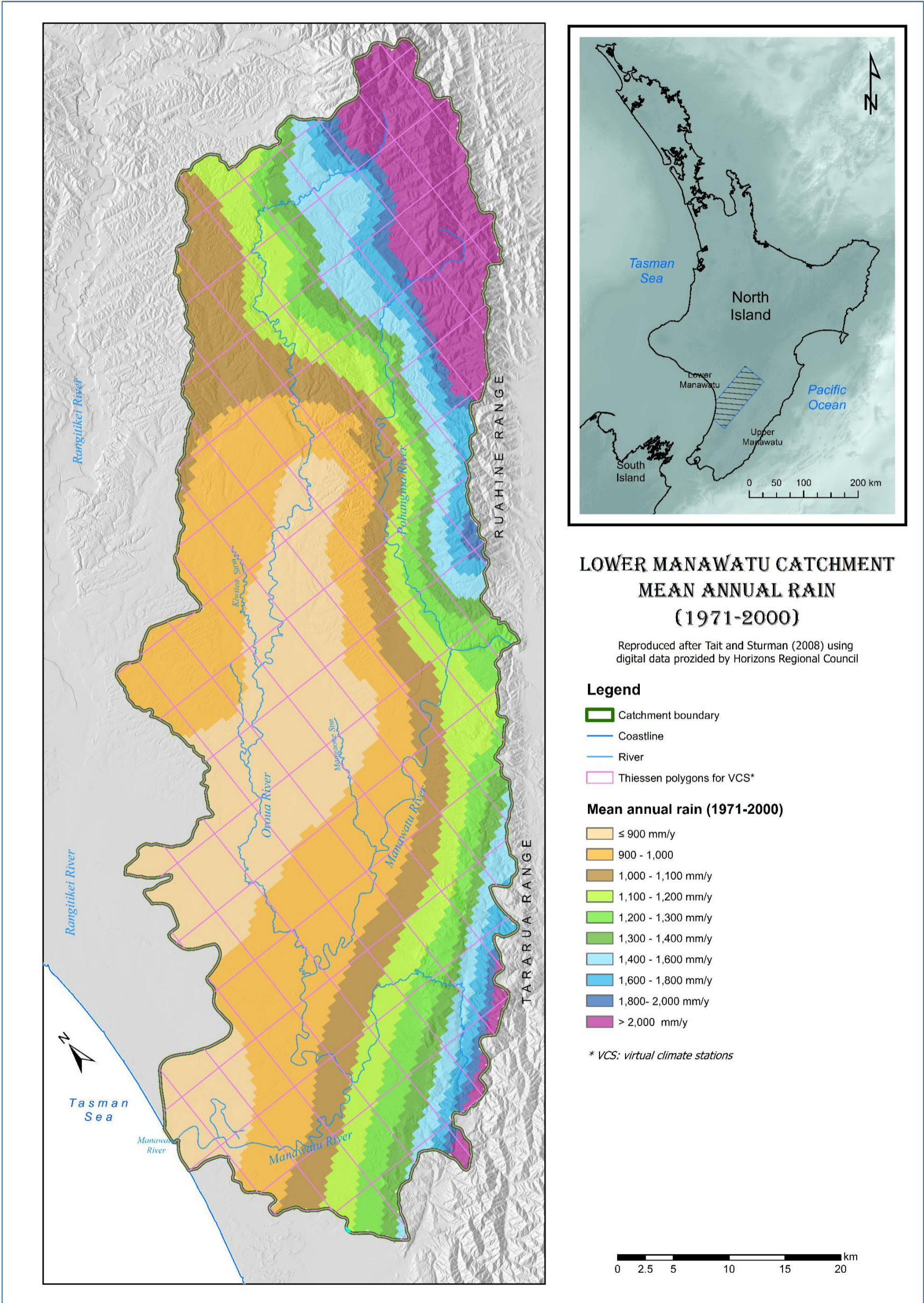
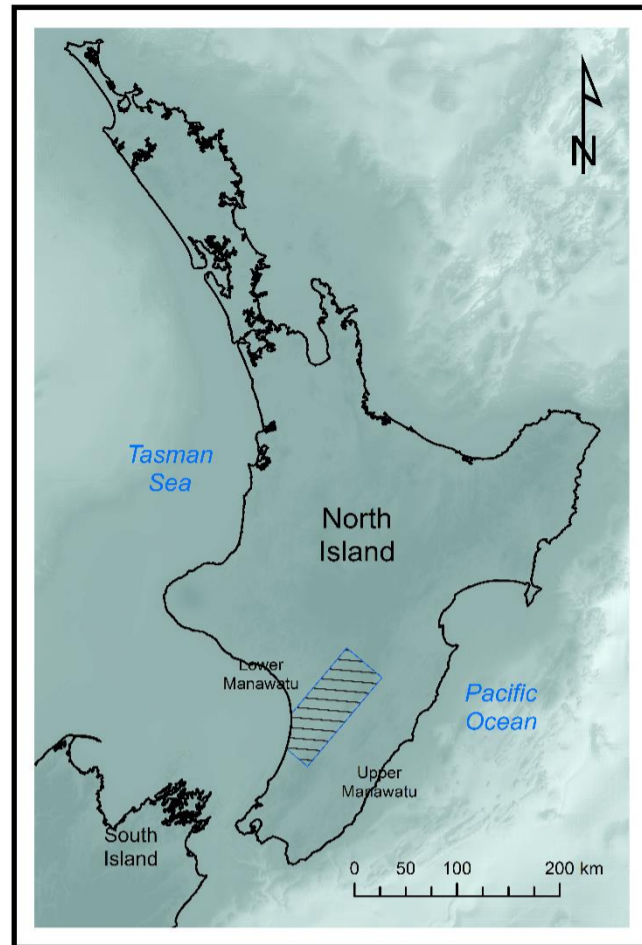
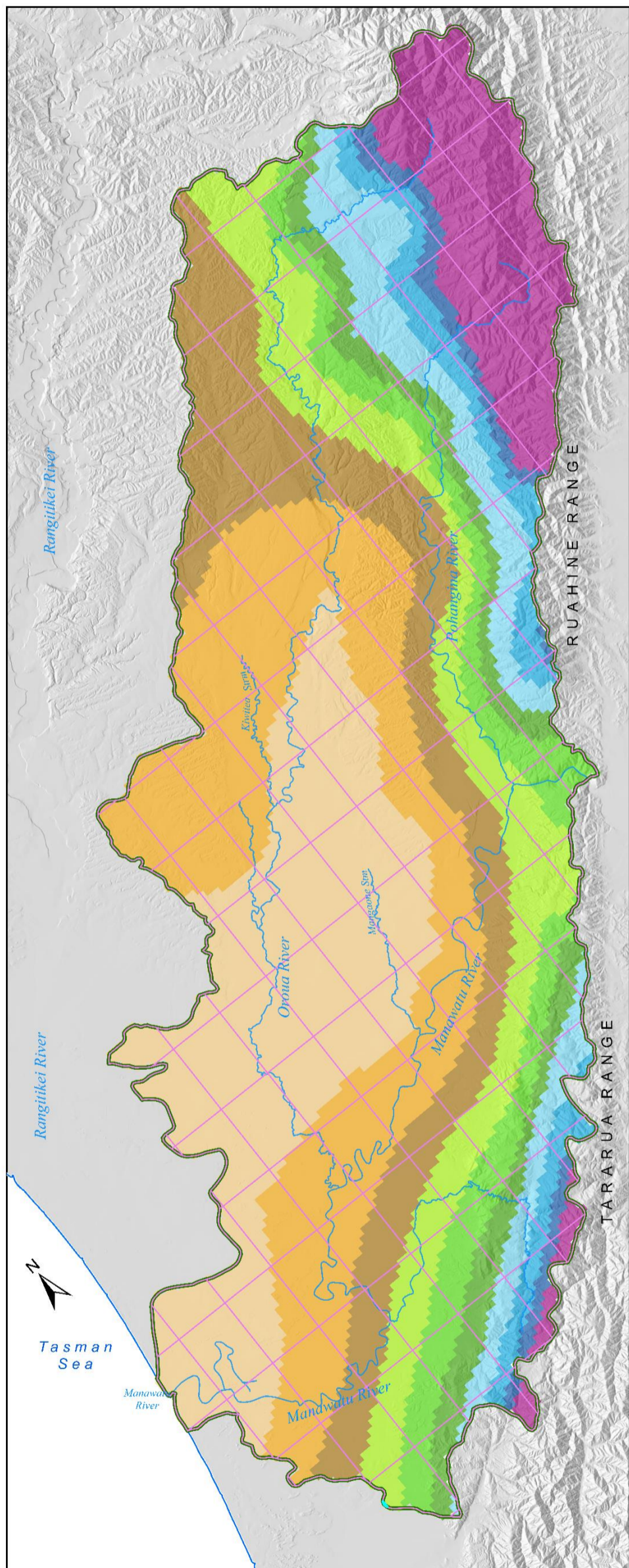


Figure A-1. Mean annual rain (in mm/y) for the 'normal' period 1971–2000 (reproduced from digital maps by Tait & Sturman, 2008).



**LOWER MANAWATU CATCHMENT  
MEDIAN ANNUAL RAIN  
(1971-2000)**

Reproduced after Tait and Sturman (2008) using digital data provided by Horizons Regional Council

**Legend**

- Catchment boundary
- Coastline
- River
- Thiessen polygons for VCS\*

**Median annual rain (1971-2000)**

- ≤ 900 mm/y
- 900 - 1,000
- 1,000 - 1,100 mm/y
- 1,100 - 1,200 mm/y
- 1,200 - 1,300 mm/y
- 1,300 - 1,400 mm/y
- 1,400 - 1,600 mm/y
- 1,600 - 1,800 mm/y
- 1,800 - 2,000 mm/y
- > 2,000 mm/y

\* VCS: virtual climate stations

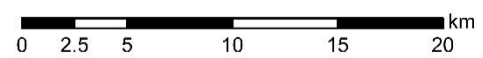
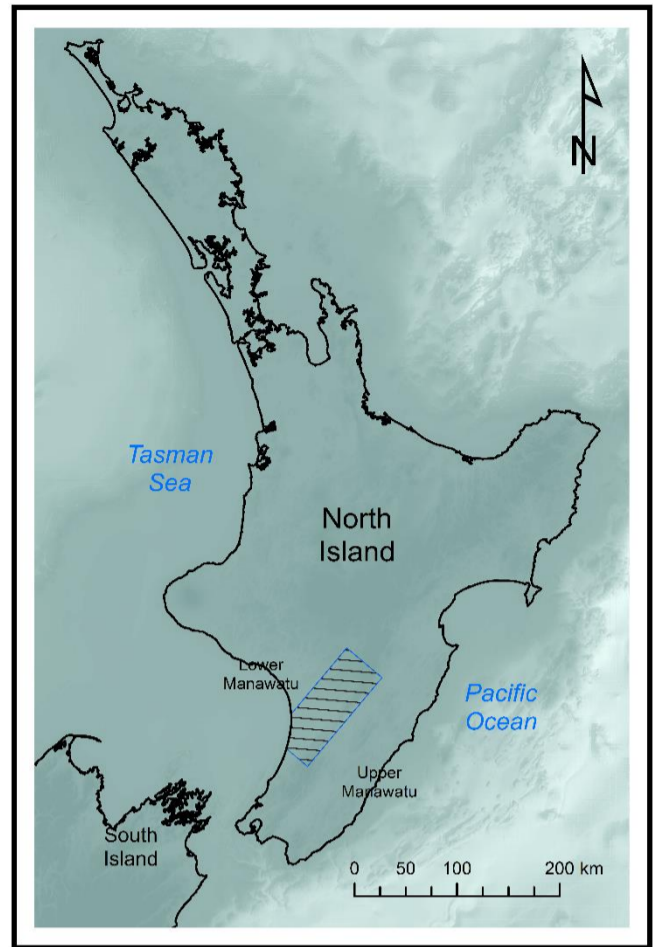
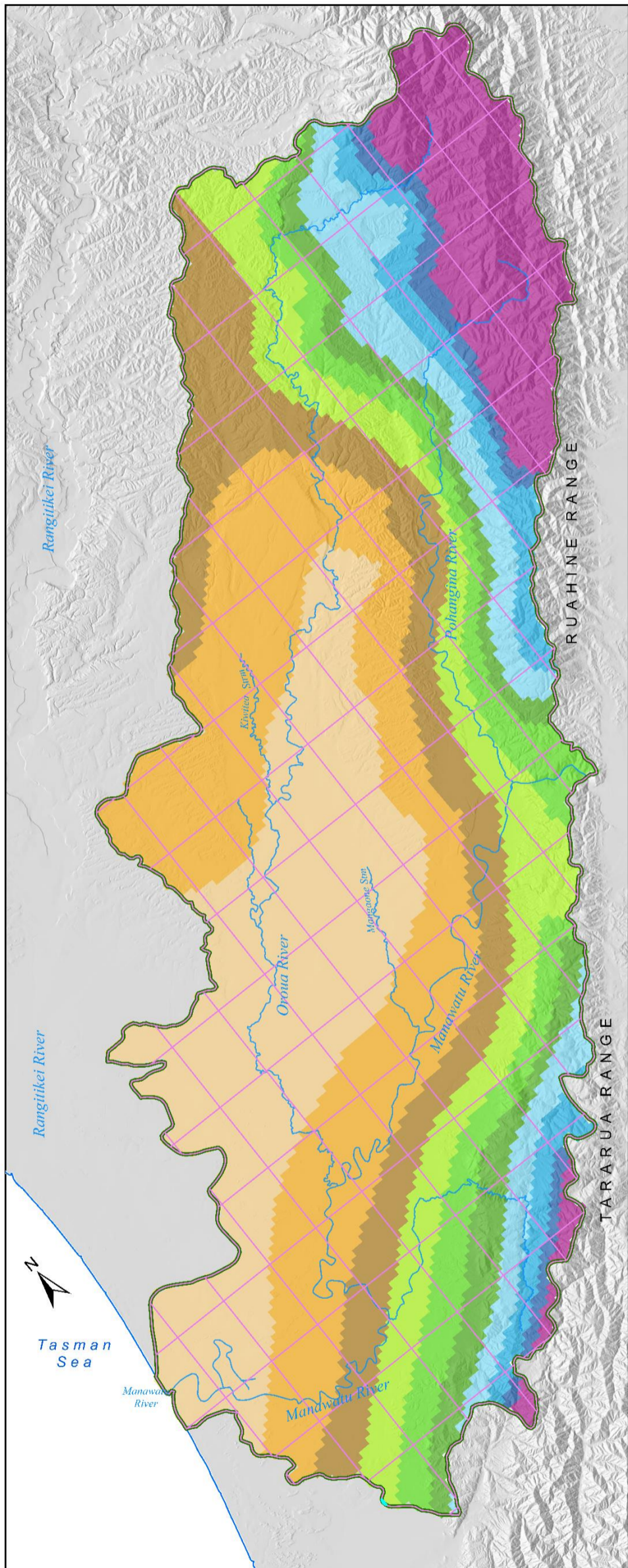


Figure A-2. Median annual rain (in mm/y) for the 'normal' period 1971-2000 (reproduced from digital maps by Tait & Sturman, 2008).



**LOWER MANAWATU CATCHMENT  
MEAN ANNUAL RAIN  
(1978-2007)**

Reproduced after Tait and Sturman (2008) using digital data provided by Horizons Regional Council

**Legend**

- Catchment boundary
- Coastline
- River
- Thiessen polygons for VCS\*

**Mean annual rain (1978-2007)**

- ≤ 900 mm/y
- 900 - 1,000
- 1,000 - 1,100 mm/y
- 1,100 - 1,200 mm/y
- 1,200 - 1,300 mm/y
- 1,300 - 1,400 mm/y
- 1,400 - 1,600 mm/y
- 1,600 - 1,800 mm/y
- 1,800 - 2,000 mm/y
- > 2,000 mm/y

\* VCS: virtual climate stations

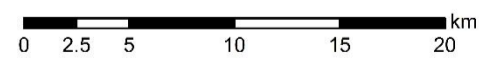


Figure A-3. Mean annual rain (in mm/y) for the period 1978–2007 (reproduced from digital maps by Tait & Sturman, 2008).

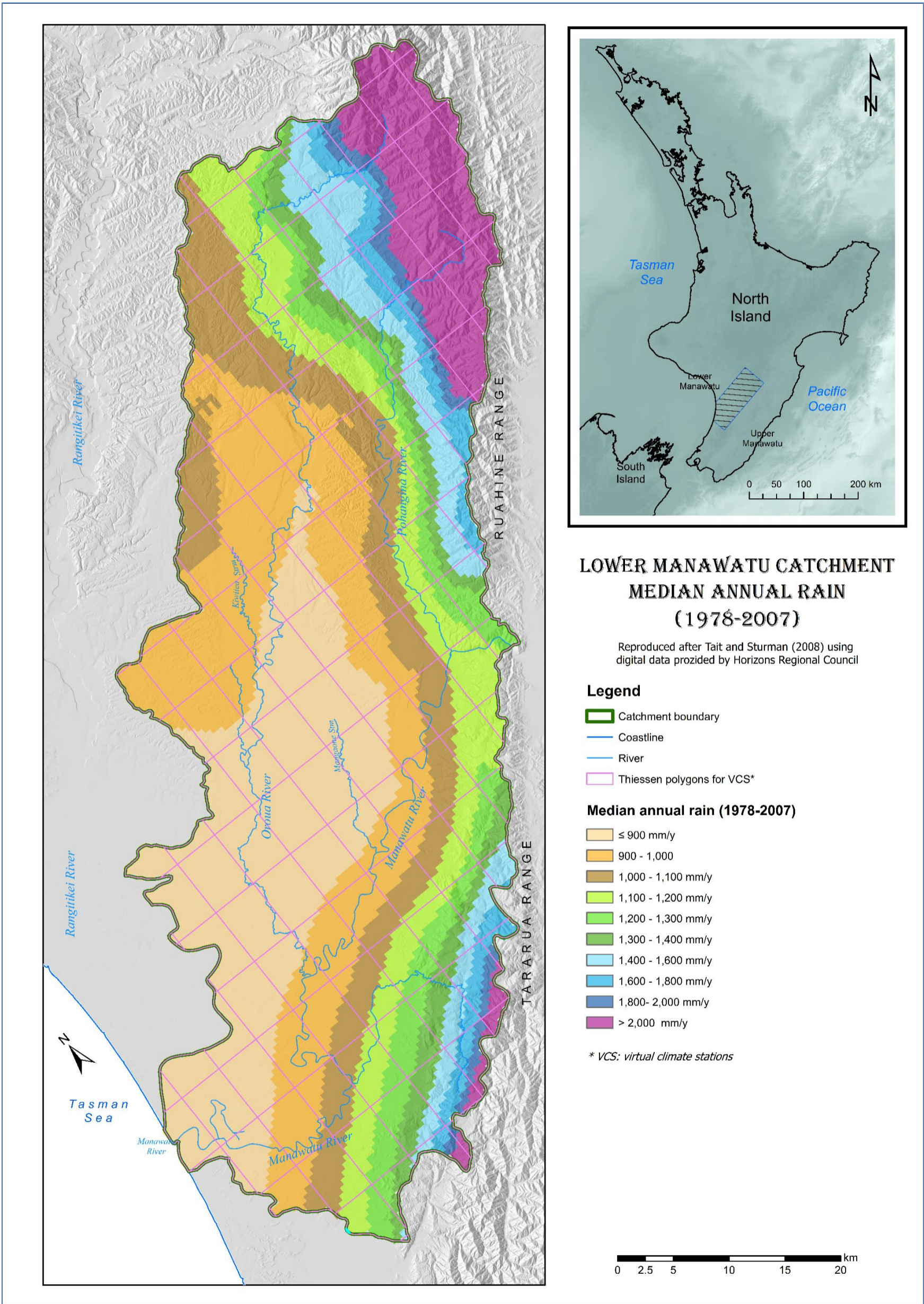


Figure A-4. Median annual rain (in mm/y) for the period 1978–2007 (reproduced from digital maps by Tait & Sturman, 2008).

## Appendix B Surface water hydrographs

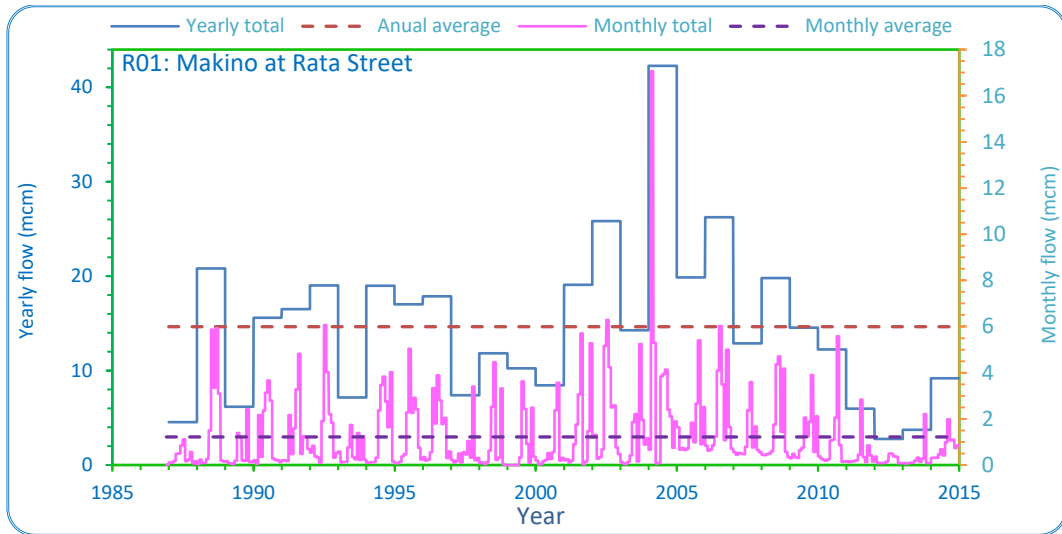


Figure B-1. Yearly and monthly total and average flow calculated for Makino Stream at Rata Street (Site R01 in the map in Figure 5-5).

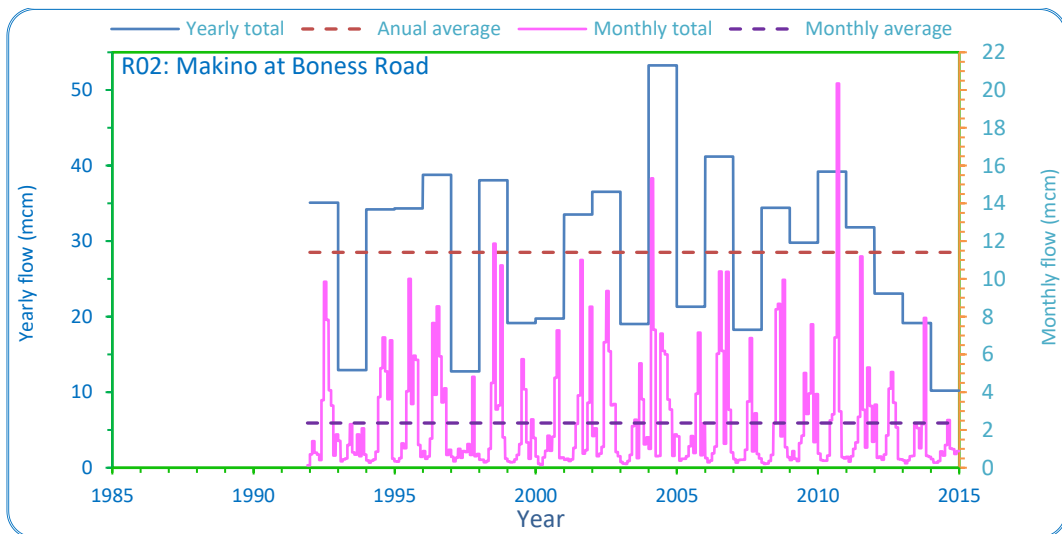


Figure B-2. Yearly and monthly total and average flow calculated for Makino Stream at Boness Road (Site R02 in the map in Figure 5-5).

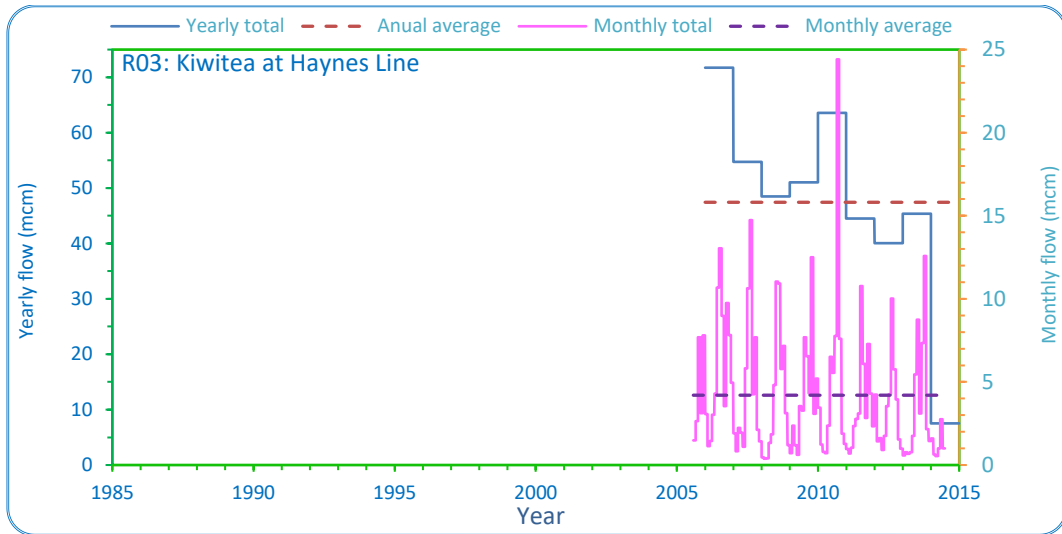


Figure B-3. Yearly and monthly total and average flow calculated for Kiwitea Stream at Haynes Line (Site R03 in the map in Figure 5-5).

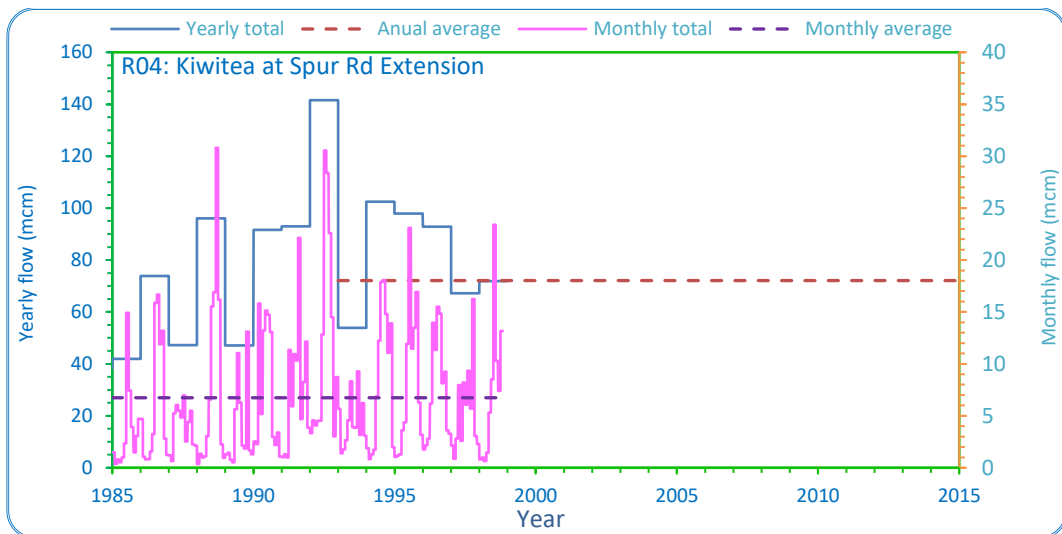


Figure B-4. Yearly and monthly total and average flow calculated for Kiwitea Stream at Spur Road Extension (Site R04 in the map in Figure 5-5).

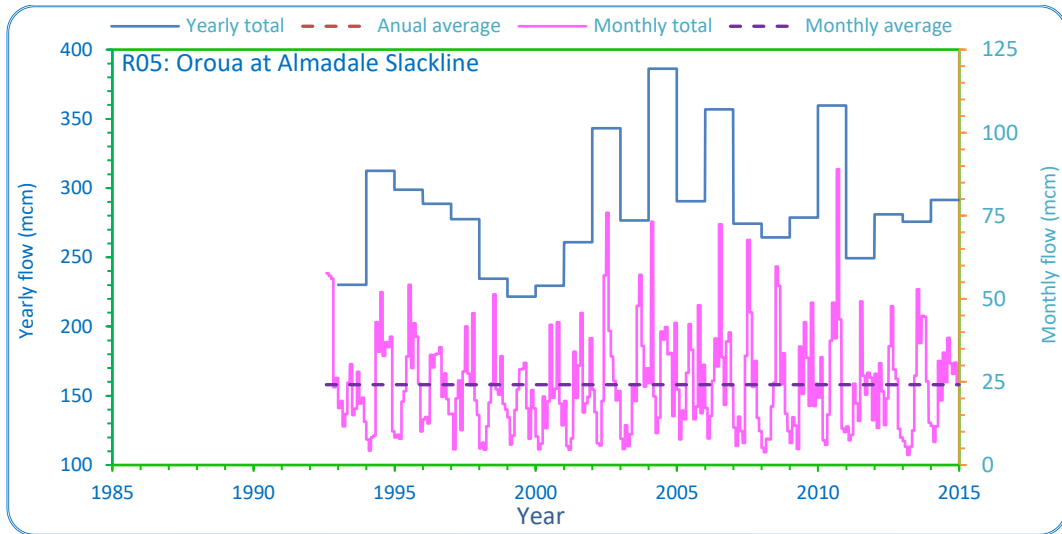


Figure B-5. Yearly and monthly total and average flow calculated for Oroua Stream at Almadale Slackline (Site R05 in the map in Figure 5-5).

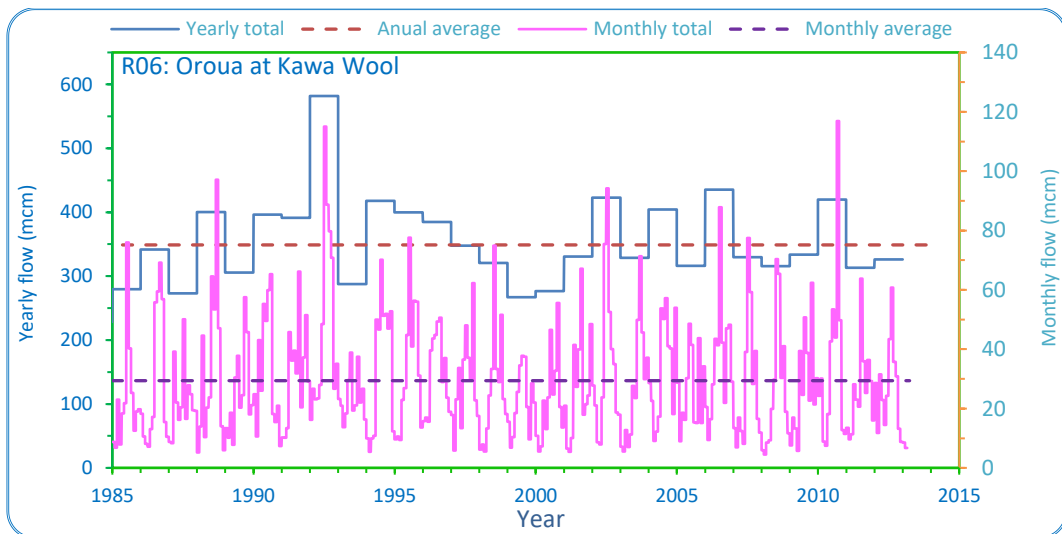


Figure B-6. Yearly and monthly total and average flow calculated for Oroua River at Kawa Wool (Site R06 in the map in Figure 5-5).

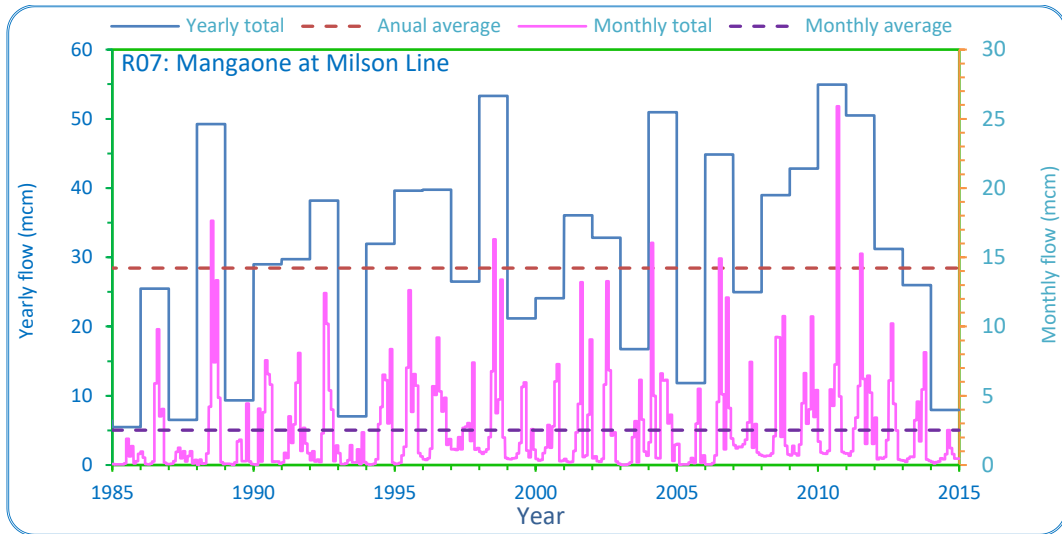


Figure B-7. Yearly and monthly total and average flow calculated for Mangaone Stream at Milson Line (Site R07 in the map in Figure 5-5).

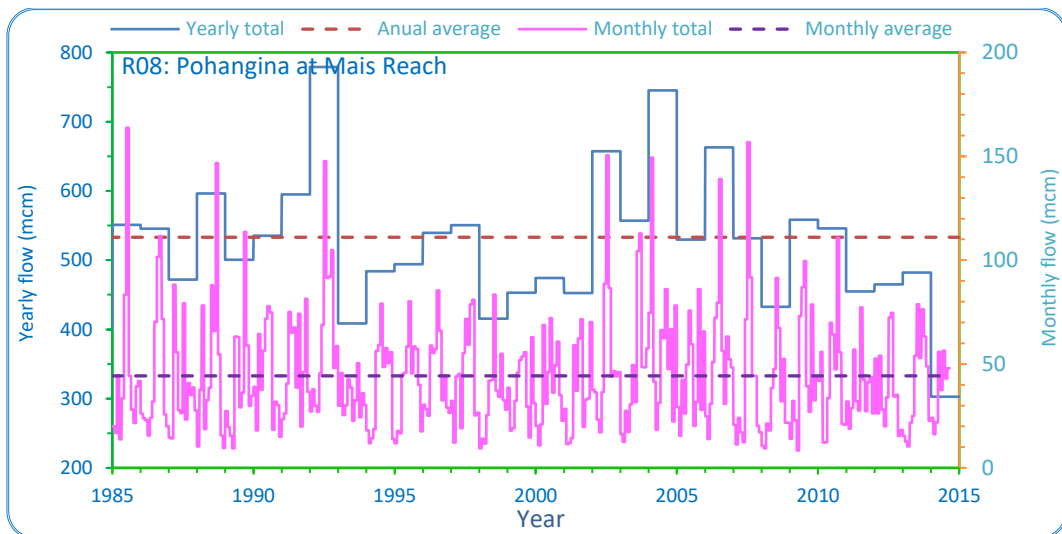


Figure B-8. Yearly and monthly total and average flow calculated for Pohangina River at Mais Reach (Site R08 in the map in Figure 5-5).

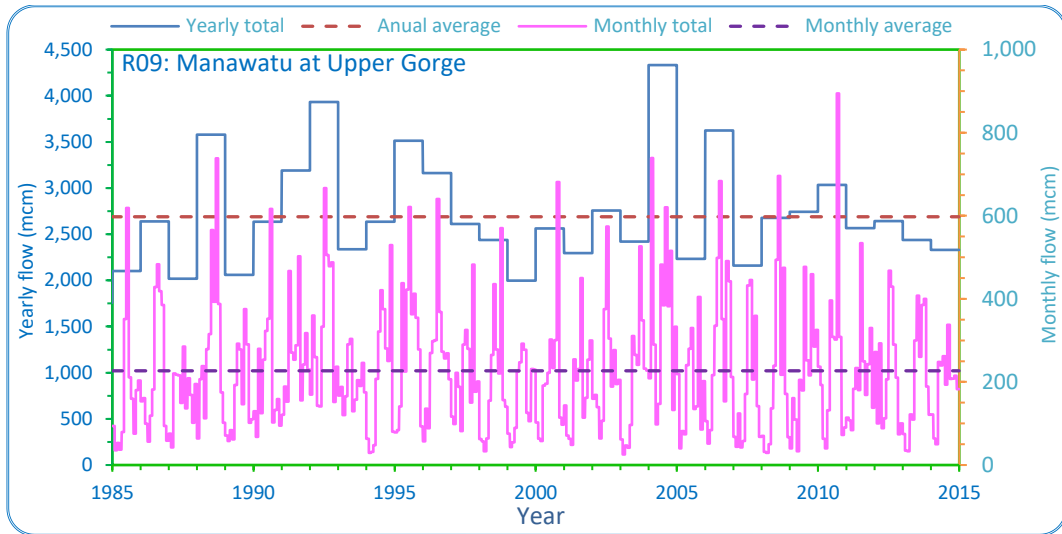


Figure B-9. Yearly and monthly total and average flow calculated for Manawatu River at Upper Gorge (Site R09 in the map in Figure 5-5).

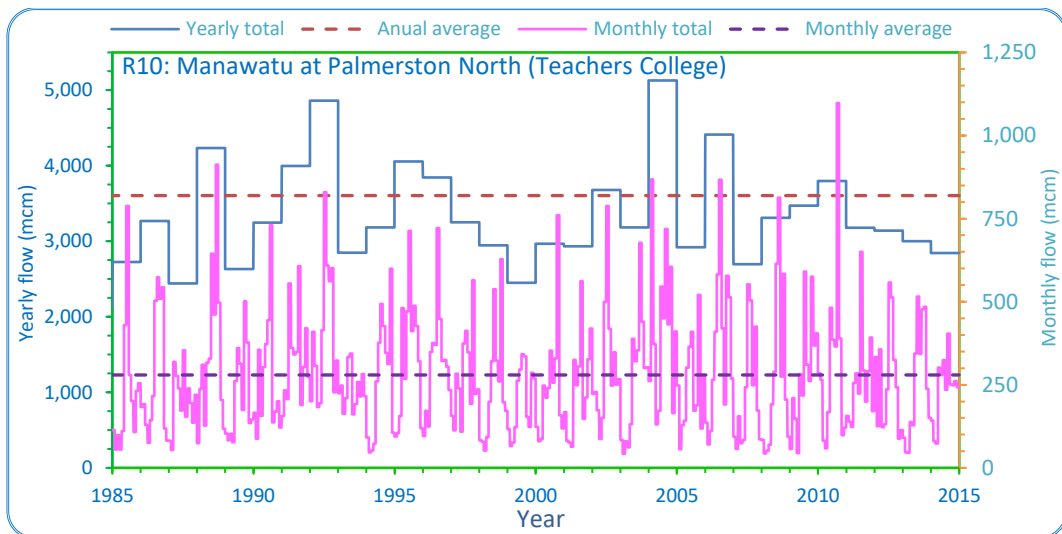


Figure B-10. Yearly and monthly total and average flow calculated for Manawatu River at Palmerston North Teachers College (Site R10 in the map in Figure 5-5).

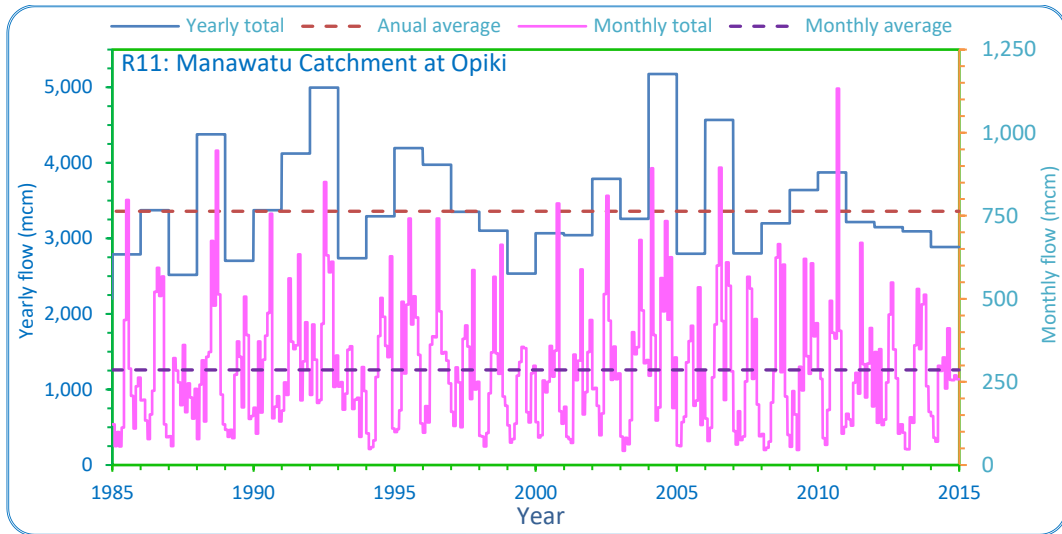


Figure B-11. Yearly and monthly total and average flow calculated for Manawatu River at Opiki (Site R11 in the map in Figure 5-5).

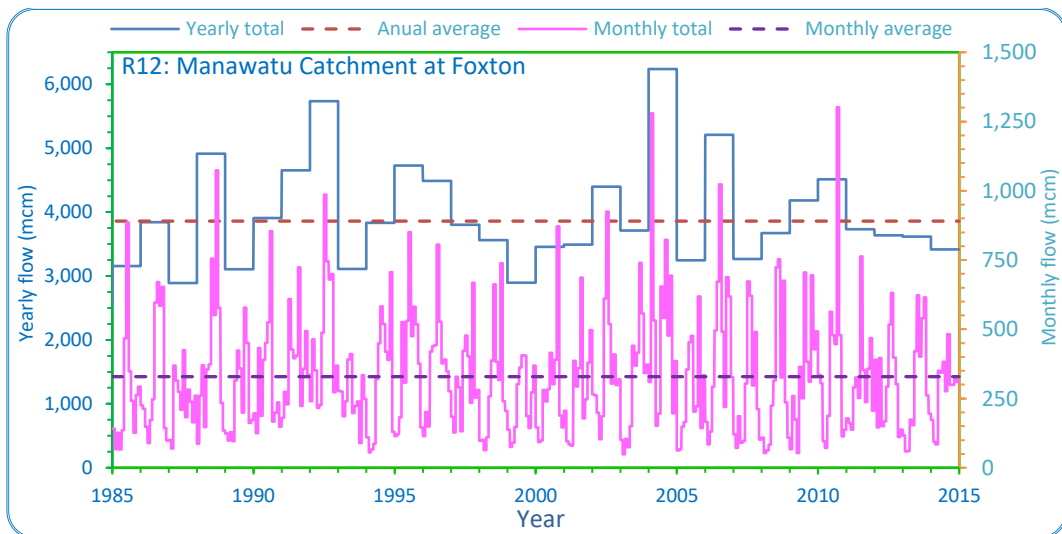


Figure B-12. Yearly and monthly total and average flow calculated for Manawatu River at Foxton (Site R12 in the map in Figure 5-5).

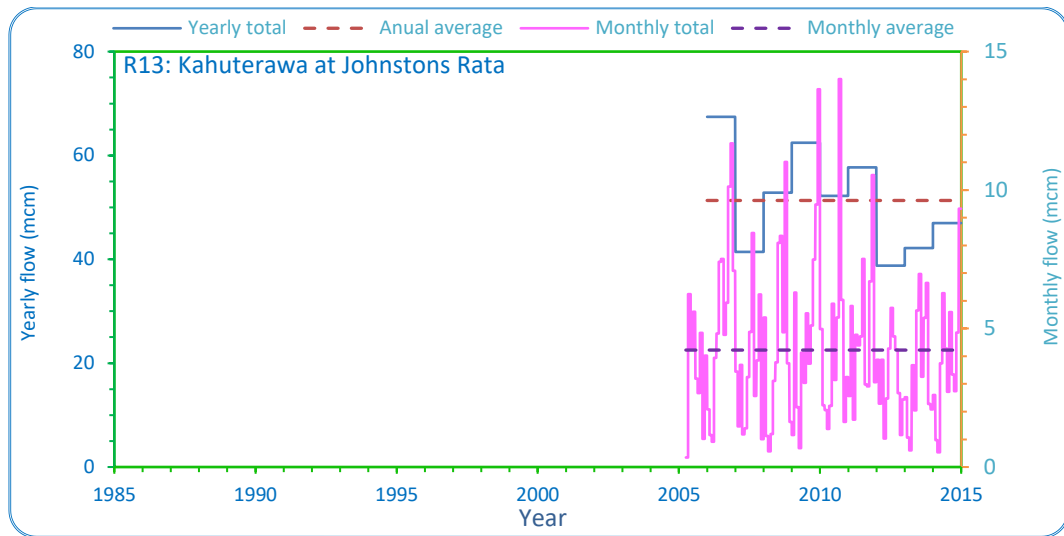


Figure B-13. Yearly and monthly total and average flow calculated for Kahuterawa Stream at Johnstons Rata (Site R13 in the map in Figure 5-5).

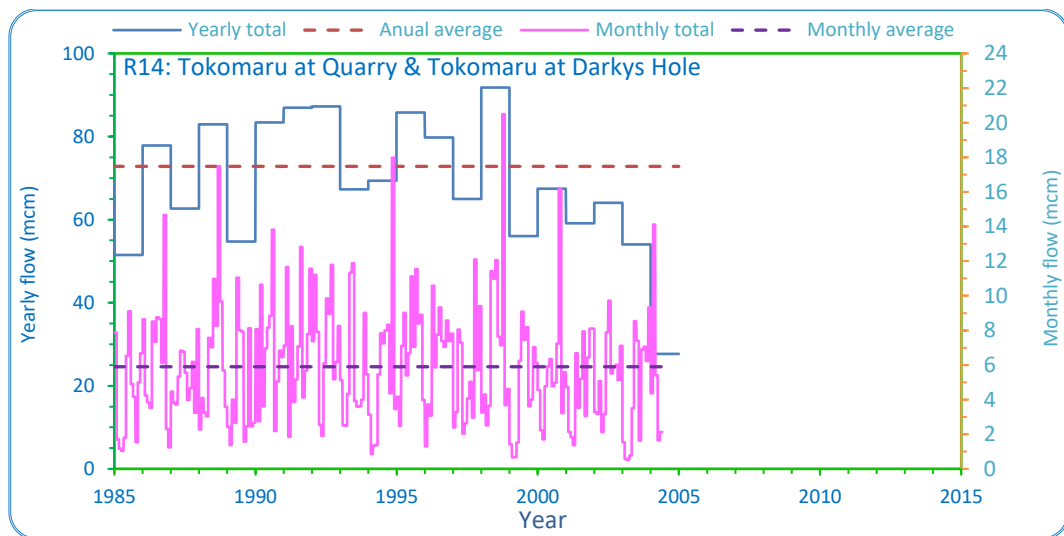


Figure B-14. Yearly and monthly total and average flow calculated for Tokomaru at Quarry and Tokomaru at Darkys Hole (Site R14 in the map in Figure 5-5).

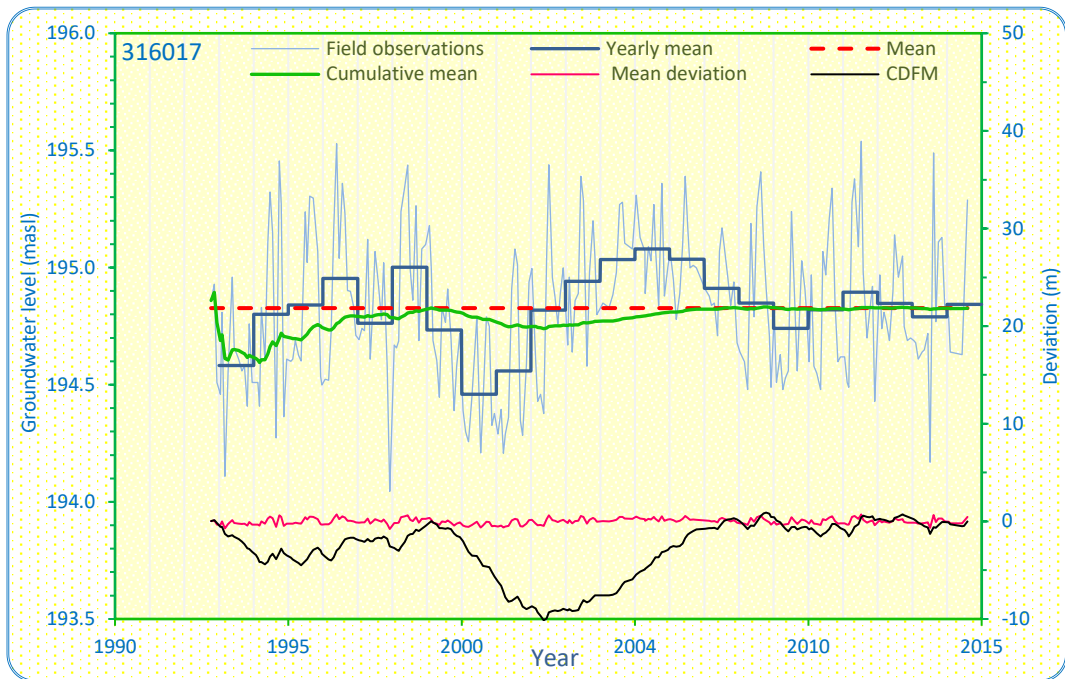
## Appendix C Groundwater level data and hydrographs

Table C-1. Summary of groundwater level monitoring records<sup>70</sup> in the LMC.

Figure number	Well ID	NZMG position			Measurement point		Well depth (m)	Screen position (masl)			Examined record length		Number of Readings	Groundwater level (masl)				GWL STDEV (m)
		Easting	Northing	Info source	Level (masl)	Info source		Top	Middle	Bottom	From	To		Min	Max	Mean	Median	
D-1	316017	2738281	6116317	Handheld GPS	202.01	Survey	85.00	120.01	118.51	117.01	9/10/1992	5/08/2014	254	194.05	195.54	194.83	194.83	0.30
D-2	316019	2738274	6116317	Handheld GPS	202.11	Survey	85.00	120.11	118.61	117.11	9/10/1992	2/12/2014	259	190.02	191.26	190.74	190.71	0.19
D-3	316031	2734564	6116317	Handheld GPS	147.34	Survey	25.90	123.44	122.44	121.44	9/10/1992	2/12/2014	259	137.64	142.42	140.42	140.29	0.83
D-4	316037	2733577	6116317	Handheld GPS	129.64	Survey	26.50	105.24	104.19	103.14	9/10/1992	2/12/2014	260	117.25	123.69	121.57	121.63	0.88
D-5	324071	2716360	6116317	Surveying GPS	28.12	Surveying GPS	170.70	-139.58	-141.08	-142.58	19/09/1990	3/12/2014	286	41.12	44.37	42.88	43.02	0.55
D-6	325009	2728348	6116317	Handheld GPS	66.96	Survey	62.30	7.66	6.16	4.66	6/03/1991	19/02/2001	113	61.38	65.02	63.64	63.97	1.01
D-7	325019	2729745	6116317	Surveying GPS	71.31	Surveying GPS	102.50	-28.19	-29.69	-31.19	9/10/1992	9/12/2013	248	39.63	64.32	47.72	46.92	4.23
D-8	325023	2723463	6116317	Handheld GPS	39.28	Survey	47.00	-4.72	-6.22	-7.72	9/10/1992	2/12/2014	261	30.05	32.88	31.49	31.52	0.56
D-9	325031	2730352	6116317	Surveying GPS	44.26	Surveying GPS	127.50	-78.54	-80.89	-83.24	8/08/1990	2/12/2014	288	46.78	49.96	49.01	49.03	0.52
D-10	325047	2729131	6116317	Surveying GPS	65.98	Surveying GPS	111.60	-39.62	-42.62	-45.62	23/06/1994	2/12/2014	226	42.80	58.61	49.13	49.16	2.49
D-11	325071	2729688	6116317	Surveying GPS	44.69	Surveying GPS	169.50	-91.31	-104.06	-116.81	8/08/1990	2/12/2014	288	48.72	51.72	50.83	50.86	0.47
D-12	325081	2724585	6116317	Handheld GPS	31.21	Survey	89.00	-54.79	-56.29	-57.79	21/08/1990	3/12/2014	284	28.53	31.82	30.35	30.28	0.69
D-13	325141	2725902	6116317	Surveying GPS	48.81	Surveying GPS	44.00	8.91	6.86	4.81	9/10/1992	7/04/2014	250	43.87	48.61	46.02	45.90	0.96
D-14	325251	2730110	6116317	Surveying GPS	93.36	Surveying GPS	46.00	53.36	50.36	47.36	22/05/1992	2/12/2014	266	89.21	93.34	92.10	92.16	0.69
D-15	325261	2723641	6116317	Surveying GPS	39.12	Surveying GPS	8.70	33.62	32.02	30.42	9/10/1992	2/12/2014	261	34.22	37.66	36.48	36.47	0.60
D-16	325351	2730247	6116317	Surveying GPS	61.43	Surveying GPS	144.00	-78.57	-80.57	-82.57	8/08/1990	2/12/2014	269	58.94	62.25	60.91	60.96	0.56
D-17	326011	2734271	6116317	Surveying GPS	58.29	Surveying GPS	113.00	-51.71	-53.21	-54.71	8/08/1990	2/12/2014	288	58.23	60.87	59.77	59.84	0.63
D-18	326061	2733901	6116317	Handheld GPS	50.79	Survey	118.95	-65.16	-66.66	-68.16	8/08/1990	10/01/2008	204	53.30	54.51	53.98	53.97	0.25
D-19	326181	2735590	6116317	Handheld GPS	64.24	Survey	135.00	-67.76	-69.26	-70.76	8/08/1990	2/12/2014	287	57.24	60.46	59.12	59.20	0.70
D-20	326191	2731628	6116317	Handheld GPS	49.46	Survey	153.75	-102.29	-103.29	-104.29	8/08/1990	5/08/2014	285	52.17	55.28	54.29	54.32	0.52
D-21	326211	2735683	6116317	Handheld GPS	111.31	Survey	118.00	-3.69	-5.19	-6.69	19/01/2001	2/12/2014	162	92.79	94.70	93.63	93.62	0.29
D-22	327037	2741611	6116317	Handheld GPS	172.00	DEM	58.60	113.90	113.65	113.40	13/11/2002	2/12/2014	139	118.22	118.92	118.57	118.57	0.14
D-23	327039	2742351	6116317	Surveying GPS	123.49	Surveying GPS	117.00	8.49	7.49	6.49	11/04/2003	8/12/2014	133	68.53	69.73	69.25	69.28	0.23
D-24	333035	2711086	6116317	Surveying GPS	35.52	Surveying GPS	45.00	-6.48	-7.98	-9.48	15/05/2008	3/12/2014	80	20.72	22.95	22.50	22.61	0.35
D-25	334001	2721746	6116317	Handheld GPS	23.61	Survey	18.00	8.61	7.11	5.61	3/09/1990	3/12/2014	284	19.07	20.96	20.24	20.27	0.32
D-26	334021	2722023	6116317	Surveying GPS	12.64	Surveying GPS	96.50	-82.86	-83.36	-83.86	3/09/1990	3/12/2014	287	12.93	18.51	17.27	17.40	0.78
D-27	334041	2715605	6116317	Surveying GPS	12.67	Surveying GPS	99.00	-82.63	-84.48	-86.33	26/10/1990	3/12/2014	265	14.11	18.21	16.83	17.03	0.74
D-28	335041	2725446	6116317	Surveying GPS	21.44	Surveying GPS	155.30	-129.86	-131.86	-133.86	21/08/1990	3/12/2014	281	25.82	28.82	27.77	27.84	0.52
D-29	335051	2724204	6116317	Surveying GPS	16.83	Surveying GPS	126.00	-106.17	-107.67	-109.17	13/08/1990	30/07/2014	281	20.20	23.86	22.76	22.91	0.65
D-30	335071	2727378	6116317	Surveying GPS	17.74	Surveying GPS	91.00	-70.26	-71.76	-73.26	21/08/1990	3/12/2014	287	21.51	25.53	24.23	24.40	0.73
D-31	335171	2724602	6116317	Surveying GPS	13.77	Surveying GPS	68.63	-51.86	-53.36	-54.86	21/08/1990	3/12/2014	285	14.70	18.19	17.05	17.25	0.66
D-32	335311	2730453	6116317	Handheld GPS	28.24	Survey	85.00	-53.76	-55.26	-56.76	21/08/1990	31/07/2014	280	29.90	32.87	31.57	31.68	0.57
D-33	335331	2727044	6116317	Surveying GPS	21.96	Surveying GPS	141.00	-117.04	-118.04	-119.04	21/08/1990	1/12/2014	286	28.25	32.62	30.69	30.77	0.83
D-34	335351	2726004	6116317	Surveying GPS	18.31	Surveying GPS	171.00	-149.69	-151.19	-152.69	13/08/1990	1/12/2014	283	25.74	32.97	29.08	29.00	1.52
D-35	335361	2728554	6116317	Surveying GPS	23.87	Surveying GPS	112.00	-85.13	-86.63	-88.13	21/08/1990	30/07/2014	280	29.19	33.21	31.62	31.83	0.80
D-36	335371	2726552	6116317	Surveying GPS	20.66	Surveying GPS	111.00	-87.34	-88.84	-90.34	21/08/1990	7/08/2014	284	24.11	27.04	25.99	26.12	0.59
D-37	335391	2729492	6116317	Handheld GPS	31.43	Survey	73.30	-39.87	-40.87	-41.87	8/08/1990	2/12/2014	289	32.68	35.61	34.54	34.66	0.60
D-38	336001	2732831	6116317	Handheld GPS	43.68	Survey	125.00	-78.32	-79.82	-81.32	8/08/1990	1/12/2014	285	46.24	50.01	48.58	48.70	0.88
D-39	336009	2735800	6116317	Surveying GPS	38.01	Surveying GPS	64.30	-23.29	-24.79	-26.29	7/02/1991	8/12/2014	279	36.00	39.12	37.96	38.03	0.61
D-40	336017	2737308	6116317	Handheld GPS	44.44	Survey	60.00	-12.56	-14.06	-15.56	7/02/1991	7/03/2000	110	41.17	43.47	42.45	42.50	0.46
D-41	336019	2735242	6116317	Surveying GPS	48.61	Surveying GPS	60.20	-8.59	-10.09	-11.59	17/04/1991	3/09/2014	277	57.26	59.49	58.49	58.49	0.47
D-42	336071	2731448	6116317	Handheld GPS	28.43	Survey	84.30	-52.88	-54.38	-55.88	7/02/1991	8/12/2014	282	31.58	42.43	39.01	39.38	1.43

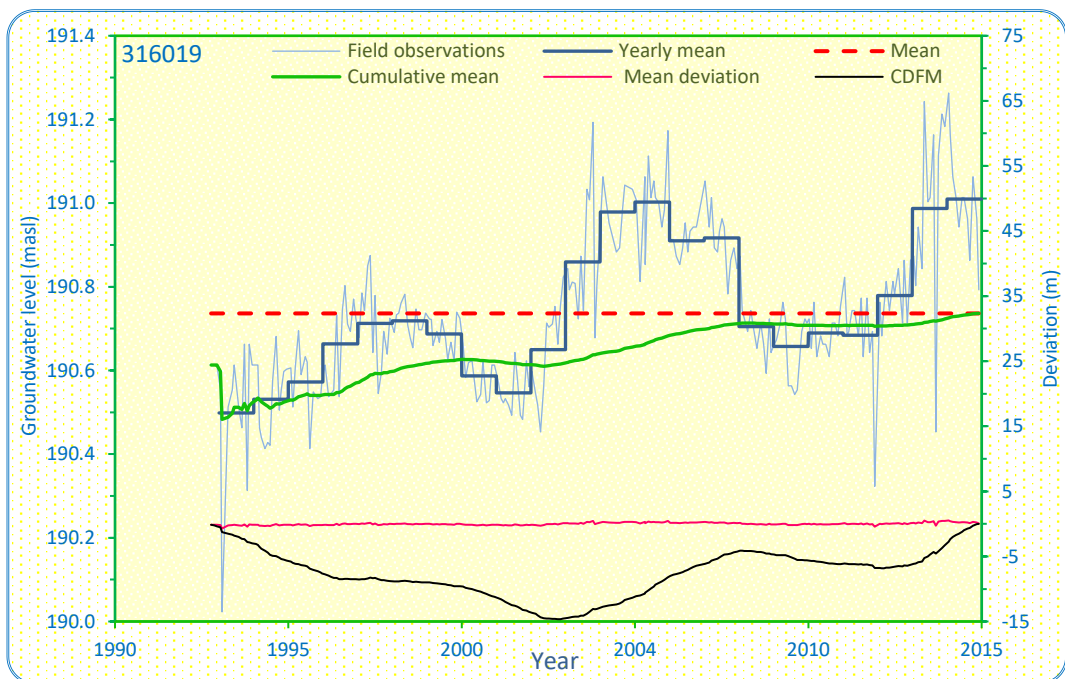
<sup>70</sup> Yellow highlighted text indicates estimated values, or value dependent on other estimated values.

Figure number	Well ID	NZMG position			Measurement point		Well depth (m)	Screen position (masl)			Examined record length		Number of Readings	Groundwater level (masl)				GWL STDEV (m)
		Easting	Northing	Info source	Level (masl)	Info source		Top	Middle	Bottom	From	To		Min	Max	Mean	Median	
D-43	336113	2735033	6116317	Handheld GPS	34.49	Survey	34.00	2.49	1.49	0.49	24/03/1992	8/12/2014	267	27.47	36.66	31.96	32.74	2.91
D-44	336121	2731895	6116317	Handheld GPS	29.30	Survey	68.63	-36.33	-37.83	-39.33	7/02/1991	20/11/2009	226	33.41	38.39	36.88	37.14	0.99
D-45	336181	2735888	6116317	Surveying GPS	36.25	Surveying GPS	72.10	-32.85	-34.35	-35.85	7/02/1991	1/08/2014	271	41.25	48.42	46.17	46.35	1.17
D-46	336203	2739023	6116317	Surveying GPS	44.77	Surveying GPS	63.00	-15.73	-16.98	-18.23	9/09/1994	8/12/2014	223	41.67	47.03	45.01	45.18	0.80
D-47	336333	2735006	6116317	Surveying GPS	57.79	Surveying GPS	96.00	-35.21	-36.71	-38.21	6/09/1996	8/12/2014	203	49.59	52.87	51.88	51.95	0.60
D-48	336371	2736935	6116317	Surveying GPS	39.08	Surveying GPS	54.80	-12.72	-14.22	-15.72	8/03/1991	1/08/2014	278	43.22	49.13	46.57	46.65	1.20
D-49	336401	2738005	6116317	Handheld GPS	41.76	Survey	45.70	-0.94	-2.44	-3.94	23/09/1992	8/12/2014	255	42.02	49.03	46.49	46.66	1.25
D-50	336421	2735200	6116317	Surveying GPS	36.70	Surveying GPS	71.00	-31.30	-32.80	-34.30	7/02/1991	1/08/2014	276	36.75	40.23	38.90	39.00	0.66
D-51	336441	2731967	6116317	Handheld GPS	29.84	Survey	72.00	-39.16	-40.66	-42.16	7/02/1991	31/07/2014	280	32.12	37.75	35.81	36.07	1.15
D-52	336481	2735150	6116317	Surveying GPS	33.07	Surveying GPS	48.00	-7.93	-11.43	-14.93	7/02/1991	8/12/2014	281	34.40	38.14	36.98	37.08	0.60
D-53	336541	2734971	6116317	Surveying GPS	36.98	Surveying GPS	75.50	-35.52	-37.02	-38.52	7/02/1991	8/12/2014	288	36.65	40.17	38.94	39.06	0.65
D-54	336571	2735044	6116317	Surveying GPS	43.56	Surveying GPS	49.00	-2.44	-3.94	-5.44	7/02/1991	8/12/2014	282	43.91	48.74	46.62	46.79	0.99
D-55	336581	2736639	6116317	Surveying GPS	43.83	Surveying GPS	120.30	-74.97	-75.72	-76.47	18/04/1991	8/12/2014	282	47.50	53.47	50.57	50.69	1.37
D-56	336651	2738427	6116317	Handheld GPS	43.81	Survey	20.00	26.81	25.31	23.81	25/06/1991	8/12/2014	273	39.46	42.52	41.04	41.01	0.49
D-57	337001	2744112	6116317	Handheld GPS	55.08	Survey	40.00	18.08	16.58	15.08	7/02/1991	8/12/2014	241	55.98	61.74	58.97	59.00	0.90
D-58	337003	2740464	6116317	Surveying GPS	46.75	Surveying GPS	81.00	-31.25	-32.75	-34.25	8/03/1991	8/12/2014	282	47.87	51.14	49.93	49.96	0.51
D-59	337021	2740394	6116317	Surveying GPS	44.61	Surveying GPS	27.10	19.51	18.51	17.51	7/02/1991	8/12/2014	273	46.46	49.43	48.34	48.38	0.53
D-60	337031	2741732	6116317	Surveying GPS	48.71	Surveying GPS	80.83	-29.12	-30.62	-32.12	7/02/1991	1/08/2014	278	53.56	63.43	59.07	60.13	2.55
D-61	337041	2741818	6116317	Surveying GPS	48.72	Surveying GPS	99.00	-47.28	-48.78	-50.28	7/02/1991	8/12/2014	280	62.14	65.90	64.07	64.03	0.72
D-62	342001	2704483	6116317	Surveying GPS	15.31	Surveying GPS	80.00	-61.69	-63.19	-64.69	19/02/1991	4/11/2014	273	4.44	8.47	7.31	7.57	0.83
D-63	342051	2703360	6116317	Surveying GPS	6.95	Surveying GPS	65.50	-52.45	-55.50	-58.55	19/02/1991	5/12/2014	280	7.87	9.85	8.88	8.90	0.36
D-64	342091	2703738	6116317	Surveying GPS	3.57	Surveying GPS	160.00	-153.43	-154.93	-156.43	19/02/1991	5/12/2014	280	9.73	13.91	12.43	12.55	0.80
D-65	343101	2711435	6116317	Surveying GPS	26.51	Surveying GPS	41.30	-11.69	-13.24	-14.79	19/02/1991	5/12/2014	276	14.87	20.07	18.42	18.51	0.61
D-66	344001	2715768	6116317	Surveying GPS	4.77	Surveying GPS	153.50	-144.74	-146.74	-148.74	13/08/1990	30/09/2014	281	5.48	14.04	12.67	12.99	1.24
D-67	344007	2718282	6116317	Surveying GPS	7.97	Surveying GPS	149.00	-137.03	-139.03	-141.03	12/08/1991	1/12/2014	276	8.74	15.18	11.88	11.21	1.89
D-68	344041	2714987	6116317	Surveying GPS	5.39	Surveying GPS	68.40	-60.01	-61.51	-63.01	13/08/1990	8/01/2014	275	6.73	9.90	8.89	8.90	0.52
D-69	344051	2721233	6116317	Surveying GPS	12.86	Surveying GPS	137.00	-121.14	-122.64	-124.14	13/08/1990	30/07/2014	282	19.43	23.09	21.38	21.34	0.72
D-70	345001	2726823	6116317	Surveying GPS	24.77	Surveying GPS	135.00	-99.23	-104.73	-110.23	13/08/1990	30/07/2014	282	25.46	36.50	30.40	30.08	3.12
D-71	345009	2727234	6116317	Handheld GPS	31.90	Survey	29.40	3.50	3.00	2.50	21/11/1996	1/12/2014	209	30.90	32.21	31.61	31.63	0.30
D-72	345011	2722414	6116317	Surveying GPS	14.25	Surveying GPS	135.00	-117.76	-119.26	-120.76	13/08/1990	1/12/2014	288	19.11	22.92	21.56	21.54	0.68
D-73	345021	2722208	6116317	Surveying GPS	8.80	Surveying GPS	92.40	-81.90	-82.75	-83.60	13/08/1990	1/12/2014	285	11.06	21.61	15.03	14.83	3.08
D-74	345031	2726749	6116317	Surveying GPS	23.88	Surveying GPS	129.00	-100.12	-102.62	-105.12	13/08/1990	30/07/2014	282	26.68	36.34	32.99	32.88	1.56
D-75	345041	2729264	6116317	Surveying GPS	36.49	Surveying GPS	165.51	-126.02	-127.52	-129.02	13/08/1990	1/12/2014	285	41.01	49.03	45.52	45.43	3.32
D-76	345071	2724304	6116317	Surveying GPS	15.52	Surveying GPS	85.00	-66.48	-67.98	-69.48	13/08/1990	1/12/2014	288	19.19	22.90	21.15	21.19	0.58
D-77	345111	2724301	6116317	Surveying GPS	16.09	Surveying GPS	111.00	-91.91	-93.41	-94.91	13/08/1990	1/12/2014	287	19.87	23.48	22.41	22.50	0.63
D-78	345151	2723416	6116317	Handheld GPS	14.79	Survey	78.00	-62.31	-62.76	-63.21	22/02/1991	10/12/2014	279	26.62	28.89	27.82	27.81	0.41
D-79	346031	2734540	6116317	Handheld GPS	57.34	DEM	47.28	13.06	11.56	10.06	7/02/1991	8/12/2014	279	65.29	71.07	69.63	69.60	1.00
D-80	352051	2703128	6116317	Surveying GPS	11.95	Surveying GPS	44.20	-29.25	-30.75	-32.25	19/02/1991	5/12/2014	277	2.90	5.51	4.70	4.78	0.51
D-81	353291	2709290	6116317	Surveying GPS	46.51	Surveying GPS	46.50	3.01	1.51	0.01	22/02/1991	10/12/2014	276	11.19	15.33	14.02	14.10	0.41
D-82	354003	2714870	6116317	Surveying GPS	18.06	Surveying GPS	85.00	-63.94	-65.44	-66.94	19/03/1991	11/03/2002	132	21.56	22.73	22.26	22.25	0.17
D-83	354005	2713445	6116317	Surveying GPS	5.74	Surveying GPS	165.50	-138.66	-149.21	-159.76	16/12/1993	10/12/2014	245	11.74	21.66	18.40	19.58	2.61
D-84	354011	2714255	6116317	Handheld GPS	5.05	Survey	36.50	-28.45	-29.95	-31.45	22/02/1991	10/12/2014	273	5.05	7.18	5.97	6.01	0.38



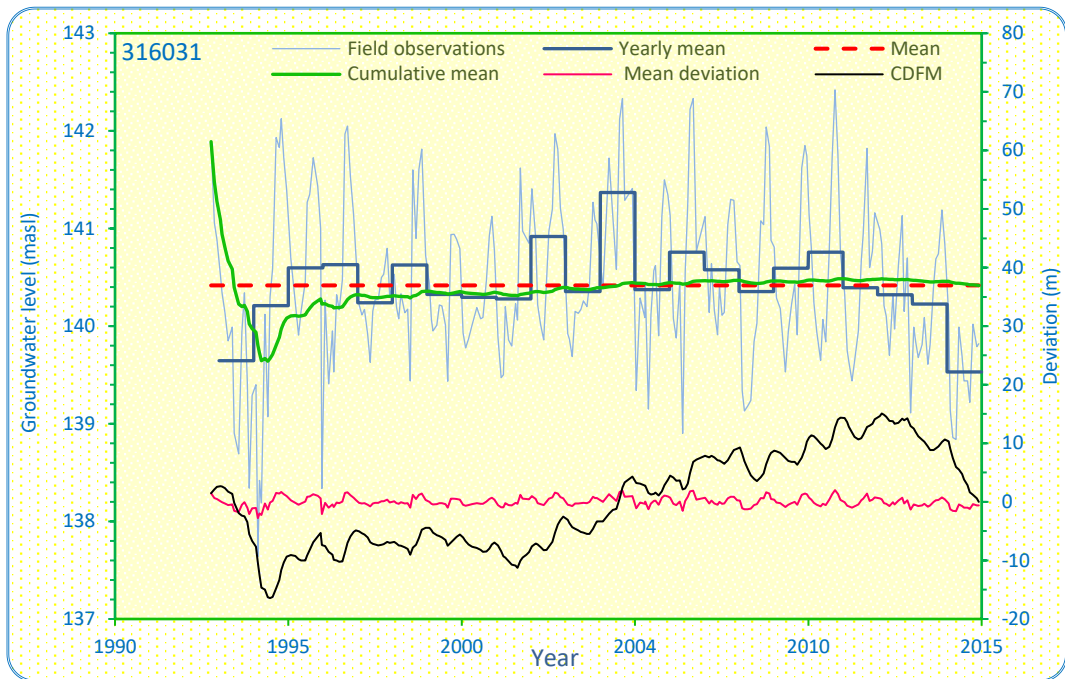
Elevation (masl)	Screen extent (mbgl)	Groundwater level		Area	Trend/comments
		Mean (masl)	STDEV (m)		
202.01	12–15	194.83	0.30		Steady

Figure C-1. Groundwater level hydrographs for Well 316017.



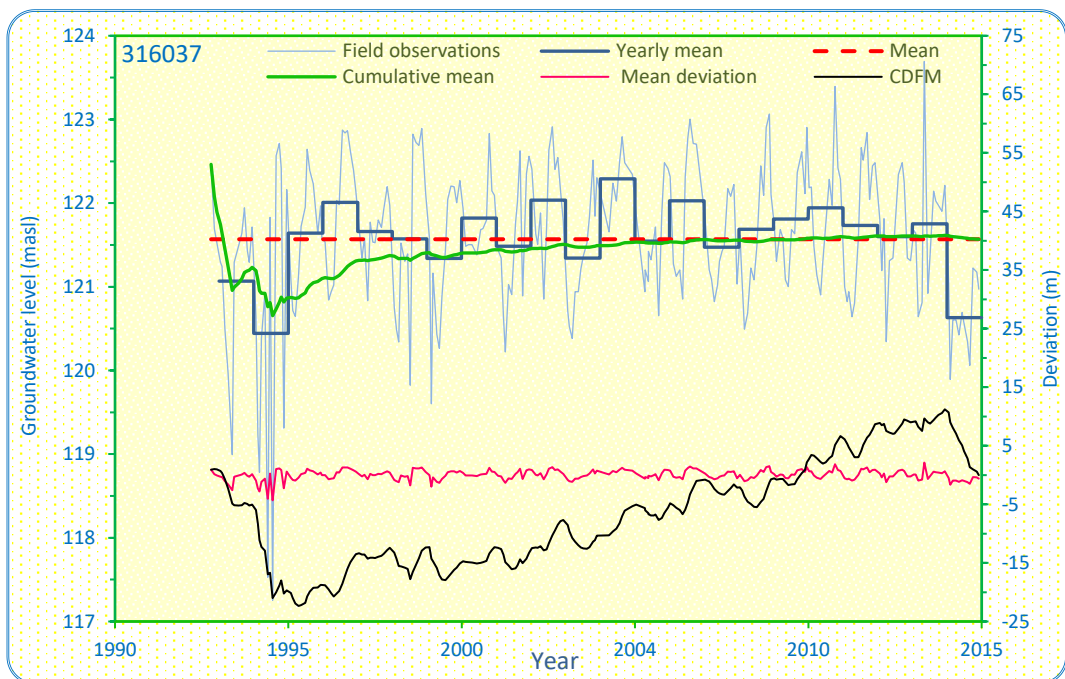
Elevation (masl)	Screen extent (mbgl)	Groundwater level		Area	Trend/comments
		Mean (masl)	STDEV (m)		
202.11	27–30	190.74	0.19		Steady

Figure C-2. Groundwater level hydrographs for Well 316019.



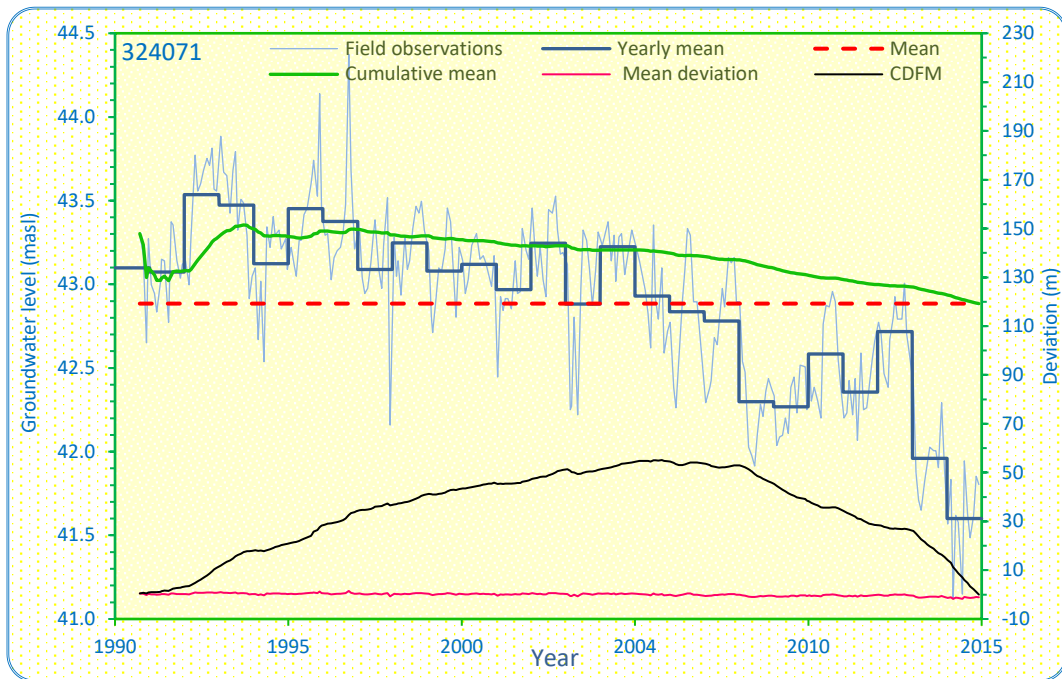
Elevation (masl)	Screen extent (mbgl)	Groundwater level		Area	Trend/comments
		Mean (masl)	STDEV (m)		
147.34	23.9–25.9	140.40	0.87		Steady

Figure C-3. Groundwater level hydrographs for Well 316031.



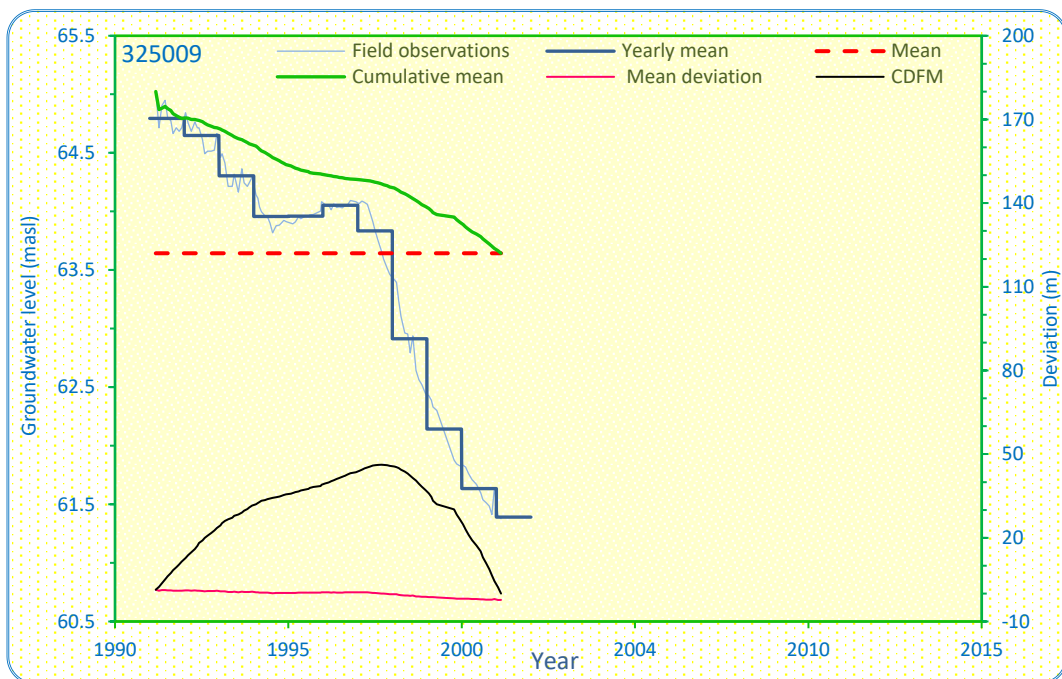
Elevation (masl)	Screen extent (mbgl)	Groundwater level		Area	Trend/comments
		Mean (masl)	STDEV (m)		
129.64	24.4–26.5	121.57	0.88		Steady

Figure C-4. Groundwater level hydrographs for Well 316037.



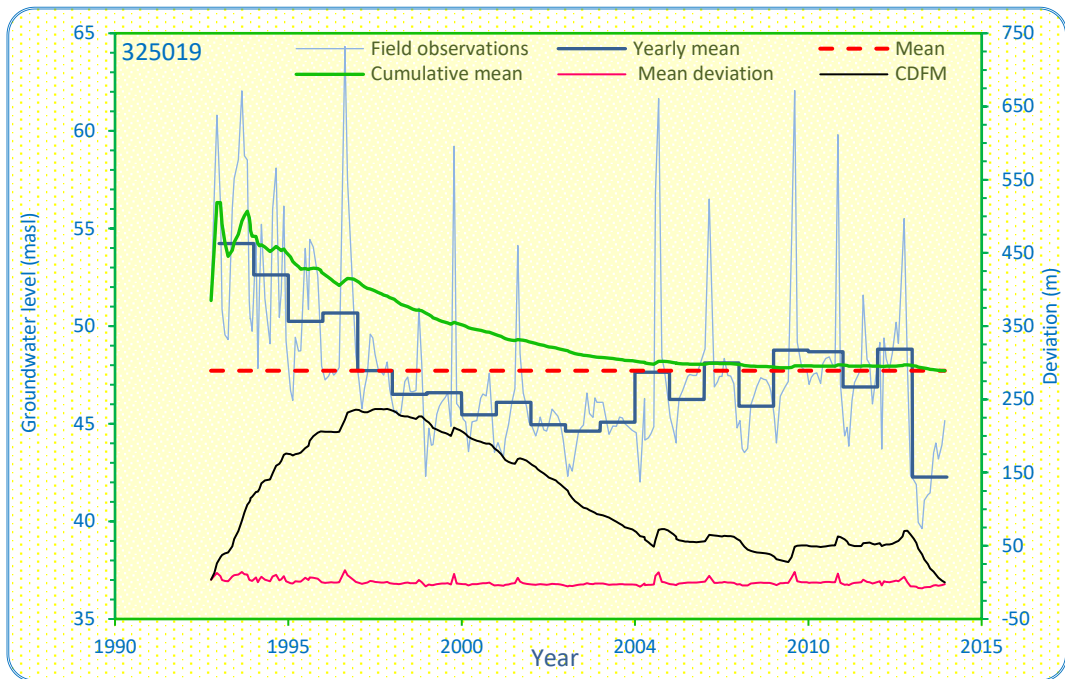
Elevation (masl)	Screen extent (mbgl)	Groundwater level		Area	Trend/comments
		Mean (masl)	STDEV (m)		
28.12	167.7–170.7	42.88	0.55		Declining

Figure C-5. Groundwater level hydrographs for Well 324071.



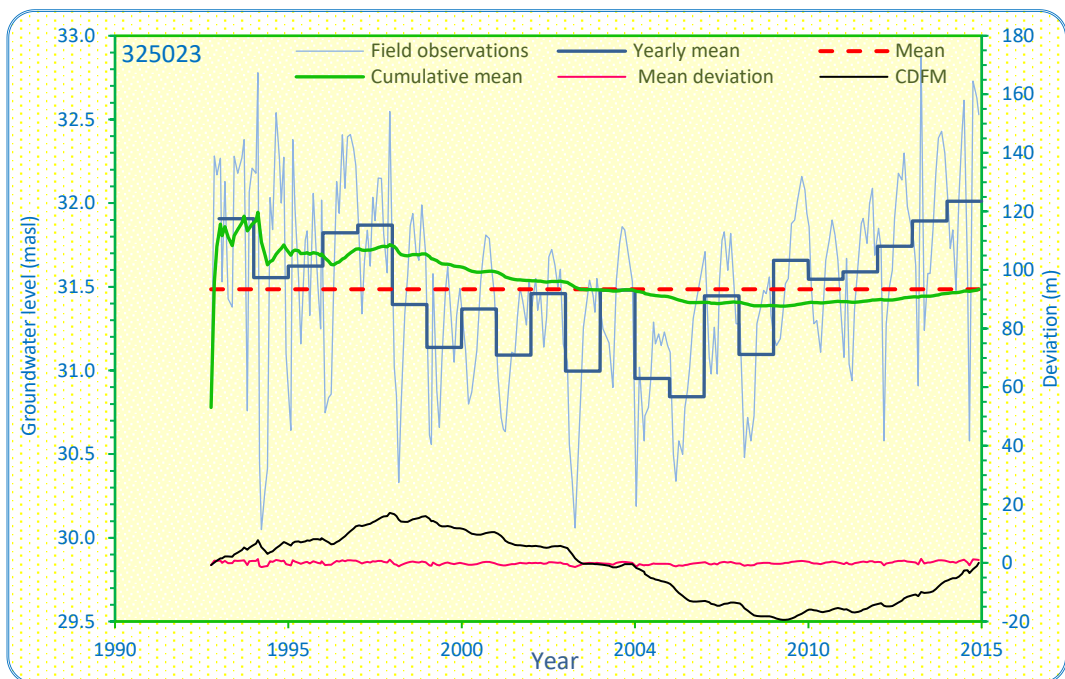
Elevation (masl)	Screen extent (mbgl)	Groundwater level		Area	Trend/comments
		Mean (masl)	STDEV (m)		
66.96	59.3–62.3	63.64	1.01		Old, short record

Figure C-6. Groundwater level hydrographs for Well 325009.



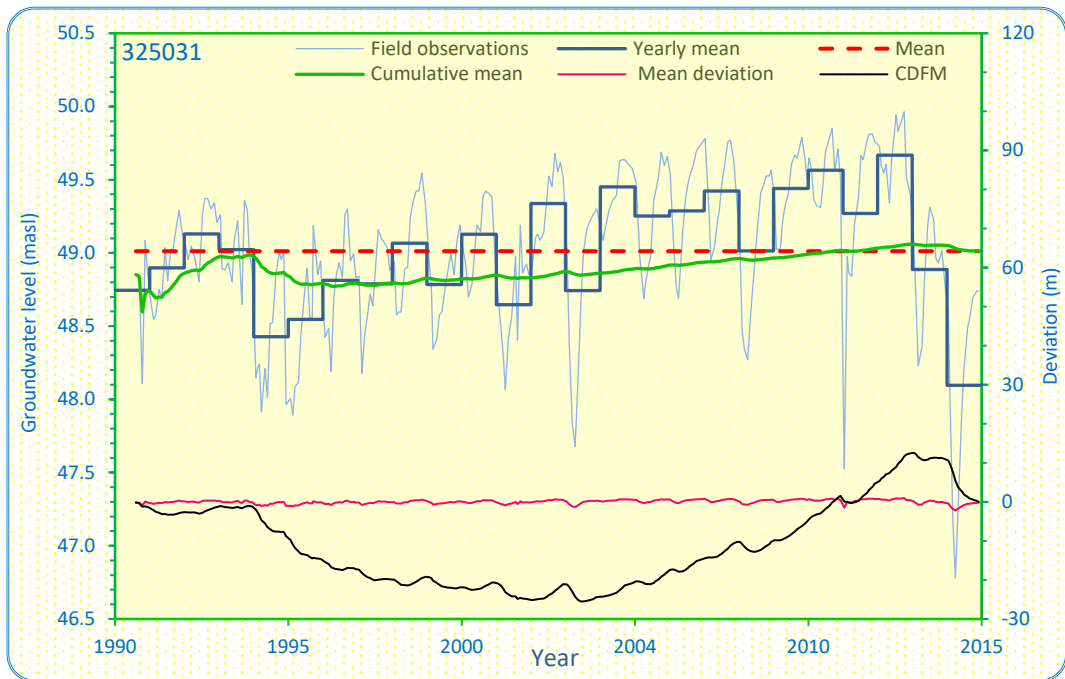
Elevation (masl)	Screen extent (mbgl)	Groundwater level		Area	Trend/comments
		Mean (masl)	STDEV (m)		
71.31	99.5–102.5	47.72	4.23		Declining

Figure C-7. Groundwater level hydrographs for Well 325019.



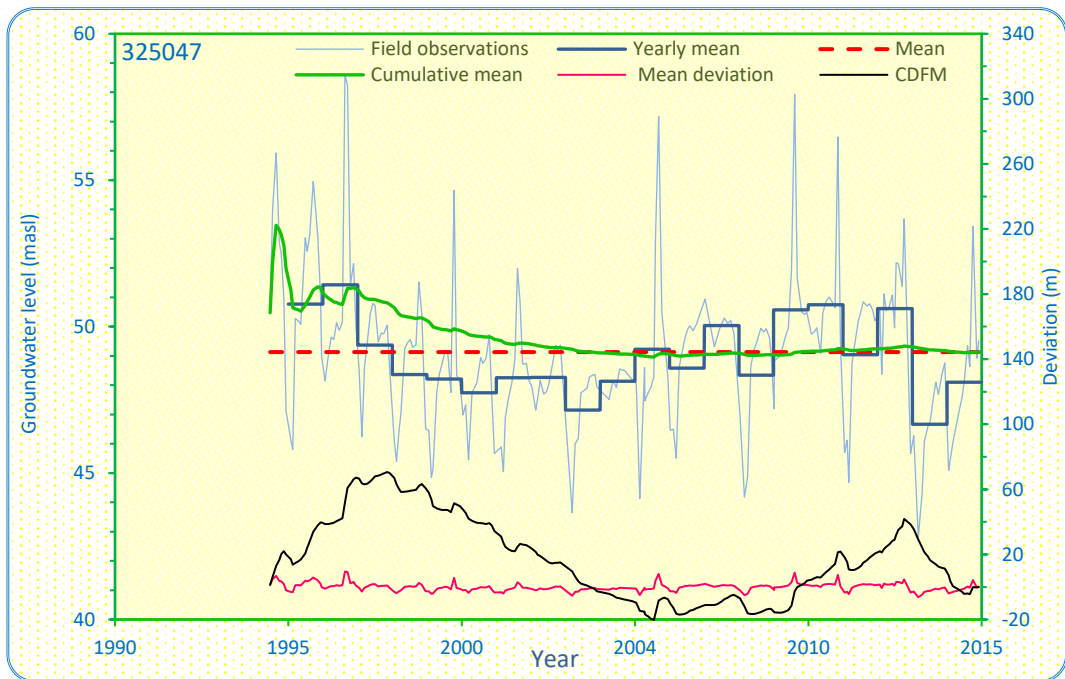
Elevation (masl)	Screen extent (mbgl)	Groundwater level		Area	Trend/comments
		Mean (masl)	STDEV (m)		
39.28	44–47	31.49	0.56		Steady

Figure C-8. Groundwater level hydrographs for Well 325023.



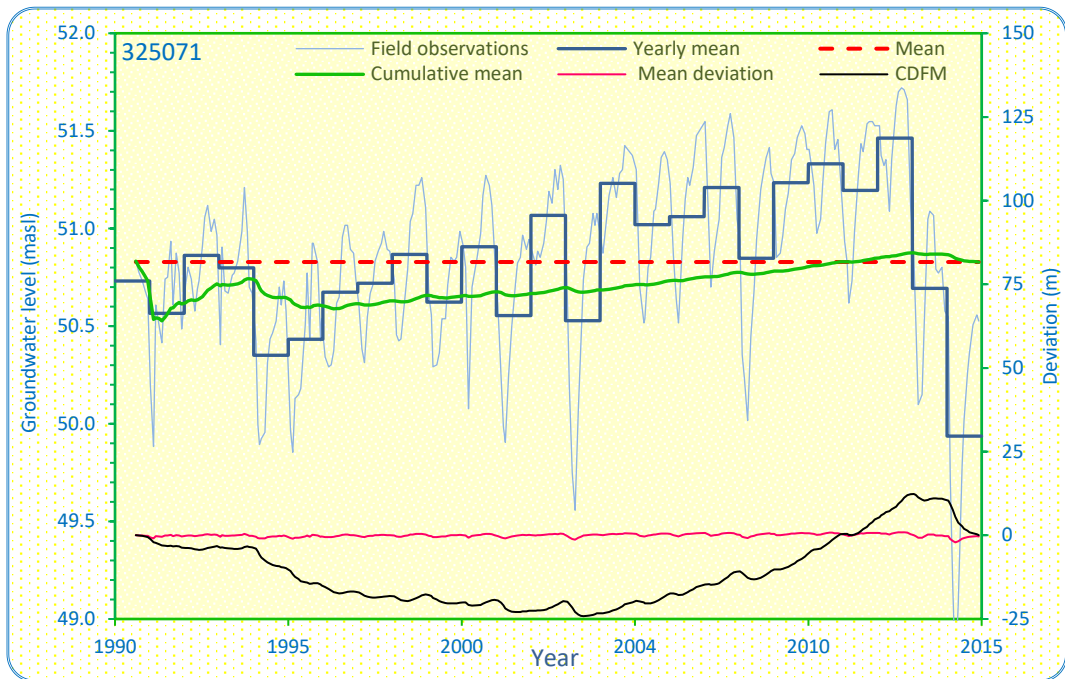
Elevation (masl)	Screen extent (mbgl)	Groundwater level		Area	Trend/comments
		Mean (masl)	STDEV (m)		
44.26	122.8–127.5	49.01	0.52		Steady

Figure C-9. Groundwater level hydrographs for Well 325031.



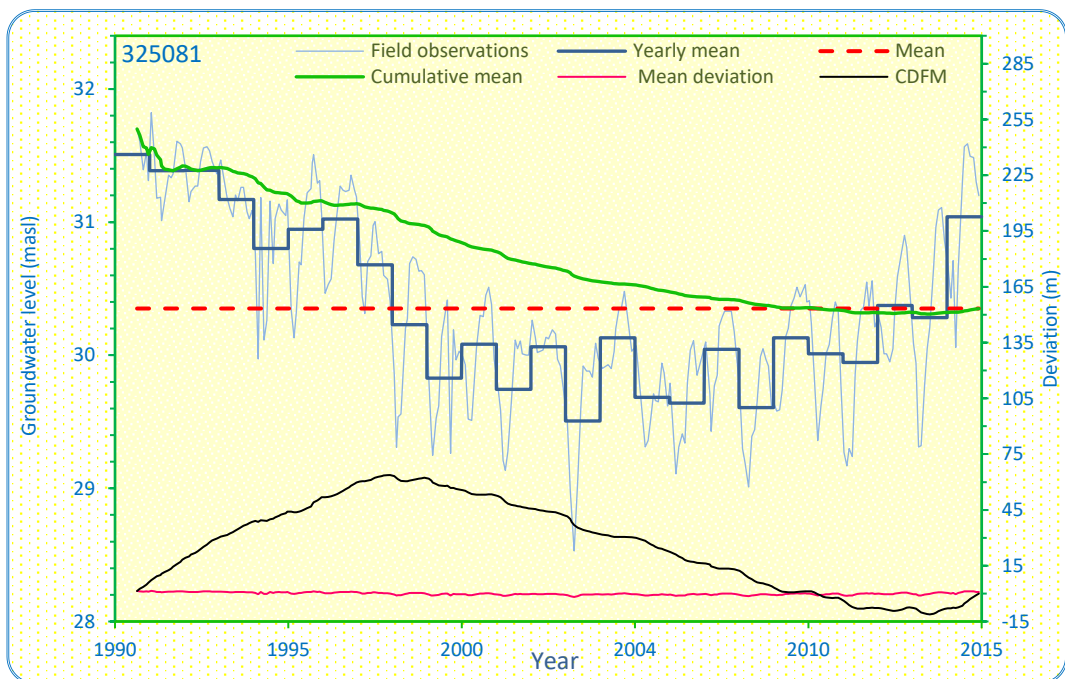
Elevation (masl)	Screen extent (mbgl)	Groundwater level		Area	Trend/comments
		Mean (masl)	STDEV (m)		
65.98	105.6–111.6	49.13	2.49		Steady

Figure C-10. Groundwater level hydrographs for Well 325047.



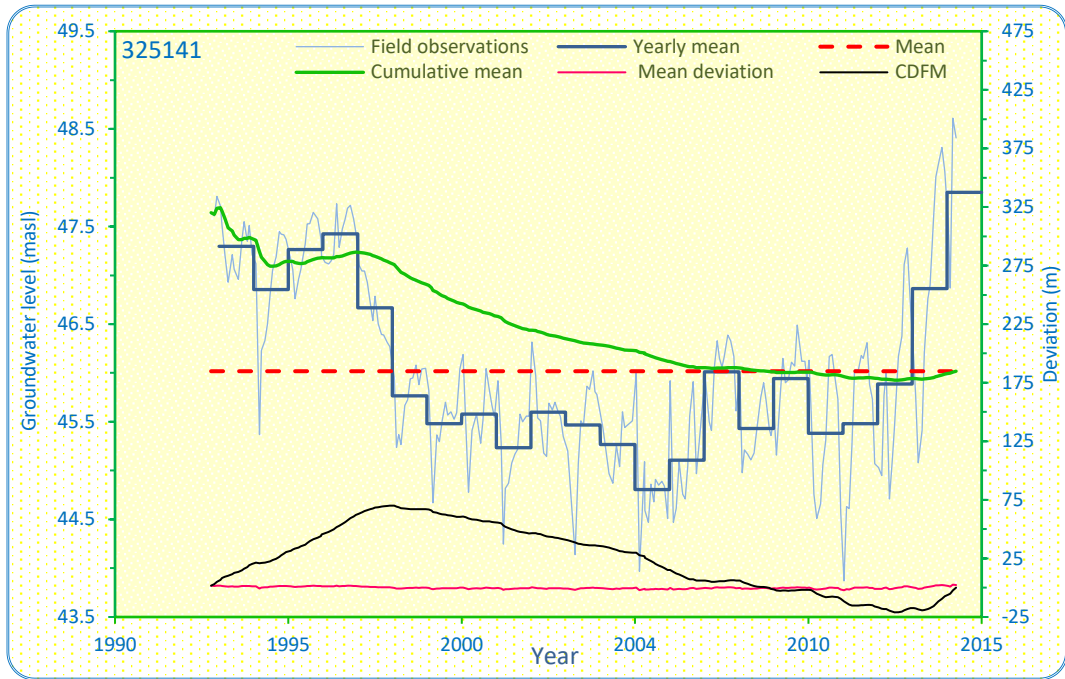
Elevation (masl)	Screen extent (mbgl)	Groundwater level		Area	Trend/comments
		Mean (masl)	STDEV (m)		
44.69	136–169.5	50.83	0.47		Steady

Figure C-11. Groundwater level hydrographs for Well 325071.



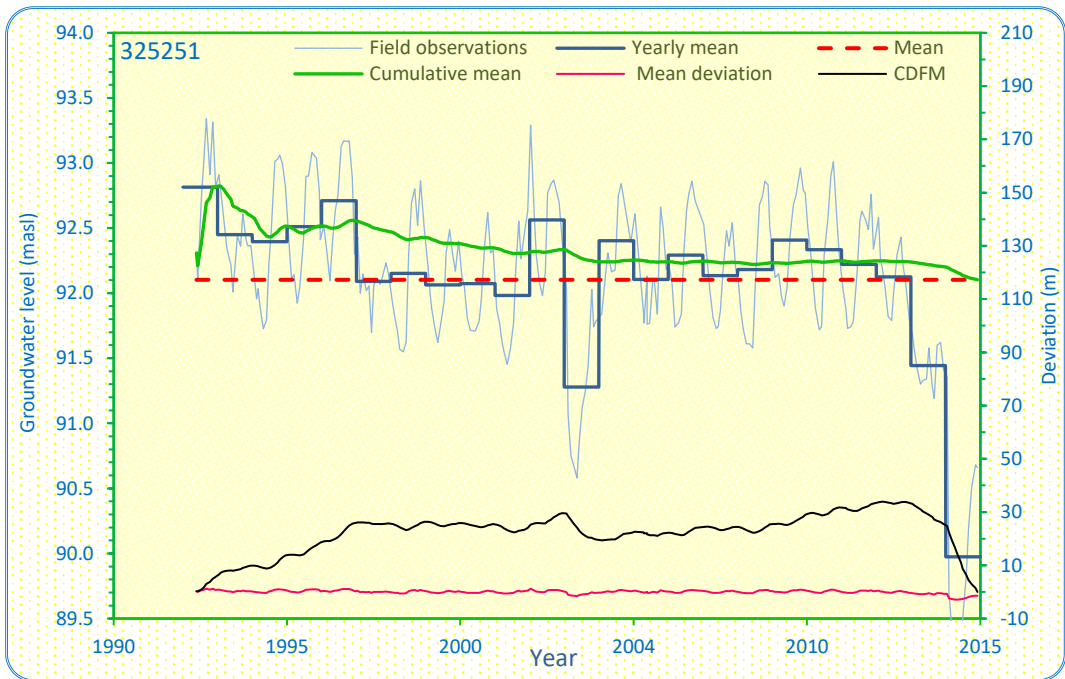
Elevation (masl)	Screen extent (mbgl)	Groundwater level		Area	Trend/comments
		Mean (masl)	STDEV (m)		
31.21	86–89	30.35	0.69		Steady

Figure C-12. Groundwater level hydrographs for Well 325081.



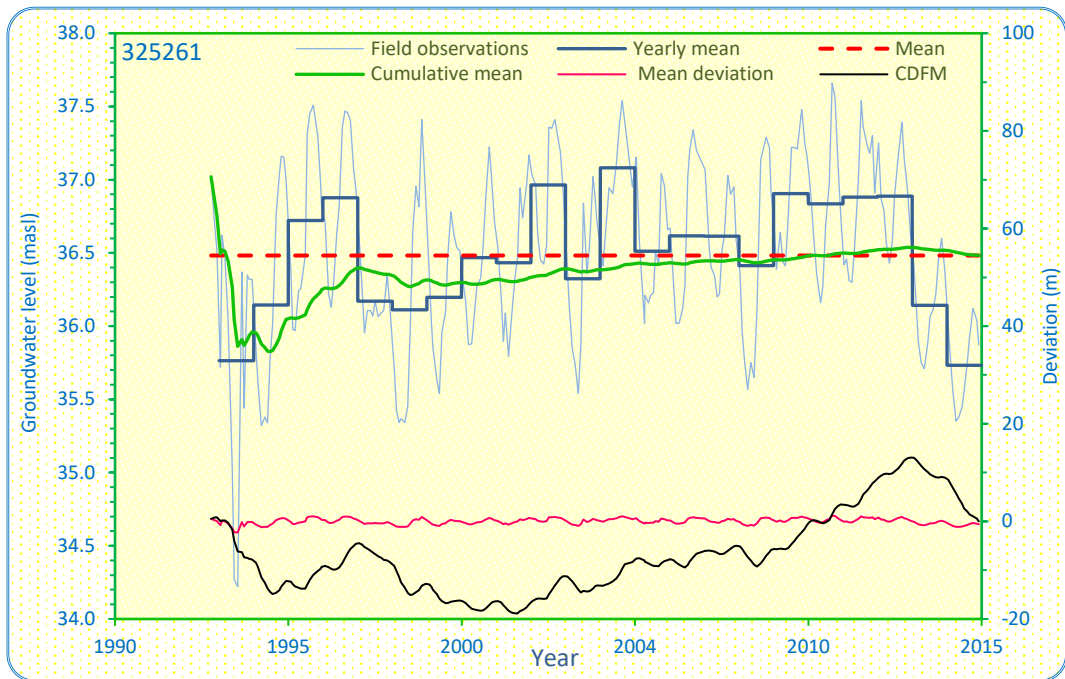
Elevation (masl)	Screen extent (mbgl)	Groundwater level		Area	Trend/comments
		Mean (masl)	STDEV (m)		
48.81	39.9-44	46.02	0.96		Steady

Figure C-13. Groundwater level hydrographs for Well 325141.



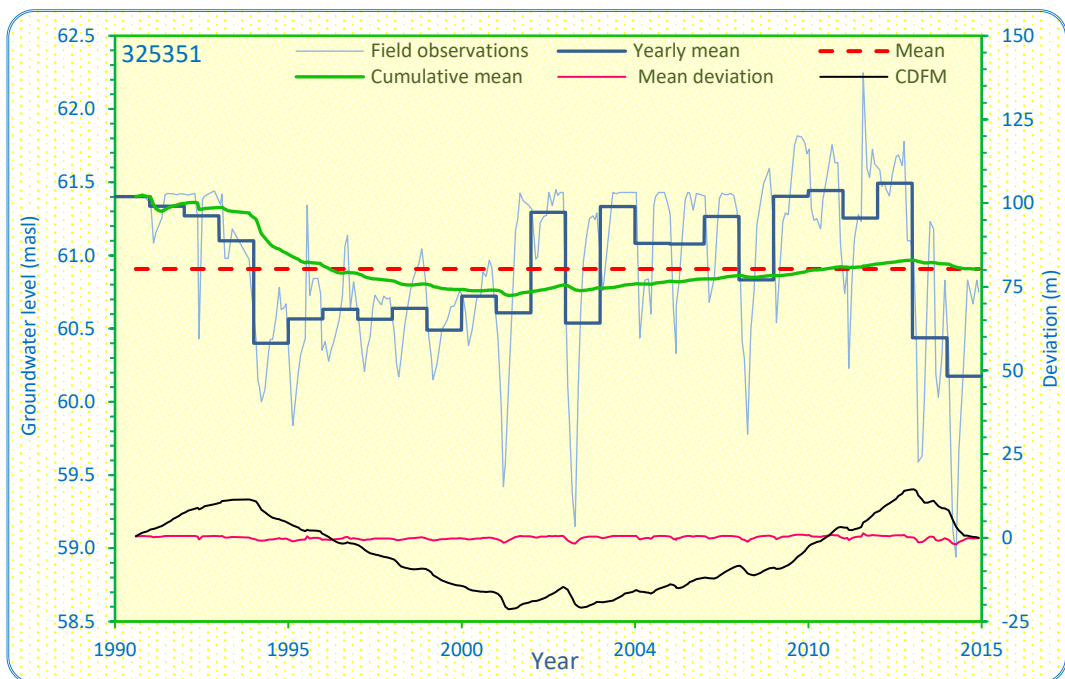
Elevation (masl)	Screen extent (mbgl)	Groundwater level		Area	Trend/comments
		Mean (masl)	STDEV (m)		
93.36	40-46	92.10	0.69		Declining

Figure C-14. Groundwater level hydrographs for Well 325251.



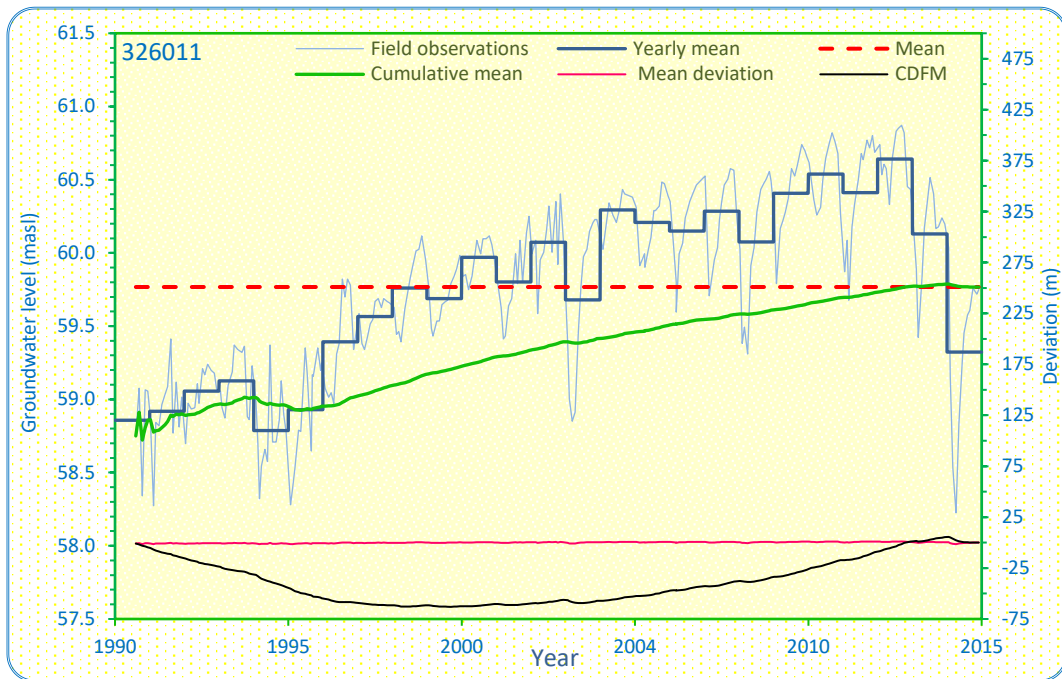
Elevation (masl)	Screen extent (mbgl)	Groundwater level		Area	Trend/comments
		Mean (masl)	STDEV (m)		
39.12	5.5–8.7	36.48	0.60		Steady

Figure C-15. Groundwater level hydrographs for Well 325261.



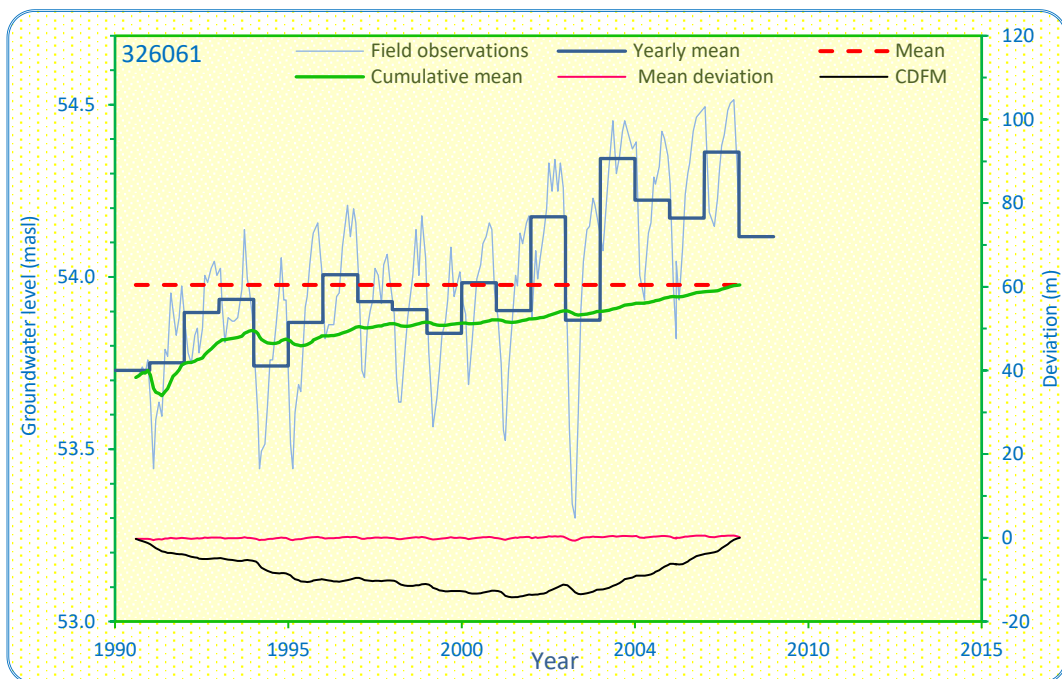
Elevation (masl)	Screen extent (mbgl)	Groundwater level		Area	Trend/comments
		Mean (masl)	STDEV (m)		
61.43	140–144	60.91	0.56		Steady

Figure C-16. Groundwater level hydrographs for Well 325351.



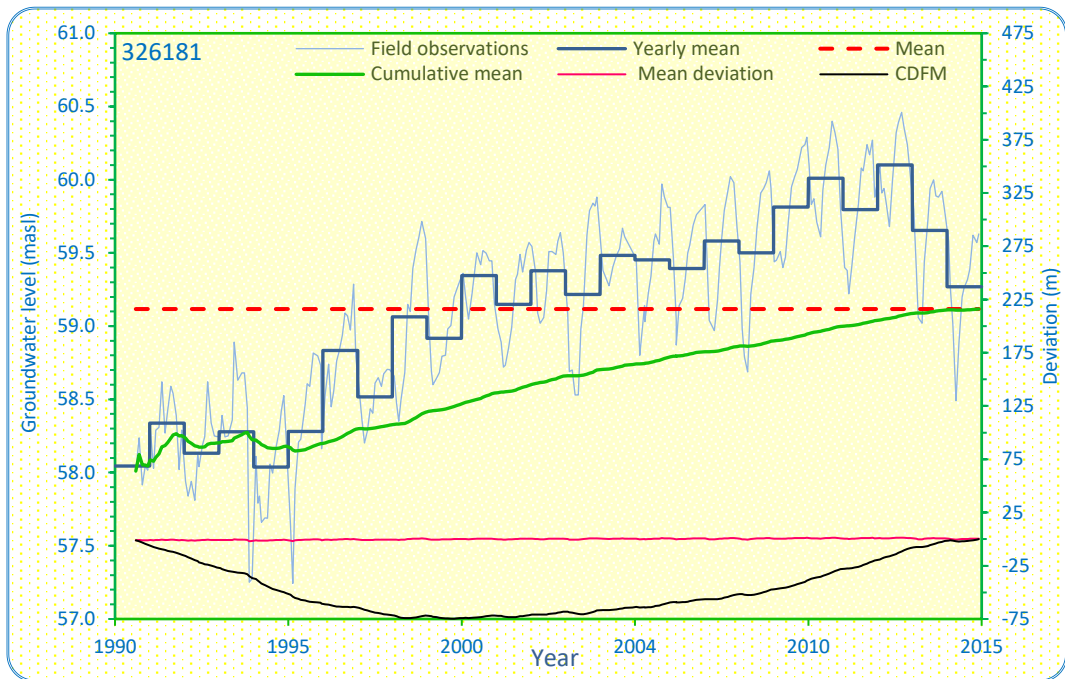
Elevation (masl)	Screen extent (mbgl)	Groundwater level		Area	Trend/comments
		Mean (masl)	STDEV (m)		
58.29	110–113	59.77	0.63		Rising

Figure C-17. Groundwater level hydrographs for Well 326011.



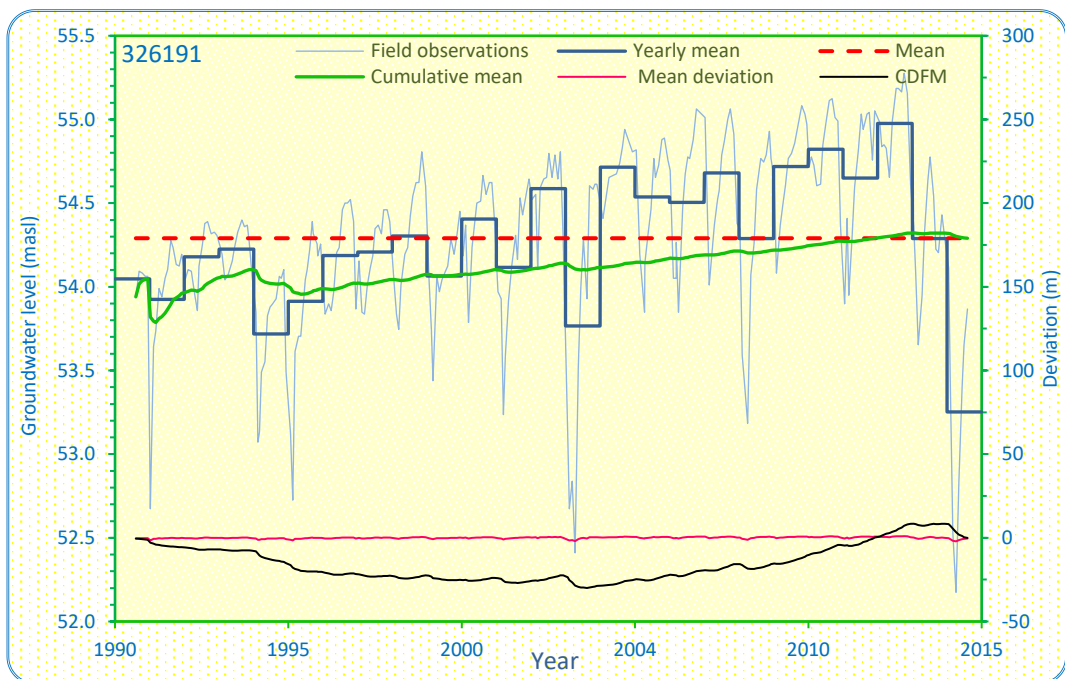
Elevation (masl)	Screen extent (mbgl)	Groundwater level		Area	Trend/comments
		Mean (masl)	STDEV (m)		
50.79	115.95–118.95	53.98	0.25		Steady

Figure C-18. Groundwater level hydrographs for Well 326061.



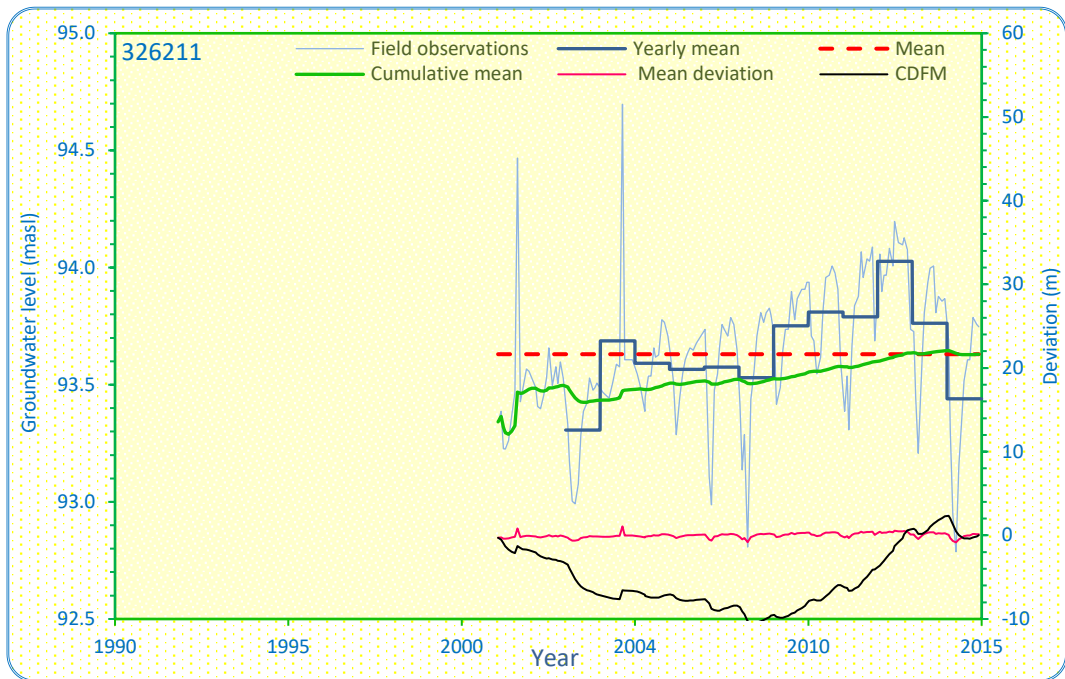
Elevation (masl)	Screen extent (mbgl)	Groundwater level		Area	Trend/comments
		Mean (masl)	STDEV (m)		
64.24	132–135	59.12	0.70		Rising

Figure C-19. Groundwater level hydrographs for Well 326181.



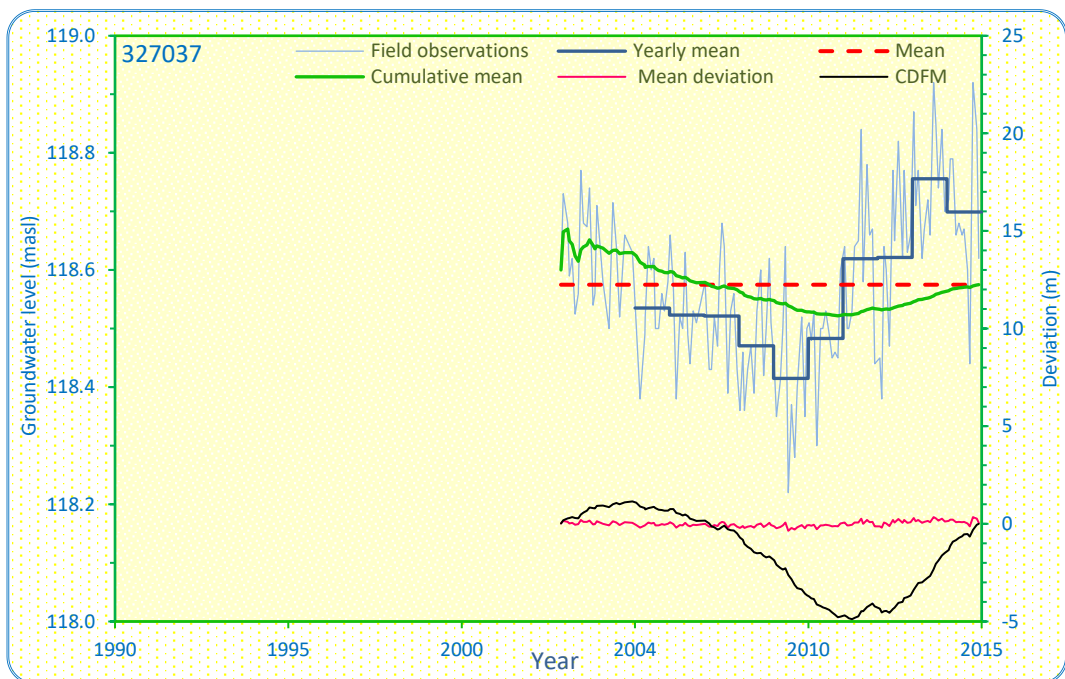
Elevation (masl)	Screen extent (mbgl)	Groundwater level		Area	Trend/comments
		Mean (masl)	STDEV (m)		
49.46	151.75–153.75	54.29	0.52		Steady

Figure C-20. Groundwater level hydrographs for Well 326191.



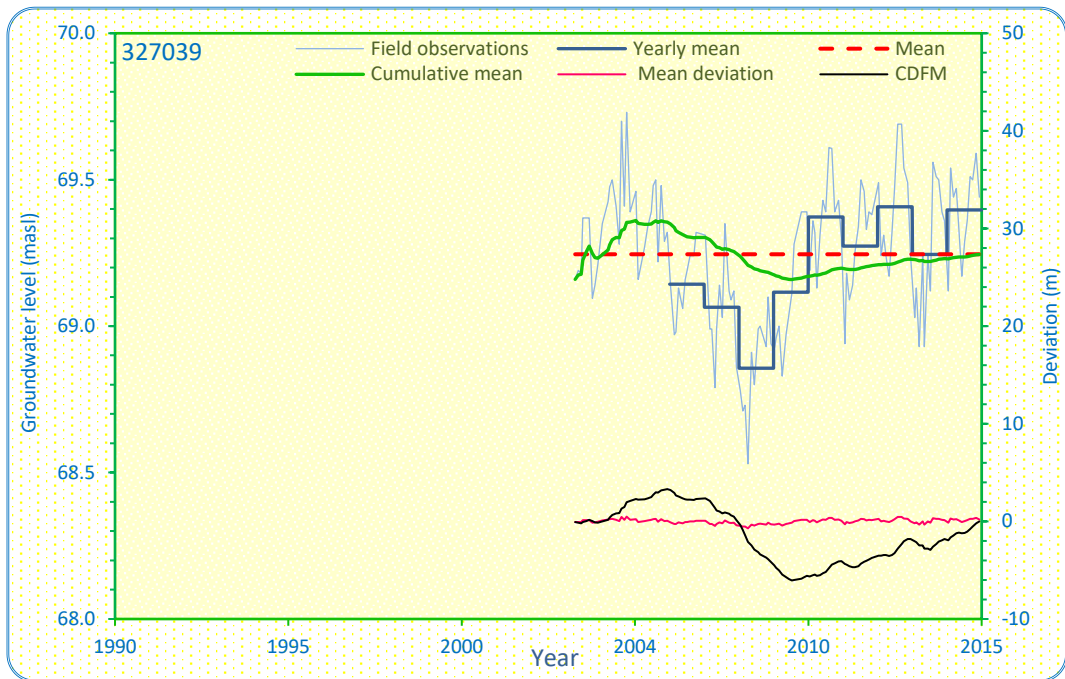
Elevation (masl)	Screen extent (mbgl)	Groundwater level		Area	Trend/comments
		Mean (masl)	STDEV (m)		
111.31	115-118	93.63	0.29		Steady

Figure C-21. Groundwater level hydrographs for Well 326211.



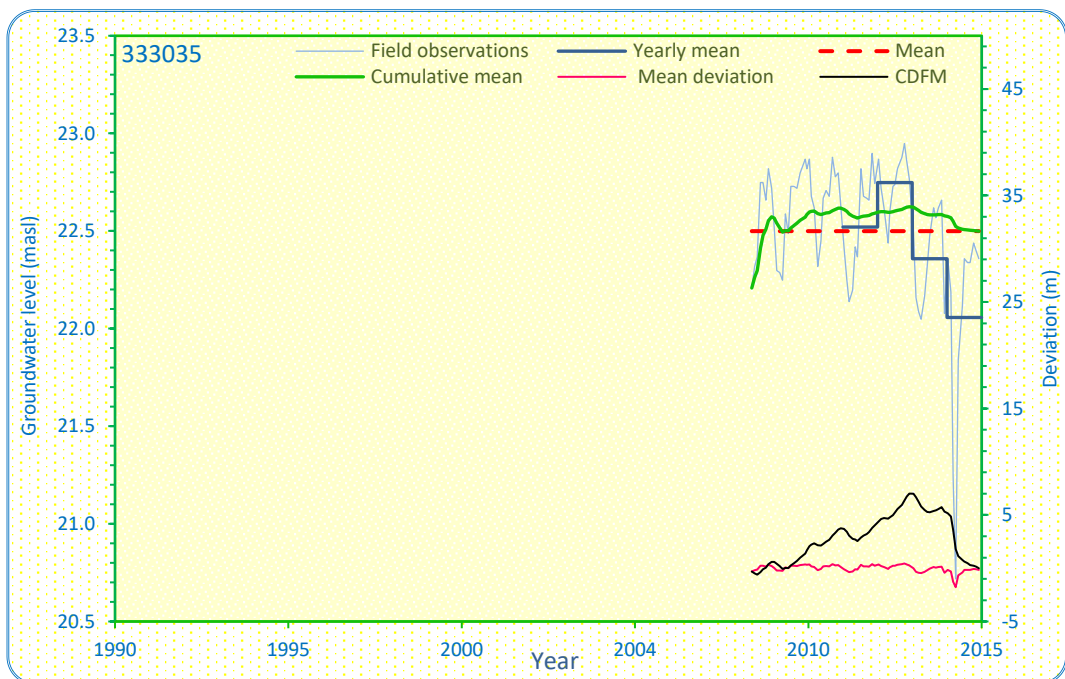
Elevation (masl)	Screen extent (mbgl)	Groundwater level		Area	Trend/comments
		Mean (masl)	STDEV (m)		
159.31	58.1-58.6	118.30	1.85		Steady

Figure C-22. Groundwater level hydrographs for Well 327037.



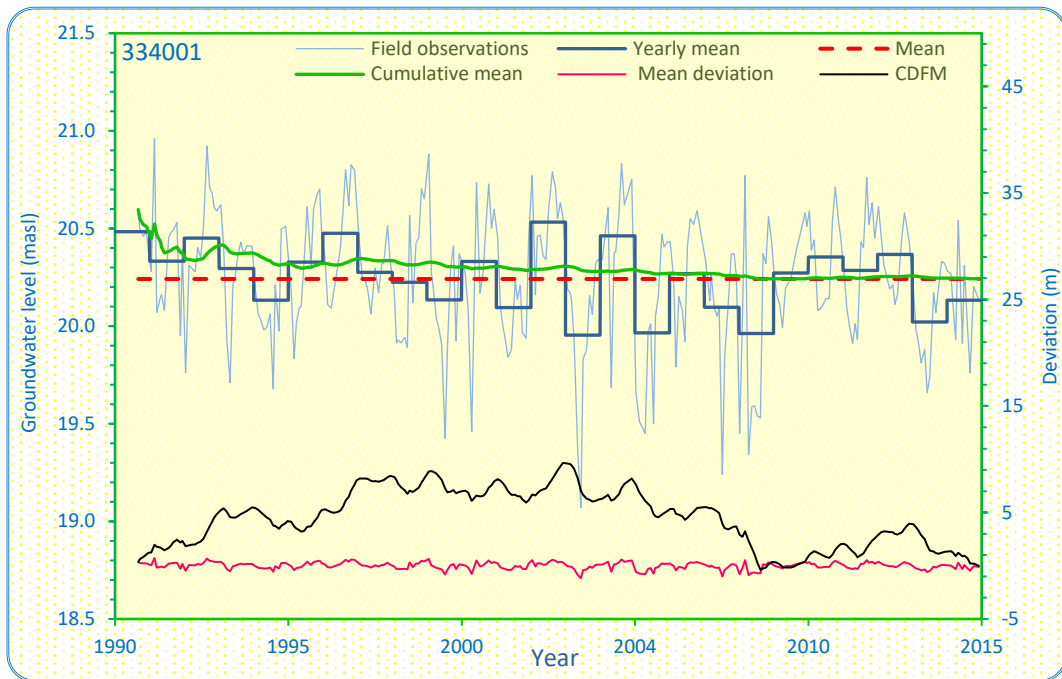
Elevation (masl)	Screen extent (mbgl)	Groundwater level		Area	Trend/comments
		Mean (masl)	STDEV (m)		
123.49	115-117	69.25	0.23		Steady

Figure C-23. Groundwater level hydrographs for Well 327039.



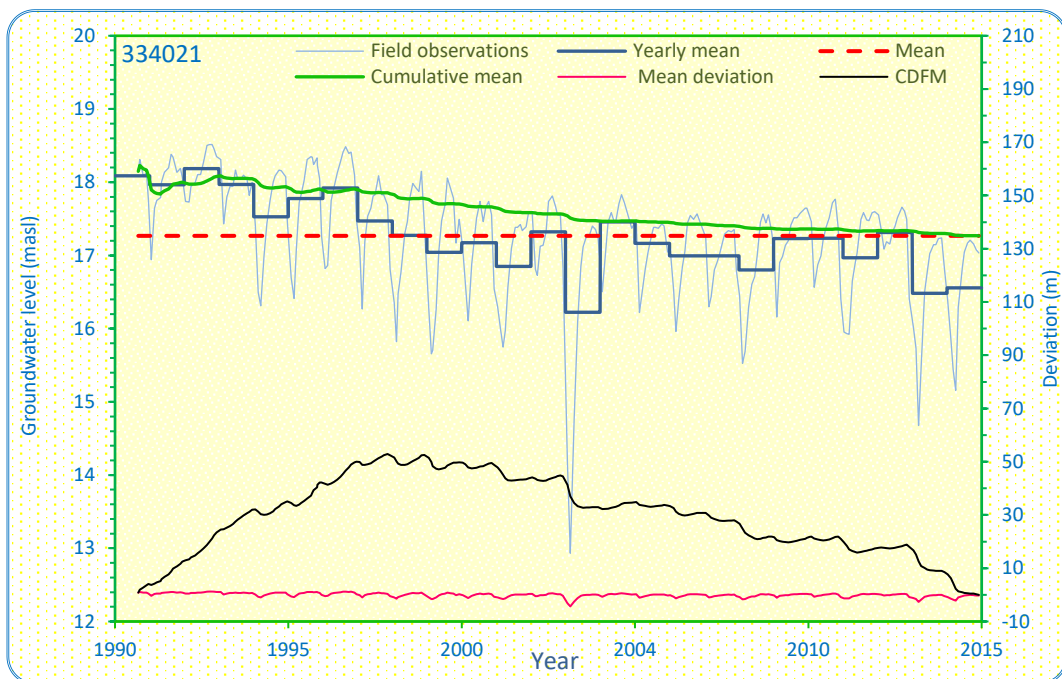
Elevation (masl)	Screen extent (mbgl)	Groundwater level		Area	Trend/comments
		Mean (masl)	STDEV (m)		
35.52	42-45	22.50	0.35		Short record

Figure C-24. Groundwater level hydrographs for Well 333035.



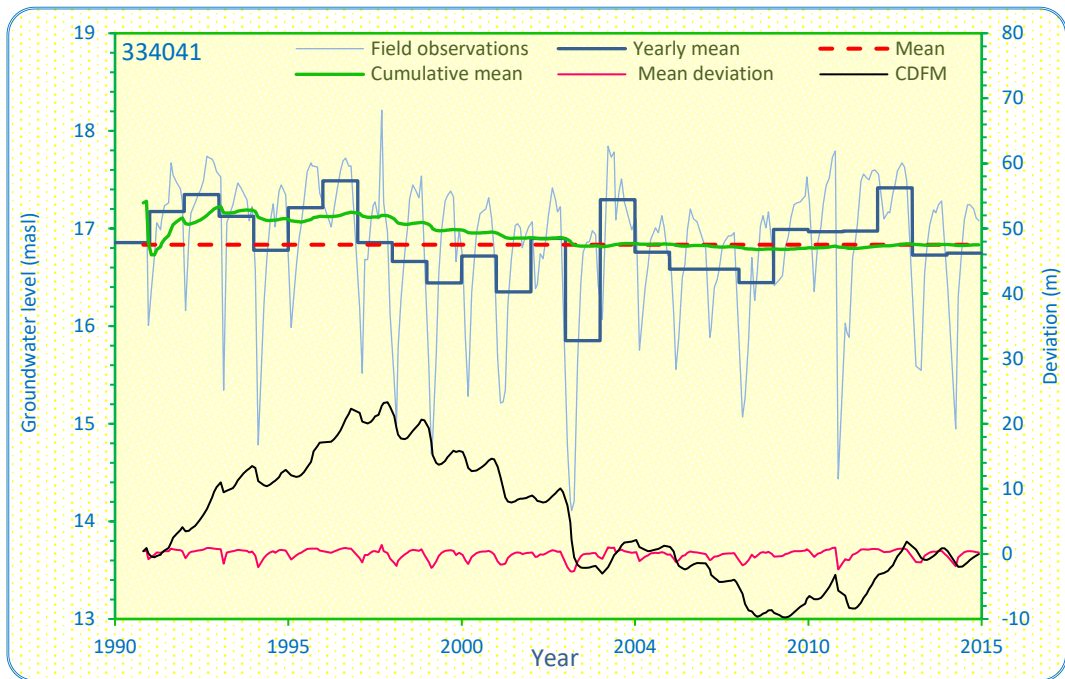
Elevation (masl)	Screen extent (mbgl)	Groundwater level		Area	Trend/comments
		Mean (masl)	STDEV (m)		
23.61	15–18	20.24	0.32		Steady

Figure C-25. Groundwater level hydrographs for Well 334001.



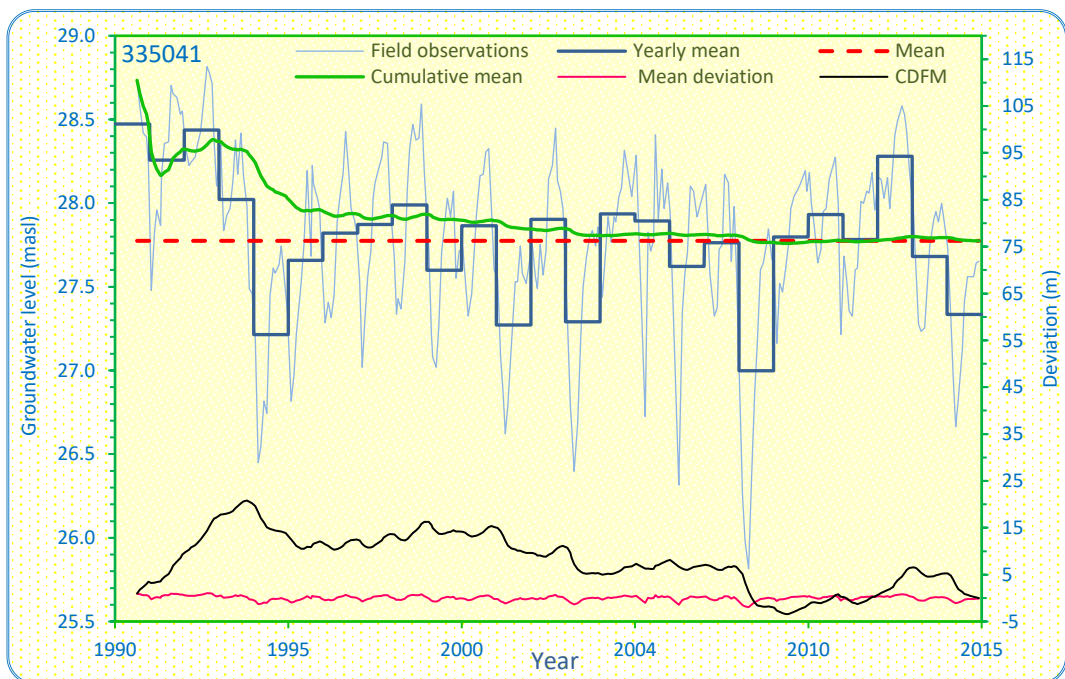
Elevation (masl)	Screen extent (mbgl)	Groundwater level		Area	Trend/comments
		Mean (masl)	STDEV (m)		
12.64	95.5–96.5	17.27	0.78		Declining

Figure C-26. Groundwater level hydrographs for Well 334021.



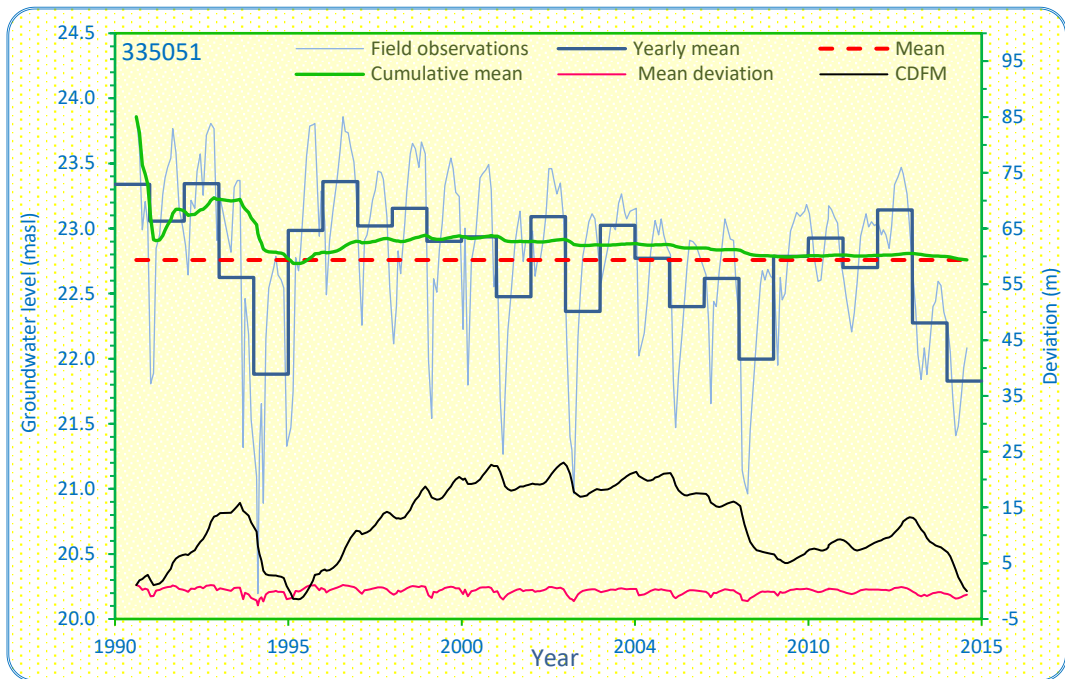
Elevation (masl)	Screen extent (mbgl)	Groundwater level		Area	Trend/comments
		Mean (masl)	STDEV (m)		
12.67	95.3-99	16.83	0.74		Steady

Figure C-27. Groundwater level hydrographs for Well 334041.



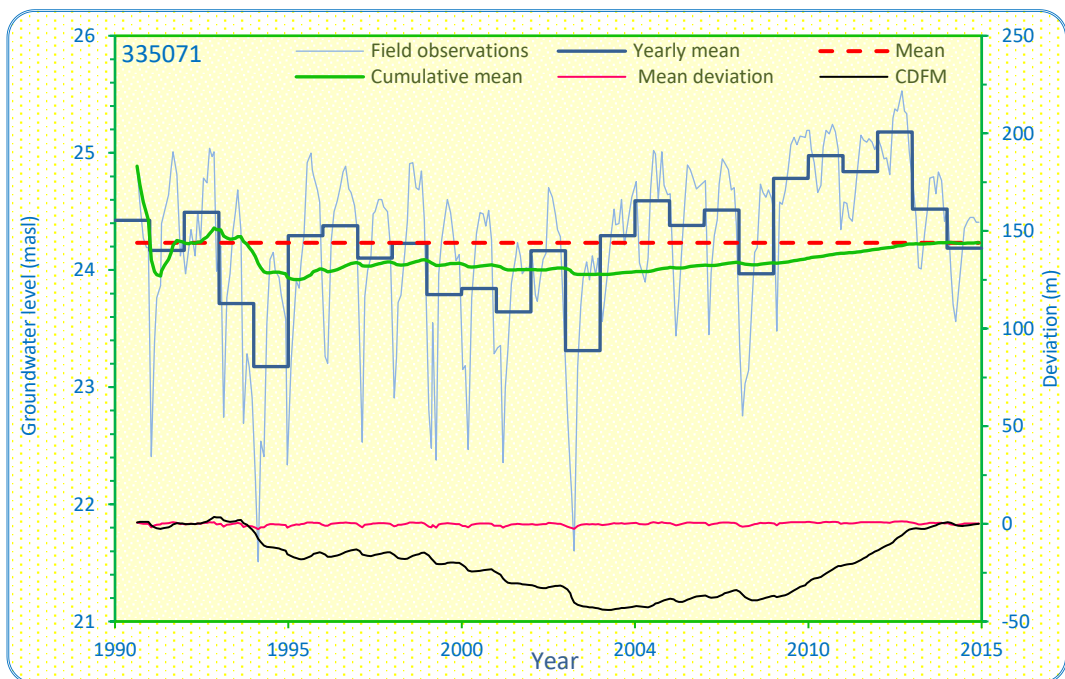
Elevation (masl)	Screen extent (mbgl)	Groundwater level		Area	Trend/comments
		Mean (masl)	STDEV (m)		
21.44	151.3-155.3	27.77	0.52		Steady

Figure C-28. Groundwater level hydrographs for Well 335041.



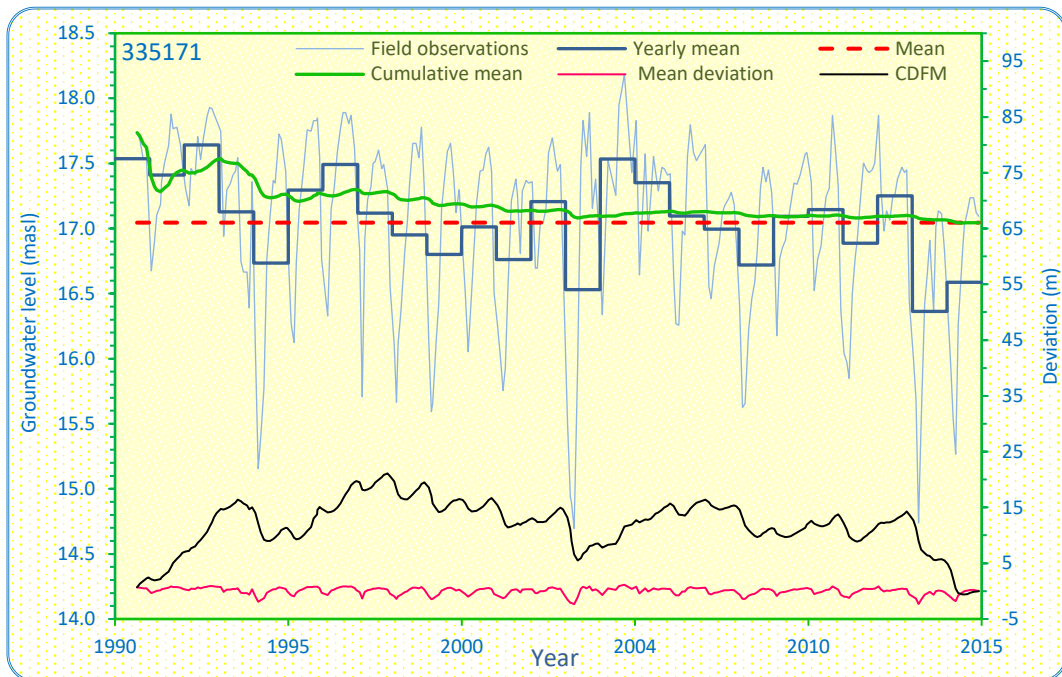
Elevation (masl)	Screen extent (mbgl)	Groundwater level		Area	Trend/comments
		Mean (masl)	STDEV (m)		
16.83	123-126	22.76	0.65		Steady

Figure C-29. Groundwater level hydrographs for Well 335051.



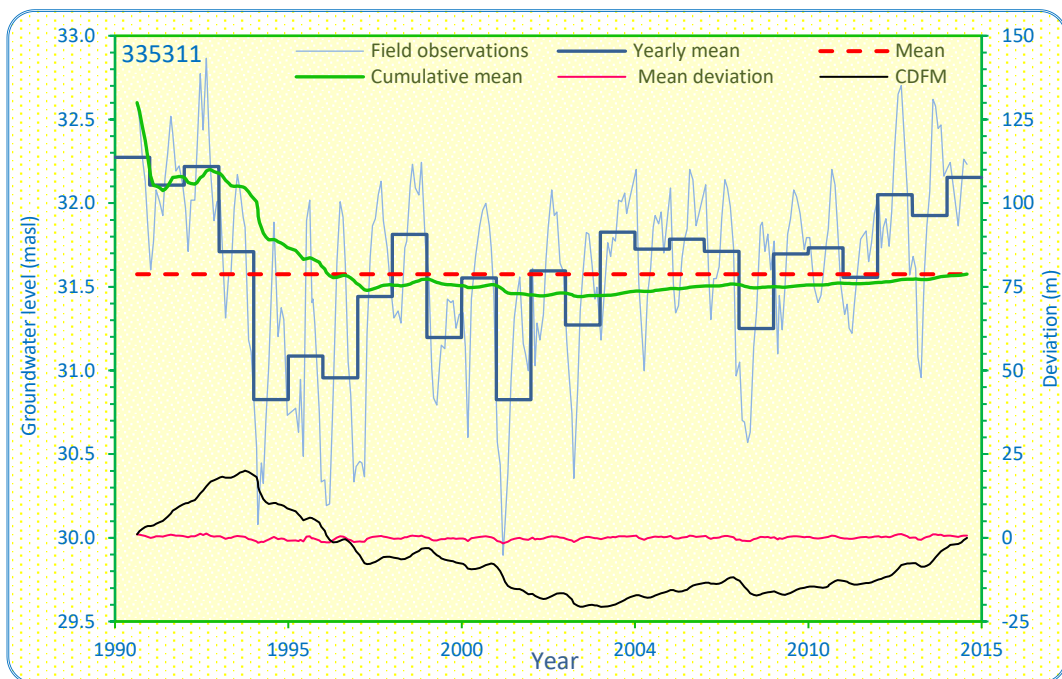
Elevation (masl)	Screen extent (mbgl)	Groundwater level		Area	Trend/comments
		Mean (masl)	STDEV (m)		
17.74	88-91	24.23	0.73		Steady

Figure C-30. Groundwater level hydrographs for Well 335071.



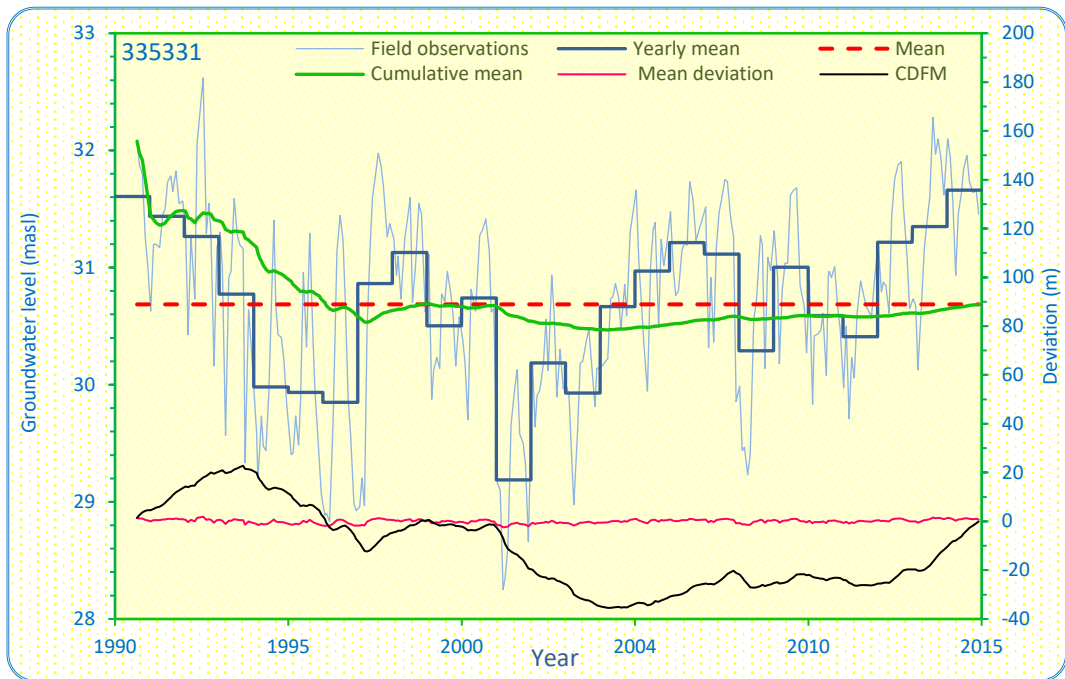
Elevation (masl)	Screen extent (mbgl)	Groundwater level		Area	Trend/comments
		Mean (masl)	STDEV (m)		
13.77	65.63–68.63	17.05	0.66		Steady

Figure C–31. Groundwater level hydrographs for Well 335171.



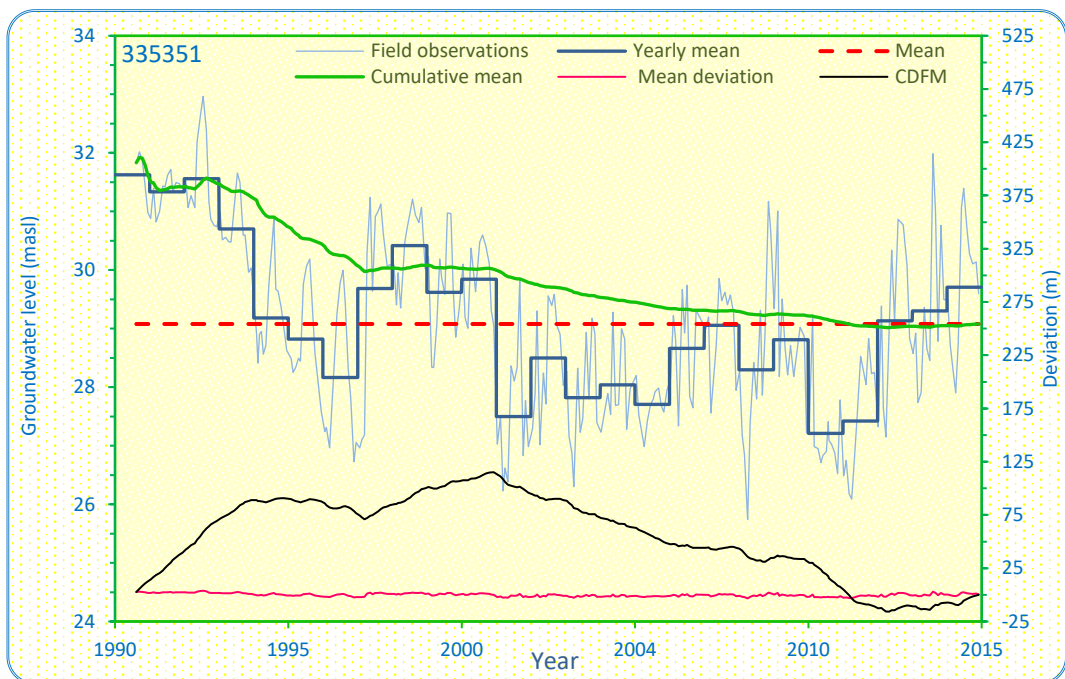
Elevation (masl)	Screen extent (mbgl)	Groundwater level		Area	Trend/comments
		Mean (masl)	STDEV (m)		
28.24	82–85	31.57	0.57		Steady

Figure C–32. Groundwater level hydrographs for Well 335311.



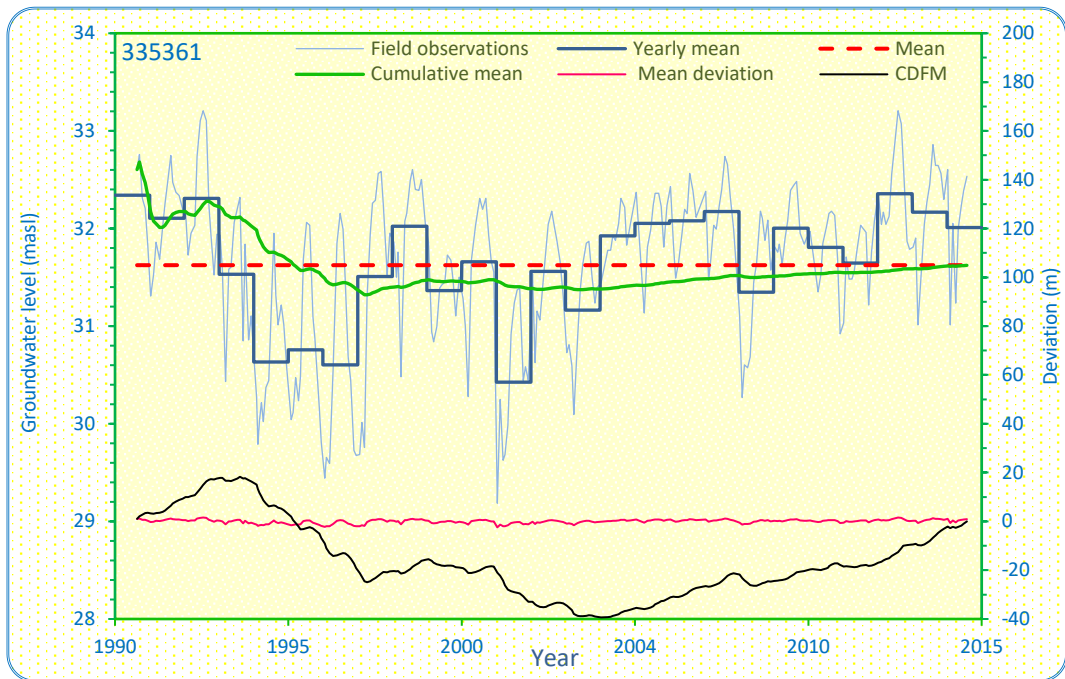
Elevation (masl)	Screen extent (mbgl)	Groundwater level		Area	Trend/comments
		Mean (masl)	STDEV (m)		
21.96	139–141	30.69	0.83		Steady

Figure C–33. Groundwater level hydrographs for Well 335331.



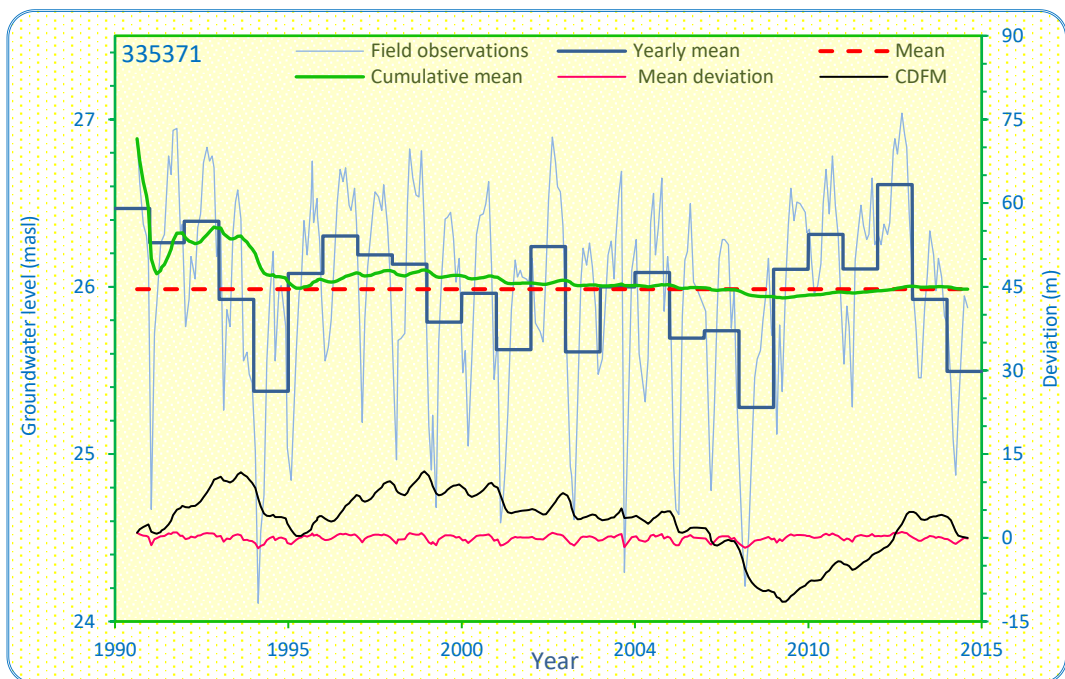
Elevation (masl)	Screen extent (mbgl)	Groundwater level		Area	Trend/comments
		Mean (masl)	STDEV (m)		
18.31	168–171	29.08	1.52		Declining

Figure C–34. Groundwater level hydrographs for Well 335351.



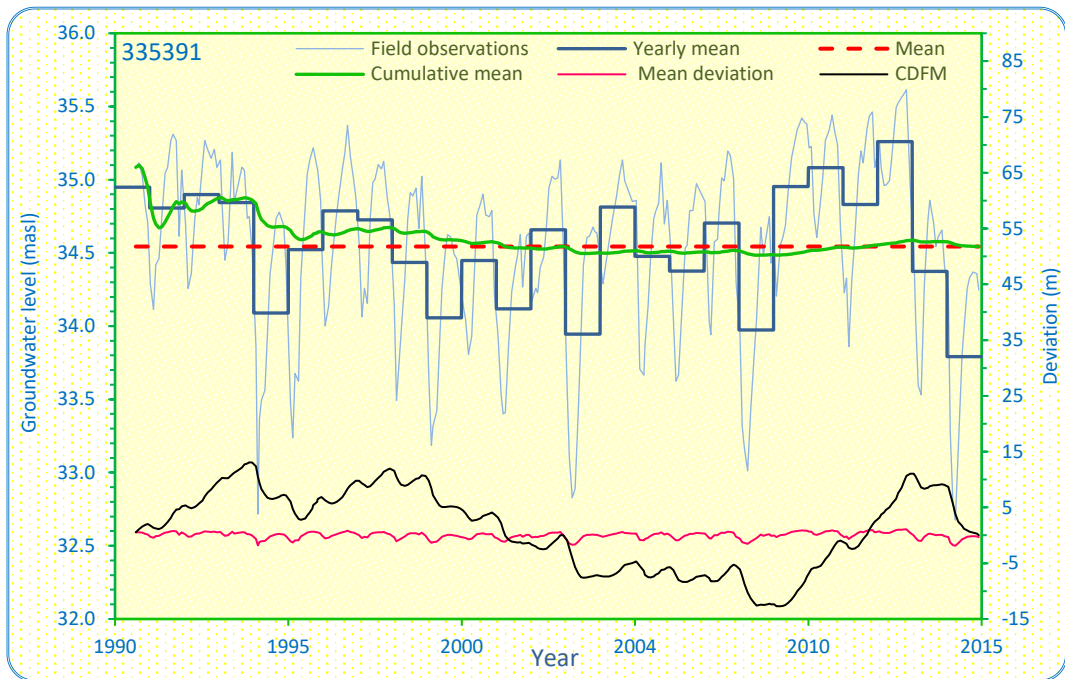
Elevation (masl)	Screen extent (mbgl)	Groundwater level		Area	Trend/comments
		Mean (masl)	STDEV (m)		
23.87	109–112	31.62	0.80		Steady

Figure C–35. Groundwater level hydrographs for Well 335361.



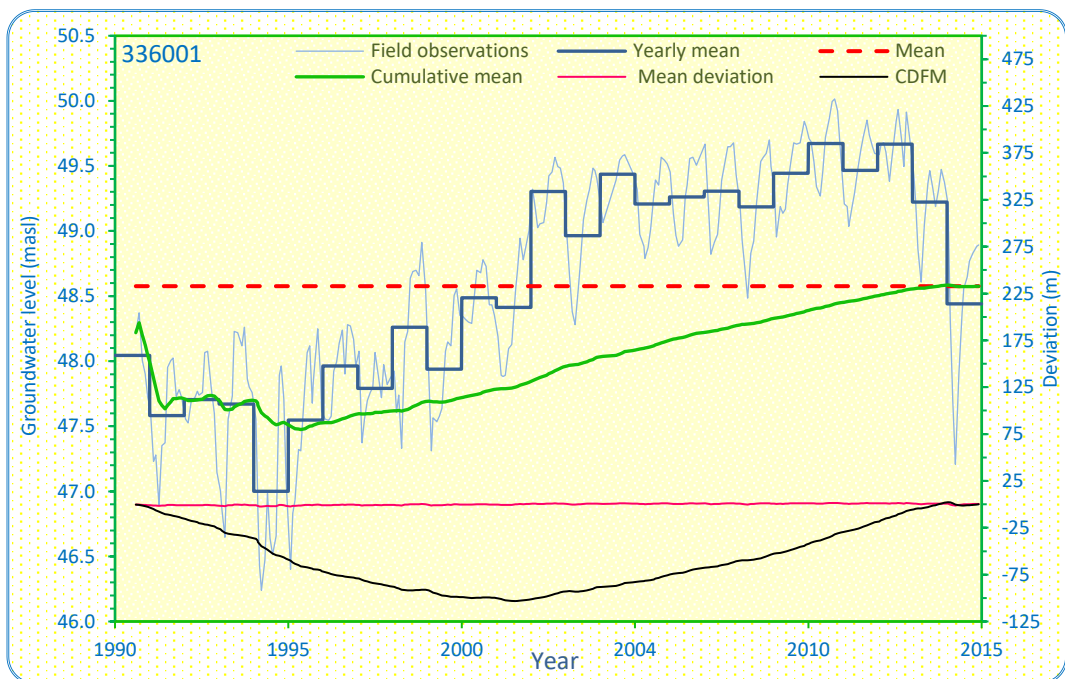
Elevation (masl)	Screen extent (mbgl)	Groundwater level		Area	Trend/comments
		Mean (masl)	STDEV (m)		
20.66	108–111	25.99	0.59		Steady

Figure C–36. Groundwater level hydrographs for Well 335371.



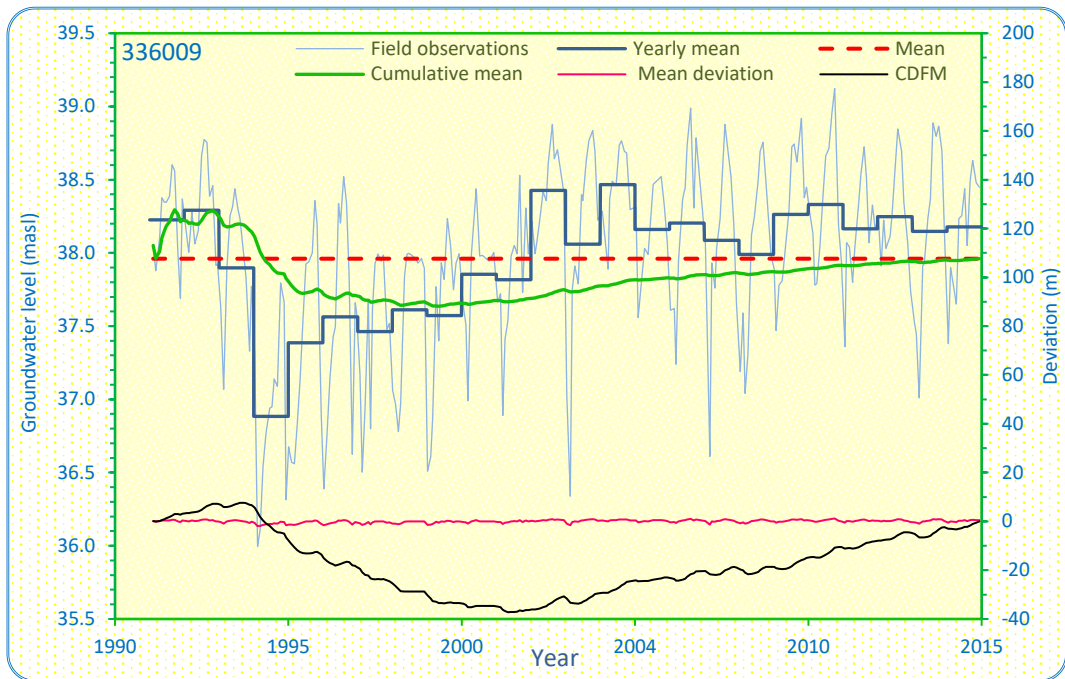
Elevation (masl)	Screen extent (mbgl)	Groundwater level		Area	Trend/comments
		Mean (masl)	STDEV (m)		
31.43	71.3–73.3	34.54	0.60		Steady

Figure C–37. Groundwater level hydrographs for Well 335391.



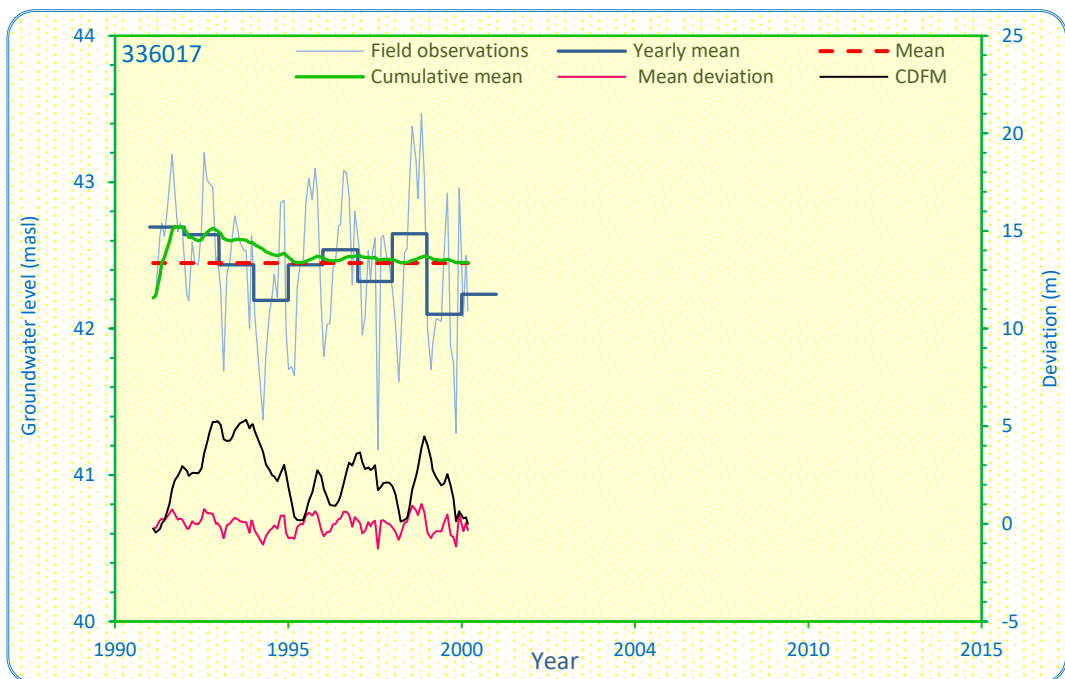
Elevation (masl)	Screen extent (mbgl)	Groundwater level		Area	Trend/comments
		Mean (masl)	STDEV (m)		
43.68	122–125	48.58	0.88		Rising

Figure C–38. Groundwater level hydrographs for Well 336001.



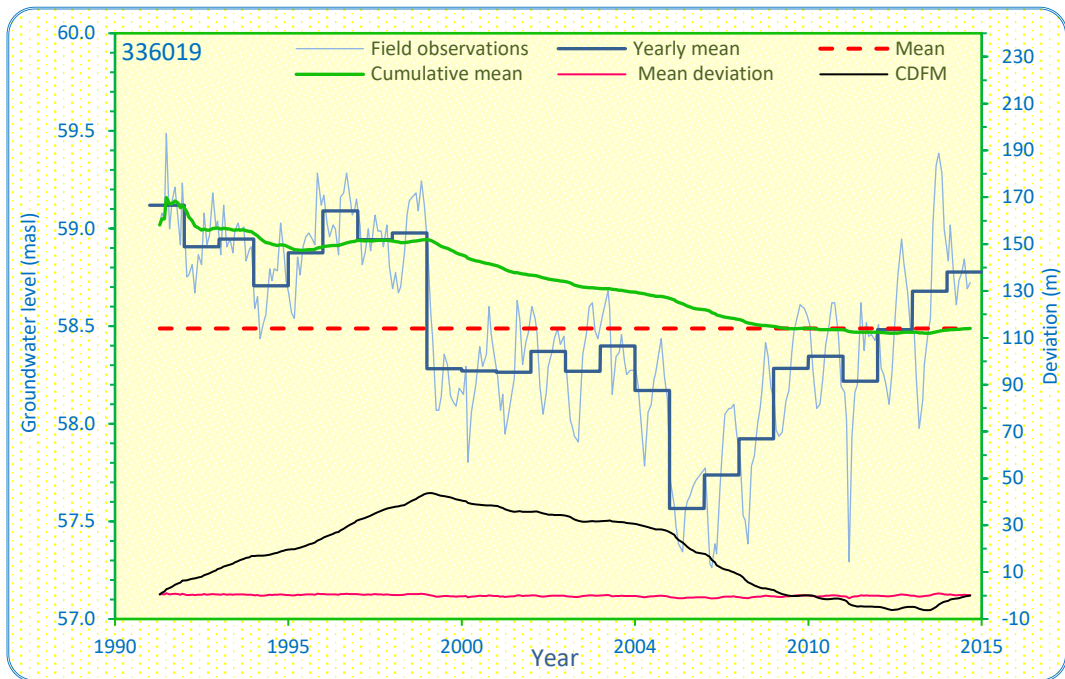
Elevation (masl)	Screen extent (mbgl)	Groundwater level		Area	Trend/comments
		Mean (masl)	STDEV (m)		
38.01	61.3–64.3	37.96	0.61		Steady

Figure C–39. Groundwater level hydrographs for Well 336009.



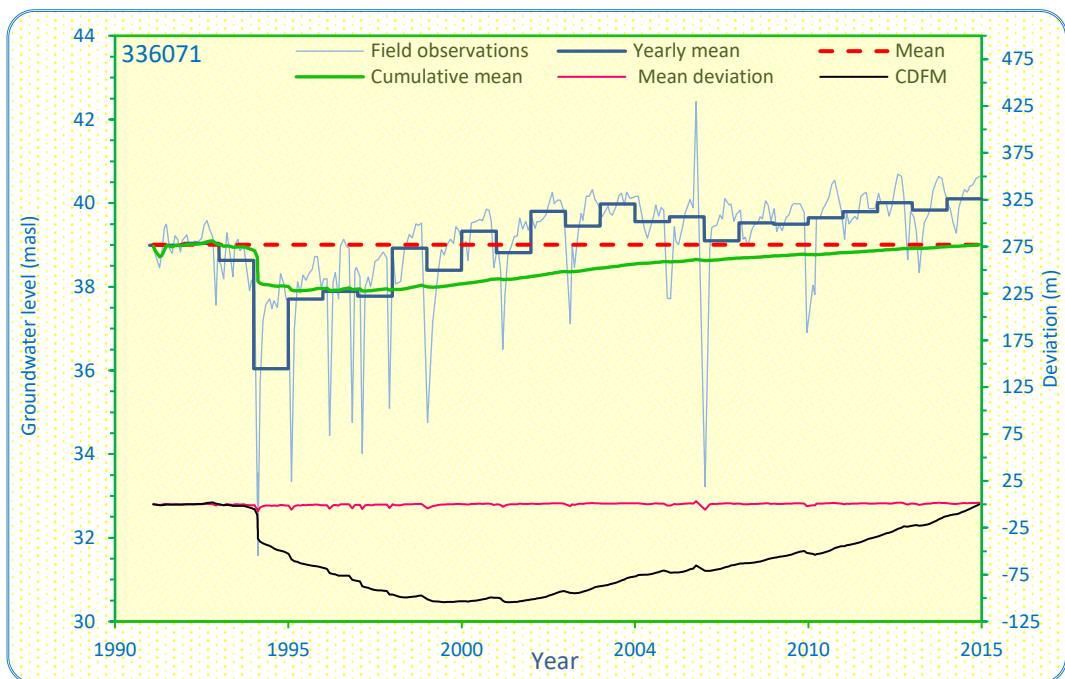
Elevation (masl)	Screen extent (mbgl)	Groundwater level		Area	Trend/comments
		Mean (masl)	STDEV (m)		
44.44	57–60	42.45	0.46		Old, short record

Figure C–40. Groundwater level hydrographs for Well 336017.



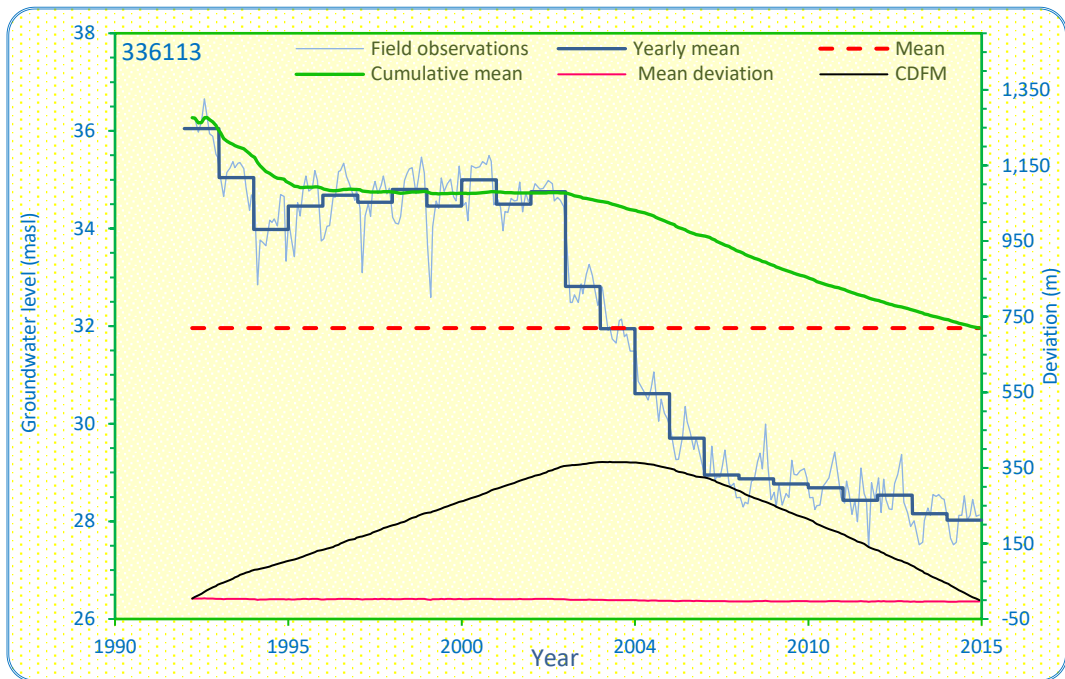
Elevation (masl)	Screen extent (mbgl)	Groundwater level		Area	Trend/comments
		Mean (masl)	STDEV (m)		
48.61	57.2–60.2	58.49	0.47		Steady

Figure C-41. Groundwater level hydrographs for Well 336019.



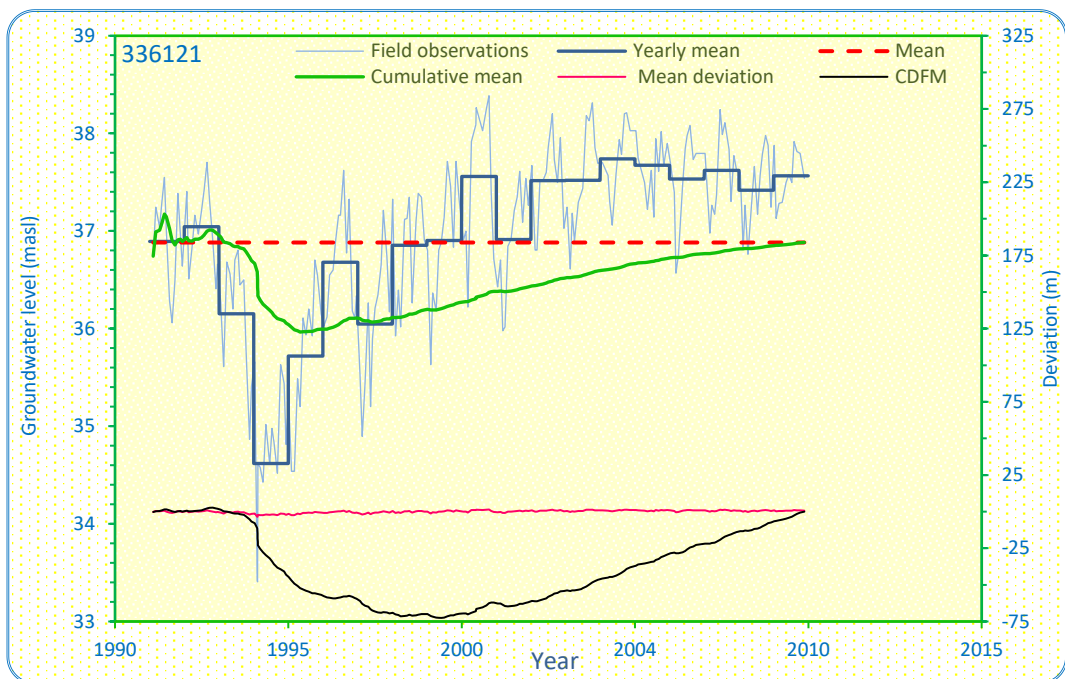
Elevation (masl)	Screen extent (mbgl)	Groundwater level		Area	Trend/comments
		Mean (masl)	STDEV (m)		
28.43	81.3–84.3	39.01	1.43		Rising

Figure C-42. Groundwater level hydrographs for Well 336071.



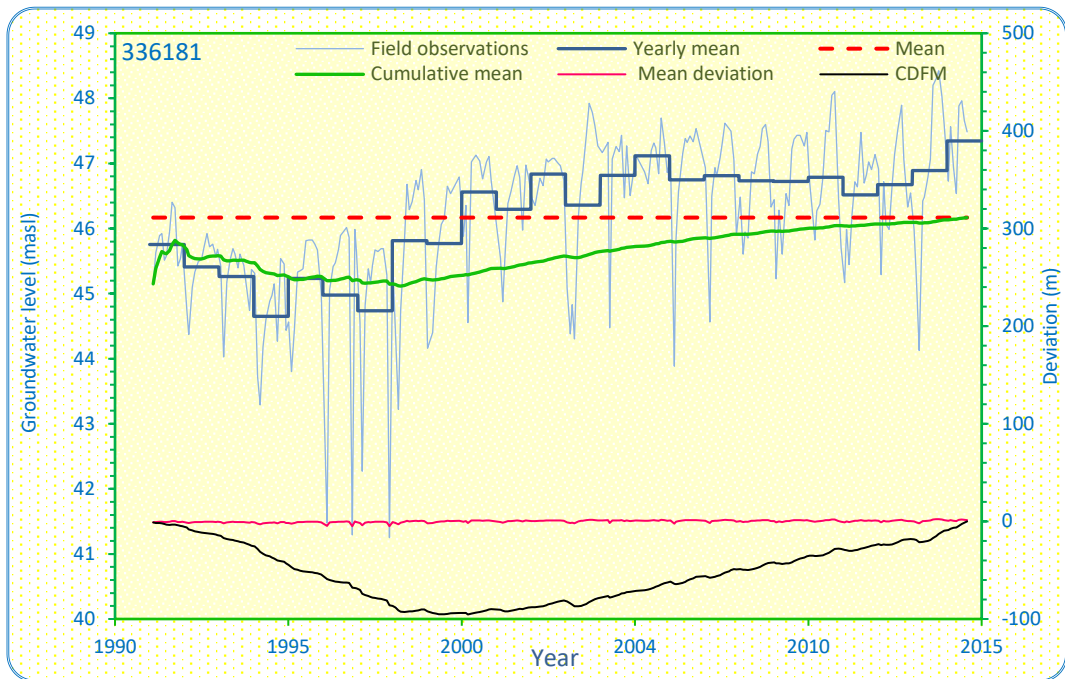
Elevation (masl)	Screen extent (mbgl)	Groundwater level		Area	Trend/comments
		Mean (masl)	STDEV (m)		
34.49	32–34	31.96	2.91		Declining

Figure C-43. Groundwater level hydrographs for Well 336113.



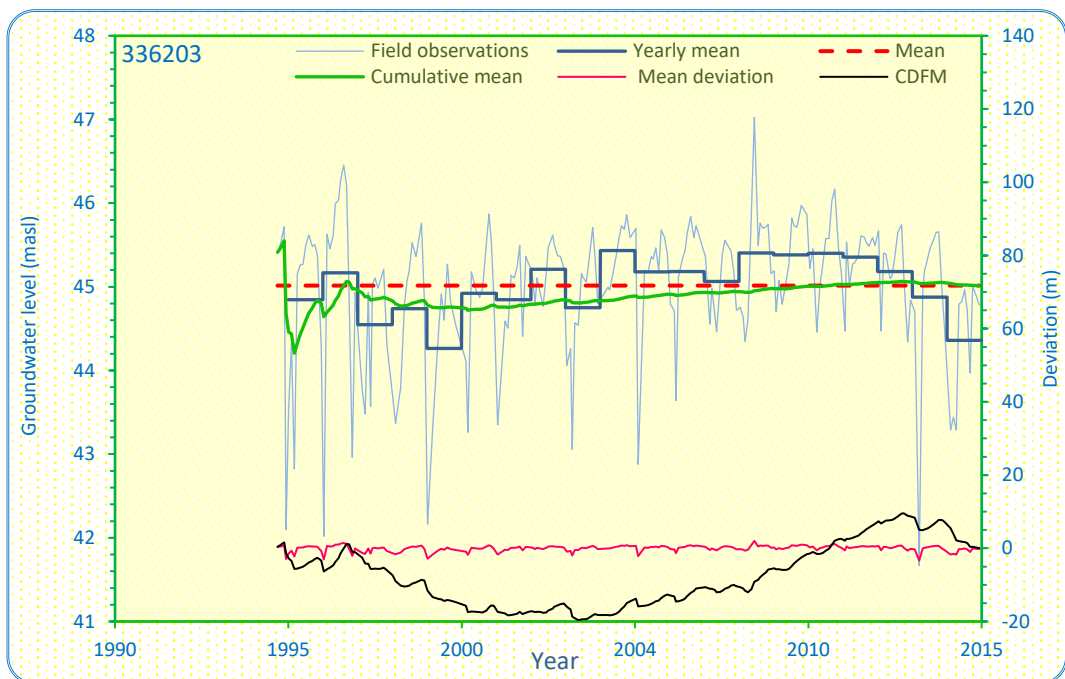
Elevation (masl)	Screen extent (mbgl)	Groundwater level		Area	Trend/comments
		Mean (masl)	STDEV (m)		
29.30	65.63–68.63	36.88	0.99		Steady

Figure C-44. Groundwater level hydrographs for Well 336121.



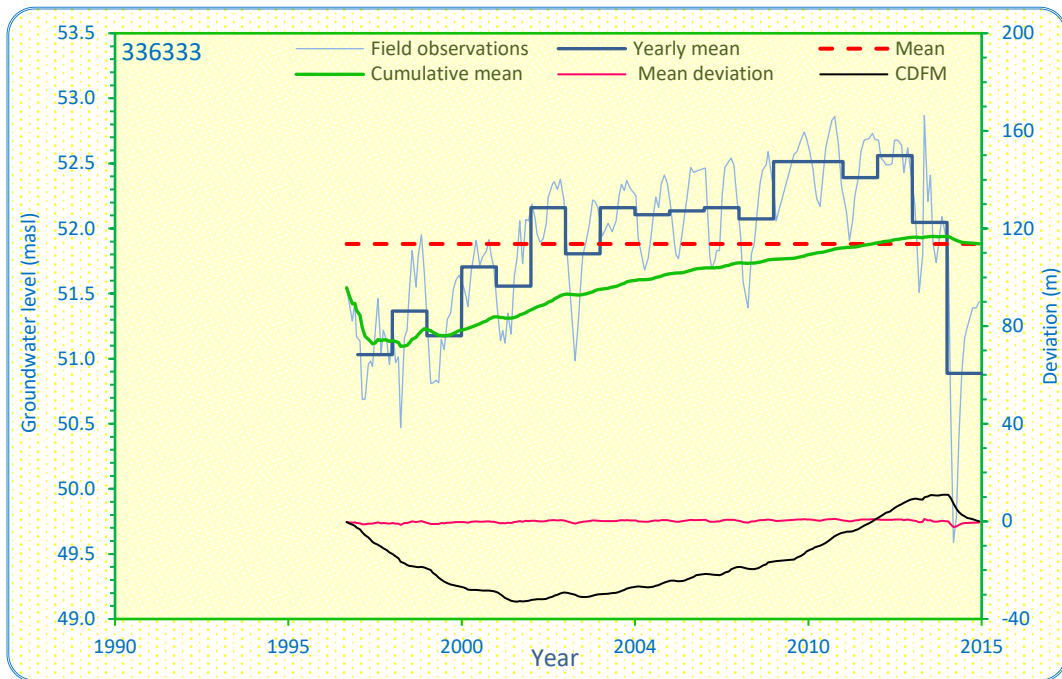
Elevation (masl)	Screen extent (mbgl)	Groundwater level		Area	Trend/comments
		Mean (masl)	STDEV (m)		
36.25	69.1–72.1	46.17	1.17		Steady

Figure C–45. Groundwater level hydrographs for Well 336181.



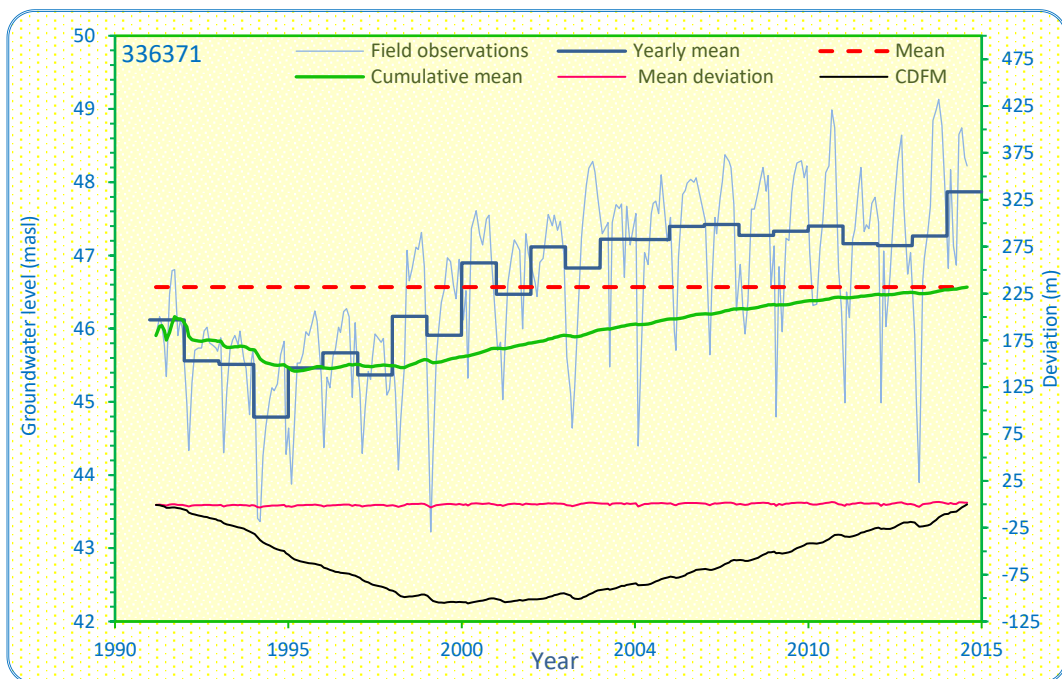
Elevation (masl)	Screen extent (mbgl)	Groundwater level		Area	Trend/comments
		Mean (masl)	STDEV (m)		
44.77	60.5–63	45.01	0.80		Steady

Figure C–46. Groundwater level hydrographs for Well 336203.



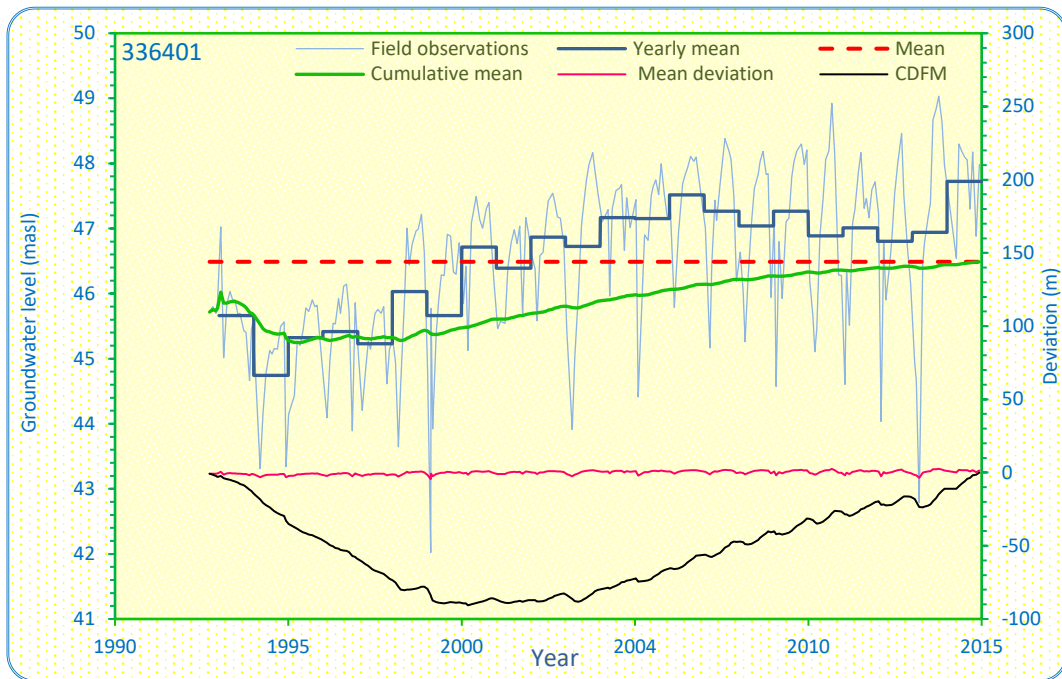
Elevation (masl)	Screen extent (mbgl)	Groundwater level		Area	Trend/comments
		Mean (masl)	STDEV (m)		
57.79	93-96	51.88	0.60		Rising

Figure C-47. Groundwater level hydrographs for Well 336333.



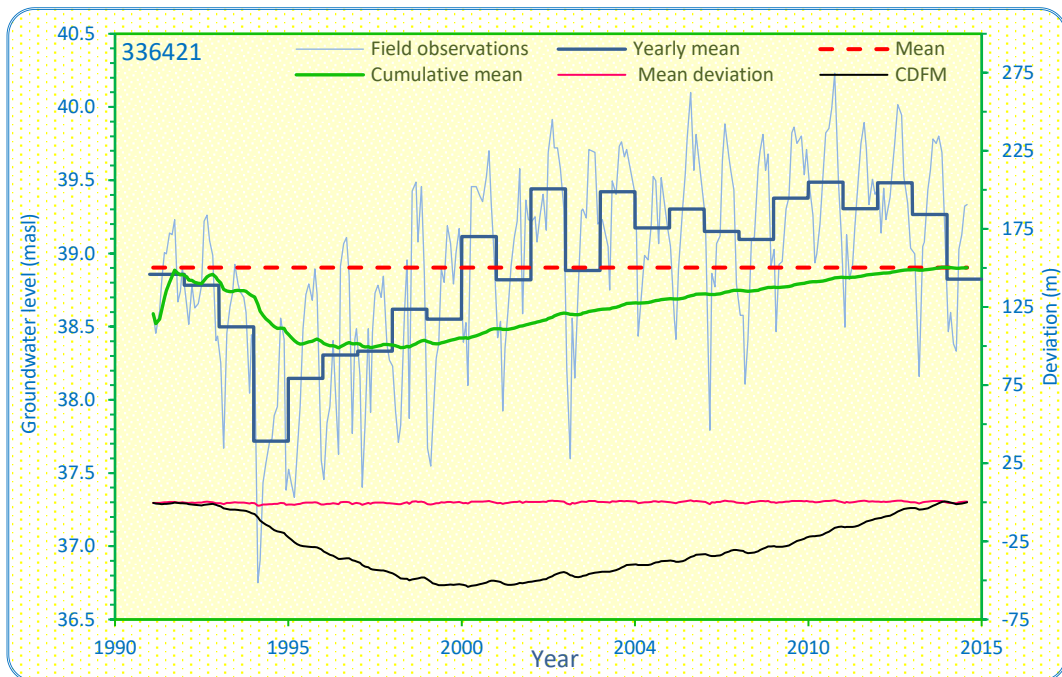
Elevation (masl)	Screen extent (mbgl)	Groundwater level		Area	Trend/comments
		Mean (masl)	STDEV (m)		
39.08	51.8-54.8	46.57	1.20		Rising

Figure C-48. Groundwater level hydrographs for Well 336371.



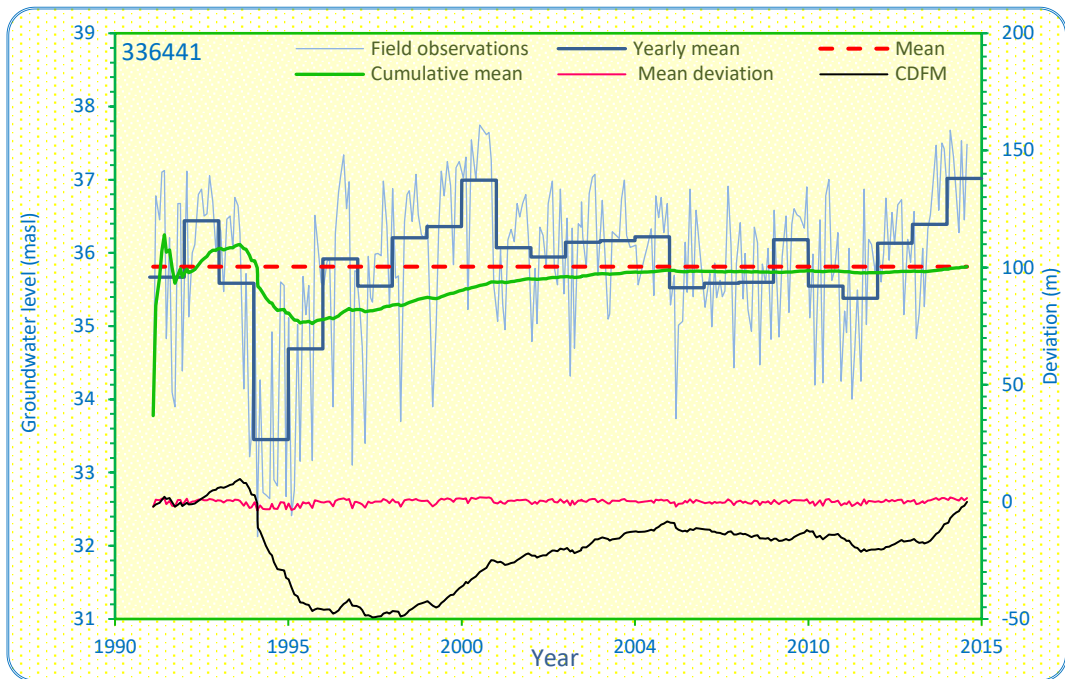
Elevation (masl)	Screen extent (mbgl)	Groundwater level		Area	Trend/comments
		Mean (masl)	STDEV (m)		
41.76	42.7–45.7	46.49	1.25		Rising

Figure C-49. Groundwater level hydrographs for Well 336401.



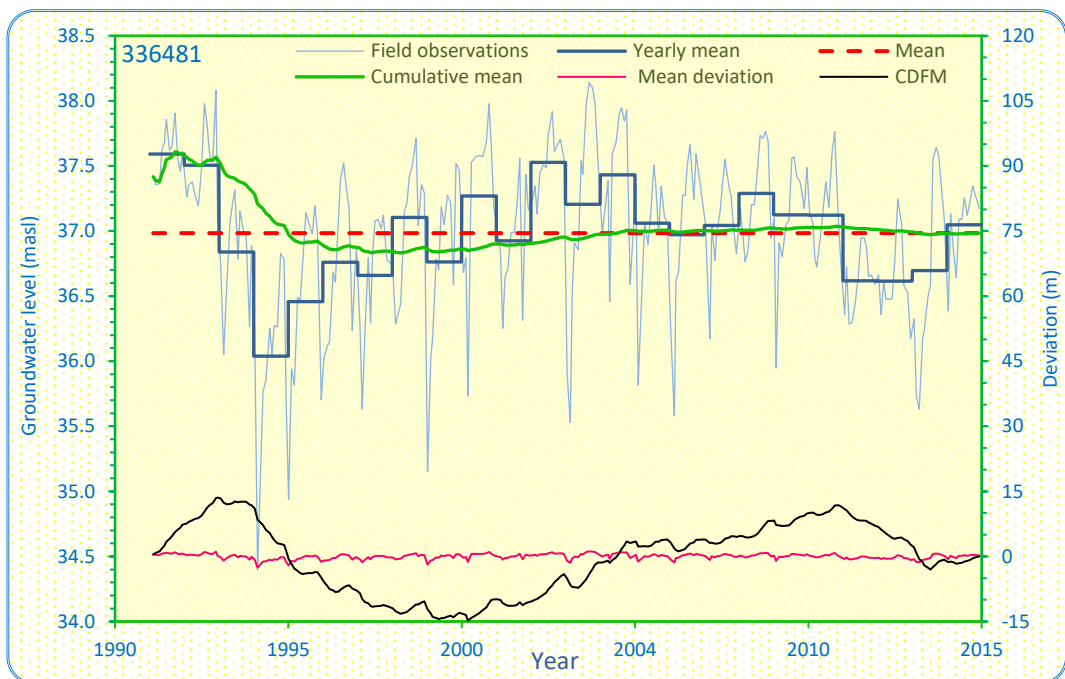
Elevation (masl)	Screen extent (mbgl)	Groundwater level		Area	Trend/comments
		Mean (masl)	STDEV (m)		
36.70	68–71	38.90	0.66		Rising

Figure C-50. Groundwater level hydrographs for Well 336421.



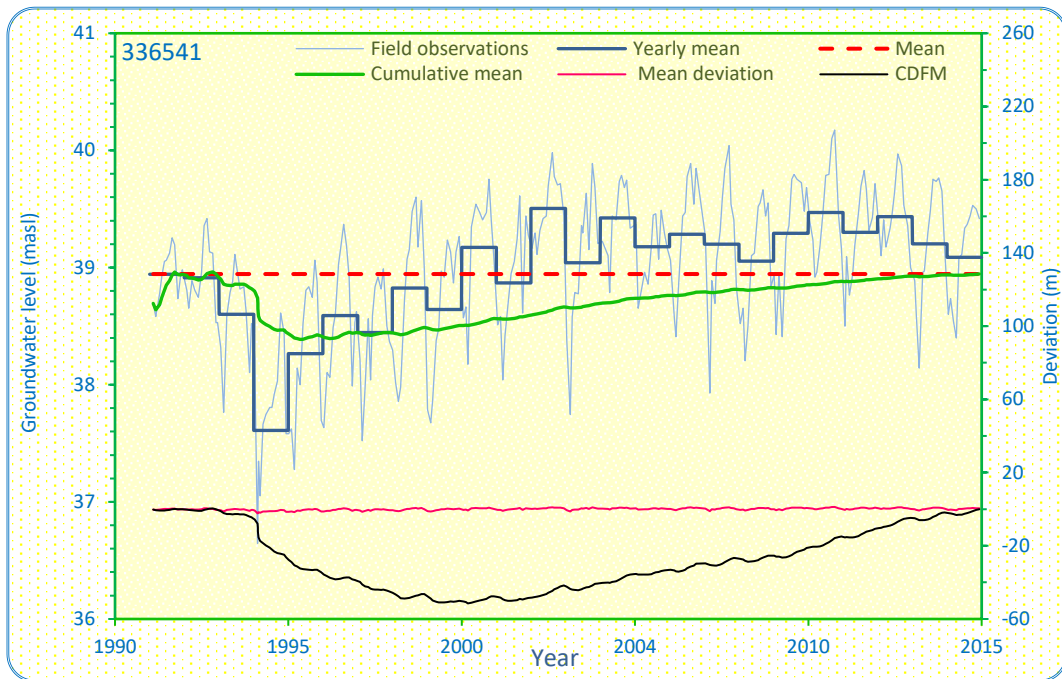
Elevation (masl)	Screen extent (mbgl)	Groundwater level		Area	Trend/comments
		Mean (masl)	STDEV (m)		
29.84	69–72	35.81	1.15		Steady

Figure C-51. Groundwater level hydrographs for Well 336441.



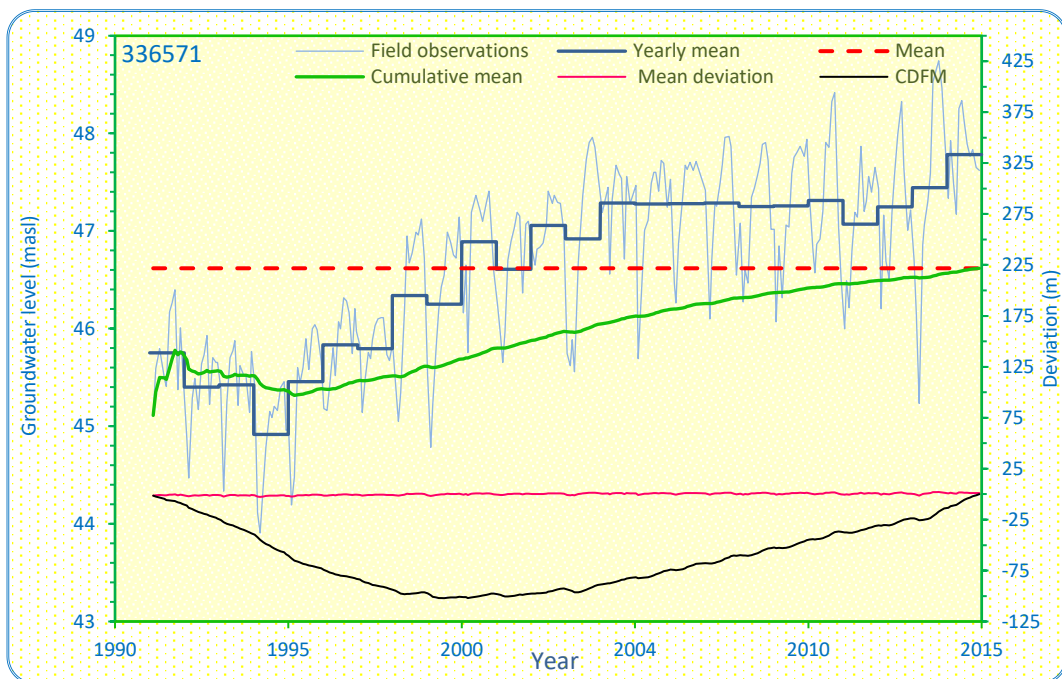
Elevation (masl)	Screen extent (mbgl)	Groundwater level		Area	Trend/comments
		Mean (masl)	STDEV (m)		
33.07	41–48	36.98	0.60		Steady

Figure C-52. Groundwater level hydrographs for Well 336481.



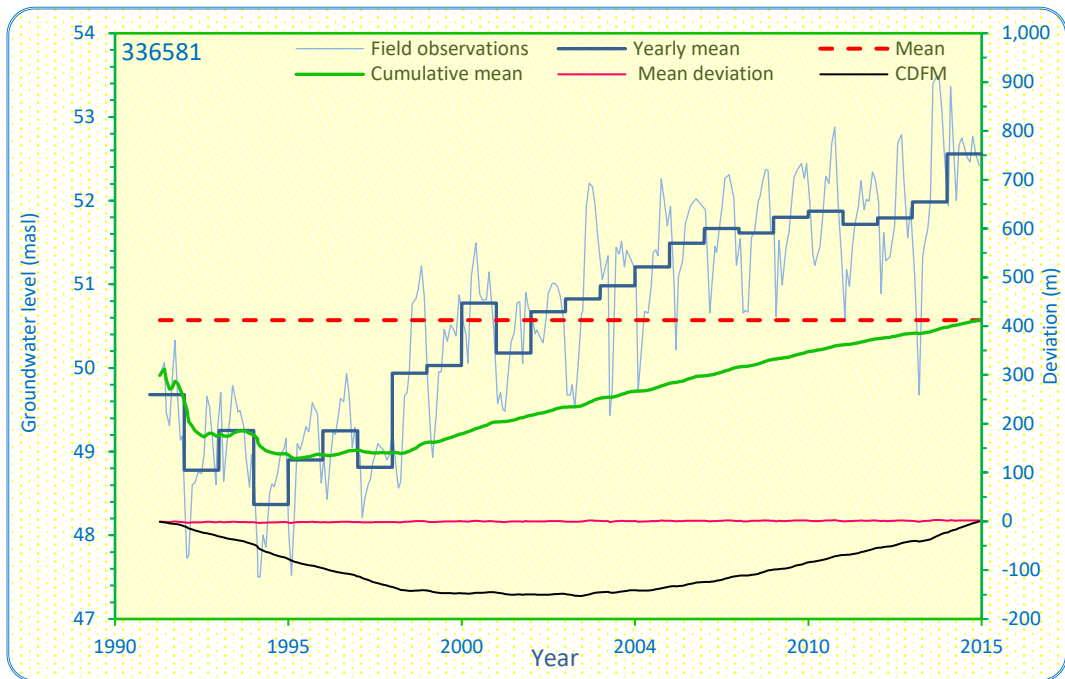
Elevation (masl)	Screen extent (mbgl)	Groundwater level		Area	Trend/comments
		Mean (masl)	STDEV (m)		
36.98	72.5–75.5	38.94	0.65		Rising

Figure C-53. Groundwater level hydrographs for Well 336541.



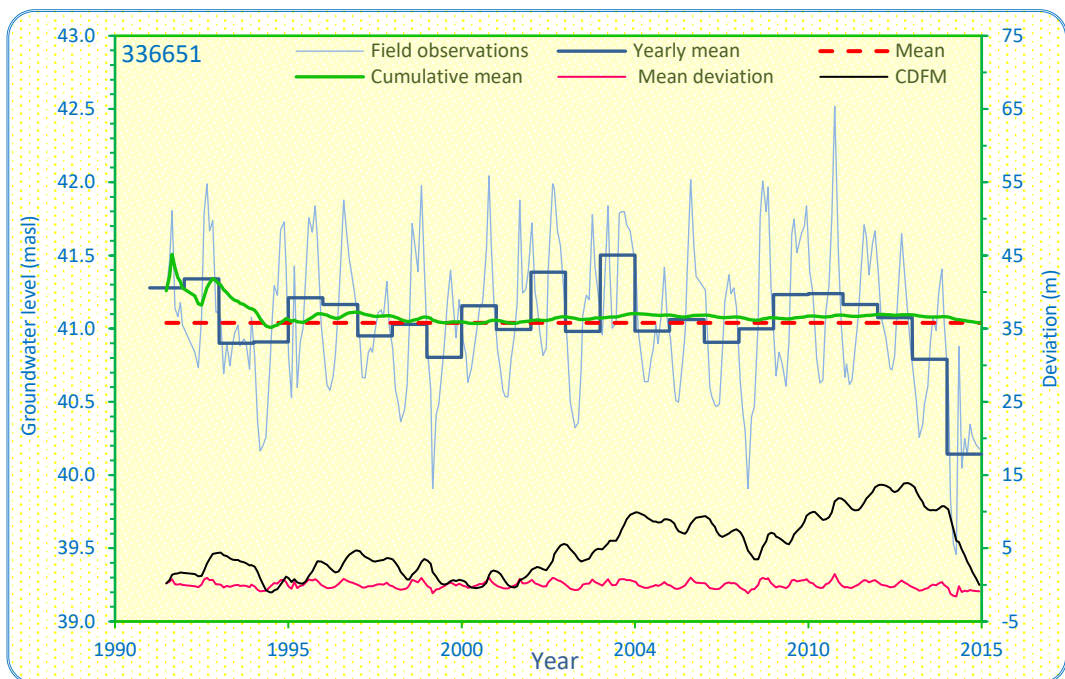
Elevation (masl)	Screen extent (mbgl)	Groundwater level		Area	Trend/comments
		Mean (masl)	STDEV (m)		
43.56	46–49	46.62	0.99		Rising

Figure C-54. Groundwater level hydrographs for Well 336571.



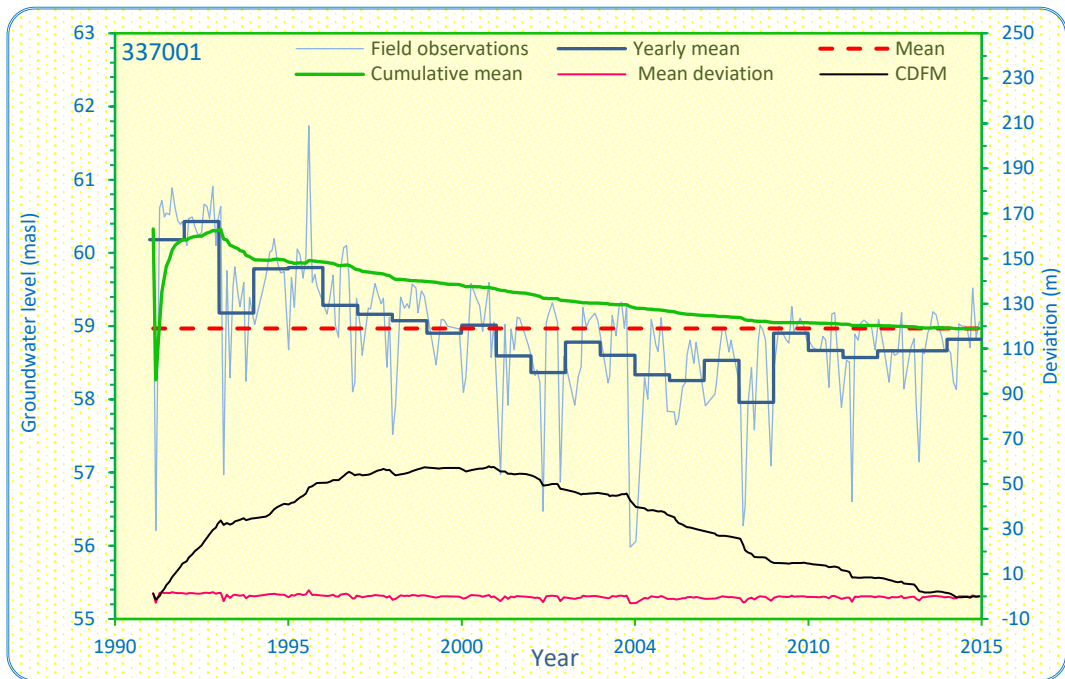
Elevation (masl)	Screen extent (mbgl)	Groundwater level		Area	Trend/comments
		Mean (masl)	STDEV (m)		
43.83	118.8–120.3	50.57	1.37		Rising

Figure C-55. Groundwater level hydrographs for Well 336581.



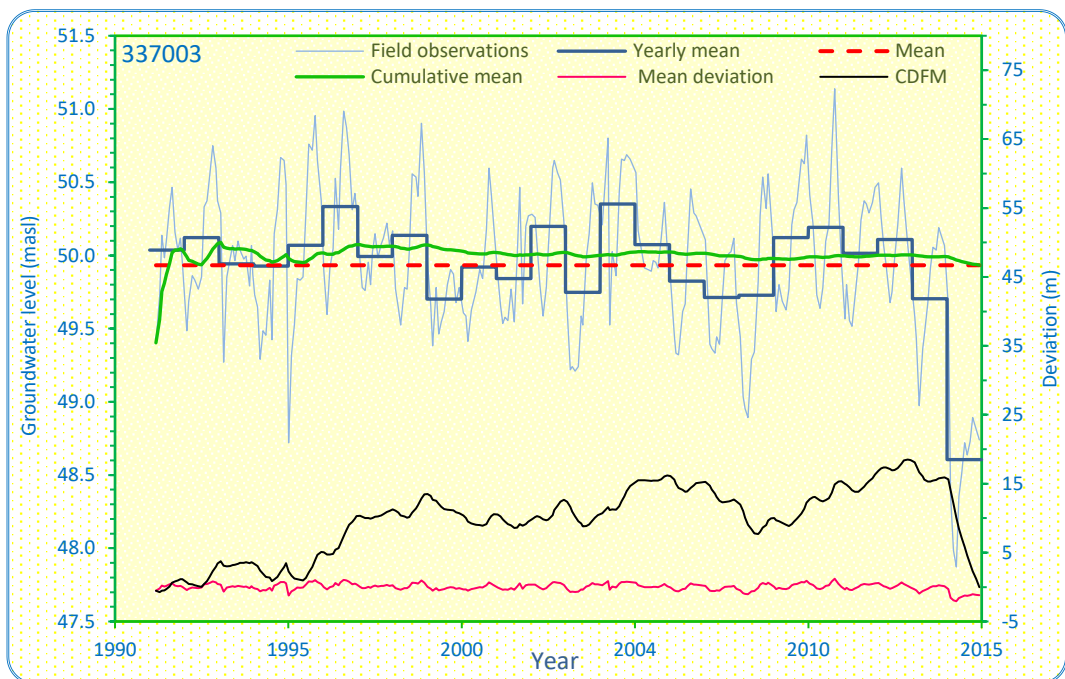
Elevation (masl)	Screen extent (mbgl)	Groundwater level		Area	Trend/comments
		Mean (masl)	STDEV (m)		
43.81	17–20	41.04	0.49		Steady

Figure 9-1. Groundwater level hydrographs for Well 336651.



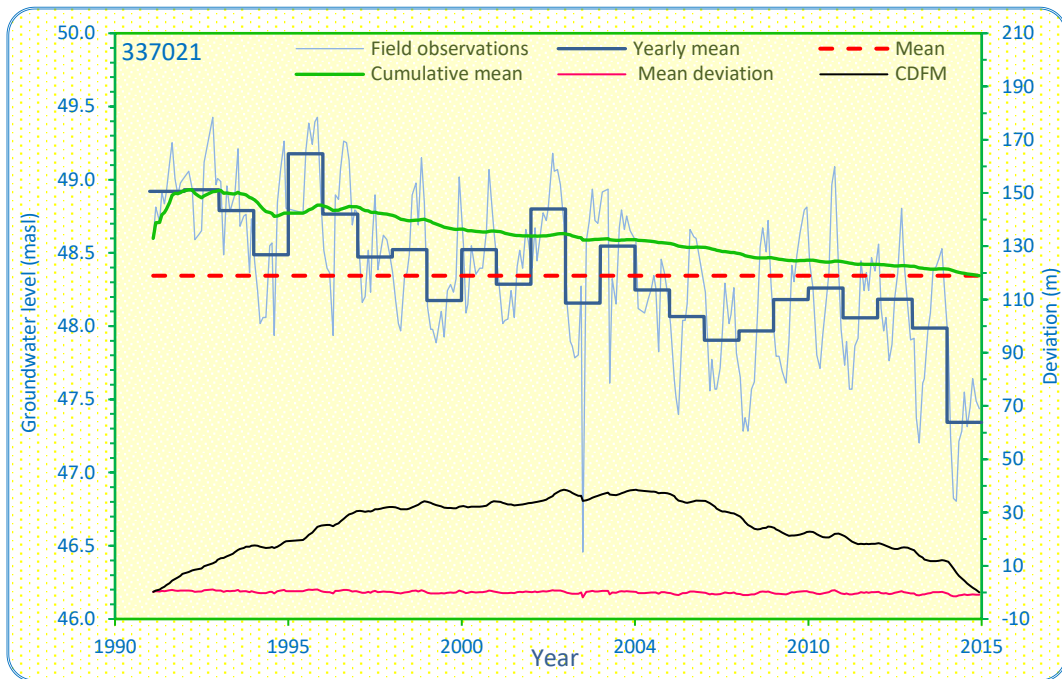
Elevation (masl)	Screen extent (mbgl)	Groundwater level		Area	Trend/comments
		Mean (masl)	STDEV (m)		
55.08	37-40	58.97	0.90		Declining

Figure C-57. Groundwater level hydrographs for Well 337001.



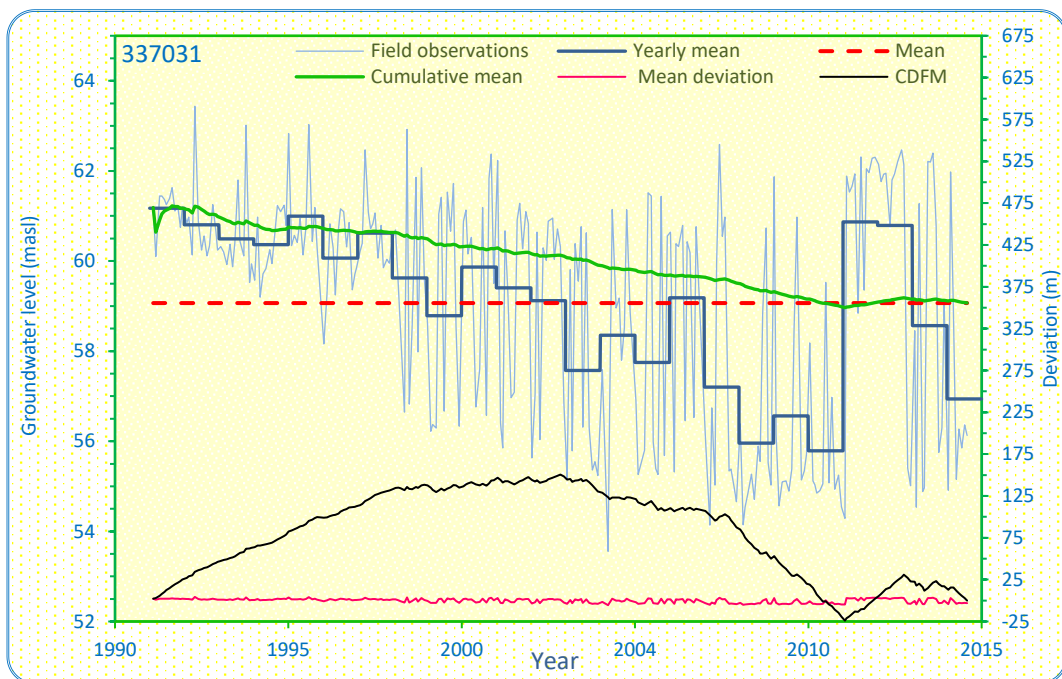
Elevation (masl)	Screen extent (mbgl)	Groundwater level		Area	Trend/comments
		Mean (masl)	STDEV (m)		
46.75	78-81	49.93	0.51		Steady

Figure C-58. Groundwater level hydrographs for Well 337003.



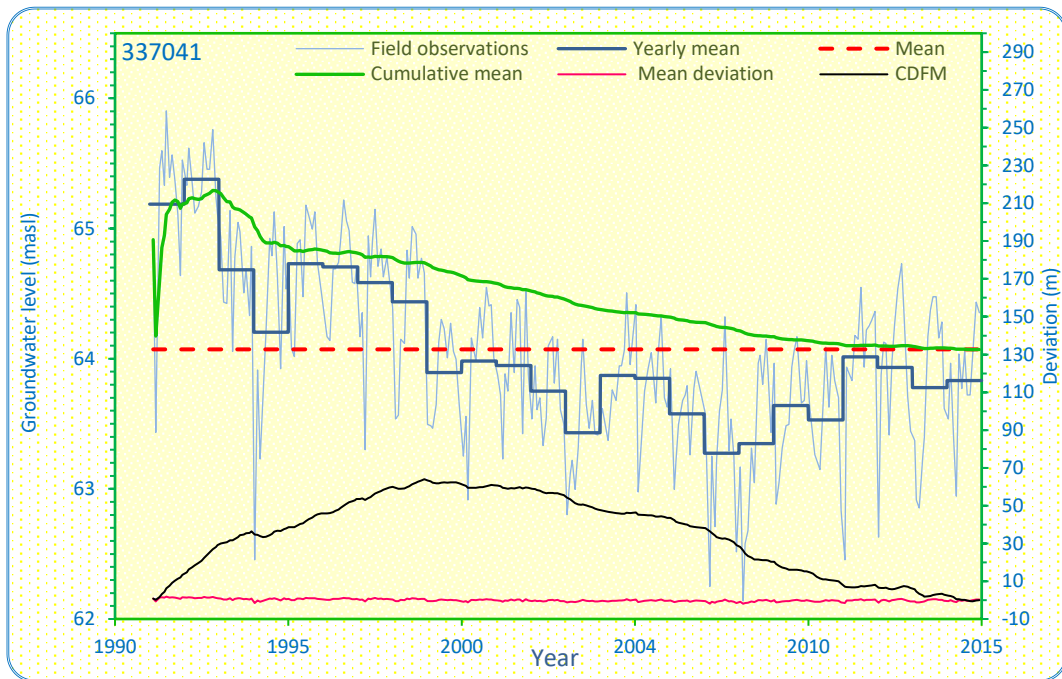
Elevation (masl)	Screen extent (mbgl)	Groundwater level		Area	Trend/comments
		Mean (masl)	STDEV (m)		
44.61	25.1–27.1	48.34	0.53		Declining

Figure C-59. Groundwater level hydrographs for Well 337021.



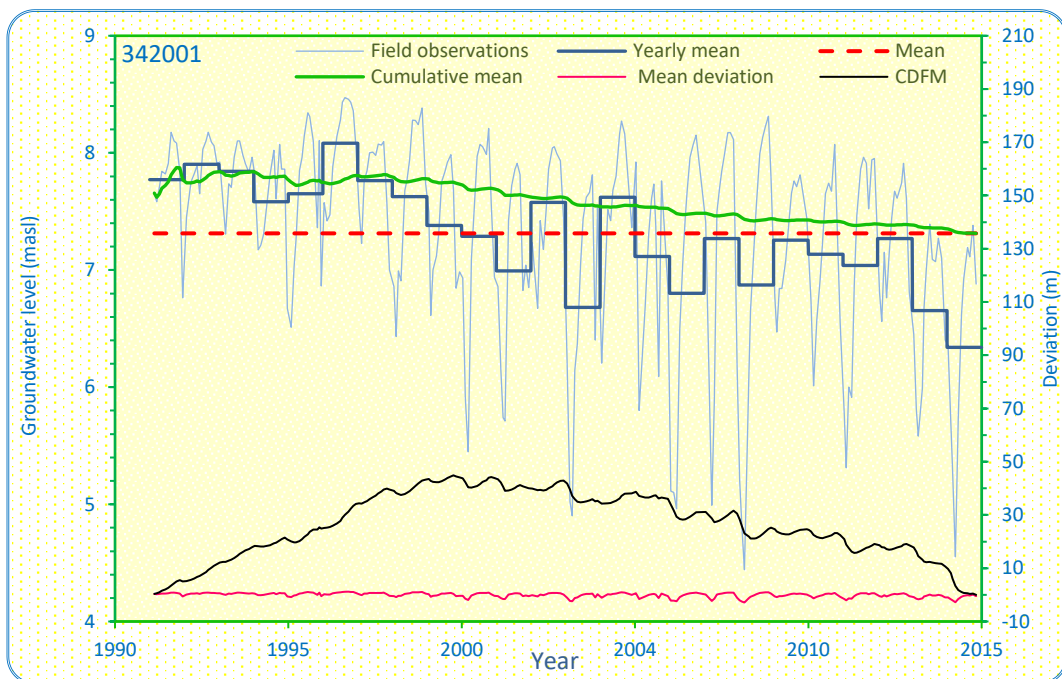
Elevation (masl)	Screen extent (mbgl)	Groundwater level		Area	Trend/comments
		Mean (masl)	STDEV (m)		
48.71	77.83–80.83	59.07	2.55		Declining

Figure C-60. Groundwater level hydrographs for Well 337031.



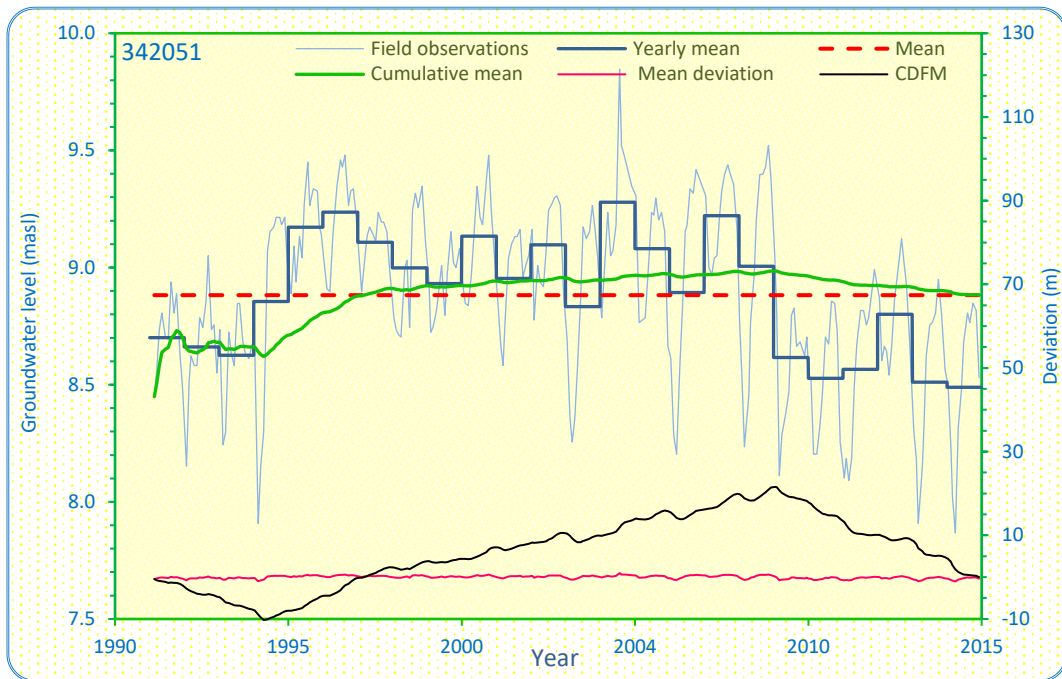
Elevation (masl)	Screen extent (mbgl)	Groundwater level		Area	Trend/comments
		Mean (masl)	STDEV (m)		
48.72	96-99	64.07	0.72		Declining

Figure C-61. Groundwater level hydrographs for Well 337041.



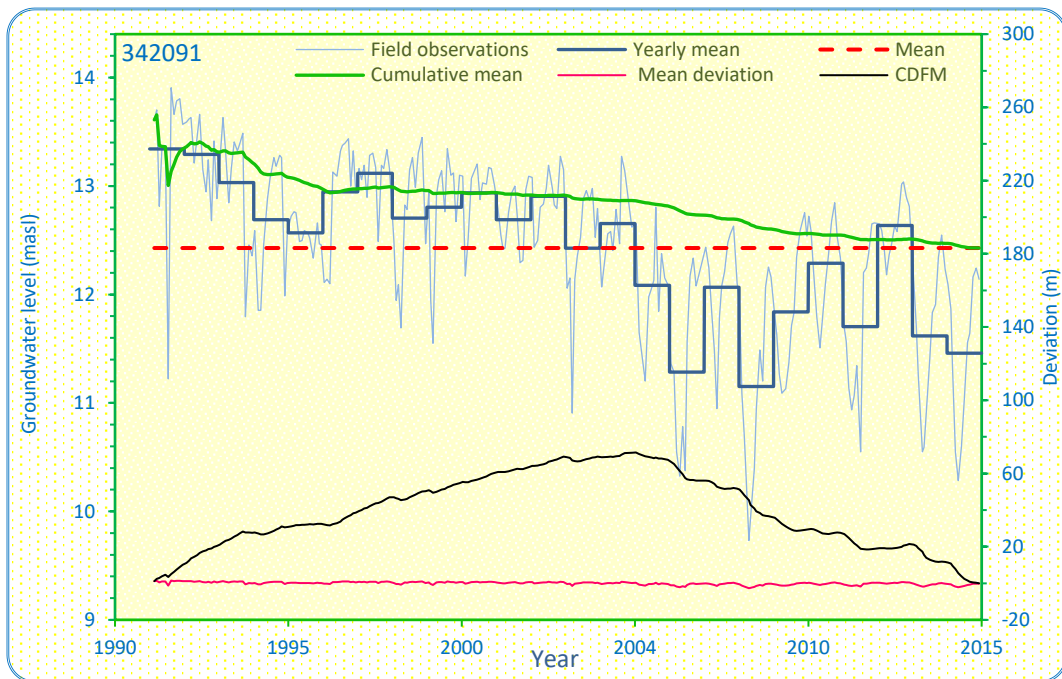
Elevation (masl)	Screen extent (mbgl)	Groundwater level		Area	Trend/comments
		Mean (masl)	STDEV (m)		
15.31	77-80	7.31	0.83		Declining

Figure C-62. Groundwater level hydrographs for Well 342001.



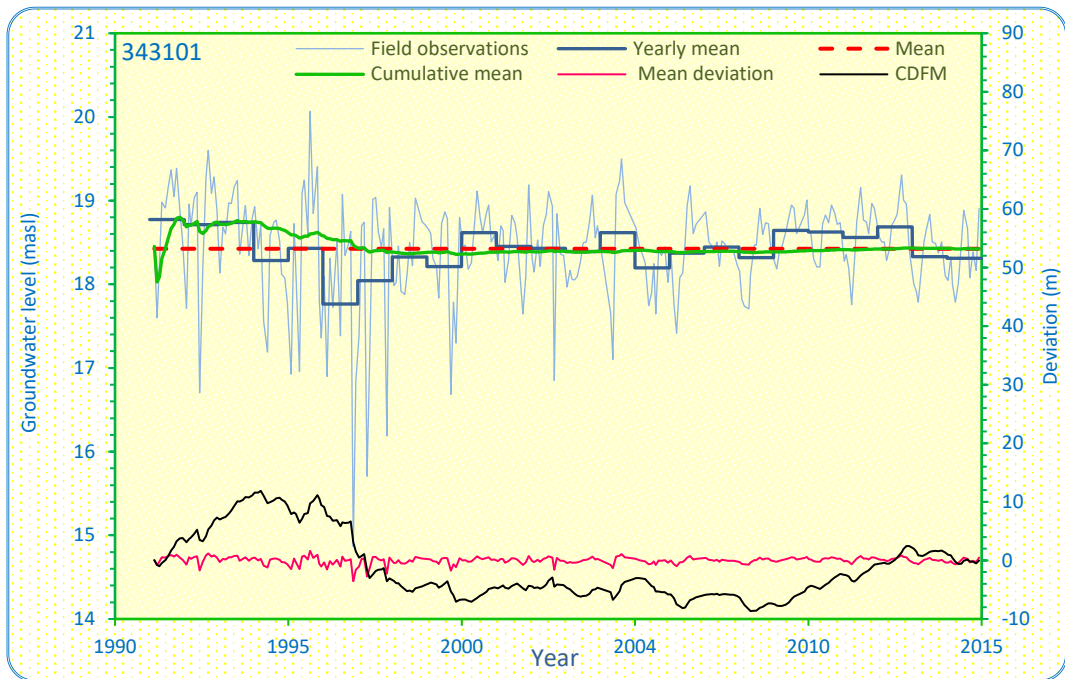
Elevation (masl)	Screen extent (mbgl)	Groundwater level		Area	Trend/comments
		Mean (masl)	STDEV (m)		
6.95	59.4–65.5	8.88	0.36		Steady

Figure C-63. Groundwater level hydrographs for Well 342051.



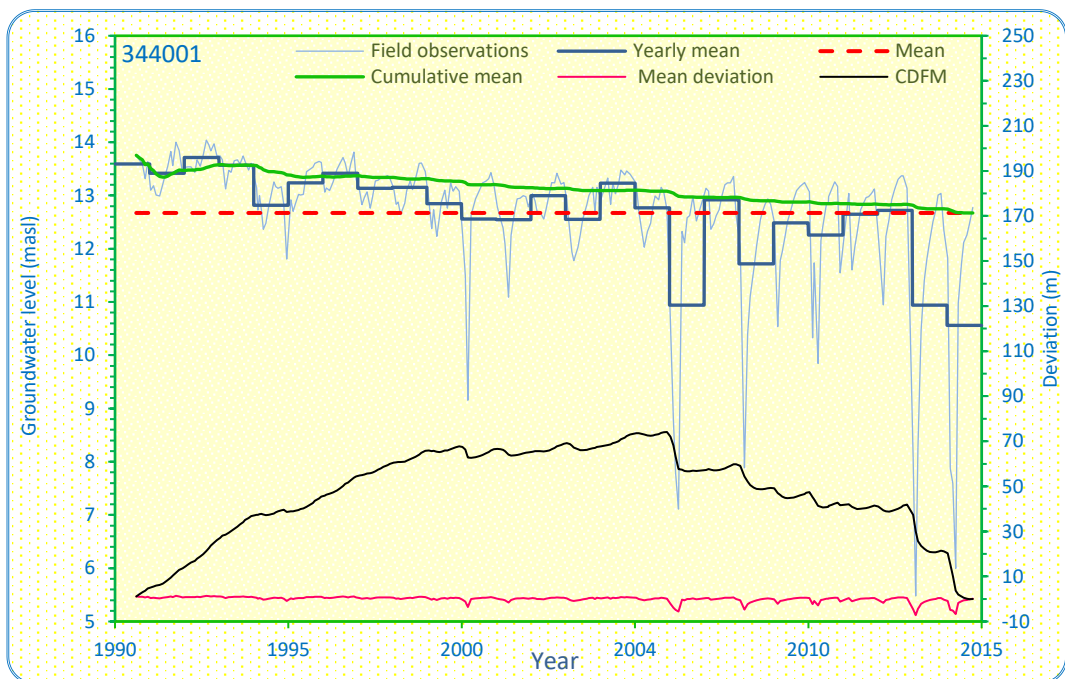
Elevation (masl)	Screen extent (mbgl)	Groundwater level		Area	Trend/comments
		Mean (masl)	STDEV (m)		
3.57	157–160	12.43	0.80		Declining

Figure C-64. Groundwater level hydrographs for Well 342091.



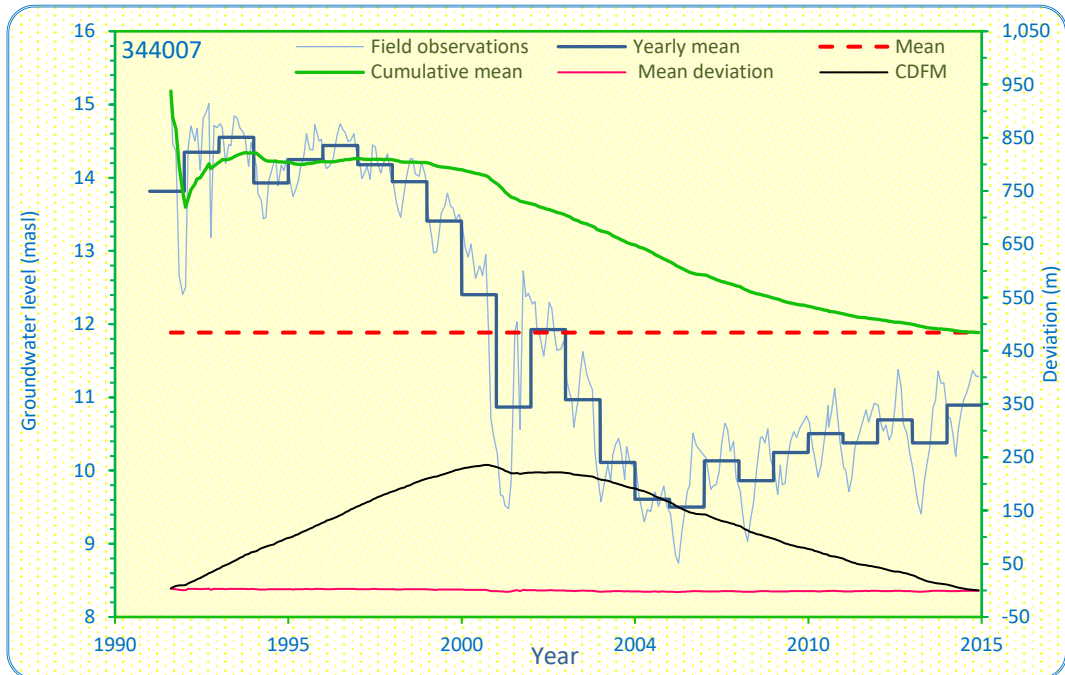
Elevation (masl)	Screen extent (mbgl)	Groundwater level		Area	Trend/comments
		Mean (masl)	STDEV (m)		
26.51	38.2–41.3	18.42	0.61		Steady

Figure C-65. Groundwater level hydrographs for Well 343101.



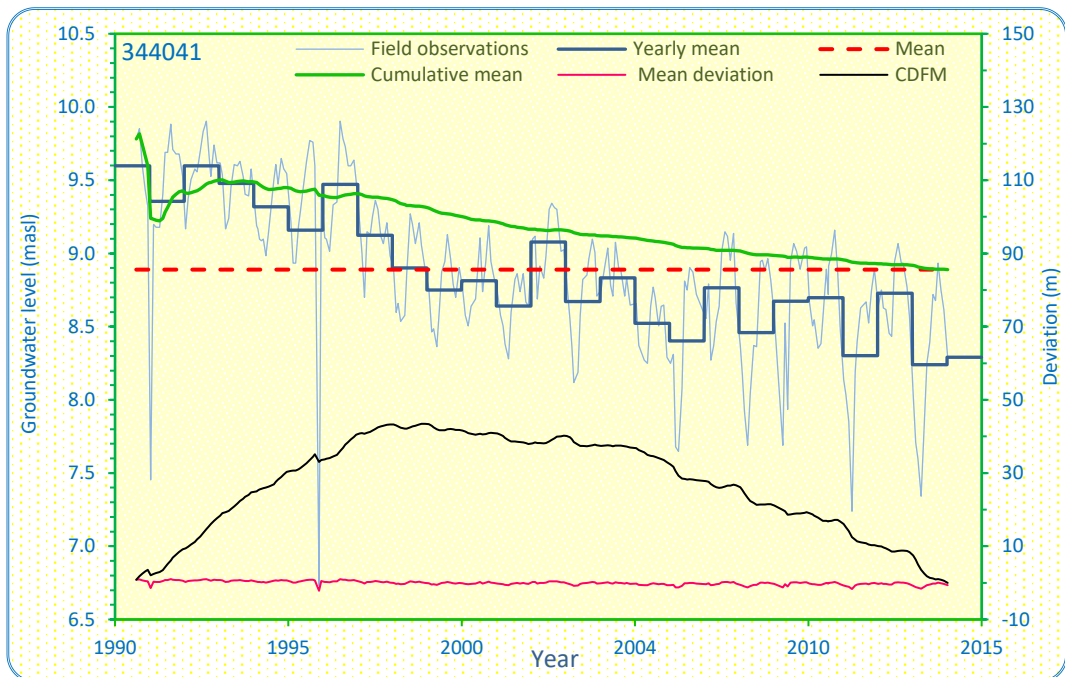
Elevation (masl)	Screen extent (mbgl)	Groundwater level		Area	Trend/comments
		Mean (masl)	STDEV (m)		
4.77	149.5–153.5	12.67	1.24		Declining

Figure C-66. Groundwater level hydrographs for Well 344001.



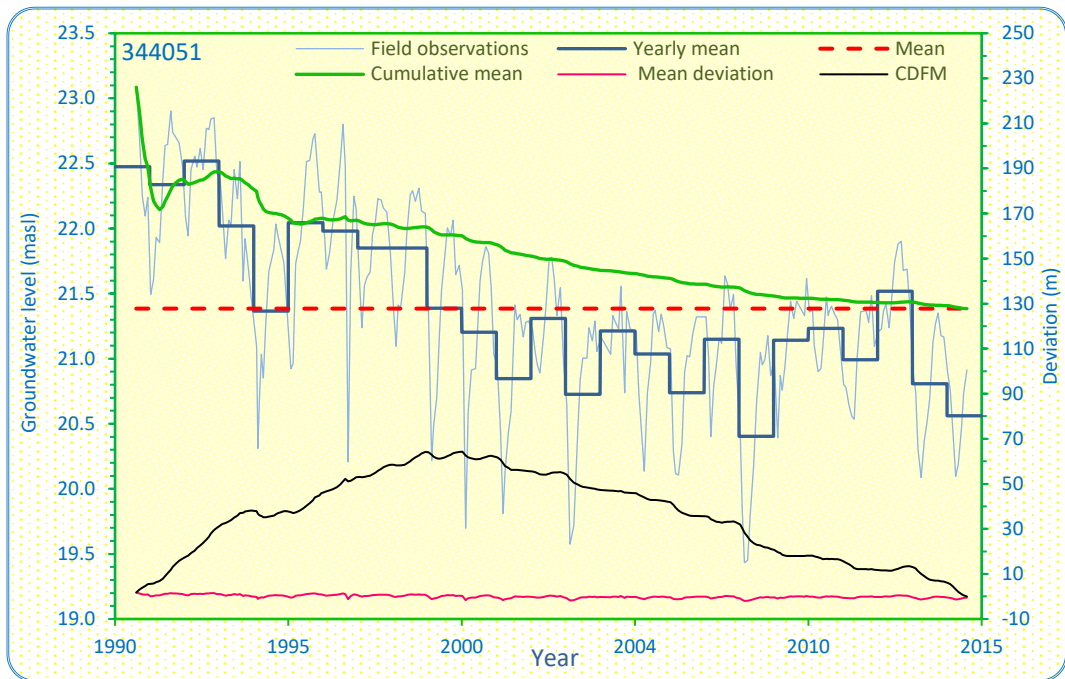
Elevation (masl)	Screen extent (mbgl)	Groundwater level		Area	Trend/comments
		Mean (masl)	STDEV (m)		
7.97	145-149	11.88	1.89		Declining

Figure C-67. Groundwater level hydrographs for Well 344007.



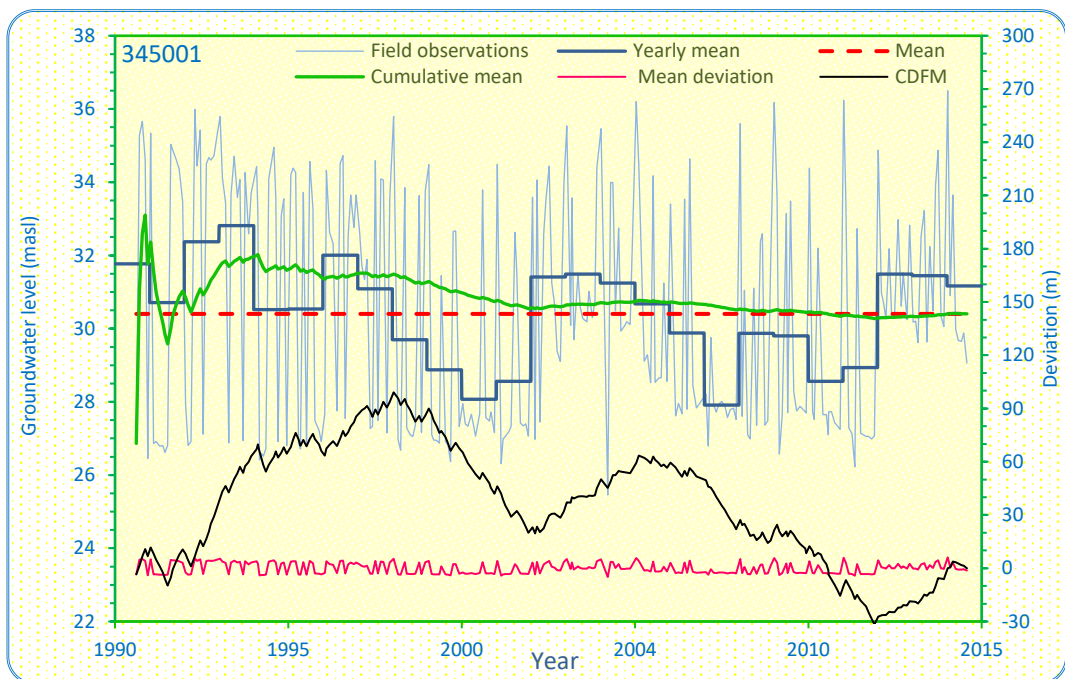
Elevation (masl)	Screen extent (mbgl)	Groundwater level		Area	Trend/comments
		Mean (masl)	STDEV (m)		
5.39	65.4-68.4	8.89	0.52		Declining

Figure C-68. Groundwater level hydrographs for Well 344041.



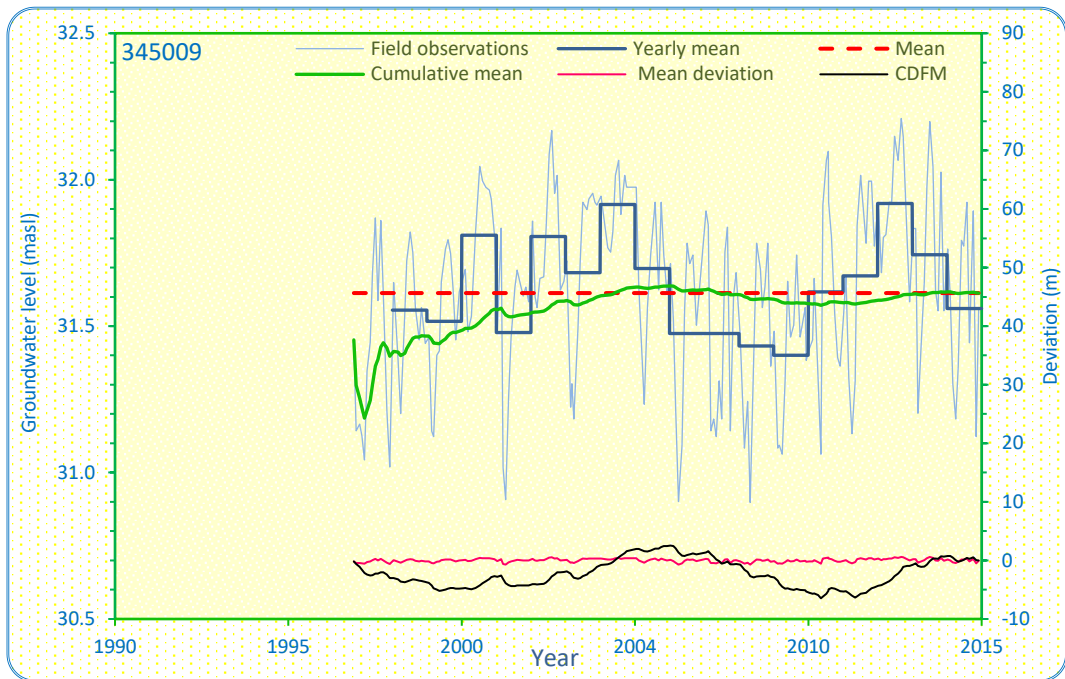
Elevation (masl)	Screen extent (mbgl)	Groundwater level		Area	Trend/comments
		Mean (masl)	STDEV (m)		
12.86	134–137	21.38	0.72		Declining

Figure C-69. Groundwater level hydrographs for Well 344051.



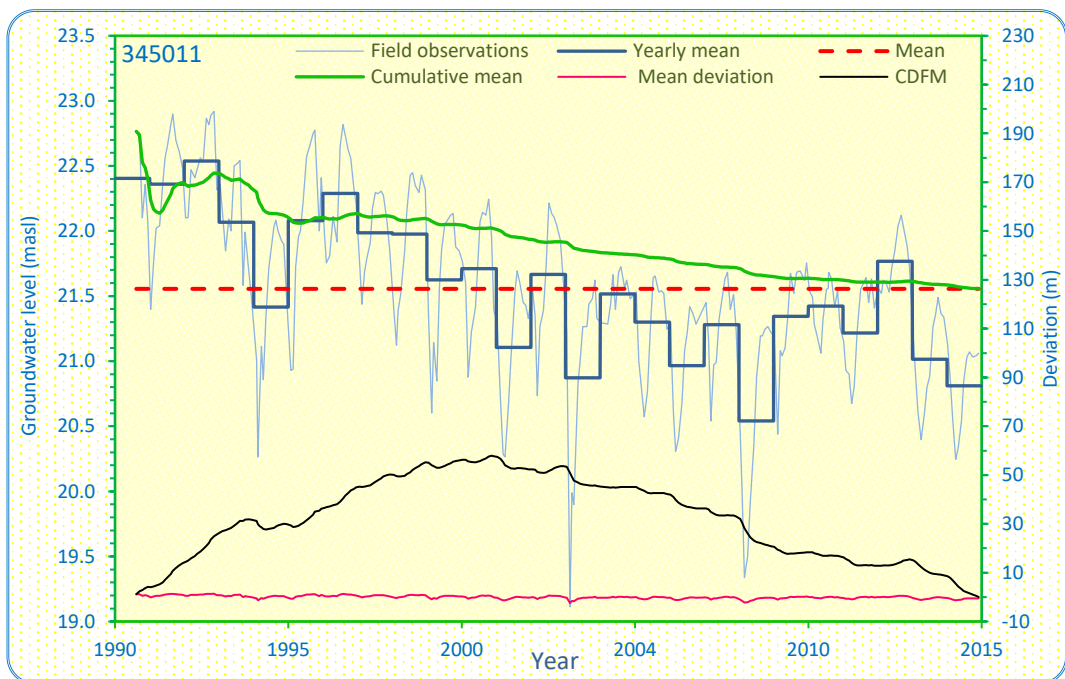
Elevation (masl)	Screen extent (mbgl)	Groundwater level		Area	Trend/comments
		Mean (masl)	STDEV (m)		
24.77	124–135	30.40	3.12		Steady

Figure C-70. Groundwater level hydrographs for Well 345001.



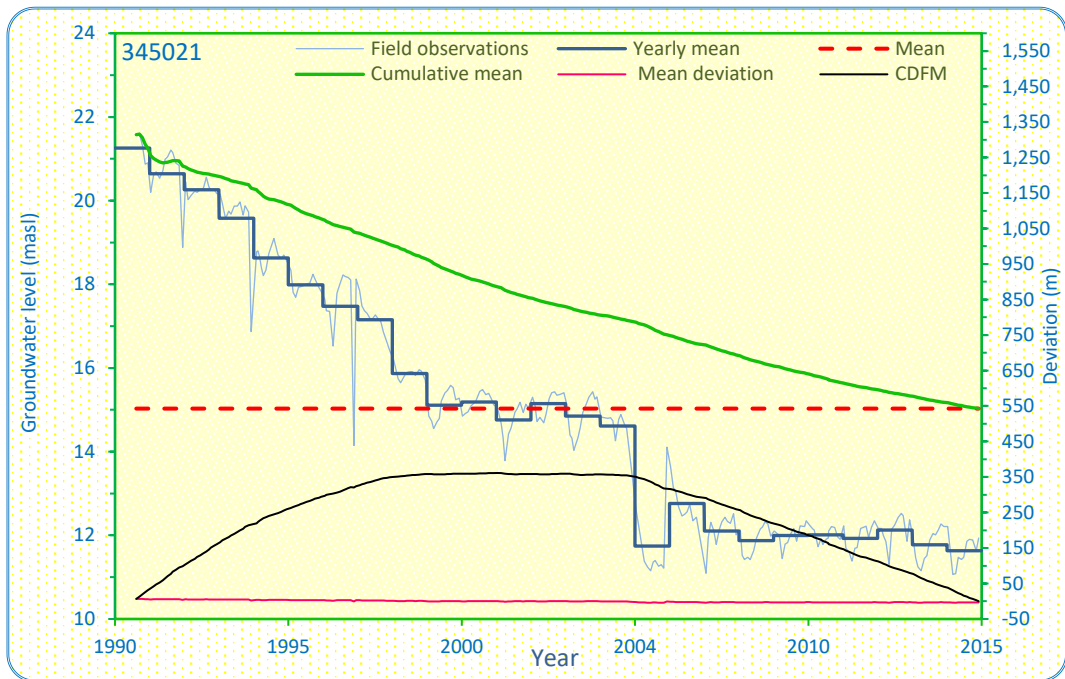
Elevation (masl)	Screen extent (mbgl)	Groundwater level		Area	Trend/comments
		Mean (masl)	STDEV (m)		
31.90	28.4–29.4	31.61	0.30		Steady

Figure C-71. Groundwater level hydrographs for Well 345009.



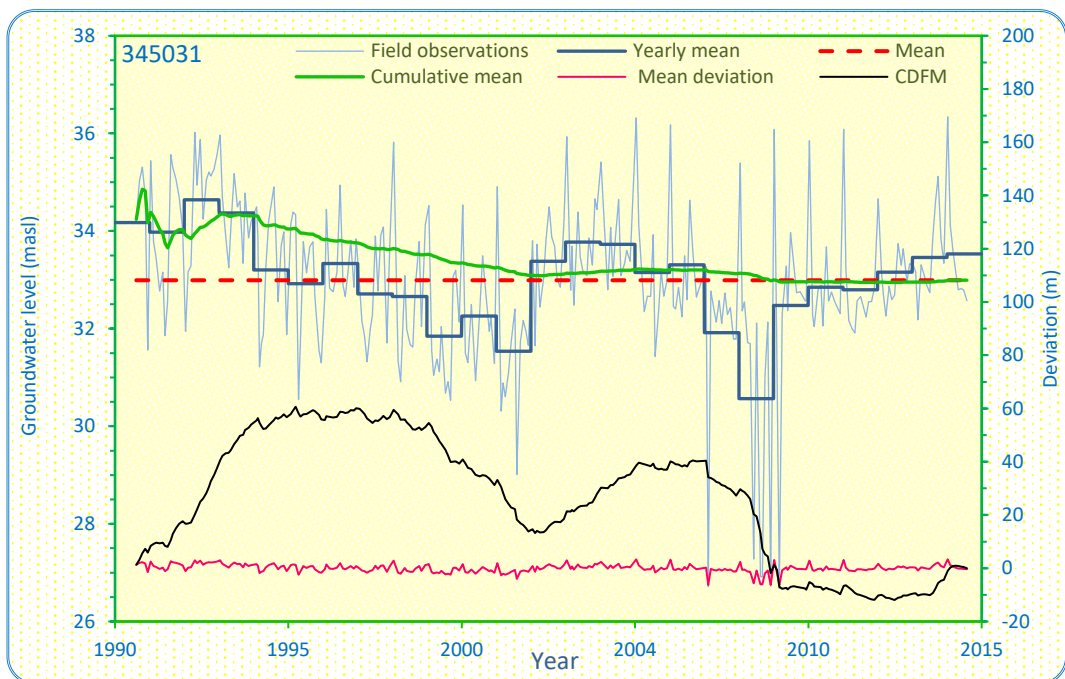
Elevation (masl)	Screen extent (mbgl)	Groundwater level		Area	Trend/comments
		Mean (masl)	STDEV (m)		
14.25	132–135	21.56	0.68		Declining

Figure C-72. Groundwater level hydrographs for Well 345011.



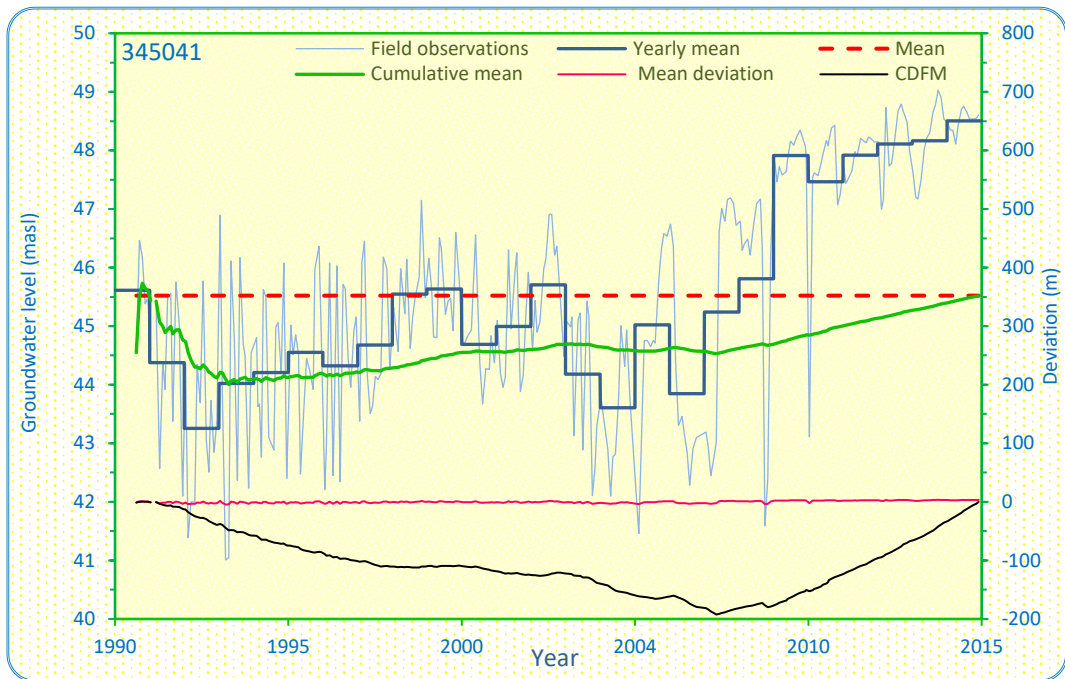
Elevation (masl)	Screen extent (mbgl)	Groundwater level		Area	Trend/comments
		Mean (masl)	STDEV (m)		
8.80	90.7–92.4	15.03	3.08		Declining

Figure C-73. Groundwater level hydrographs for Well 345021.



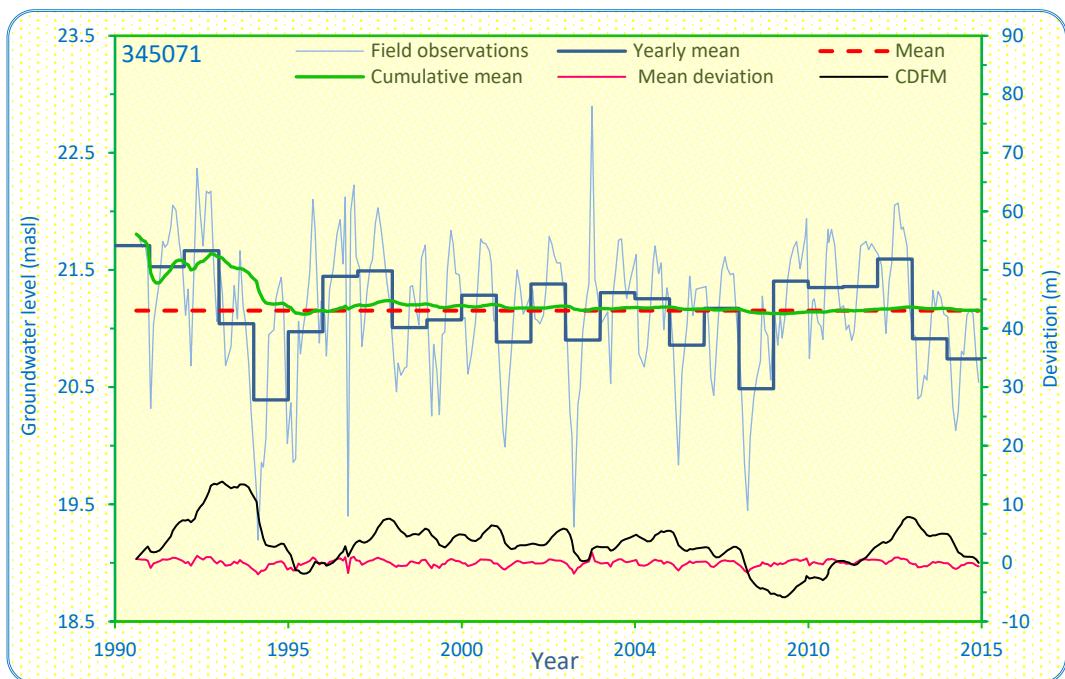
Elevation (masl)	Screen extent (mbgl)	Groundwater level		Area	Trend/comments
		Mean (masl)	STDEV (m)		
23.88	124–129	32.99	1.56		Steady

Figure C-74. Groundwater level hydrographs for Well 345031.



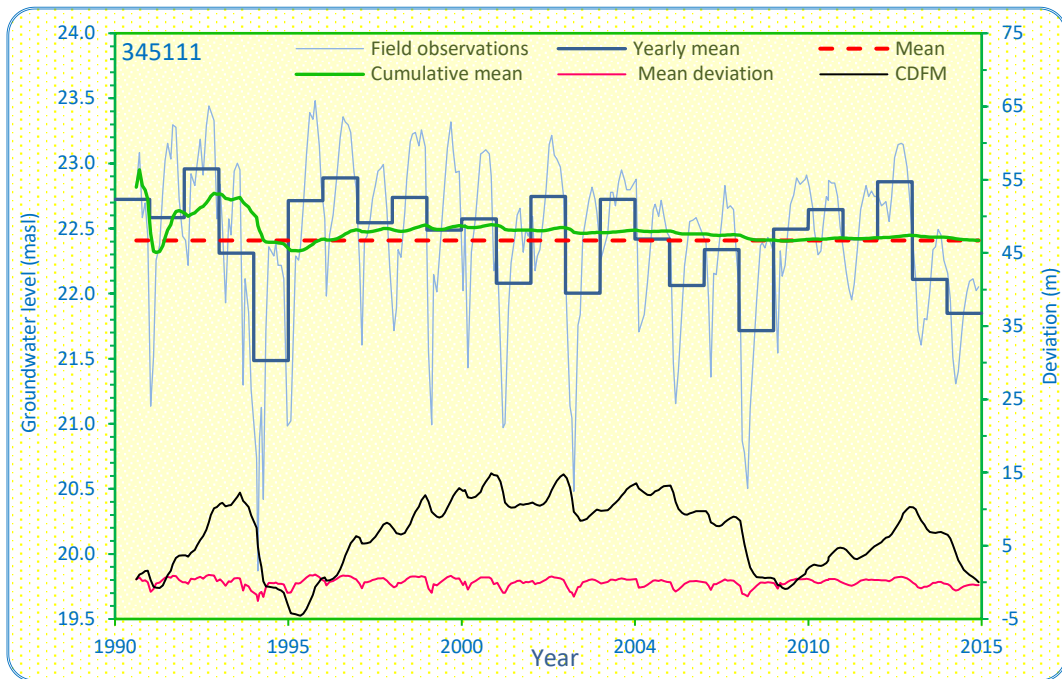
Elevation (masl)	Screen extent (mbgl)	Groundwater level		Area	Trend/comments
		Mean (masl)	STDEV (m)		
36.49	162.51–165.51	45.50	2.03		Rising

Figure C-75. Groundwater level hydrographs for Well 345041.



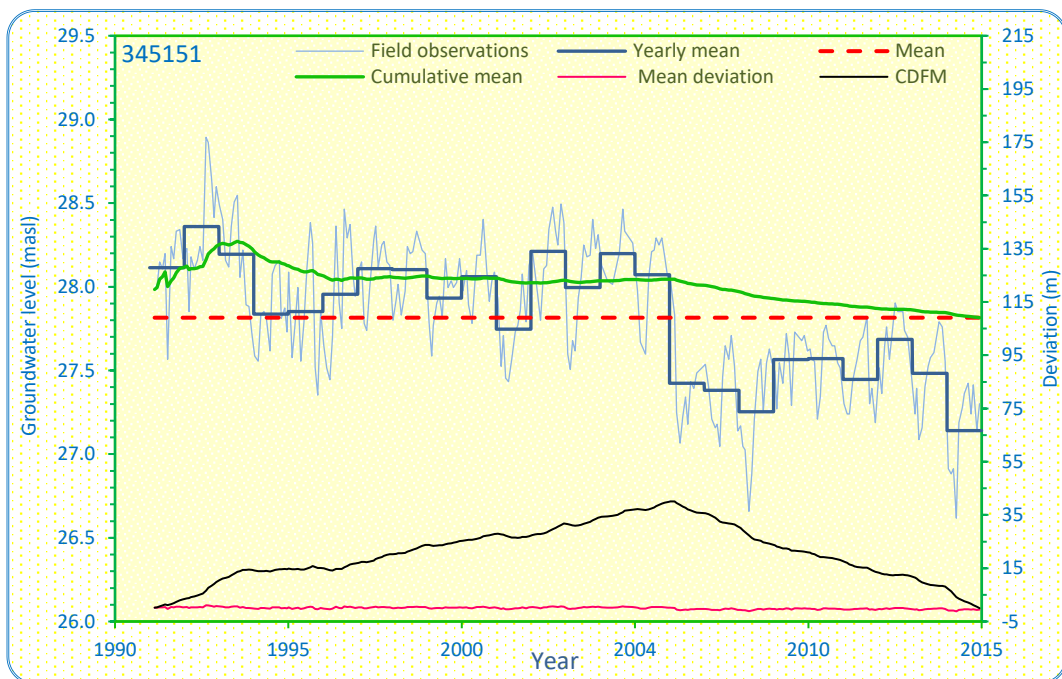
Elevation (masl)	Screen extent (mbgl)	Groundwater level		Area	Trend/comments
		Mean (masl)	STDEV (m)		
15.52	82–85	21.15	0.58		Steady

Figure C-76. Groundwater level hydrographs for Well 345071.



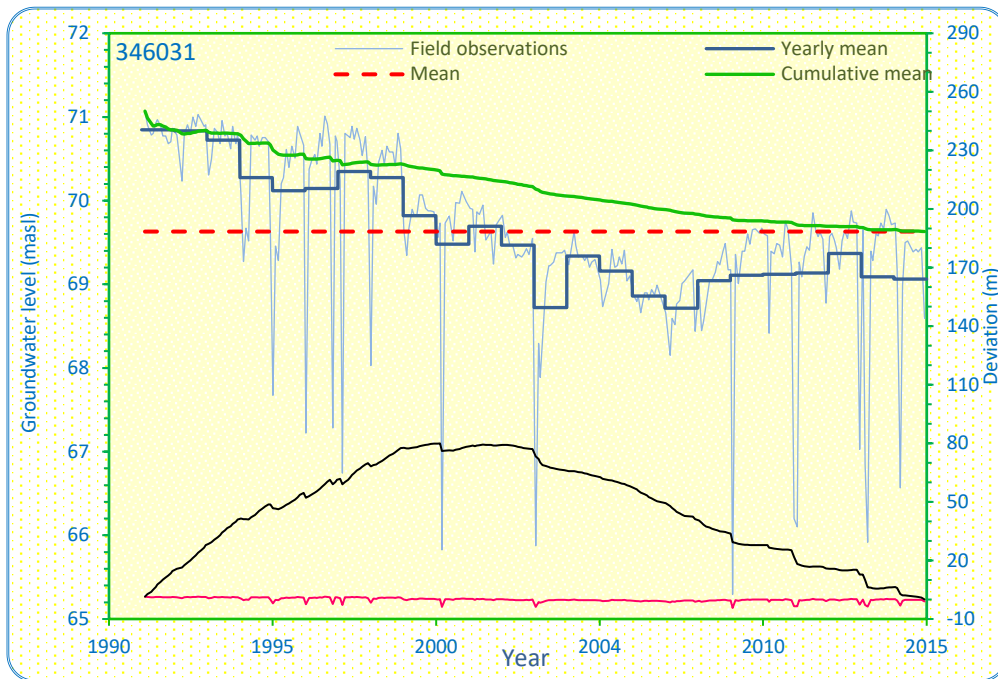
Elevation (masl)	Screen extent (mbgl)	Groundwater level		Area	Trend/comments
		Mean (masl)	STDEV (m)		
16.09	108-111	22.41	0.63		Steady

Figure C-77. Groundwater level hydrographs for Well 345111.



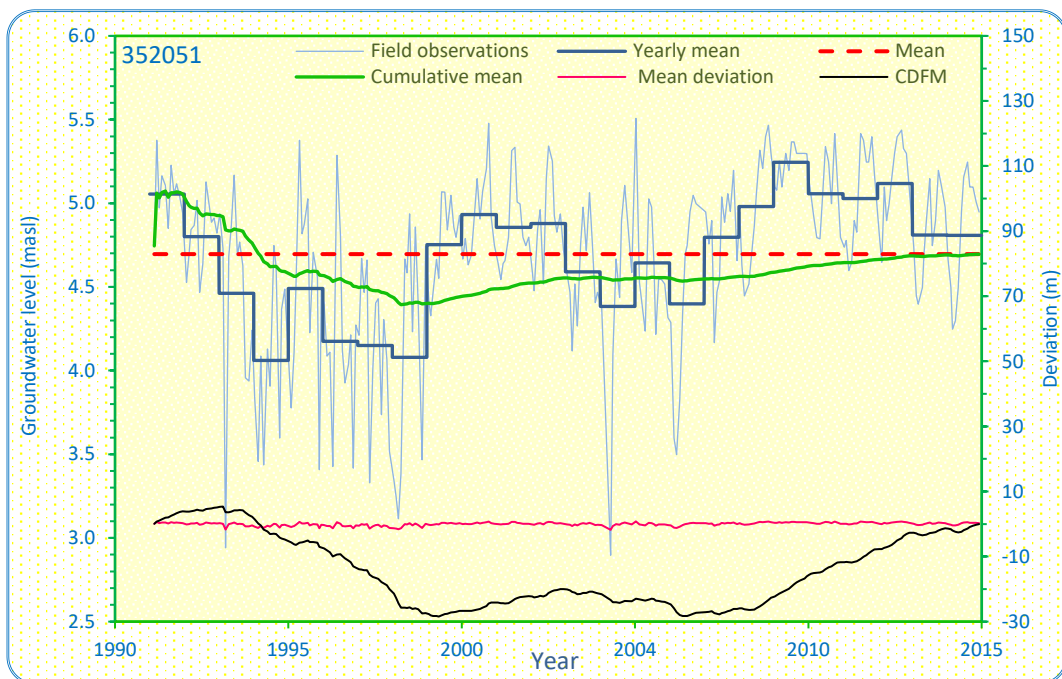
Elevation (masl)	Screen extent (mbgl)	Groundwater level		Area	Trend/comments
		Mean (masl)	STDEV (m)		
14.79	77.1-78	27.82	0.41		Declining

Figure C-78. Groundwater level hydrographs for Well 345151.



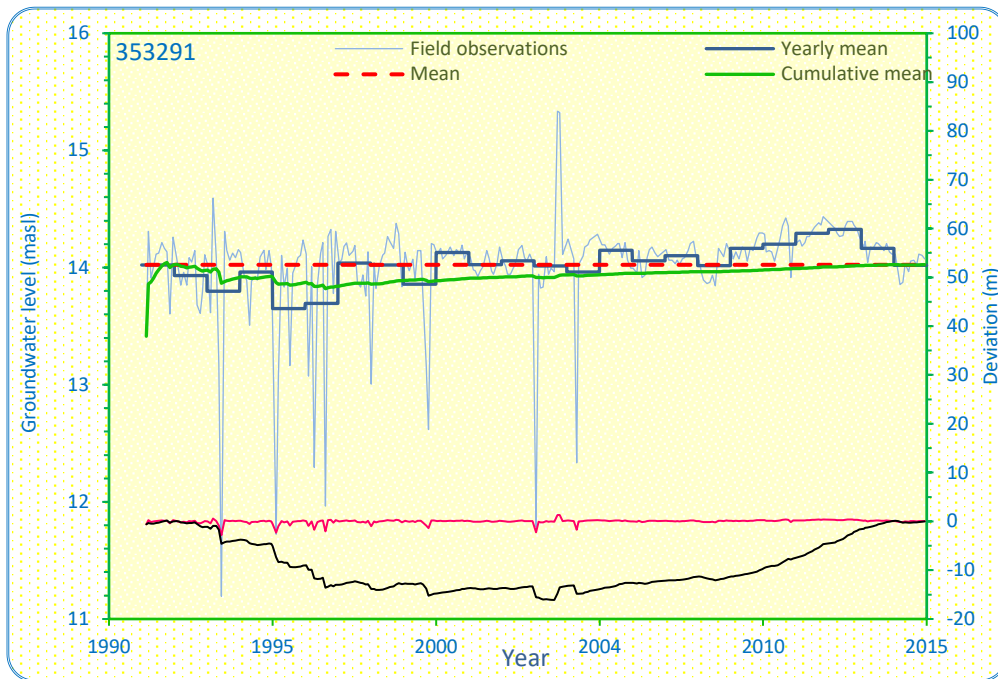
Elevation (masl)	Screen extent (mbgl)	Groundwater level		Area	Trend/comments
		Mean (masl)	STDEV (m)		
86.51	44.28-47.28	69.84	2.70		Declining

Figure C-79. Groundwater level hydrographs for Well 346031.



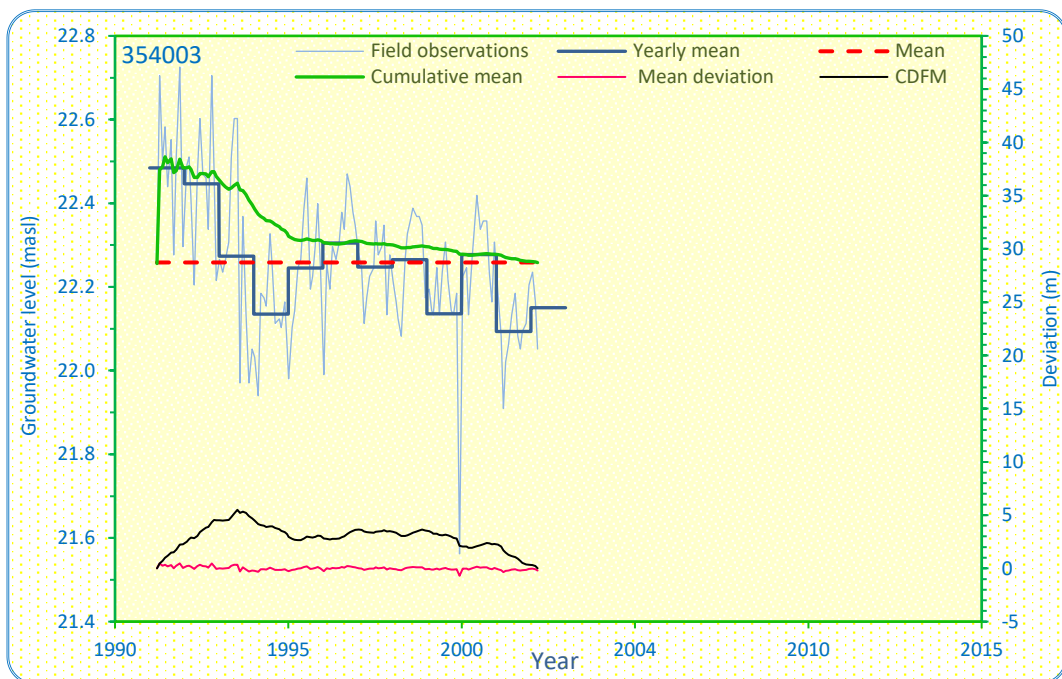
Elevation (masl)	Screen extent (mbgl)	Groundwater level		Area	Trend/comments
		Mean (masl)	STDEV (m)		
11.95	41.2-44.2	4.70	0.51		Steady

Figure C-80. Groundwater level hydrographs for Well 352051.



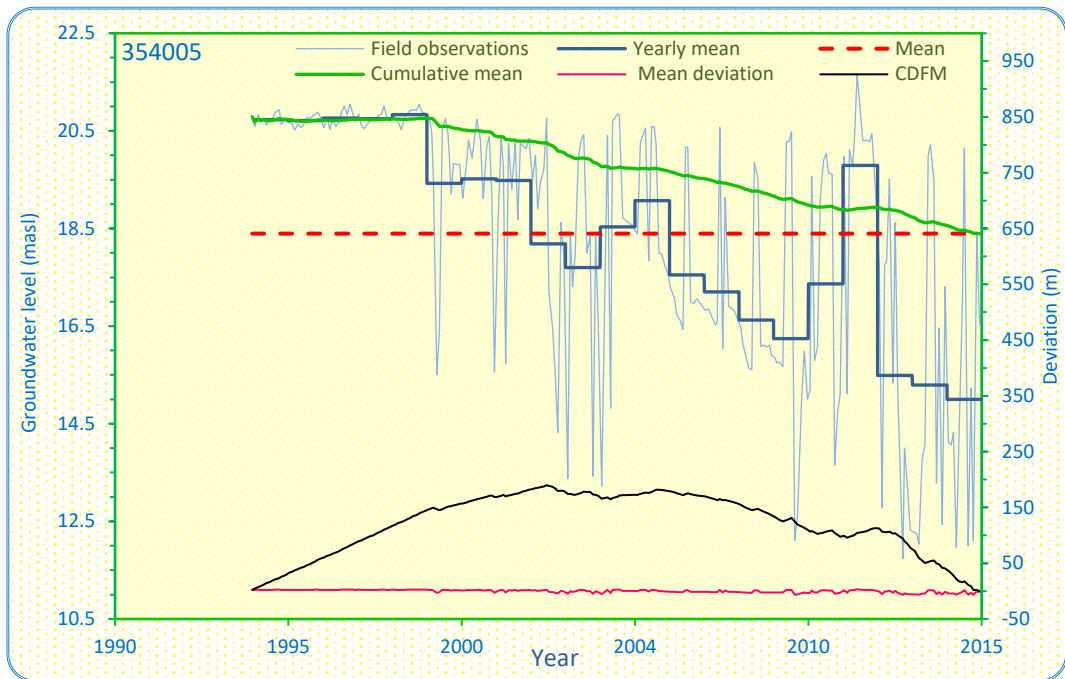
Elevation (masl)	Screen extent (mbgl)	Groundwater level		Area	Trend/comments
		Mean (masl)	STDEV (m)		
46.51	43.5–46.5	14.02	0.41		Steady

Figure C-81. Groundwater level hydrographs for Well 353291.



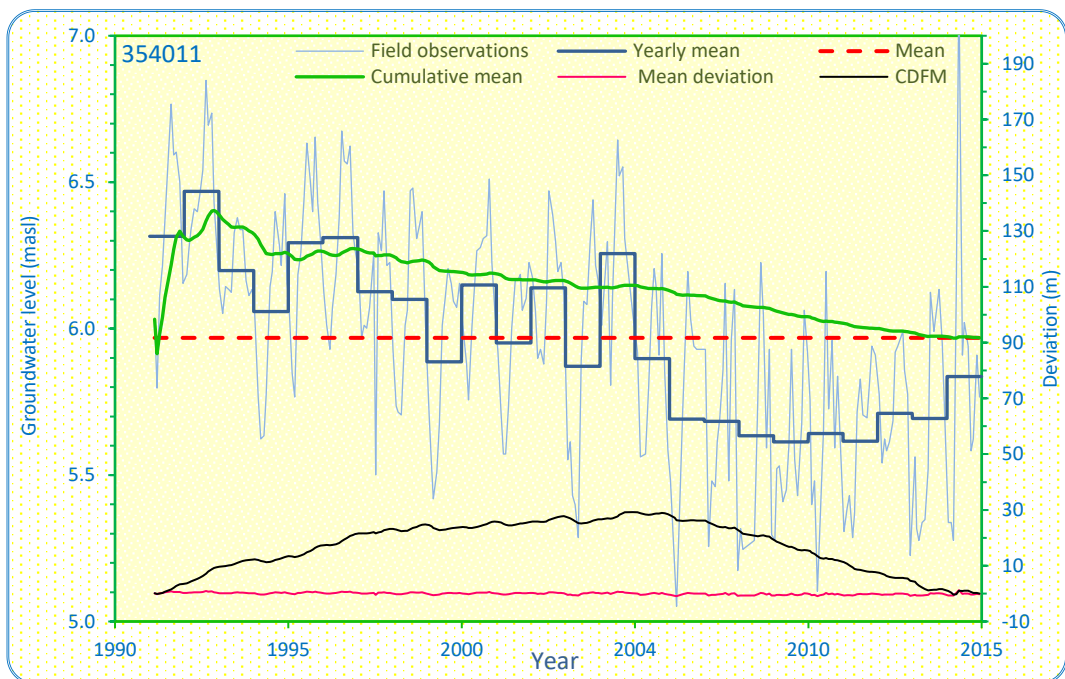
Elevation (masl)	Screen extent (mbgl)	Groundwater level		Area	Trend/comments
		Mean (masl)	STDEV (m)		
18.06	77–80	22.26	0.17		Old, short record

Figure C-82. Groundwater level hydrographs for Well 354003.



Elevation (masl)	Screen extent (mbgl)	Groundwater level		Area	Trend/comments
		Mean (masl)	STDEV (m)		
5.74	144.4–165.5	18.40	2.61		Declining

Figure C-83. Groundwater level hydrographs for Well 354005.



Elevation (masl)	Screen extent (mbgl)	Groundwater level		Area	Trend/comments
		Mean (masl)	STDEV (m)		
5.05	33.5–36.5	5.97	0.38		Declining

Figure C-84. Groundwater level hydrographs for Well 354011.

## Appendix D Groundwater quality data

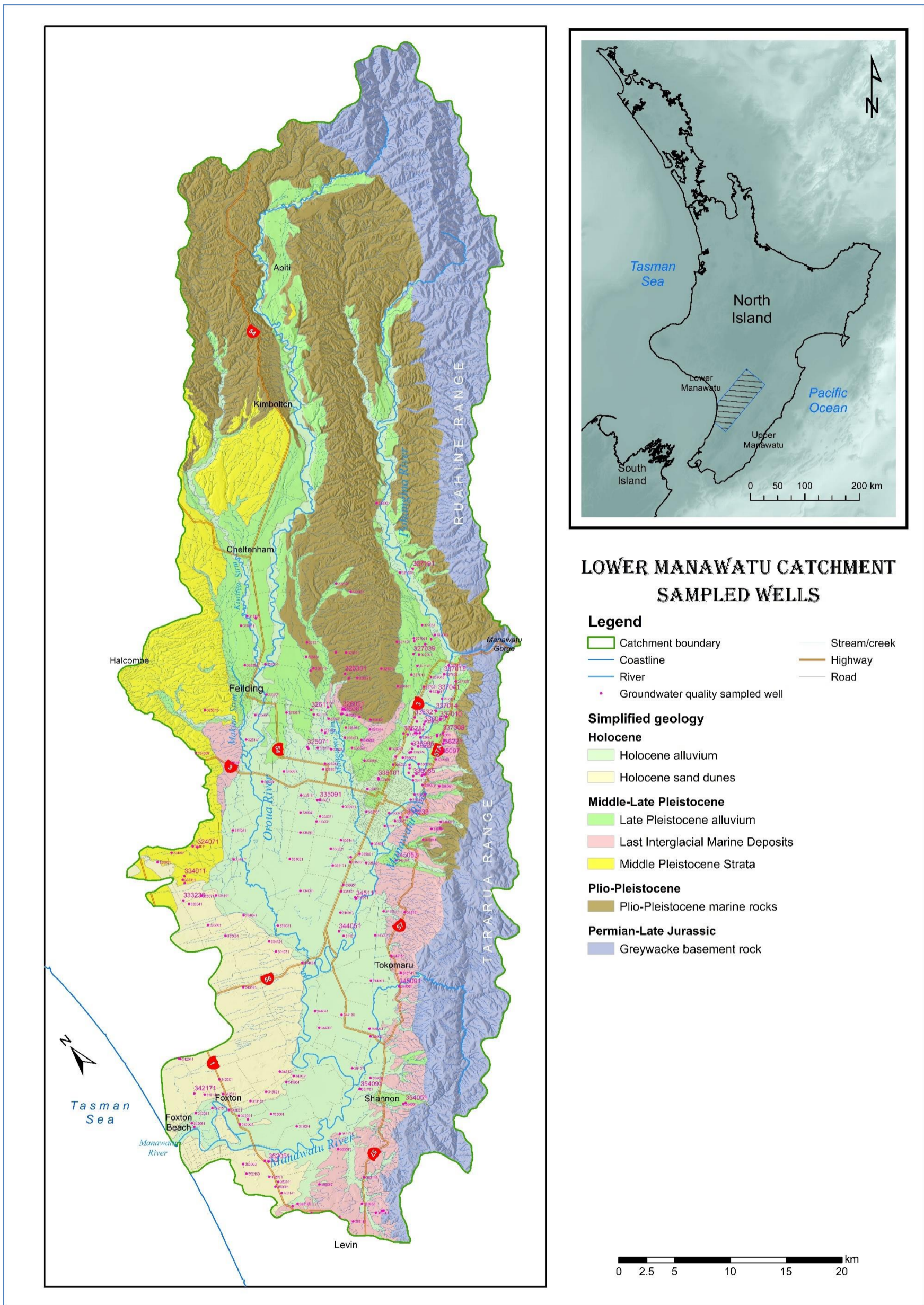


Figure D-1: Map showing locations of groundwater quality samples listed in Chapter 7 and Appendix D.



Well	Location Classification	NZMG		Elevation (masl)	Well Nominal Depth (m)	Well Screens			All Samples			Acceptable Samples		
		Easting	Northing			Number	From	To	Number	From	To	Number	From	To
325091	LMC	2726679	6098520	33.96	169.30	1	167.30	169.30	1	03/04/1989	03/04/1989	1	03/04/1989	03/04/1989
325121	LMC	2729667	6098660	44.67	165.00				1	27/02/1989	27/02/1989	1	27/02/1989	27/02/1989
325141	LMC	2725902	6102868	48.81	44.00	1	39.90	44.00	3	29/07/1987	11/08/1987	1	11/08/1987	11/08/1987
325221	LMC	2729900	6104800	73.11	100.00				1	30/03/1989	30/03/1989	1	30/03/1989	30/03/1989
325251	LMC	2730110	6108063	93.36	46.00	1	40.00	46.00	4	11/09/1984	30/03/1989	1	30/03/1989	30/03/1989
325351	LMC	2730247	6102416	61.43	144.00	1	140.00	144.00	1	01/05/1989	01/05/1989	1	01/05/1989	01/05/1989
325361	LMC	2727968	6104045	60.84	65.00	1	59.00	65.00	1	24/04/1989	24/04/1989	1	24/04/1989	24/04/1989
325381	LMC	2723349	6102334	60.01	62.80	1	60.80	62.80	1	09/06/2003	09/06/2003	1	09/06/2003	09/06/2003
326011	LMC	2734271	6098740	58.29	113.00				1	02/03/1989	02/03/1989	1	02/03/1989	02/03/1989
326021	LMC	2732780	6099561	50.44	30.00				2	09/03/1989	01/11/1995	1	09/03/1989	09/03/1989
326041	LMC	2739280	6099950	145.16	90.89				1	06/03/1989	06/03/1989	1	06/03/1989	06/03/1989
326061	LMC	2733901	6099145	50.79	118.95				2	19/07/1965	20/03/1989	1	19/07/1965	19/07/1965
326071	LMC	2737100	6100700	93.92	33.55				1	06/03/1989	06/03/1989	1	06/03/1989	06/03/1989
326091	LMC	2734300	6099400	58.99	207.71				5	29/07/1969	20/11/1995	1	02/03/1989	02/03/1989
326099	LMC	2734000	6099100	50.00	102.10				2	24/01/1990	14/09/1993	1	14/09/1993	14/09/1993
326101	LMC	2739400	6097800	107.86	108.28				1	09/03/1989	09/03/1989	1	09/03/1989	09/03/1989
326103	LMC	2734400	6099300	56.26	201.80	1	198.80	201.80	1	31/05/1996	31/05/1996	1	31/05/1996	31/05/1996
326113	LMC	2732014	6100697	54.95	199.00	1	190.00	199.00	2	30/07/1999	19/03/2001	1	30/07/1999	30/07/1999
326117	LMC	2732097	6101164	58.39	360.90	1	354.40	360.90	2	30/11/2000	19/03/2001	1	30/11/2000	30/11/2000
326119	LMC	2734644	6103883	76.00	122.00	1	116.00	122.00	1	18/06/2003	18/06/2003	1	18/06/2003	18/06/2003
326131	LMC	2734800	6105100	90.30	12.20				3	29/09/1994	15/03/1995	1	14/03/1995	14/03/1995
326141	LMC	2737800	6103100	111.70	92.11				1	09/03/1989	09/03/1989	1	09/03/1989	09/03/1989
326151	LMC	2737100	6103700	98.45	102.00				1	09/03/1989	09/03/1989	1	09/03/1989	09/03/1989
326171	LMC	2735000	6097900	57.76	103.00				1	02/03/1989	02/03/1989	1	02/03/1989	02/03/1989
326181	LMC	2735590	6097071	64.24	135.00				1	07/02/1989	07/02/1989	1	07/02/1989	07/02/1989
326191	LMC	2731628	6099141	49.46	153.75	1	151.75	153.75	3	19/06/1985	09/04/1996	1	19/06/1985	19/06/1985
326211	LMC	2735683	6106044	111.31	118.00				3	09/03/1989	15/03/1995	2	09/03/1989	06/06/1989
326211	LMC	2735683	6106044	111.31	118.00				3	09/03/1989	15/03/1995	2	09/03/1989	06/06/1989
326231	LMC	2731582	6106960	93.71	35.10	1	33.10	35.10	1	30/03/1989	30/03/1989	1	30/03/1989	30/03/1989
326241	LMC	2734300	6103900	80.34	23.70	1	21.70	23.70	3	25/09/1987	06/06/1989	2	06/03/1989	06/06/1989
326241	LMC	2734300	6103900	80.34	23.70	1	21.70	23.70	3	25/09/1987	06/06/1989	2	06/03/1989	06/06/1989
326301	LMC	2736500	6101700	84.98	124.00				1	06/03/1989	06/03/1989	1	06/03/1989	06/03/1989
326311	LMC	2731722	6098785	47.42	152.30	1	150.30	152.30	1	23/07/1987	23/07/1987	1	23/07/1987	23/07/1987
326321	LMC	2736492	6101178	90.81	158.30	1	154.20	158.30	3	04/08/1988	06/03/1989	1	06/03/1989	06/03/1989
326331	LMC	2733397	6100383	56.96	85.90	1	81.80	85.90	2	31/08/1988	02/03/1989	1	02/03/1989	02/03/1989
326361	LMC	2733441	6097951	50.70	63.50	1	61.50	63.50	1	10/06/2003	10/06/2003	1	10/06/2003	10/06/2003
327001	LMC	2742679	6098753	118.71	95.00				1	20/03/1989	20/03/1989	1	20/03/1989	20/03/1989
327003	LMC	2744900	6099200	63.18	51.00				1	25/05/1990	25/05/1990	1	25/05/1990	25/05/1990
327005	LMC	2746100	6105500	90.03	92.60				3	03/06/1992	14/03/1995	1	14/03/1995	14/03/1995
327011	LMC	2744400	6099100	84.14	42.00				1	13/03/1989	13/03/1989	1	13/03/1989	13/03/1989
327037	LMC	2741611	6107000	172.00	58.60	1	58.10	58.60	2	03/12/2002	06/12/2006	1	03/12/2002	03/12/2002
327039	LMC	2742351	6099119	123.49	117.00	1	115.00	117.00	1	11/06/2003	11/06/2003	1	11/06/2003	11/06/2003

Well	Location Classification	NZMG		Elevation (masl)	Well Nominal Depth (m)	Well Screens			All Samples			Acceptable Samples		
		Easting	Northing			Number	From	To	Number	From	To	Number	From	To
327041	LMC	2741000	6097800	105.56	120.17				1	20/03/1989	20/03/1989	1	20/03/1989	20/03/1989
327051	LMC	2744600	6100600	94.24	40.10	1	37.00	40.10	1	13/03/1989	13/03/1989	1	13/03/1989	13/03/1989
327071	LMC	2743700	6099100	83.13	68.63				1	13/03/1989	13/03/1989	1	13/03/1989	13/03/1989
327081	LMC	2743272	6100159	131.42	110.00				1	13/03/1989	13/03/1989	1	13/03/1989	13/03/1989
327091	LMC	2743134	6099949	131.05	110.00				1	13/03/1989	13/03/1989	1	13/03/1989	13/03/1989
327121	LMC	2741900	6100900	130.00	25.92				2	14/03/1995	15/03/1995	1	14/03/1995	14/03/1995
327131	LMC	2741100	6108400	154.25	133.00				1	30/03/1989	30/03/1989	1	30/03/1989	30/03/1989
327141	LMC	2741930	6098073	109.04	111.00	1	105.00	111.00	1	20/03/1989	20/03/1989	1	20/03/1989	20/03/1989
327191	LMC	2747200	6105000	97.47	14.00				3	02/10/1994	15/03/1995	1	14/03/1995	14/03/1995
333001	LMC	2713177	6090586	20.63	113.00				2	06/03/1989	21/03/2006	1	06/03/1989	06/03/1989
333011	LMC	2713465	6096884	17.91	83.00				2	16/02/1989	22/05/2006	1	16/02/1989	16/02/1989
333041	LMC	2712502	6094872	22.03	182.00	1	152.60	182.00	2	02/03/1989	29/03/2006	1	02/03/1989	02/03/1989
333048	Within 2 km	2710600	6089500	26.00					1	22/03/1977	22/03/1977	1	22/03/1977	22/03/1977
333050	Within 2 km	2708100	6087500	22.00	23.00				2	01/01/1975	12/10/1977	1	12/10/1977	12/10/1977
333061	LMC	2712600	6092327	18.42	97.00				2	09/02/1989	12/05/2006	1	09/02/1989	09/02/1989
333068	Within 2 km	2710609	6090171	30.48	41.00				2	27/01/1975	06/12/1976	1	06/12/1976	06/12/1976
333071	LMC	2713788	6094724	18.91	131.00				3	02/03/1989	29/03/2006	2	02/03/1989	06/06/1989
333071	LMC	2713788	6094724	18.91	131.00				3	02/03/1989	29/03/2006	2	02/03/1989	06/06/1989
333081	LMC	2713415	6096557	16.97	28.00				1	16/02/1989	16/02/1989	1	16/02/1989	16/02/1989
333094	Within 2 km	2708300	6090100	25.00	50.00				3	29/05/1975	19/10/1977	2	06/12/1976	19/10/1977
333094	Within 2 km	2708300	6090100	25.00	50.00				3	29/05/1975	19/10/1977	2	06/12/1976	19/10/1977
333096	Within 2 km	2709040	6094504	34.18	46.00				2	22/03/1977	22/09/1977	2	22/03/1977	22/09/1977
333096	Within 2 km	2709040	6094504	34.18	46.00				2	22/03/1977	22/09/1977	2	22/03/1977	22/09/1977
333110	Within 2 km	2711000	6089400	27.00	8.00				4	01/05/1975	10/02/1981	2	22/03/1977	19/10/1977
333110	Within 2 km	2711000	6089400	27.00	8.00				4	01/05/1975	10/02/1981	2	22/03/1977	19/10/1977
333236	LMC	2712323	6095434	23.67	54.00				1	08/05/1989	08/05/1989	1	08/05/1989	08/05/1989
334011	LMC	2713792	6097044	19.07	113.00				2	16/02/1989	23/03/2006	1	16/02/1989	16/02/1989
334021	LMC	2722023	6092152	12.64	96.50	1	95.50	96.50	2	27/02/1989	31/10/1995	1	27/02/1989	27/02/1989
334031	LMC	2717361	6088272	12.26	125.00				1	13/02/1989	13/02/1989	1	13/02/1989	13/02/1989
334041	LMC	2715605	6090956	12.67	99.00	1	95.30	99.00	2	16/02/1989	15/05/2006	1	16/02/1989	16/02/1989
334051	LMC	2719772	6097406	18.81	95.00				1	13/02/1989	13/02/1989	1	13/02/1989	13/02/1989
334071	LMC	2718147	6095372	20.00	68.63				1	16/02/1989	16/02/1989	1	16/02/1989	16/02/1989
334091	LMC	2720920	6089360	9.49	19.00	1	18.00	19.00	25	29/02/1988	01/08/2007	1	28/05/2002	28/05/2002
334101	LMC	2714849	6093908	16.68	71.00				2	13/02/1989	17/05/2006	1	13/02/1989	13/02/1989
334121	LMC	2715852	6087685	13.12	63.00				2	13/02/1989	12/05/2006	1	13/02/1989	13/02/1989
335001	LMC	2727104	6088478	21.13	82.10				1	20/02/1989	20/02/1989	1	20/02/1989	20/02/1989
335011	LMC	2727320	6094624	22.00	94.00				2	01/01/1901	27/02/1989	1	27/02/1989	27/02/1989
335041	LMC	2725446	6094738	21.44	155.30	1	151.30	155.30	3	18/06/1984	29/01/1999	1	07/02/1989	07/02/1989
335051	LMC	2724204	6087297	16.83	126.00				2	13/04/1989	29/01/1999	1	13/04/1989	13/04/1989
335091	LMC	2727500	6094500	27.79	80.00				1	03/04/1989	03/04/1989	1	03/04/1989	03/04/1989
335101	LMC	2723673	6086974	13.98	123.00				1	01/11/1995	01/11/1995	1	01/11/1995	01/11/1995
335131	LMC	2730008	6090991	26.09	148.54				6	17/10/1969	01/11/1995	3	23/09/1993	01/11/1995

Well	Location Classification	NZMG		Elevation (masl)	Well Nominal Depth (m)	Well Screens			All Samples			Acceptable Samples		
		Easting	Northing			Number	From	To	Number	From	To	Number	From	To
335131	LMC	2730008	6090991	26.09	148.54				6	17/10/1969	01/11/1995	3	23/09/1993	01/11/1995
335131	LMC	2730008	6090991	26.09	148.54				6	17/10/1969	01/11/1995	3	23/09/1993	01/11/1995
335141	LMC	2726620	6090506	17.04	50.00				1	20/02/1989	20/02/1989	1	20/02/1989	20/02/1989
335161	LMC	2726480	6095876	27.03	68.63				1	07/02/1989	07/02/1989	1	07/02/1989	07/02/1989
335171	LMC	2724602	6089231	13.77	68.63				2	01/05/1989	31/10/1995	1	01/05/1989	01/05/1989
335221	LMC	2725428	6090500	14.50	114.00	1	111.00	114.00	1	20/02/1989	20/02/1989	1	20/02/1989	20/02/1989
335241	LMC	2729931	6096667	38.00	100.58	1	97.54	100.58	1	20/04/1989	20/04/1989	1	20/04/1989	20/04/1989
335261	LMC	2724282	6093366	16.73	95.77				1	27/02/1989	27/02/1989	1	27/02/1989	27/02/1989
335291	LMC	2726317	6088776	17.90	237.00	2	169.00	237.00	1	20/02/1989	20/02/1989	1	20/02/1989	20/02/1989
335301	LMC	2726032	6093210	19.66	32.00	1	31.40	32.00	1	27/02/1989	27/02/1989	1	27/02/1989	27/02/1989
335311	LMC	2730453	6088953	28.24	85.00				1	01/05/1989	01/05/1989	1	01/05/1989	01/05/1989
335331	LMC	2727044	6087486	21.96	141.00	1	139.00	141.00	2	13/04/1989	29/01/1999	1	13/04/1989	13/04/1989
335351	LMC	2726004	6088453	18.31	171.00				4	13/04/1989	28/01/1999	2	13/04/1989	06/09/1993
335351	LMC	2726004	6088453	18.31	171.00				4	13/04/1989	28/01/1999	2	13/04/1989	06/09/1993
335361	LMC	2728554	6088463	23.87	112.00				2	07/02/1989	29/01/1999	1	07/02/1989	07/02/1989
335371	LMC	2726552	6093332	20.66	111.00				2	07/02/1989	31/10/1995	1	07/02/1989	07/02/1989
335391	LMC	2729492	6096409	31.43	73.30	1	71.30	73.30	5	23/10/1987	31/10/1995	2	03/04/1989	06/06/1989
335391	LMC	2729492	6096409	31.43	73.30	1	71.30	73.30	5	23/10/1987	31/10/1995	2	03/04/1989	06/06/1989
335431	LMC	2728700	6092700	21.57	136.00				2	17/05/1989	15/01/2002	1	17/05/1989	17/05/1989
336001	LMC	2732831	6094613	43.68	125.00				3	06/03/1970	31/10/1996	1	27/02/1989	27/02/1989
336004	LMC	2735625	6090697	36.49	72.00				3	01/08/1990	16/09/1994	1	14/10/1993	14/10/1993
336017	LMC	2737308	6093930	44.44	60.00				1	13/05/1991	13/05/1991	1	13/05/1991	13/05/1991
336022	LMC	2737328	6092483	41.03	61.00				1	13/05/1991	13/05/1991	1	13/05/1991	13/05/1991
336024	LMC	2736543	6092512	39.34	55.00				1	13/05/1991	13/05/1991	1	13/05/1991	13/05/1991
336035	LMC	2737814	6094014	42.27	88.00				1	09/09/1991	09/09/1991	1	09/09/1991	09/09/1991
336039	LMC	2739262	6093780	43.54					1	13/05/1991	13/05/1991	1	13/05/1991	13/05/1991
336041	LMC	2738217	6093317	42.37	78.00				2	16/02/1989	31/10/1995	1	16/02/1989	16/02/1989
336050	LMC	2739027	6093684	43.37	100.00				1	13/05/1991	13/05/1991	1	13/05/1991	13/05/1991
336060	LMC	2738688	6094288	45.08	15.00				1	13/05/1991	13/05/1991	1	13/05/1991	13/05/1991
336061	LMC	2736500	6088550	78.46	58.50				1	27/03/2002	27/03/2002	1	27/03/2002	27/03/2002
336069	LMC	2737800	6090600	49.56	36.00				1	05/08/1991	05/08/1991	1	05/08/1991	05/08/1991
336071	LMC	2731448	6088704	28.43	84.30				3	11/07/1984	04/10/1993	2	11/07/1984	04/10/1993
336071	LMC	2731448	6088704	28.43	84.30				3	11/07/1984	04/10/1993	2	11/07/1984	04/10/1993
336078	LMC	2735637	6092613	37.76	65.00				1	13/05/1991	13/05/1991	1	13/05/1991	13/05/1991
336079	LMC	2735400	6089600	35.68					1	09/09/1991	09/09/1991	1	09/09/1991	09/09/1991
336080	LMC	2736351	6091256	38.02	70.00				1	09/09/1991	09/09/1991	1	09/09/1991	09/09/1991
336081	LMC	2731500	6089600	28.28	166.84				2	16/10/1969	06/04/1989	1	06/04/1989	06/04/1989
336085	LMC	2735286	6090751	31.70	38.00				1	09/09/1991	09/09/1991	1	09/09/1991	09/09/1991
336088	LMC	2737061	6093037	39.91	60.00				1	13/05/1991	13/05/1991	1	13/05/1991	13/05/1991
336091	LMC	2732700	6092500	35.00	151.59				1	20/03/1984	20/03/1984	1	20/03/1984	20/03/1984
336097	LMC	2738143	6090678	52.66	90.00				2	09/09/1991	04/04/1996	1	09/09/1991	09/09/1991
336101	LMC	2732772	6092609	35.72	130.15	1	126.00	130.15	4	22/09/1993	01/11/1995	1	22/07/1994	22/07/1994







Well	Location Classification	NZMG		Elevation (masl)	Well Nominal Depth (m)	Well Screens			All Samples			Acceptable Samples		
		Easting	Northing			Number	From	To	Number	From	To	Number	From	To
337005	LMC	2743665	6094800	51.08	83.00	1	77.00	83.00	39	05/12/1990	17/08/2004	25	13/12/1990	17/08/2004
337005	LMC	2743665	6094800	51.08	83.00	1	77.00	83.00	39	05/12/1990	17/08/2004	25	13/12/1990	17/08/2004
337005	LMC	2743665	6094800	51.08	83.00	1	77.00	83.00	39	05/12/1990	17/08/2004	25	13/12/1990	17/08/2004
337005	LMC	2743665	6094800	51.08	83.00	1	77.00	83.00	39	05/12/1990	17/08/2004	25	13/12/1990	17/08/2004
337005	LMC	2743665	6094800	51.08	83.00	1	77.00	83.00	39	05/12/1990	17/08/2004	25	13/12/1990	17/08/2004
337005	LMC	2743665	6094800	51.08	83.00	1	77.00	83.00	39	05/12/1990	17/08/2004	25	13/12/1990	17/08/2004
337005	LMC	2743665	6094800	51.08	83.00	1	77.00	83.00	39	05/12/1990	17/08/2004	25	13/12/1990	17/08/2004
337005	LMC	2743665	6094800	51.08	83.00	1	77.00	83.00	39	05/12/1990	17/08/2004	25	13/12/1990	17/08/2004
337006	LMC	2739300	6092200	51.20					1	05/08/1991	05/08/1991	1	05/08/1991	05/08/1991
337007	LMC	2743283	6095927	52.39	85.00	1	79.00	85.00	1	15/08/1990	15/08/1990	1	15/08/1990	15/08/1990
337008	LMC	2739800	6092000	57.41	50.00				1	05/08/1991	05/08/1991	1	05/08/1991	05/08/1991
337010	LMC	2740400	6093100	54.56	35.00				1	05/08/1991	05/08/1991	1	05/08/1991	05/08/1991
337011	LMC	2741361	6095539	46.66	25.40				1	20/02/1989	20/02/1989	1	20/02/1989	20/02/1989
337012	LMC	2741000	6092900	59.75	35.00				1	05/08/1991	05/08/1991	1	05/08/1991	05/08/1991
337014	LMC	2740600	6093900	55.66					1	05/08/1991	05/08/1991	1	05/08/1991	05/08/1991
337015	LMC	2743282	6095969	52.41	84.70	2	75.70	84.70	2	18/03/1991	01/01/1994	1	18/03/1991	18/03/1991
337018	LMC	2742200	6096500	62.74					1	09/09/1991	09/09/1991	1	09/09/1991	09/09/1991
337023	LMC	2739500	6091400	62.83	60.00				1	09/09/1991	09/09/1991	1	09/09/1991	09/09/1991
337031	LMC	2741732	6094389	48.71	80.83				2	07/02/1989	31/10/1995	1	07/02/1989	07/02/1989
337041	LMC	2741818	6095040	48.72	99.00				2	16/12/1969	07/02/1989	1	07/02/1989	07/02/1989
337051	LMC	2741139	6096263	60.56	61.00				1	20/03/1989	20/03/1989	1	20/03/1989	20/03/1989
337064	LMC	2739206	6091223	60.58	32.50	1	31.50	32.50	1	27/03/2002	27/03/2002	1	27/03/2002	27/03/2002
337067	LMC	2739207	6092097	51.85	49.50	1	46.60	49.50	1	27/03/2002	27/03/2002	1	27/03/2002	27/03/2002
342001	LMC	2704483	6081080	15.31	80.00				2	13/03/1989	02/03/2006	1	13/03/1989	13/03/1989
342002	LMC	2703300	6076800	10.00					1	30/10/1996	30/10/1996	1	30/10/1996	30/10/1996
342011	LMC	2703903	6079869	11.88	72.00				2	09/03/1989	02/03/2006	1	09/03/1989	09/03/1989
342041	LMC	2702980	6084733	9.51	26.00				1	06/03/1989	06/03/1989	1	06/03/1989	06/03/1989
342051	LMC	2703360	6078432	6.95	65.50	1	59.40	65.50	37	15/06/1988	16/08/2004	3	29/04/1991	21/10/1991
342051	LMC	2703360	6078432	6.95	65.50	1	59.40	65.50	37	15/06/1988	16/08/2004	3	29/04/1991	21/10/1991
342051	LMC	2703360	6078432	6.95	65.50	1	59.40	65.50	37	15/06/1988	16/08/2004	3	29/04/1991	21/10/1991
342061	LMC	2700054	6079648	2.67	67.10				5	04/11/1969	24/08/1993	1	13/03/1989	13/03/1989
342081	LMC	2700919	6080108	4.83	28.50	1	26.50	28.50	3	04/11/1983	02/03/2006	1	09/03/1989	09/03/1989
342091	LMC	2703738	6077464	3.57	160.00				7	04/11/1969	19/05/2006	2	07/12/1984	30/03/1989
342091	LMC	2703738	6077464	3.57	160.00				7	04/11/1969	19/05/2006	2	07/12/1984	30/03/1989
342097	LMC	2702893	6084888	10.36	192.00	1	183.00	192.00	2	14/04/2003	10/03/2006	1	14/04/2003	14/04/2003
342105	LMC	2700021	6079231	2.73	205.00	3	168.20	205.00	5	26/11/2002	22/11/2006	1	26/11/2002	26/11/2002
342141	LMC	2702598	6080882	10.18	66.00	1	60.00	66.00	2	09/03/1989	26/03/1990	1	09/03/1989	09/03/1989
342151	LMC	2702346	6079509	6.90	60.00	1	57.00	60.00	2	09/03/1989	08/05/2006	1	09/03/1989	09/03/1989
342161	LMC	2704138	6076691	4.80	51.00				3	14/04/2003	10/05/2006	1	14/04/2003	14/04/2003
342171	LMC	2701955	6081547	7.64	51.30	1	45.20	51.30	2	09/03/1989	09/03/2006	1	09/03/1989	09/03/1989
343021	LMC	2706986	6077528	14.31	66.00				2	20/03/1989	10/05/2006	1	20/03/1989	20/03/1989
343031	LMC	2709787	6077039	3.56	46.00				1	30/03/1989	30/03/1989	1	30/03/1989	30/03/1989

Well	Location Classification	NZMG		Elevation (masl)	Well Nominal Depth (m)	Well Screens			All Samples			Acceptable Samples		
		Easting	Northing			Number	From	To	Number	From	To	Number	From	To
343051	LMC	2708919	6077031	7.19	167.43				2	20/03/1989	22/02/2006	1	20/03/1989	20/03/1989
343061	Within 2 km	2708299	6084377	26.98	38.20	1	31.30	38.20	4	06/03/1989	23/02/2006	1	06/03/1989	06/03/1989
343101	LMC	2711435	6086030	26.51	41.30	1	38.20	41.30	3	02/03/1989	15/03/2006	2	02/03/1989	13/03/1989
343101	LMC	2711435	6086030	26.51	41.30	1	38.20	41.30	3	02/03/1989	15/03/2006	2	02/03/1989	13/03/1989
343121	LMC	2709086	6078129	12.09	75.00	1	71.00	75.00	4	03/05/1983	18/05/2006	1	20/03/1989	20/03/1989
343151	LMC	2705362	6077796	10.98	56.90				2	20/03/1989	01/03/2006	1	20/03/1989	20/03/1989
343155	Within 2 km	2706857	6086664	22.26	169.80	1	166.80	169.80	1	14/04/2003	14/04/2003	1	14/04/2003	14/04/2003
343161	Within 2 km	2707884	6084262	26.86	54.00				2	06/03/1989	11/05/2006	1	06/03/1989	06/03/1989
343171	Within 2 km	2707280	6086805	24.57	120.00	1	114.60	120.00	4	09/02/1989	23/02/2006	1	09/02/1989	09/02/1989
344011	LMC	2721284	6083778	13.14	29.00				1	13/02/1989	13/02/1989	1	13/02/1989	13/02/1989
344031	LMC	2715735	6086601	14.65	31.50	1	29.60	31.50	2	13/02/1989	06/06/1989	2	13/02/1989	06/06/1989
344031	LMC	2715735	6086601	14.65	31.50	1	29.60	31.50	2	13/02/1989	06/06/1989	2	13/02/1989	06/06/1989
344041	LMC	2714987	6080259	5.39	68.40				1	13/02/1989	13/02/1989	1	13/02/1989	13/02/1989
344051	LMC	2721233	6084351	12.86	137.00				2	13/04/1989	28/01/1999	1	13/04/1989	13/04/1989
344061	LMC	2720593	6079134	5.83	81.32				1	27/04/1989	27/04/1989	1	27/04/1989	27/04/1989
344081	LMC	2716900	6084300	13.18	36.00				1	30/03/1989	30/03/1989	1	30/03/1989	30/03/1989
344091	LMC	2714319	6078870	6.39	59.00				1	13/02/1989	13/02/1989	1	13/02/1989	13/02/1989
344183	LMC	2716605	6078479	7.00	154.70	1	151.70	154.70	1	14/04/2003	14/04/2003	1	14/04/2003	14/04/2003
345011	LMC	2722414	6085552	14.25	135.00				2	13/04/1989	28/01/1999	1	13/04/1989	13/04/1989
345041	LMC	2729264	6085929	36.49	165.51				7	14/07/1975	17/09/1998	1	02/12/1997	02/12/1997
345051	LMC	2725461	6083162	15.88	52.00				1	04/10/1989	04/10/1989	1	04/10/1989	04/10/1989
345053	LMC	2729236	6085940	36.06	163.90				4	04/09/1986	17/09/1998	1	06/04/1989	06/04/1989
345061	LMC	2723500	6082000	10.45	62.83				1	10/04/1989	10/04/1989	1	10/04/1989	10/04/1989
345071	LMC	2724304	6085753	15.52	85.00				1	10/04/1989	10/04/1989	1	10/04/1989	10/04/1989
345081	LMC	2722198	6077097	18.35	183.00				3	31/05/1977	23/06/1997	2	27/04/1989	23/06/1997
345081	LMC	2722198	6077097	18.35	183.00				3	31/05/1977	23/06/1997	2	27/04/1989	23/06/1997
345091	LMC	2722187	6077096	17.92	91.50				1	27/04/1989	27/04/1989	1	27/04/1989	27/04/1989
345101	LMC	2726857	6081869	28.54	36.00	1	33.00	36.00	1	13/02/1989	13/02/1989	1	13/02/1989	13/02/1989
345111	LMC	2724301	6085634	16.09	111.00				2	10/04/1989	28/01/1999	1	10/04/1989	10/04/1989
345141	LMC	2723078	6077930	35.67	205.70				3	14/01/1976	28/06/1984	1	28/06/1984	28/06/1984
345151	LMC	2723416	6079642	14.79	78.00	1	77.10	78.00	4	23/04/1987	26/03/2002	1	27/04/1989	27/04/1989
346031	LMC	2734540	6086023	57.34	47.28				4	10/02/1970	27/03/2002	3	06/04/1989	27/03/2002
346031	LMC	2734540	6086023	57.34	47.28				4	10/02/1970	27/03/2002	3	06/04/1989	27/03/2002
346031	LMC	2734540	6086023	57.34	47.28				4	10/02/1970	27/03/2002	3	06/04/1989	27/03/2002
346041	LMC	2732300	6085800	58.83	88.75				1	06/04/1989	06/04/1989	1	06/04/1989	06/04/1989
346051	LMC	2734138	6085589	96.47	104.00				1	26/03/2002	26/03/2002	1	26/03/2002	26/03/2002
352001	LMC	2702146	6070470	21.76	44.90				1	03/04/1989	03/04/1989	1	03/04/1989	03/04/1989
352003	LMC	2701230	6073883	10.77	54.90	1	51.00	54.90	1	11/08/1983	11/08/1983	1	11/08/1983	11/08/1983
352011	LMC	2702633	6070645	19.75	23.60				1	03/04/1989	03/04/1989	1	03/04/1989	03/04/1989
352021	LMC	2702915	6072851	13.89	37.50				1	03/04/1989	03/04/1989	1	03/04/1989	03/04/1989
352051	LMC	2703128	6072610	11.95	44.20				1	03/04/1989	03/04/1989	1	03/04/1989	03/04/1989
352123	LMC	2702683	6068017	7.66	50.60	1	38.60	50.60	1	14/04/2003	14/04/2003	1	14/04/2003	14/04/2003



Well	Location Classification	NZMG		Elevation (masl)	Well Nominal Depth (m)	Well Screens			All Samples			Acceptable Samples		
		Easting	Northing			Number	From	To	Number	From	To	Number	From	To
354011	LMC	2714255	6074187	5.05	36.50	1	33.50	36.50	65	01/05/1989	25/03/2008	13	08/06/1993	04/03/1997
354011	LMC	2714255	6074187	5.05	36.50	1	33.50	36.50	65	01/05/1989	25/03/2008	13	08/06/1993	04/03/1997
354011	LMC	2714255	6074187	5.05	36.50	1	33.50	36.50	65	01/05/1989	25/03/2008	13	08/06/1993	04/03/1997
354011	LMC	2714255	6074187	5.05	36.50	1	33.50	36.50	65	01/05/1989	25/03/2008	13	08/06/1993	04/03/1997
354011	LMC	2714255	6074187	5.05	36.50	1	33.50	36.50	65	01/05/1989	25/03/2008	13	08/06/1993	04/03/1997
354011	LMC	2714255	6074187	5.05	36.50	1	33.50	36.50	65	01/05/1989	25/03/2008	13	08/06/1993	04/03/1997
354011	LMC	2714255	6074187	5.05	36.50	1	33.50	36.50	65	01/05/1989	25/03/2008	13	08/06/1993	04/03/1997
354011	LMC	2714255	6074187	5.05	36.50	1	33.50	36.50	65	01/05/1989	25/03/2008	13	08/06/1993	04/03/1997
354011	LMC	2714255	6074187	5.05	36.50	1	33.50	36.50	65	01/05/1989	25/03/2008	13	08/06/1993	04/03/1997
354011	LMC	2714255	6074187	5.05	36.50	1	33.50	36.50	65	01/05/1989	25/03/2008	13	08/06/1993	04/03/1997
354011	LMC	2714255	6074187	5.05	36.50	1	33.50	36.50	65	01/05/1989	25/03/2008	13	08/06/1993	04/03/1997
354021	LMC	2717338	6075320	4.12	32.00				1	10/04/1989	10/04/1989	1	10/04/1989	10/04/1989
354031	LMC	2715706	6068786	52.38	62.00	1	60.00	62.00	1	10/04/1989	10/04/1989	1	10/04/1989	10/04/1989
354051	LMC	2715914	6068725	47.65	26.01				2	28/06/1995	14/04/2003	1	14/04/2003	14/04/2003
354061	LMC	2714953	6072473	5.35	88.00				1	27/04/1989	27/04/1989	1	27/04/1989	27/04/1989
354063	LMC	2717723	6075907	5.07	175.00	1	160.00	175.00	2	14/04/2003	12/05/2003	2	14/04/2003	12/05/2003
354063	LMC	2717723	6075907	5.07	175.00	1	160.00	175.00	2	14/04/2003	12/05/2003	2	14/04/2003	12/05/2003
354081	LMC	2713559	6072334	4.41	157.08				1	30/03/1989	30/03/1989	1	30/03/1989	30/03/1989
354091	LMC	2713617	6072264	4.73	108.30	2	87.60	108.30	2	30/03/1989	23/01/2003	1	30/03/1989	30/03/1989
363001	Within 2 km	2705893	6061382	57.66	45.00	1	42.00	45.00	6	13/04/1989	16/12/1999	1	13/04/1989	13/04/1989
363011	LMC	2704770	6064643	46.06	36.00	1	30.00	36.00	1	13/04/1989	13/04/1989	1	13/04/1989	13/04/1989
363021	Within 2 km	2704700	6061600	47.00	107.97				1	22/08/1980	22/08/1980	1	22/08/1980	22/08/1980
363055	LMC	2707100	6064300	28.72	21.30				3	25/08/1987	13/04/1989	1	13/04/1989	13/04/1989
363101	LMC	2707544	6062894	43.37	115.00				4	30/01/1984	15/10/1985	1	10/02/1984	10/02/1984
363161	LMC	2705494	6063610	35.04	23.00	1	17.00	23.00	7	13/04/1989	14/12/1999	1	13/04/1989	13/04/1989
363251	Within 2 km	2704865	6061400	48.41	30.00	1	28.00	30.00	2	17/05/1988	15/05/1989	1	15/05/1989	15/05/1989
363271	LMC	2708092	6062687	50.80	51.20	1	48.10	51.20	1	15/05/1989	15/05/1989	1	15/05/1989	15/05/1989
363273	LMC	2708200	6062600	84.00					1	15/05/1989	15/05/1989	1	15/05/1989	15/05/1989

Table D-2: Complete, acceptable groundwater quality data in the Lower Manawatu Catchment until the end of 2007. All concentrations in mg/L<sup>71</sup>.

Sample #	Well ID	Temp (°C)	EC (µS/cm)	TDS	pH	Ca	Mg	Na	K	Fe	Mn	B	HCO <sub>3</sub>	CO <sub>2</sub>	SO <sub>4</sub>	Cl	F	Br	Nh <sub>4</sub>	NO <sub>2</sub>	NO <sub>3</sub>	PO <sub>4</sub>	CAB (%)	Representative
1	316001		263		7.00	17.22	10.93	20.00		0.19	0.98		106.06	22.00	3.00	25.00					1.329		1.97	Y
2	316037		299	223	6.10	16.82	7.53	24.00	1.80				43.89	57.00	10.00	29.00			0.026		62.000	0.061	-3.71	N
3	316037	14.0	301		6.10	16.42	7.05	26.00	2.00				43.89	57.00	11.00	28.00				0.003	48.714	0.061	1.12	N
4	316037	14.0	303		6.10	14.42	8.75	24.00	1.80				43.89	57.00	10.00	27.00					57.571	0.061	-1.72	N
5	316037		292		6.10	17.22	6.56	26.00	2.00	0.10			41.45	54.00	12.00	28.00					57.571	0.061	-1.27	N
6	316037		291		6.10	17.22	7.05	25.00	2.10				40.23	52.00	12.00	26.00					53.143	0.061	1.59	N
7	316037		293		6.10	16.82	6.32	26.00	2.00				41.45	54.00	12.00	25.00			0.026		53.143	0.061	0.99	N
8	316037		290		6.20	18.02	6.07	26.00	1.90		0.02		37.79	39.00	12.00	26.00					48.714	0.061	3.83	N
9	316037		293		6.00	16.82	6.80	26.00	2.10	0.05			43.89	72.00	11.00	25.00					53.143	0.061	1.44	N
10	316037		286		6.20	16.82	6.80	26.00	2.20	0.04			40.23	42.00	11.00	27.00					53.143	0.021	1.56	N
11	316037	16.5	294		6.20	17.62	6.32	25.00	2.30	0.04			46.33	48.00	11.00	24.00			0.039		53.143	0.037	0.45	N
12	316037		287		6.50	17.62	6.32	25.00	2.00	0.03			42.67	22.00	9.30	24.00					57.571	0.104	0.78	N
13	316037		283		6.00	17.22	6.56	26.00	2.20	0.06			42.67	70.00	11.00	24.00			0.026		57.571	0.040	1.03	N
14	316037		284		6.20	16.82	6.80	27.00	2.20		0.02		41.45	43.00	12.00	25.00				0.010	53.143	0.080	2.70	N
15	316037		287		6.00	17.22	6.56	24.00	2.20	0.06			41.45	68.00	11.00	24.00			0.064	0.010	53.143	0.064	1.15	N
16	316037		283		6.00	16.02	7.29	26.00	2.20				41.45	68.00	12.00	25.00			0.013		53.143	0.049	1.87	N
17	316037		280		6.20	17.62	6.56	24.00	2.10	0.03		0.021	40.23	50.00	12.00	26.00		0.14			55.357	0.061	-0.37	Y
18	316037		281		6.10	20.82	4.37	27.00	2.30	0.06			41.45	54.00	12.00	25.00					55.800	0.058	1.90	N
19	316037		284		6.20	16.82	7.05	25.00	2.20				39.01	40.00	12.00	26.00					56.243		0.65	N
20	316037		292	199	6.10	14.82	8.02	24.00	1.90	0.02	0.01		41.45	54.00	11.00	27.00			0.051		54.029		-0.99	N
21	316037	18.4	291		6.47	17.22	7.05	24.80	2.44				41.45		13.00	28.00	0.18				54.029	0.772	-0.60	N
22	316041		265	170	6.40	14.02	8.50	22.00	2.70	2.70	1.07		79.24	52.00	15.00	30.00	0.19		0.007				-0.66	Y
23	318001		375	231	8.10	26.43	8.26	32.00	7.00	0.07	0.10		177.99	6.00	25.00	13.00	0.18						-3.19	Y
24	323001		595	224	8.10	57.27	19.92	24.00	13.00	0.44	0.06		273.08	4.00	13.00	45.00	0.09						-1.20	Y
25	323021		860	391	7.95	96.12	29.64	32.00	12.50	0.60	0.18		341.35	6.00	63.00	72.00							0.05	Y
26	323027		750			94.51	30.61	29.50	7.60			0.040	329.16		65.00	67.00							0.43	Y
27	323092		303		8.30	37.65	6.32	14.00	8.90	1.49	0.07	0.036	160.92		8.00	15.00							0.12	Y
28	323166	14.1	1430		6.60	51.26	57.34	110.00	6.40	3.29			360.86		80.00	210.00							-4.97	Y
29	324009		445			53.66	13.36	16.50	5.50			0.030	231.63		13.00	33.00							-3.76	Y
30	324011		560	165	8.05	66.88	15.55	20.00	6.70	0.11	0.15		232.85	3.00	27.00	40.00	0.18						1.35	Y
31	324011		460		8.20	60.07	15.69	20.00	6.90	0.10	0.02		247.48		31.00	36.00		0.10	0.450		0.443		-3.52	N
32	324041		550		8.10	56.07	19.44	20.00		0.37	0.05		232.85	3.00	24.00	41.00							-1.91	N
33	324041		540	329	8.05	58.87	18.46	22.00	8.00	0.54	0.06		235.29	3.00	23.00	41.00	0.17						1.14	Y
34	324057		760			98.92	26.72	30.00	6.10			0.028	329.16		64.00	80.00							-2.21	Y
35	324071		589		7.90	68.08	17.01	22.00	6.80	0.37	0.04		241.39	5.00	40.00	38.00			0.669			0.123	0.56	Y
36	325013		850			104.12	26.72	49.00	4.90			0.025	402.31		57.00	88.00							-3.07	Y

<sup>71</sup> For wells and samples locations, see map in Figure D-1 in Appendix D.

Sample #	Well ID	Temp (°C)	EC (µS/cm)	TDS	pH	Ca	Mg	Na	K	Fe	Mn	B	HCO <sub>3</sub>	CO <sub>2</sub>	SO <sub>4</sub>	Cl	F	Br	NH <sub>4</sub>	NO <sub>2</sub>	NO <sub>3</sub>	PO <sub>4</sub>	CAB (%)	Representative
37	325031		510	326	8.20	59.27	12.63	25.00	3.60	1.08	0.07		199.94	2.00	21.00	51.00	0.10						0.23	Y
38	325071		380	145	8.25	42.85	9.96	18.00	3.10	0.27	0.04		174.33	2.00	7.00	32.00	0.10						-1.11	N
39	325071		360	208	8.30	41.65	9.48	17.00	2.90	0.90	0.07		160.92	1.00	8.00	28.00	0.07						1.07	Y
40	325081		345	226	7.30	26.43	13.36	21.00	3.80	3.50	0.75		171.90	14.00	0.10	24.00	0.14						-0.97	Y
41	325091		595	356	7.60	55.67	20.89	30.00	3.90	1.30	1.20		257.23	11.00	13.00	52.00	0.19						-0.44	Y
42	325121		415	117	8.25	48.86	11.42	18.00	3.10	0.81	0.04		181.65	2.00	14.00	36.00	0.09						-0.52	Y
43	325141		256		7.30	29.24	14.82	20.00	2.90	1.87	0.45		163.36	12.00	1.00	28.00				0.085	0.089		1.84	Y
44	325221		325	202	7.20	21.63	14.82	18.50	3.40	3.60	1.04		160.92	17.00	0.10	24.00	0.12			0.003			-1.94	Y
45	325251		270	160	6.70	20.42	9.23	17.50	2.10	0.30	1.25		109.72	36.00	1.00	27.00	0.12			0.003			0.25	Y
46	325351		275	166	7.30	20.42	10.20	16.00	3.20	5.10	0.63		137.76	11.00	0.10	21.00	0.21						-3.93	Y
47	325361		260		6.70	23.03	9.74	20.00	2.00	0.39	0.53		146.29		0.87	26.00	0.12			0.003			-4.61	Y
48	325381		710			55.67	29.15	50.00	5.10			0.026	341.35		0.90	85.00							-3.42	Y
49	326011		440	237	8.10	44.85	13.36	25.00	3.70	0.11	0.17		185.31	2.00	15.00	38.00	0.19						1.10	Y
50	326021		1065	732	7.20	65.68	38.87	78.00	7.70	4.40	2.30		235.29	24.00	25.00	217.00	0.20			0.003			-2.10	Y
51	326041		490	332	7.25	44.85	16.52	29.00	4.20	1.30	1.62		171.90	16.00	30.00	45.00	0.27						2.64	Y
52	326061		580	300	8.10	60.07	7.77	28.00	4.20	0.15	0.30		190.18	6.00	24.00	41.00	0.10		0.167				1.95	Y
53	326071		745	460	6.90	30.44	30.86	65.00	3.50	6.00	0.34		134.10	28.00	53.00	126.00	0.34			0.007			0.86	Y
54	326091		310	221	8.20	37.24	6.56	15.00	2.90	0.01	0.05		138.98	1.00	10.00	21.00	0.07						0.75	Y
55	326099		440		8.30	50.06	13.98	27.00	3.00	0.10	0.12		209.69		25.00	44.00		0.10					-2.96	Y
56	326101		495	209	7.75	53.26	14.33	24.00	4.30	0.57	0.66		195.06	6.00	25.00	41.00	0.24						1.19	Y
57	326103		282		8.20	36.84	4.37	13.00	2.70	0.04	0.04		134.10	2.00	9.00	18.00							-1.05	Y
58	326113		212	142	8.30	25.63	4.86	7.90	1.90		0.04		107.28		5.00	6.00			0.077				0.96	Y
59	326117		342	225	8.20	41.37	5.42	14.40	2.82	0.03	0.02	0.014	163.36	2.00	16.30	16.80			0.450				-4.21	Y
60	326119		450			45.65	14.58	25.00	3.00			0.018	201.15		24.00	43.00							-3.81	Y
61	326131		705		6.60	26.03	19.68	77.00	3.20	3.00	0.27		107.28	44.00	41.00	133.00			0.090		0.089	0.031	-0.12	Y
62	326141		425	197	7.30	40.05	12.88	22.00	4.10	4.60	0.59		158.49	13.00	22.00	40.00	0.20						-0.77	Y
63	326151		405	319	7.15	34.84	10.69	26.00	3.80	4.90	0.58		141.42	16.00	16.00	45.00	0.18						-0.95	Y
64	326171		445	178	7.90	41.65	12.15	30.00	3.20	0.32	0.58		174.33	4.00	14.00	47.00	0.30			0.003			-0.11	Y
65	326181		335	227	8.10	41.25	8.02	13.00	2.20	0.17	0.03		143.86	2.00	16.00	22.00	0.10						0.42	Y
66	326191		233		8.03	28.43	6.32	9.00	2.30	0.07	0.04		117.04	2.00	6.00	10.00				0.003	0.089		1.32	Y
67	326211		480	187	7.50	51.26	12.88	25.50	2.70	2.20	0.56		176.77	9.00	25.00	47.00	0.15			0.003			0.55	Y
68	326211		485	269	7.60	50.86	13.85	28.00	2.50	2.00	0.51		181.65	7.00	24.00	46.00	0.20						1.90	N
69	326231		310	194	6.90	20.02	11.90	21.00	2.70	2.60	0.60		126.79	26.00	1.00	32.00	0.16			0.003			-0.68	Y
70	326241		1005	560	6.80	49.26	42.52	79.00	6.20	9.80	1.57		179.21	47.00	34.00	209.00	0.24			0.046			0.05	Y
71	326241		1020	650	6.90	47.66	41.06	77.00	6.10	12.50	1.50		188.96	39.00	30.00	205.00	0.18						-1.29	N
72	326301		395	221	7.40	35.24	10.20	25.00	3.70	1.50	0.24		143.86	9.00	15.00	39.00	0.20						0.13	Y
73	326311		253		7.90	32.44	6.56	9.50	2.30	0.18	0.04		129.23	3.00	9.10	7.00				0.003	0.089		2.42	Y
74	326321		310	216	7.90	37.24	8.99	12.00	2.50	0.16	0.12		132.88	3.00	25.00	13.00	0.23						1.90	Y
75	326331		550	310	7.90	54.06	19.19	30.00	4.00	0.33	0.22		202.37	4.00	29.00	53.00	0.14						2.42	Y

Sample #	Well ID	Temp (°C)	EC (µS/cm)	TDS	pH	Ca	Mg	Na	K	Fe	Mn	B	HCO <sub>3</sub>	CO <sub>2</sub>	SO <sub>4</sub>	Cl	F	Br	NH <sub>4</sub>	NO <sub>2</sub>	NO <sub>3</sub>	PO <sub>4</sub>	CAB (%)	Representative	
76	326361		530			53.26	20.17	29.00	3.90			0.017	225.54		42.00	53.00							-3.30	Y	
77	327001		240	172	7.10	16.42	9.23	12.50	3.20	2.60	0.39		99.97	13.00	7.00	20.00	0.14							-3.16	Y
78	327003		521		7.79	56.87	14.33	26.00	4.90	0.74	0.77		230.41	7.50	34.00	32.00								-1.07	Y
79	327005		236		6.90	13.62	6.32	22.00	2.70	4.40	0.61		115.82	24.00	8.00	12.00			0.540		0.089	0.429		-3.88	Y
80	327011		525	301	7.45	52.86	16.76	26.00	4.80	0.14	0.34		181.65	11.00	47.00	40.00	0.27			0.003	5.669			0.91	Y
81	327037		411		6.90	18.42	14.82	36.00	4.60	0.10	0.30		99.97	21.00	18.00	61.00			0.039			0.037		1.17	Y
82	327039		316			22.43	14.58	17.50	3.80			0.024	146.29		11.00	23.00								-1.53	Y
83	327041		495	326	7.20	41.65	15.06	30.00	4.30	1.80	1.30		173.12	18.00	27.00	55.00	0.16							-2.25	Y
84	327051		255	153	7.00	16.42	10.20	14.00	3.40	3.50	0.64		108.50	18.00	3.00	22.00	0.17			0.013				-2.22	Y
85	327071		285	224	6.70	15.62	12.63	16.50	3.40	11.50	0.61		99.97	33.00	20.00	23.00	0.19							-1.50	Y
86	327081		340	225	7.10	26.03	12.88	16.50	4.30	5.40	0.60		143.86	19.00	12.00	27.00	0.17							-2.79	Y
87	327091		255	182	7.20	17.22	10.20	13.00	3.20	4.60	0.40		112.16	12.00	2.00	19.00	0.17							-1.47	Y
88	327121		382		7.10	22.03	16.28	28.00	2.50	0.64	0.38		124.35	16.00	28.00	35.00			0.051		2.746			0.92	Y
89	327131		460	313	7.65	48.86	14.33	23.00	6.10	0.68	0.79		199.94	7.00	25.00	31.00	0.19							1.08	Y
90	327141		440	287	7.50	38.05	16.03	22.00	4.70	1.10	0.82		176.77	9.00	16.00	38.00	0.21							-0.09	Y
91	327191		170		6.50	13.22	3.89	13.00	1.70	1.60	0.54		68.27	35.00	6.00	14.00			0.154			0.521		-1.57	Y
92	333001		950	572	7.70	91.31	41.55	45.00	8.30	2.10	0.37		401.09	13.00	26.00	95.00	0.19			0.003				1.75	Y
93	333011		855	339	7.10	64.08	37.90	46.00	5.50	12.80	0.37		301.12	39.00	46.00	90.00	0.18							0.15	Y
94	333041		615	216	8.20	60.87	21.62	26.00	11.60	0.07	0.05		291.37	3.00	14.00	46.00	0.16							-0.96	Y
95	333048	14.8	790		6.40	18.42	25.75	90.00	5.40	4.10			180.43		2.00	164.00								-3.63	Y
96	333050	13.6	470		7.20	42.45	13.61	29.00	6.50	3.02			214.57		1.00	44.00								-1.20	Y
97	333061		755	192	7.80	72.89	28.18	40.00	6.20	0.66	0.26		334.04	9.00	17.00	67.00	0.13							0.87	Y
98	333068	16.2	630		8.00	44.05	43.73	31.00	6.00				380.37		1.00	34.00								0.58	Y
99	333071		755	196	7.90	78.09	29.64	29.00	9.20	7.20	0.99		325.51	7.00	46.00	60.00	0.20		3.857					-0.97	Y
100	333071		770	432	7.90	75.29	33.04	31.00	9.00	0.72	0.16		319.41	7.00	41.00	59.00	0.20							1.91	N
101	333081		1015	636	7.70	96.12	43.73	48.00	7.00	2.40	0.87		382.80	13.00	72.00	100.00	0.21			0.003				0.32	Y
102	333094	15.4	480		6.90	36.84	24.30	23.00	4.90				175.55		5.00	66.00								1.23	Y
103	333094	13.6	550		7.40	2.40	2.92	3.00	0.50				24.38		2.00	4.00								-4.84	N
104	333096	16.0	335		6.70	15.22	17.98	20.00	16.40	4.14			131.66		4.00	42.00								1.47	Y
105	333096	10.4	290		6.60	15.22	11.18	18.00	17.00	0.24			90.21		8.00	36.00								4.25	N
106	333110	14.8	915		6.60	26.43	43.73	77.00	29.00	4.10			248.70		37.00	152.00								-0.69	Y
107	333110	14.6	930		6.60	34.44	30.61	72.00	33.00	2.74			238.95		47.50	144.00								-4.39	N
108	333236		1045	510	7.80	110.53	38.87	50.00	6.90	1.80	0.80		399.87	10.00	56.00	111.00	0.21							0.98	Y
109	334011		745	471	8.05	81.70	26.72	28.00	10.00	0.25	0.07		297.47	4.00	48.00	59.00	0.21							1.38	Y
110	334021		410	273	7.40	28.03	17.01	26.00	4.90	3.90	0.63		209.69	14.00	0.10	27.00	0.22							-1.77	Y
111	334031		845	482	7.50	73.69	39.12	39.00	6.50	3.00	0.67		387.68	20.00	0.10	82.00	0.20							0.51	Y
112	334041		960	413	7.60	69.28	42.76	58.00	10.80	2.10	0.53		440.10	18.00	0.10	97.00	0.19							-0.90	Y
113	334051		1010	631	7.50	80.10	48.10	52.00	9.90	4.00	0.56		396.21	21.00	59.00	103.00	0.20							-0.75	Y
114	334071		800	400	7.70	80.10	31.58	38.00	6.70	1.28	0.39		393.78	13.00	0.10	65.00	0.18			0.003				0.78	Y

Sample #	Well ID	Temp (°C)	EC (µS/cm)	TDS	pH	Ca	Mg	Na	K	Fe	Mn	B	HCO <sub>3</sub>	CO <sub>2</sub>	SO <sub>4</sub>	Cl	F	Br	NH <sub>4</sub>	NO <sub>2</sub>	NO <sub>3</sub>	PO <sub>4</sub>	CAB (%)	Representative	
115	334091		440		6.70	36.04	15.55	28.00	4.50	5.90	1.23	0.041	196.28	60.00	1.00	46.00		0.15	2.443			4.015	-1.39	Y	
116	334101		900	575	7.70	90.91	39.12	38.00	7.10	6.00	0.57		370.61	12.00	49.00	77.00	0.20			0.003				1.71	Y
117	334121		575	331	7.60	43.25	24.30	31.00	6.60	2.40	0.26		265.77	11.00	0.10	51.00	0.23			0.003				-1.06	Y
118	335001		315	200	7.90	35.24	8.26	15.00	3.50	0.31	0.08		156.05	3.00	0.10	21.00	0.20							0.45	Y
119	335011		505	343	7.50	49.26	15.79	25.00	5.10	2.30	0.53		199.94	10.00	0.10	62.00	0.17							-0.53	Y
120	335041		615	357	7.70	64.48	20.65	28.00	4.50	1.38	0.46		266.99	9.00	15.00	51.00	0.20							0.99	Y
121	335051		380	250	7.70	43.25	8.99	17.00	4.80	0.34	0.14		187.74	6.00	0.10	28.00	0.07							-1.43	Y
122	335091		585	368	7.65	56.47	16.28	26.00	4.70	0.74	0.42		212.13	8.00	0.10	78.00	0.16							-2.44	Y
123	335101		306	210	8.20	36.04	6.56	15.00	2.50	0.06	0.03		141.42	1.50	11.00	19.00			0.386					-0.46	Y
124	335131		210		8.30	25.63	5.39	13.00	2.40				128.01		3.70	9.60	1.50			0.257				-2.01	N
125	335131		269		8.00	31.64	5.10	15.00	2.00				120.69	2.00	11.00	15.00			0.360	0.033				1.34	N
126	335131		250	170	8.20	28.03	5.10	12.00	2.30				123.13	5.00	4.00	10.00			0.257					0.33	Y
127	335141		415	263	7.50	40.05	12.39	22.00	4.20	0.93	0.29		185.31	10.00	0.10	29.00	0.20			0.003				2.84	Y
128	335161		445	266	7.70	42.05	13.12	24.00	4.80	0.97	0.53		208.47	7.00	0.10	35.00	0.21			0.003				-0.71	Y
129	335171		465	278	7.35	43.65	14.82	23.00	5.30	2.70	0.55		203.59	15.00	0.10	47.00	0.21							-1.43	Y
130	335221		460	287	7.70	44.85	16.03	22.00	4.30	0.97	0.37		210.91	7.00	0.10	41.00	0.21							0.10	Y
131	335241		425	271	7.70	46.46	11.66	20.00	4.80	0.62	0.17		196.28	6.00	0.10	35.00	0.20							0.76	Y
132	335261		430	260	7.60	42.05	11.18	25.00	6.00	0.80	0.23		223.10	9.00	0.10	27.00	0.16							-1.86	Y
133	335291		335	219	8.25	39.25	9.23	14.00	3.60	0.05	0.02		164.58	2.00	8.00	20.00	0.17							-0.13	Y
134	335301		645	80	6.90	40.45	25.27	43.00	6.30	12.00	1.90		291.37	60.00	0.10	67.00	0.21			0.033				-4.22	Y
135	335311		245	146	8.10	27.23	5.83	12.00	2.50	2.30	0.02		125.57	2.00	2.00	14.00	0.23							-1.43	Y
136	335331		305	177	8.10	35.64	7.29	14.00	2.90	0.11	0.04		152.39	2.00	1.00	17.00	0.18							1.04	Y
137	335351		305	152	8.10	35.64	7.29	14.00	2.90	0.42	0.04		152.39	2.00	4.00	18.00	0.16							-0.45	Y
138	335351		330		6.90	32.04	9.39	23.00	3.20	1.00	0.32		154.83		19.00	29.00			0.154					-4.14	N
139	335361		265	178	8.10	30.84	6.32	12.00	2.70	0.04	0.03		134.10	2.00	2.00	13.00	0.18							0.82	Y
140	335371		445	295	7.50	45.25	13.36	20.00	4.80	1.29	0.53		185.31	10.00	0.10	49.00	0.14			0.003				-0.81	Y
141	335391		610		7.70	59.67	17.25	27.00	4.80	1.10	0.38		212.13	7.00	0.10	82.00	0.10							-0.85	N
142	335391		610	395	7.70	59.67	17.74	28.00	5.00	2.30	0.43		217.00	7.00	0.10	81.00	0.15							-0.52	Y
143	335431		470		7.80	50.06	12.88	22.00	3.50	0.46	0.12		193.84		8.00	47.00			0.707					-0.71	Y
144	336001		430	290	8.20	50.06	9.96	22.00	3.00	2.40	0.08		175.55	2.00	21.00	36.00	0.10							0.24	Y
145	336004		210		8.10	26.63	4.29	11.00	2.50	0.20	0.02		119.47		9.20	7.30			0.643		1.771			-3.47	Y
146	336017	14.5	398	256	7.90	42.85	10.69	20.00	2.80		0.06		164.58	3.00	15.00	34.00			0.386			0.307		-0.12	Y
147	336022	14.0	230	171	8.10	27.63	5.34	10.00	1.90	0.07	0.00		113.38	1.00	10.00	9.00			0.463	0.003				-0.39	Y
148	336024	13.5	362	227	7.90	41.25	8.02	18.00	2.50	0.11	0.04		151.17	3.00	13.00	27.00			0.463	0.003				0.78	Y
149	336035	13.5	257	190	7.90	31.24	5.34	10.00	2.30	0.09	0.00		121.91	2.50	12.00	11.00			0.489	0.003				-1.31	Y
150	336039	14.0	270	185	8.10	32.84	6.07	10.00	2.60	0.01	0.00		117.04	2.00	21.00	9.00			0.437	0.003				0.58	Y
151	336041		220	130	8.10	26.43	4.62	9.00	1.70	0.01	0.02		104.84	1.00	11.00	8.00	0.13							-0.92	Y
152	336050	15.0	268	182	8.20	33.64	6.32	10.00	1.50	0.04	0.04		131.66	1.00	11.00	10.00			0.643			0.184		0.05	Y
153	336060	14.0	538	325	6.50	36.44	17.01	39.00	3.80	1.80	0.36		128.01	42.00	43.00	66.00			0.154			0.429	1.59	Y	

Sample #	Well ID	Temp (°C)	EC (µS/cm)	TDS	pH	Ca	Mg	Na	K	Fe	Mn	B	HCO <sub>3</sub>	CO <sub>2</sub>	SO <sub>4</sub>	Cl	F	Br	NH <sub>4</sub>	NO <sub>2</sub>	NO <sub>3</sub>	PO <sub>4</sub>	CAB (%)	Representative
154	336061		225		7.40	18.02	7.29	13.60	5.41	1.40	0.23	0.028	117.04	7.60	5.00	8.00			1.041	0.010	0.354	0.116	-0.56	Y
155	336069	14.5	230	190	7.75	23.63	5.10	14.00	4.20	0.29	0.05		123.13	4.00	4.00	8.00			1.543	0.003			-0.26	Y
156	336071		262		7.85	33.64	5.34	12.00	2.30	0.05	0.04		138.98	4.00	12.00	13.00							-3.49	Y
157	336071		220		8.10	27.23	4.19	12.00	4.10	0.80	0.03		131.66		9.00	7.20			0.771				-4.47	N
158	336078	13.5	370	232	8.05	42.85	7.53	18.00	2.50	0.04	0.00		156.05	2.00	13.00	28.00			0.450	0.003			-0.18	Y
159	336079	14.0	268	184	7.45	31.64	5.10	13.00	2.50	0.34	0.00		125.57	7.30	9.00	14.00			0.489	0.003			-0.24	Y
160	336080	14.0	234	176	7.90	28.43	4.13	11.00	2.40	0.09	0.00		112.16	2.30	12.00	8.00			0.617	0.003			-0.33	Y
161	336081		265	195	7.95	32.44	4.37	12.00	3.50	0.16	0.03		128.01	2.00	12.00	12.00	0.14						-1.83	Y
162	336085	14.0	331	223	7.85	40.05	7.29	15.00	2.60	0.11	0.00		145.08	3.40	12.00	24.00			0.437	0.003			0.19	Y
163	336088	13.5	372	228	7.95	40.45	8.99	18.00	2.60	0.12	0.05		152.39	3.00	12.00	29.00			0.386	0.003			0.58	Y
164	336091	13.9	290		8.10	34.84	6.07	15.00	2.50		0.02		137.76	2.00	10.50	16.50				0.003			0.22	Y
165	336097	14.5	273	204	7.90	27.23	5.34	22.00	3.00	0.06	0.03		138.98	2.90	10.00	12.00			0.797	0.003			0.14	Y
166	336101		300		8.10	35.64	6.07	16.00	2.50				134.10	2.00	10.00	20.00			0.489				1.13	Y
167	336113		313		8.20	39.65	7.05	14.00	2.80				150.95		10.00	16.00							1.65	N
168	336113		300		8.00	34.44	6.80	14.00	2.70	0.10	0.08		142.95		9.50	17.20			0.463				-1.16	N
169	336113		300		8.10	36.04	6.80	13.60	2.70		0.04		150.95		13.00	20.00			0.476				-4.59	N
170	336113		310		8.10	40.05	7.19	13.60	2.80	0.06	0.05		140.95		11.00	21.00			0.411				1.91	N
171	336113		310		8.10	38.05	6.88	15.10	2.60	0.28	0.06		143.95		11.00	20.00			0.450				0.55	N
172	336113		320	283	8.00	38.05	6.97	13.10	2.70	0.08	0.04		143.95		11.00	22.00			0.450				-1.55	N
173	336113		300	285	8.00	38.05	7.09	13.60	2.50	0.04	0.02		145.95		11.00	20.00			0.476	0.016			-0.76	N
174	336113		310		8.00	39.45	6.68	14.10	2.80				143.95		11.40	22.30			0.437		0.080		-0.37	N
175	336113		320	290	8.30	40.17	7.51	14.10	3.13				148.95		10.90	21.30			0.424	0.026	0.213		0.65	N
176	336113		320	281	8.00	37.12	7.51	14.10	2.80				151.95		2.50	20.80				0.043	0.089		0.38	N
177	336113		320	291	8.14	39.45	7.80	14.00	2.70	0.07			144.95		12.20	22.80				0.007	0.044		0.22	N
178	336113		310	291	8.02	38.53	7.51	14.20	3.20	0.11			148.95		12.60	21.40			0.476	0.007	0.044		-1.05	N
179	336113		310		8.08	38.85	7.77	14.60	2.90	0.07	0.06		136.96		11.00	21.70	0.09	0.08	0.437				3.16	N
180	336113		310	298	8.02	42.57	7.90	14.60	3.00	0.09	0.06		151.95		11.80	21.30	0.08	0.08	0.437				2.18	N
181	336113		300		8.14	40.97	7.12	15.50	3.30	0.04	0.05		146.95		11.88	21.20	0.08	0.07	0.386		0.009		2.03	N
182	336113		320		7.81	38.45	6.83	12.80	4.70	0.11	0.06		144.95		11.32	21.70	0.08	0.07	0.411		0.031		-1.05	N
183	336113		330		8.06	40.05	8.36	14.40	2.70	0.20	0.05		146.95		11.90	22.00	0.07	0.08	0.193				1.57	N
184	336113		300		8.04	39.45	7.29	14.10	3.00	0.14	0.06		145.95		11.80	21.00	0.10	0.07	0.039				0.43	N
185	336113		320		8.09	41.25	7.05	14.40	2.60	0.07	0.05		148.95		11.70	21.00	0.08	0.07	0.386				0.81	N
186	336113		320		8.07	39.77	7.51	14.10	2.80	0.08	0.05		147.95		11.70	22.00	0.09	0.08	0.386				-0.03	Y
187	336113		320		8.22	41.97	7.39	14.70	2.70	0.09	0.05		152.95		11.40	21.00			0.489				1.10	N
188	336113		320		8.30	40.05	7.29	15.30	2.70	0.11	0.05		149.95		11.70	19.90	0.06	0.07					1.06	N
189	336113		310		8.04	41.05	7.29	15.50	2.80	0.08	0.05		147.95		11.90	21.00					0.797		1.74	N
190	336113		260		8.01	41.05	7.29	15.20	2.80	0.04	0.06		149.95		11.80	21.00			0.399				1.27	N
191	336113		310		7.80	40.05	7.29	15.60	2.80	0.08	0.05		145.95		11.50	20.00	0.07	0.06	0.424		0.531		2.20	N
192	336113		300		7.99	39.05	7.29	15.30	2.90	0.03	0.05		146.95		11.80	21.00	0.09	0.11	0.424				0.63	N

Sample #	Well ID	Temp (°C)	EC (µS/cm)	TDS	pH	Ca	Mg	Na	K	Fe	Mn	B	HCO <sub>3</sub>	CO <sub>2</sub>	SO <sub>4</sub>	Cl	F	Br	NH <sub>4</sub>	NO <sub>2</sub>	NO <sub>3</sub>	PO <sub>4</sub>	CAB (%)	Representative
193	336113		200		7.99	39.05	7.29	14.90	2.90	0.09	0.05		146.29		11.60	21.00	0.10	0.07	0.437				0.60	N
194	336113		310		8.11	37.97	7.00	14.80	2.70	0.07	0.05		146.29		11.60	21.00	0.10	0.08	0.077				-0.76	N
195	336113		310		7.99	38.05	7.00	14.50	2.80	0.05	0.05		151.90		11.20	20.00	0.10	0.18					-1.71	N
196	336113		320		8.07	39.05	7.19	14.70	2.90	0.07	0.05		146.90		11.60	20.00	0.10	0.08	0.463		0.310		0.55	N
197	336113		300		7.81	37.04	7.00	14.70	2.40	0.10	0.05		146.90		11.70	20.00	0.08	0.08	0.386		0.221		-1.48	N
198	336113		330		7.40	36.04	6.78	14.40	2.80	0.04	0.05		143.98		11.50	19.60	0.09	0.07	0.334				-1.58	N
199	336113		300		7.60	37.04	6.77	14.20	2.80	0.06	0.05		143.95		10.90	19.60	0.10	0.04	0.386				-0.71	N
200	336113		300		7.51	37.04	7.17	14.20	3.00	0.05	0.05		143.95		10.70	19.70	0.08	0.08	0.411				-0.08	N
201	336113		270		7.98	37.04	6.97	13.60	2.80	0.10	0.05		144.95		10.90	20.00	0.08	0.05	0.450				-1.30	N
202	336113		290		7.72	35.04	6.77	13.50	2.90	0.07	0.05		143.95		10.30	19.30	0.08	0.10	0.411		0.044		-2.49	N
203	336113		280		8.00	36.04	6.87	13.20	2.70	0.04	0.05		140.95		10.50	19.40	0.09		0.373				-1.13	N
204	336113		260		8.06	35.04	6.57	13.50	3.10	0.04	0.05		143.95		10.50	19.50	0.08	0.05	0.437				-2.83	N
205	336113		290		8.00	34.04	6.18	13.30	2.90	0.04	0.04		138.96		10.60	19.00	0.08		0.437				-2.97	N
206	336113		300		7.80	37.04	6.97	13.20	2.90	0.04	0.05		137.96		10.10	18.60	0.12		0.424				1.23	N
207	336113		300		7.91	37.04	6.87	13.40	2.70	0.03	0.04		138.96		9.90	18.20	0.11		0.424				1.14	N
208	336113		290		7.94	37.04	6.77	13.10	2.60	0.04	0.05		139.95		10.00	18.60	0.08		0.399				0.25	N
209	336113				8.06	34.04	6.38	13.20	2.60	0.05	0.05		139.95		10.00	18.40	0.09		0.399				-2.68	N
210	336113				7.96	35.04	6.38	12.60	3.00	0.04	0.05		138.96		9.90	18.10	0.13		0.437				-1.64	N
211	336113				8.04	34.04	6.28	13.00	2.70	0.02	0.04		139.95		9.80	17.80	0.12		0.437				-2.58	N
212	336114		370	236	7.10	40.85	8.75	16.00	2.10	0.93	0.08		145.08	19.00	19.00	29.00			0.283	0.013	0.354	0.153	-1.26	N
213	336114	15.5	391		7.40	43.25	8.75	20.00	2.70	0.12	0.12		153.61	10.00	21.00	32.00			0.334	0.010	0.310	0.153	-0.60	N
214	336114	15.5	385		7.00	39.25	10.20	17.00	2.30	0.20			149.95	25.00	20.00	30.00			0.334		0.664	0.153	-1.84	N
215	336114		396		7.30	40.45	12.39	20.00	2.70	2.80	0.14		156.05	13.00	20.00	34.00			0.411		0.487		0.45	N
216	336114		396		7.30	40.45	12.39	20.00	2.70	2.80	0.14		156.05	13.00	20.00	34.00			0.411		0.487	0.215	0.45	N
217	336114		377		7.10	42.45	8.99	19.00	2.60	0.55	0.14		151.17	20.00	21.00	30.00			0.334	0.003	0.620	0.184	-0.27	Y
218	336114		400		7.50	44.85	8.99	20.00	2.60	0.81	0.10		159.70	8.30	19.00	31.00			0.411			0.184	0.34	N
219	336114		394		7.50	44.85	7.53	20.00	2.60	0.21	0.09		149.95	7.80	19.00	31.00			0.450			0.215	0.89	N
220	336114		404		7.70	46.06	9.48	19.00	2.90	0.31	0.08		162.14	5.30	18.00	32.00			0.450			0.307	0.55	N
221	336114		392		7.50	44.85	8.26	21.00	2.90	2.30	0.09		160.92	8.30	20.00	37.00			0.411			0.242	-2.40	N
222	336114	15.7	408		7.60	47.26	8.50	20.00	2.90	0.13	0.08		163.36	6.70	16.00	31.00			0.450			0.248	1.48	N
223	336114		406		7.70	42.05	10.93	20.50	2.80	0.07	0.07		158.49	5.20	17.00	31.00			0.437			0.270	1.74	N
224	336114		390		7.60	46.86	8.26	20.00	2.80	0.06	0.07		167.02	7.00	17.00	32.00			0.424	0.007		0.276	-0.44	N
225	336114		389		7.80	46.46	8.99	22.00	2.80	0.07	0.07		164.58	4.30	16.00	31.00			0.450	0.003		0.291	2.27	N
226	336114		386		7.80	45.65	8.99	20.00	2.80	0.09	0.06		164.58	4.30	17.00	30.00			0.463	0.007	0.177	0.325	0.75	N
227	336114		387		7.80	47.26	6.80	20.00	2.80	1.20	0.06		163.36	4.20	17.00	31.00			0.463	0.003		0.279	-0.60	N
228	336114		380		7.40	44.85	8.75	19.00	2.80	0.06	0.09	0.014	154.83	8.00	18.00	31.00		0.12	0.424			0.307	0.91	N
229	336114		369		7.40	45.25	7.29	20.00	2.80	0.08	0.07		152.39	10.00	19.00	29.00			0.386	0.016	0.443	0.224	1.08	N
230	336114		379		7.90	45.25	8.99	20.00	2.90	0.18	0.09		153.61	3.00	17.00	31.00			0.489				2.55	N
231	336114		365		7.80	42.85	9.96	20.00	2.80	0.16	0.07		157.27	4.10	17.00	31.00			0.527				1.21	N

Sample #	Well ID	Temp (°C)	EC (µS/cm)	TDS	pH	Ca	Mg	Na	K	Fe	Mn	B	HCO <sub>3</sub>	CO <sub>2</sub>	SO <sub>4</sub>	Cl	F	Br	NH <sub>4</sub>	NO <sub>2</sub>	NO <sub>3</sub>	PO <sub>4</sub>	CAB (%)	Representative
232	336141		420	276	8.00	46.86	9.96	22.00	2.80	0.26	0.09		170.68	3.00	16.00	36.00	0.13			0.003			0.48	Y
233	336151		269	237	8.20	29.64	2.92	28.00	2.70	0.03	0.00		137.76	2.00	14.00	11.00	0.08		0.797	0.003			2.49	N
234	336151		295	228	8.15	28.83	3.16	28.00	2.70	0.01	0.02		141.42	2.00	12.00	15.00	0.08						-0.09	Y
235	336181		240	177	8.25	28.83	5.34	12.00	2.40	0.64	0.03		121.91	1.00	7.00	10.00	0.13						0.74	Y
236	336200		482		7.90	57.67	11.90	28.00	3.20	0.21	0.16		196.28	4.50	23.00	44.00	0.20		0.141				2.18	Y
237	336201		332		7.00	29.24	7.53	20.00	2.40	1.90	0.32		106.06	17.00	24.00	28.00			0.193		0.841	0.215	-0.52	Y
238	336211		425	278	8.00	44.45	10.93	26.00	2.90	0.50	0.11		174.33	3.00	14.00	38.00	0.17			0.003			1.20	Y
239	336221	14.5	2	247	8.10	36.04	5.83	22.00	2.80	0.04	0.03		154.83	2.00	11.00	17.00			0.823	0.003			0.93	Y
240	336223		229		8.40	28.43	5.83	10.00	1.90			0.012	110.94	1.00	9.70	7.10			0.823				3.51	Y
241	336233	21.0	238	162	8.10	19.62	3.64	22.00	6.60	0.06	0.03		136.54	1.50	2.00	10.00	0.13		2.186		0.886		-3.44	Y
242	336241		495	132	8.15	51.66	16.03	27.00	3.70	0.12	0.14		188.96	2.00	26.00	48.00	0.12			0.003			1.71	N
243	336241		495	315	8.10	50.86	14.33	27.00	3.70	0.15	0.14		187.74	2.00	26.00	45.00	0.11						1.00	Y
244	336245		203		8.40	24.03	4.86	9.50	1.70		0.02		109.72	0.70	10.00	5.40			0.604				-2.45	Y
245	336253	14.0	218		8.00	28.03	4.86	11.00	1.90	0.01	0.00		118.25	2.00	13.00	7.00			0.849	0.003			-1.71	N
246	336253		247		8.00	30.04	4.86	12.00	1.70				117.04	2.00	12.00	10.00			0.540				0.28	Y
247	336253		251	170	8.10	30.44	5.10	12.00	0.08		0.02		120.69	1.50	12.00	9.00			0.386				-0.39	N
248	336271		225	135	8.10	25.63	4.37	10.50	3.40	0.34	0.03		114.60	1.00	5.00	8.00	0.14						-0.58	Y
249	336321		280	176	8.10	35.24	5.83	10.50	1.70	0.09	0.03		121.91	2.00	23.00	10.00	0.13						-0.37	Y
250	336333		422		8.00	44.45	11.42	26.00	3.10	0.20	0.16		180.43	3.00	13.00	36.00			0.167	0.007		0.377	1.45	N
251	336333		422		7.90	44.05	12.63	25.00	3.10	1.30	0.16		185.31	3.80	14.00	35.00			0.206	0.003		0.365	1.01	N
252	336333		423		7.90	38.45	15.55	26.00	3.10	0.21	0.15		181.65	3.80	14.00	39.00			0.180			0.328	0.45	N
253	336333		420		7.80	44.05	12.15	25.00	3.10	0.20	0.16	0.020	174.33	3.50	14.00	39.00		0.12	0.180			0.368	1.34	N
254	336333		415		8.10	44.05	12.88	26.00	3.10	0.19	0.15		169.46	2.00	15.00	38.00			0.180			0.328	3.55	N
255	336333		420		7.90	43.25	12.88	26.00	3.10	0.32	0.18		171.90	4.00	14.00	38.00			0.167				2.87	N
256	336333		384		7.90	41.25	14.09	26.00	3.10	0.20	0.15		173.12	4.00	15.00	39.00			0.193				2.05	N
257	336333	13.0	438	298	7.80	40.85	14.09	24.00	2.60	0.03	0.10		175.55	4.60	15.00	40.00			0.141				-0.11	Y
258	336361		260	198	8.20	33.64	5.34	11.00	2.00	0.04	0.02		121.91	1.00	12.00	12.00	0.13						1.18	Y
259	336391		250	186	8.00	30.44	5.10	12.00	2.50	0.29	0.02		124.35	2.00	7.00	10.00	0.14						1.17	Y
260	336401		230	180	8.15	28.03	5.10	10.00	1.90	0.72	0.03		113.38	1.00	8.00	9.00	0.13			0.003			0.51	Y
261	336421		415	184	8.10	46.86	9.48	24.00	2.80	0.10	0.07		165.80	23.00	17.00	35.00	0.14						2.11	Y
262	336441		270	123	8.10	32.84	5.59	12.00	2.40	0.14	0.03		129.23	2.00	5.00	13.00	0.15						1.76	N
263	336441		265		8.00	31.64	5.83	12.00	2.50	0.08	0.04		131.66	2.50	7.80	18.00	0.10		0.553	0.010			-3.36	N
264	336441		268		7.90	33.24	5.34	12.00	2.50	0.07	0.05		131.66	3.00	7.50	13.50	0.04		0.707	0.003			-0.20	Y
265	336441		267		7.90	31.64	5.10	11.50	2.40	0.10	0.05		129.23		7.00	13.30			0.527				-1.52	N
266	336442	19.7	227	154	8.10	25.23	4.86	12.00	4.30	0.06	0.06		117.04	1.50	5.00	9.00	0.17		1.286				0.32	Y
267	336451		250	172	8.10	29.24	4.86	10.50	3.20	0.12	0.04		123.13	2.00	7.00	11.00	0.09						-1.58	Y
268	336471		670	321	7.70	63.68	23.81	36.00	4.50	1.03	0.53		254.80	8.00	30.00	67.00	0.16			0.003			0.94	Y
269	336481		335	184	8.10	38.85	8.02	15.00	2.60	0.01	0.05		142.64	2.00	4.00	24.00	0.13			0.003			3.41	Y
270	336491		235	184	8.10	28.03	4.86	10.00	1.60	0.01	0.03		106.06	1.00	15.00	9.00	0.18						-0.65	Y

Sample #	Well ID	Temp (°C)	EC (µS/cm)	TDS	pH	Ca	Mg	Na	K	Fe	Mn	B	HCO <sub>3</sub>	CO <sub>2</sub>	SO <sub>4</sub>	Cl	F	Br	NH <sub>4</sub>	NO <sub>2</sub>	NO <sub>3</sub>	PO <sub>4</sub>	CAB (%)	Representative		
271	336511		230	173	8.25	27.63	4.86	11.00	2.20	0.19	0.02		117.04	1.00	8.00	9.00	0.13							-0.54	Y	
272	336571		245		8.00	29.64	4.86	11.00	3.00	0.13	0.00		121.91	2.00	10.00	8.00				0.003	0.177				-0.02	Y
273	336591		660	275	7.80	63.28	21.14	36.00	4.10	5.40	0.47		237.73	6.00	32.00	68.00	0.10			0.003					0.67	Y
274	336996		214		8.20	27.23	4.62	11.00	1.80				112.16		11.00	7.00			0.501						-0.04	Y
275	337001		230	176	8.30	29.24	5.59	9.00	1.20	0.03	0.06		114.60	0.50	9.00	7.00	0.15			0.003					1.69	Y
276	337005		727	433	7.55	2.00	1.46	145.00	7.00	2.10	0.12		252.36	15.00	0.10	95.00				0.016					-0.83	N
277	337005	17.0	711		7.60	2.00	1.21	135.00	6.50	2.14	0.12		245.04	10.00	0.10	90.00			4.629	0.003					-2.49	N
278	337005		707	456	7.55	2.80	1.21	139.00	7.80	1.59	0.15		249.92	11.70	0.10	90.00			4.500	0.007					-1.16	N
279	337005		692	432	7.60	2.40	0.97	138.00	7.70	1.52	0.13		248.70	10.20	0.10	85.00			4.500	0.007					-0.60	N
280	337005	18.0	647		7.64	2.00	0.97	126.00	6.20	1.40	0.15		231.63	8.70	1.00	82.00			4.371						-2.61	N
281	337005	15.0	639		7.69	2.00	1.21	121.00	6.10	2.50	0.16		234.07		1.00	81.00			4.500						-4.45	N
282	337005	17.5	637		7.80	2.40	1.21	127.00	5.60	1.70	0.13		236.51		1.00	78.00			4.243						-1.76	N
283	337005				7.70	2.00	1.21	128.00	6.30	2.20	0.18		236.51	7.70	2.00	84.00			4.243						-2.94	N
284	337005	16.0	665		7.80	1.20	1.70	134.00	6.80	1.30	0.20		240.17	6.00	2.00	79.00			4.500						-0.03	Y
285	337005		672		7.60	2.00	1.70	144.00	7.70	3.60	0.22		245.04	10.00	1.00	80.00			4.629						3.13	N
286	337005		669		7.80	3.20	0.97	135.00	7.30	1.10	0.22		247.48	6.40	4.00	82.00			4.629	0.010					-1.21	N
287	337005		677		7.70	2.40	1.46	140.00	10.50	3.90	0.24		249.92	8.20	2.00	82.00			4.629						1.13	N
288	337005		665		7.70	2.80	1.21	140.00	6.50	2.40	0.21		245.04	7.90	4.00	82.00			4.757						0.64	N
289	337005		678		7.60	3.20	0.97	132.00	8.50	3.60	0.22		245.04	10.00	2.00	82.00			5.143		0.443				-1.43	N
290	337005		655		7.50	2.00	1.70	140.00	8.00	3.80	0.24		246.26	13.00	3.00	91.00			4.371						-1.00	N
291	337005		674		7.70	2.00	1.70	140.00	8.40	3.30	0.22		248.70	8.10	2.00	78.00			4.757						1.76	N
292	337005		679		7.80	2.40	1.46	137.00	8.00	3.80	0.22		249.92	6.50	2.90	85.00			5.400		0.044				-1.17	N
293	337005		674		7.70	2.80	1.21	135.00	7.90	2.00	0.23		257.23	8.00	4.00	80.00			4.629	0.003					-1.88	N
294	337005		680	0.9	7.60	2.40	1.70	130.00	7.90	3.50	0.24		252.36	10.00	4.00	79.00			4.629	0.010	0.044				-2.65	N
295	337005		677		7.60	2.40	1.46	140.00	8.30	4.00	0.24		256.02	11.00	3.00	77.00			5.143	0.010					0.85	N
296	337005		691		7.60	3.60	0.73	140.00	8.10	3.50	0.23		256.02	11.00	2.00	82.00			5.014		0.044				-0.12	N
297	337005		670		7.50	3.20	1.21	135.00	7.70	2.10	0.26	0.844	251.14	10.00	4.00	93.00		0.33	4.976						-3.76	N
298	337005		198	0.3	7.60	3.60	0.97	150.00	8.00	1.80	0.24		243.82	10.00	4.10	90.00			5.529						2.71	N
299	337005		700		7.60	3.60	1.70	145.00	8.20	1.03	0.21		243.82	10.00	4.30	92.00			5.014		0.221				1.12	N
300	337005	15.0	760	517	7.60	2.00	3.16	150.00	9.00	3.67	0.28		268.21	11.10	3.00	102.00			5.400						-1.53	N
301	337006	14.0	264	207	8.20	32.84	5.34	12.00	1.90	0.04	0.03		131.66	1.50	10.00	10.00			0.720	0.003					0.01	Y
302	337007		238		8.30	30.04	5.10	8.50	2.50	0.01	0.05		113.38	1.00	12.00	9.00			0.630	0.003					-0.21	Y
303	337008	12.0	296	229	8.20	30.84	4.13	24.00	2.30	0.01	0.00		148.73	1.50	13.00	10.00			0.656	0.003					-0.15	Y
304	337010	14.0	291	228	8.20	36.04	6.56	13.00	2.00	0.11	0.02		142.64	1.50	12.00	12.00			0.797	0.003					0.49	Y
305	337011		355	249	7.80	38.85	10.45	16.00	2.90	0.20	0.12		148.73	4.00	19.00	24.00	0.19			0.003					0.82	Y
306	337012	14.5	337	240	8.20	32.04	5.10	30.00	2.40	0.01	0.00		153.61	1.50	10.00	22.00			0.900	0.003					0.57	Y
307	337014	15.5	275	209	8.20	35.24	5.83	11.00	1.60	0.01	0.00		132.88	1.50	12.00	10.00			0.579	0.003					0.87	Y
308	337015		241	170	8.29	30.84	5.10	9.00	1.30	0.01	0.06		121.91	1.00	11.00	6.80			0.656	0.003					-0.75	Y
309	337018	13.0	291	214	7.90	36.84	6.32	13.00	2.40	0.04	0.00		138.98	2.90	13.00	16.00			0.193	0.003					-0.25	Y

Sample #	Well ID	Temp (°C)	EC (µS/cm)	TDS	pH	Ca	Mg	Na	K	Fe	Mn	B	HCO <sub>3</sub>	CO <sub>2</sub>	SO <sub>4</sub>	Cl	F	Br	NH <sub>4</sub>	NO <sub>2</sub>	NO <sub>3</sub>	PO <sub>4</sub>	CAB (%)	Representative
310	337023	14.0	650	418	8.15	23.23	2.67	121.00	3.70	0.06	0.00		309.66	3.60	0.10	56.00			1.697	0.003			0.60	Y
311	337031		245	169	8.25	30.44	6.07	9.00	1.40	0.01	0.06		128.01	1.00	8.00	7.00	0.13			0.003			-0.33	Y
312	337041		240	186	8.20	30.44	5.83	8.00	1.20	0.03	0.05		124.35	1.00	5.00	9.00	0.15						-0.40	Y
313	337051		455	169	7.60	46.46	12.39	23.00	3.60	4.00	0.37		173.12	7.00	24.00	41.00	0.22						-0.71	Y
314	337064		318		8.20	34.04	5.34	25.10	2.51	0.03	0.04	0.036	165.80	1.70	9.00	13.00			0.861			0.147	0.35	Y
315	337067		262		8.20	31.24	6.32	12.50	2.56	0.04	0.04	0.016	126.79	1.30	14.00	8.00			0.591			0.113	1.75	Y
316	342001		760	317	7.10	39.25	28.67	83.00	8.70	5.90	0.20		452.29	59.00	0.10	30.00	0.16						-0.68	Y
317	342002		136		5.80	8.81	2.43	11.50	1.60	0.28			24.38	63.00	5.00	14.00					16.829		0.46	Y
318	342011		920	572	7.40	27.63	21.87	130.00	12.00	2.90	0.37		509.59	33.00	0.10	45.00	0.29			0.003			-2.58	Y
319	342041		515	224	7.60	54.87	12.39	32.00	7.30	2.60	0.54		256.02	11.00	0.10	39.00	0.38			0.003			0.35	Y
320	342051	15.0	525		7.50	32.44	17.01	43.00	13.50	1.02	0.17		287.71	15.00	0.10	24.00			3.009	0.043			-1.53	N
321	342051		471	292	7.50	27.63	15.55	41.00	12.60	1.10	0.31		262.11	14.00	0.10	20.00			3.471	0.003			-1.02	N
322	342051		477	288	7.60	29.64	14.09	40.00	13.40	1.11	0.25		256.02	10.50	0.10	21.00			3.471	0.003			-0.73	Y
323	342061		700	316	7.90	11.21	11.66	120.00	8.00	0.63	0.11		363.30	8.00	0.10	46.00	0.37						-2.19	Y
324	342081		650	207	7.50	80.10	11.66	33.50	8.00	3.60	1.15		295.03	15.00	0.10	60.00	0.29			0.003			0.67	Y
325	342091		307		8.00	21.23	4.13	25.00	19.60	0.08	0.00		184.09	4.00	0.10	9.00			4.243	0.003	0.089		-4.58	N
326	342091		315	208	8.20	20.82	4.62	26.00	17.50	0.07	0.00		175.55	2.00	0.10	10.00	0.13						-2.67	Y
327	342097		446			42.85	14.58	31.40	9.72			0.078	243.82		1.00	23.00							2.98	Y
328	342105				7.60	20.42	11.18	62.00	11.60		0.05		268.21	11.00	1.00	19.00	0.19		3.857				-0.21	Y
329	342141		610	389	7.50	22.43	18.46	76.00	11.00	4.80	0.37		349.89	18.00	0.10	24.00	0.46						-1.49	Y
330	342151		825	502	7.60	18.02	21.14	120.00	15.00	1.40	0.38		440.10	18.00	0.10	47.00	0.34						-1.79	Y
331	342161		396			23.23	15.79	35.20	12.90			0.088	220.66		0.60	17.00							2.50	Y
332	342171		660	381	7.80	67.68	26.00	24.00	14.00	0.86	0.15		370.61	10.00	0.10	31.00	0.22			0.003			-0.24	Y
333	343021		385	240	7.80	34.04	9.23	25.00	10.00	0.92	0.10		213.35	6.00	0.10	17.00	0.14						-2.27	Y
334	343031		735	416	7.30	57.67	21.14	59.00	9.30	5.90	0.91		397.43	33.00	0.10	38.00	0.16			0.003			-1.11	Y
335	343051		490	298	7.90	49.66	14.09	27.00	6.80	0.26	0.16		260.89	5.00	0.10	30.00	0.15						-1.37	Y
336	343061		430	251	7.20	35.64	16.03	20.00	8.30	7.40	1.31		220.66	23.00	0.10	24.00	0.76			0.016			-1.37	Y
337	343101		740	200	7.10	57.67	36.93	48.00	4.90	4.00	1.80		435.23	57.00	0.10	32.00	0.24			0.010			0.56	Y
338	343101		750	468	7.10	56.07	36.93	50.00	4.90	4.10	1.80		435.23	57.00	0.10	32.00	0.28						0.61	N
339	343121		620	317	7.00	41.65	17.01	66.00	7.10	19.00	0.84		345.01	56.00	0.10	30.00	0.15						0.21	Y
340	343151		555	333	7.50	39.65	23.57	36.00	14.00	0.37	0.25		331.60	17.00	0.10	21.00	0.26			0.003			-1.58	Y
341	343155		330			29.64	7.53	24.70	14.70			0.096	186.53		0.80	12.00							1.96	Y
342	343161		475	314	7.05	37.24	26.24	21.00	4.10	6.10	0.22		262.11	38.00	0.10	22.00	0.40			0.010			1.18	Y
343	343171		505	191	8.10	50.46	15.79	25.00	9.50	0.17	0.12		266.99	3.00	0.10	29.00	0.13						-0.47	Y
344	344011		535	317	8.50	61.67	15.06	29.00	4.90	1.07	0.21		236.51	1.00	0.10	44.00	0.28			0.003	4.429		4.71	Y
345	344031		990	606	6.90	67.28	40.57	82.00	10.60	17.80	2.14		586.40	121.00	0.10	40.00	0.26			0.003			-0.98	Y
346	344031		1015	492	6.80	62.47	40.82	84.00	12.00	18.50	2.20		614.44	160.00	0.10	39.00	0.29						-3.41	N
347	344041		635	366	7.40	53.26	22.11	39.00	7.30	2.40	0.42		351.11	23.00	0.10	29.00	0.23						-1.66	Y
348	344051		430	274	7.70	48.46	11.90	20.00	5.20	0.52	0.17		218.22	7.00	0.10	31.00	0.14						-0.60	Y

Sample #	Well ID	Temp (°C)	EC (µS/cm)	TDS	pH	Ca	Mg	Na	K	Fe	Mn	B	HCO <sub>3</sub>	CO <sub>2</sub>	SO <sub>4</sub>	Cl	F	Br	NH <sub>4</sub>	NO <sub>2</sub>	NO <sub>3</sub>	PO <sub>4</sub>	CAB (%)	Representative		
349	344061		315	203	7.60	32.44	8.02	15.00	4.80	0.48	0.16		165.80	7.00	0.10	16.00	0.09							-1.89	Y	
350	344081		910	558	6.85	56.07	32.80	82.00	9.10	22.00	2.10		520.56	118.00	0.10	52.00	0.23			0.007					-3.65	Y
351	344091		625	369	7.40	54.06	21.38	40.00	7.00	3.50	0.29		349.89	23.00	0.10	25.00	0.27								-0.52	Y
352	344183		323			30.84	10.69	20.50	8.31			0.041	177.99		0.50	18.00									1.25	Y
353	345011		380	213	7.50	38.05	10.69	19.00	5.90	1.40	0.37		187.74	10.00	0.10	27.00	0.10								-1.13	Y
354	345041		241		8.00	25.63	2.92	16.00	4.80	0.06	0.03		125.57	2.10	4.00	8.00			1.414		0.221	0.215			-0.70	Y
355	345051		260	213	7.90	22.83	5.10	20.00	5.40	0.19	0.06		140.20	3.00	0.10	14.00	0.17			0.003					-2.43	Y
356	345053		225	183	8.00	25.23	2.92	16.00	4.60	0.09	0.03		123.13	2.00	2.00	10.00	0.10								-0.63	Y
357	345061		310		7.90	36.04	6.56	16.00	3.90	0.16	0.04		163.36	3.00	0.10	18.00	0.09			0.046	0.709				-1.04	Y
358	345071		385	274	7.80	38.85	9.72	23.00	5.50	10.60	0.36		213.35	6.00	0.10	20.00	0.04								-2.32	Y
359	345081		370	249	8.20	15.22	1.70	57.00	9.50	0.16	0.02		206.03	2.00	0.10	16.00	0.18								-2.80	N
360	345081		377		7.90	13.62	3.40	58.00	9.40	0.14	0.03		204.81	4.20	2.00	13.00			2.700			0.307			-0.57	Y
361	345091		375	183	8.00	14.02	2.67	59.00	9.50	0.06	0.02		207.25	3.00	0.10	17.00	0.24								-1.97	Y
362	345101		745	464	7.85	14.82	4.62	134.00	7.90	0.44	0.09		293.81	7.00	0.10	93.00	0.23			0.007					-2.00	Y
363	345111		330	239	7.40	32.84	9.23	17.00	5.30	1.20	0.30		170.68	11.00	0.10	22.00	0.16								-2.19	Y
364	345141		574		8.40	7.61	0.97	134.00	17.00	0.08	0.03		357.20	2.00	0.10	31.00				0.003	0.133				-0.08	Y
365	345151		285	124	8.00	18.82	3.40	33.00	7.80	0.30	0.04		164.58	3.00	0.10	9.00	0.13								-1.72	Y
366	346031		370	235	8.10	28.03	2.92	48.00	3.10	0.09	0.04		179.21	2.00	3.00	26.00	0.10								0.96	N
367	346031		362		7.70	26.83	3.16	47.00	3.40	0.15	0.03		175.55	6.00	3.50	24.00	0.12		0.026	0.003	1.771				1.00	N
368	346031		362		8.00	27.23	2.92	45.40	3.22	0.11	0.04	0.094	180.43	3.00	4.00	23.00			0.939			0.150			-0.46	Y
369	346041		500	323	8.00	38.85	4.37	60.00	4.50	0.30	0.07		220.66	4.00	0.10	50.00	0.08								-0.06	Y
370	346051		335		8.00	27.63	3.89	37.60	4.12	0.28	0.01	0.072	163.36	2.70	5.00	19.00			0.077		4.119	0.208			0.81	Y
371	352001		425	270	7.10	25.63	15.55	39.00	4.80	5.50	0.23		199.94	26.00	0.10	36.00	0.21			0.003					0.96	Y
372	352003			272	6.92	27.71	13.99	40.40	2.51	1.41	1.20		187.99		2.60	36.90				0.007	0.186				2.07	Y
373	352011		310	170	7.10	17.22	9.48	31.00	3.50	1.04	0.42		129.23	17.00	0.10	31.00	0.22			0.003					1.36	Y
374	352021		315	221	7.20	22.43	8.99	25.00	3.30	1.40	1.60		114.60	12.00	0.10	39.00	0.34			0.003					0.84	Y
375	352051		455	288	7.05	27.23	13.85	46.00	5.30	4.60	0.39		198.72	29.00	0.10	46.00	0.27			0.007					0.85	Y
376	352123		560			41.25	21.87	45.20	8.04			0.028	226.76		0.60	69.00									3.02	Y
377	352131		245	175	7.20	13.62	7.77	22.00	4.50	1.50	0.25		110.94	11.00	0.10	21.00	0.10								-0.45	Y
378	352133		347			22.43	7.77	39.90	3.40			0.050	123.13		1.50	43.00									4.66	Y
379	352141		3050		7.60	56.07	43.73	520.00	31.00				646.13		9.00	660.00									0.70	Y
380	352211		310	235	6.85	17.62	11.18	26.00	2.70	0.73	0.74		89.00	21.00	3.00	43.00	0.29			0.026	3.676				3.54	Y
381	352241		595	164	7.20	54.87	17.74	44.00	6.10	2.00	0.53		304.78	32.00	0.10	40.00	0.33								1.14	Y
382	352251		330	215	7.20	12.82	9.23	42.00	2.60	0.01	0.00		99.97	10.00	7.00	33.00	0.09					24.357			2.88	Y
383	352271		6300		7.50	224.27	126.34	750.00	40.00				160.92		9.00	1,880.00						0.886			-0.57	Y
384	352271		5775	1659	7.55	220.26	116.62	700.00	34.00	2.00	0.68		162.14	7.00	0.10	1,930.00	0.13								-4.76	N
385	352271	14.0	5151		7.60	171.81	99.85	600.00	35.00	2.24	0.44		156.05	6.00	0.10	1,500.00			####	0.003					-1.23	N
386	352271		5952	3698	7.45	204.25	112.97	701.00	35.50	1.31	0.65		175.55	10.00	0.10	1,775.00			####	0.003					-1.98	N
387	352271		5840	3573	7.50	210.25	111.76	721.00	35.30	1.31	0.60		169.46	8.80	0.10	1,820.00			####	0.003					-2.04	N

Sample #	Well ID	Temp (°C)	EC (µS/cm)	TDS	pH	Ca	Mg	Na	K	Fe	Mn	B	HCO <sub>3</sub>	CO <sub>2</sub>	SO <sub>4</sub>	Cl	F	Br	NH <sub>4</sub>	NO <sub>2</sub>	NO <sub>3</sub>	PO <sub>4</sub>	CAB (%)	Representative
388	352271		5950	3380	7.60	211.45	119.53	692.00	31.00	1.80	0.61		188.96	7.80	3.00	1,843.00			####				-3.63	N
389	352271		6130	3531	7.50	220.26	119.05	780.00	34.00	1.10	0.72		187.74	9.70	1.00	1,929.00			####				-1.70	N
390	352271		6240	3533	7.50	226.27	114.19	820.00	38.00	1.30	0.69		197.50	10.00	1.00	1,840.00			####				1.93	N
391	352291		213		7.00	11.21	7.29	21.00	1.10	0.01	0.06		95.09	20.00	2.00	16.00			0.090				1.18	Y
392	352301		305	207	7.00	17.62	8.75	27.00	3.40	4.60	0.82		91.43	15.00	0.10	47.00	0.35			0.003			0.60	Y
393	352341		345	203	7.30	15.62	12.15	30.00	2.70	0.06	0.14		91.43	8.00	19.00	48.00	0.14						-1.49	Y
394	352451		438			27.23	14.58	48.50	4.78			0.052	203.59		0.60	37.00							4.32	Y
395	353001		475	183	7.50	32.84	13.12	40.00	10.00	1.40	0.28		247.48	13.00	0.10	30.00	0.16			0.003			-1.98	Y
396	353015	15.0	312		6.70	13.22	11.42	24.00	1.90	0.23			53.64	18.00	8.00	23.00					62.000	0.092	-0.05	Y
397	353015		291		6.80	12.82	10.93	24.00	2.00	0.10			48.76	13.00	7.00	24.00					57.571	0.123	1.62	N
398	353015		301		6.80	15.22	10.20	25.00	2.10	0.34			49.98	13.00	10.00	25.00					57.571	0.092	1.47	N
399	353015		292		6.80	14.82	8.99	24.00	1.90	0.06			51.20	13.00	7.00	22.00			0.026		57.571	0.092	0.74	N
400	353015		289		6.80	14.42	9.23	25.00	1.80	0.09			48.76	13.00	8.00	20.00					57.571	0.092	3.04	N
401	353015		290		6.70	14.82	8.75	24.00	2.00	0.04			51.20	17.00	7.00	23.00					57.571	0.092	-0.16	N
402	353015		281		6.90	12.01	10.20	24.00	2.10	0.06			49.98	10.00	7.00	22.00					57.571	0.116	0.45	N
403	353015	15.5	283		6.70	14.02	8.99	25.00	2.20				49.98	16.00	7.00	21.00			0.064		57.571	0.129	1.92	N
404	353015		280		6.80	14.42	8.75	24.50	2.10	0.07			49.98	13.00	6.70	23.00			0.026		57.571	0.104	0.45	N
405	353015		278		6.70	14.02	8.75	24.00	2.00				51.20	17.00	7.00	24.00			0.026		57.571	0.113	-1.49	N
406	353015		274		6.70	14.02	8.50	25.00	2.10				49.98	16.00	7.00	21.00			0.013		53.143	0.123	2.54	N
407	353015		273		6.70	14.02	8.50	24.00	2.10				48.76	16.00	7.00	23.00			0.064		53.143	0.138	0.93	N
408	353015		272		6.70	12.82	9.72	25.00	2.00	0.85			49.98	16.00	7.00	24.00			0.039		53.143	0.126	1.55	N
409	353015		270		6.70	13.22	8.50	24.00	1.90	0.03		0.013	48.76	15.00	7.00	24.00		0.18			54.471	0.123	-0.99	N
410	353015		267		6.80	13.62	8.02	25.00	2.00				46.33	12.00	8.20	23.00					54.029	0.116	0.56	N
411	353015		268		6.70	13.62	8.26	25.00	1.90				46.33	15.00	6.60	25.00					54.029		0.44	N
412	353015	15.2	276	188	6.70	12.41	8.99	23.00	1.80	0.02	0.00		51.20	16.80	6.70	26.00					48.271		-1.73	N
413	353067		505		6.40	19.62	17.01	54.00	3.40	0.20	0.14		57.30	40.00	28.00	49.00					117.357		0.18	Y
414	353084		280			18.02	6.32	28.40	11.00			0.119	164.58		0.70	8.50							-0.28	Y
415	353101		260	194	7.00	15.22	10.93	17.00	1.90	0.06	0.00		84.12	14.00	3.00	19.00	0.06			0.003	30.114		-0.32	Y
416	353171		270	210	7.75	12.41	4.62	31.00	9.30	0.22	0.06		153.61	4.00	0.10	10.00	0.10						-4.02	Y
417	354011		320		7.60	26.03	8.60	24.00	7.90	1.55	0.35		170.95		2.00	17.00			3.343				-1.07	N
418	354011		320		7.40	24.43	7.48	24.20	8.60	0.80			173.94		3.00	17.50			3.651				-4.60	N
419	354011		320			23.50	8.60	24.00	8.60	0.15			180.00		1.50	14.40			2.540		0.010		-3.73	N
420	354011		320			23.50	8.60	24.00	8.60	0.15			180.00		1.50	14.40			2.540		0.010		-3.58	N
421	354011		320	310	7.50	23.51	8.58	24.00	8.60	0.20			179.94		1.50	14.00			3.214		0.053		-3.73	N
422	354011		320	310	7.50	23.51	8.58	24.00	8.60	0.20			179.94		1.50	14.00			3.214		0.053		-3.58	N
423	354011		330	310	7.60	24.63	8.09	23.30	8.68	0.20			177.94		2.20	16.40			3.639	0.036	0.545		-4.64	N
424	354011		310	316	7.40	23.43	9.31	24.20	8.70				179.94		3.00	17.30					0.089		-4.34	N
425	354011		320	310	7.43	25.43	9.18	24.40	8.40	0.42			171.94		2.50	16.90				0.007	0.044		-0.71	Y
426	354011		320	319	7.43	25.11	9.18	24.20	8.30	0.34			177.94		2.70	16.70			4.114	0.007	0.018		-2.54	N

Sample #	Well ID	Temp (°C)	EC (µS/cm)	TDS	pH	Ca	Mg	Na	K	Fe	Mn	B	HCO <sub>3</sub>	CO <sub>2</sub>	SO <sub>4</sub>	Cl	F	Br	NH <sub>4</sub>	NO <sub>2</sub>	NO <sub>3</sub>	PO <sub>4</sub>	CAB (%)	Representative
427	354011		300		7.43	24.43	9.72	24.30	8.50	0.15	0.40		163.95		0.30	16.30	0.20	0.08	4.577				2.17	N
428	354011		330		7.79	27.55	9.50	26.10	9.30	0.16	0.51		175.94		0.01	16.00	0.20	0.07	3.600		0.022		2.82	N
429	354011		330		7.08	24.03	7.97	21.70	6.20	1.70	0.40		166.95		0.02	16.70	0.20	0.08	3.857		0.027		-4.07	N
430	354021		430	252	7.05	38.45	13.12	25.00	5.90	3.90	0.92		224.32	33.00	0.10	27.00	0.10			0.016			-2.36	Y
431	354031		1395	826	7.40	10.01	4.86	290.00	8.60	2.40	0.13		446.20	29.00	0.10	242.00	0.32						-1.46	Y
432	354051		192			7.21	7.05	17.70	1.44			0.017	69.49		6.80	20.00							-2.74	Y
433	354061		240	167	7.80	18.42	4.86	15.00	8.90	1.34	0.11		132.88	3.00	0.10	8.00	0.12			0.010			-4.49	Y
434	354063		270			27.63	6.80	14.10	8.31			0.040	142.64		1.10	13.00							0.67	N
435	354063		270			27.63	6.80	14.10	8.31			0.040	142.64		1.10	13.00							0.67	Y
436	354081		255	164	8.00	23.23	4.86	14.50	10.30	0.12	0.02		140.20	2.00	0.10	10.00	0.11						-2.56	Y
437	354091		260	175	7.90	24.03	4.86	14.00	10.00	0.19	0.02		137.76	3.00	0.10	11.00	0.13						-2.12	Y
438	363001		175	137	6.35	7.61	4.13	19.00	1.20	0.12	0.00		40.23	30.00	1.00	19.00	0.07			0.003	21.700		0.33	Y
439	363011		325	219	6.80	18.02	12.39	27.00	2.30	0.45	0.00		106.06	28.00	9.00	34.00	0.07			0.007	14.614		0.50	Y
440	363021		172		6.70	9.61	5.59	17.00	1.20	0.01	0.00		47.55	15.00	7.50	15.00			0.026	0.003	28.786		-3.21	Y
441	363055		280	206	6.30	15.22	9.23	21.00	1.70	0.11			43.89	36.00	4.00	25.00	0.06			0.003	55.800		1.40	Y
442	363101		4469		6.90	160.19	29.15	700.00		4.80	1.30		186.53	50.00	2.00	1,320.00			1.671		0.886		0.61	Y
443	363161		420	260	6.60	24.03	13.85	32.00	2.50	0.95	0.02		54.86	23.00	5.00	34.00	0.06			0.007	94.329		4.27	Y
444	363251		195	160	6.70	9.61	5.83	18.00	1.30	0.43	0.00		45.11	15.00	2.00	16.00	0.09			0.003	30.114		1.65	Y
445	363271		955	375	7.00	46.06	18.46	115.00	6.60	7.70	0.55		286.49	47.00	0.10	178.00	0.21						-3.90	Y
446	363273		205	145	6.95	10.81	7.29	18.00	1.40	0.01	0.00		79.24	15.00	4.00	18.00	0.10			0.007	3.011		0.50	Y

Table D-3: Main calculated characteristics of representative groundwater quality samples.

Well ID	Short type	Long type	Expanded Durov diagram field	Redox <sup>72</sup> water type	SAR <sup>73</sup>	TDS <sup>74</sup> (mg/L)	Density (kg/m <sup>3</sup> )	pCO <sub>2</sub> (atm) <sup>75</sup>	Total Hardness (mg/L)	Carbonate Hardness (mg/L as CaCO <sub>3</sub> )	Calcite Saturation Index	Dolomite Saturation Index	Gypsum Saturation Index	Anhydrite Saturation Index	Halite Saturation Index
316001	Mg-HCO3	Mg-Na-Ca-HCO3-Cl	2	X	0.928	183.54	1.000146	0.09626	87.93639	86.91279	-1.1961	-2.3058	-3.5597	-3.7969	-7.8379
316037	Na-NO3	Na-Ca-Mg-NO3-Cl-HCO3	8	B	1.239	184.03	1.000141	0.23037	70.95461	32.9669	-2.3949	-4.936	-2.924	-3.1612	-7.7372
316041	Na-HCO3	Na-Ca-Mg-HCO3-Cl	2	X	1.144	171.66	1.000137	0.28630	69.95401	64.93485	-2.0108	-3.9561	-2.94	-3.1772	-7.716
318001	Na-HCO3	Na-Ca-HCO3	2	X	1.392	289.86	1.000229	0.01283	99.93118	99.93118	0.2649	0.3105	-2.5073	-2.7445	-7.9274
323001	Ca-HCO3	Ca-Mg-HCO3-Cl	2	X	0.696	445.36	1.000354	0.01969	224.8548	223.7756	0.7389	1.3075	-2.5561	-2.7933	-7.5298
323021	Ca-HCO3	Ca-Mg-HCO3-Cl	1	X	0.732	646.61	1.000533	0.03476	361.7826	279.7194	0.8573	1.4912	-1.746	-1.9831	-7.2179
323027	Ca-HCO3	Ca-Mg-HCO3-Cl	1	X	0.675	623.42	1.000518		361.7563	269.7295	-0.0978	-0.4004	-1.7331	-1.9702	-7.2839
323092	Ca-HCO3	Ca-HCO3	1	X	0.556	250.83	1.000200	0.00732	119.9447	119.9447	0.578	0.6686	-2.8418	-3.079	-8.2215
323166	Na-Cl	Na-Mg-Cl-HCO3	5	X	2.509	875.86	1.000692	0.82262	363.8192	295.7034	-0.8404	-1.4372	-1.9368	-2.1873	-6.2147
324009	Ca-HCO3	Ca-Mg-HCO3	1	X	0.522	366.68	1.000292		188.857	188.857	-0.4225	-1.1643	-2.5423	-2.7795	-7.8206
324011	Ca-HCO3	Ca-Mg-HCO3-Cl	1	X	0.573	409.16	1.000336	0.01883	230.8532	190.8086	0.6897	1.0328	-2.1694	-2.4065	-7.6591
324041	Ca-HCO3	Ca-Mg-HCO3-Cl	1	X	0.641	406.79	1.000331	0.01903	222.84	192.8067	0.6417	1.0667	-2.29	-2.5271	-7.6065
324057	Ca-HCO3	Ca-Mg-HCO3-Cl	1	X	0.691	634.93	1.000522		356.7549	269.7295	-0.0782	-0.44	-1.719	-1.9561	-7.1998
324071	Ca-HCO3	Ca-Mg-HCO3	1	X	0.618	433.94	1.000357	0.02758	239.8544	197.8016	0.5593	0.8023	-2.0023	-2.2395	-7.6422
325013	Ca-HCO3	Ca-Mg-Na-HCO3-Cl	1	X	1.108	732.07	1.000591		369.7297	329.6693	0.0205	-0.2643	-1.7639	-2.001	-6.9495
325031	Ca-HCO3	Ca-Na-Mg-HCO3-Cl	1	X	0.769	372.54	1.000302	0.01145	199.8513	163.8357	0.7274	1.0708	-2.3089	-2.546	-7.4533
325071	Ca-HCO3	Ca-Mg-Na-HCO3-Cl	1	X	0.619	268.02	1.000216	0.00732	142.9267	131.8677	0.6116	0.868	-2.8195	-3.0567	-7.8699
325081	Ca-HCO3	Ca-Mg-Na-HCO3	2	X	0.831	260.73	1.000204	0.07819	120.9145	120.9145	-0.5244	-1.0607	-4.8954	-5.1326	-7.8426
325091	Ca-HCO3	Ca-Mg-Na-HCO3-Cl	2	X	0.870	432.89	1.000347	0.05864	224.8535	210.7886	0.2162	0.2923	-2.5633	-2.8005	-7.3702
325121	Ca-HCO3	Ca-Mg-HCO3-Cl	1	X	0.602	313.12	1.000253	0.00927	168.8985	148.8507	0.6689	0.9941	-2.5359	-2.7731	-7.741
325141	Ca-HCO3	Ca-Mg-Na-HCO3-Cl	2	X	0.752	259.50	1.000207	0.07430	133.9328	133.8658	-0.5061	-1.0228	-3.8612	-4.0983	-7.7982
325221	Mg-HCO3	Mg-Ca-Na-HCO3-Cl	2	X	0.751	243.50	1.000191	0.09215	114.9449	114.9449	-0.7347	-1.3494	-4.9737	-5.2109	-7.8959
325251	Ca-HCO3	Ca-Na-Mg-HCO3-Cl	2	X	0.807	187.10	1.000148	0.19868	88.92637	88.92637	-1.4064	-2.8741	-3.9626	-4.1998	-7.8626
325351	Ca-HCO3	Ca-Mg-Na-HCO3-Cl	2	X	0.722	208.89	1.000162	0.06266	92.91732	92.91732	-0.714	-1.4456	-4.9709	-5.2081	-8.0121
325361	Ca-HCO3	Ca-Na-Mg-HCO3-Cl	2	X	0.881	228.06	1.000176	0.26490	97.53701	97.53701	-1.2401	-2.57	-3.989	-4.2262	-7.8246
325381	Ca-HCO3	Ca-Mg-Na-HCO3-Cl	2	X	1.352	567.20	1.000441		258.8383	258.8383	-0.2767	-0.5484	-3.7603	-3.9974	-6.9435
326011	Ca-HCO3	Ca-Mg-Na-HCO3-Cl	2	X	0.842	325.41	1.000263	0.01336	166.8749	151.8477	0.4948	0.7501	-2.5452	-2.7824	-7.576
326021	Na-Cl	Na-Ca-Mg-Cl-HCO3	8	X	1.885	667.75	1.000526	0.13473	323.8064	192.8067	-0.1961	-0.3342	-2.3002	-2.5372	-6.3547
326041	Ca-HCO3	Ca-Mg-Na-HCO3-Cl	2	X	0.941	341.74	1.000281	0.08773	179.8763	140.8587	-0.3839	-0.9177	-2.2582	-2.4954	-7.4413
326061	Ca-HCO3	Ca-Na-HCO3-Cl	1	X	0.903	355.49	1.000290	0.01371	181.8515	155.8437	0.6216	0.6414	-2.231	-2.4682	-7.4968
326071	Na-Cl	Na-Mg-Ca-Cl-HCO3	8	X	1.985	443.25	1.000361	0.15322	202.9217	109.8898	-1.0386	-1.7877	-2.2284	-2.4655	-6.6546
326091	Ca-HCO3	Ca-Na-HCO3	1	X	0.596	231.75	1.000187	0.00796	119.9091	113.8858	0.4177	0.3675	-2.7444	-2.9816	-8.0447
326099	Ca-HCO3	Ca-Na-Mg-HCO3-Cl	1	X	0.870	372.83	1.000299	0.00954	182.4255	171.8276	0.7707	1.2759	-2.3008	-2.538	-7.4828
326101	Ca-HCO3	Ca-Mg-Na-HCO3-Cl	1	X	0.754	357.19	1.000292	0.03148	191.8499	159.8397	0.238	0.1908	-2.27	-2.5071	-7.5646
326103	Ca-HCO3	Ca-HCO3	1	X	0.539	218.01	1.000175	0.00768	109.9006	109.8898	0.4041	0.1686	-2.7821	-3.0193	-8.1715
326113	Ca-HCO3	Ca-HCO3	1	X	0.375	158.65	1.000128	0.00488	83.94619	83.94619	0.2705	0.1051	-3.1534	-3.3906	-8.8569
326117	Ca-HCO3	Ca-HCO3	1	X	0.559	260.94	1.000208	0.00935	125.5237	125.5237	0.5234	0.4508	-2.4998	-2.737	-8.1615
326119	Ca-HCO3	Ca-Mg-Na-HCO3-Cl	2	X	0.825	356.40	1.000285		173.8906	164.8347	-0.555	-1.3215	-2.3425	-2.5797	-7.5249
326131	Na-Cl	Na-Mg-Ca-Cl-HCO3	9	X	2.773	407.37	1.000323	0.24456	145.9193	87.91184	-1.4861	-2.8099	-2.3699	-2.607	-6.5526
326141	Ca-HCO3	Ca-Mg-Na-HCO3-Cl	2	X	0.774	299.72	1.000243	0.07209	152.9233	129.8697	-0.4029	-1.0146	-2.4127	-2.6499	-7.6072
326151	Ca-HCO3	Ca-Na-Mg-HCO3-Cl	2	X	0.988	277.93	1.000222	0.09086	130.9132	115.8837	-0.6518	-1.5329	-2.5911	-2.8283	-7.4806
326171	Ca-HCO3	Ca-Na-Mg-HCO3-Cl	2	X	1.052	322.64	1.000258	0.01992	153.9121	142.8567	0.2458	0.2419	-2.5981	-2.8353	-7.4039
326181	Ca-HCO3	Ca-HCO3	1	X	0.485	246.43	1.000202	0.01037	135.9216	117.8818	0.3714	0.3171	-2.5121	-2.7493	-8.0893

<sup>72</sup> Redox water type: B = weakly oxidised, x= redox conflict.<sup>73</sup> SAR: sodium adsorption ratio.<sup>74</sup> TDS: total dissolved solids.<sup>75</sup> pCO<sub>2</sub>: CO<sub>2</sub> soil gas partial pressure, atm: atmosphere (pressure measurement unit).

Well ID	Short type	Long type	Expanded Durov diagram field	Redox <sup>72</sup> water type	SAR <sup>73</sup>	TDS <sup>74</sup> (mg/L)	Density (kg/m <sup>3</sup> )	pCO <sub>2</sub> (atm) <sup>75</sup>	Total Hardness (mg/L)	Carbonate Hardness (mg/L as CaCO <sub>3</sub> )	Calcite Saturation Index	Dolomite Saturation Index	Gypsum Saturation Index	Anhydrite Saturation Index	Halite Saturation Index
326191	Ca-HCO3	Ca-Mg-HCO3	1	X	0.398	179.18	1.000145	0.00991	96.93956	95.90379	0.083	-0.2021	-3.0456	-3.2828	-8.5819
326211	Ca-HCO3	Ca-Na-Mg-HCO3-Cl	1	X	0.825	341.27	1.000279	0.05073	180.8938	144.8547	-0.0634	-0.4423	-2.2769	-2.5141	-7.4777
326231	Ca-HCO3	Ca-Mg-Na-HCO3-Cl	2	X	0.918	215.57	1.000169	0.14486	98.91372	98.91372	-1.1622	-2.2664	-3.9892	-4.2264	-7.7132
326241	Mg-Cl	Mg-Na-Ca-Cl-HCO3	8	X	1.991	599.48	1.000479	0.25777	297.8538	146.8527	-0.8299	-1.4386	-2.2757	-2.5127	-6.3625
326301	Ca-HCO3	Ca-Na-Mg-HCO3-Cl	2	X	0.954	272.20	1.000219	0.05197	129.8952	117.8818	-0.3889	-1.0323	-2.6115	-2.8487	-7.5591
326311	Ca-HCO3	Ca-Mg-HCO3	1	X	0.398	196.22	1.000160	0.01476	107.9325	105.8938	0.0478	-0.3138	-2.8217	-3.0589	-8.7158
326321	Ca-HCO3	Ca-Mg-HCO3	1	X	0.458	231.84	1.000194	0.01518	129.9071	108.8908	0.0988	-0.1354	-2.3574	-2.5946	-8.3514
326331	Ca-HCO3	Ca-Mg-Na-HCO3-Cl	2	X	0.892	391.76	1.000322	0.02312	213.8419	165.8336	0.3957	0.6273	-2.2215	-2.4587	-7.3602
326361	Ca-HCO3	Ca-Mg-Na-HCO3-Cl	2	X	0.859	426.88	1.000347		215.8779	184.8146	-0.4622	-1.0621	-2.0751	-2.3122	-7.3769
327001	Ca-HCO3	Ca-Mg-Na-HCO3-Cl	2	X	0.612	168.46	1.000133	0.07206	78.94583	78.94583	-1.1376	-2.2421	-3.2	-3.4373	-8.1364
327003	Ca-HCO3	Ca-Mg-Na-HCO3	1	X	0.798	398.51	1.000324	0.03391	200.8574	188.8106	0.367	0.4208	-2.1233	-2.3604	-7.6401
327005	Na-HCO3	Na-Ca-Mg-HCO3	2	X	1.236	181.09	1.000140	0.13232	59.98661	59.98661	-1.3528	-2.7556	-3.2121	-3.4493	-8.1117
327011	Ca-HCO3	Ca-Mg-Na-HCO3-Cl	1	B	0.798	375.01	1.000312	0.05849	200.8498	148.8507	-0.1034	-0.4218	-2.0134	-2.2505	-7.5429
327037	Na-Cl	Na-Mg-Ca-Cl-HCO3	5	X	1.514	252.85	1.000202	0.11421	106.9355	81.91783	-1.3219	-2.4546	-2.801	-3.0382	-7.2053
327039	Mg-HCO3	Mg-Ca-Na-HCO3-Cl	2	X	0.707	238.63	1.000190		115.9535	115.9535	-0.9639	-1.8311	-2.9209	-3.1581	-7.939
327041	Ca-HCO3	Ca-Na-Mg-HCO3-Cl	2	X	1.013	346.29	1.000278	0.09913	165.8849	141.8577	-0.4598	-1.0774	-2.3282	-2.5653	-7.3387
327051	Mg-HCO3	Mg-Ca-Na-HCO3-Cl	2	X	0.669	177.71	1.000139	0.09847	82.93679	82.93679	-1.2032	-2.3296	-3.5726	-3.8098	-8.0469
327071	Mg-HCO3	Mg-Ca-Na-HCO3-Cl	2	X	0.753	191.31	1.000155	0.18102	90.93861	81.91782	-1.575	-2.9593	-2.7921	-3.0293	-7.9597
327081	Ca-HCO3	Ca-Mg-Na-HCO3-Cl	2	X	0.661	242.74	1.000193	0.10370	117.9416	117.8818	-0.8085	-1.6388	-2.821	-3.0582	-7.8954
327091	Ca-HCO3	Ca-Mg-Na-HCO3-Cl	2	X	0.614	176.95	1.000139	0.06422	84.93288	84.93288	-0.9684	-1.8805	-3.7284	-3.9656	-8.1426
327121	Mg-HCO3	Mg-Na-Ca-HCO3-Cl	2	B	1.103	258.96	1.000211	0.08964	121.9499	101.8978	-0.9568	-1.7616	-2.5433	-2.7805	-7.5564
327131	Ca-HCO3	Ca-Mg-Na-HCO3	1	X	0.744	348.42	1.000284	0.04062	180.8713	163.8357	0.1166	-0.0149	-2.2988	-2.5359	-7.703
327141	Ca-HCO3	Ca-Mg-Na-HCO3-Cl	2	X	0.754	311.76	1.000251	0.05073	160.8934	144.8547	-0.1807	-0.4523	-2.5792	-2.8164	-7.6305
327191	Ca-HCO3	Ca-Na-HCO3-Cl	2	X	0.808	120.24	1.000095	0.19593	48.99062	48.99062	-1.9733	-4.1949	-3.3139	-3.5511	-8.2659
333001	Ca-HCO3	Ca-Mg-HCO3-Cl	2	X	0.980	708.44	1.000575	0.07263	398.7832	328.6703	0.6589	1.2635	-2.168	-2.4051	-6.9534
333011	Ca-HCO3	Ca-Mg-Na-HCO3-Cl	2	X	1.126	590.78	1.000482	0.21707	315.8232	246.7525	-0.1936	-0.3303	-2.0306	-2.2676	-6.9603
333041	Ca-HCO3	Ca-Mg-HCO3-Cl	2	X	0.729	471.62	1.000376	0.01668	240.8317	238.7605	0.8806	1.6012	-2.5122	-2.7493	-7.4876
333048	Na-Cl	Na-Mg-Cl-HCO3	9	X	3.176	486.00	1.000365	0.65188	151.9057	147.8517	-1.6855	-3.0203	-3.8259	-4.0753	-6.3841
333050	Ca-HCO3	Ca-Na-Mg-HCO3-Cl	2	X	0.991	351.13	1.000275	0.12286	161.9152	161.9152	-0.4414	-1.1925	-3.724	-3.9756	-7.4326
333061	Ca-HCO3	Ca-Mg-Na-HCO3-Cl	2	X	1.008	565.44	1.000455	0.04805	297.8136	273.7255	0.6115	1.0975	-2.3889	-2.626	-7.1454
333068	Mg-HCO3	Mg-Ca-HCO3	2	X	0.792	540.15	1.000431	0.03452	289.8325	289.8325	0.5978	1.4236	-3.8182	-4.0649	-7.5386
333071	Ca-HCO3	Ca-Mg-HCO3-Cl	2	X	0.709	581.49	1.000472	0.03719	316.7953	266.7324	0.7161	1.2985	-1.9422	-2.1793	-7.3346
333081	Ca-HCO3	Ca-Mg-HCO3-Cl	2	X	1.019	749.87	1.000619	0.06932	419.7542	313.6854	0.6446	1.2337	-1.7241	-1.9611	-6.9064
333094	Mg-HCO3	Mg-Ca-Na-HCO3-Cl	2	X	0.722	335.59	1.000270	0.20057	191.9002	143.8557	-0.8683	-1.7027	-3.1084	-3.3568	-7.3642
333096	Mg-HCO3	Mg-Na-Ca-HCO3-Cl	2	X	0.822	247.27	1.000193	0.23841	111.9525	107.8918	-1.5349	-2.7736	-3.52	-3.7672	-7.6106
333110	Mg-Cl	Mg-Na-Cl-HCO3	5	X	2.136	613.86	1.000480	0.56694	245.8682	203.7956	-1.2288	-2.0332	-2.4745	-2.7239	-6.4958
333236	Ca-HCO3	Ca-Mg-HCO3-Cl	2	X	1.042	773.38	1.000635	0.05752	435.7132	327.6714	0.8207	1.4751	-1.7778	-2.0148	-6.8444
334011	Ca-HCO3	Ca-Mg-HCO3-Cl	1	X	0.688	551.10	1.000455	0.02406	313.7887	243.7555	0.8439	1.4901	-1.9006	-2.1377	-7.356
334021	Mg-HCO3	Mg-Ca-Na-HCO3	2	X	0.956	312.95	1.000244	0.07576	139.9242	139.9242	-0.3279	-0.5879	-4.8969	-5.1341	-7.7037
334031	Ca-HCO3	Ca-Mg-HCO3-Cl	2	X	0.914	628.29	1.000501	0.11126	344.821	317.6813	0.3769	0.7658	-4.6387	-4.8758	-7.0734
334041	Mg-HCO3	Mg-Ca-Na-HCO3-Cl	2	X	1.351	718.23	1.000564	0.10033	348.7938	348.7938	0.4919	1.0619	-4.682	-4.9191	-6.832
334051	Ca-HCO3	Ca-Mg-Na-HCO3-Cl	2	X	1.134	748.51	1.000609	0.11371	397.7619	324.6743	0.3891	0.843	-1.8802	-2.1172	-6.8579
334071	Ca-HCO3	Ca-Mg-HCO3-Cl	2	X	0.910	615.44	1.000491	0.07130	329.7924	322.6764	0.62	1.1235	-4.594	-4.8311	-7.1837
334091	Ca-HCO3	Ca-Mg-Na-HCO3-Cl	2	X	0.982	330.00	1.000257	0.35541	153.9033	153.9033	-0.9507	-1.9819	-3.8002	-4.0374	-7.4428
334101	Ca-HCO3	Ca-Mg-HCO3-Cl	2	X	0.839	671.95	1.000554	0.06711	387.7872	303.6954	0.6232	1.1669	-1.8893	-2.1264	-7.1164
334121	Ca-HCO3	Ca-Mg-Na-HCO3-Cl	2	X	0.935	422.25	1.000332	0.06059	207.894	207.894	0.1292	0.2939	-4.7734	-5.0106	-7.3625
335001	Ca-HCO3	Ca-Mg-Na-HCO3	1	X	0.591	239.35	1.000190	0.01783	121.9133	121.9133	0.1559	-0.0328	-4.7651	-5.0023	-8.0448
335011	Ca-HCO3	Ca-Mg-Na-HCO3-Cl	2	X	0.793	357.36	1.000283	0.05738	187.8764	163.8357	-0.0221	-0.2531	-4.6915	-4.9286	-7.3667
335041	Ca-HCO3	Ca-Mg-HCO3-Cl	1	X	0.777	450.82	1.000364	0.04835	245.8482	218.7806	0.3879	0.5674	-2.4512	-2.6884	-7.4106
335051	Ca-HCO3	Ca-HCO3-Cl	1	X	0.614	289.95	1.000229	0.03400	144.9028	144.9028	0.1135	-0.1698	-4.7037	-4.9408	-7.8708

Well ID	Short type	Long type	Expanded Durov diagram field	Redox <sup>72</sup> water type	SAR <sup>73</sup>	TDS <sup>74</sup> (mg/L)	Density (kg/m <sup>3</sup> )	pCO <sub>2</sub> (atm) <sup>75</sup>	Total Hardness (mg/L)	Carbonate Hardness (mg/L as CaCO <sub>3</sub> )	Calcite Saturation Index	Dolomite Saturation Index	Gypsum Saturation Index	Anhydrite Saturation Index	Halite Saturation Index
335091	Ca-HCO3	Ca-Mg-Na-HCO3-Cl	1	X	0.784	393.84	1.000310	0.04310	207.8824	173.8257	0.2013	0.1483	-4.6511	-4.8883	-7.2534
335101	Ca-HCO3	Ca-Na-HCO3	1	X	0.603	231.90	1.000186	0.00810	116.915	115.8837	0.4115	0.3693	-2.7154	-2.9526	-8.0878
335131	Ca-HCO3	Ca-Na-HCO3	1	X	0.547	184.82	1.000147	0.00705	90.92196	90.92196	0.2645	0.0749	-3.2255	-3.4627	-8.4567
335141	Ca-HCO3	Ca-Mg-Na-HCO3-Cl	2	X	0.779	293.25	1.000234	0.05318	150.9073	150.9073	-0.1259	-0.4764	-4.7432	-4.9804	-7.7449
335161	Ca-HCO3	Ca-Mg-Na-HCO3-Cl	2	X	0.828	327.75	1.000258	0.03775	158.9011	158.9011	0.1359	0.0514	-4.7359	-4.9731	-7.6281
335171	Ca-HCO3	Ca-Mg-Na-HCO3-Cl	2	X	0.768	337.67	1.000266	0.08253	169.8877	166.8326	-0.2082	-0.6006	-4.728	-4.9651	-7.5203
335221	Ca-HCO3	Ca-Mg-Na-HCO3-Cl	2	X	0.718	339.40	1.000269	0.03819	177.8603	172.8267	0.1628	0.1645	-4.7222	-4.9594	-7.5994
335241	Ca-HCO3	Ca-Mg-Na-HCO3-Cl	1	X	0.680	314.50	1.000250	0.03554	163.8976	160.8387	0.1547	-0.0057	-4.6917	-4.9289	-7.7067
335261	Ca-HCO3	Ca-Na-Mg-HCO3	2	X	0.885	334.59	1.000261	0.05086	150.9192	150.9192	0.0677	-0.1546	-4.7312	-4.9683	-7.7224
335291	Ca-HCO3	Ca-Mg-HCO3	1	X	0.522	258.83	1.000208	0.00840	135.9097	134.8647	0.5523	0.7631	-2.8367	-3.0739	-8.0987
335301	Mg-HCO3	Mg-Ca-Na-HCO3-Cl	2	X	1.307	473.73	1.000366	0.33289	204.8986	204.8986	-0.5623	-1.0437	-4.8106	-5.0477	-7.1047
335311	Ca-HCO3	Ca-Na-HCO3	1	X	0.544	189.36	1.000150	0.00905	91.92934	91.92934	0.1634	-0.0571	-3.5399	-3.7771	-8.311
335331	Ca-HCO3	Ca-Na-HCO3	1	X	0.558	230.40	1.000184	0.01099	118.9204	118.9204	0.3472	0.2913	-3.7569	-3.9942	-8.1655
335351	Ca-HCO3	Ca-HCO3	1	X	0.558	234.38	1.000187	0.01099	118.9204	118.9204	0.345	0.2869	-3.1574	-3.3946	-8.1411
335361	Ca-HCO3	Ca-HCO3	1	X	0.514	201.14	1.000161	0.00967	102.9528	102.9528	0.2399	0.077	-3.4981	-3.7354	-8.3452
335371	Ca-HCO3	Ca-Mg-HCO3-Cl	1	X	0.671	317.96	1.000252	0.05318	167.873	151.8477	-0.0808	-0.4064	-4.7067	-4.9439	-7.5616
335391	Ca-HCO3	Ca-Mg-Na-HCO3-Cl	1	X	0.818	408.66	1.000324	0.03929	221.8738	177.8217	0.2792	0.3177	-4.6382	-4.8754	-7.2066
335431	Ca-HCO3	Ca-Mg-Na-HCO3-Cl	1	X	0.717	337.99	1.000270	0.02788	177.8997	158.8407	0.2696	0.2354	-2.7738	-3.011	-7.5404
336001	Ca-HCO3	Ca-Na-HCO3-Cl	1	X	0.743	317.67	1.000258	0.01005	165.8857	143.8557	0.6144	0.8143	-2.3508	-2.588	-7.6544
336004	Ca-HCO3	Ca-Na-HCO3	1	X	0.522	182.81	1.000145	0.00861	84.09612	84.09612	0.1335	-0.2407	-2.8803	-3.1175	-8.6302
336017	Ca-HCO3	Ca-Mg-Na-HCO3-Cl	1	X	0.708	290.31	1.000234	0.01880	150.8992	134.8647	0.1612	-0.0799	-2.5322	-2.7823	-7.7041
336022	Ca-HCO3	Ca-HCO3	1	X	0.456	177.71	1.000144	0.00817	90.91136	90.91136	0.0383	-0.445	-2.8221	-3.0731	-8.5666
336024	Ca-HCO3	Ca-Na-HCO3-Cl	1	X	0.672	261.41	1.000211	0.01727	135.9216	123.8758	0.1027	-0.3222	-2.5907	-2.8424	-7.8441
336035	Ca-HCO3	Ca-HCO3	1	X	0.435	194.28	1.000157	0.01393	99.91879	99.8998	-0.0874	-0.7585	-2.7003	-2.9521	-8.4806
336039	Ca-HCO3	Ca-HCO3	1	X	0.421	198.99	1.000165	0.00844	106.9145	95.90379	0.1124	-0.3159	-2.449	-2.7	-8.5706
336041	Ca-HCO3	Ca-HCO3	1	X	0.425	165.72	1.000135	0.00756	84.95484	84.95484	0.076	-0.3207	-2.8027	-3.04	-8.6767
336050	Ca-HCO3	Ca-HCO3	1	X	0.415	204.77	1.000166	0.00754	109.9392	107.8918	0.2882	0.0598	-2.7211	-2.9704	-8.5273
336060	Ca-HCO3	Ca-Na-Mg-HCO3-Cl	5	X	1.337	333.41	1.000275	0.36737	160.9083	104.8948	-1.44	-3.019	-2.1741	-2.425	-7.1315
336061	Ca-HCO3	Ca-Mg-Na-HCO3	2	X	0.683	175.79	1.000138	0.04228	74.95615	74.95615	-0.7284	-1.5661	-3.3018	-3.539	-8.497
336069	Ca-HCO3	Ca-Na-HCO3	1	X	0.681	183.61	1.000144	0.01987	79.94337	79.94337	-0.3251	-1.1164	-3.2776	-3.5278	-8.4718
336071	Ca-HCO3	Ca-HCO3	1	X	0.507	217.26	1.000174	0.01782	105.9071	105.9071	0.0406	-0.4335	-2.6918	-2.929	-8.3472
336078	Ca-HCO3	Ca-Na-HCO3-Cl	1	X	0.667	268.38	1.000216	0.01262	137.8978	127.8718	0.2779	-0.0152	-2.5778	-2.8296	-7.8288
336079	Ca-HCO3	Ca-Na-HCO3	1	X	0.566	201.30	1.000162	0.04043	99.9294	99.9294	-0.5071	-1.6157	-2.821	-3.072	-8.2638
336080	Ca-HCO3	Ca-Na-HCO3	1	X	0.510	178.74	1.000144	0.01281	87.92907	87.92907	-0.1502	-0.9465	-2.7286	-2.9796	-8.5763
336081	Ca-HCO3	Ca-HCO3	1	X	0.525	204.46	1.000164	0.01303	98.922	98.922	0.0916	-0.4027	-2.6993	-2.9365	-8.3804
336085	Ca-HCO3	Ca-HCO3-Cl	1	X	0.572	246.46	1.000199	0.01860	129.924	118.8808	0.0353	-0.4772	-2.6304	-2.8814	-7.974
336088	Ca-HCO3	Ca-Na-Mg-HCO3-Cl	1	X	0.667	263.82	1.000213	0.01552	137.9165	124.8747	0.146	-0.1772	-2.6358	-2.8876	-7.8134
336091	Ca-HCO3	Ca-Na-HCO3	1	X	0.617	223.17	1.000180	0.00993	111.9048	111.9048	0.2051	-0.1577	-2.7308	-2.9819	-8.133
336097	Ca-HCO3	Ca-Na-HCO3	2	X	1.009	219.35	1.000174	0.01588	89.9133	89.9133	-0.0783	-0.6638	-2.8432	-3.0933	-8.1042
336101	Ca-HCO3	Ca-Na-HCO3	1	X	0.652	224.80	1.000181	0.00967	113.9009	109.8898	0.2902	0.0972	-2.7563	-2.9935	-8.0369
336113	Ca-HCO3	Ca-HCO3	1	X	0.538	246.39	1.000199	0.01143	130.1305	121.2384	0.3421	0.2459	-2.6579	-2.8951	-8.0533
336114	Ca-HCO3	Ca-Na-HCO3-Cl	1	X	0.691	276.17	1.000225	0.10898	142.9067	123.8758	-0.5897	-1.5699	-2.3933	-2.6304	-7.793
336141	Ca-HCO3	Ca-Na-HCO3-Cl	1	X	0.762	304.43	1.000247	0.01549	157.9012	139.8597	0.3874	0.388	-2.4862	-2.7233	-7.653
336151	Ca-HCO3	Ca-Na-HCO3	2	X	1.322	231.19	1.000183	0.00909	84.93617	84.93617	0.2737	-0.1269	-2.7535	-2.9907	-7.917
336181	Ca-HCO3	Ca-Na-HCO3	1	X	0.539	187.61	1.000151	0.00622	93.90552	93.90552	0.317	0.1878	-2.976	-3.2132	-8.4575
336200	Ca-HCO3	Ca-Na-HCO3-Cl	1	X	0.877	364.39	1.000298	0.02243	192.8555	160.8387	0.421	0.4422	-2.2739	-2.5111	-7.4675
336201	Ca-HCO3	Ca-Na-Mg-HCO3-Cl	2	X	0.853	218.27	1.000178	0.09626	103.939	86.91279	-0.9878	-2.2816	-2.4589	-2.6961	-7.7942
336211	Ca-HCO3	Ca-Na-Mg-HCO3-Cl	1	X	0.906	310.79	1.000251	0.01582	155.8789	142.8567	0.3733	0.4232	-2.5677	-2.8049	-7.5573
336221	Ca-HCO3	Ca-Na-HCO3	1	X	0.897	250.32	1.000200	0.01116	113.9115	113.9115	0.2726	-0.0448	-2.7075	-2.9576	-7.9574
336223	Ca-HCO3	Ca-Mg-HCO3	1	X	0.446	174.73	1.000143	0.00401	94.92352	90.9088	0.4142	0.4269	-2.8397	-3.0769	-8.6845

Well ID	Short type	Long type	Expanded Durov diagram field	Redox <sup>72</sup> water type	SAR <sup>73</sup>	TDS <sup>74</sup> (mg/L)	Density (kg/m <sup>3</sup> )	pCO <sub>2</sub> (atm) <sup>75</sup>	Total Hardness (mg/L)	Carbonate Hardness (mg/L as CaCO <sub>3</sub> )	Calcite Saturation Index	Dolomite Saturation Index	Gypsum Saturation Index	Anhydrite Saturation Index	Halite Saturation Index
336233	Ca-HCO3	Ca-Na-HCO3	2	X	1.197	203.60	1.000154	0.00984	63.93089	63.93089	0.0767	-0.2784	-3.6662	-3.9003	-8.1945
336241	Ca-HCO3	Ca-Mg-Na-HCO3-Cl	1	X	0.861	354.74	1.000290	0.01353	185.8616	153.8457	0.5422	0.8206	-2.2729	-2.51	-7.4727
336245	Ca-HCO3	Ca-HCO3	1	X	0.462	165.82	1.000133	0.00396	79.95397	79.95397	0.3439	0.2803	-2.884	-3.1212	-8.8231
336253	Ca-HCO3	Ca-Na-HCO3	1	X	0.536	188.18	1.000152	0.01062	94.94974	94.94974	0.0729	-0.3604	-2.725	-2.9622	-8.458
336271	Ca-HCO3	Ca-Na-HCO3	1	X	0.505	171.64	1.000137	0.00826	81.93014	81.93014	0.1039	-0.2754	-3.1548	-3.3921	-8.6095
336321	Ca-HCO3	Ca-HCO3	1	X	0.432	208.31	1.000173	0.00879	111.9154	99.8998	0.2425	-0.0115	-2.398	-2.6352	-8.5197
336333	Ca-HCO3	Ca-Mg-Na-HCO3-Cl	2	X	0.826	312.23	1.000251	0.02525	159.8979	143.8557	0.0417	-0.2038	-2.56	-2.8124	-7.5529
336361	Ca-HCO3	Ca-HCO3	1	X	0.465	198.02	1.000162	0.00698	105.9071	99.8998	0.3277	0.1417	-2.689	-2.9262	-8.4184
336391	Ca-HCO3	Ca-Na-HCO3	1	X	0.530	191.53	1.000154	0.01129	96.93523	96.93523	0.106	-0.2789	-2.9535	-3.1907	-8.4581
336401	Ca-HCO3	Ca-HCO3	1	X	0.456	175.54	1.000142	0.00728	90.92196	90.92196	0.1809	-0.0929	-2.9228	-3.16	-8.5811
336421	Ca-HCO3	Ca-Na-HCO3-Cl	1	X	0.836	301.08	1.000245	0.01195	155.9263	135.8637	0.4718	0.5357	-2.4595	-2.6967	-7.6272
336441	Ca-HCO3	Ca-HCO3	1	X	0.510	206.50	1.000165	0.01504	104.9091	104.9091	0.0657	-0.3779	-2.8954	-3.1326	-8.3297
336442	Ca-HCO3	Ca-Na-HCO3	1	X	0.573	178.88	1.000141	0.00844	82.94813	82.94813	0.0999	-0.2347	-3.1648	-3.4029	-8.5004
336451	Ca-HCO3	Ca-HCO3	1	X	0.474	189.02	1.000151	0.00888	92.95362	92.95362	0.1834	-0.1271	-2.9674	-3.2046	-8.474
336471	Ca-HCO3	Ca-Mg-Na-HCO3-Cl	2	X	0.977	479.95	1.000391	0.04614	256.8535	208.7906	0.3514	0.5613	-2.1719	-2.409	-7.1861
336481	Ca-HCO3	Ca-Mg-Na-HCO3-Cl	1	X	0.572	235.24	1.000191	0.01028	129.9333	116.8827	0.3503	0.3014	-3.1288	-3.366	-7.9877
336491	Ca-HCO3	Ca-HCO3	1	X	0.459	174.73	1.000143	0.00765	89.93451	86.9128	0.1005	-0.2754	-2.6522	-2.8894	-8.5815
336511	Ca-HCO3	Ca-Na-HCO3	1	X	0.507	179.86	1.000145	0.00597	88.93645	88.93645	0.284	0.0992	-2.93	-3.1673	-8.5398
336571	Ca-HCO3	Ca-HCO3	1	X	0.494	188.59	1.000152	0.01106	93.95168	93.95168	0.0862	-0.328	-2.808	-3.0452	-8.5923
336591	Ca-HCO3	Ca-Mg-Na-HCO3-Cl	2	X	1.001	462.35	1.000377	0.03419	244.8701	194.8046	0.4201	0.6499	-2.139	-2.3761	-7.1783
336996	Ca-HCO3	Ca-Na-HCO3	1	X	0.513	175.31	1.000142	0.00642	86.95094	86.95094	0.2117	-0.0616	-2.7957	-3.0329	-8.6485
337001	Ca-HCO3	Ca-HCO3	1	X	0.400	175.78	1.000144	0.00521	95.95712	93.90582	0.3455	0.2586	-2.8593	-3.0965	-8.7365
337005	Na-HCO3	Na-HCO3-Cl	3	X	18.442	469.37	1.000339	0.03454	9.988607	9.988607	-1.3085	-2.2402	-4.9336	-5.1807	-6.5201
337006	Ca-HCO3	Ca-HCO3	1	X	0.512	204.47	1.000165	0.00754	103.911	103.911	0.2652	-0.0655	-2.7661	-3.0171	-8.445
337007	Ca-HCO3	Ca-HCO3	1	X	0.377	181.15	1.000147	0.00516	95.93719	92.90684	0.3502	0.2163	-2.7255	-2.9627	-8.6527
337008	Ca-HCO3	Ca-Na-HCO3	1	X	1.077	233.66	1.000186	0.00852	93.94234	93.94234	0.255	-0.2047	-2.6801	-2.9339	-8.1408
337010	Ca-HCO3	Ca-HCO3	1	X	0.523	225.04	1.000182	0.00817	116.915	116.8827	0.3312	0.1157	-2.6629	-2.9139	-8.334
337011	Ca-HCO3	Ca-Mg-HCO3	1	X	0.588	260.13	1.000213	0.02139	139.9312	121.8777	0.0625	-0.1608	-2.4702	-2.7074	-7.9631
337012	Ca-HCO3	Ca-Na-HCO3	2	X	1.299	256.05	1.000202	0.00880	100.9274	100.9274	0.3165	0.0365	-2.7952	-3.0454	-7.7105
337014	Ca-HCO3	Ca-HCO3	1	X	0.452	209.14	1.000170	0.00761	111.9154	108.8908	0.3175	0.0714	-2.6676	-2.9159	-8.4878
337015	Ca-HCO3	Ca-HCO3	1	X	0.396	186.61	1.000151	0.00567	97.93329	97.93329	0.382	0.2687	-2.7544	-2.9916	-8.7501
337018	Ca-HCO3	Ca-HCO3	1	X	0.521	226.74	1.000184	0.01588	117.9236	113.8858	0.0212	-0.5481	-2.6161	-2.8686	-8.207
337023	Na-HCO3	Na-HCO3-Cl	3	X	6.339	518.06	1.000385	0.01989	68.94737	68.94737	0.3822	0.0197	-4.9901	-5.2409	-6.714
337031	Ca-HCO3	Ca-Mg-HCO3	1	X	0.390	190.05	1.000154	0.00653	100.9262	100.9262	0.3588	0.3035	-2.9002	-3.1375	-8.7379
337041	Ca-HCO3	Ca-Mg-HCO3	1	X	0.348	183.97	1.000148	0.00712	99.93874	99.93874	0.3018	0.1716	-3.0993	-3.3365	-8.6792
337051	Ca-HCO3	Ca-Mg-Na-HCO3-Cl	1	X	0.774	323.79	1.000263	0.03946	166.9011	141.8577	-0.0103	-0.3102	-2.3251	-2.5623	-7.5796
337064	Ca-HCO3	Ca-Na-HCO3	1	X	1.056	255.69	1.000202	0.00949	106.9052	106.9052	0.4532	0.3888	-2.8276	-3.0648	-8.0298
337067	Ca-HCO3	Ca-Na-HCO3	1	X	0.533	202.02	1.000165	0.00726	103.9509	103.8958	0.3112	0.2142	-2.6553	-2.8925	-8.5391
342001	Na-HCO3	Na-Mg-Ca-HCO3	2	X	2.457	642.17	1.000494	0.32605	215.8933	215.8933	-0.2114	-0.273	-4.8609	-5.0979	-7.176
342002	Na-HCO3	Na-Ca-HCO3-Cl-NO3	8	B	0.885	84.55	1.000065	0.35070	31.98008	19.97988	-3.2717	-6.8201	-3.5273	-3.7646	-8.311
342011	Na-HCO3	Na-HCO3	3	X	4.486	746.49	1.000560	0.18411	158.9221	158.9221	-0.0216	0.1422	-5.0103	-5.2473	-6.8076
342041	Ca-HCO3	Ca-Na-HCO3-Cl	1	X	1.015	402.06	1.000317	0.05836	187.8852	187.8852	0.2238	0.0871	-4.6527	-4.8899	-7.4623
342051	Na-HCO3	Na-Ca-Mg-HCO3	2	X	1.515	377.72	1.000288	0.05836	131.9274	131.9274	-0.0286	-0.0944	-4.8836	-5.1208	-7.6288
342061	Na-HCO3	Na-HCO3	3	X	5.990	560.64	1.000415	0.04151	75.94412	75.94412	-0.0306	0.2438	-5.3302	-5.5672	-6.8203
342081	Ca-HCO3	Ca-Na-HCO3-Cl	1	X	0.926	488.68	1.000388	0.08467	247.8339	241.7575	0.3282	0.1055	-4.5342	-4.7713	-7.2635
342091	Na-HCO3	Na-Ca-HCO3	3	X	1.343	254.72	1.000191	0.01005	70.95714	70.95714	0.2794	0.1922	-4.9651	-5.2023	-8.1244
342097	Ca-HCO3	Ca-Na-Mg-HCO3	2	X	1.057	366.45	1.000290		166.9042	166.9042	-0.4906	-1.1645	-3.7401	-3.9773	-7.6964
342105	Na-HCO3	Na-Ca-HCO3	3	X	2.739	397.45	1.000298	0.06114	96.94941	96.94941	-0.1684	-0.3129	-4.032	-4.2692	-7.4813
342141	Na-HCO3	Na-Mg-HCO3	3	X	2.878	502.34	1.000381	0.10041	131.9173	131.9173	-0.1362	-0.0712	-5.0374	-5.2745	-7.2999
342151	Na-HCO3	Na-Mg-HCO3	3	X	4.544	661.70	1.000495	0.10033	131.9403	131.9403	-0.0584	0.2396	-5.1701	-5.4071	-6.8186

Well ID	Short type	Long type	Expanded Durov diagram field	Redox <sup>72</sup> water type	SAR <sup>73</sup>	TDS <sup>74</sup> (mg/L)	Density (kg/m <sup>3</sup> )	pCO <sub>2</sub> (atm) <sup>75</sup>	Total Hardness (mg/L)	Carbonate Hardness (mg/L as CaCO <sub>3</sub> )	Calcite Saturation Index	Dolomite Saturation Index	Gypsum Saturation Index	Anhydrite Saturation Index	Halite Saturation Index
342161	Na-HCO3	Na-Mg-Ca-HCO3	2	X	1.381	325.47	1.000253		122.928	122.928	-0.7844	-1.4518	-4.1932	-4.4303	-7.7726
342171	Ca-HCO3	Ca-Mg-HCO3	2	X	0.629	533.62	1.000423	0.05331	275.8446	275.8446	0.6374	1.147	-4.6298	-4.8669	-7.6975
343021	Ca-HCO3	Ca-Na-HCO3	2	X	0.981	308.86	1.000239	0.03069	122.9101	122.9101	0.1643	0.0476	-4.7996	-5.0368	-7.9193
343031	Ca-HCO3	Ca-Na-Mg-HCO3	2	X	1.689	582.81	1.000452	0.18077	230.8724	230.8724	0.1054	0.0611	-4.6875	-4.9246	-7.2193
343051	Ca-HCO3	Ca-Na-Mg-HCO3	2	X	0.871	388.69	1.000305	0.02981	181.88	181.88	0.4859	0.7117	-4.6912	-4.9283	-7.6484
343061	Ca-HCO3	Ca-Mg-Na-HCO3	2	X	0.699	325.51	1.000255	0.12635	154.8801	154.8801	-0.4047	-0.8722	-4.8027	-5.0399	-7.8703
343101	Mg-HCO3	Mg-Ca-Na-HCO3	2	X	1.214	615.08	1.000487	0.31375	295.8384	295.8384	-0.0675	-0.0424	-4.7215	-4.9585	-7.388
343121	Na-HCO3	Na-Ca-Mg-HCO3	2	X	2.177	507.02	1.000392	0.31311	173.9079	173.9079	-0.3768	-0.8571	-4.7882	-5.0253	-7.2669
343151	Ca-HCO3	Ca-Mg-Na-HCO3	2	X	1.119	466.18	1.000362	0.09517	195.908	195.908	0.0847	0.2296	-4.8117	-5.0488	-7.6833
343155	Ca-HCO3	Ca-Na-HCO3	2	X	1.049	275.99	1.000214		104.9371	104.9371	-0.7365	-1.7837	-3.9337	-4.1709	-8.0723
343161	Mg-HCO3	Mg-Ca-HCO3	2	X	0.644	373.20	1.000298	0.21201	200.8801	200.8801	-0.4777	-0.8227	-4.8218	-5.059	-7.8929
343171	Ca-HCO3	Ca-Mg-Na-HCO3	2	X	0.787	396.97	1.000312	0.01925	190.8705	190.8705	0.6923	1.1684	-4.6933	-4.9305	-7.6975
344011	Ca-HCO3	Ca-Na-Mg-HCO3-Cl	1	B	0.859	395.95	1.000319	0.00679	215.8375	193.8056	1.093	1.8661	-4.6269	-4.8641	-7.4538
344031	Na-HCO3	Na-Ca-Mg-HCO3	2	X	1.949	827.21	1.000644	0.66997	334.793	334.793	-0.1	-0.1331	-4.701	-4.938	-7.0686
344041	Ca-HCO3	Ca-Mg-Na-HCO3	2	X	1.134	502.11	1.000393	0.12685	223.8598	223.8598	0.1289	0.162	-4.7033	-4.9404	-7.5119
344051	Ca-HCO3	Ca-Mg-HCO3	1	X	0.667	335.02	1.000265	0.03951	169.8753	169.8753	0.2143	0.1045	-4.681	-4.9182	-7.7608
344061	Ca-HCO3	Ca-Mg-Na-HCO3	1	X	0.611	242.25	1.000190	0.03780	113.9395	113.9395	-0.1468	-0.6158	-4.794	-5.0312	-8.1621
344081	Na-HCO3	Na-Ca-Mg-HCO3	2	X	2.151	752.87	1.000578	0.66732	274.8539	274.8539	-0.265	-0.4767	-4.7468	-4.9838	-6.9496
344091	Ca-HCO3	Ca-Mg-Na-HCO3	2	X	1.166	497.70	1.000391	0.12641	222.8524	222.8524	0.1346	0.1523	-4.6955	-4.9327	-7.565
344183	Ca-HCO3	Ca-Na-Mg-HCO3	2	X	0.811	266.87	1.000210		120.9327	120.9327	-0.7417	-1.6592	-4.1296	-4.3668	-7.9781
345011	Ca-HCO3	Ca-Mg-Na-HCO3-Cl	1	X	0.701	288.58	1.000227	0.05388	138.9226	138.9226	-0.1382	-0.543	-4.7553	-4.9925	-7.8379
345041	Ca-HCO3	Ca-Na-HCO3	1	X	0.799	188.56	1.000147	0.01140	75.96429	75.96429	0.0445	-0.5692	-3.2514	-3.4886	-8.4273
345051	Ca-HCO3	Ca-Na-HCO3	2	X	0.985	207.80	1.000160	0.01602	77.94726	77.94726	-0.06	-0.4858	-4.9113	-5.1485	-8.0894
345053	Ca-HCO3	Ca-Na-HCO3	1	X	0.804	183.98	1.000144	0.01117	74.96623	74.96623	0.0312	-0.5891	-3.5565	-3.7937	-8.33
345061	Ca-HCO3	Ca-Na-HCO3	1	X	0.644	244.81	1.000193	0.01866	116.915	116.915	0.1861	-0.0821	-4.7524	-4.9896	-8.0834
345071	Ca-HCO3	Ca-Na-Mg-HCO3	2	X	0.855	310.56	1.000242	0.03069	136.9277	136.9277	0.2182	0.1205	-4.7513	-4.9885	-7.8861
345081	Na-HCO3	Na-HCO3	3	X	3.642	306.93	1.000227	0.02340	47.97263	47.97263	-0.1379	-0.5925	-3.8504	-4.0875	-7.6652
345091	Na-HCO3	Na-HCO3	3	X	3.785	309.78	1.000230	0.01881	45.96718	45.96718	-0.0225	-0.4788	-5.1392	-5.3764	-7.5415
345101	Na-HCO3	Na-HCO3-Cl	3	X	7.790	548.48	1.000403	0.03766	55.98633	55.98633	-0.0447	-0.3085	-5.1966	-5.4337	-6.4665
345111	Ca-HCO3	Ca-Mg-Na-HCO3	1	X	0.675	257.31	1.000201	0.06166	119.9159	119.9159	-0.332	-0.9307	-4.7975	-5.0347	-7.9713
345141	Na-HCO3	Na-HCO3	3	X	12.159	548.02	1.000401	0.01291	22.97892	22.97892	0.2799	-0.0402	-5.4807	-5.7178	-6.9401
345151	Na-HCO3	Na-Ca-HCO3	3	X	1.839	236.83	1.000179	0.01494	60.94732	60.94732	0.0204	-0.4165	-4.9939	-5.2311	-8.0646
346031	Na-HCO3	Na-Ca-HCO3	3	X	2.208	287.23	1.000220	0.01637	79.9565	79.9565	0.201	-0.2815	-3.266	-3.5032	-7.5253
346041	Na-HCO3	Na-Ca-HCO3-Cl	3	X	2.435	378.56	1.000290	0.02003	114.9158	114.9158	0.4171	0.1724	-4.7624	-4.9995	-7.0764
346051	Na-HCO3	Na-Ca-HCO3	3	B	1.775	264.87	1.000205	0.01483	84.9455	84.9455	0.1685	-0.2286	-3.1582	-3.3954	-7.6886
352001	Na-HCO3	Na-Mg-Ca-HCO3-Cl	2	X	1.500	321.23	1.000250	0.14413	127.9289	127.9289	-0.686	-1.3044	-4.9325	-5.1697	-7.4032
352003	Na-HCO3	Na-Ca-Mg-HCO3-Cl	2	X	1.561	312.29	1.000245	0.20511	126.7004	126.7004	-0.8576	-1.7275	-3.4817	-3.7189	-7.3768
352011	Na-HCO3	Na-Ca-Mg-HCO3-Cl	2	X	1.489	221.75	1.000172	0.09316	81.97054	81.97054	-1.0172	-2.0098	-5.0448	-5.282	-7.557
352021	Ca-HCO3	Ca-Na-Mg-HCO3-Cl	2	X	1.128	213.76	1.000167	0.06562	92.95415	92.95415	-0.8557	-1.8248	-4.9355	-5.1727	-7.5513
352051	Na-HCO3	Na-Ca-Mg-HCO3-Cl	2	X	1.790	337.47	1.000261	0.16073	124.9267	124.9267	-0.715	-1.4391	-4.9095	-5.1466	-7.2263
352123	Ca-HCO3	Ca-Na-Mg-HCO3-Cl	2	X	1.416	412.74	1.000326		192.9058	185.8136	-0.5528	-1.096	-4.008	-4.2452	-7.0673
352131	Na-HCO3	Na-Ca-Mg-HCO3-Cl	2	X	1.178	180.03	1.000139	0.06353	65.95247	65.95247	-1.07	-2.1	-5.1171	-5.3544	-7.8692
352133	Na-HCO3	Na-Ca-HCO3-Cl	3	X	1.851	241.18	1.000189		87.9346	87.9346	-1.0307	-2.2377	-3.7674	-4.0046	-7.3083
352141	Na-Cl	Na-Cl-HCO3	9	X	12.648	1,965.93	1.001461	0.14729	319.824	319.824	0.4559	1.0954	-2.979	-3.2155	-5.0924
352211	Na-HCO3	Na-Mg-Ca-HCO3-Cl	2	B	1.192	196.49	1.000156	0.11409	89.96304	72.92684	-1.4166	-2.7472	-3.5583	-3.7955	-7.4908
352241	Ca-HCO3	Ca-Na-Mg-HCO3	2	X	1.321	467.92	1.000368	0.17452	209.8971	209.8971	-0.1111	-0.4273	-4.6778	-4.9149	-7.3181
352251	Na-HCO3	Na-Mg-HCO3-Cl	3	B	2.184	231.07	1.000178	0.05724	69.96335	69.96335	-1.1564	-2.1719	-3.3221	-3.5593	-7.3973
352271	Na-Cl	Na-Ca-Cl	9	X	9.930	3,191.42	1.002409	0.04618	1079.395	131.8677	0.2624	0.571	-2.5954	-2.8312	-4.5218
352291	Na-HCO3	Na-Mg-Ca-HCO3-Cl	2	X	1.200	153.78	1.000120	0.08630	57.96429	57.96429	-1.4129	-2.7291	-3.8849	-4.1221	-8.0043
352301	Na-HCO3	Na-Ca-Mg-HCO3-Cl	2	X	1.313	195.66	1.000152	0.08298	79.9651	74.92484	-1.2513	-2.5231	-5.0264	-5.2636	-7.4348

Well ID	Short type	Long type	Expanded Durov diagram field	Redox <sup>72</sup> water type	SAR <sup>73</sup>	TDS <sup>74</sup> (mg/L)	Density (kg/m <sup>3</sup> )	$pCO_2$ (atm) <sup>75</sup>	Total Hardness (mg/L)	Carbonate Hardness (mg/L as CaCO <sub>3</sub> )	Calcite Saturation Index	Dolomite Saturation Index	Gypsum Saturation Index	Anhydrite Saturation Index	Halite Saturation Index
352341	Na-HCO3	Na-Mg-Ca-HCO3-Cl	5	X	1.384	219.04	1.000174	0.04159	88.96371	74.92484	-1.0224	-1.8705	-2.8258	-3.063	-7.384
352451	Na-HCO3	Na-Ca-Mg-HCO3-Cl	2	X	1.865	336.34	1.000264		127.9302	127.9302	-0.7551	-1.4968	-4.1334	-4.3705	-7.298
353001	Na-HCO3	Na-Ca-Mg-HCO3	2	X	1.492	373.71	1.000287	0.07102	135.9209	135.9209	-0.0984	-0.3098	-4.841	-5.0782	-7.4744
353015	Na-NO3	Na-Mg-Ca-NO3-HCO3-Cl	8	B	1.167	197.18	1.000151	0.09713	79.9719	43.9559	-1.9722	-3.8004	-3.2245	-3.4737	-7.7796
353067	Na-NO3	Na-Mg-Ca-NO3-Cl	9	B	2.154	345.69	1.000264	0.20702	118.9401	46.95288	-2.0409	-3.8607	-2.594	-2.8312	-7.1259
353084	Na-HCO3	Na-Ca-HCO3	3	X	1.466	237.64	1.000181		70.96521	70.96521	-0.9909	-2.1527	-4.1721	-4.4093	-8.1557
353101	Mg-HCO3	Mg-Ca-Na-HCO3-Cl	2	B	0.812	181.35	1.000141	0.07634	82.94612	68.93085	-1.3416	-2.5434	-3.5991	-3.8363	-8.0246
353171	Na-HCO3	Na-Ca-HCO3	3	X	1.907	221.14	1.000165	0.02479	49.97305	49.97305	-0.4283	-1.0009	-5.1587	-5.3959	-8.0437
354011	Ca-HCO3	Ca-Na-Mg-HCO3	2	X	1.055	258.81	1.000201	0.05798	101.2213	101.2213	-0.4075	-0.9731	-3.5005	-3.7377	-7.9278
354021	Ca-HCO3	Ca-Na-Mg-HCO3	2	X	0.888	334.01	1.000260	0.18144	149.9186	149.9186	-0.5144	-1.211	-4.7684	-5.0055	-7.7224
354031	Na-HCO3	Na-HCO3-Cl	3	X	18.810	1,002.09	1.000728	0.16121	44.97218	44.97218	-0.5404	-1.1073	-5.4618	-5.6987	-5.7402
354051	Na-HCO3	Na-Mg-Ca-HCO3-Cl	2	X	1.123	129.71	1.000101		46.9963	46.9963	-1.7338	-3.1942	-3.5291	-3.7663	-7.9786
354061	Ca-HCO3	Ca-Na-HCO3	2	X	0.803	188.29	1.000143	0.01911	65.95627	65.95627	-0.2652	-0.8245	-4.9856	-5.2228	-8.4539
354063	Ca-HCO3	Ca-Na-Mg-HCO3	2	X	0.623	213.62	1.000168		96.91835	96.91835	-0.868	-2.0609	-3.8008	-4.038	-8.2756
354081	Ca-HCO3	Ca-Na-HCO3	2	X	0.714	203.30	1.000156	0.01272	77.95786	77.95786	0.0473	-0.2993	-4.9013	-5.1385	-8.3743
354091	Ca-HCO3	Ca-Na-HCO3	2	X	0.681	201.88	1.000156	0.01574	79.95397	79.95397	-0.0435	-0.4962	-4.887	-5.1242	-8.3483
363001	Na-HCO3	Na-Ca-Mg-HCO3-Cl-NO3	9	B	1.378	113.94	1.000086	0.16309	35.98036	32.96691	-2.5783	-5.139	-4.307	-4.5443	-7.9645
363011	Na-HCO3	Na-Mg-Ca-HCO3-Cl	2	B	1.199	223.46	1.000176	0.15256	95.93949	86.91279	-1.3883	-2.6557	-3.0832	-3.3204	-7.5782
363021	Na-HCO3	Na-Ca-Mg-HCO3-NO3-Cl	5	B	1.079	132.26	1.000101	0.08609	46.97763	38.96091	-2.0665	-4.0854	-3.3515	-3.5887	-8.1186
363055	Na-NO3	Na-Ca-Mg-NO3-HCO3-Cl	8	B	1.048	175.90	1.000134	0.19962	75.95168	35.96391	-2.3155	-4.565	-3.461	-3.6983	-7.8114
363101	Na-Cl	Na-Cl	9	X	13.357	2,400.42	1.001788	0.21311	519.6298	152.8467	-0.3505	-1.1487	-3.2534	-3.4896	-4.6814
363161	Na-NO3	Na-Ca-Mg-NO3-Cl-HCO3	8	B	1.287	260.64	1.000200	0.12506	116.9423	44.9549	-1.746	-3.4476	-3.2194	-3.4567	-7.5045
363251	Na-HCO3	Na-Mg-Ca-HCO3-NO3-Cl	8	B	1.131	128.06	1.000098	0.08168	47.96507	36.96292	-2.0849	-4.1037	-3.921	-4.1582	-8.065
363271	Na-Cl	Na-Ca-Cl-HCO3	9	X	3.621	650.92	1.000489	0.26000	190.8773	190.8773	-0.4386	-0.9884	-4.7884	-5.0255	-6.2643
363273	Na-HCO3	Na-Mg-Ca-HCO3-Cl	2	B	1.037	141.86	1.000111	0.08069	56.96623	56.96623	-1.5547	-2.9973	-3.5945	-3.8317	-8.0189

Table D-4: Well clusters used for checking groundwater quality–depth relationship.

Cluster	Well ID	Easting	Northing	Elevation (masl)	Well Depth (m)	Well bottom level (masl)	Dominant cation–anion
Ashhurst	327011	2744400	6099100	84.14	42.00	42.14	Ca–HCO <sub>3</sub>
	327003	2744900	6099200	63.10	51.00	12.18	Ca–HCO <sub>3</sub>
	327071	2743700	6099100	83.13	68.63	14.50	Mg–HCO <sub>3</sub>
	327001	2742679	6098753	118.71	95.00	23.71	Ca–HCO <sub>3</sub>
Bunynthorpe	326021 <sup>76</sup>	2732780	6099561	50.44	30.00	20.44	Na–Cl
	336471	2732800	6097300	45.47	48.00	-2.53	Ca–HCO <sub>3</sub>
	326361	2733441	6097951	50.69	63.50	-12.80	Ca–HCO <sub>3</sub>
	326331 <sup>76</sup>	2733397	6100383	56.96	85.90	-28.94	Ca–HCO <sub>3</sub>
	336333	2735006	6096447	57.79	96.00	-38.21	Ca–HCO <sub>3</sub>
	326099	2734000	6099100	55.16	102.10	-46.94	Ca–HCO <sub>3</sub>
	326171 <sup>76</sup>	2735000	6097900	57.76	103.00	-45.24	Ca–HCO <sub>3</sub>
	326011 <sup>76</sup>	2734271	6098740	58.29	113.00	-54.71	Ca–HCO <sub>3</sub>
	336200	2733800	6096200	54.67	113.30	-58.62	Ca–HCO <sub>3</sub>
	326061	2733901	6099145	50.79	118.95	-68.16	Ca–HCO <sub>3</sub>
	326181 <sup>76</sup>	2735590	6097071	64.24	135.00	-70.76	Ca–HCO <sub>3</sub>
	326311	2731722	6098785	47.41	152.30	-104.88	Ca–HCO <sub>3</sub>
	326191	2731628	6099141	49.46	153.75	-104.29	Ca–HCO <sub>3</sub>
	326103	2734400	6099300	56.26	201.80	-145.54	Ca–HCO <sub>3</sub>
326091 <sup>76</sup>	2734300	6099400	58.98	207.71	-148.72	Ca–HCO <sub>3</sub>	
Staces/Pinfold Rds	336114	2735675	6091722	36.83	12.30	24.53	Ca–HCO <sub>3</sub>
	336113	2735033	6090471	34.49	34.00	0.49	Ca–HCO <sub>3</sub>
	336085	2735286	6090751	31.70	38.00	-6.30	Ca–HCO <sub>3</sub>
	336481	2735150	6091214	33.07	48.00	-14.93	Ca–HCO <sub>3</sub>
	336004	2735625	6090697	36.49	72.00	-35.51	Ca–HCO <sub>3</sub>
	336181	2735888	6090262	36.25	72.10	-35.85	Ca–HCO <sub>3</sub>
	336511	2735500	6091500	35.61	97.00	-61.39	Ca–HCO <sub>3</sub>
Massey	346031	2734540	6086023	57.33	47.28	10.06	Na–HCO <sub>3</sub>
	346041	2732300	6085800	58.83	88.75	-29.92	Na–HCO <sub>3</sub>
	346051	2734138	6085589	96.47	104.00	-7.53	Na–HCO <sub>3</sub>
	336151	2733492	6086070	81.94	200.00	-118.05	Ca–HCO <sub>3</sub>
Glen Oroua	333081	2713415	6096557	16.97	28.00	-11.03	Ca–HCO <sub>3</sub>
	333236	2712323	6095434	23.67	54.00	-30.33	Ca–HCO <sub>3</sub>
	333011	2713465	6096884	17.91	83.00	-65.09	Ca–HCO <sub>3</sub>
	334011	2713792	6097044	19.07	113.00	-93.93	Ca–HCO <sub>3</sub>
	333071	2713788	6094724	18.91	131.00	-112.09	Ca–HCO <sub>3</sub>
	333041	2712502	6094872	22.03	182.00	-159.97	Ca–HCO <sub>3</sub>
Himatangi	333050	2708100	6087500	25.591	23.00	2.59	Ca–HCO <sub>3</sub>
	343061	2708299	6084377	26.98	38.20	-11.22	Ca–HCO <sub>3</sub>
	343161	2707884	6084262	26.86	54.00	-27.15	Mg–HCO <sub>3</sub>
	343171	2707280	6086805	24.57	120.00	-95.43	Ca–HCO <sub>3</sub>
	343155	2706857	6086664	22.26	169.80	-147.54	Ca–HCO <sub>3</sub>

<sup>76</sup> Also considered by Lieffering (1990).

Appendix D: Groundwater quality data

Cluster	Well ID	Easting	Northing	Elevation (masl)	Well Depth (m)	Well bottom level (masl)	Dominant cation-anion
Foxton	342081	2700919	6080108	4.83	28.50	-23.67	Ca-HCO <sub>3</sub>
	342161	2704138	6076691	4.80	51.00	-46.20	Na-HCO <sub>3</sub>
	342171	2701955	6081547	7.64	51.30	-43.66	Ca-HCO <sub>3</sub>
	343151	2705362	6077796	10.98	56.90	-45.92	Ca-HCO <sub>3</sub>
	342151	2702346	6079509	6.901	60.00	-53.10	Na-HCO <sub>3</sub>
	342051	2703360	6078432	6.95	65.50	-58.55	Na-HCO <sub>3</sub>
	342141	2702598	6080882	10.18	66.00	-55.82	Na-HCO <sub>3</sub>
	342061	2700054	6079648	2.67	67.10	-64.44	Na-HCO <sub>3</sub>
	342011	2703903	6079869	11.88	72.00	-60.12	Na-HCO <sub>3</sub>
	342001	2704483	6081080	15.31	80.00	-64.69	Na-HCO <sub>3</sub>
	342091	2703738	6077464	3.57	160.00	-156.43	Na-HCO <sub>3</sub>
	342105	2700021	6079231	2.73	205.00	-202.27	Na-HCO <sub>3</sub>
Poroutawhao	352211	2700700	6069700	25.56	18.00	7.56	Na-HCO <sub>3</sub>
	352301	2702300	6071500	23.16	20.40	2.76	Na-HCO <sub>3</sub>
	352011	2702633	6070645	19.75	23.60	-3.85	Na-HCO <sub>3</sub>
	352251	2702201	6068147	8.66	33.90	-25.24	Na-HCO <sub>3</sub>
	352341	2701900	6067400	13.70	37.50	-23.80	Na-HCO <sub>3</sub>
	352001	2702146	6070470	21.76	44.90	-23.15	Na-HCO <sub>3</sub>
	352123	2702683	6068017	7.66	50.60	-42.95	Ca-HCO <sub>3</sub>
	352141	2702214	6069684	21.54	64.00	-42.46	Na-Cl
	352451	2699716	6069177	18.28	67.75	-49.47	Na-HCO <sub>3</sub>
	352291	2703100	6066596	21.41	76.30	-54.89	Na-HCO <sub>3</sub>
	352131	2702509	6066162	22.23	109.29	-87.06	Na-HCO <sub>3</sub>

Table D-5: Wells exceeding DWSNZ 2005 MAVs and/or GVs.

Well ID	TDS	pH	Hardness	Na	Cl	Fe	Mn	NH4	NO3	Number of parameters exceeding MAV and/or GV
316001							>MAV & > GV			1
316037		<GV								1
316041		<GV				>GV	>MAV & > GV	>GV		4
318001							>GV			1
323001			>GV			>GV	>GV			3
323021			>GV			>GV	>GV			3
323027			>GV							1
323092						>GV	>GV			2
323166		<GV	>GV			>GV				3
324011			>GV				>GV			2
324041			>GV			>GV	>GV			3
324057			>GV							1
324071			>GV			>GV				2
325013			>GV							1
325031						>GV	>GV			2
325071						>GV	>GV			2
325081						>GV	>MAV & > GV			2
325091			>GV			>GV	>MAV & > GV			3
325121						>GV				1
325141						>GV	>MAV & > GV			2
325221						>GV	>MAV & > GV	>GV		3

Well ID	TDS	pH	Hardness	Na	Cl	Fe	Mn	NH4	NO3	Number of parameters exceeding MAV and/or GV
325251		<GV				>GV	>MAV & > GV			3
325351						>GV	>MAV & > GV			2
325361		<GV				>GV	>MAV & > GV			3
325381			>GV							1
326011							>GV			1
326021			>GV			>GV	>MAV & > GV			3
326041						>GV	>MAV & > GV			2
326061							>GV			1
326071		<GV	>GV			>GV	>GV			4
326091							>GV			1
326099							>GV			1
326101						>GV	>MAV & > GV			2
326117								>GV		1
326119								>GV	>MAV	2
326131		<GV				>GV	>GV			3
326141						>GV	>MAV & > GV			2
326151						>GV	>MAV & > GV			2
326171						>GV	>MAV & > GV			2
326211						>GV	>MAV & > GV			2
326231		<GV				>GV	>MAV & > GV			3
326241		<GV	>GV			>GV	>MAV & > GV			4
326301						>GV	>GV			2

Well ID	TDS	pH	Hardness	Na	Cl	Fe	Mn	NH4	NO3	Number of parameters exceeding MAV and/or GV
326321							>GV			1
326331			>GV			>GV	>GV			3
326361			>GV							1
327001						>GV	>GV			2
327003			>GV			>GV	>MAV & > GV			3
327005		<GV				>GV	>MAV & > GV			3
327011			>GV				>GV			2
327037		<GV					>GV			2
327041						>GV	>MAV & > GV			2
327051						>GV	>MAV & > GV			2
327071		<GV				>GV	>MAV & > GV			3
327081						>GV	>MAV & > GV			2
327091						>GV	>GV			2
327121						>GV	>GV			2
327131						>GV	>MAV & > GV			2
327141						>GV	>MAV & > GV			2
327191		<GV				>GV	>MAV & > GV			3
333001			>GV			>GV	>GV			3
333011			>GV			>GV	>GV			3
333041			>GV				>GV			2
333048		<GV				>GV				2
333050						>GV				1

Well ID	TDS	pH	Hardness	Na	Cl	Fe	Mn	NH4	NO3	Number of parameters exceeding MAV and/or GV
333061			>GV			>GV	>GV			3
333068			>GV							1
333071			>GV			>GV	>MAV & > GV			3
333081			>GV			>GV	>MAV & > GV			3
333094		<GV								1
333096		<GV				>GV				2
333110		<GV	>GV			>GV				3
333236			>GV			>GV	>MAV & > GV			3
334011			>GV			>GV	>GV			3
334021						>GV	>MAV & > GV			2
334031			>GV			>GV	>MAV & > GV			3
334041			>GV			>GV	>MAV & > GV			3
334051			>GV			>GV	>MAV & > GV			3
334071			>GV			>GV	>GV			3
334091		<GV				>GV	>MAV & > GV			3
334101			>GV			>GV	>MAV & > GV			3
334121			>GV			>GV	>GV			3
335001						>GV	>GV			2
335011						>GV	>MAV & > GV			2
335041			>GV			>GV	>MAV & > GV			3
335051						>GV	>GV			2
335091			>GV			>GV	>MAV & > GV			3

Well ID	TDS	pH	Hardness	Na	Cl	Fe	Mn	NH4	NO3	Number of parameters exceeding MAV and/or GV
335141						>GV	>GV			2
335161						>GV	>MAV & > GV			2
335171						>GV	>MAV & > GV			2
335221						>GV	>GV	>GV	>MAV	4
335241						>GV	>GV			2
335261						>GV	>GV			2
335301		<GV	>GV			>GV	>MAV & > GV			4
335311						>GV				1
335351						>GV				1
335371						>GV	>MAV & > GV			2
335391			>GV			>GV	>MAV & > GV			3
335431						>GV	>GV			2
336001						>GV	>GV			2
336017							>GV			1
336060		<GV				>GV	>GV			3
336061						>GV	>GV			2
336069						>GV	>GV			2
336079						>GV				1
336088							>GV			1
336113							>GV			1
336114						>GV	>GV			2
336141						>GV	>GV			2

Well ID	TDS	pH	Hardness	Na	Cl	Fe	Mn	NH4	NO3	Number of parameters exceeding MAV and/or GV
336181						>GV				1
336200						>GV	>GV			2
336201						>GV	>GV			2
336211						>GV	>GV			2
336241							>GV			1
336271						>GV				1
336333							>GV			1
336391						>GV				1
336401						>GV				1
336421							>GV			1
336441							>GV			1
336442							>GV			1
336471			>GV			>GV	>MAV & > GV			3
336481							>GV			1
336591			>GV			>GV	>MAV & > GV			3
337001							>GV			1
337005						>GV	>GV			2
337007							>GV			1
337011							>GV			1
337012								>GV	>MAV	2
337015							>GV			1
337018								>GV		1

Well ID	TDS	pH	Hardness	Na	Cl	Fe	Mn	NH4	NO3	Number of parameters exceeding MAV and/or GV
337031							>GV			1
337041							>GV			1
337051						>GV	>GV			2
342001			>GV			>GV	>GV			3
342002		<GV				>GV				2
342011						>GV	>GV			2
342041						>GV	>MAV & > GV			2
342051						>GV	>GV			2
342061						>GV	>GV			2
342081			>GV			>GV	>MAV & > GV			3
342105							>GV			1
342141						>GV	>GV			2
342151						>GV	>GV			2
342171			>GV			>GV	>GV			3
343021						>GV	>GV			2
343031			>GV			>GV	>MAV & > GV			3
343051						>GV	>GV			2
343061						>GV	>MAV & > GV			2
343101			>GV			>GV	>MAV & > GV			3
343121						>GV	>MAV & > GV			2
343151						>GV	>GV			2
343161			>GV			>GV	>GV			3

Well ID	TDS	pH	Hardness	Na	Cl	Fe	Mn	NH4	NO3	Number of parameters exceeding MAV and/or GV
343171							>GV			1
344011			>GV			>GV	>GV			3
344031		<GV	>GV			>GV	>MAV & > GV			4
344041			>GV			>GV	>MAV & > GV			3
344051						>GV	>GV			2
344061						>GV	>GV			2
344081		<GV	>GV			>GV	>MAV & > GV			4
344091			>GV			>GV	>GV			3
345011						>GV	>GV			2
345051							>GV			1
345071						>GV	>GV			2
345101						>GV	>GV			2
345111						>GV	>GV			2
345151						>GV				1
346031							>GV			1
346041						>GV	>GV			2
346051						>GV				1
352001						>GV	>GV			2
352003		<GV				>GV	>MAV & > GV			3
352011						>GV	>MAV & > GV			2
352021						>GV	>MAV & > GV			2
352051						>GV	>GV			2

Well ID	TDS	pH	Hardness	Na	Cl	Fe	Mn	NH4	NO3	Number of parameters exceeding MAV and/or GV
352131						>GV	>GV			2
352141	>GV		>GV	>GV	>GV					4
352211		<GV				>GV	>MAV & > GV			3
352241			>GV			>GV	>MAV & > GV	>GV		4
352271	>GV		>GV	>GV	>GV					4
352291							>GV			1
352301						>GV	>MAV & > GV			2
352341							>GV			1
353001						>GV	>GV			2
353015		<GV				>GV				2
353067		<GV					>GV			2
353171						>GV	>GV			2
354011						>GV				1
354021						>GV	>MAV & > GV			2
354031	>GV			>GV		>GV	>GV			4
354061						>GV	>GV			2
363001		<GV						>GV	>MAV	3
363011		<GV				>GV				2
363021		<GV						>GV	>MAV	3
363055		<GV								1
363101	>GV	<GV	>GV	>GV	>GV	>GV	>MAV & > GV			7
363161		<GV				>GV				2

Well ID	TDS	pH	Hardness	Na	Cl	Fe	Mn	NH4	NO3	Number of parameters exceeding MAV and/or GV
363251		<GV				>GV				2
363271						>GV	>MAV & > GV			2
363273		<GV								1

## Appendix E LMC groundwater model data and figures

Table E-1: Observation wells and head data used in model calibration<sup>77</sup>.

Well Name	Easting (X)	Northing (Y)	Screen		Mean observed head		
			Top	Bottom	Height	Confidence (%)	Std Dev
316017	2738281	6116317	175.01	172.01	201.42	50	0.51
316019	2738274	6116322	175.11	172.11	197.01	50	0.19
324061	2722300	6108500	-18.45	-21.45	81.87	75	0.64
324071	2716360	6098295	-139.58	-142.58	39.96	75	1.03
325003	2723385	6106235	-36.06	-39.06	79.87	75	1.51
325007	2728800	6108200	-47.15	-50.15	82.54	75	2.67
325019	2729745	6104072	-28.19	-31.19	47.18	95	4.23
325023	2723463	6100651	-4.72	-7.72	29.65	95	0.62
325031	2730352	6098190	-78.54	-83.24	48.37	95	0.53
325071	2729688	6098834	-91.31	-124.81	49.27	95	0.47
325081	2724585	6099046	-54.79	-57.79	33.94	75	1.87
325211	2729900	6104000	61.06	58.06	65.88	75	0.57
325251	2730110	6108063	53.36	47.36	92.08	95	0.69
325261	2723641	6100688	33.62	30.42	35.11	95	0.60
325351	2730247	6102416	-78.57	-82.57	57.51	95	1.65
325361	2727968	6104045	1.84	-4.16	59.52	95	4.09
326011	2734271	6098740	-51.71	-54.71	53.59	75	0.63
326061	2733901	6099145	-65.16	-68.16	58.43	75	0.25
326181	2735590	6097071	-67.76	-70.76	55.45	75	0.70
326191	2731628	6099141	-102.29	-104.29	51.44	95	0.52
326201	2731188	6099656	-115.19	-118.19	54.74	75	0.28
326211	2735683	6106044	-3.69	-6.69	87.78	75	0.58
326321	2736492	6101178	-63.39	-67.49	63.87	95	0.80
327001	2742679	6098753	26.71	23.71	57.91	75	0.15
327037	2741611	6107000	100.89	100.39	105.58	95	0.18
327039	2742351	6099119	8.49	6.49	61.81	95	0.23
333035	2711086	6095657	-6.48	-9.48	24.00	75	0.35
334021	2722023	6092152	-82.86	-83.86	15.87	95	0.78
334041	2715605	6090956	-82.63	-86.33	23.69	95	0.74
335041	2725446	6094738	-129.86	-133.86	26.59	95	0.52
335051	2724204	6087297	-106.17	-109.17	23.80	75	0.65
335071	2727378	6091887	-70.26	-73.26	24.81	75	0.73
335161	2726480	6095876	-38.60	-41.60	26.17	75	0.42
335171	2724602	6089231	-51.86	-54.86	17.98	75	0.81
335331	2727044	6087486	-117.04	-119.04	28.73	95	0.83
335351	2726004	6088453	-149.69	-152.69	30.65	75	1.70
335361	2728554	6088463	-85.13	-88.13	29.67	75	0.80
335371	2726552	6093332	-87.34	-90.34	23.31	75	0.59
335391	2729492	6096409	-39.87	-41.87	37.45	95	0.60
336001	2732831	6094613	-78.32	-81.32	45.78	75	0.88
336007	2738892	6094889	-25.12	-28.22	53.19	95	0.89
336009	2735800	6093068	-23.29	-26.29	38.29	95	4.51
336017	2737308	6093930	-12.56	-15.56	38.85	75	0.46
336023	2738480	6093205	-15.53	-18.53	49.20	75	1.20
336121	2731895	6088519	-36.33	-39.33	45.66	75	0.99
336141	2736368	6092569	-1.27	-4.27	34.82	75	0.47
336203	2739023	6094570	-15.73	-18.23	49.29	95	2.60
336271	2734300	6089400	-85.28	-88.28	46.58	75	1.44
336301	2731600	6092000	-66.04	-69.04	34.85	75	0.28

<sup>77</sup> All elevations in metres above mean sea level (masl).

Appendix E: LMC groundwater model data and figures

Well Name	Easting (X)	Northing (Y)	Screen		Mean observed head		
			Top	Bottom	Height	Confidence (%)	Std Dev
336333	2735006	6096447	-35.21	-38.21	53.69	95	0.60
336371	2736935	6091665	-12.72	-15.72	43.42	95	1.20
336401	2738005	6092984	-0.94	-3.94	41.81	95	1.25
336421	2735200	6093085	-31.30	-34.30	40.94	95	0.66
336431	2737661	6092472	-9.81	-11.81	43.17	95	0.64
336441	2731967	6088627	-39.16	-42.16	44.79	75	1.15
336511	2735500	6091500	-58.39	-61.39	43.01	75	0.59
336541	2734971	6092983	-35.52	-38.52	40.95	95	0.65
336571	2735044	6088801	-2.44	-5.44	43.67	95	0.99
336581	2736639	6093824	-74.97	-76.47	46.17	95	1.37
336641	2738927	6094267	-13.82	-16.82	46.13	75	0.35
336651	2738427	6094684	26.81	23.81	49.21	75	0.51
337003	2740464	6095659	-31.25	-34.25	57.21	75	0.51
337005	2743665	6094800	-25.92	-31.92	77.03	95	2.15
337041	2741818	6095040	-47.28	-50.28	68.39	75	1.00
342001	2704483	6081080	-61.69	-64.69	10.64	75	0.91
342051	2703360	6078432	-52.45	-58.55	9.61	95	0.36
342091	2703738	6077464	-153.43	-156.43	16.03	75	0.80
343101	2711435	6086030	-11.69	-14.79	30.00	95	0.61
344001	2715768	6078616	-144.74	-148.74	15.98	95	1.24
344007	2718282	6081688	-137.03	-141.03	12.93	95	1.89
344041	2714987	6080259	-60.01	-63.01	13.55	75	0.52
344051	2721233	6084351	-121.14	-124.14	22.72	75	0.82
345009	2727234	6081937	3.50	2.50	30.45	95	0.30
345011	2722414	6085552	-117.76	-120.76	21.75	75	0.68
345101	2726857	6081869	-4.46	-7.46	37.21	95	0.87
345151	2723416	6079642	-62.31	-63.21	32.74	95	0.45
352051	2703128	6072610	-29.25	-32.25	8.95	75	0.55
353291	2709290	6066220	3.01	0.01	10.67	75	3.93
354003	2714870	6070659	-8.94	-11.94	23.36	50	0.17
354005	2713445	6071256	-138.66	-159.76	23.25	95	2.65

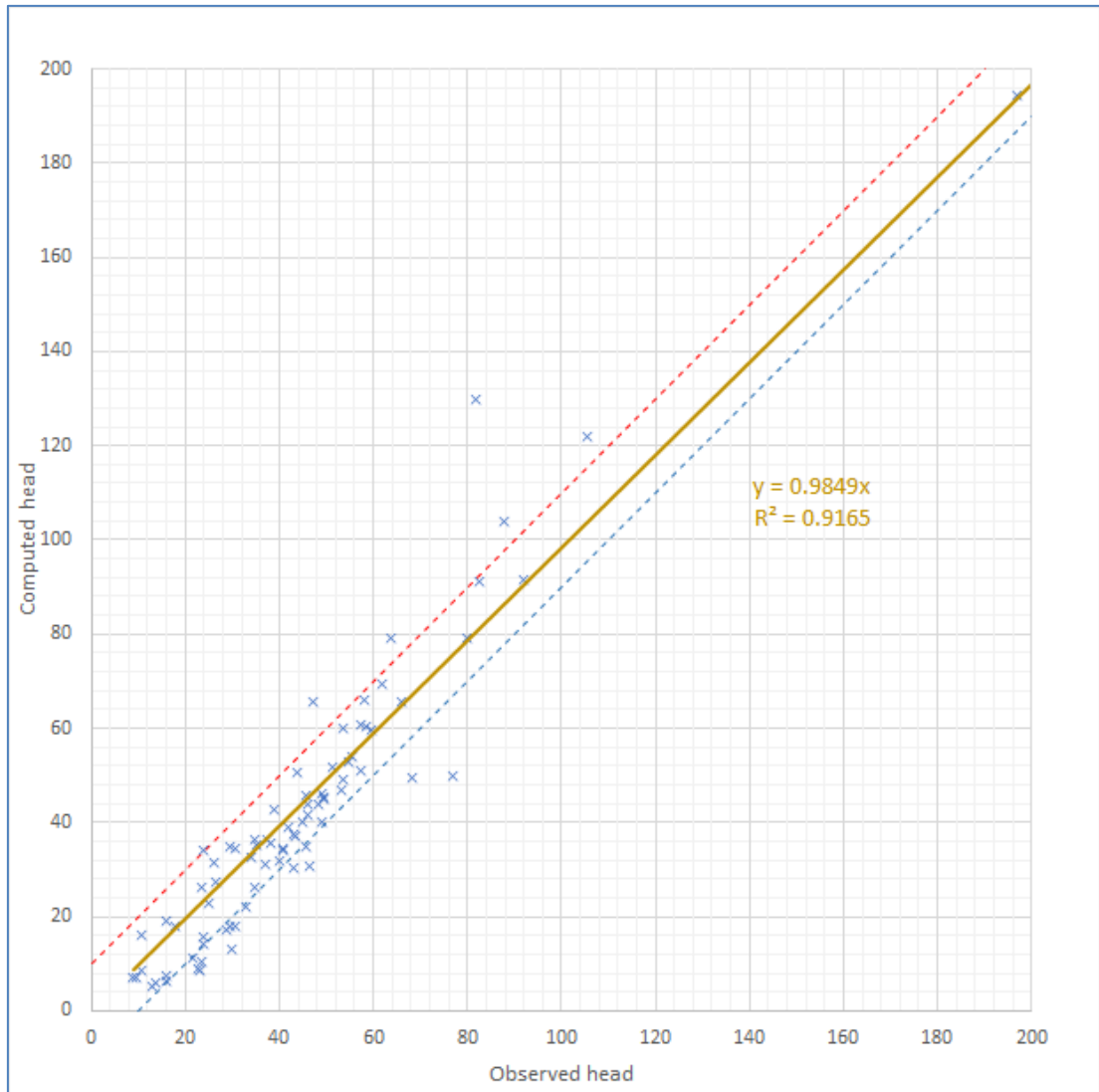


Figure E-1. Scatter plot of measured heads against model calculated heads from automated estimation of hydraulic conductivity assuming homogeneous geological strata and river/stream bed conductance values from Figure 8-9. The brown solid line represents the data linear trend, the red dashed line represents 10 m model overestimation, and the blue dashed line represents 10 m model underestimation. The trend line equation and linear regression goodness-of-fit ( $R^2$ ) are shown on the graph.

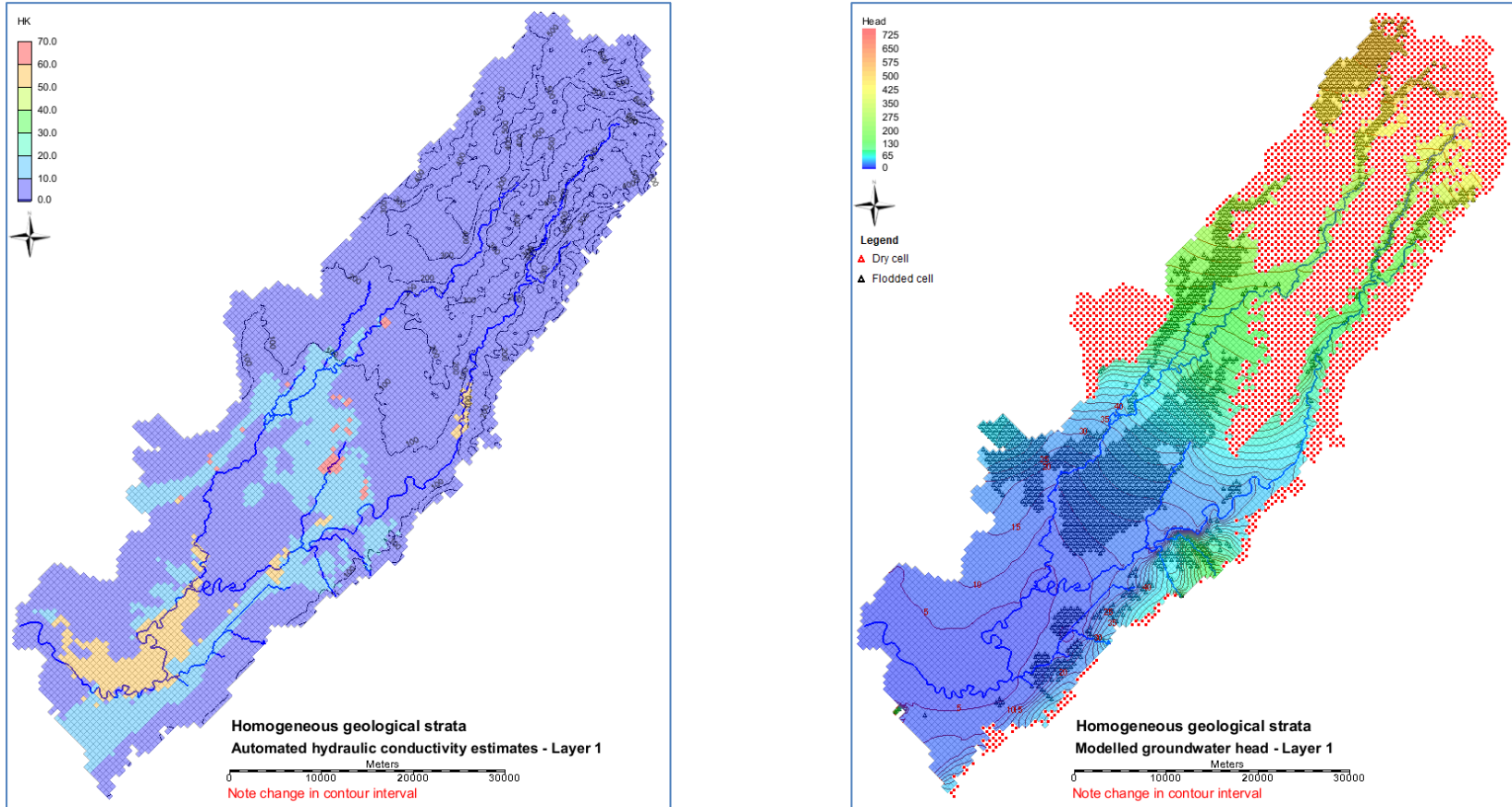


Figure E-2. Contour map of top elevation, automated estimates of horizontal hydraulic conductivity and computed groundwater head for model layer 1 assuming homogeneity of geological strata.

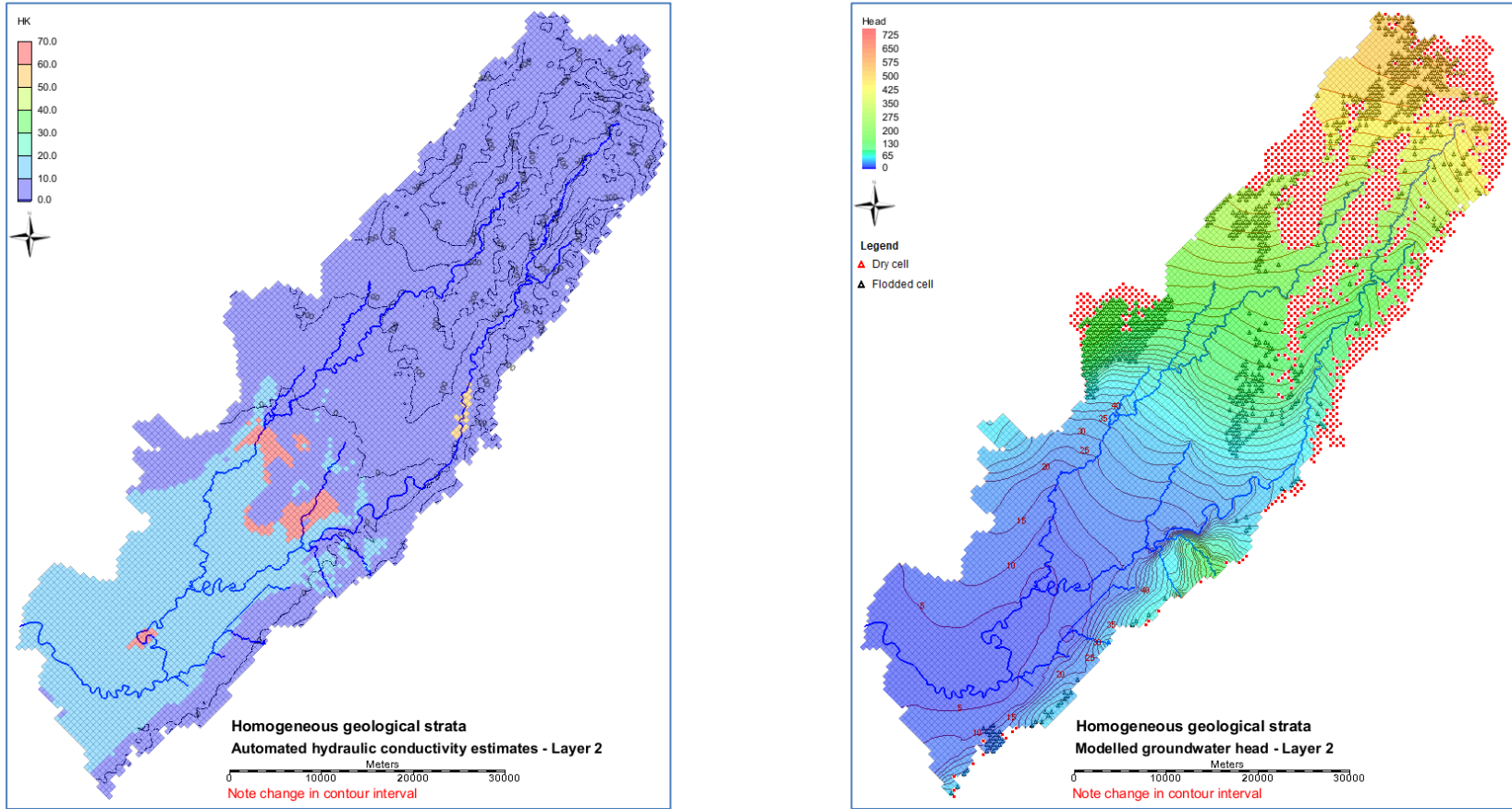


Figure E-3. Contour map of top elevation, automated estimates of horizontal hydraulic conductivity and computed groundwater head for model layer 2 assuming homogeneity of geological strata.

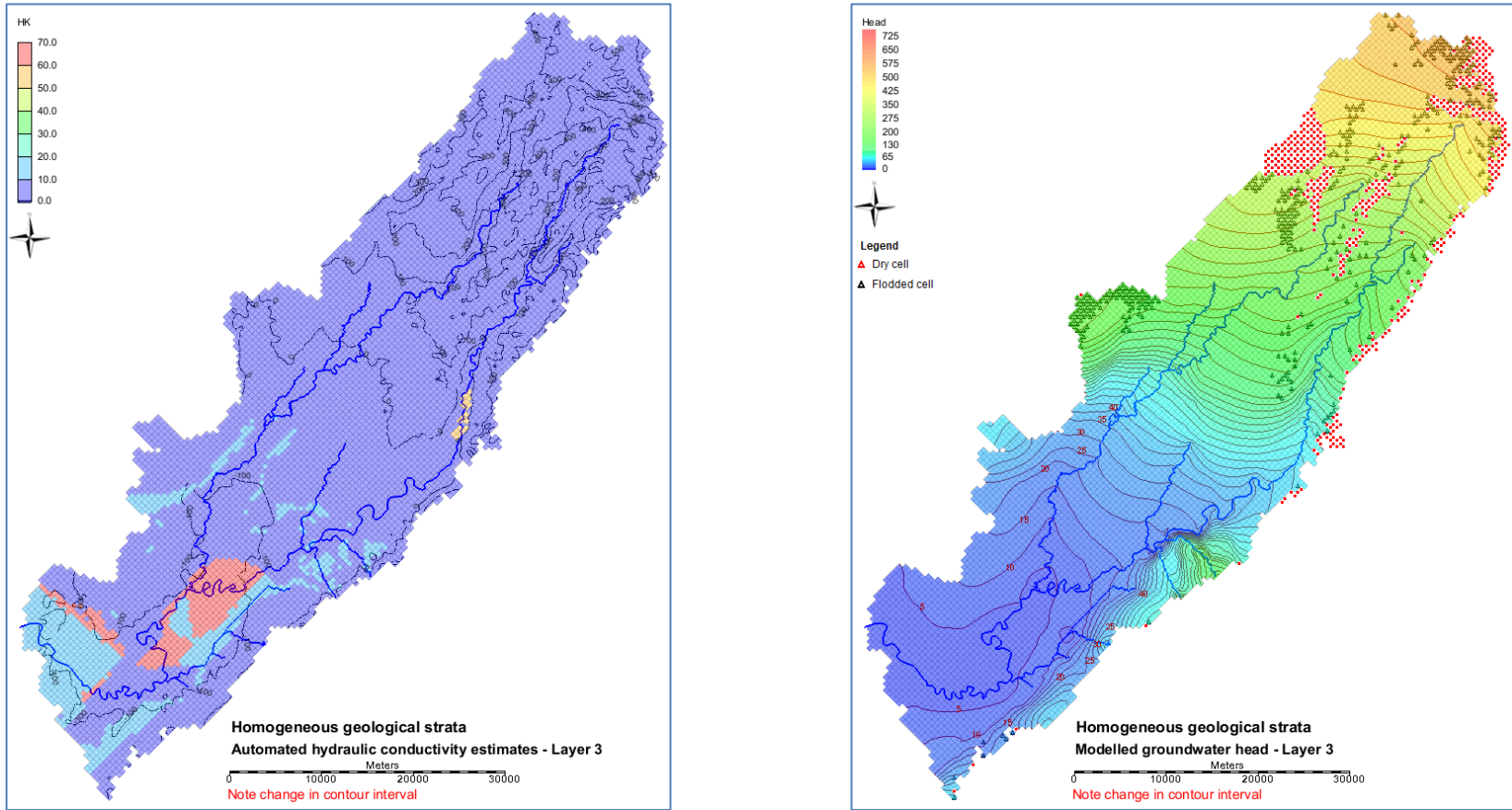


Figure E-4. Contour map of top elevation, automated estimates of horizontal hydraulic conductivity and computed groundwater head for model layer 3 assuming homogeneity of geological strata.

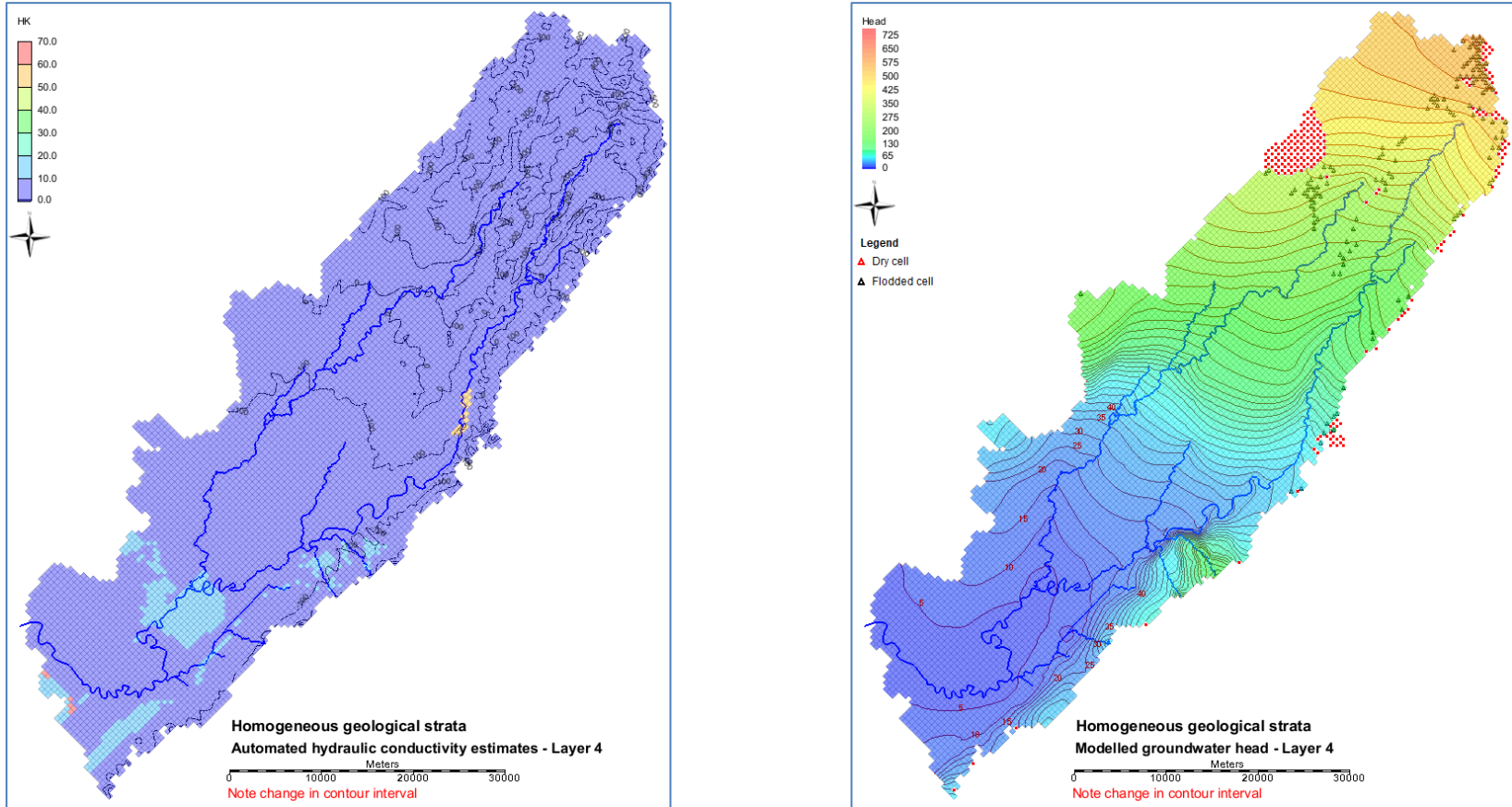


Figure E-5. Contour map of top elevation, automated estimates of horizontal hydraulic conductivity and computed groundwater head for model layer 4 assuming homogeneity of geological strata.

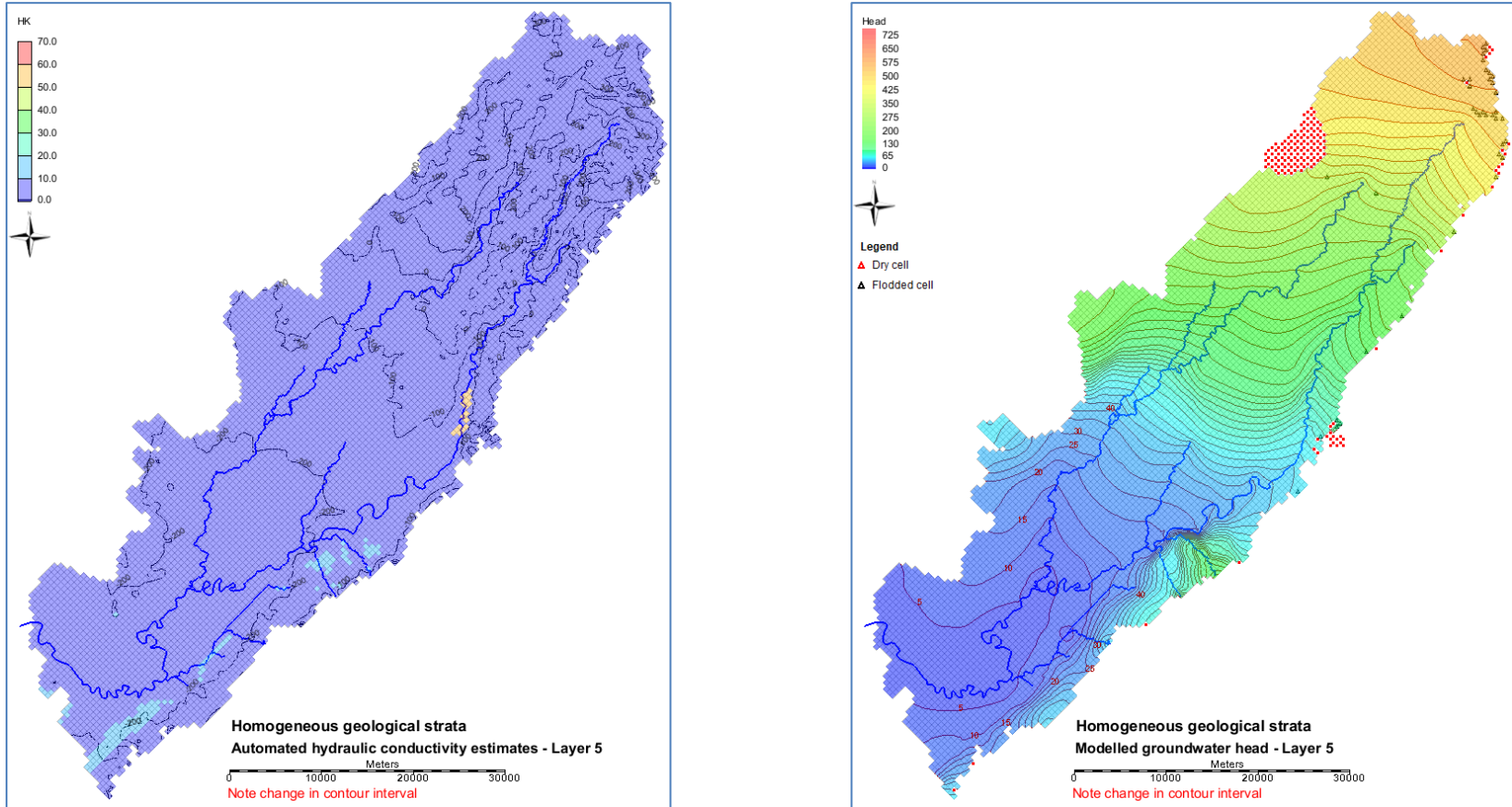


Figure E-6. Contour map of top elevation, automated estimates of horizontal hydraulic conductivity and computed groundwater head for model layer 5 assuming homogeneity of geological strata.

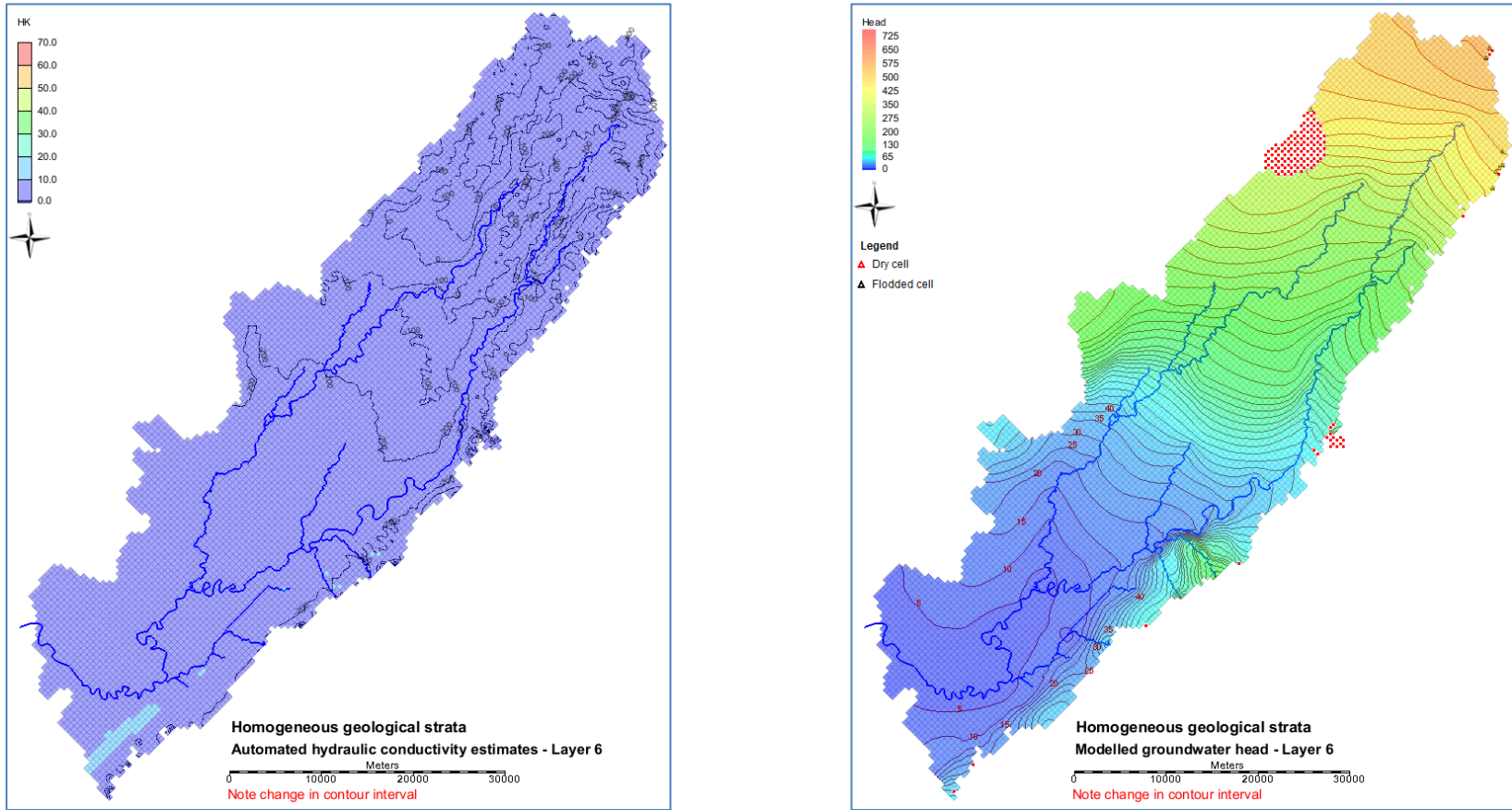


Figure E-7. Contour map of top elevation, automated estimates of horizontal hydraulic conductivity and computed groundwater head for model layer 6 assuming homogeneity of geological strata.

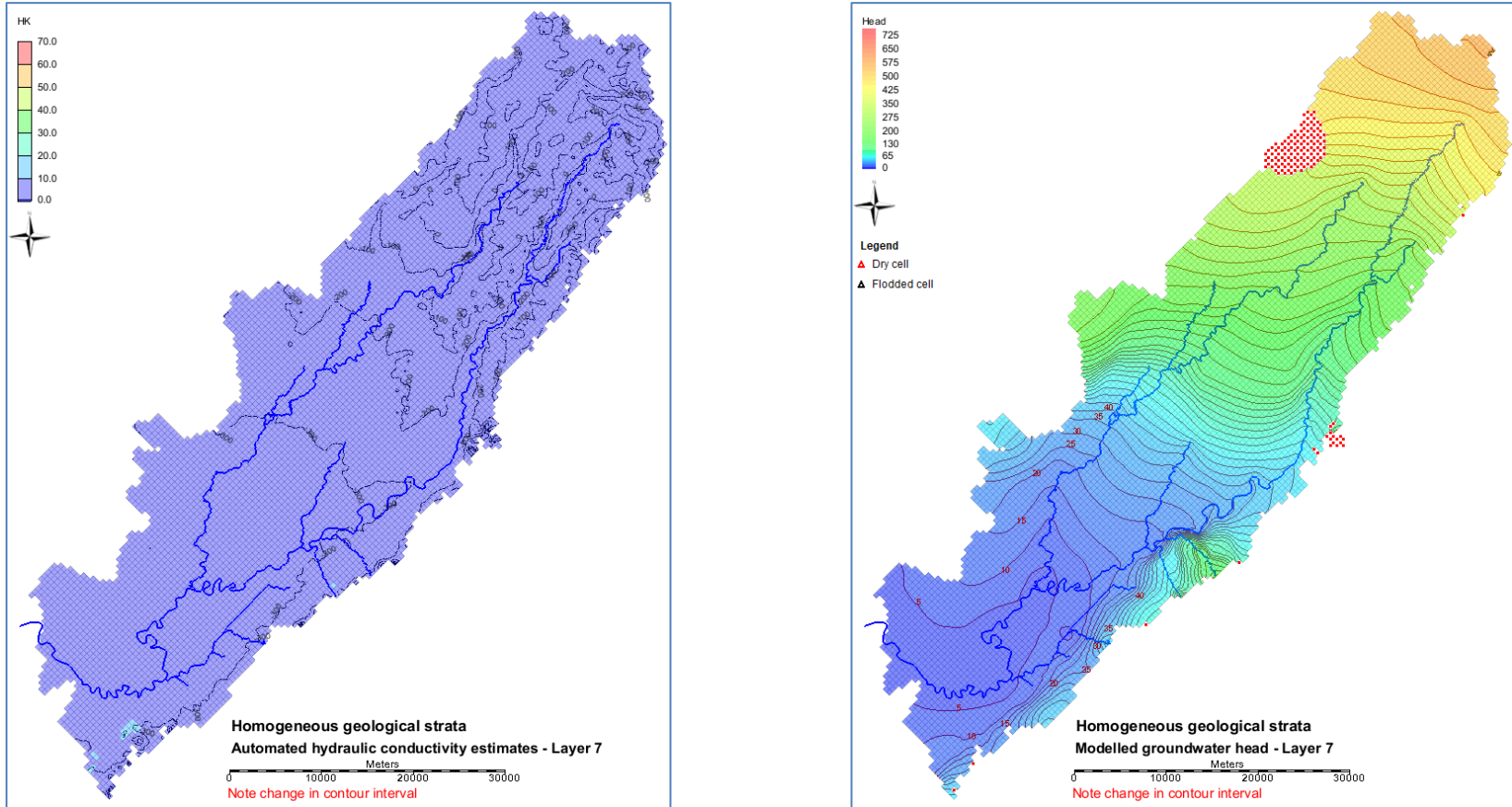


Figure E-8. Contour map of top elevation, automated estimates of horizontal hydraulic conductivity and computed groundwater head for model layer 7 assuming homogeneity of geological strata.

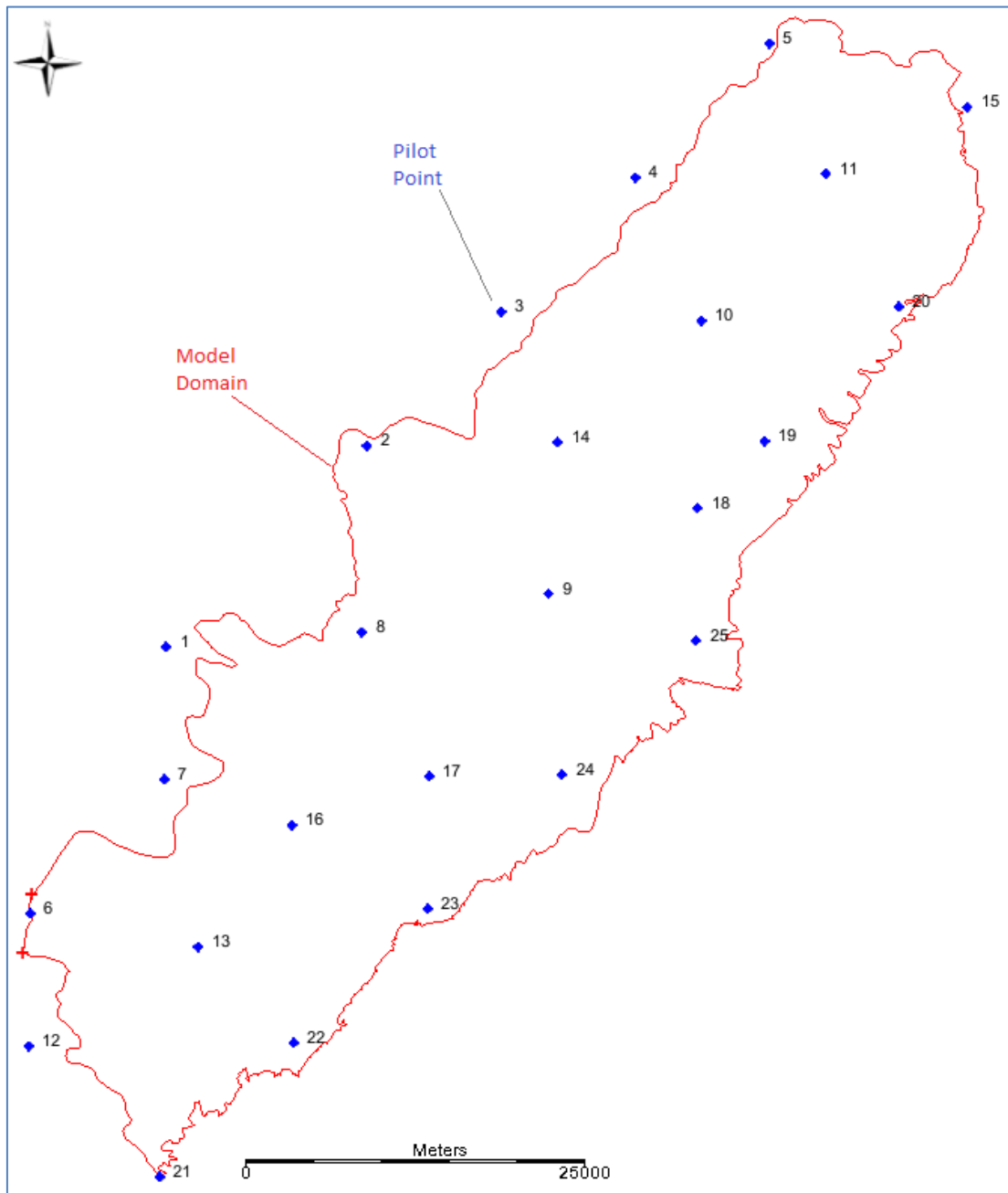


Figure E-9. Map showing the distribution of pilot points for use in automated estimation of hydraulic conductivity assuming heterogeneous geological strata. Labels are point ids.

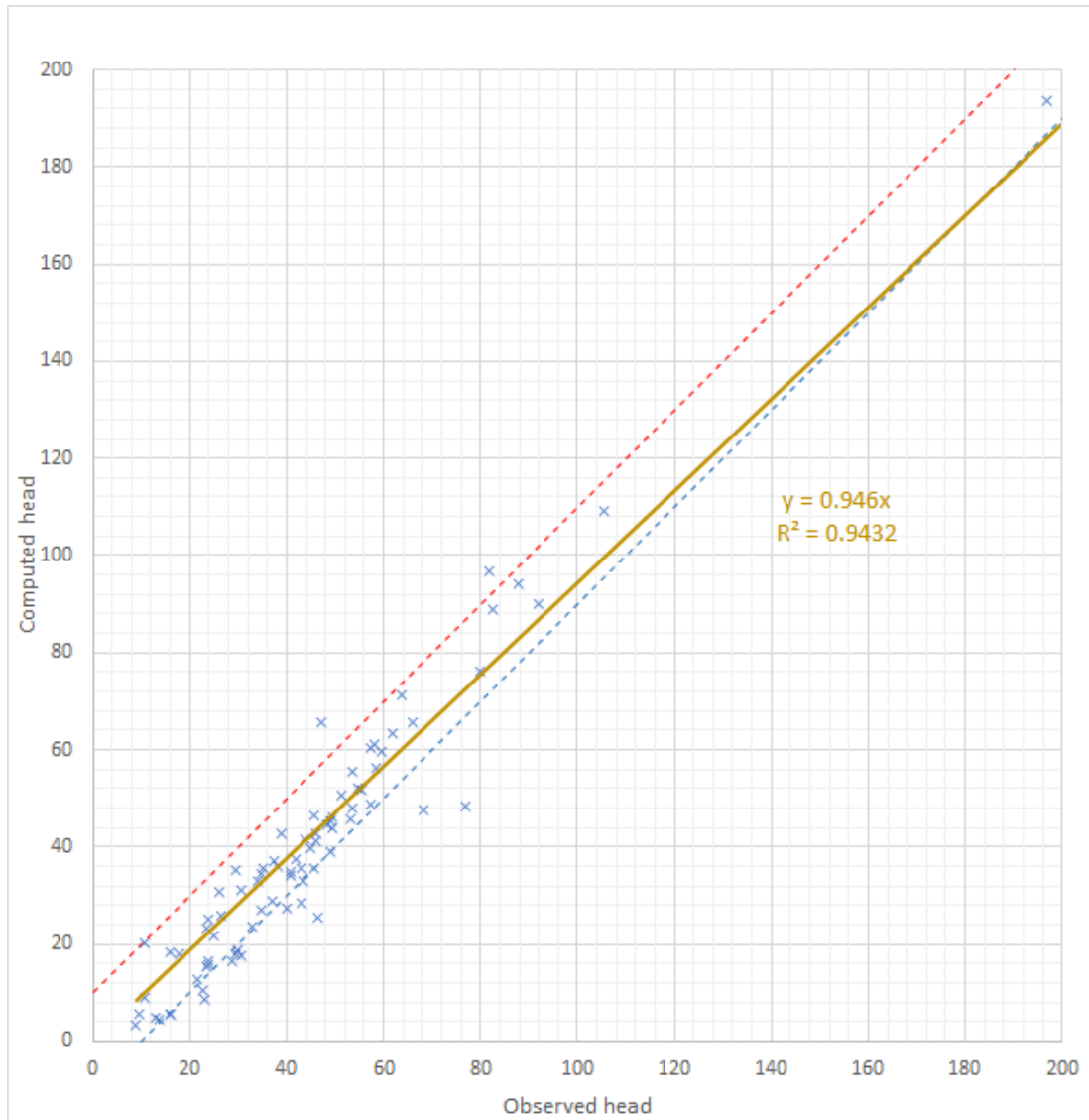


Figure E-10. Scatter plot of measured heads against model calculated heads from automated estimation of hydraulic conductivity assuming heterogeneous geological strata and using river/stream bed conductance values from Figure 8-9. The brown solid line represents the data linear trend, the red dashed line represents 10 m model overestimation, and the blue dashed line represents 10 m model underestimation. The trend line equation and linear regression goodness-of-fit ( $R^2$ ) are shown on the graph.

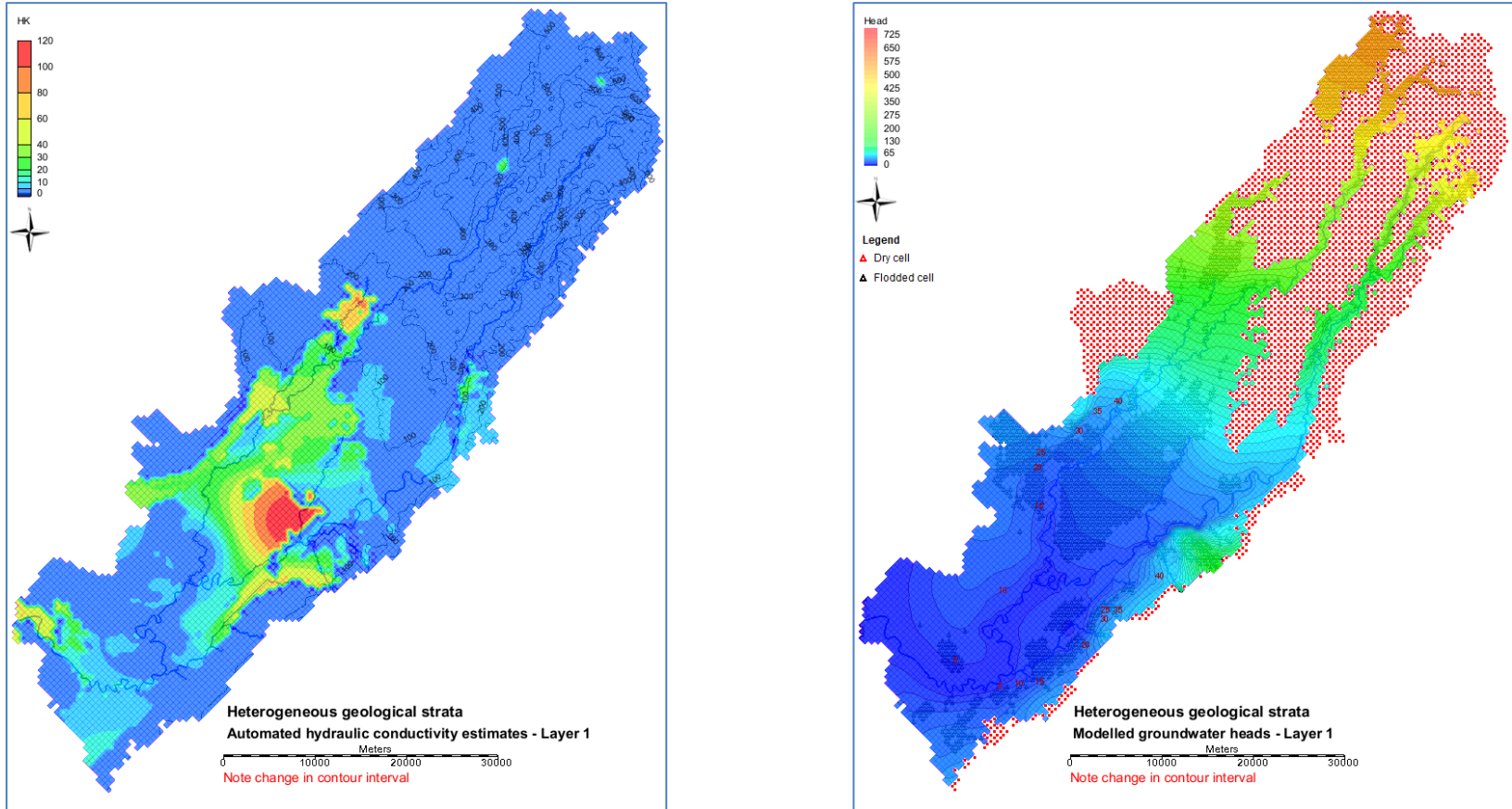


Figure E-11. Contour map of top elevation, automated estimates of horizontal hydraulic conductivity and computed groundwater head for model layer 1 assuming heterogeneity of geological strata.

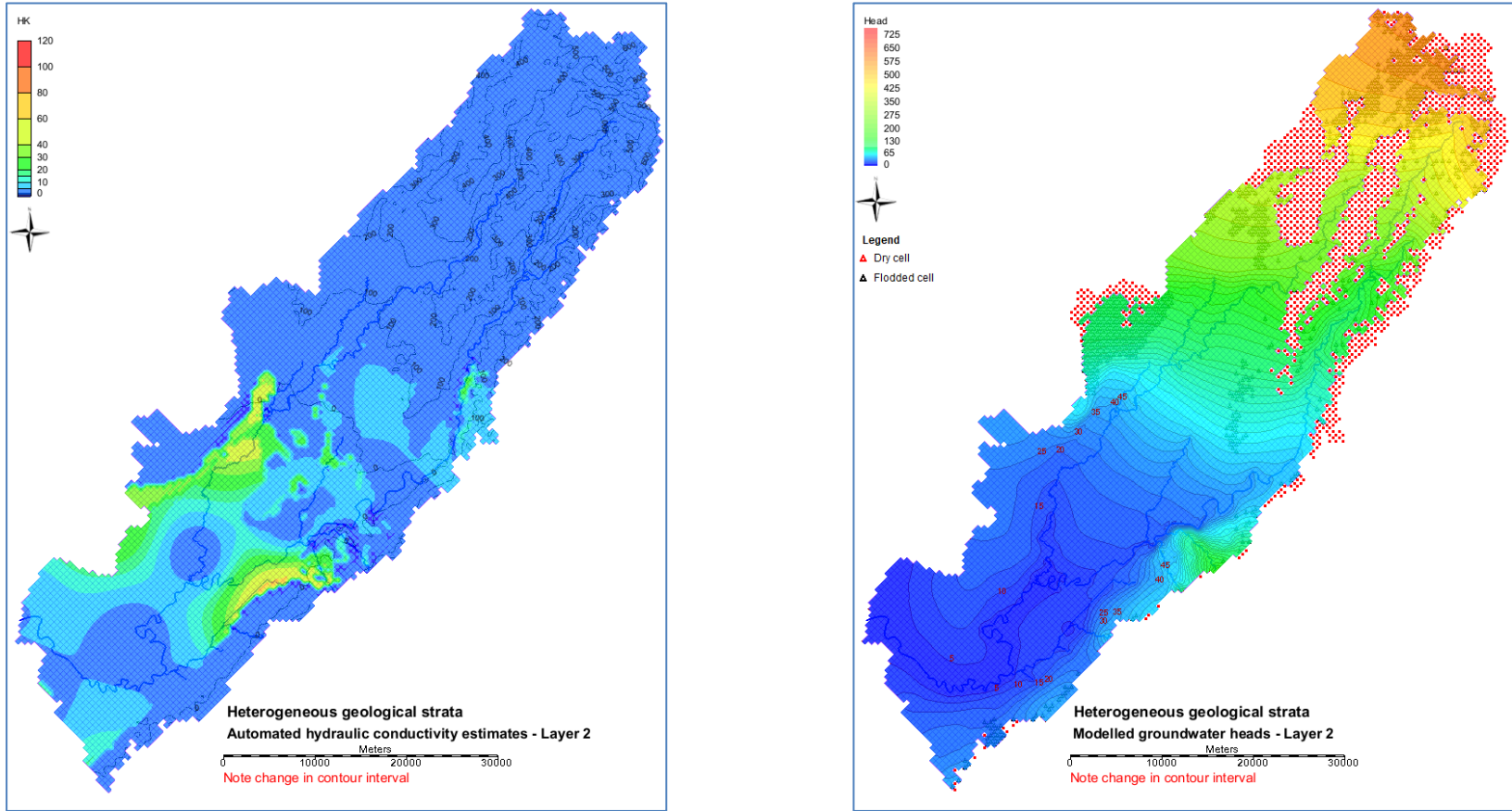


Figure E-12. Contour map of top elevation, automated estimates of horizontal hydraulic conductivity and computed groundwater head for model layer 2 assuming heterogeneity of geological strata.

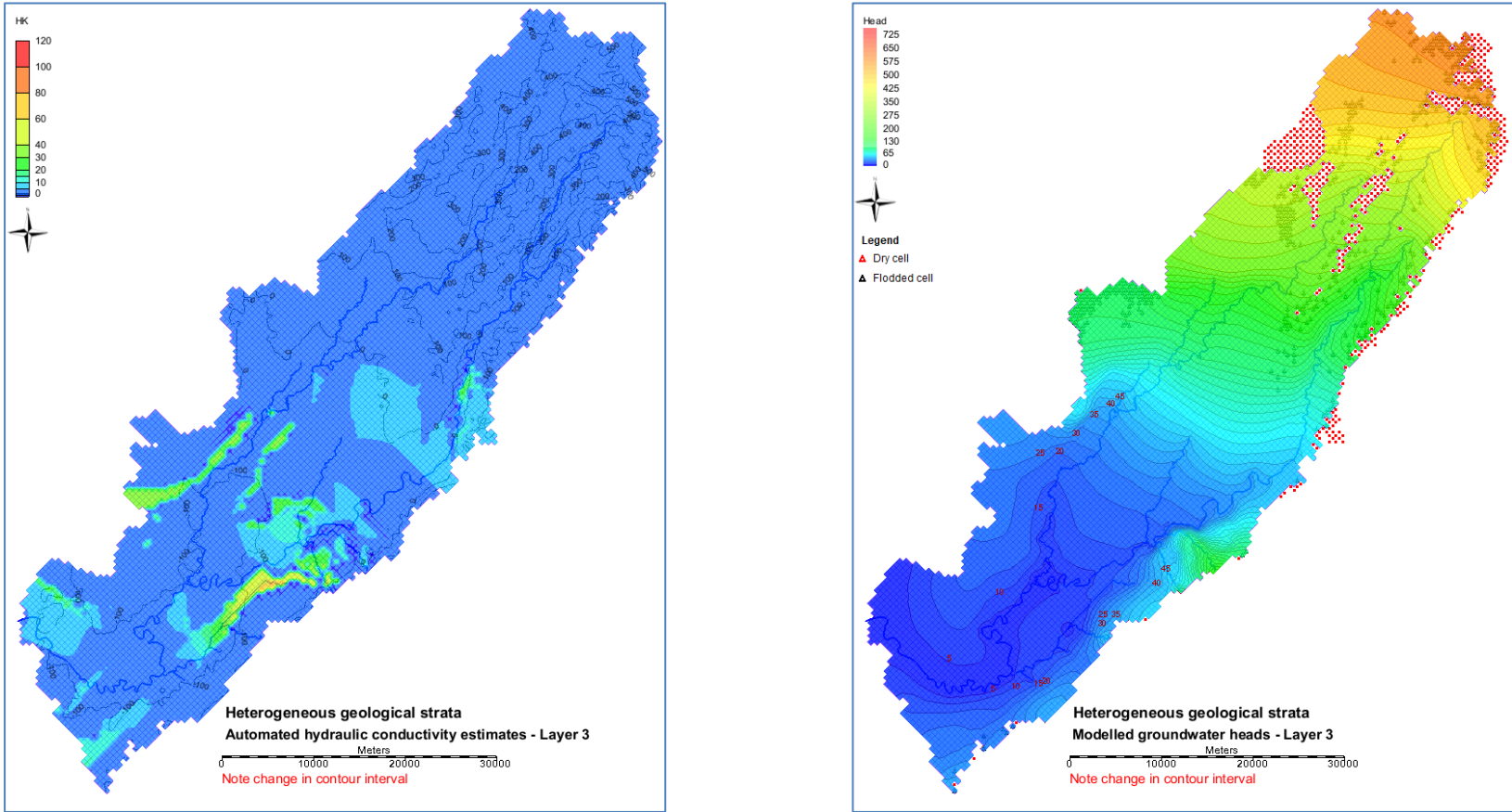


Figure E-13. Contour map of top elevation, automated estimates of horizontal hydraulic conductivity and computed groundwater head for model layer 3 assuming heterogeneity of geological strata.

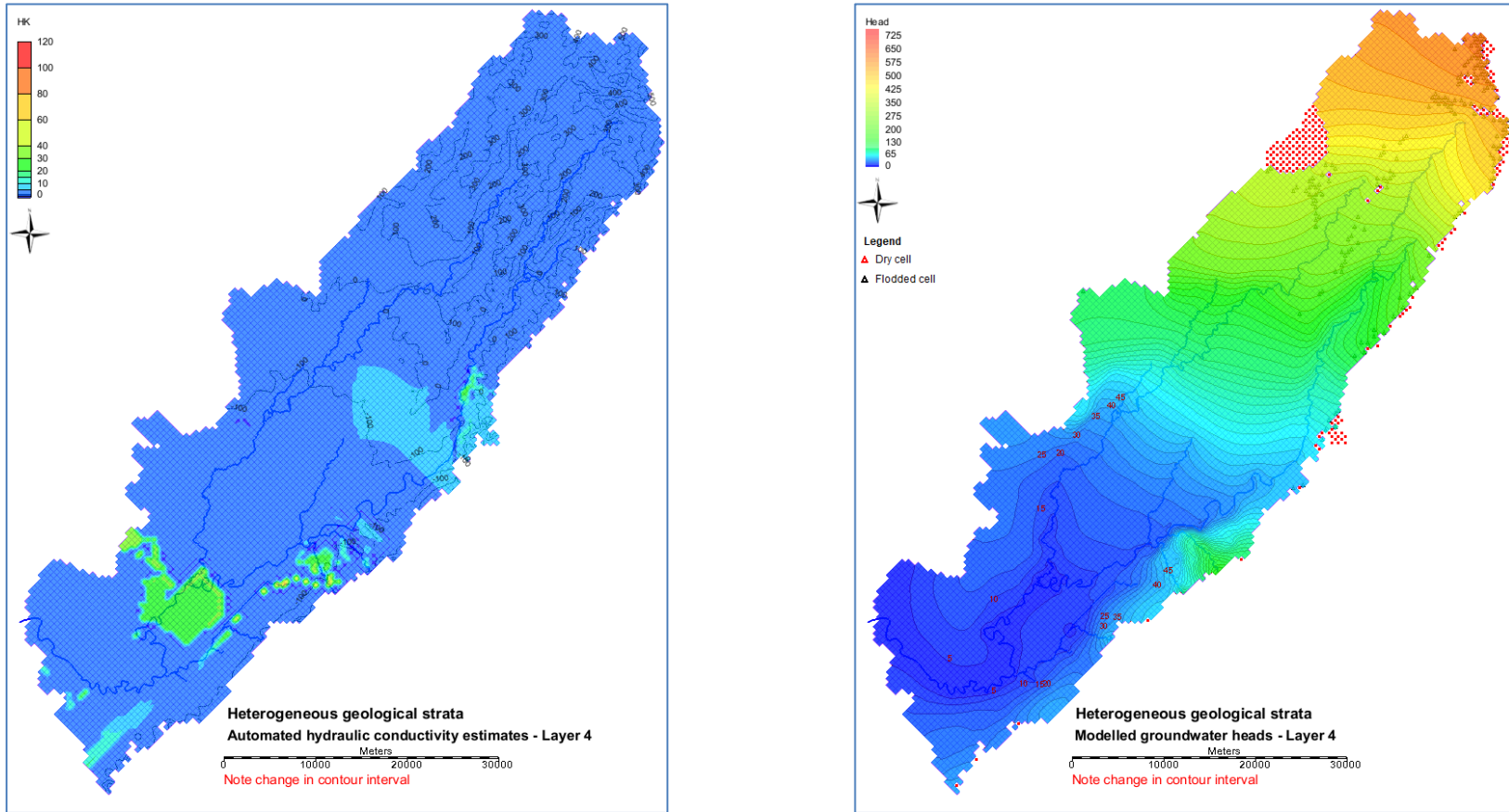


Figure E-14. Contour map of top elevation, automated estimates of horizontal hydraulic conductivity and computed groundwater head for model layer 4 assuming heterogeneity of geological strata.

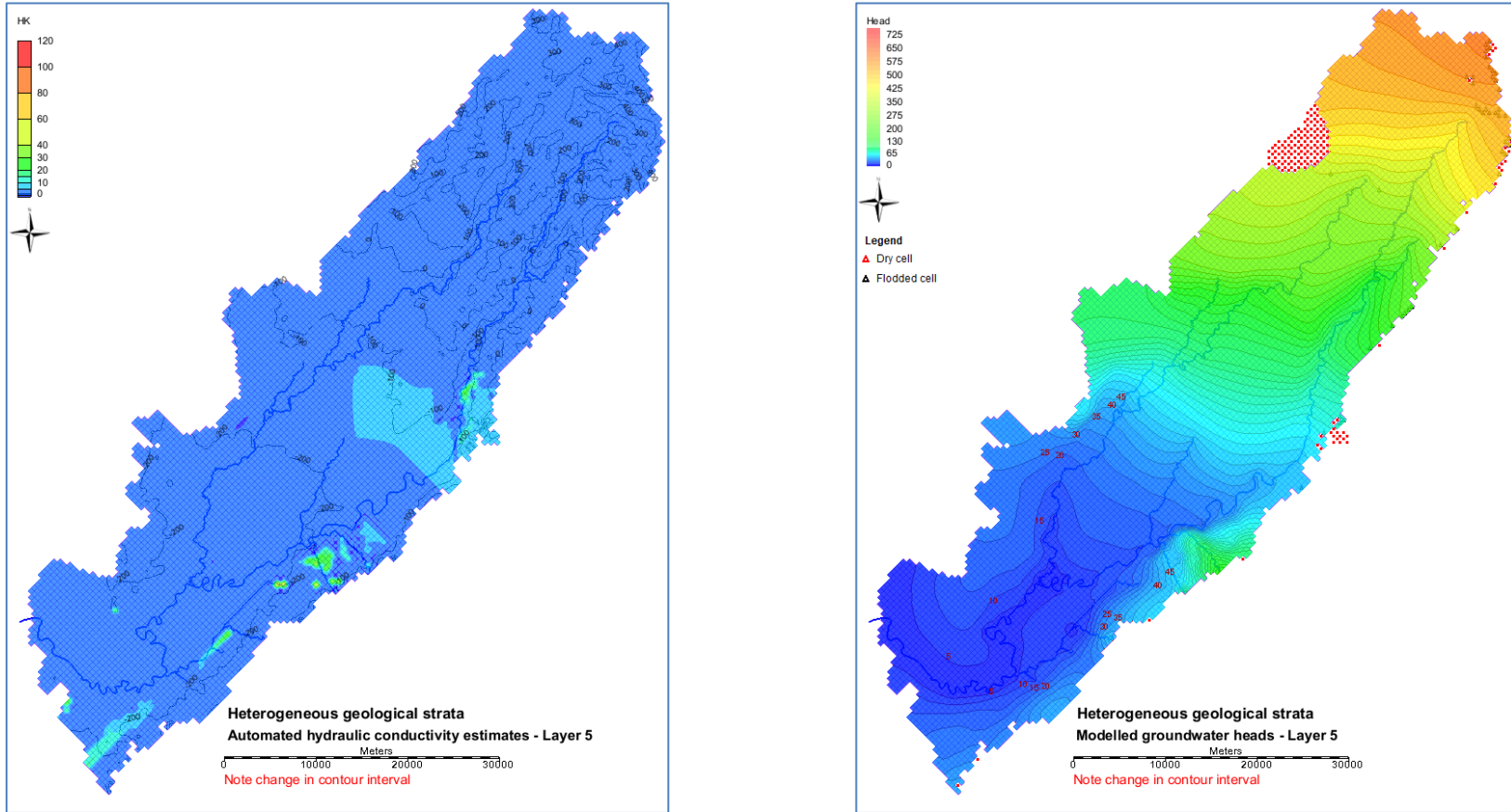


Figure E-15. Contour map of top elevation, automated estimates of horizontal hydraulic conductivity and computed groundwater head for model layer 5 assuming heterogeneity of geological strata.

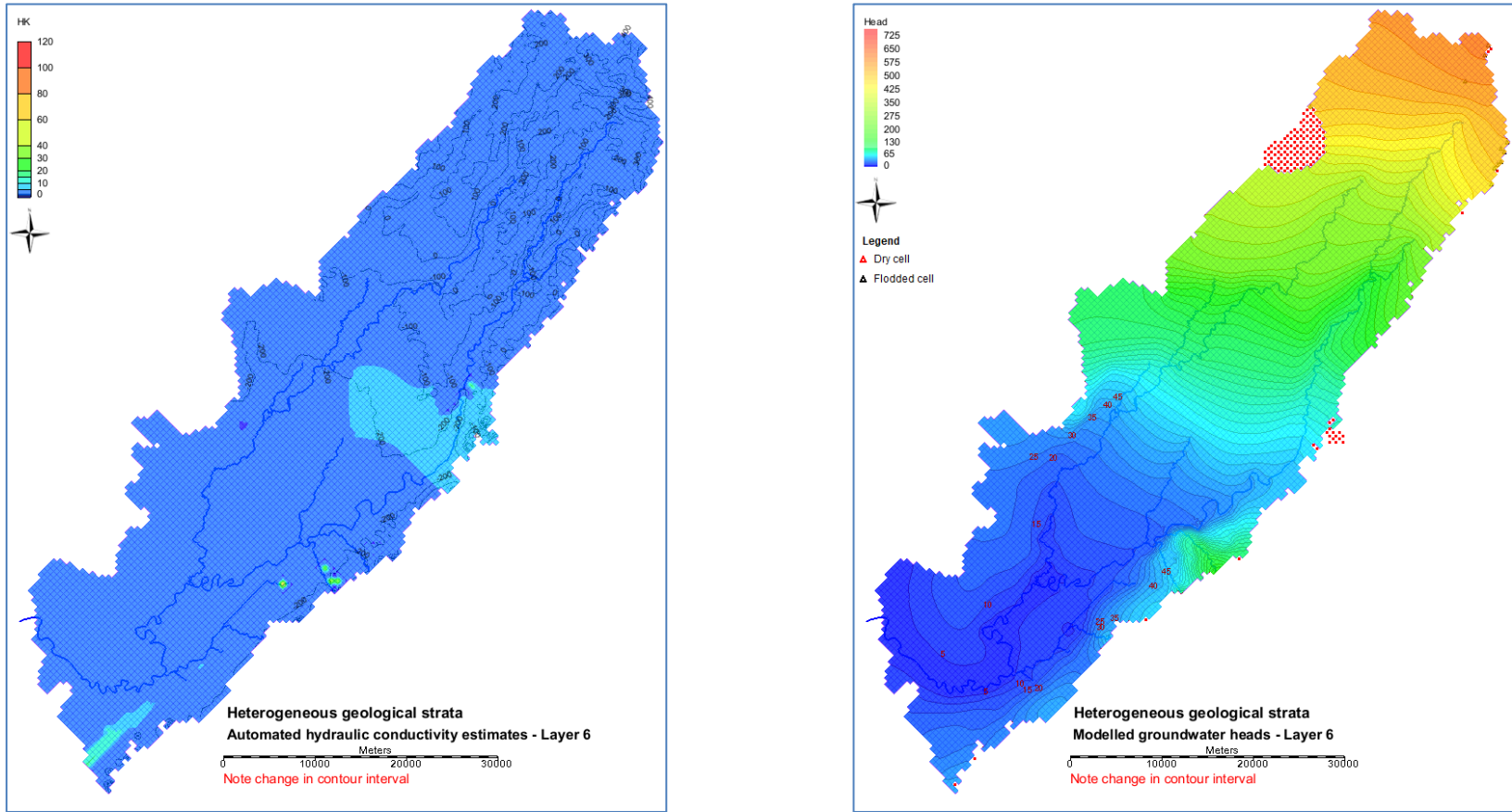


Figure E-16. Contour map of top elevation, automated estimates of horizontal hydraulic conductivity and computed groundwater head for model layer 6 assuming heterogeneity of geological strata.

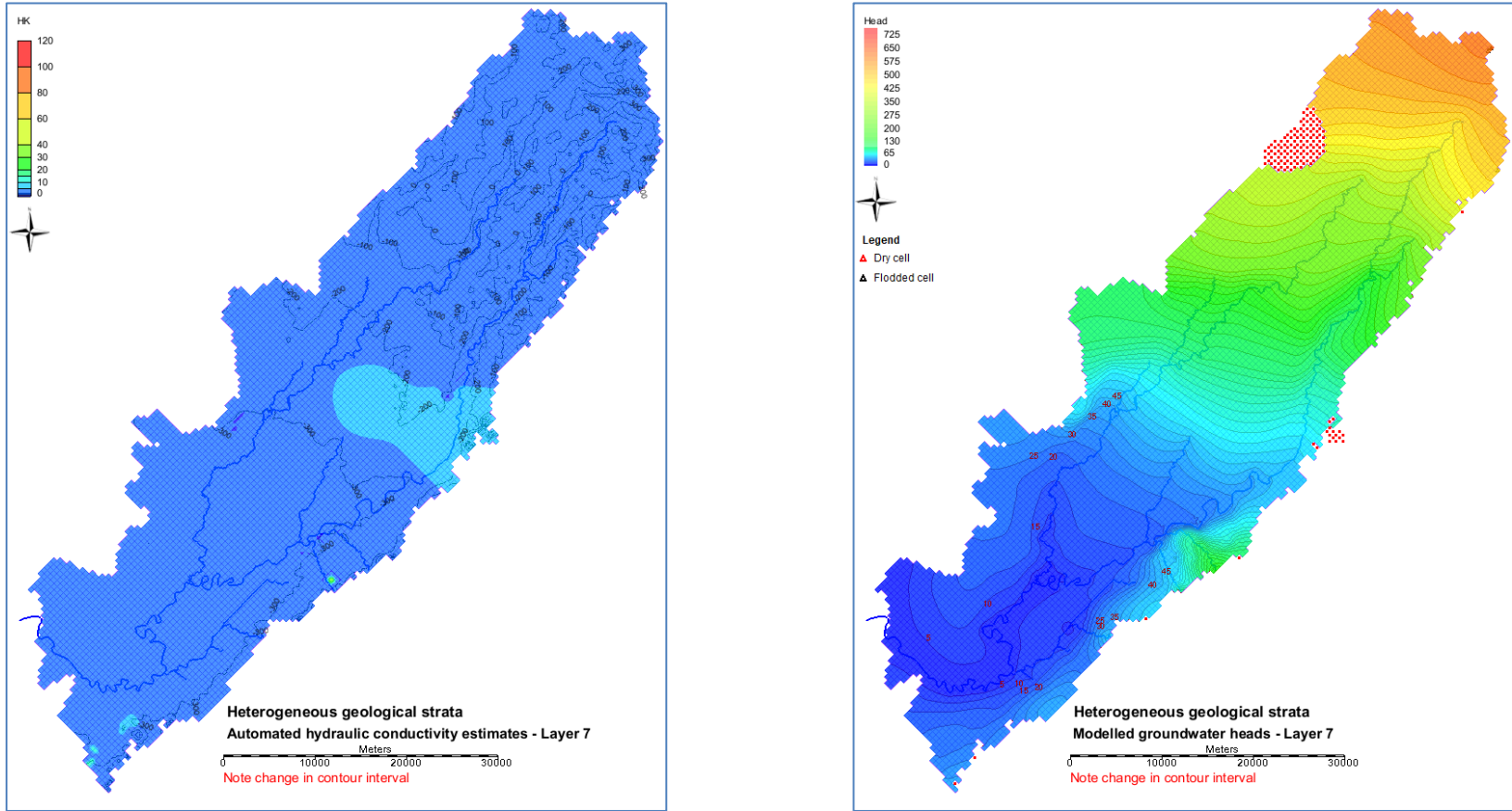


Figure E-17. Contour map of top elevation, automated estimates of horizontal hydraulic conductivity and computed groundwater head for model layer 7 assuming heterogeneity of geological strata.